

# Oxidation of Organic Compounds

Volume II. Gas-Phase Oxidations, Homogeneous  
and Heterogeneous Catalysis,  
Applied Oxidations and Synthetic  
Processes

Proceedings of the International  
Oxidation Symposium, arranged  
by Stanford Research Institute,  
in San Francisco, Calif.

Aug. 28-Sept. 1, 1967

**Frank R. Mayo**

*General Chairman*

ADVANCES IN CHEMISTRY SERIES

76

AMERICAN CHEMICAL SOCIETY

WASHINGTON, D.C. 1968

Copyright © 1968

American Chemical Society

All Rights Reserved

Library of Congress Catalog Card 967-7520

PRINTED IN THE UNITED STATES OF AMERICA

**American Chemical Society  
Library  
1155 16th St., N.W.  
Washington, D.C. 20036**

# Advances in Chemistry Series

Robert F. Gould, *Editor*

## *Advisory Board*

Sidney M. Cantor

Frank G. Ciapetta

William von Fischer

Edward L. Haenisch

Edwin J. Hart

Stanley Kirschner

John L. Lundberg

Harry S. Mosher

Edward E. Smissman

AMERICAN CHEMICAL SOCIETY PUBLICATIONS



## FOREWORD

**ADVANCES IN CHEMISTRY SERIES** was founded in 1949 by the American Chemical Society as an outlet for symposia and collections of data in special areas of topical interest that could not be accommodated in the Society's journals. It provides a medium for symposia that would otherwise be fragmented, their papers distributed among several journals or not published at all. Papers are refereed critically according to ACS editorial standards and receive the careful attention and processing characteristic of ACS publications. Papers published in **ADVANCES IN CHEMISTRY SERIES** are original contributions not published elsewhere in whole or major part and include reports of research as well as reviews since symposia may embrace both types of presentation.

# Rate Constants in the Gas-Phase Oxidation of Alkanes and Alkyl Radicals

JOHN H. KNOX

The University of Edinburgh, Edinburgh, Scotland

*Data on alkyl radical oxidation between 300° and 800°K. have been studied to establish which of the many elementary reactions proposed for systems containing alkyl radicals and oxygen remain valid when considered in a broad framework, and the rate constants of the most likely major reactions have been estimated. It now seems that olefin formation in autocatalytic oxidations at about 600°K. occurs largely by decomposition of peroxy radicals rather than by direct abstraction of H from an alkyl radical by oxygen. This unimolecular decomposition apparently competes with H abstraction by peroxy radicals and mutual reaction of peroxy radicals. The position regarding other peroxy radical isomerization and decomposition reactions remains obscured by the uncertain effects of reaction vessel surface in oxidations of higher alkanes at 500°–600°K.*

The oxidation of hydrocarbons in the gas phase has been studied intensively for over 70 years, yet the mechanism of the process is still poorly understood. Free radicals are certainly involved, but the identity of the elementary steps and their rate constants are in many cases uncertain. The papers in this section were chosen to cover the oxidation of alkyl and other simple organic radicals over a wide range of conditions in order that areas of agreement and divergence of views could be exposed and in the hope that a self-consistent mechanism for gas phase oxidations might emerge.

Two quotations from recent reviews are particularly relevant to any discussion of oxidation mechanisms:

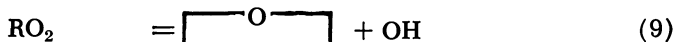
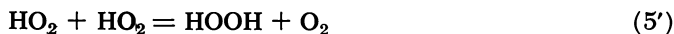
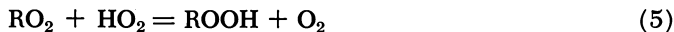
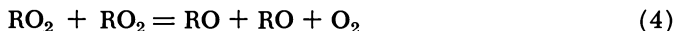
“It is as easy to derive a rate constant for a chemical reaction which does not occur as for one which does occur” (41).

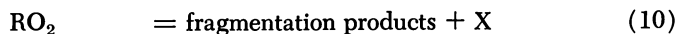
“If there are more than two free radical intermediates, the mechanism (of a reaction) cannot be deduced by a kinetic study based upon analysis of all products and reactants” (32)—the uncertainty principle of reaction mechanism.

Kineticists interested in oxidation have too often failed to appreciate the importance of the second statement and have claimed validity for mechanisms on the grounds that they explain the products and certain basic features of the over-all kinetics of the reactions: they have thus fallen into the trap described in the first quotation. There are indeed few reactions in oxidation about whose importance we can be certain, and even fewer whose rate constants can be stated with any conviction. Nevertheless, the papers presented here, along with other relevant information, allow one to make first some qualitative, and later some quantitative statements about the elementary reactions occurring in oxidation systems.

### *Probable Reactions in Gas-Phase Oxidations*

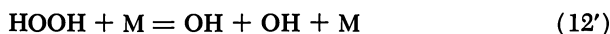
When alkyl radicals are generated in oxygen, there are only a few primary reactions, but the radical products of these reactions evidently undergo many reactions. The elementary steps 0 to 11 are thought to include most of those which are plausible at temperatures between 25° and 600°C. We denote an unspecified radical by X, an alkyl radical by R, an olefin by A, a carbonyl compound by AO, and an oxygen-containing heterocyclic compound by  $\boxed{\text{O}}$ . Primes on symbols denote species with fewer (usually one fewer) C atoms than the parent alkane or alkyl radical. Reaction 11 is the intramolecular abstraction of H from some point in the peroxy radical.





Although Reactions 8 to 10 have been written as distinct unimolecular processes, it is possible that they may occur *via* Reaction 11, followed by decomposition of the QOOH radical. Reactions 9 to 11 are to be regarded as reaction types rather than as single reactions—*i.e.*, each represents several distinct elementary processes.

Oxidations will be chain reactions when one or more of Reactions 7 to 10 are faster than Reactions 4 to 6 combined. They will be autocatalytic when products such as ROOH and HOOH pyrolyze to give new free radicals by reactions such as 12 and 12', or when products such as aldehydes and olefins react with oxygen to give new free radicals by reactions such as 13.



### ***Effect of Temperature on Dominant Reactions***

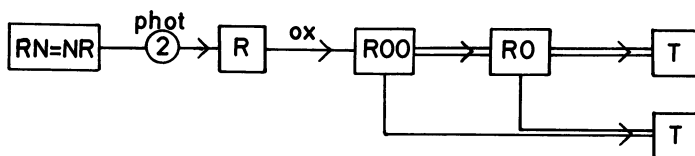
**At 25° to 50°C.** At ambient temperatures Reactions 7 to 10 are slow compared with Reactions 4 to 6 because of their relatively high activation energies, and the alkyl radicals to be oxidized must be generated photochemically or by some other external agency. The oxidations proceed essentially by nonchain free radical processes—*i.e.*, by Reactions 2 and 4 to 6. Typical of such studies are those of Calvert and co-workers (18, 19, 51, 52) on the photo-oxidation of azoalkanes, and of Nalbandyan and co-workers (43) on the mercury-photosensitized oxidation of alkanes. The important reactions are probably represented by Schemes A and B shown in Figure 1. Although Nalbandyan has suggested that the Hg-photosensitized oxidations are chain reactions at room temperature, this seems unlikely in view of the relative unreactivity of peroxy radicals in abstraction reactions. Although the main product at 25°C. is the alkyl hydroperoxide, which presumably arises from Reaction 5, other minor products occur, and other mutual reactions of radicals ought to be added as minor reactions in Scheme B.

In Schemes A and B and those following, the symbols in boxes represent reactive intermediates, starting materials, termination products (T), or branching intermediates (B); single arrows represent elementary reactions consuming one molecule of intermediate; double arrows represent elementary reactions consuming two molecules of intermediate;

② → represents a reaction producing two molecules of intermediate. The descriptions on the arrows give the type of reaction involved: phot = photolysis, Hg phot = mercury-photosensitized decomposition, ox = reaction with oxygen, abs = H atom abstraction from the substrate, pyr = pyrolysis, and wall = reaction on wall.

0 – 50°C

SCHEME A



SCHEME B

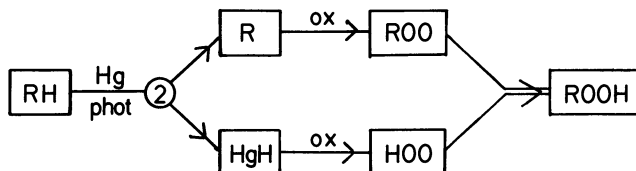


Figure 1. Photo-oxidation of azoalkanes and mercury-photo-sensitized oxidation of alkanes

The mechanisms for ambient temperature oxidations become more complex as the alkyl radical R becomes more complex and as the reactions proceed. Thus, with azo-2-methylpropane (52) the pyrolysis of the *tert*-butoxy radical must be included, and in all but the initial stages, reactions of alkoxy radicals with products containing weak C—H bonds must be included. Numerous tertiary reactions can then occur. As with most free radical systems, useful information can be obtained only if the degree of conversion of the starting material is kept low.

**At 100° to 150°C.** In this range of temperature chain oxidation by Reactions 2 and 7 can occur. Conditions favoring chain reaction are (1) low rates of initiation, which give low radical concentrations and favor Reaction 7 relative to Reactions 4 to 6, (2) high pressures which favor Reaction 7, and (3) high temperatures which increase the rate of

Reaction 7 more than that of Reaction 4. Conditions 1 and 3 will, however, conflict if reactions are thermally initiated (*e.g.*, peroxide decomposition) since the rate of initiation will probably rise faster than the rate of Reaction 7, and the lower temperatures may be more conducive to chain reaction. These features are clearly brought out by the work of Allara, Mill, Hendry, and Mayo (1). The oxidation of 2-methylpropane was initiated by pyrolysis of azo-isobutyronitrile or di-*tert*-butyl peroxide. At 100°C. and high pressure the reaction proceeded by chains of moderate length (50 units at 22 atm.), the length increasing with pressure. At 155°C. when the initiation rate is much higher, the chain length measured as (rate of consumption of alkane)/(rate of generation of radicals by initiation) was around unity at 1 atm. pressure. At the lower temperature the major chain product was hydroperoxide, but at 155°C. the main products were derivable from the *tert*-butoxy radical, as shown in Figure 2. The yield of 2-methylpropene, an important product of the

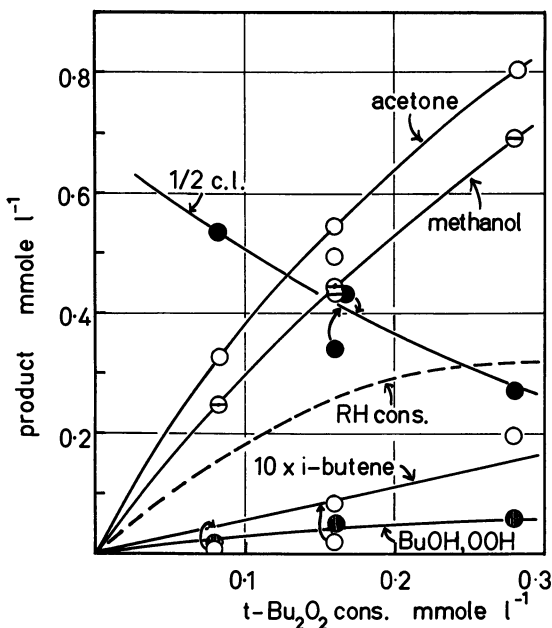


Figure 2. Product development in oxidation of 2-methylpropane at 155°C. initiated by di-*tert*-butyl peroxide

Data from Ref. 1 and private communication

BuOH,OOH represents sum of alcohol and peroxide

RH consumption calculated from products

c.l. represents chain length =  $\frac{[RH \text{ consumed}]}{[2(Bu_2O_2) \text{ consumed}]}$



about 450°C. Reaction 12'. It is not, however, the purpose of this paper to discuss the nature of the branching reactions in alkane combustion. These have been given more than their due share of attention elsewhere.

It is in the region 250° to 400°C. that Johnston's uncertainty principle has so often been ignored. Although Reactions 8 to 11 can explain the formation of the observed products, this is no guarantee that they in fact occur, and there is a great need for careful independent experiments in this area.

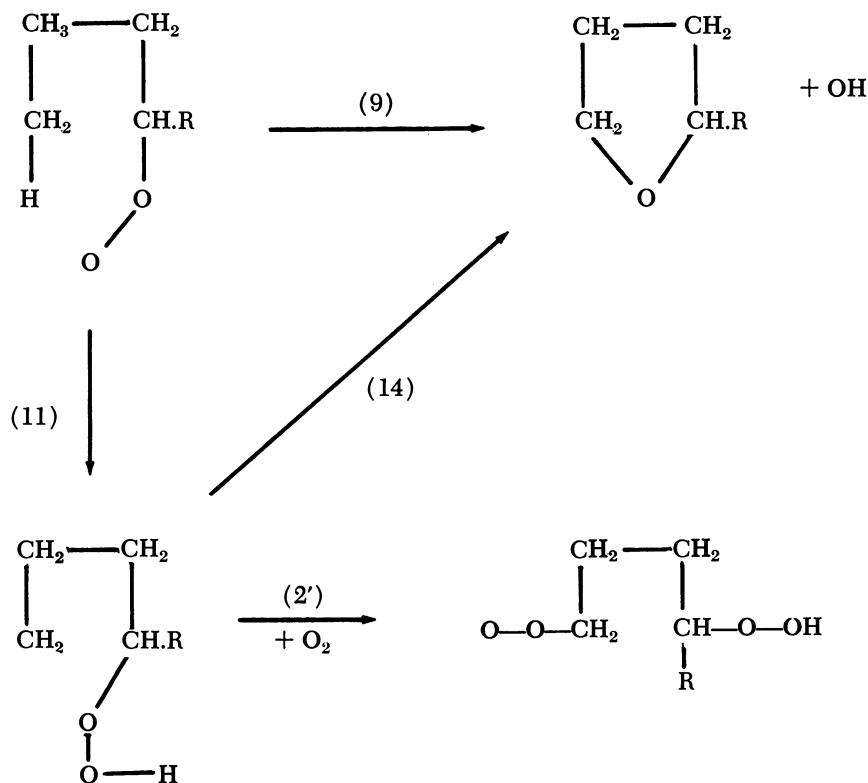
Until recently the major problems in the study of combustion have been analytical since it is essential to determine products in the earliest stages of reaction when secondary reactions involving products can be shown to be unimportant. Generally this implies reactant consumptions below 0.1 or 1%. Only gas chromatography is capable of adequate sensitivity, selectivity, and quantitative accuracy under these conditions. However, even gas chromatography has not been able to deal effectively with the analysis of peroxides, and there is need for more work in this field.

By studying the earliest stages of the autocatalytic combustion of the simpler alkanes, ethane (40), propane (39), and 2-methylpropane (28, 58), it has been shown that about 80% of the initial reaction product is the olefin with the same carbon number as the original alkane (we term this the "conjugate olefin"), and that the remainder of the products form a complex mixture whose composition depends strongly on the nature of the reaction vessel surface (28). We interpret this to mean that there are two basic homogeneous processes, one forming the conjugate olefin, either Reaction 3 or Reaction 2 followed by Reaction 8, and one forming an unstable product which is readily destroyed at the walls. The latter may well be a hydroperoxide, and the second homogeneous process Reaction 7.

Zeelenberg (57) pointed out that if this view were correct, all products from the slow combustion of neopentane should belong to the surface-sensitive group since there was no conjugate olefin for neopentane. Zeelenberg (56) had previously investigated the oxidation of neopentane using an unspecified reaction vessel surface. Turner (55) re-investigated the reaction using two different surfaces. The percentage yields of the three major initial products are given in Table I. These initial fractional yields clearly depend on the surface used and support our contention regarding the nature of the reaction. All the initial products from the neopentane oxidation at about 250°C. arise on the walls of the reaction vessel from some precursor probably formed homogeneously.

With hydrocarbons containing straight chains of five or more carbon atoms (and probably of four carbon atoms also), the initial products at

about 250°C. often contain considerable proportions of oxygen heterocycles, particularly furans (24, 42). It is plausible that they arise either by direct decomposition of peroxy radicals or by internal H abstraction, followed by decomposition of the resulting QOOH or hydroperoxide radical.



Bailey (4, 5) favors the first alternative and Fish (23) the second. The two possibilities can be distinguished if Reaction 14 can be made to compete with a reaction such as the further addition of oxygen, Reaction 2'. This reaction seems well established by Cartlidge and Tipper's (16) isolation of di- and higher hydroperoxides from the oxidation of heptane at 240° to 310°C. A careful investigation of the dependence of the ratio (heterocycles)/(polyperoxides) ought to resolve the problem, provided that the heterocycles arise in true homogeneous reactions, a point which has not yet been proved.

The initial stages of combustion of an alkane between 250° and 400°C. can probably be represented reasonably completely by Scheme D shown in Figure 4. The major points for argument are (1) whether the

conjugate olefin arises from the direct Reaction 3 or from Reaction 2 followed by Reaction 8, and (2) whether the heterocyclic and other minor products arise from homogeneous reactions such as 9 to 11 or from heterogeneous destruction of an unstable intermediate such as a peroxide formed by Reaction 7.

As oxidations proceed, the over-all process becomes increasingly complex as olefins and other primary products, being more reactive than

**Table I. Effect of Surface on Initial Product Distribution in the Oxidation of Neopentane**

Investigator Reaction vessel	Zeelenberg (56) Unspecified	Turner (55) 500 ml. spherical borosilicate glass	
		Clean	HF-treated
Temperature, °C.	260	255	255
RH:O <sub>2</sub>	1:3	2:1	2:1
Pressure, mm. Hg	400	225	225
Initial % age yields of major products			
2-Methylpropene	0 <sup>a</sup>	41	20
Isobutyraldehyde	75	40	55
Acetone	15	12	15
Others	10	7	10
Conversion, %	0.1	From initial gradients: below 0.1%	

<sup>a</sup> Values taken from figure in Ref. 56.

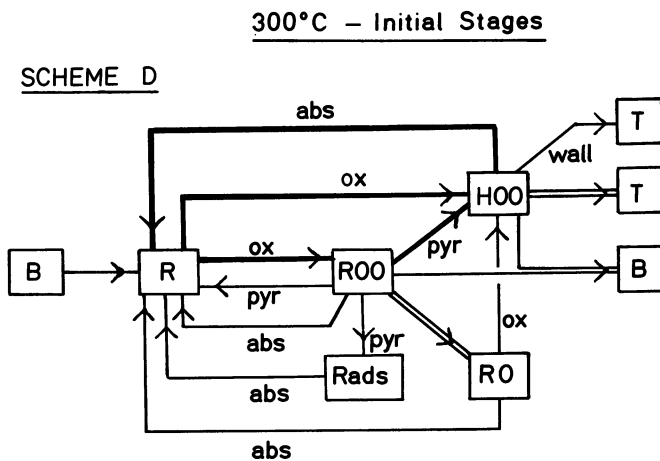


*Figure 4. Low temperature autocatalytic oxidation of alkanes. Heavy lines represent main oxidation route for ethane, propane, and 2-methylpropane.*

the parent alkane, begin to play an important part in the reaction. Until the initial stages of the reaction are clearly understood, there seems little chance of understanding the later stages.

At 350° to 500°C. Above *ca.* 400°C. the combustion of alkanes appears to become simpler. H-abstraction reactions and radical pyrolysis will become faster, so that mutual reactions of radicals should become less important. The homogeneous decomposition of peroxides will be fast (14, 36), and heterogeneous processes will be unimportant. The over-all reactions should therefore become much less sensitive to walls and conditioning procedures, as is observed. The formation of high yields of olefins has long been taken as a characteristic of the "high temperature combustion regime." Shtern (50), for instance, has argued that propene, a major product from all stages of the oxidation of propane above 400°C., arises from the pyrolysis of propyl by loss of H, and ethylene by loss of methyl. The first of these views is almost certainly incorrect since below 600°C. loss of H by an alkyl radical is far too slow to compete with reaction with oxygen (34) even on the most conservative estimate of the rate of 3 or of 2 + 8. The view that all olefins arise from pyrolysis also conflicts with the data obtained in Edinburgh, which showed that initially propene was the major oxidation product from propane even at 320°C. (39). Satterfield and Reid (49) added support to the view that olefins were major products only above 400°C. by their analysis of analytical data from several investigations of propane combustion. They showed that the ratio (propene)/(propane converted to other products including CO, CO<sub>2</sub>) rose with temperature according to an Arrhenius equation

$$\text{Log } k(\text{propene})/k(\text{other products}) = 6.6 - 19,000/2.303 RT$$

They considered that the two competing reactions were Reactions 3 and 2, respectively—Reaction 3 having 19 kcal. more activation energy than 2, and a vastly greater *A* factor. While the activation energy difference might be acceptable, the *A* factor ratio is not. Benson has suggested that the equation can be reinterpreted (12) in terms of a competition between Reactions 2, -2, 3, and 7. Unfortunately, this explanation must also be considered incorrect since both Benson and the original authors have misinterpreted the original data. Our work has shown that the fractional yield of conjugate olefin from the oxidation of a simple olefin exceeds about 80% in the initial stages of oxidation at all temperatures above 300°C., but thereafter it drops rapidly until the ratio (conjugate olefin)/(alkane) becomes roughly stationary (39, 40), when some 10% of alkane has been consumed. The stationary concentration ratio is about 10% at 300°C. and rises with temperature with an activation energy of about 7 kcal. per mole (15). The data used by Satterfield and

Reid were obtained at indeterminate stages of reaction when neither condition held and probably have no simple interpretation. What is clear is that the initial yield of olefin is very high above 300°C. but exceedingly small at 155°C. (1).

It appears that there is little change in the homogeneous part of the combustion of the simpler alkanes above 300°C. in the early stages of reaction. Phenomena such as the negative temperature coefficient and cool flames which indicate important changes of mechanism at around 400°C. are probably associated with changes in the importance of certain secondary reactions. Recently several explanations (11, 38) along these lines have been advanced, and particular attention is drawn here to that of Barnard for the negative temperature coefficient in the combustion of ketones (11).

**At 500° to 600°C.** Alkane combustion at 500° to 600°C. has been studied directly by Sampson (48) using a high speed flow reactor, and indirectly by Baldwin (6-8, 10) using the elegant technique of adding traces of alkanes to slowly oxidizing hydrogen + oxygen whose mechanism is well understood. The work of Sampson showed that the reaction probably occurred by a radical - molecule chain reaction similar to that operating in the hydrogen + oxygen reaction. This is shown by Schemes E and F of Figure 5. For alkanes other than ethane, pyrolysis of the alkyl radicals will occur to a large extent before oxidation and the oxidation mechanism, Scheme G, is somewhat more complex.

Somewhere in the temperature range 450° to 600°C. pyrolysis must compete on nearly equal terms with oxidation of alkyl radicals. The work of Baldwin is therefore particularly important since the rate constants for pyrolysis of alkyl radicals are reasonably well established. There is therefore the strong possibility that we shall soon possess rate constants for oxidation reactions of alkyl radicals at high temperatures. Examination of the oxidation products of the higher alkanes by the Baldwin method should go far toward resolving the problem of the source of fragmentation products at lower temperatures.

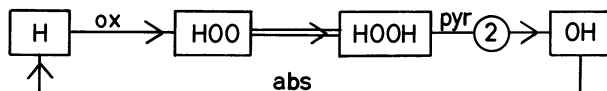
### ***Numerical Values for Rate Constants***

There is little firm information on the rate constants for the majority of Reactions 1 to 11, but if the mechanisms proposed above are broadly correct, a number of quantitative deductions may be made which set limits on several of the values.

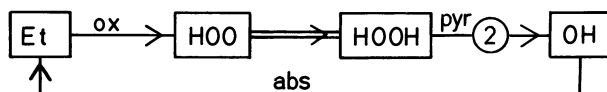
**Reactions 4 to 6.** In the hydrogen + oxygen reaction in boric acid-coated vessels at about 500°C. the mutual reaction of HOO competes with H-abstraction from H<sub>2</sub> (9). The latter reaction causes the slow

500–600°C

## SCHEME E



## SCHEME F



## SCHEME G

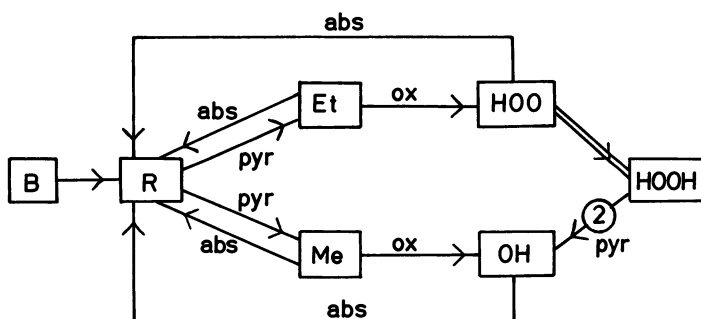


Figure 5. High temperature oxidation

*E*, Hydrogen  
*F*, Ethane  
*G*, Higher alkanes

autocatalysis, and its rate can be obtained relative to Reaction 5' by analyzing the reaction during the induction period. The parameter derivable is  $k_7/k_5^{1/2}$ . The value of  $k_5'$  is probably about  $10^{9.3}$  mole<sup>-1</sup> liter sec.<sup>-1</sup> (25), very close to the rate constant for the isoelectronic reaction, the disproportionation of ethyl radicals (34) for which  $k = 10^{9.4}$ . (Where not stated, the units of bimolecular reaction rate constants are mole<sup>-1</sup> liter

sec.<sup>-1</sup>, and of unimolecular reaction rate constants sec.<sup>-1</sup>; activation energies are in cal. mole<sup>-1</sup>.) According to the Arrhenius equation,  $k_7$  is then:

$$\text{Log } k_7 = (10.2 \pm 1.1) - (25,000 \pm 4000)/2.303RT$$

where the error limits are to be taken together. The A factor seems unduly high for a bimolecular reaction involving a polyatomic nonlinear free radical, and it seems likely that log A and E may both be rather high. We should therefore prefer to take as the best Arrhenius equation:

$$\text{Log } k_7 = 8.8 - 20,000/2.303RT$$

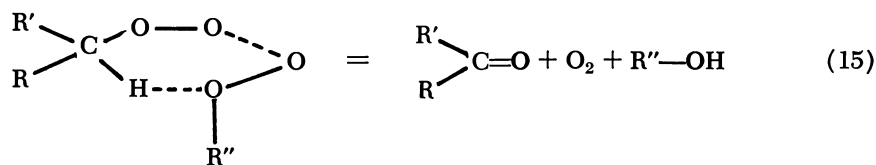
Heicklen (29) argues that Reactions 4 to 6 have similar rate constants at room temperature:

$$\text{Log } k_4 = \text{log } k_5 = \text{log } k_6 = 9.5 \pm 0.3$$

Such values are derived mainly from photo-oxidation studies and depend upon the rate of mutual reaction of methoxy radicals. They seem plausible, except possibly for  $k_4$ . Reaction 4 differs from the others in that it is almost thermoneutral and must pass through a transition state ROO—OOR which is likely to redissociate preferentially into the original fragments since  $D(\text{ROO—OOR}) = 5$  kcal. per mole (14). The value of  $k_4$  might therefore be lower than the others. There is some evidence that this is true. In the gamma-ray (31) and mercury-photosensitized (43) oxidations of alkanes, hydroperoxides are the major products at low temperatures. The simplest explanation of this is that they arise from Reaction 5 (see Figure 1). However, for this to be true, Reactions 4 and probably 5' must have much lower rate constants than Reaction 5. Evidence from studies in the liquid phase presented by Ingold (30) and by Sajus (47) shows that mutual reactions of ROO which are terminating are indeed slow and have considerable activation energies. The range of their rate constants can be expressed by the Arrhenius equation:

$$\text{Log } k_t = 10 - (4,000 \text{ to } 10,000)/2.303RT$$

that is, they lie between about  $10^4$  and  $10^8$  at 300°K. and are much lower than  $10^{9.5}$  proposed by Heicklen for Reaction 4. However, the termination reaction is not Reaction 4, but probably 15 as proposed by Russell (46, 53) which involves a ring transition state.



Although the partial O—H bond may not be required in Reaction 4, and  $A_4$  may slightly exceed  $A_{15}$ ,  $E_4$  is likely to be at least as large as  $E_{15}$  since

Reaction 4 is much less exothermic than 15. Thus, Reaction 4 could well be very slow, and its rate constant is still uncertain. This is unfortunate since the most likely way of obtaining  $k_7$  is by setting up competition between Reactions 4 and 7 so as to yield the rate constant ratio  $k_7/k_4^{1/2}$ .

**Reactions 2, -2, and 3.** The equilibrium constant for Reaction 2 has been independently estimated by Knox (37) and by Benson (12). For nonconjugated radicals it is probably given within a factor of 3 by

$$\text{Log } K_2 = \log k_2/k_{-2} = -5.2 + 29,000/2.303RT$$

the value of  $k_{-2}$  is then obtainable from  $K_2$  and  $k_2$ . The rate of addition of oxygen to alkyl radicals has been measured for ethyl in three studies. Dingley and Calvert (18) obtained a value of  $k_2 = 10^{9.6}$  from a study of the photo-oxidation of azoethane by flash photolysis; Goldfinger *et al.* (26) obtained  $10^{8.7}$  from a study of the oxygen-inhibited chlorination of ethane, and Avramenko and Kolesnikova (2) obtained  $10^{9.1}$  from a fast flow experiment. Thus, the true value probably lies in the range:

$$\text{Log } k_2 = 9.1 \pm 0.5$$

and

$$\text{Log } k_{-2} = 14.3 \pm 0.5 - 29,000/2.303 RT$$

Above 300°C. the effective reaction of an alkyl radical with oxygen may be Reaction 3 rather than 2 because of the reversibility of Reaction 2. If it is assumed that Reaction 3 is important at about 450°C., its rate can be estimated from the competition between pyrolysis and oxidation of alkyl radicals. Falconer and Knox (21) observed that the ratio of (propene)/(ethylene) from the oxidation of propane between 435° and 475°C. increased with oxygen concentration and decreased with temperature—the apparent activation energy difference for the two reactions forming the olefins being  $27 \pm 5$  kcal. per mole. They interpreted this result in terms of a competition between Reactions 1 and 3. The observed ratio (propene)/(ethylene) was 3.5 at 435°C. and 10 mm. of Hg pressure. If  $\log k_1(\text{propyl}) = 13.2 - 30,000/2.303RT$ , the value for the *n*-propyl radical (34), then  $\log k_3 = 8.0$ . If the *A* factor is  $10^{9.5}$ , we derive the Arrhenius equation

$$\text{Log } k_3 = 9.5 - 5,000/2.303RT$$

The activation energy difference  $E_1 - E_3 = 25$  kcal per mole then agrees with the experimental value.

**Reaction 7.** The Arrhenius parameters for the H-abstraction reactions of peroxy radicals may be estimated from general considerations. Generally H-abstraction reactions by polyatomic radicals have *A* factors in the range  $10^{7.5}$  to  $10^{8.5}$ —*e.g.*,  $\text{CH}_3$  (54),  $\text{CF}_3$  (3, 45),  $\text{CH}_3\text{O}$  (27). The activation energies for such reactions depend upon the type of radical

and upon the type of bond being broken. For a given radical reacting with members of a homologous series it is expected that a smooth variation of  $E$  with  $\Delta H$  will be observed, such as is embodied in the Evans-Polanyi relation (20)

$$E = a\Delta H + c$$

where  $a$  and  $c$  are constants. Clearly the Evans-Polanyi relation cannot hold over more than a restricted range of  $\Delta H$  since when  $\Delta H$  is large and positive,  $E$  must approach  $\Delta H$  and  $a$  must tend to unity, while when  $\Delta H$  is large and negative  $E$  must approach zero and consequently also  $a$ . Thus, a smooth curve is expected for any extended range of  $\Delta H$ , as is shown clearly in Figure 6 for the reactions of halogen atoms (22) where  $\Delta H$  ranges from  $-13$  to  $+33$  kcal. per mole, and  $a$  changes from near zero to near unity. The data for other radicals (33), while less extensive, show similar features. Figure 6 also shows that for highly reactive species like the halogens the change of gradient around thermoneutrality is rapid, but for less reactive species like  $\text{CH}_3$  it is more gradual. For such radicals the Evans-Polanyi relation may be expected to hold within experimental error over a range of, say, 20 kcal. per mole in  $\Delta H$ . The selectivity of a given radical with respect to different members of a homologous series will to a first approximation be related to  $a$ . It is clear from Figure 6 that the selectivity of an unreactive radical like methyl will be less than that of a reactive radical like Br for reactions of the same endothermicity; thus, selectivity cannot be used as a simple measure of the general reactivity or the endothermicity of a radical reaction. When considering the ROO radical it seems reasonable to suppose that its electrophilicity will be similar to that of the RO radical in reactions of the same  $\Delta H$ , and hence that the  $E$ 's for ROO radicals should lie on an extension of the curve for the RO radical, the reactions of ROO being about 22 kcal. per mole more endothermic. The region of interest in oxidation reactions is shown shaded in Figure 6. Within this region the change of gradient is slight, and the  $E$ 's can be represented by the Evans-Polanyi relation

$$E_7 = 0.60\Delta H_7 + 10,000 \text{ cal. per mole}$$

This equation gives roughly the same activation energies as one proposed by Benson (12) in which  $a = 1.0$  and  $c = 6,000$  cal. per mole. However, so high a value for  $a$  does not seem reasonable.

The Arrhenius parameters suggested for Reaction 7 are then given by the Arrhenius equation

$$\text{Log } k_7 = 8.0 \pm 0.5 - (10,000 + 0.60\Delta H_7)/2.303 RT$$

This equation agrees well with the only value for  $k_7$  which can be derived from experimental data directly. In the work of Allara *et al.* (1) on the oxidation of 2-methylpropane at  $100^\circ\text{C}$ . it is possible, as described

above, to derive a value of  $k_7/k_4^{1/2} = 10^{-3.4}$ . If  $k_4 = 10^{9.5}$ , then  $k_7 = 10^{1.3}$ . For 2-methylpropane Reaction 7 is nearly thermoneutral, and so  $E_7$  should be about 10 kcal. per mole. This would then lead to  $A_7 = 10^{7.2}$ , which is in reasonable agreement with the proposed equation. This value gives some support to Heicklen's value for  $k_4$  since a lower value of  $k_4$  would give a lower value of  $k_7$ , which seems unlikely.

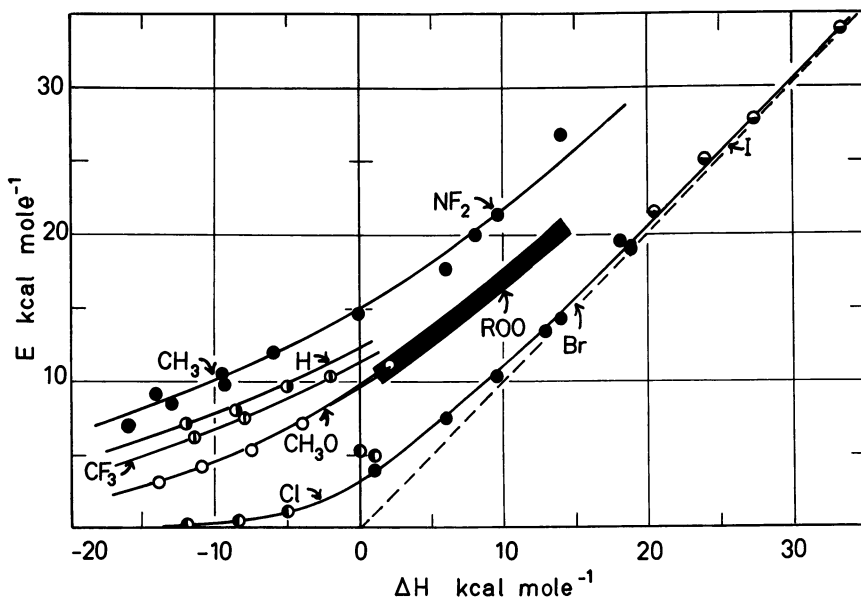


Figure 6. Dependence of activation energy,  $E$ , on heat of reaction,  $\Delta H$ , for various radicals

Shaded area represents supposed distribution of  $E$  and  $\Delta H$  for ROO radicals

For the reaction of  $\text{HO}_2$  with  $\text{H}_2$  the Evans-Polanyi relation predicts  $E_7 = 25$  kcal. per mole. This in excellent agreement with Baldwin's value (9) but not in very good agreement with the more reasonable value of  $E_7 = 20$  kcal. per mole required to bring the  $A$  factor down to a reasonable level. It could, however, be argued that  $\text{HO}_2$  is somewhat more reactive than  $\text{RO}_2$  and that a lower activation energy is in order; 20 kcal. per mole is still about 6 kcal. per mole more than the endothermicity of the reaction.

**Reactions 3 and 8.** One of the more puzzling features of the oxidation of 2-methylpropane between  $155^\circ$  and  $300^\circ\text{C}$ . is the remarkable transition from a reaction producing about 1% or less 2-methylpropene at  $155^\circ\text{C}$ . to one producing 80% 2-methylpropene at  $300^\circ\text{C}$ . If the olefin and other products arise from the same two competing Reactions 3 and

2 at both temperatures, then the change in product distribution demands the Arrhenius equation

$$\text{Log } k_3/k_2 = 7.5 - 18,000/2.303 RT$$

Such an equation is unacceptable since, if  $k_2 = 10^9$ , then  $A_3 = 10^{16.5}$ , which is impossible. The explanation must therefore be unsound. The transition in products must have some other explanation.

A more acceptable explanation is obtained if the competing reactions are Reactions 7 and 8. At 300°C., on this assumption, (rate of 8)/(rate of 7) = (2-methylpropene)/(other products)  $\approx 4$  on the basis of initial product analysis. At 155°C. the rate ratio is obtained not from the ratio (2-methylpropene)/(other products) but from the ratio (2-methylpropene)/(*tert*-butyl hydroperoxide) since a large part of the oxygenates arise from Reaction 4 (*see* Figures 2 and 3) and its successors. Although precise figures for the hydroperoxide are not given by Allara *et al.*, it is stated that the peroxide yield was about half of (peroxide + *tert*-butyl alcohol). Bearing in mind that there is some uncertainty as to whether the 2-methylpropene arises homogeneously or heterogeneously, we can only make an upper estimate of the rate ratio of 0.1. With (RH) =  $10^{-2}$  mole per liter the change in product distribution now demands

$$\text{Log } k_8/k_7 = 3.4 - 12,500/2.303 RT$$

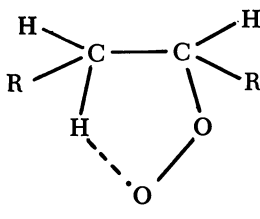
If

$$\text{Log } k_7 = 7.2 - 10,000/2.303 RT$$

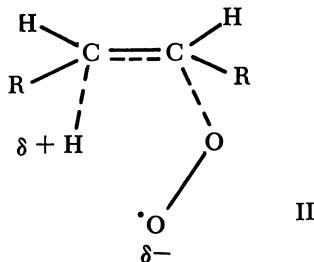
we obtain

$$\text{Log } k_8 = 10.6 - 22,500/2.303 RT$$

The value of  $A_8$  seems too low since calculations by the method of O'Neal and Benson (44) suggest that it should lie between  $10^{12.3}$  and  $10^{13.4}$ , depending upon whether the transition state complex is the relatively rigid form (I) or the looser, but highly polarized form (II).



I



II

The A factor and activation energy are probably both higher, in agreement with the view that much of the 2-methylpropene found at 155°C. was formed heterogeneously. Taking  $A_8 = 10^{12.5}$  gives  $E_8 = 27.5$

kcal. per mole, and a predicted ratio of (2-methylpropene)/(peroxide) of  $10^{-3.9}$  at  $155^{\circ}\text{C}$ .

This explanation for the transition in the yields of products is not entirely satisfactory for two reasons. First, there is little evidence for any dependence of the ratio of (conjugate olefin)/(other products) on the alkane pressure in oxidations above  $300^{\circ}\text{C}$ . The little evidence which exists suggests that there is no dependence, whereas the explanation in terms of Reactions 7 and 8 demands that the minor products should increase relative to the conjugate olefin in direct proportion to (RH). On the other hand the variation in (RH) which can be used is small since the over-all rate of oxidation depends upon (RH) to a high power; further, the indeterminate effects of heterogeneous reactions might obscure the changes in the homogeneous reaction. Likewise, the predicted effect of temperature on the ratio (conjugate olefin)/(other products) is much greater than that observed either for ethane (40) or 2-methylpropane (28) and if the explanation advanced above is correct, one has to suppose that changes in the heterogeneous part of the reaction which produces 2-methylpropene must almost exactly compensate for changes in the homogeneous part.

It might be argued that the addition of Reaction 3 might solve the difficulty. Unfortunately as now shown, Reaction 3 has little effect on the situation and indeed is probably not required to explain any of the observations.

At temperatures around  $300^{\circ}\text{C}$ . Reaction -2 is much faster than Reaction 8, and hence all other reactions of peroxy radicals at this temperature. Reaction 2 may therefore be considered to be in equilibrium at this temperature for the simpler alkanes (ethane, propane, 2-methylpropane, neopentane) and therefore

$$\begin{aligned} \text{(Rate of 8)}/\text{(rate of 3)} &= k_8(\text{ROO})/k_3(\text{R})(\text{O}_2) \\ &= k_8K_2/k_3 \\ &= 10^{-2.2} \exp(+7000/RT) \end{aligned}$$

The two rates are thus equal at about  $400^{\circ}\text{C}$ ., and Reaction 3, if it occurred, would slowly take over from  $2 + 8$  at above this temperature. The rate of Reaction 3 relative to 7 would show an activation energy difference of about 24 kcal. per mole, so that it gives no help in explaining the apparent lack of dependence of (conjugate olefin)/(other products) on temperature.

For temperatures above  $400^{\circ}\text{C}$ . it might be argued that because Reaction 2 is highly reversed, Reaction 8 could not compete effectively with Reaction 1, and that Reaction 3 is required to explain why any reaction with oxygen occurs above about  $400^{\circ}\text{C}$ . The rate of radical pyrolysis relative to Reaction 8 when Reaction 2 is in equilibrium and

(O<sub>2</sub>) = 10<sup>-2</sup> mole per liter is given by:

$$\begin{aligned} (\text{Rate of 1})/(\text{rate of 8}) &= k_1/(K_2k_8(\text{O}_2)) \\ &= 10^{7.9} \exp(-32,000/RT) \end{aligned}$$

whereas

$$(\text{Rate of 1})/(\text{rate of 3}) = 10^{5.7} \exp(-25,000/RT)$$

Either of these expressions would fit the data of Falconer and Knox (21) within their experimental error, and it therefore seems that Reaction 3 is unnecessary to explain any of the observations. Until more precise data are available on the relative rates of oxidation and pyrolysis, it will not be possible to decide whether it occurs or not.

**Reactions 9 to 11.** These reactions are relatively unimportant with the simpler alkanes since the conjugate olefin is the major product at all temperatures when the over-all processes are autocatalytic and since the minor products, at least in part, arise from heterogeneous processes. They may well be important with alkanes containing four or more C atoms in a straight chain. Typical results for the distribution of initial products from the oxidations of 1-pentane (35) and 2-methylpentane (24) are given in Table II. Although oxygen-containing heterocycles are important initial products, particularly from 2-methylpentane, there is little

**Table II. Initial Oxidation Products of Higher Alkanes**

Investigator	Kinnear and Turner (35)	Kinnear and Turner (35)	Fish (24) <sup>a</sup>	
Temperature, °C.	230	270	291	
Alkane	<i>1-Pentane</i>	<i>1-Pentane</i>	<i>2-Methylpentane</i>	
Olefins (conjugate)				
Pentenenes	6 <sup>c</sup>	22	Hexenes	0
Oxygen heterocycles				
2-Methyl THF <sup>b</sup>	2	13	2,2-Dimethyl THF	15
Propene oxide	3	2	2,4-Dimethyl THF	35
Ketones				
Acetone	49	33	Acetone	9
Methyl ethyl K	17	6	Methyl <i>n</i> -propyl K	8
Aldehydes				
Acetaldehyde	10	6	Acetaldehyde	10
Propionaldehyde	7	6	Propionaldehyde	3
<i>n</i> -Valeraldehyde	4	3	<i>n</i> -Butyraldehyde	14
Others				
Lower olefins	1	3	Lower olefins	3
Unidentified	1	5		

<sup>a</sup> Data taken by analysis of Figure 2 of (24).

<sup>b</sup> THF = tetrahydrofuran.

<sup>c</sup> Relative yields.

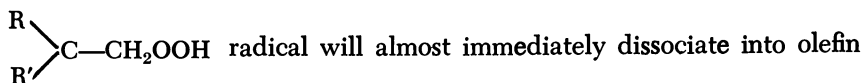
relation between the results of the two investigations, which leads one to suspect that surface reactions may again be important in these oxidations. The two sets of data are different in two particular respects: Kinneer and Turner found substantial yields of pentenes and small yields of heterocycles from 1-pentane at 270°C. Fish found no hexenes but large amounts of heterocycles in the products of oxidation of 2-methylpentane at 285°C.; the hexenes arose only after a substantial build up of heterocycles. These divergences are difficult to explain, and further experiments are required, particularly concerning the role of surface in these oxidations, before the importances of the homogeneous and heterogeneous oxidation routes are clearly established.

While there are clearly serious interpretational problems in the combustion of the higher alkanes at below 300°C., the work of Baldwin *et al.* (7) gives most valuable information on the high temperature oxidation of one higher alkane, neopentane. When traces of neopentane were added to oxidizing hydrogen + oxygen at 480°C. the initial products from the neopentane were equal amounts of 2-methylpropene and 3,3-dimethyloxetane. These products contrast sharply with those found at about 300°C. (Table I). Using the value for  $K_2$  and the experimental oxygen pressure of 70 mm. of Hg, it is found that  $(ROO)/(R) = 3$ . If the 2-methylpropene arises from Reaction 1, and the oxetane arises from Reaction 9, and if, furthermore,  $k_1(\text{neopentyl}) = k_1(n\text{-propyl}) = 10^{4.5}$  at 480°C., then  $k_9(\text{oxetane}) = 10^{4.0}$ . If  $A_9(\text{oxetane})$  is between  $10^{12}$  and  $10^{13}$ ,  $E_9(\text{oxetane})$  is between 28 and 34 kcal. per mole. This activation energy is thus comparable with  $E_{.2}$  and  $E_8$ . It is, however, much higher than the value proposed by Fish (23), who suggests  $k_9(\text{oxetane}) = 10^{11} \exp(-13,000/RT)$ .

Other evidence that peroxy radical rearrangements are essentially high temperature phenomena is the formation of methyl ethyl ketone in cool flames where the carbon atom of the carbonyl group was originally tertiary in the alkane (17). Since cool flame temperatures are around 500°C., heterogeneous processes are unlikely, and all products must presumably arise homogeneously.

Reaction 11 seems well established by the work of Cartledge and Tipper (16). The polyhydroperoxides found by them in the oxidation products of 1-heptane presumably arose from Reaction 11 followed by further addition of oxygen to the QOOH radical to give OOOOH. The A factor for Reaction 11 is likely to be around  $10^{12}$ , with the activation energy being somewhat greater than for the corresponding intermolecular H abstraction. If Reaction 8 indeed occurs *via* Reaction 11, then  $E_{11}$  for abstraction from the beta position is 22 to 27 kcal. per mole, which is 7 to 12 kcal. greater than the activation energy for abstraction of a primary H atom according to the Evans-Polanyi relation derived

above. The difference corresponds reasonably with the strain energy of a five-membered ring (13). Unlike other QOOH radicals, the



radical will almost immediately dissociate into olefin and HO<sub>2</sub> since the C—O bond strength is only about 12 kcal. per mole (12, 37).

The apparently high activation energies for formation of the oxygen heterocycles probably reflect the difficulty of decomposition of the other QOOH radicals rather than the difficulty of their formation. If the decomposition of QOOH to an oxygen containing heterocycle had an A factor of 10<sup>13</sup>, this reaction would compete with its further oxidation at 280°C. only if its activation energy were below about 15 kcal. per mole. Since the activation energies are apparently greater than this, the heterocycles are probably formed in some other way at this temperature. At about 500°C. it becomes possible for the decomposition of QOOH to compete with their oxidation.

### Literature Cited

- (1) Allara, D. L., Mill, T., Hendry, D. G., Mayo, F. R., *ADVAN. CHEM. SER.* **76**, 40 (1968).
- (2) Avramenko, L. I., Kolesnikova, R. V., *Izvest. Nauk SSSR Otdel. Khim. Nauk* **806**, 989 (1960).
- (3) Ayscough, P. B., *J. Phys. Chem.* **24**, 944 (1956).
- (4) Bailey, H. C., *ADVAN. CHEM. SER.* **75**, 138 (1968).
- (5) Bailey, H. C., Norrish, R. G. W., *Proc. Roy. Soc. A* **212**, 311 (1952).
- (6) Baldwin, R. R., *Trans. Faraday Soc.* **60**, 527 (1964).
- (7) Baldwin, R. R., Everett, C. J., Hopkins, D. E., Walker, R. W., *ADVAN. CHEM. SER.* **76**, 124 (1968).
- (8) Baldwin, R. R., Jackson, D., Walker, R. W., Webster, S. J., "Tenth Symposium (International) on Combustion," p. 423, Combustion Institute, Pittsburgh, 1965.
- (9) Baldwin, R. R., Jackson, D., Walker, R. W., Webster, S. J., *Trans. Faraday Soc.* **63**, 1665 (1967).
- (10) Baldwin, R. R., Walker, R. W., *Trans. Faraday Soc.* **60**, 1236 (1964).
- (11) Barnard, J. A., *ADVAN. CHEM. SER.* **76**, 98 (1968).
- (12) Benson, S. W., *J. Am. Chem. Soc.* **87**, 972 (1965).
- (13) Benson, S. W., *J. Chem. Phys.* **34**, 521 (1961).
- (14) *Ibid.* **40**, 1007 (1964).
- (15) Carabine, M. J., Knox, J. H., *J. Chem. Soc.* **1963**, 862.
- (16) Cartlidge, J., Tipper, C. F. H., *Anal. Chim. Acta* **22**, 106 (1960).
- (17) Cullis, C. F., Hardy, F. R. F., Turner, D. W., *Proc. Roy. Soc. A* **244**, 573 (1958).
- (18) Dingley, D. P., Calvert, J. G., *J. Am. Chem. Soc.* **85**, 856 (1963).
- (19) Drever, D. F., Calvert, J. G., *J. Am. Chem. Soc.* **84**, 1362 (1962).
- (20) Evans, M. G., Polanyi, M., *Trans. Faraday Soc.* **34**, 11 (1938).
- (21) Falconer, J. W., Knox, J. H., *Proc. Roy. Soc. A* **250**, 493 (1959).
- (22) Fettis, G. C., Knox, J. H., "Progress in Reaction Kinetics," Vol. 2, p. 1, Pergamon Press, London, 1964.

- (23) Fish, A., *ADVAN. CHEM. SER.* **76**, 69 (1968).
- (24) Fish, A., *Proc. Roy. Soc.* **A298**, 204 (1967).
- (25) Foner, S. N., Hudson, R. L., *ADVAN. CHEM. SER.* **36**, 34 (1962).
- (26) Goldfinger, P., Huybrechts, G., Martens, G., Meyers, L., Olbregts, J., *Trans. Faraday Soc.* **61**, 1933 (1965).
- (27) Gray, P., Shaw, R., Thynne, J. C. J., "Progress in Reaction Kinetics," Vol. 4, p. 63, Pergamon Press, London, 1967.
- (28) Hay, J., Knox, J. H., Turner, J. M. C., "Tenth Symposium (International) on Combustion," p. 331, Combustion Institute, Pittsburgh, 1965.
- (29) Heicklen, J., *ADVAN. CHEM. SER.* **76**, 23 (1968).
- (30) Howard, J. A., Schwalm, W. J., Ingold, K. U., *ADVAN. CHEM. SER.* **75**, 6 (1968).
- (31) Johnston, G. R. A., Salmon, G. A., *J. Phys. Chem.* **65**, 177 (1961).
- (32) Johnston, H. S., Cramarossa, F., "Advances in Photochemistry," Vol. 4, p. 1, Interscience, New York, 1966.
- (33) Kerr, J. A., *Chem. Rev.* **66**, 465 (1966).
- (34) Kerr, J. A., Trotman-Dickenson, A. F., "Progress in Reaction Kinetics," Vol. 1, p. 106, Pergamon Press, London, 1961.
- (35) Kinnear, C. G., Turner, J. M. C., private communication.
- (36) Kirk, A. D., Knox, J. H., *Trans. Faraday Soc.* **56**, 1296 (1960).
- (37) Knox, J. H., *Combust. Flame* **9**, 297 (1965).
- (38) Knox, J. H., "Photochemistry and Reaction Kinetics," p. 250, Cambridge University Press, Cambridge, 1967.
- (39) Knox, J. H., *Trans. Faraday Soc.* **55**, 1362 (1959); **56**, 1225 (1960).
- (40) Knox, J. H., Wells, C. H. J., *Trans. Faraday Soc.* **59**, 2786, 2801 (1963).
- (41) McMillan, G. R., Calvert, J. G., "Oxidation and Combustion Reviews," Vol. 1, p. 83, Elsevier, London, New York, 1965.
- (42) Minkoff, G. J., Tipper, C. F. H., "Chemistry of Combustion Reactions," p. 120, Butterworth & Co., London, 1962.
- (43) Nalbandyan, A. B., "Preprint, International Oxidation Symposium," Vol. I, p. 397, 1967.
- (44) O'Neal, H. E., Benson, S. W., *J. Phys. Chem.* **71**, 1903 (1967).
- (45) Pritchard, G. O., Pritchard, H. O., Schiff, H. I., Trotman-Dickenson, A. F., *Trans. Faraday Soc.* **52**, 849 (1956).
- (46) Russell, G. A., *J. Am. Chem. Soc.* **79**, 3871 (1957).
- (47) Sajus, L., *ADVAN. CHEM. SER.* **75**, 59 (1968).
- (48) Sampson, R., *J. Chem. Soc.* **1963**, 5095.
- (49) Satterfield, C. N., Reid, R. C., *J. Phys. Chem.* **59**, 283 (1955).
- (50) Shtern, V. Ya., "Gas Phase Oxidation of Hydrocarbons," p. 332, Pergamon Press, London, 1964.
- (51) Slater, D. H., Calvert, J. G., *ADVAN. CHEM. SER.* **76**, 58 (1968).
- (52) Thomas, S. S., Calvert, J. G., *J. Am. Chem. Soc.* **84**, 4207 (1962).
- (53) Traylor, T. G., Russell, G. A., *J. Am. Chem. Soc.* **87**, 3698 (1965).
- (54) Trotman-Dickenson, A. F., "Gas Kinetics," Butterworth & Co., London, 1955.
- (55) Turner, J. M. C., private communication.
- (56) Zeelenberg, A. P., *Rec. Trav. Chim. Pays-Bas* **81**, 720 (1962).
- (57) Zeelenberg, A. P., "Tenth Symposium (International) on Combustion," p. 340, Combustion Institute, Pittsburgh.
- (58) Zeelenberg, A. P., Bickel, A. F., *J. Chem. Soc.* **1961**, 4014.

RECEIVED November 6, 1967.

# Gas-Phase Reactions of Alkylperoxy and Alkoxy Radicals

JULIAN HEICKLEN\*

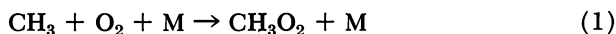
Aerospace Corp., El Segundo, Calif. 90045

*Small alkylperoxy and alkoxy radicals can decompose unimolecularly, though their rate constants are often in the second-order region. They abstract hydrogen atoms from alkanes, aldehydes, esters, and acids, add to olefins, and may react with O<sub>2</sub>. Furthermore, interactions with other radicals can lead to disproportionation or combination. These reactions are reviewed, and particular attention is given to CH<sub>3</sub>O<sub>2</sub> and CH<sub>3</sub>O; a number of rate constants are estimated.*

This paper discusses the reactions of alkylperoxy and alkoxy radicals in the slow oxidation of hydrocarbons. These reactions were reviewed recently by McMillan and Calvert (29). However, since that review, more reliable information has become available on the thermochemistry of these radicals and on dissociation energies of the species formed by oxidation and is summarized in two papers by Benson (2, 3). Furthermore, Hoare (21) has critically discussed the oxidation of methane. Based on these reviews, as well as more recent data, some deductions can be made concerning the important reactions and their rate constants.

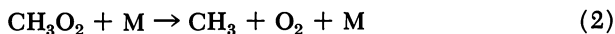
## *Unimolecular Reactions of RO<sub>2</sub>*

Alkylperoxy radicals are produced from the reaction of the corresponding alkyl radical with O<sub>2</sub>. In particular for methyl radicals, the reaction is known to be third order:



\* Present address, Department of Chemistry, The Pennsylvania State University, University Park, Pa. 16802.

The rate constant is about  $3 \times 10^{10} M^{-2} \text{ sec.}^{-1}$ , independent of temperature (29) from 25° to 225°C. The reverse reaction,



must proceed with an activation energy  $E_2$ , similar to the dissociation energy (3) of 26 kcal. per mole and a pre-exponential factor of about  $10^{15.8} M^{-1} \text{ sec.}^{-1}$  as computed from  $k_1$  and the equilibrium constant. (Subscripts on  $E$ ,  $A$ , and  $k$  refer to reaction numbers.)

Another reaction of  $\text{CH}_3$  with  $\text{O}_2$  that is often invoked is



Much of the evidence for Reaction 3 is indirect. The best evidence is from the work of McKellar and Norrish (25), who studied the flash photolysis of  $\text{CH}_3\text{I}$  in the presence of  $\text{O}_2$  and observed the HO radical by absorption spectroscopy. When a mixture of 5 torr of  $\text{CH}_3\text{I}$  and 50 torr of  $\text{O}_2$  was irradiated, the HO absorption intensity reached a maximum in 30  $\mu\text{sec}$ . It is difficult to understand this result unless Reaction 3 is utilized. However, McGarvey and McGrath (24) have flash-photolyzed mixtures of  $\text{CH}_3\text{ONO}$  and  $\text{O}_2$  and found HO to be produced rapidly. In this system, the primary cleavage gives  $\text{CH}_3\text{O}^*$  (excited  $\text{CH}_3\text{O}$ ) and NO. There are no methyl radicals, so an alternative route to Reaction 3 must be responsible for HO production. Perhaps this alternative route could be important in McKellar and Norrish's experiment also.

The rate data for Reaction 3 are summarized by McMillan and Calvert (29). The results are greatly scattered, but a number of investigations report  $k_3 \sim 6 \times 10^7 M^{-1} \text{ sec.}^{-1}$ . This value is surely an upper limit, and there is considerable evidence (29) that the rate constant is much smaller. Benson and Spokes (4) suggest an upper limit one tenth as large at temperatures from 600° to 1450°K. If we adopt the value  $6 \times 10^7 M^{-1} \text{ sec.}^{-1}$ ,  $k_3$  can have little or no activation energy, as it is difficult to believe that the pre-exponential factor can be much larger than  $6 \times 10^7 M^{-1} \text{ sec.}^{-1}$ . On the other hand, if  $k_3$  is much smaller than  $10^7 M^{-1} \text{ sec.}^{-1}$ , it could have an activation energy, but it would be too slow to compete with Reaction 1 at pressures above about 10 torr.

In thermal reactions at pressures above 10 torr, there is much evidence (21) that  $\text{CH}_3$  reacts with  $\text{O}_2$  to produce  $\text{CH}_2\text{O}$  and HO radicals above about 400°C. Furthermore, Miyama and Takeyama (31) monitored HO production in the shock-induced oxidation of  $\text{CH}_4$  and observed that the induction time for HO production had an activation energy of 21.5 kcal. per mole. Reaction 3 may proceed with a 21 kcal. per mole activation energy, or HO production may be *via*

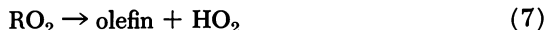


Another possible decomposition reaction of  $\text{CH}_3\text{O}_2$  is



However, this reaction is endothermic by 55 kcal. per mole, so it cannot be important.

For alkylperoxy radicals larger than  $\text{CH}_3\text{O}_2$ , the decomposition reactions are first-order. Two important reactions are



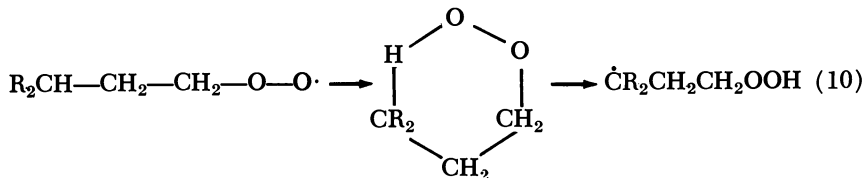
The rate constants for Reactions 6 and 7 can be estimated from thermodynamic data and the rate constants for



When R is  $\text{C}_2\text{H}_5$ ,  $k_8$  is  $10^{8.8} \text{ M}^{-1} \text{ sec}^{-1}$  independent of temperature (29). Combining this value with the equilibrium constant (3) for Reactions 6 and 8, we find  $k_6 = 10^{14.4} \exp(-28,000/RT) \text{ sec}^{-1}$ . The rate constants for other alkyl radicals should be similar.

The importance of Reaction 7 can be estimated from the following considerations. When R is  $\text{C}_2\text{H}_5$ , then  $k_8/k_9$  is greater than  $10^3$  at room temperature (29). Since  $k_8 = 10^{8.8} \text{ M}^{-1} \text{ sec}^{-1}$  and the pre-exponential factor for Reaction 9 must be about  $10^9 \text{ M}^{-1} \text{ sec}^{-1}$ , the activation energy  $E_9$  for Reaction 9 must exceed 4.4 kcal. per mole. On the other hand, it cannot be much larger than this because Reaction 9 is important at moderate temperatures. Benson's calculations (3) yield about 4 kcal. per mole. A value of 5 kcal. per mole is adopted here. If the intermediate to product formation is the same in Reactions 7 and 9, then by straightforward manipulation of thermodynamic data,  $k_7$  is  $k_6 k_9 / k_8 \sim 10^{14.6} \exp(-33,000/RT) \text{ sec}^{-1}$ .

The rate constants for  $\text{CH}_3\text{O}_2$  and  $\text{C}_2\text{H}_5\text{O}_2$  decompositions are summarized in Table I. For larger alkylperoxy radicals, rearrangements can also occur. For example, if a 3-hydrogen is present, internal abstraction can occur *via* a six-membered ring intermediate:



Benson (3) has estimated  $k_{10} \sim 10^{11} \exp(-15,000/RT) \text{ sec}^{-1}$ .

Table I. Unimolecular Decompositions of RO<sub>2</sub>

Reaction	$\Delta H_{298^\circ K.}$ Kcal./Mole	$E,$ Kcal./Mole	$A^a$
$CH_3O_2 + M \xrightarrow{2} CH_3 + O_2 + M$	26	26	$10^{15.8}$
$CH_3O_2 + M \xrightarrow{4} CH_2O + HO + M$	-25	~47	—
$CH_3O_2 + M \xrightarrow{5} CH_3O + O + M$	55	Not important	
$C_2H_5O_2 \xrightarrow{6} C_2H_5 + O_2$	28	28	$10^{14.4}$
$C_2H_5O_2 \xrightarrow{7} C_2H_4 + HO_2$	19.5	~33	$10^{14.6}$

<sup>a</sup> Units are  $M^{-1} \text{ sec.}^{-1}$  for second-order reactions and  $\text{sec.}^{-1}$  for first-order reactions.

### Reactions of RO<sub>2</sub> with Molecules

Hydroperoxides can be formed *via* hydrogen-atom abstraction by RO<sub>2</sub>. The RO<sub>2</sub>—H bond strength is about 90 kcal. per mole; consequently, many such abstractions will be endothermic. Benson (3) has estimated an activation energy of 6 kcal. per mole for exothermic abstractions and  $6 + \Delta H$  for endothermic reactions. The pre-exponential factors should be about  $10^{8.0} M^{-1} \text{ sec.}^{-1}$ —*i.e.*, about a factor of 2 lower than hydrogen-atom abstraction by CH<sub>3</sub> radicals. Some typical abstraction reactions are listed in Table II.

Table II. Reactions of RO<sub>2</sub> with Molecules

Reaction	$\Delta H_{298^\circ K.}$ Kcal./Mole	$\sim E,$ Kcal./Mole	$\sim A,$ $M^{-1} \text{ sec.}^{-1}$
$RO_2 + CH_4 \rightarrow RO_2H + CH_3$	12	18	$10^{8.0}$
$RO_2 + C_2H_6 \rightarrow RO_2H + C_2H_5$	8	14	$10^{8.0}$
$RO_2 + C_3H_8 \rightarrow RO_2H + i-C_3H_7$	5	11	$10^{8.0}$
$RO_2 + CH_2O \rightarrow RO_2H + HCO$	-3	6	$10^{8.0}$
$RO_2 + \text{olefin} \xrightarrow{11} \text{adduct}$	-12	6	$10^{8.5}$
$RO_2 + O_2 \xrightarrow{12} RO + O_3$	29	35	$10^{8.5}$

The RO<sub>2</sub> radical can add to olefins:



The rate constant for Reaction 11 has been estimated (3) to be  $10^{8.5} \times \exp(-6000/RT) M^{-1} \text{ sec.}^{-1}$ .

A reaction often postulated is (23)



However, this reaction is endothermic by 29 kcal. per mole and should have an activation energy  $\sim 35$  kcal. per mole. Consequently it cannot be important. Even if the  $\text{RO}_2$  still retained the energy of the  $\text{R}-\text{O}_2$  bond—*i.e.*,  $\sim 27$  kcal. per mole—the reaction would still be energetically unfavorable. Furthermore, its preexponential factor should be about  $10^{8.5} \text{ M}^{-1} \text{ sec}^{-1}$ , so that only about one in  $10^3$  collisions would be sterically favorable. The other collisions would deactivate.

### Reactions of $\text{RO}_2$ with Radicals

There are no experimental values for absolute rate constants of radical- $\text{RO}_2$  reactions. However, it is now generally accepted that two important reactions are



Other possible radical reactions of  $\text{RO}_2$  are



Reactions 16b and 16c initially must form an excited  $\text{RO}_2\text{R}$  molecule as a precursor to products.

Reasonable rate constants can be deduced by comparison with the reactions



The value of  $k_{18b}$  is  $10^{8.8} \text{ M}^{-1} \text{ sec}^{-1}$  when  $\text{R} = \text{CH}_3$ ;  $k_{18a}/k_{18b}$  is approximately 10 for  $\text{R} = \text{CH}_3$ ,  $\text{C}_2\text{H}_5$ , or  $i\text{-C}_3\text{H}_7$ . Furthermore, Heicklen and Johnston (18) found  $k_{15}/k_{13}^{1/2}k_{18a}^{1/2}$  to be 0.15 for  $\text{R} = \text{CH}_3$  or  $\text{C}_2\text{H}_5$ . Now  $k_{16a}$  and  $k_{14}$  should be similar to  $k_{18a}$ , except that the symmetry reduction will reduce them by a factor of 2. The constant  $k_{15}$  will be further reduced by an additional factor of about 2 because of the increased complexity of the radicals. Thus, it is estimated that  $k_{14} \sim k_{16a} \sim 10^{9.5}$  and  $k_{15} \sim 10^{9.2} \text{ M}^{-1} \text{ sec}^{-1}$  when  $\text{R} = \text{CH}_3$ . For somewhat larger radicals, the rate constants probably are not too much different. This value for  $k_{15}$ , when combined with the known values for  $k_{18b}$ ,

$k_{18a}/k_{18b}$ , and  $k_{15}/k_{13}^{1/2}k_{18a}^{1/2}$ , yields  $k_{13} = 10^{10.2} M^{-1} \text{ sec}^{-1}$ . This is a surprisingly large rate constant for a reaction such as 13, the value being similar to that for  $\text{CH}_3$  recombination. Consequently, this value must be considered an upper limit. If the value of  $10^{10.6} M^{-1} \text{ sec}^{-1}$  is used for  $k_{18a}$  as deduced from the results of Quee and Thynne (33), then  $k_{15}$  should be about  $10^{10.0} M^{-1} \text{ sec}^{-1}$ , and  $k_{13}$  becomes  $10^{10.4} M^{-1} \text{ sec}^{-1}$ , which is even larger than before. These results are inconsistent with liquid-phase results, where  $k_{13}$  has been found to be much smaller and proceeds with an activation energy of 5 to 10 kcal. per mole. The liquid-phase results seem more reasonable.

Reactions 16b and 16c proceed through an excited peroxide intermediate. The sum of their rate constants should be similar to  $k_{18b} \sim 10^{8.8} M^{-1} \text{ sec}^{-1}$ .

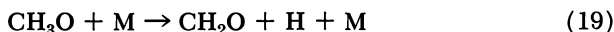
Reaction 17a has been proposed by Linnett and his co-workers (1, 12). However, it is this author's opinion (17) that this reaction cannot be important. Presumably it would proceed by replacement of the  $\text{O}_2$  group by the HO radical; the steric factor should be prohibitively small. There appears to be no information concerning Reaction 17b. The suggested rate constants for some  $\text{CH}_3\text{O}_2$ -radical reactions are listed in Table III.

**Table III. Reactions of  $\text{CH}_3\text{O}_2$  with Radicals**

<i>Reaction</i>	<i>Log (k, M<sup>-1</sup> sec.<sup>-1</sup>)</i>
13 $2\text{CH}_3\text{O}_2 \rightarrow 2\text{CH}_3\text{O} + \text{O}_2$	~10.2
14 $\text{CH}_3\text{O}_2 + \text{HO}_2 \rightarrow \text{CH}_3\text{OOH} + \text{O}_2$	~9.5
15 $\text{CH}_3\text{O}_2 + \text{CH}_3\text{O} \rightarrow \text{CH}_3\text{OOH} + \text{CH}_2\text{O}$	~9.2
17a $\text{CH}_3\text{O}_2 + \text{HO} \rightarrow \text{CH}_3\text{OH} + \text{O}_2$	<7
16 $\text{CH}_3\text{O}_2 + \text{CH}_3 \rightarrow \text{CH}_3\text{OOCH}_3 \text{ or } 2\text{CH}_3\text{O}$	~8.8
16a $\text{CH}_3\text{O}_2 + \text{R} \rightarrow \text{CH}_3\text{OOH} + \text{olefin}$	~9.5

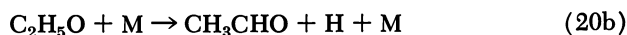
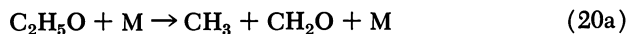
### *Unimolecular Decompositions of RO*

The methoxy radical can decompose *via*



The reaction is endothermic by 29 kcal. per mole; there appears to be no direct experimental evidence concerning Reaction 19.

For ethoxy radicals, two modes of decomposition can be envisioned:



Gray (15) reported that  $\text{C}_2\text{H}_5\text{O}$  radicals generated by the photolysis of  $\text{C}_2\text{H}_5\text{ONO}_2$  can decompose by both paths. He calculated  $\Delta H = 11$  and  $13$  kcal. per mole, respectively, for Reactions 20a and 20b. He further estimated the respective activation energies to be  $21$  and  $23$  kcal. per mole. A more accurate estimate for  $E_{20a}$  can be made from Wijnen's (38) results on the photolysis of  $10^{-3}M$  ethyl propionate between  $15^\circ$  and  $195^\circ\text{C}$ . From the competition between Reaction 20a and



he found  $E_{20a} - E_{21} = 7.5$  kcal. per mole. His results also give  $E_{21} \sim 5.5$  kcal. per mole and  $A_{20a}/A_{21} = 10^{4.3}$  ( $A$  is the pre-exponential factor). Thus,  $E_{20a}$  is  $13$  kcal. per mole and, if  $A_{21} \sim 10^{8.3} M^{-1} \text{sec}^{-1}$ ,  $A_{20a}$  is approximately  $10^{12.6} M^{-1} \text{sec}^{-1}$ . Wijnen reported that there was no evidence for Reaction 20b, and that he felt that this reaction could not be important relative to 20a.

The decomposition of  $i\text{-C}_3\text{H}_7\text{O}$  between  $160^\circ$  and  $200^\circ\text{C}$ . was studied in the pyrolysis of  $20$  to  $230$  torr of  $i\text{-C}_3\text{H}_7\text{NO}$  by Phillips and his co-workers (9, 13). The decomposition was estimated from the competition



It was assumed that Reactions 22 and 23 were the only sources of  $\text{CH}_3\text{CHO}$  and  $(\text{CH}_3)_2\text{CO}$ , respectively, and that  $k_{23} = 10^{10} M^{-1} \text{sec}^{-1}$ . Reaction 22 was found to be in the transition region with  $k_{22^\infty} = 10^{11.8} \exp(-17,300/RT) \text{sec}^{-1}$  and  $k_{22^0} = 10^{10.1} \exp(-8300/RT) M^{-1} \text{sec}^{-1}$ . The Arrhenius parameters for  $k_{22^0}$  are abnormally low and should be used with caution.

The rate constant for the decomposition of *tert*-butoxy radicals



has been reported in a number of studies (6, 7, 26, 30, 37), which assumed Reaction 24a to be in the first-order region. However, more recent work (14, 20, 32) has shown that the reactions may be in the falloff region at the pressures and temperatures employed in the thermal decomposition of di-*tert*-butyl peroxide.

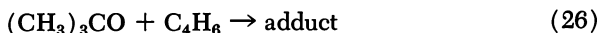
The first estimates were made by Volman and co-workers. Brinton and Volman (7) studied the thermal decomposition of di-*tert*-butyl peroxide between  $129^\circ$  and  $154^\circ\text{C}$ . in the presence of ethyleneimine.

From the competition between Reaction 24a and Reaction 25a



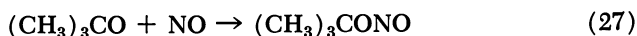
they found  $E_{24a} - E_{25a} = 12$  kcal. per mole; thus  $E_{24a}$  is greater than 12 kcal. per mole, and they estimated it to be about 17 kcal. per mole.

At about the same time, Volman and Graven (37) examined the photolysis of di-*tert*-butyl peroxide-butadiene mixtures at 60° to 100°C. In this system, a competition exists between Reaction 24a and



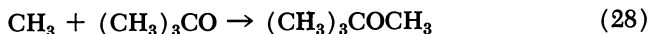
They found  $E_{24a} - E_{26} = 5.8$  kcal. per mole.  $E_{26}$  had been estimated from a number of studies. Volman and Graven used a value of 5.4 kcal. per mole to deduce  $E_{24a} = 11.2 \pm 2.0$  kcal. per mole.

Birss, Danby, and Hinshelwood (6) investigated the thermal decomposition of di-*tert*-butyl peroxide from 130° to 170°C. in the presence of NO. In that investigation, Reaction 24a was in competition with

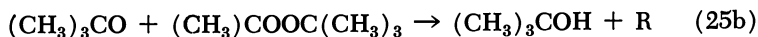


Their results showed considerable scatter, but a rough estimate of  $E_{24a} \sim 13.2 \pm 2.4$  kcal. per mole was made.

McMillan and Wijnen (30) made a crude estimate for  $E_{24a} \sim 9 \pm 2$  kcal. per mole in the photolysis of di-*tert*-butyl peroxide at 25° and 55°C. from the competition between



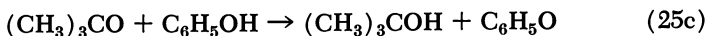
At 25°C.,  $k_{24b}k_{29}^{1/2}/k_{28}$  was found to be  $0.021 M^{1/2} \text{ sec.}^{1/2}$ . The most likely value for  $E_{24b}$  is 12 kcal. per mole; for  $k_{29}$ ,  $10^{10.34} M^{-1} \text{ sec.}^{-1}$ ; and for  $k_{28}$ ,  $10^{9.2} M^{-1} \text{ sec.}^{-1}$ . Then the pre-exponential factor for Reaction 24 is  $10^{11.2} \text{ sec.}^{-1}$ . Another estimate can be made from the same study where the competition between 24b and 25b



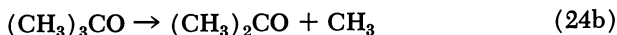
gave  $k_{24b}/k_{25b} = 10^{0.6} \exp(-3000/RT) M$ . Since the pre-exponential factor for Reaction 25b must be about  $10^{8.0} M^{-1} \text{ sec.}^{-1}$ , the pre-exponential factor for Reaction 24b becomes  $10^{8.6} \text{ sec.}^{-1}$ , in poor agreement with the other estimate of  $10^{11.2} \text{ sec.}^{-1}$ . The experiments of McMillan and Wijnen were repeated in more detail between 25° and 79°C. by McMillan (26); by the first analysis as above, he estimated  $k_{24b} \sim 10^{11} \exp(-11,000/RT) \text{ sec.}^{-1}$ .

Mulcahy and Williams (32) looked at the thermal decomposition of di-*tert*-butyl peroxide at 482°, 516°, and 547°K. in the presence of  $\text{C}_6\text{H}_5\text{OH}$ . Reaction 24a was definitely in the second-order region. At

482°K. the pressure corresponding to a factor of 2 decrease in the first-order rate constant was 80 torr. By a suitable manipulation of their data, they could study the competition between Reactions 24a and 25c:



in both the first- and second-order regions of 24a. For the first-order reaction



$E_{24\text{b}} - E_{25\text{c}}$  was estimated to be 11 kcal. per mole. The pre-exponential factor for 25c should be about  $10^{8.0} M^{-1} \text{ sec}^{-1}$ . At 482°K.,  $k_{25\text{c}}/k_{24\text{b}}$  was  $70 M^{-1}$ , so that the pre-exponential factor for 24b is about  $10^{11.2} \text{ sec}^{-1}$ , in excellent agreement with that obtained from the photolysis experiments.

The summary of all the data gives a best estimate of  $k_{24\text{b}} = 10^{11.2} \times \exp(-12,000/RT) \text{ sec}^{-1}$ . The pre-exponential factor is considerably smaller than the expected value of  $\sim 10^{14} \text{ sec}^{-1}$ . The reason for the discrepancy is not known. The activation energy is considerably greater than the dissociation energy for Reaction 24a of about 4 kcal. per mole computed from the heat of formation of *tert*-C<sub>4</sub>H<sub>9</sub>O given by Benson (2).

The tertiary pentoxy radical can decompose by two paths (11, 28):



The ratio  $k_{30\text{a}}/k_{30\text{b}}$  is not known precisely, but it is large.

Estimates for rate parameters for various decompositions are summarized in Table IV.

### *Reactions of RO with Molecules*

Methoxy radicals can abstract a hydrogen atom, and several such reactions have been studied. Wijnen examined the photolysis of CH<sub>3</sub>COOCH<sub>3</sub> and CH<sub>3</sub>COOCD<sub>3</sub> from 29° to 217° and 145° to 350°C., respectively (39, 41). The rate constant for abstraction of a hydrogen atom from the substrate by methoxy can be deduced from the competition



or



together with the reaction



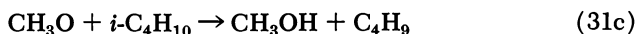
Wijnen's data yielded  $k_{31a}k_{29}^{1/2}/k_{32a} = 10^{1.85} \exp(-4500/RT)$  and  $k_{31b}k_{29}^{1/2}/k_{32b} = 10^{2.09} \exp(-5000/RT) M^{-1/2} \text{ sec.}^{-1/2}$ . Unfortunately, no reasonable choice of rate constants can lead to the computed pre-exponential factors. Shaw and Trotman-Dickenson (34) reanalyzed Wijnen's data and concluded that the activation energy should be about 7.1 kcal. per mole. If so, then  $k_{31a}k_{29}^{1/2}/k_{32a} = 10^{3.28} \exp(-7100/RT) M^{-1} \text{ sec.}^{-1}$ . This expression leads to a reasonable pre-exponential factor of  $10^{7.9}$  for  $k_{31a}$  when combined with the values of  $10^{10.3}$  and  $10^{9.8} M^{-1} \text{ sec.}^{-1}$  for  $k_{29}$  and  $k_{32a}$ , respectively.

Table IV. Unimolecular Decomposition of RO

Reaction	$\Delta H_{298}^{\circ K.},$ Kcal./ Mole	$E,$ Kcal./ Mole	$A^a$	Ref.
19 $\text{CH}_3\text{O} + \text{M} \rightarrow \text{CH}_2\text{O} + \text{H} + \text{M}$	29	—	—	—
20a $\text{C}_2\text{H}_5\text{O} + \text{M} \rightarrow \text{CH}_3 + \text{CH}_2\text{O} + \text{M}$	13	13	$10^{12.6}$	(38)
20b $\text{C}_2\text{H}_5\text{O} + \text{M} \rightarrow \text{CH}_3\text{CHO} + \text{H} + \text{M}$	15	—	—	—
22 $i\text{-C}_3\text{H}_7\text{O} \rightarrow \text{CH}_3 + \text{CH}_3\text{CHO}$	—	17.3	$10^{11.8}$	(9)
22 $i\text{-C}_3\text{H}_7\text{O} + \text{M} \rightarrow \text{CH}_3 + \text{CH}_3\text{CHO} + \text{M}$	—	8.3	$10^{10.1}$	(9)
24b $\text{tert-C}_4\text{H}_9\text{O} \rightarrow \text{CH}_3 + (\text{CH}_3)_2\text{CO}$	4	12	$10^{11.2}$	(6, 7, 26, 30, 32, 37)

<sup>a</sup> Units are  $M^{-1} \text{ sec.}^{-1}$  for second-order reactions and  $\text{sec.}^{-1}$  for first-order reactions.

Berces and Trotman-Dickenson (5) pyrolyzed dimethyl peroxide and di-*tert*-butyl peroxide at 190° to 260°C. in the presence of *i*-C<sub>4</sub>H<sub>10</sub>. The ratio  $k_{31c}k_{29}^{1/2}/k_{32a}$  was deduced where Reaction 31c is



From the values of  $10^{10.3}$  and  $10^{9.8} M^{-1} \text{ sec.}^{-1}$  for  $k_{29}$  and  $k_{32a}$ , respectively,  $k_{31c}$  can be computed to be  $10^{7.6} \exp(-4100/RT) M^{-1} \text{ sec.}^{-1}$ .

Shaw and Trotman-Dickenson (34) investigated the simultaneous reaction of methoxy radicals with two hydrocarbons. The methoxy radicals were generated by pyrolysis of either CH<sub>3</sub>ONO at 300° to 400°C.

or  $\text{CH}_3\text{OOCH}_3$  at 200° to 300°C. They measured the rate of consumption of each hydrocarbon and, thus, determined their relative reaction rate constants with methoxy radicals. The absolute rate constants can be obtained by comparison to that for 2-methylpropane (Table V). The results are reasonable except for  $n\text{-C}_4\text{H}_{10}$ , where the listed Arrhenius parameters must be too low.

Thynne and Gray (36) pyrolyzed  $\text{CH}_3\text{OOCH}_3$  at 124° to 185°C. in the presence of methyl formate. Thus, they were able to obtain  $k_{31d}k_{29}^{1/2}/k_{32a}$ , where Reaction 31d is



Table V. Arrhenius Parameters for the Reaction

RH	31		
	$\text{CH}_3\text{O} + \text{RH} \rightarrow \text{CH}_3\text{OH} + \text{R}$		
	$\text{Log}(A, M^{-1} \text{sec}^{-1})$	$E, \text{Kcal./Mole}$	Ref.
$\text{CH}_3\text{COOCH}_3$	7.9	7.1	(34, 39, 41)
$\text{C}_2\text{H}_6$	8.1	7.1	(5, 34)
$\text{C}_3\text{H}_8$	7.9	5.2	(5, 34)
$n\text{-C}_4\text{H}_{10}$	7.1	2.9	(5, 34)
$i\text{-C}_4\text{H}_{10}$	7.6	4.1	(5, 34)
$neo\text{-C}_5\text{H}_{12}$	8.4	7.3	(5, 34)
$c\text{-C}_3\text{H}_6$	8.8	9.7	(5, 34)
$\text{HCOOCH}_3$	8.8	8.2	(36)
$\text{CH}_3\text{OCO}_2\text{CH}_3$	7.85	5.9	(33)
$\text{CH}_2\text{O}$	7.1	3.0	(22)

Using the previously mentioned values for  $k_{29}$  and  $k_{32a}$  yields  $k_{31d} = 10^{8.8} \times \exp(-8200/RT) M^{-1} \text{sec}^{-1}$ . In a similar study, Quee and Thynne (33) photolyzed  $\text{CH}_3\text{OCO}_2\text{CH}_3$  between 41° and 93°C. and were able to estimate  $k_{31e}k_{29}^{1/2}/k_{32a}$  where Reaction 31e is

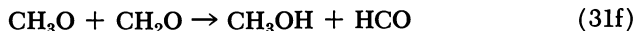


With the previously mentioned values of  $k_{29}$  and  $k_{32a}$ ,  $k_{31e}$  is  $10^{7.85} \times \exp(-5920/RT) M^{-1} \text{sec}^{-1}$ .

Hoare and Wellington (22) produced  $\text{CH}_3\text{O}$  radicals from the photochemical (50° and 100°C.) and thermal (135°C.) decompositions of di-*tert*-butyl peroxide in the presence of  $\text{O}_2$ . The initially formed *tert*-butoxy radicals decomposed to acetone plus methyl radicals, and the methyl radicals oxidized to methoxy radicals. Formaldehyde and  $\text{CH}_3\text{OH}$  were products of the reaction; the formation of the former was inhibited, and the latter was enhanced as the reaction proceeded. If the sole fate of  $\text{CH}_3\text{O}$  were either



or



and if the only source of CO were from the HCO radical, and if every HCO radical eventually produced CO, then  $k_{31f}/k_{18c}^{1/2}$  could be estimated from the expression

$$k_{31f}/k_{18c}^{1/2} = \sqrt{2R\{\text{CO}\}}/[\text{CH}_2\text{O}](R\{\text{CH}_3\text{O}\} - R\{\text{CO}\})$$

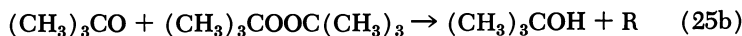
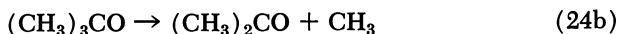
where  $R\{\text{CO}\}$  is the rate of CO production and  $R\{\text{CH}_3\text{O}\}$  is the rate of  $\text{CH}_3\text{O}$  production. The function  $R\{\text{CH}_3\text{O}\}$  is equal to twice the rate of peroxide decomposition. By using the above expression, Hoare and Wellington found  $k_{31f}/k_{18c}^{1/2} = 150 \exp(-3000/RT) M^{-1/2} \text{ sec.}^{-1/2}$ . If  $k_{18c}$  is taken to be  $10^{9.8} M^{-1} \text{ sec.}^{-1}$ , then  $k_{31f} = 10^{7.08} \exp(-3000/RT) M^{-1} \text{ sec.}^{-1}$ . Since there are many questionable assumptions in the derivation of  $k_{31f}$ , its Arrhenius parameters are subject to considerable uncertainty. The pre-exponential factor of  $10^{7.08}$  is probably too small by at least an order of magnitude.

Wijnen (38) photolyzed  $\text{C}_2\text{H}_5\text{COOC}_2\text{H}_5$  between  $15^\circ$  and  $195^\circ\text{C}$ . In a manner analogous to his studies on  $\text{CH}_3\text{COOCH}_3$ , he deduced the activation energy to be 5.5 kcal. per mole for



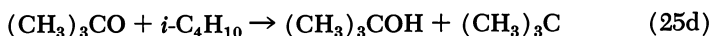
The pre-exponential factor for this reaction should be about  $10^{8.0} M^{-1} \text{ sec.}^{-1}$ .

McMillan and Wijnen (30) have studied the competition



from the photolysis of di-*tert*-butyl peroxide at  $25^\circ$  to  $79^\circ\text{C}$ . They found  $E_{24b} - E_{25b} = 3$  kcal. per mole. Using the value of  $E_{24b} \sim 12$  kcal. per mole, we find  $E_{25b} \sim 9$  kcal. per mole. Unfortunately, however, the value of  $A_{24b}/A_{25b}$ , found is inconsistent with the value of  $A_{24b} = 10^{11.2} M^{-1} \text{ sec.}^{-1}$ .  $E_{25b}$  is probably much lower than 9 kcal. per mole.

In a similar study, but with *i*- $\text{C}_4\text{H}_{10}$  present, McMillan (26) studied the competition between Reaction 24b and



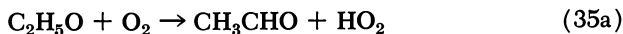
Assuming  $k_{24b} = 10^{11.2} \exp(-12,000/RT) \text{ sec.}^{-1}$ , we can deduce  $k_{25d}$  to be  $\sim 10^{8.0} \exp(-5000/RT) M^{-1} \text{ sec.}^{-1}$ .

Thynne (35) found that ethoxy radicals add to  $\text{C}_2\text{H}_4$  at  $70^\circ$  and  $160^\circ\text{C}$ ..



He estimated the reaction to be exothermic by about 13 kcal. per mole. The Arrhenius parameters should be similar to those for  $\text{RO}_2$  addition to olefins—*i.e.*,  $k_{34} \sim 10^{8.5} \exp(-6000/RT) M^{-1} \text{sec}^{-1}$ .

The reaction of alkoxy radicals with  $\text{O}_2$  has been postulated in many studies (29). Cerfontain and Kutschke (8), in the photolysis of  $(\text{C}_2\text{H}_5)_2\text{N}_2$ , estimated the relative importance between



and



Their computations showed that  $k_{35a}$  was roughly equal to  $k_{36}$  at both  $118^\circ$  and  $152^\circ\text{C}$ . However, their system was complex, and they made a number of assumptions. For example, they neglected the reactions of  $\text{HO}_2$  radicals, which must almost surely be incorrect. Nevertheless,  $k_{36}$  can be assumed equal to  $k_{33}$  by analogy. Thus, if Cerfontain and Kutschke's conclusion is correct, then  $k_{36} \sim k_{35a} \sim 10^{8.0} \exp(-5500/RT) M^{-1} \text{sec}^{-1}$ . The reactions of  $\text{C}_2\text{H}_5\text{O}$  radicals with molecules are summarized in Table VI.

The competition



was studied by Heicklen and Johnston (18) in the photo-oxidation of RI at  $25^\circ\text{C}$ . They found  $k_{35b}/k_{18a}^{1/2} = 1.97 \times 10^{-2}$  and  $4 \times 10^{-2} M^{-1/2} \text{sec}^{-1/2}$ , respectively, for  $\text{R} = \text{CH}_3$  and  $\text{C}_2\text{H}_5$ . Since  $k_{18a}$  is  $10^{9.8} M^{-1} \text{sec}^{-1}$ ,  $k_{35b}$  is  $10^{3.2} M^{-1} \text{sec}^{-1}$  at  $25^\circ\text{C}$ , which is compatible with the expression  $k_{35b} = 10^{8.0} \exp(-6500/RT) M^{-1} \text{sec}^{-1}$ .

### Reactions of RO with Radicals

There are no directly measured rate constants for radical-radical reactions involving RO radicals. These radicals can react with themselves in two ways.



The pre-exponential factor for the reverse of Reaction 18b was determined by Hanst and Calvert (16) to be  $10^{15.4} \text{sec}^{-1}$  for  $\text{R} = \text{CH}_3$ . Berces and Trotman-Dickenson (5) estimate the standard entropy of  $\text{CH}_3\text{OOCH}_3$  and  $\text{CH}_3\text{O}$  to be about 73 and 54.7 cal. per mole- $^\circ\text{K}$ ., respectively. With these values,  $k_{18b}$  can be computed to be  $10^{8.8} M^{-1} \text{sec}^{-1}$

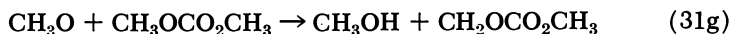
(not  $10^{10.0}$  as deduced by Berces and Trotman-Dickenson) for methoxy radicals.

Table VI. Some Reactions of  $C_2H_5O$  with Molecules

Reaction	$\sim E,$ Kcal./Mole	$\sim A,$ $M^{-1} \text{ sec.}^{-1}$
33		
$C_2H_5O + C_2H_5CO_2C_2H_5 \rightarrow C_2H_5OH + R$	5.5	$10^8$
34		
$C_2H_5O + C_2H_4 \rightarrow C_2H_5OC_2H_4$	6.0	$10^{8.5}$
35a		
$C_2H_5O + O_2 \rightarrow CH_3CHO + HO_2$	5.5	$10^8$

The ratio  $k_{18a}/k_{18b}$  was found to be between 9 and 12 at room temperature for  $R = CH_3, C_2H_5,$  or  $i-C_3H_7$  (19). Thus,  $k_{18a} = 10^{9.8} M^{-1} \text{ sec.}^{-1}$  for  $CH_3O$  radicals. Other estimates for  $k_{18a}/k_{18b}$  are higher. Dever and Calvert (10), in their study of methyl radical oxidation at  $25^\circ C.$ , did not find  $CH_3OOCH_3$  as a product. Thus, they concluded that  $k_{18a}/k_{18b} > 60$ .

Quee and Thynne (33) photolyzed dimethyl carbonate between  $41^\circ$  and  $93^\circ C.$  They assumed that essentially all the methanol was produced from the reactions



An additional amount of  $CH_3OH$  could come from the secondary reactions of  $CH_3O$  with  $CH_2O$ , but the investigators argued that it should be negligible at  $41^\circ C.$  Their conclusions, of course, depend on the validity of their argument. They further assumed that all the  $CH_3OCH_3$  and  $C_2H_6$  came, respectively, from the reactions



Thus, they were able to evaluate  $k_{18c}k_{29}/k_{32a}^2 = 18.5$ . With  $k_{29} = 10^{10.3}$  and  $k_{32a} = 10^{9.8}$ ,  $k_{18a}$  would be  $10^{10.6} M^{-1} \text{ sec.}^{-1}$ . However, this value is on the high side and probably reflects that other radical-radical reactions could be producing  $CH_3OH$ —e.g.,  $CH_3O + CH_2OCO_2CH_3 \rightarrow CH_3OH + R$ . A similar analysis from Wijnen's results (40) leads to  $k_{18a} \sim 10^{10.3} M^{-1} \text{ sec.}^{-1}$  for  $CD_3O$  radicals.

With alkyl radicals, the analogous reactions are



Reaction 37c cannot be important when R' is CH<sub>3</sub>. The rate constant for 37a can be estimated to be  $2k_{18a}^{1/2}k_{38}^{1/2}$  where Reaction 38 is



For R = CH<sub>3</sub>,  $k_{18a}$  is  $10^{8.8}$  and  $k_{38}$  is  $10^{10.3} M^{-1} \text{ sec}^{-1}$ ; thus,  $k_{37a}$  is approximately  $10^{9.8} M^{-1} \text{ sec}^{-1}$ . The ratio  $k_{37b}/k_{37a}$  has been reported to be 1.6 for CH<sub>3</sub>-CH<sub>3</sub>O (33, 36, 39), 1.4 for CH<sub>3</sub>-CD<sub>3</sub>O (40, 41), 1.3 for C<sub>2</sub>H<sub>5</sub>-C<sub>2</sub>H<sub>5</sub>O (38), and 3.4 for CH<sub>3</sub>-(CH<sub>3</sub>)<sub>2</sub>CHO (27). For C<sub>2</sub>H<sub>5</sub>-C<sub>2</sub>H<sub>5</sub>O,  $k_{37c}/k_{37a}$  is  $2.3 \pm 0.3$  (38). Consequently, when R is CH<sub>3</sub>,  $k_{37b}$  is approximately  $10^{10.0} M^{-1} \text{ sec}^{-1}$ .

**Table VII. Disproportionation-Recombination Ratios Involving Alkoxy Radicals**

Reaction	$k_a/k_b$	R
18a 2RO → ROH + R'R''CO	(a) } (b) }	CH <sub>3</sub> , C <sub>2</sub> H <sub>5</sub> , <i>i</i> -C <sub>3</sub> H <sub>7</sub>
18b → ROOR		
37b R + RO → RH + R'R''CO	(a) } (b) }	CH <sub>3</sub> , C <sub>2</sub> H <sub>5</sub>
37a → ROR		
37b CH <sub>3</sub> + (CH <sub>3</sub> ) <sub>2</sub> CHO → CH <sub>4</sub> + (CH <sub>3</sub> ) <sub>2</sub> CO	(a) } (b) }	3.4
37a → (CH <sub>3</sub> ) <sub>2</sub> CHOCH <sub>3</sub>		
37c C <sub>2</sub> H <sub>5</sub> O + C <sub>2</sub> H <sub>5</sub> → C <sub>2</sub> H <sub>5</sub> OH + C <sub>2</sub> H <sub>4</sub>	(a) } (b) }	2.3
37a → (C <sub>2</sub> H <sub>5</sub> ) <sub>2</sub> O		

**Table VIII. Some Rate Constants for Reactions of CH<sub>3</sub>O with Radicals**

Reaction	Log ( $k, M^{-1} \text{ sec}^{-1}$ )
18b 2CH <sub>3</sub> O → (CH <sub>3</sub> O) <sub>2</sub>	8.8
18c 2CH <sub>3</sub> O → CH <sub>3</sub> OH + CH <sub>2</sub> O	9.8 to 10.6
32a CH <sub>3</sub> O + CH <sub>3</sub> → CH <sub>3</sub> OCH <sub>3</sub>	9.8
37b CH <sub>3</sub> O + CH <sub>3</sub> → CH <sub>2</sub> O + CH <sub>4</sub>	10.0

The rate constant for atom transfer between two radicals is about 30 times larger than the pre-exponential factor for hydrogen-atom transfer from a molecule to a radical. Some rate constant data are summarized in Tables VII and VIII.

### *Acknowledgment*

The author thanks Barbara Peer for assistance with the manuscript and Ed Smith for his literature search. He also appreciates a number of useful suggestions and revisions which were proposed by S. W. Benson and J. H. Knox. R. R. Baldwin pointed out an error in the original manuscript. Financial support through Air Force Contract 04(695)-1001 is gratefully acknowledged.

### *Literature Cited*

- (1) Barber, M., Farren, J., Linnett, J. W., *Proc. Roy. Soc. (London)* **A272**, 306 (1963).
- (2) Benson, S. W., *J. Am. Chem. Soc.* **86**, 3922 (1964).
- (3) *Ibid.* **87**, 972 (1965).
- (4) Benson, S. W., Spokes, unpublished results.
- (5) Berces, T., Trotman-Dickenson, A. F., *J. Chem. Soc.* **1961**, 348.
- (6) Birss, F. W., Danby, C. J., Hinshelwood, C., *Proc. Roy. Soc. (London)* **A239**, 154 (1957).
- (7) Brinton, R. K., Volman, D. H., *J. Chem. Phys.* **20**, 25 (1952).
- (8) Cerfontain, H., Kutschke, K. O., *J. Am. Chem. Soc.* **84**, 4017 (1962).
- (9) Cox, D. L., Livermore, R. H., Phillips, L., *J. Chem. Soc.-Phys. Org.* **1966**, 245.
- (10) Dever, D. F., Calvert, J. G., *J. Am. Chem. Soc.* **84**, 1362 (1962).
- (11) Durant, D., McMillan, G. R., *J. Phys. Chem.* **70**, 2709 (1966).
- (12) Farren, J., Gilbert, J. R., Linnett, J. W., Read, I. A., *Trans. Faraday Soc.* **60**, 740 (1964).
- (13) Ferguson, J. M., Phillips, L., *J. Chem. Soc.* **1965**, 4416.
- (14) Flowers, M., Batt, L., Benson, S. W., *J. Chem. Phys.* **37**, 2662 (1962).
- (15) Gray, J. A., Thesis, University of London, England, 1950.
- (16) Hanst, P., Calvert, J. G., *J. Phys. Chem.* **63**, 104 (1959).
- (17) Heicklen, J., *J. Chem. Phys.* **42**, 1853 (1965).
- (18) Heicklen, J., Johnston, H. S., *J. Am. Chem. Soc.* **84**, 4030 (1962).
- (19) Heicklen, J., Johnston, H. S., Newton, J., *Bull. Soc. Chim. Belges* **71**, 744 (1962).
- (20) Hershenson, H., Benson, S. W., *J. Chem. Phys.* **37**, 1889 (1962).
- (21) Hoare, D. E., "Low Temperature Oxidation," W. Jost, ed., Chap. 6, Gordon and Breach, New York, 1966.
- (22) Hoare, D. E., Wellington, C. A., 8th Symposium on Combustion, Pasadena, Calif., 1960, p. 472, 1962.
- (23) Leighton, P. A., "Photochemistry of Air Pollution," p. 215, Academic Press, New York, 1961; also references quoted therein.
- (24) McGarvey, J. J., McGrath, W. D., *Trans. Faraday Soc.* **60**, 2196 (1964).
- (25) McKellar, J. F., Norrish, R. G. W., *Proc. Roy. Soc. (London)* **A263**, 51 (1961).
- (26) McMillan, G. R., *J. Am. Chem. Soc.* **82**, 2422 (1960).
- (27) *Ibid.* **83**, 3018 (1961).

- (28) *Ibid.* **84**, 2514 (1962).
- (29) McMillan, G. R., Calvert, J. G., *Oxidation Combust. Rev.* **1**, 83 (1965).
- (30) McMillan, G. R., Wijnen, M. H. J., *Can. J. Chem.* **36**, 1227 (1958).
- (31) Miyama, H., Takeyama, T., *J. Chem. Phys.* **40**, 2049 (1964).
- (32) Mulcahy, M. F. R., Williams, D. J., *Australian J. Chem.* **17**, 1291 (1964).
- (33) Quee, M. J. Y., Thynne, J. C. J., *Trans. Faraday Soc.* **62**, 3154 (1966).
- (34) Shaw, R., Trotman-Dickenson, A. F., *J. Chem. Soc.* **1960**, 3210.
- (35) Thynne, J. C. J., *J. Chem. Soc., Suppl. 1* **1964**, 5882.
- (36) Thynne, J. C. J., Gray, P., *Trans. Faraday Soc.* **59**, 1149 (1963).
- (37) Volman, D. H., Graven, W. M., *J. Am. Chem. Soc.* **75**, 3111 (1953).
- (38) Wijnen, M. H. J., *J. Am. Chem. Soc.* **82**, 3034 (1960).
- (39) Wijnen, M. H. J., *J. Chem. Phys.* **27**, 710 (1957).
- (40) *Ibid.* **28**, 271 (1958).
- (41) *Ibid.* **28**, 939 (1958).

RECEIVED October 9, 1967.

## Low Temperature Gas- and Liquid-Phase Oxidations of Isobutane

DAVID L. ALLARA, THEODORE MILL, DALE G. HENDRY,  
and FRANK R. MAYO

Stanford Research Institute, Menlo Park, Calif. 94025

*The rates and products of oxidations of isobutane were studied in both liquid (50 to 100°C.) and gas (100-155°C.) phases over wide ranges of concentrations and rates of chain initiation. Depending on these variables, the oxidation may yield as the principal product tert-butyl hydroperoxide, tert-butyl alcohol, acetone, and methanol, or (at higher temperatures) isobutylene. The effects of phase change alone are surprisingly small. High concentrations of isobutane and low rates of initiation favor formation of hydroperoxide. Low concentrations and higher temperatures favor formation of methanol and acetone. Changes in both reaction rates and products are explained by measured competitions between hydrogen abstraction and interactions of tert-butylperoxy radicals, between terminating and non-terminating reactions of the same radicals, and between hydrogen abstraction and cleavage reactions of tert-butoxy radicals.*

Earlier fundamental studies of autoxidations of hydrocarbons have concentrated on liquid-phase oxidations below 100°C., gas-phase oxidations above 200°C., and reactions of alkyl radicals with oxygen in the gas phase at 25°C. To investigate the transitions between these three regions, we have studied the oxidation of isobutane (2-methylpropane) between 50° and 155°C., emphasizing the kinetics and products. Isobutane was chosen because its oxidation has been studied in both the gas and liquid phases (9, 34, 36), and both the products and intermediate radicals are simple and known. Its physical properties make both gas- and liquid -phase studies feasible at 100°C. where primary oxidation products are stable and initiation and oxidation rates are convenient.

### Experimental

**Materials.** Isobutane (Phillips research grade) of 99.9 mole % purity was degassed through several freeze-thaw cycles and stored in a 2-liter bulb on the vacuum line. Analysis by gas liquid partition chromatography (GLPC) indicated no more than 0.2% impurity and no detectable isobutylene. Oxygen of 99.6 mole % purity was passed through liquid nitrogen and also stored in a 2-liter bulb. Di-*tert*-butyl peroxide (Lucidol) was distilled under vacuum; no *tert*-butyl alcohol or acetone was detected.

2,2'-Azobis(2-methylpropionitrile) (ABN) was Eastman White Label material recrystallized from alcohol. 1,1'-Azobis(cyclohexane-1-carbonitrile) (ABC) was prepared according to the directions in "Organic Syntheses" (26).

**Oxidation Procedures.** A vacuum line capable of giving a vacuum of  $10^{-5}$  torr was used in the preparation and analysis of all reactions. Liquid-phase experiments at 50°, 80°, and 100°C. were done in 20-ml. borosilicate glass vessels with glass break seals. The vessels were cleaned by repeated acetone rinses, then a water rinse, and evacuation with gentle heating. Isobutane, measured in a larger calibrated vessel, was frozen into this flask *via* a capillary sidearm with stopcock, and a known amount of oxygen was forced into the flask with the Toepler pump. Initiator was then injected from a tared microliter syringe through another capillary sidearm fitted with a serum cap. After the flask was charged, both capillary arms were sealed off, and the flask was immersed in the oil bath. The vessel was shaken to equilibrate gas and liquid phases. Essentially all reaction occurred in the liquid phase because of the small proportion of isobutane and absence of initiator in the gas phase. Oxidation was stopped by cooling the flasks to 25°C.

For the analysis, vessels were sealed on the vacuum line, flask contents were frozen at -195°C., the seal was broken, and noncondensable gases were moved to a gas buret with a Toepler pump. After the volume of the noncondensables was determined, they were analyzed by circulation through a Cu-CuO furnace at 265°C., where oxygen was removed as CuO and CO was oxidized to CO<sub>2</sub>. This gas was frozen at -195°C. and residual noncondensables (methane or nitrogen) were measured in the gas buret. The original carbon monoxide was estimated as CO<sub>2</sub> by warming the furnace trap to -80°C. and measuring CO<sub>2</sub> (and total noncondensable gases which usually were not significant) in the gas buret. For ABN and ABC initiators, a correction was applied for N<sub>2</sub> evolution. In some of the experiments isobutane was distilled from the reaction vessel at -80°C., and the residual products were dissolved in benzene. In other experiments all the reaction mixture was distilled into a trap; benzene or xylene was added, and analyses were performed directly on the chilled solutions. One portion of the product solution was analyzed for hydroperoxide by either the Wibaut (33) or Hiatt (15) iodine titration method; another was treated with triphenylphosphine to reduce the hydroperoxide to alcohol, then analyzed by GLPC on a 1.5-meter column of Carbowax 20M on Chromosorb.

Gas-phase experiments at 100°C. were made up and analyzed as described above. In the high pressure experiments the reacted mixture

was distilled into a trap, solvent was added, and the chilled reaction solutions were analyzed directly. No isobutylene was found by GLPC on a 1.5-meter column of dimethylsulfolane on Chromosorb at 70°C.

Gas-phase experiments at 155°C. were carried out in a 250-ml. cylindrical Vycor reactor in a hot-air furnace. Later experiments were done in a 500-ml. borosilicate glass flask heated in an oil bath. With either system, di-*tert*-butyl peroxide, oxygen, and isobutane were metered into the reaction vessel in that order by expansion from the vacuum line; the pressure of each component was measured using a mercury or oil manometer. Mercury vapor was excluded from the reaction vessel.

Experiments were terminated by expanding the contents of the 155°C. reaction vessel into the analytical side of the vacuum line, which contained a detachable GLPC sampling bulb in parallel with two liquid nitrogen traps and in series with a Toepler pump, gas buret, and Cu-CuO furnace. The noncondensable gases were estimated as described above. Corrections were applied for that portion of the reaction mixture diverted to the GLPC sampling bulb.

Condensable products were analyzed by GLPC using the contents of the sampling bulb to which was added a known amount of 2-methyl-2-butene as internal standard. Isobutylene and CO<sub>2</sub> were measured on the dimethylsulfolane column. Oxygenated products were measured with a 3-meter *N,N*-dimethylstearamide on Chromosorb column at 75°C. or with the Carbowax 20M column at 80°C. A 1.5-meter all-glass column containing didecyl phthalate on Fluoropak was used at 90°C. to separate and analyze mixtures containing *tert*-butyl alcohol and *tert*-butyl hydroperoxide.

### **Liquid-Phase Oxidations at 50° to 100°C.**

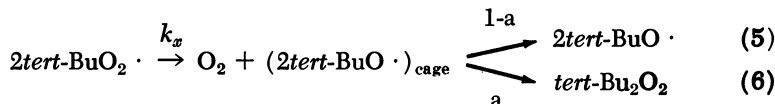
In 1961, Winkler and Hearne (34) reported the oxidation of isobutane by air at 125°C. with *tert*-BuO<sub>2</sub>H or *tert*-Bu<sub>2</sub>O<sub>2</sub> as initiator. They obtained the best yields of *tert*-Bu<sub>2</sub>OH at the lowest rates of oxidation. In one experiment, 7.6% conversion in 6 hours of 800 grams of isobutane (with 4 grams of *tert*-BuO<sub>2</sub>H) gave 75% yield of *tert*-BuO<sub>2</sub>H, 21% *tert*-BuOH, about 2% acetone, and 1% (iso-BuO<sub>2</sub>H + iso-BuOH). At this temperature, slow decomposition of *tert*-BuO<sub>2</sub>H caused a steady increase with time in the proportion of *tert*-BuOH and acetone in the products. Winkler and Hearne suggested no termination process, but they used Reactions 3, 4, 5, and 7 for chain propagation.

Our own liquid-phase studies were carried out at 50°–100°C., where the products are stable (16, 17). We obtained more information on radical interactions and determined the effects of dilution with CCl<sub>4</sub>. Our oxidations were carried out by heating known amounts of isobutane, initiator, and oxygen (sometimes with solvents) in sealed glass tubes as described above. Nearly all conversions of isobutane were kept below 1%. Experimental data are summarized in Table I.

**Experiments without Solvents.** At our rates of initiation, yields of hydroperoxide,  $\text{tert-BuO}_2\text{H}/(\Delta\text{O}_2)$ , in liquid-phase runs were about 75% at 50°, 90 to 93% at 100°C. *tert*-Butyl alcohol was a major product only at 50°C. with a high rate of initiation (Run 91); acetone was a minor product under all conditions. The termination product, 39% of the expected di-*tert*-butyl peroxide, was detected in Run 91 where ABN was used as the initiator.

A log-log plot of rate of oxygen uptake,  $R_o$ , vs. rate of initiation,  $R_i$ , in the absence of solvent at 50°C. gives a slope ranging from 0.48 at low [ABN] to about 0.57 at high [ABN] and averaging 0.53. A similar plot for 100°C. has a slope of 0.42. Although this test is inexact (*cf.* Equations 8 and 11 and discussion of Figure 1), most chain terminations involve two radicals.

**Simplest Mechanism.** The kinetics and products of the liquid-phase oxidation of neat isobutane (*tert*-BuH) are largely explained by the following steps. (We have found no significant reactions of primary C—H bonds.) Similar steps also apply to the liquid-phase oxidation of cumene (6, 12).



According to this scheme,  $k_x$  is the rate constant for Reactions 5 and 6 together, and  $a$  represents the fraction of these interactions that terminate. (The step represented by  $k_x$  can be further broken down to include  $\text{tert-Bu}_2\text{O}_4$  as intermediate.) Reactions 3, 5, and 6 have also been studied at 25°C. in the gas phase by photogeneration of *tert*-butyl radicals in the presence of oxygen (24). The competition between Reactions 5 and 6 is demonstrated by product studies on our Experiment 91 and measured as indicated below.

From Reactions 1 to 7

$$\frac{-d[\text{O}_2]}{dt} = \frac{\Delta[\text{O}_2]}{\Delta t} = R_o = \frac{R_i}{2a} + \left(\frac{R_i}{2ak_x}\right)^{1/2} k_p [\text{tert-BuH}] \quad (8)$$

Table I. Liquid-Phase

Expt. No.	[In] <sub>o</sub> , mM	[Iso-BuH] <sub>o</sub> , M	Solvent	Time, Min.
50°C., ABN Initiator				
7	5.1	8.91	None	1428
11	9.7	8.91	None	480
87	42	8.91	None	1230
89	48	8.91	None	606
103	102	8.91	None	1248
91	48	8.91	None	1194
13	10.0	2.06	CCl <sub>4</sub>	1452
9	9.8	4.99	CCl <sub>4</sub>	978
80°C., ABC Initiator				
88	12	8.12	None	318
100°C., <i>tert</i> -Bu <sub>2</sub> O <sub>2</sub> Initiator				
32	1.81	7.46	None	60
35	3.54	7.46	None	85.8
13A	61.9	7.46	None	129.0
11A	66.4	7.46	None	118.8
6	0.92	0.48	CCl <sub>4</sub>	891.0
5	0.92	0.68	CCl <sub>4</sub>	835.2
3	4.00	1.47	CCl <sub>4</sub>	609.0
4	2.62	4.30	CCl <sub>4</sub>	118.2

<sup>a</sup>  $R_i$  is rate of initiation,  $R_o$  is rate of oxygen absorption.  $R_i$  is calculated from  $2ek_d[\text{In}]_{av}$ ; at 50°,  $e = 0.60$ ,  $k_d = 1.30 \times 10^{-4}/\text{min.}$  (31); at 80°,  $e = 0.61$ ,  $k_d = 5.05 \times 10^{-4}/\text{min.}$  (35); at 100°,  $e = 1.0$ ,  $k_d = 4.08 \times 10^{-5}/\text{min.}$  (our value). Values of  $R_i$  at 50° for CCl<sub>4</sub> runs are corrected for solvent effects using available data at 60° (see 10) and 30.9 kcal. per mole activation energy for decomposition of ABN (18).

where  $R_i$  is rate of production of initiating radicals ( $\text{In} \cdot$ ). The last term is the oxygen uptake associated with formation of hydroperoxide; it includes  $\text{InO}_2\text{H}$  from Reactions 1a and 2 when  $\text{In} \cdot$  is an alkyl radical, not when  $\text{In} \cdot$  is an alkoxy radical. The  $R_i/2a$  term is the sum of two others,  $R_i/2 + R_i(1-a)/2a$ , corresponding to oxygen absorbed and appearing in *tert*-Bu<sub>2</sub>O<sub>2</sub> and *tert*-BuOH, respectively, as a result of radical interactions (Reactions 5 and 6).

Equation 8 can be written as

$$R_o = \frac{R_i}{2a} + \frac{\Delta[\text{tert-BuO}_2\text{H}]}{\Delta t} \quad \text{or} \quad \Delta\text{O}_2 = \frac{e\Delta[\text{Initiator}]}{a} + \Delta[\text{tert-BuO}_2\text{H}]$$

where  $e$  is the fraction of initiator decompositions that initiate chains. Thus,  $a$  can be evaluated from the hydroperoxide titer. For neat isobutane experiments in Table I, values of 0.128, 0.119, 0.127, 0.124, 0.11,

## Oxidations of Isobutane

$\Delta[\text{O}_2]$ , mM	Rate <sup>a</sup> $\times 10^6$ , Moles/L./Min.		Products, <sup>b</sup> mM		$\text{O}_2$ Acctd. for, %
	$R_i$	$R_o$	<i>tert</i> -BuO <sub>2</sub> H	<i>tert</i> -BuOH	
50°C., ABN Initiator					
32.7	0.72	23.0			
16.9	1.45	35.2			
89.5	6.0	72	58.5		
47.1	7.2	78.5	30.2		
42.1	1.45	33.7			
88.0	6.94	73.8	55.5	45	91°
9.01	1.20	6.2			
17.2	1.20	17.7			
80°C., ABC Initiator					
76.8	8.4	242	66.4		
100°C., <i>tert</i> -Bu <sub>2</sub> O <sub>2</sub> Initiator					
4.94	0.148	84			
8.62	0.288	100	5.05		
44.8	5.06	347	40.2	1.8	92
42.2	5.41	355	39.3	3.4	97
2.01	0.075	2.3			
3.96	0.075	4.7			
18.8	0.327	30.8			
8.41	0.214	71.1			

<sup>b</sup> Products by GLPC analysis except for hydroperoxide, which is by iodometric titration (15, 33).

<sup>c</sup> Includes  $\sim 3$  mM acetone [much of which may have come from Me<sub>2</sub>C(CN)O<sub>2</sub>H] and 1.6 mM *tert*-Bu<sub>2</sub>O<sub>2</sub> found.

and 0.072 were thus calculated from Experiments 89, 87, and 91 at 50°C., Experiment 88 at 80°C., and Experiments 11A and 13A at 100°C., respectively, using values of  $e$  given in the footnote to Table I. The average value of  $a$  at 50° and 80°C. is 0.125 and at 100°C. is 0.091, suggesting a slight temperature dependence. [The separation of two *tert*-BuO· radicals, Reaction 5, should have an activation energy of about 2 kcal. per mole, corresponding to diffusion from a solvent cage, while combination 6 should have almost no activation energy. However, Thomas (28) reports  $E_5 - E_6 = 5.3$  kcal. per mole.] From the induced decomposition of *tert*-butyl hydroperoxide in benzene solution at 45° and 100°C., values of  $a = 0.10$  to 0.12 (7, 14) and 0.04 (17), respectively, have been reported. These values are in fair agreement except at 100°C., where our value of  $a$  depends on the small difference between  $\Delta\text{O}_2$  and  $\Delta\text{tert-BuO}_2\text{H}$ . The good agreement between values of  $a$  obtained at 50 to 80°C. over a wide range of reaction times shows that *tert*-BuO<sub>2</sub>H is stable, and the

agreement among values determined by different methods shows that Reactions 1 to 7 and Equation 8 are good approximations for oxidation products in neat isobutane.

Equation 8 is less satisfactory when it is applied to rates of oxidation. The open circles and squares in Figure 1 are plots of  $R_o$  against  $R_i^{1/2}$  at  $50^\circ$  and  $100^\circ$  from Table I. Thus, when the  $R_i/2a$  term is neglected,  $R_o$  is proportional to  $R_i^{1/2}$ . However, when we incorporate the  $R_i/2a$  term (solid circles and squares), considerable curvature appears, corresponding to unexpectedly high rates of chain termination (larger  $a$ 's) at higher rates of initiation.

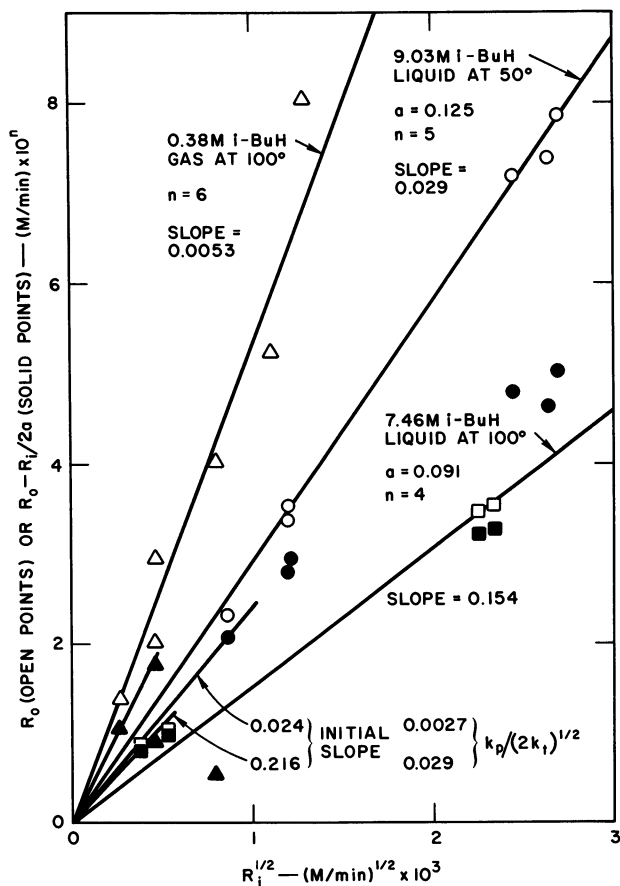


Figure 1. Rates of oxidation of isobutane as a function of rate of initiation (Equation 8). Reaction temperature and constant concentration indicated for each set of points

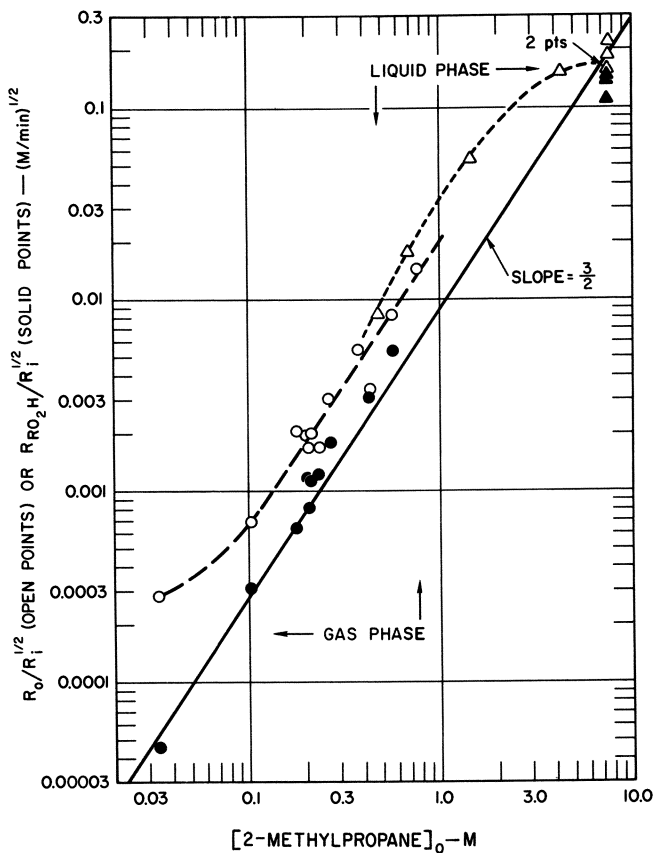
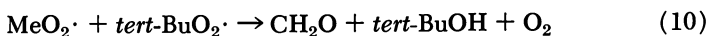


Figure 2. Rates of oxidation of isobutane at 100°C.

Equation 8 fails in two other ways when isobutane is diluted with carbon tetrachloride. The first is of secondary interest here: dilution of a hydrocarbon by a solvent often results in a rate decrease at high hydrocarbon concentrations so that the oxidation appears to be less than first order in hydrocarbon (10, 11, 19). Carbon tetrachloride shows a small effect of this kind at 100°C. but no obvious effect at 50°C. The more interesting failures of Equation 8 appear at lower hydrocarbon concentrations. For the 100°C. oxidations in Table I, the log-log plot in Figure 2 of  $R_o/R_i^{1/2}$  vs.  $[tert\text{-BuH}]_0$  shows a rate proportional to  $[tert\text{-BuH}]^{1.5}$  at high dilution, to  $[tert\text{-BuH}]^{1.0}$  at 1.5 to 4M, and to less than first power at higher concentrations (first failure above). In the absence of solvation effects, a plot of  $R_o$  vs.  $[tert\text{-BuH}]$  at constant  $R_i$  should be a straight line with intercept  $R_i/2a$  at  $[tert\text{-BuH}] = 0$ . However, for carbon tetrachloride at 50°, the rates at 2 and 5M isobutane (Table I) extrapolate to a slightly negative intercept.

**Modified Mechanism.** The failures of Equation 8 at low [*tert*-BuH] and high rates of initiation are ascribed mostly to Reactions 9 and 10.



Traylor and Russell (30) have shown recently that similar reactions for the cumyloxy radical are important in cumene oxidation at 60°C., and Hendry (12) has provided some quantitative data. At low concentrations of hydrocarbon, Reaction 9 is favored over Reaction 7 (propagation by *tert*-BuO·), and significant numbers of methyl radicals are formed and converted to MeO<sub>2</sub>· radicals. Chain termination thus shifts from the slow termination by 2 *tert*-BuO<sub>2</sub>· (Reaction 6) to Reaction 10, which has a rate constant several hundredfold larger (21). The apparent order of the oxidation in isobutane is then 3/2; a similar relation applies to gas-phase oxidations and is discussed there.

At low rates of initiation in neat isobutane, most of the *tert*-BuO<sub>2</sub>· radicals propagate by Reaction 4 instead of Reactions 5 and 6; any MeO<sub>2</sub>· radicals formed are more likely to propagate than to terminate with other radicals and so Equation 8 is a good approximation. As the rate of initiation increases, the effects of Reactions 9 and 10 on rates of oxidation become apparent. They have less effect on yields of hydroperoxides because the oxygen consumed in all the terminations is less affected (*cf.* also our finding only 39% of the expected *tert*-Bu<sub>2</sub>O<sub>2</sub> in Experiment 91, Table I).

The maximum increase in termination rate arising from Reaction 10 is a factor of  $(2 - a)/a$ , shown as follows. The rate of destruction of radicals by Reaction 10 is  $2k_{10}[\textit{tert}\text{-BuO}_2\cdot][\text{MeO}_2\cdot] = R_{t10}$ . If we assume that all *tert*-BuO· radicals produced from *tert*-BuO<sub>2</sub>· radicals (Reaction 5) eventually lead to termination *via* Reaction 9 and make the reasonable assumption that the slowest step in this sequence is Reaction 5, then at the steady state  $k_{10}[\textit{tert}\text{-BuO}_2\cdot][\text{MeO}_2\cdot] = 2k_x(1 - a)[\textit{tert}\text{-BuO}_2\cdot]^2 = R_{t10}/2$ . Since the contribution of Reaction 6 to the total termination rate is  $2ak_x[\textit{tert}\text{-BuO}_2\cdot]^2 = R_{t6}$ , intervention of Reaction 10 increases the chain termination rate by a maximum factor of  $(R_{t6} + R_{t10})/R_t = (2 - a)/a$ . Thus, at low isobutane concentrations the chain lengths are shorter and the over-all oxidation rate is slower than one would predict from Equation 8. At 100°C. where  $a \simeq 0.09$ , the maximum termination rate *via* Reactions 10 and 6 could be 21 times as fast as *via* Reaction 6 alone, and the oxidation rate would be  $21^{-1/2}$ , or 0.22 times as fast. Since  $a$  decreases slightly with increasing temperature, this factor of 21 will increase with increasing temperature.

**Some Rate Constants and Activation Energies.** When we apply Equation 8 to the initial slopes of the corrected liquid-phase curves in

Figure 1,  $k_p/(2k_6)^{1/2}$  at 50° is 0.0027 ( $M \text{ min.}$ )<sup>-1/2</sup>; the single value at 80°C. is 0.0103, and the initial value at 100°C. is 0.029. The 50° and 100°C. points then give an activation energy of  $11.3 \pm 1$  kcal. per mole, and if  $E_t = 9 \pm 1$  kcal. per mole, then  $E_p = 15.8 \pm 1.5$  kcal. per mole. [ $E_t = 9$  is an average of  $10.2 \pm 1$  kcal. per mole (28) and  $7.6 \pm 1.5$  kcal. per mole (12).] This is a surprisingly high value of  $E_p$  for a radical abstraction reaction that is close to thermoneutral (5), in view of earlier estimates of  $E_p \sim 8$  to 10 kcal. for exothermic abstractions by polyatomic radicals from polyatomic molecules (3). While these calculations based on initial slopes of the  $R_o - R_i/2a$  curves in Figure 1 appear to be significant, in all other experiments in this paper, the observed termination constant is complex and has not been evaluated.

A value of 0.06 ( $M \text{ min.}$ )<sup>-1/2</sup> for  $k_p/(2k_6)^{1/2}$  calculated from the data of Winkler and Hearne (34) in *tert*-Bu<sub>2</sub>O<sub>2</sub>-initiated oxidations at both 110° and 125°C. agrees with our extrapolated values, although the high conversions in their experiments lead to some uncertainty. Equation 8 predicts initial RO<sub>2</sub>H/ROH ratios obtained under their conditions within experimental error (+5%). For calculations from their data, values of  $k_d$  for *tert*-Bu<sub>2</sub>O<sub>2</sub> were taken as  $1.6 \times 10^{-6}$  per second at 110°C. and  $6.3 \times 10^{-6}$  at 125°C. (2).

### **Gas-Phase Oxidations at 100°C.**

Gas-phase oxidations of isobutane at 100°C. were carried out with di-*tert*-butyl peroxide as initiator as described above. These are summarized in Figure 2, and most are detailed in Table II. Even though conversions were held below 1%, long reaction times (up to 100 hours) were required because of the slow decomposition of the initiator.

These oxidations are essentially homogeneous and not autocatalytic. Adding borosilicate glass wool to Experiment 32B increased the surface area by a factor of 100 to 1000 (depending on variations in the diameters of individual strands) but had no significant effect on either the rate of oxidation or the yield of hydroperoxide. The comparative insensitivity of rate to amount of added *tert*-butyl hydroperoxide can be seen by comparing Experiment 17D with other similar experiments. The somewhat higher yield of hydroperoxide found in Experiment 17D rather than in 17C could be within experimental error.

A log-log plot of the rates of oxidation ( $R_o$ ) vs. the rates of initiation ( $R_i$ ) for 380 mM 2-methylpropane experiments in Table II gave a slope of 0.45 to 0.55 for the initiator dependence. [Although Figure 1 supports the same relation, the result is misleading. When we replace  $R_o$  by  $R_o - R_i/2a$  in the plot, using the liquid-phase value  $a = 0.091$ , the ordinates become smaller (solid triangles) or negative (not shown). To

obtain reasonable ordinates we need values of  $a$  in the gas about twice as large as in the liquid phase, but  $a$  is expected to be very small in the gas phase if  $\text{MeO}_2\cdot$  radicals are not involved.] The log-log plot of  $R_o/R_i^{1/2}$  vs.  $[\text{tert-BuH}]$  in Figure 2 gives a slope of 1.3 to 1.5 for isobutane dependence above 0.1M isobutane, but a lower slope at lower concentrations. Thus, the rate law  $R_o = kR_i^{0.45-0.55}[\text{tert-BuH}]^{1.3-1.5}$  applies to the gas-phase oxidation at 100°C. at concentrations above 0.1M (pressures above 3 atm.) as well as in the  $\text{CCl}_4$  solution. The same mechanism presumably applies and is now supported both quantitatively and qualitatively by the product studies below.

Table II. Rates of Gas-Phase Oxidations of Isobutane at 100°C.

Run No.	[ <i>tert</i> - $\text{Bu}_2\text{O}_2$ ] <sub>o</sub> , mM	[ <i>Iso</i> - $\text{BuH}$ ] <sub>o</sub> , mM	[ $\text{O}_2$ ] <sub>o</sub> , mM	Time, Min.	$\Delta[\text{O}_2]$ , mM	$\text{RO}_2\text{H}^a$ Yield, %	$\text{Rate}^b \times 10^8$ , Moles/L./Min.	
							$R_i$	$R_o$
32A	0.881	33.7 <sup>c</sup>	9.85	6025	0.455	16	6.0	7.5
31C	0.942	103	9.76	1666	0.317	45	7.7	19
3A	0.810	179	9.15	990	0.525	30	6.6	53
17C	1.08	208	9.72	990	0.422	49	8.8	43
32B <sup>d</sup>	1.03	214	9.92	200	0.446	56	8.4	50
17D <sup>e</sup>	0.961	233	9.89	990	0.422	71	7.9	41
17F	0.980	427	10.02	982	0.941	92	8.0	95
50	0.983	568	10.40	920	2.18	64	8.0	237
66	1.001	755	9.62	622	2.56		8.2	412
18	0.803	378	9.78	1691	2.35		6.6	139
108	2.51	375	9.52	1000	2.01		20.5	201
84	2.65	389	11.28	935	2.75		21.6	295
74	7.78	380	10.72	600	2.41		63.5	402
100	15.2	376	8.84	408	2.15		123	525
94	20.2	281	8.60	275	2.21		165	804

<sup>a</sup>  $[\text{RO}_2\text{H}]$  determined by iodometric titration (15, 33)/ $\Delta\text{O}_2$ .

<sup>b</sup> See footnote <sup>a</sup>, Table I.

<sup>c</sup> Corresponds to pressure of 1.03 atm.

<sup>d</sup> Contains 0.497 mM *tert*- $\text{BuO}_2\text{H}$ .

<sup>e</sup> Glass wool added; surface-volume ratio increased 100 to 1000.

Results of product studies of three experiments in Table II are given in Table III. Hydroperoxide yields based on  $\Delta\text{O}_2$  vary from 7 to 92%, and the yields increase with increasing isobutane pressure, although there is some scatter that may be caused by wall decomposition. From the yields of methanol and *tert*-butyl alcohol after reduction, nearly all of the hydroperoxide formed at high isobutane pressures is *tert*-butyl hydroperoxide. The yields of hydroperoxide at high isobutane pressures are comparable to those found in the liquid phase at 50° and 100°C. (Table I) and those reported by Winkler and Hearne for liquid-phase runs at 125°C. (34).

The total isobutane which reacts is measured by the sum of the *tert*-BuO<sub>2</sub>H, *tert*-BuOH, and acetone. In the following discussion of the methyl (corresponding to acetone) and oxygen balances, we assume that one mole of formaldehyde is formed for each mole of *tert*-Bu<sub>2</sub>O<sub>2</sub> decomposed, according to Reactions 1 and 10. In Experiments 32A, 31C, and 17C, respectively, 57, 95, and 91% of the oxygen consumed plus the oxygen in the initiating *tert*-BuO· radicals appears in the listed products and assumed formaldehyde. The shortage of oxygen and the excess (118%) of methyl radical products in Experiment 32A suggests that some acetone was oxidized. From the shortage of methyl radical products and satisfactory (at first sight) experimental oxygen balance in Experiments 31C and 17C, we conclude that the experimental ΔO<sub>2</sub>'s are too low and that the missing material is in undetected oxidation products of methyl radicals.

Table III shows that chains are carried by both alkylperoxy and alkoxy radicals. However, some of the *tert*-BuOH came from the initiation and termination steps, and the methyl radical balance is unsatisfactory.

We now use the following reasonable simplifying assumptions to consider why oxidation rates in both the gas phase and dilute solution are proportional to [*tert*-BuH]<sup>3/2</sup>—*i.e.*, all the interactions represented by *k<sub>x</sub>* are nonterminating (Reaction 5), all termination is by Reaction 10, no methylperoxy radicals propagate (because they terminate so fast), and all initiation is by *tert*-BuO· radicals from *tert*-Bu<sub>2</sub>O<sub>2</sub>. Then Relation 8 is replaced by

$$R_o = \frac{R_i}{2} + \left( \frac{R_i F}{2k_5} \right)^{1/2} k_p [\textit{tert}\text{-BuH}] + \frac{R_i F}{2} \quad (11)$$

where  $F = (k_7 [\textit{tert}\text{-BuH}] - k_9) / 2k_9$  and  $(R_i F / 2k_5)^{1/2} = [\text{RO}_2\cdot]$ . The terms on the right side of Relation 11 correspond to the oxygen associated, respectively, with the chain termination products, with formation of *tert*-butyl hydroperoxide, and with formation of *tert*-BuOH (by Reaction 7, not 10) and acetone. For 50 to 100% cleavage of *tert*-BuO· radicals, *F* ranges from 1 to 1/2. For low extents of cleavage,  $F \simeq k_7 [\textit{tert}\text{-BuH}] / 2k_9$  (the isobutane favors propagation of *tert*-BuO· radicals over their cleavage). Under such conditions, the rate of formation of *tert*-BuO<sub>2</sub>H, the second term on the right, is 3/2-order in isobutane and half-order in *R<sub>i</sub>*. Figure 2 shows how this relation fits well in gas-phase oxidations over a 22-fold change in [*tert*-BuH]. The other terms in Equation 11 are only 0 to 1-order in isobutane and are responsible for the differences between the *R<sub>o</sub>* and *R<sub>RO<sub>2</sub>H</sub>* plots in Figure 2.

#### **Effect of Phase Change at 100°C.**

Figure 2 shows that with about 0.5*M* isobutane at 100°C. the rates and rate laws for oxidation in the gas phase and in solution are similar.

However, the following considerations suggest that this similarity must be caused by a fortuitous compensation of several effects. There are two reasons to expect a higher rate in the gas phase.

(1) From the results of Walling and Wagner (32), with cyclohexane as hydrogen donor at 100°C., we calculate that  $k_7/k_9$  for *tert*-BuO· radicals is 13 times as large in the gas phase as in benzene solution. Several halogenated and aromatic solvents gave the same results. [Our own gas-phase data in Table III show that  $k_7/k_9$  decreases and approaches the expected liquid-phase value, 0.72 (1) as the pressure of isobutane gas increases from 1 to 6.5 atm.] The relatively higher cleavage of *tert*-BuO radicals in solution should increase the rate of chain termination by Reaction 10 and hence reduce the rate of oxidation of isobutane (but by no more than the factor of 4.6 calculated earlier).

(2) The absence of a cage effect in the gas phase (13, 23) should increase the proportion of nonterminating interactions (Reactions 5 and the analog of 10) and then increase the rate of oxidation.

We can suggest only one phase effect that might offset these effects. In the autoxidation of several hydrocarbons, Howard and Ingold (21) found solvent effects on  $k_p$  and  $k_t$  consistent with previously reported solvent effects on over-all rates (10, 19). We might then expect (25) that  $k_p$  would be slightly larger and/or  $k_t$  slightly smaller in the gas phase than in alkanes.

**Table III. Products of Gas-Phase Oxidations of 2-Methylpropane at 100°C.**

(Concentrations, mM; additional data in Table II)

Run No.	$\Delta$ , [tert-Bu <sub>2</sub> O <sub>2</sub> ]	$\Delta$ [O <sub>2</sub> ]	Products Found					$\Delta$ [tert-BuH] <sup>c</sup>	$k_7/k_9$ <sup>d</sup>
			RO <sub>2</sub> H <sup>a</sup>	tert-BuOH <sup>b</sup>	Ace-tone	MeOH	CO		
32A	0.181	0.455	0.073	0.091	0.224	0.035	0.049	0.10	12.0
31C	0.064	0.317	0.144	0.173	0.163	0.038	0	0.37	10.3
17C	0.044	0.422	0.206	0.196	0.167	0.020	0	0.505	5.6

<sup>a</sup> By iodometric titration (33).

<sup>b</sup> Corrected for *tert*-BuOH formed from reduction of *tert*-BuO<sub>2</sub>H by triphenylphosphine, assuming all hydroperoxide is *tert*-BuO<sub>2</sub>H.

<sup>c</sup> Calculated from products.

<sup>d</sup> Calculated from  $k_7/k_9 = \Delta \text{tert-BuOH} / \Delta \text{AcMe}[\text{tert-BuH}]$ .

#### Gas-Phase Oxidations at 155°C.

Several mixtures of isobutane, *tert*-Bu<sub>2</sub>O<sub>2</sub>, and oxygen were heated for 20 to 40 minutes at 155°C. (half-life of initiator, 36 minutes) and analyzed for oxygen consumption and products. Results are shown in Table IV.

Experiment 51 serves as a control in the presence of oxygen and absence of isobutane. Although only 44% of the *tert*-Bu<sub>2</sub>O<sub>2</sub> is

calculated to have decomposed, 50% of the initial peroxide was found as acetone, only 1.5% as *tert*-BuOH. Of the methyl groups expected to correspond to the acetone, 55% appear as methanol, 23% as CO; formaldehyde (undetermined) could account for much of the remainder.

Table IV. Oxidations of Isobutane at 155°C.

	Run Number					
	51	45	49	65	57	47
	Time, Min.					
	30	20	40	40	40	100
Reactants, mM in 253-ml. Vessel						
Isobutane	0	12.30 <sup>a</sup>	12.0	23.1	21.1	12.7
<i>tert</i> -Bu <sub>2</sub> O <sub>2</sub>	0.33	0.26	0.295	0.32	0.427	0.33
O <sub>2</sub>	0.968	0.862	0.925	1.10	1.31	0.941
Products, mM						
ΔO <sub>2</sub>	0.21	0.35	0.423	0.664	0.720	0.762
Δ <i>tert</i> -Bu <sub>2</sub> O <sub>2</sub> calcd. <sup>b</sup>	0.145	0.083	0.159	0.172	0.230	0.282
CO	0.0771	0.0439	0.039	0.0494	0.063	0.14
CO <sub>2</sub>	—	0.02	0.047	0.0660	0.095	0.091
Acetone	0.33	0.326	0.541	0.636	0.786	0.806
MeOH	0.18	0.247	0.443	0.534	0.747	0.69
<i>tert</i> -(BuOH + BuO <sub>2</sub> H) <sup>c</sup>	0.004	0.019	0.055	0.0759	0.099	0.058
<i>Iso</i> -C <sub>4</sub> H <sub>8</sub>	0	0.001	0.002	0.0099	0.015	0.02
RO <sub>2</sub> H <sup>d</sup>			0.043			
Δ <i>tert</i> -BuH calcd.		0.18	0.28	0.38	0.44	0.32
ΣC <sub>1</sub> (without CH <sub>2</sub> O)	0.26	0.31	0.53	0.65	0.91	0.92
Rates, Moles/Liter/Min. × 10 <sup>5</sup>						
R <sub>i av</sub> = 2ΔBu <sub>2</sub> O <sub>2</sub> /time	1.06	0.83	0.80	0.86	1.15	0.56
R <sub>o</sub> = ΔO <sub>2</sub> /time	0.70	1.75	1.06	1.7	1.8	0.77
(R <sub>o</sub> /R <sub>i</sub> )	(0.66)	2.10	1.32	1.98	1.57	1.37
Δ-BuH/2Δ-Bu <sub>2</sub> O <sub>2</sub>		1.1	0.9	1.1	1.0	0.57

<sup>a</sup> Corresponds to pressure of 328 torr.

<sup>b</sup> From (27),  $k_d = 0.0192/\text{min}$ .

<sup>c</sup> Not separated by GLPC.

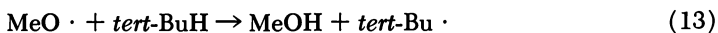
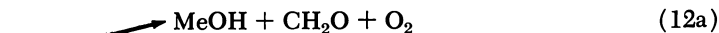
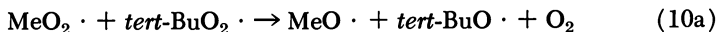
<sup>d</sup> Iodometric titration (33).

When isobutane is added to such an experiment, acetone and methanol are still the major products, and the concentrations of all products increase with the concentrations of isobutane and *tert*-Bu<sub>2</sub>O<sub>2</sub>. About one molecule of isobutane is consumed per initiating *tert*-BuO· radical. The higher consumption of oxygen is due mostly to oxidation of the initiating fragments (Experiment 51).

Comparison of Experiments 45, 49, and 47, which differ reaction times, shows that the rates of formation of most product  $R_i$  decrease gradually with time. CO might be both a primary and secondary product, but the yields of isobutylene increase with time, indicating that it is partly a secondary product.

In Experiment 49, about 10% of the oxygen reacting appeared as hydroperoxide. The latter is probably *tert*-BuO<sub>2</sub>H since this has a measured half-life of about 30 minutes in our system at 155°C.; indications are that methyl hydroperoxide is less stable (22). In Experiment 49, up to 80% of the *tert*-BuOH + *tert*-BuO<sub>2</sub>H (not distinguished by our GLPC) could be *tert*-BuO<sub>2</sub>H; peroxide analyses are not available for the other experiments.

The short kinetic chain lengths and different product mix at 155°C. in comparison with runs at 100°C. (Tables II and III) have three origins: generally lower concentrations of isobutane at 155°C., higher rates of initiation, and more cleavage of *tert*-BuO· radicals. To Reactions 1 to 7, 9, and 10 at 100°C., we need to add at 155°C. the terminating Reaction 12a, the nonterminating Reactions 10a and 12b, and the propagation Reaction 13.

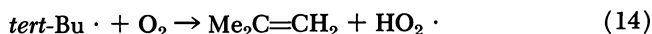


In Experiment 49, which has the best analyses and material balance, initiation by 32 μmoles of *tert*-BuO· radicals per 100 ml. of reaction mixture resulted in the reaction of 28 μmoles of isobutane to give mostly acetone and methanol. Of the 28 μmoles of *tert*-BuO<sub>2</sub>· resulting from attack on isobutane, no more than 4.3 (15%) abstracted hydrogen from isobutane to give *tert*-BuO<sub>2</sub>H; most of them reacted with other peroxy radicals to produce *tert*-BuO· radicals (as by Reaction 5), but some may have terminated chains (as by Reaction 10). The greater prominence of Reaction 5 at 155°C. as compared with 100°C. (Table II) is caused partly by the lower concentration of isobutane (12 to 23 mM instead of 34 to several hundred) but mostly by much higher radical concentrations and rates of chain initiation ( $R_i = \sim 10^{-5}$  instead of  $\sim 10^{-7}M$  per minute). Nearly all the *tert*-BuO· radicals cleaved to acetone and methyl radicals (Reaction 9). Since the amount of *tert*-BuOH found is only about one-tenth of what might result from termination by Reaction 10, we cannot be sure that much of the little *tert*-BuOH came from Reaction 7. The high extent of cleavage at 155°C. is partly caused by lower concentration of isobutane, but mostly by the activation energy difference,  $E_9 - E_7$ .

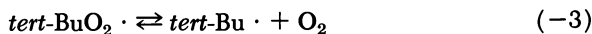
54  $\mu$ moles of methyl radicals formed (equivalent to the ac-44 appeared as methanol. Since there were only 31  $\mu$ moles of initiating radicals and of chain termination products, nearly all chain propagation involved methoxy radicals and nearly all chain termination involved  $\text{MeO}_2 \cdot$  or  $\text{MeO} \cdot$  radicals or their oxidation products. The 10  $\mu$ moles of missing methyl radicals ( $\text{AcMe} - \text{MeOH}$ ) are insufficient to permit one mole of formaldehyde to be formed in each of the 16 terminating radical interactions (10 and 12a) and so other terminations involving peroxy radicals derived from formaldehyde and formic acid must have occurred, producing some of the carbon oxides found. These considerations (with assignment of the *tert*-BuOH to termination by 10) permit only 15 of the 44  $\mu$ moles of methanol to be associated with chain termination; the remaining 29  $\mu$ moles of methanol must have been formed by Reaction 13 from methoxy radicals formed in nonterminating Reactions 10a and 12b. Just about 50% of interactions involving  $\text{MeO}_2 \cdot$  radicals must have been nonterminating. Still higher proportions of methyl radicals were converted to methanol in Experiments 65 and 57. These results contrast sharply with those in the liquid phase at or below 100°C., where essentially all interactions involving primary and secondary alkylperoxy radicals are terminating.

### Other Oxidations

At 300°C. and above isobutylene becomes the major product of the gas-phase oxidation of isobutane (9, 36), apparently by Reaction 14.



Benson (4) has suggested that the competition between Reaction 14 and the dissociation



is governed partly by propagation Reaction 4. Since in our 155°C. experiments some of the isobutylene may be a secondary product (from wall reactions) and its yields are erratic (0.6 to 2.9%), we have not estimated any of the ratios of rate constants above.

Our results and explanations have a close parallel in the work of Thomas and Calvert (24, 29); in their photogeneration of *tert*-butyl radicals in the presence of 1 atm. of oxygen at 25°C., 70% of the resulting *tert*-BuO<sub>2</sub>· radicals reacted with each other or with MeO<sub>2</sub>· radicals to give *tert*-BuO· radicals and oxygen (nonterminating). About 70% of the resulting *tert*-BuO· radicals cleaved to acetone and Me· radicals; the latter reacted with oxygen and then with other alkylperoxy

radicals to give  $\text{MeO}\cdot$  radicals (nonterminating). Most of the remaining 30% of  $\text{tert-BuO}_2\cdot$  and  $\text{tert-BuO}\cdot$  radicals terminated with  $\text{MeO}\cdot$  radicals to give  $\text{tert-BuO}_2\text{H}$ ,  $\text{tert-BuOH}$ , and formaldehyde. Thus, all interactions of  $\text{MeO}_2\cdot$  and  $\text{tert-BuO}_2\cdot$  are nonterminating; nearly all the terminating reactions involve  $\text{MeO}\cdot$  radicals and produce formaldehyde.

In neither study has there been any need to introduce either homogeneous (8, 36) or heterogeneous (9) rearrangements of alkylperoxy radicals in order to explain the results.

Since product distributions depend on the relative rates of competing reactions, effects of temperature on products depend on differences in activation energies,  $\Delta E$ . For each pair of competing reactions of the  $\text{tert-BuO}_2\cdot$  radicals, the following  $\Delta E$  values (in kilocalories per mole) and qualitative effects of increasing temperature are estimated. Some of these values were considered under "Liquid-Phase Oxidations."

(1) Propagation by a  $\text{tert-BuO}_2\cdot$  radical increases faster than nonterminating interactions of two  $\text{tert-BuO}_2\cdot$  radicals:  $E_4 - E_5 = 2$  to 5 kcal. per mole in the liquid phase and 7.5 in the gas phase. Propagation increases faster than termination in the liquid phase,  $E_4 - E_8 = 7.5$ , and in the gas phase Reaction 6 is negligible.

(2) Nonterminating interactions of two  $\text{tert-BuO}_2\cdot$  radicals increase faster than terminating interactions:  $E_5 - E_6 = 2$  to 5 in the liquid phase.

(3) Cleavage of  $\text{tert-BuO}\cdot$  radicals increases faster than abstraction:  $E_9 - E_7 = 8$  to 10 (32).

(4) Propagation by a  $\text{MeO}_2\cdot$  radical increases faster than termination between  $\text{MeO}_2\cdot$  and  $\text{tert-BuO}_2\cdot$  radicals:  $E_4' - E_{10} \simeq 12$ , from  $E_4' = E_4 = 16.5$  kcal. per mole and  $E_{10} \simeq 4$  kcal. per mole, based on the value 4.3 kcal. per mole for Tetralin (20).

(5) Nonterminating interactions of  $\text{MeO}_2\cdot$  radicals increase faster than do terminating interactions:  $E_{12b} - E_{12a} = E_{10a} - E_{10} = 4.6$ . [ $E_{12f} \simeq E_{10a} \simeq E_5 = 8.6$  kcal. per mole;  $E_{12a} \simeq E_{10} \simeq 4$  kcal. per mole. Unpublished results of Allara and Irwin (1) indicate that the ratio of terminating to nonterminating interactions is independent of phase.]

The observed differences in product distribution between the 100° and 155°C. oxidations are consistent with the above relations. Above 155°C., increasing amounts of isobutylene are formed, and pyrolysis of  $\text{tert-BuO}_2\text{H}$  (17) increases the number of  $\text{tert-BuO}\cdot$  radicals in the system and affects the rate of initiation.

### Acknowledgment

We acknowledge the able assistance of Tim Delaney, Gerald Stevenson, and Katherine Irwin, who did much of the experimental work. John H. Knox read our original manuscript very carefully and made numerous useful suggestions.

Our work on gas-phase oxidations at 100°C. was supported by the US Army Edgewood Arsenal under Contract DA18-108-AMC-202(A). The remainder of the work was part of an industrially sponsored oxidation program.

### Literature Cited

- (1) Allara, D. L., Irwin, K. C., unpublished work.
- (2) Batt, L., Benson, S. W., *J. Chem. Phys.* **36**, 845 (1962).
- (3) Benson, S. W., *Ind. Eng. Chem.* **56**, 24 (1964).
- (4) Benson, S. W., *J. Am. Chem. Soc.* **87**, 972 (1965).
- (5) Benson, S. W., *J. Chem. Educ.* **42**, 502 (1965).
- (6) Blanchard, H. S., *J. Am. Chem. Soc.* **81**, 4573 (1959).
- (7) Factor, A., Russell, C. A., Traylor, T. G., *Ibid.*, **87**, 3692 (1965).
- (8) Fish, A., *Quart. Revs.* **18**, 243 (1964).
- (9) Hay, J., Knox, J. H., Turner, J. M. C., Tenth Symposium (International) on Combustion, pp. 331-340, Combustion Institute, 1965.
- (10) Hendry, D. G., Russell, G. A., *J. Am. Chem. Soc.* **86**, 2368 (1964).
- (11) Hendry, D. G., Mayo, F. R., Schuetzle, D., *Ind. Eng. Chem.*, in press.
- (12) Hendry, D. G., *J. Am. Chem. Soc.* **69**, 5433 (1967).
- (13) Herk, L., Feld, M., Szwarc, M., *Ibid.*, **83**, 3993 (1956).
- (14) Hiatt, R., Cliphsham, J., Visser, T., *Can. J. Chem.* **42**, 2754 (1964).
- (15) Hiatt, R., Gould, C. W., Mayo, F. R., *J. Org. Chem.* **29**, 3461 (1964).
- (16) Hiatt, R., Irwin, K. C., *Ibid.*, in press.
- (17) Hiatt, R., Mill, T., Irwin, K. C., Castleman, J. K., *Ibid.*, in press.
- (18) Howard, J. A., Ingold, K. U., *Can. J. Chem.* **40**, 1851 (1962).
- (19) *Ibid.*, **42**, 1044, 1250 (1964).
- (20) *Ibid.*, **43**, 2729, 2737 (1965).
- (21) *Ibid.*, **44**, 1119 (1966).
- (22) Kutschke, K. O., private communication.
- (23) Lyon, R. K., Levy, D. H., *J. Am. Chem. Soc.* **83**, 4390 (1961).
- (24) McMillan, G. R., Calvert, J. G., in "Oxidation and Combustion Reviews," p. 84, D. F. H. Tipper, ed., Elsevier, New York, 1965.
- (25) Mayo, F. R., *J. Am. Chem. Soc.* **69**, 2654 (1967).
- (26) Rabjohn, N., ed., "Organic Syntheses," Coll. Vol. IV, p. 66, Wiley, New York, 1963.
- (27) Raley, J. R., Vaughan, W. E., Rust, F. F., *J. Am. Chem. Soc.* **70**, 88 (1948).
- (28) Thomas, J. R., *Ibid.*, **67**, 3935 (1965).
- (29) Thomas, S. S., Calvert, J. G., *Ibid.*, **74**, 4207 (1962).
- (30) Traylor, T. G., Russell, C. A., *Ibid.*, **87**, 3698 (1965).
- (31) Van Sickle, D. E., Mayo, F. R., Arluck, R. M., *Ibid.*, **87**, 4832 (1965).
- (32) Walling, C., Wagner, P. J., *Ibid.*, **86**, 3368 (1964).
- (33) Wibaut, J. P., van Leeuwen, H. B., van der Wal, B., *Rec. Trav. Chim.* **73**, 1033 (1954).
- (34) Winkler, D. E., Hearne, G. W., *Ind. Eng. Chem.* **53**, 655 (1961).
- (35) Wu, C., Hammond, G. S., Wright, J. M., *J. Am. Chem. Soc.* **82**, 5386 (1960).
- (36) Zeelenberg, A. P., Bickel, A. F., *J. Chem. Soc.* **1961**, 4014.

RECEIVED December 4, 1967.

# The Photo-Oxidation of 1,1'-Azoisobutane

## Reactions of the Isobutyl Free Radical with Oxygen

DAVID H. SLATER and JACK G. CALVERT

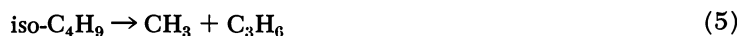
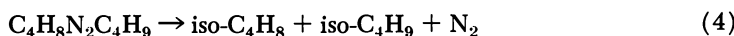
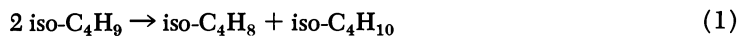
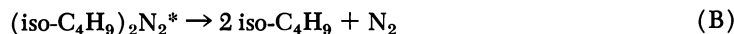
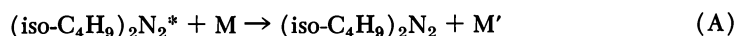
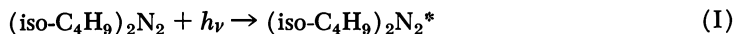
Evans Chemical Laboratory, The Ohio State University, Columbus, Ohio 43210

*A study has been made of the photo-oxidation of 1,1'-azoisobutane in experiments at 3660 Å. and full mercury arc and at temperatures from 308° to 405°K. The data prove the unimportance of energy transfer and singlet oxygen involvement for this system. The rates of products and their quantum yields are consistent with a mechanism involving the reactions of the isobutyl free radical with oxygen. A kinetic analysis of the data give  $k_7 + k_8 \cong 2.6 \times 10^9$  cc./mole-sec. (308–405°K.) and  $k_8/(k_7 + k_8) \cong 0.10$  (313°K.);  $\text{iso-C}_4\text{H}_9 + \text{O}_2 \rightarrow \text{iso-C}_4\text{H}_9\text{O}_2$  (7);  $\text{iso-C}_4\text{H}_9 + \text{O}_2 \rightarrow \text{iso-C}_4\text{H}_8 + \text{HO}_2$  (8). The product distribution suggests that the isobutyl peroxy and/or isobutoxy free radicals are unstable toward a decomposition reaction even at 308°K. for our conditions.*

The mechanism of the reaction of the simple alkyl free radicals with oxygen at and near room temperature is of special interest to the scientists concerned with the reactions in the polluted atmosphere. Photolysis of many of the atmospheric pollutants through sunlight absorption results in the formation of alkyl free radicals. In previous studies from this laboratory we have been concerned with evaluating the primary and secondary reactions of these free radicals with oxygen and determining the rate constants of the various steps in the reaction mechanism. Studies of the methyl (4, 10, 21, 23), ethyl (5), and *tert*-butyl (24) free radicals with oxygen have been reported in experiments near room temperature. Through these studies some additional insight into the nature and the reactivity of the various intermediate species and final products is gained.

Recently we have reported a study of the 3660-Å. photolysis of 1,1'-azoisobutane (20). Product rates and quantum yields were consistent

with the following reaction mechanism:



$(\text{iso-C}_4\text{H}_9)_2\text{N}_2^*$  represents an excited 1,1'-azoisobutane molecule of undefined nature.

The work showed clearly that the photolysis of 1,1'-azoisobutane was an excellent source of isobutyl radicals. In view of these findings we have used 1,1'-azoisobutane—oxygen mixture photolysis to study the reactions of the isobutyl free radical with oxygen. Some new kinetic data concerning the low temperature oxidation of this interesting radical have been found, and these are reported.

### **Experimental**

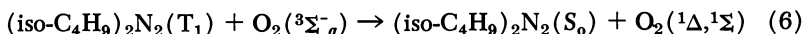
The 3660-A. photolysis system used in the rate studies was similar to that used previously by us (16, 20, 22). In one series of very high intensity experiments designed to study the reaction,  $\text{iso-C}_4\text{H}_9 + \text{O}_2 \rightarrow \text{iso-C}_4\text{H}_9\text{O}_2$ , the full mercury arc spectrum of a 200-watt PEK point source lamp was focused on the cell. Intensities were sufficiently high (about  $10^{16}$  absorbed quanta per sec.) so that a readily measurable rate of octane product formation was achieved even in runs with significant quantities of added oxygen. Products were analyzed using gas chromatographic and mass spectrometric methods. The fraction of the products not condensed at liquid nitrogen temperature was analyzed on a 1/8 in.  $\times$  6 ft. chromatographic column, filled with Linde Molecular Sieve, 5A, 90/100 mesh, operated at 60°C., and a Gow-Mac thermal conductivity detector (JDC-301). The condensible fraction was analyzed using a capillary column, 100 ft. long, 0.02 in. diameter, coated with squalane and temperature programmed, 25–125°C. at 10° per min. In this case a flame ionization detector was employed. Areas of the eluted product peaks were integrated automatically from the detector signal with an electronic integrator (Infotronics, CRS-11HSB). Products responsible for the individual elution peaks were identified using a Bendix time-of-flight mass spectrometer with rapid photographic recording of the osciloscopic trace of the mass spectra. Matching of the unknown spectrum with that of a known sample allowed unambiguous identification of most of the products.

The 1,1'-azoisobutane reactant purchased from Merck, Sharp, and Dohme (stated purity 99%) was further purified by chromatographic separation on an Autoprep instrument equipped with a Xf-1150 column operated at 140°C. The purified sample showed no impurities chromatographically at the photochemical product peak regions. It was stored at -78°C. in a darkened sample bulb sealed to the photolysis system.

The light intensity was estimated in several experiments using azomethane photolysis as an actinometer. The quantum yield of nitrogen was taken as unity (13). Azomethane was prepared by a modification of the method of Renaud and Leitch (18).

### Results and Discussion

**Mechanism of the Photo-Oxidation.** A major question must be answered satisfactorily before one can legitimately use data from the azoisobutane-oxygen mixture photolysis to derive information concerning the reactions of the isobutyl free radicals with oxygen. Do the products we observe actually arise from radical-oxygen interaction, or do they result from an excited azoisobutane molecule reaction with oxygen? One must face this question initially with considerable uncertainty since a recent study (20) showed that a relatively long-lived excited state participated in Reactions A and B. It was found that  $k_B \leq 4.5 \times 10^9 e^{-4.8/RT}$  sec.<sup>-1</sup>. These data coupled with the lack of observable fluorescence in azoisobutane and the theoretical radiative lifetime of the excited singlet state of azoisobutane, argue strongly against the participation of the first excited singlet in Reactions A and B. The first excited triplet or the vibrationally excited ground state singlet seem to be the favored reactant. If the excited state responsible for B is the triplet, then the currently popular, possible energy transfer Reaction 6 may occur in this system (7):

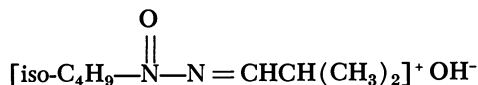


If Reaction 6 occurred in our system, the products observed would be those resulting from the singlet oxygen-azoisobutane interaction, and the photo-oxidation results would not be relevant to reactions of the isobutyl radical with oxygen.

We have tested for the possible occurrence of Reaction 6 in two direct ways.

First, singlet oxygen was prepared using a modification of the sodium hypochlorite-hydrogen peroxide method (1, 3, 8, 14). In a Y-tube, thoroughly degassed solutions of NaOCl (5.5% solution) and H<sub>2</sub>O<sub>2</sub> (30% solution) were mixed in the absence of air. The released gaseous product was passed immediately through a trap cooled to liquid nitrogen temperature and into a blackened 500-cc. reaction vessel containing 6 mm. of 1,1'-azoisobutane. The total pressure in the vessel was approximately 120 mm. After 3 hours of contact at room temperature the entire reaction mixture was analyzed chromatographically in a way identical to that used in the photochemical runs.

There were no significant quantities of nitrogen, acetone, or other light products observed, but some azoisobutane was consumed during the reaction. The nature of the heavy products of the reaction remains uncertain. It has been suggested (9) that a possible product of the singlet oxygen-1,1'-azoisobutane reaction would be:



However, it is evident that the products of the singlet oxygen reaction with azoisobutane are not those of the photo-oxidation of the azoisobutane.

The occurrence of Reaction 6 was also tested by studying the effect of oxygen concentration on the quantum yield of nitrogen in 1,1'-azoisobutane photolysis at 3660 Å. Table I shows these results. There is very little suppression of the nitrogen quantum yield as the concentration of oxygen is increased in Runs 1-6. What little inhibition occurs is that expected from the effect of oxygen acting as M in the collisional deactivation step A of the photolysis mechanism. If Reaction 6 were important for this system, a dramatic decrease in  $\Phi_{\text{N}_2}$  would be expected since singlet oxygen does not generate nitrogen from azoisobutane. In fact all the data prove that Reaction 6 is unimportant for our conditions and that the oxidation products observed are derived from the isobutyl radical reactions with oxygen following Reaction B.

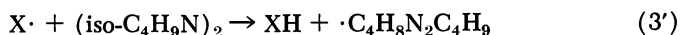
**Rate Constants for the Primary Reactions of the Isobutyl Free Radical with Oxygen.** The major primary reaction of the simple alkyl free radicals near room temperature is the association with oxygen, Reaction 7a.



The alternative Reaction 8a involving H atom abstraction by oxygen and olefin production is unimportant at low temperatures for the simple free radicals studied. For both ethyl (5) and *tert*-butyl (24) free radicals, Reaction 7a dominates; the rate of Reaction 8a is immeasurably slow at 25°C.

However, the isobutyl radical represents a special case where the occurrence of Reaction 8a at room temperature is more favorable. The enthalpy changes for Reactions 8a involving *tert*-butyl, ethyl, and isobutyl free radicals are: -5.8, -8.8, and -12.6 kcal./mole, respectively. Insofar as the over-all enthalpy change is reflected in the minimum potential energy at the transition state involved in Reaction 8a, we would expect  $k_{8a}$  for isobutyl to be the largest for the free radicals considered. This

appears to be the case. A small but significant yield of isobutene is found in the oxygen-containing runs. No octane is detectable in the runs at low intensity and high oxygen pressure, so that formation of isobutene by the disproportionation reaction of isobutyl radicals is unimportant. An alternative source of isobutene, as a referee has suggested, could be Reaction 3' followed by Reaction 4.



Where  $X\cdot$  might be an alkoxy radical RO. Previous work (20) on the reactions of isobutyl radicals indicate that Reaction 4 only becomes an important source of isobutene at temperatures above 150°C. Thus, experimental evidence suggests convincingly that Reactions 1 and 4 would not contribute significantly to the isobutene yield.

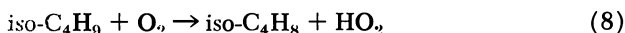
**Table I. Quantum Yields ( $\Phi$ ) of Products of the 3660-Å. Photolysis of 1,1'-Azoisobutane in Mixtures with Oxygen<sup>b</sup>**

Run	Concn., $\times 10^7$ , moles/cc.		$I_{\text{obs}}/I_0$	$\Phi_{\text{Products}}$				$k_8/(k_7 + k_8)^a$
	$\text{Bu}_2\text{N}_2$	$\text{O}_2$		$\text{N}_2$	$i\text{-C}_4\text{H}_8$	$i\text{-C}_4\text{H}_{10}$	$\text{Me}_2\text{CO}$	
1	3.03	0.00	0.130	0.069	—	—	—	—
2	2.98	6.86	0.126	0.065	0.013	—	0.065	0.10
3	3.10	3.10	0.130	0.108	0.020	<0.007	0.087	0.09
4	3.13	0.58	0.132	0.088	0.023	<0.008	0.094	0.13
5	3.19	2.16	0.136	0.105	0.017	<0.008	0.060	0.08
6	2.52	8.30	0.110	0.057	0.011	—	0.047	0.10

<sup>a</sup> Calculated from theoretical function,  $k_8/(k_7 + k_8) = \Phi_{\text{C}_4\text{H}_8}/2\Phi_{\text{N}_2}$ .

<sup>b</sup>  $T = 313^\circ\text{K}$ ,  $I_0 = 1.32 \times 10^{-9}$  Einsteins/cc.-sec.

From the quantum yield data of Table I we can estimate the ratio of  $k_8/(k_7 + k_8)$ . For these experiments at relatively low light intensities the butyl radical consumption by oxygen is complete, and it is highly likely that Reactions 7 and 8 are the major paths by which it reacts for these conditions.



If this mechanism choice is correct, Equation a should hold:

$$\Phi_{i\text{-C}_4\text{H}_8}/2\Phi_{\text{N}_2} = k_8/(k_7 + k_8) \quad (a)$$

In the last column of Table I Equation a is given as calculated from the experiments at 313°K. for various concentrations of azoisobutane and oxygen. The function is insensitive to the change in the ratio of the concentration of oxygen to that of azoisobutane over the range 0.18–3.3

as is required by Equation a. Thus, the data suggest the following rate constant ratio for 313°K.:

$$k_8/(k_7 + k_8) = 0.10$$

The very small isobutane yields can not be attributed to the participation of Reaction 3 since the known rate constant data are inconsistent with this. Isobutane must come from some other reactions, as yet undefined.

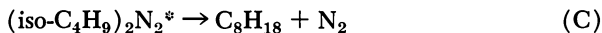
**Table II. Product Rate Data from Photolysis of 1,1'-Azoisobutane-Oxygen Mixtures Using a Full Mercury Arc**

Run	Temp., °K.	Pressure, mm.		Product Rates, moles/cc.-sec. × 10 <sup>11</sup>		(k <sub>7</sub> + k <sub>8</sub> )	
		Bu <sub>2</sub> N <sub>2</sub>	O <sub>2</sub>	N <sub>2</sub>	C <sub>8</sub> H <sub>18</sub>	cc./mole-sec. × 10 <sup>-9</sup>	(cc./mole) <sup>2</sup> sec. <sup>-1</sup> × 10 <sup>-15</sup>
7	308	6.46	3.40	4.17	0.067	2.6 <sup>a</sup>	5.0 <sup>b</sup>
8	343	5.4	0.00	6.54	6.47	—	—
9	343	5.4	0.00	6.54	2.49	—	—
10	343	3.58	8.62	5.34	0.026	2.4	4.2
11	343	5.27	5.5	4.08	0.054	2.0	4.0
12	343	5.91	3.12	2.99	0.051	2.6	6.2
13	343	6.15	1.75	3.66	0.252	2.5	6.8
14	343	7.4	3.4	4.73	0.090	2.9	5.8
15	380	6.63	2.81	4.23	0.145	2.7	6.8
16	380	6.67	3.46	4.40	0.098	2.8	6.5
17	405	6.63	2.45	4.40	0.256	2.5	6.9

<sup>a</sup> Estimates calculated assuming a second-order rate constant, Rate = [O<sub>2</sub>][Bu](k<sub>7</sub> + k<sub>8</sub>), and taking k<sub>2</sub> = 2.2 × 10<sup>13</sup> cc./mole-sec.

<sup>b</sup> Estimates calculated assuming a third-order rate constant, Rate = [O<sub>2</sub>][Bu][M](k<sub>7</sub> + k<sub>8</sub>), and taking k<sub>2</sub> = 2.2 × 10<sup>13</sup> cc./mole-sec.

In another series of runs (Table II) the high intensity, full arc photolysis of azoisobutane-oxygen mixtures was studied to estimate the rate constant sum, k<sub>7</sub> + k<sub>8</sub>. For the conditions of light intensity used, the 2,5-dimethylhexane product of the isobutyl combination reaction was formed in small but accurately measurable amounts for runs using moderate pressures of oxygen. If octane is formed only in Reaction 2, it can provide a useful monitor of the isobutyl radical concentration and allow k<sub>7</sub> + k<sub>8</sub> to be estimated from these rate data. However, if this technique is to be employed, one must evaluate carefully the importance of the possible alternative source of octane through the primary process C.



An analogous reaction of low efficiency has been postulated by Rebbert and Ausloos to explain their results from azomethane photolysis (17).

In terms of the proposed reaction mechanism the butyl radical concentration should be determined at the steady state by Equation b.

$$\frac{d[\text{Bu}\cdot]}{dt} = 0 = 2[\text{Bu}_2\text{N}_2^*]k_B - 2[\text{Bu}\cdot]^2(k_1 + k_2) - [\text{Bu}\cdot][\text{Bu}_2\text{N}_2]k_3 - [\text{Bu}\cdot]k_5 - [\text{Bu}\cdot][\text{O}_2](k_7 + k_8) \quad (\text{b})$$

If Reaction C is an unimportant source of octane compared with Reaction 2, the previously published rate data for  $k_3/k_2^{1/2}$  and  $k_5/k_2^{1/2}$  can be used together with the measured rate of octane formation of Table II to show that the third and fourth terms of Equation b are insignificant for runs at all temperatures used here. Thus, Equation b may be simplified to Equation c by eliminating these terms, substituting  $2R_{\text{N}_2}$  for  $2[\text{Bu}_2\text{N}_2^*]k_B$ ,  $2R_{\text{C}_8\text{H}_{18}}(1.075)$  for  $2[\text{Bu}\cdot]^2(k_1 + k_2)$ , and  $(R_{\text{C}_8\text{H}_{18}}/k_2)^{1/2}$  for  $[\text{Bu}\cdot]$  in the last term. It has been estimated (20) that  $k_1/k_2 = 0.075$  for the temperature range used in this study.

$$\frac{R_{\text{C}_8\text{H}_{18}}}{R_{\text{N}_2}} = \frac{k_2}{(k_7 + k_8)^2} \left\{ \frac{2R_{\text{N}_2} - 2R_{\text{C}_8\text{H}_{18}}(1.075)}{[\text{O}_2]} \right\}^2 \frac{1}{R_{\text{N}_2}} \quad (\text{c})$$

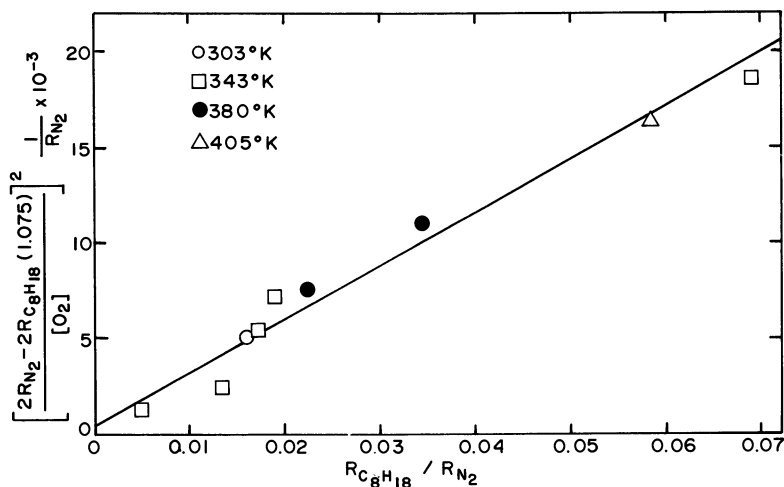


Figure 1. Test of rate function, Equation c, using rate data from the photolysis of 1,1'-azoisobutane at several temperatures

Figure 1 shows that the data of Table II at all temperatures fit the same linear plot of

$$\frac{R_{\text{C}_8\text{H}_{18}}}{R_{\text{N}_2}} \text{ vs. } \left\{ \frac{2R_{\text{N}_2} - 2R_{\text{C}_8\text{H}_{18}}(1.075)}{[\text{O}_2]} \right\}^2 \frac{1}{R_{\text{N}_2}}$$

within experimental error. Since the activation energies of Reactions 2, 7, and 8 are probably near zero, the temperature independence of Equation c is not surprising. Note that the intercept of the plot of Figure 1 with the  $x$ -axis is near zero ( $\pm 0.002$ ) within experimental error. Thus, we can conclude that the possible primary process forming octane—Reaction C—is unimportant in this system;  $\phi_C/\phi_B \leq 0.002$  for these conditions. Then the data can be used in a meaningful fashion to derive estimates of  $k_7$  and  $k_8$ .

From Equation c the useful Equation d can be derived to relate product rates to the oxygen concentration:

$$\frac{2[R_{N_2} - R_{C_8H_{18}}(1.075)]}{R_{C_8H_{18}}^{1/2}} = \frac{[O_2](k_7 + k_8)}{k_2^{1/2}} \quad (d)$$

A plot of the Equation c calculated from the data of Table II *vs.*  $[O_2]$  is shown in Figure 2. The data over the 100°C. temperature range fit the same line within the experimental error. The slope of the plot gives an estimate of  $(k_7 + k_8)/k_2^{1/2}$ :

$$(k_7 + k_8)/k_2^{1/2} = 5.5 \times 10^2 \text{ (cc./mole-sec.)}^{1/2}$$

Taking  $k_2 = 2.2 \times 10^{13}$  cc./mole-sec., the rate of association of the methyl radical (19),  $k_7 + k_8$  can be estimated:

$$k_7 + k_8 \cong 2.6 \times 10^9 \text{ cc./mole-sec. (308-405°K.)}$$

From the ratio  $k_8/(k_7 + k_8)$  at 313°K. we can calculate  $k_7$  and  $k_8$  at 313°K.:

$$k_7 \cong 2.3 \times 10^9 \text{ cc./mole-sec.}$$

$$k_8 \cong 2.3 \times 10^8 \text{ cc./mole-sec.}$$

The rate data for individual runs can be used to derive independent estimates of  $k_7 + k_8$ , and these are shown in Table II. Both rate constants for an assumed second-order and third-order rate law are shown. The second-order rate constants show the smaller deviation from constancy, but the total change in concentration of the reactants is relatively small so that the order cannot be definitely proved at present.

It is interesting to compare the present estimate of  $k_7$  for isobutyl with the analogous rate constant data for Reaction 7a involving the ethyl radical. In this case  $k_{7a}$  values range from  $7.8 \times 10^9$  (102°C.) reported by Finkelstein and Noyes to  $4.2 \times 10^{12}$  cc./mole-sec. (25°C.) given by Dingley and Calvert (5, 6, 12). The present estimate of  $k_7$  is about equal to the lowest of those reported for the ethyl radical reaction  $k_{7a}$ , but it is about  $10^{-3}$  as small as the largest estimate. In view of the complications inherent in experiments yielding the lowest estimates of  $k_{7a}$ , there is strong reason to believe that the higher estimates are more nearly correct (15). The present data for the isobutyl radical were derived in

experiments which ranged in total pressure from 9 to 12 mm. In this range the ethyl-oxygen reaction was clearly second order. Because of the increased complexity of the butyl over the ethyl radical, one expects the isobutyl-oxygen reaction to be in the second-order region for our conditions. It is possible that the smallness of  $k_7$  is a consequence of Reaction 7's being in a transition region between second- and third-order kinetics, as was observed for the methyl radical (15).

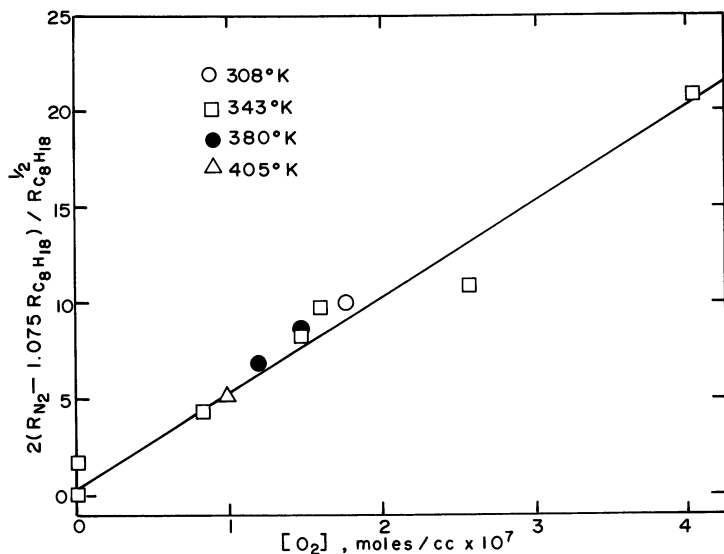
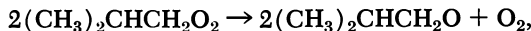


Figure 2. Test of rate function, Equation d, using rate data from the photolysis of 1,1'-azoisobutane at several temperatures

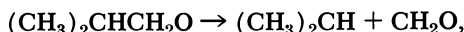
This might be the case since the full mercury arc was used in this series of experiments. Vibrationally nonequilibrated ethyl radicals were observed in azoethane photolysis at the shorter wavelength (5). It is expected that the rate constant for the reaction of a thermally equilibrated isobutyl radical with oxygen will be nearly equal to that for the ethyl radical. Certainly one should accept the present estimate of  $k_7 + k_8$  as a lower limit of the value for thermally equilibrated isobutyl radicals. We plan to test the order of the reaction more extensively and redetermine  $k_7 + k_8$  using the flash photolysis technique employed in the methyl (21) and ethyl (5) radical studies with oxygen to shed further light on this problem.

**Subsequent Reactions of the Isobutyl Peroxyl Radical.** The oxygenated products of the reaction of isobutyl with oxygen are many, and their rates were not well defined in this study. However, several of these products were identified unambiguously by chromatographic and mass

spectrometric analysis. One striking result is the small rate of formation of observed products containing the isobutyl group. Very little isobutyl alcohol, isobutyraldehyde, and isobutyl hydroperoxide were observed. Acetone and isopropyl alcohol were major products. These facts are consistent with the rapid decomposition of the isobutyl peroxy and/or isobutoxyl free radicals to generate isopropoxyl radical. This could conceivably occur through the commonly postulated path of peroxy radical reaction.



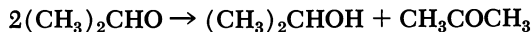
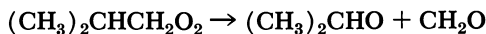
followed by decomposition of the isobutoxyl radical,



with subsequent oxidation of isopropyl to  $(\text{CH}_3)_2\text{CHO}_2$ ,  $(\text{CH}_3)_2\text{CHO}$  formation, and hence generation of acetone and isopropyl alcohol.



Alternatively a direct rearrangement of the isobutyl peroxy radical may account for the products:



A choice between these and other possible alternatives is not possible from the present data.

### *Acknowledgment*

The authors are grateful for the support of this work through a research grant from the National Center for Air Pollution Control, U.S. Public Health Service, Bethesda, Md., to William Bishop and Richard Firestone for the use of the time-of-flight instrument for product identification, and to S. W. Benson, Christopher S. Foote, and E. A. Ogryzlo for their helpful discussions with us concerning this work.

### *Literature Cited*

- (1) Arnold, S. J., Ogryzlo, E. A., Witzke, H., *J. Chem. Phys.* **40**, 1769 (1964).
- (2) Avramenko, L. I., Kolesnikova, R. V., *Izv. Akad. Nauk. SSSR Otd. Khim. Nauk* **1960**, 989, 809.
- (3) Brown, R. J., Ogryzlo, E. A., *Proc. Chem. Soc. (London)* **1964**, 117.
- (4) Dever, D. F., Calvert, J. G., *J. Am. Chem. Soc.* **84**, 1362 (1962).
- (5) Dingley, D. P., Calvert, J. G., *J. Am. Chem. Soc.* **85**, 856 (1963).
- (6) Finkelstein, A., Noyes, Jr., W. A., *Discussions Faraday Soc.* **14**, 76 (1953).
- (7) Foote, C. S., Wexler, S., *J. Am. Chem. Soc.* **86**, 3880 (1964).
- (8) *Ibid.*, p. 3879.
- (9) Foote, C. S., private communication.

- (10) Hanst, P. L., Calvert, J. G., *J. Phys. Chem.* **63**, 71 (1959).
- (11) Heicklen, J., Johnston, H. S., *J. Am. Chem. Soc.* **84**, 4394 (1962).
- (12) Jolley, J. E., *J. Am. Chem. Soc.* **79**, 1537 (1957).
- (13) Jones, M. H., Steacie, E. W. R., *J. Chem. Phys.* **21**, 1018 (1953).
- (14) Khan, A. U., Kasha, M., *J. Chem. Phys.* **39**, 2105 (1963).
- (15) McMillan, G. R., Calvert, J. G., *Oxidation Combust. Rev.* **1**, 84 (1965).
- (16) Morganroth, W. E., Calvert, J. G., *J. Am. Chem. Soc.* **88**, 5387 (1966).
- (17) Rebbert, R. E., Ausloos, P., *J. Phys. Chem.* **66**, 2253 (1962).
- (18) Renaud, R., Leitch, L. C., *Can. J. Chem.* **32**, 545 (1954).
- (19) Shepp, A., *J. Chem. Phys.* **24**, 939 (1956).
- (20) Slater, D. H., Collier, S. S., Calvert, J. G., *J. Am. Chem. Soc.* **90**, 268 (1968).
- (21) Sleppy, W. C., Calvert, J. G., *J. Am. Chem. Soc.* **81**, 769 (1959).
- (22) Smith, R. M., Calvert, J. G., *J. Am. Chem. Soc.* **78**, 2345 (1956).
- (23) Subbaratnam, N. R., Calvert, J. G., *J. Am. Chem. Soc.* **84**, 1113 (1962).
- (24) Thomas, S. S., Calvert, J. G., *J. Am. Chem. Soc.* **84**, 4207 (1962).

RECEIVED October 9, 1967.

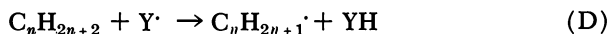
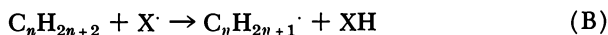
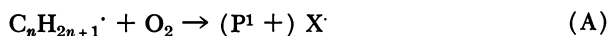
## Chain Propagation in the Oxidation of Alkyl Radicals

ANTHONY FISH

Shell Research, Ltd., Thornton Research Centre, P.O. Box 1, Chester, England

*During the gaseous oxidation of alkanes, chain propagation occurs by oxidation of alkyl radicals and their regeneration from the alkane. Routes involving intermolecular and intramolecular hydrogen abstraction by alkylperoxy radicals compete with routes via alkenes and hydroperoxy radicals. Calculation of the thermodynamic and kinetic parameters of the steps involved has enabled a single general scheme for chain propagation to be devised and the relative importances of the various chains to be assessed. At temperatures of ca. 550°K. the route via alkenes and hydroperoxy radicals is unimportant during the oxidation of large alkyl radicals but is more important for small radicals. The reasons for this are discussed.*

The primary chain-propagating cycle during the gaseous oxidation of an alkane is essentially a mechanism for oxidizing alkyl radicals and regenerating them from the alkane. Any such process can be represented by the general equations



where  $\text{X}\cdot$  and  $\text{Y}\cdot$  are free radicals capable of abstracting hydrogen from an alkane, and  $\text{P}^1$  and  $\text{P}^2$  represent stable or moderately stable products.

The natures and precise modes of formation of the radicals  $\text{X}\cdot$  and  $\text{Y}\cdot$  have aroused considerable controversy. In the liquid phase, the noncatalytic oxidation by molecular oxygen of the majority of alkanes occurs by the "hydroperoxide chain mechanism," in which the alkylperoxy

radical acts as  $X\cdot$  and no radical  $Y\cdot$  is involved. When the chain is long and the alkylperoxy radical attacks the hydrocarbon selectively—*i.e.*, always in the same skeletal position—the yield of a single monohydroperoxide approaches 100%, as evidenced by the oxidation of Tetralin (43). The success of this mechanism in describing the course of liquid-phase oxidation, together with the identification of peroxides among the products of the corresponding gas-phase reactions (1, 6, 14, 38, 49), has led to the partial acceptance of the mechanism in the gas phase also. In other gas-phase systems, however, monohydroperoxides cannot be detected even under conditions where they should definitely have been found if present (16). Again, even when such products are formed, they may arise from side reactions rather than from the primary oxidation chain. Thus, in the oxidations of ethane and 2-methylpropane, it is considered (7, 27, 39, 53) that the corresponding hydroperoxides arise from the mutual destruction of alkylperoxy and hydroperoxy radicals; in methane oxidation, methyl hydroperoxide is probably formed (26, 47) by methylperoxy radicals attacking formaldehyde (and not methane).

The second major theory of the mechanism of alkane oxidation in the gas phase is the “aldehyde” theory. The products of gaseous oxidation almost invariably contain aldehydes, and it has been proposed (41) that these are formed by decomposition of alkylperoxy radicals.

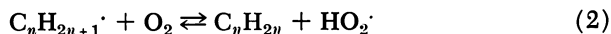
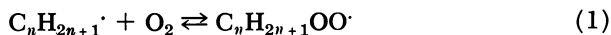
The controversy surrounding the “hydroperoxide” and “aldehyde” mechanisms of alkane oxidation has centered mainly on the nature of the degenerate-branching reaction involved. The pyrolysis of peroxides and the oxidation of aldehydes (which have a weak acyl-hydrogen bond) are both capable of acting in this capacity (4, 5, 35, 41, 44, 52), but it is not clear which route predominates. This concern with the branching step is perhaps responsible for the relative neglect of the nature of the primary propagation processes. The invention of sophisticated chromatographic techniques for analyzing the products of oxidation reactions has revived interest in the propagation steps, however. If the chains are reasonably long, almost all the material produced results from propagation steps; degenerate-branching steps are, by definition, slow and lead to very little product. Analysis of oxidation products provides, therefore, a good experimental basis from which to deduce the precise modes of oxidation and regeneration of alkyl radicals during the thermal oxidation of alkanes.

### *Oxidation of Alkyl Radicals (Step A)*

The interaction of an alkyl radical with oxygen must involve, as a first step, the formation of some species which may be formally written as  $C_nH_{2n+1} \dots O_2$ . This may be a fairly stable “thermalized” radical which can exist for relatively long periods of time, or a vibrationally

excited radical having the energy released by formation of the C—O bond randomly distributed throughout the radical, or an activated complex in which the vibrational energy is organized in a specific way and which will decompose or rearrange within the period of a single vibration. It is generally believed that at low temperatures ( $< 250^\circ\text{C}.$ )  $\text{C}_n\text{H}_{2n+1}\text{OO}\cdot$  radicals are stable, but at high temperatures ( $> 400^\circ\text{C}.$ ) an  $\text{HO}_2\cdot$  radical and an alkene are the products of alkyl radical-oxygen interactions. This is consistent with the change in the pattern of product formation with temperature; oxygenated products predominate at low temperatures but alkenes are formed in considerable yields at higher temperatures.

In the intermediate temperature range ( $250^\circ$  to  $400^\circ\text{C}.$ ), which is the region in which cool flames propagate during the oxidation of hydrocarbons, both alkenes and oxygenates are formed in significant amounts. Thus, in the oxidations of ethane (36), propane (34), and 2-methylpropane (28, 54) about 80% of the initial oxidation product is the conjugate alkene. On the other hand, the oxidations of higher alkanes such as hexane (19, 37) and 2-methylpentane (21, 24) produce a wide variety of oxygenated products and only relatively small yields of conjugate olefins. It is evident that Reactions 1 and 2:



must compete reasonably equally under these circumstances. The predominant route of oxidation will then depend on the structure of the radical  $\text{C}_n\text{H}_{2n+1}\cdot$ .

Calculating (Appendix) the thermodynamic and kinetic quantities characterizing Reactions 1 and 2 enables one to assess the competition between these reactions.

These calculations show that at  $550^\circ\text{K}.$ , alkyl radicals will react initially—*i.e.*, when the concentration of  $\text{RO}_2\cdot$  is negligible—with oxygen almost entirely to give  $\text{RO}_2\cdot$ . Of Reactions 2, as would be expected, those in which a tertiary C—H bond is broken are fastest. Even in these cases, however,  $k_1$  exceeds  $k_2$  by a factor of  $10^3$ . Recalculating these rate constants at  $700^\circ\text{K}.$  shows that the factor is still as high as  $10^2$ . The reasonably equal competition between Reactions 1 and 2, which is suggested by the nature of the products found experimentally, must depend on additional factors.

Since Reactions 1 and 2 are reversible, the effect of the reverse of Reaction 1, *i.e.*, Reaction  $-1$ , will become appreciable as the concentration of  $\text{C}_n\text{H}_{2n+1}\text{OO}\cdot$  rises ( $k_{-1} = 10^{3.8} \text{ sec.}^{-1}$ ). As Reaction 1 proceeds towards equilibrium, the importance of Reaction 2 may increase. It is

Table I. Thermodynamic and Kinetic Parameters for

Reaction	Example	$\Delta H,$ Kcal. Mole <sup>-1</sup>	$\Delta S,$ Cal. Mole <sup>-1</sup> °K. <sup>-1</sup>
1	$C_nH_{2n+1}\cdot + O_2 \rightarrow C_nH_{2n+1}OO\cdot$	-28	-32
2	$\cdot CH_2CH(CH_3)C_3H_7 + O_2 \rightarrow$ $CH_2=C(CH_3)C_3H_7 + HO_2\cdot$	-13	-0.2
2	$(CH_3)_2\dot{C}C_3H_7 + O_2 \rightarrow$ $CH_2=C(CH_3)C_3H_7 + HO_2\cdot$	-5.6	+3.2
2	$\cdot CH_2CH(CH_3)_2 + O_2 \rightarrow$ $CH_2=C(CH_3)_2 + HO_2\cdot$	-13	+0.3
2	$\cdot C(CH_3)_3 + O_2 \rightarrow$ $CH_2=C(CH_3)_2 + HO_2\cdot$	-5.6	+1.8
2	$\cdot CH_2CH_3 + O_2 \rightarrow$ $CH_2=CH_2 + HO_2\cdot$	-7.5	+0.8

necessary to consider the fates of the species X' ( $C_nH_{2n+1}OO\cdot$  and  $HO_2\cdot$ ) to assess the magnitude of this effect.

### Direct Regeneration of Alkyl Radicals (Step B)

Alkylperoxy radicals can abstract hydrogen directly from an alkane molecule (Reaction 3).



This reaction is well established at low temperatures, particularly in the liquid phase. Hydroperoxy radicals react similarly at higher temperatures (17), producing hydrogen peroxide and an alkyl radical.

### Interconversion of Chain Carriers (Step C)

**Isomerization of Alkylperoxy Radicals.** Alkylperoxy radicals can isomerize to hydroperoxyalkyl radicals (19, 25, 45, 55), which subsequently react to regenerate free radicals capable of attacking  $C_nH_{2n+2}$ .

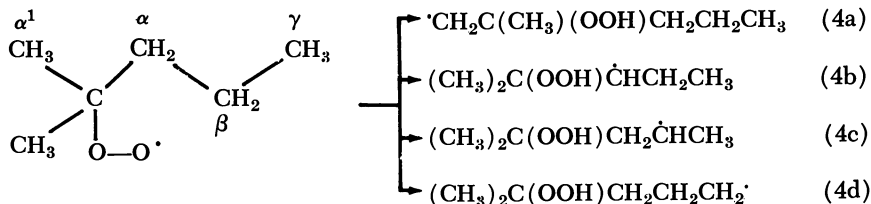
This isomerization occurs by intramolecular transfer of a hydrogen atom or an alkyl group, the former occurring much more frequently (24, 25). Alkylperoxy radicals containing several carbon atoms may isomerize by hydrogen transfer by each of several different routes, to give several hydroperoxyalkyl radicals. For the 2-methylpentyl-2-peroxy radical, for example, four routes can be distinguished. The energy requirements of these differ for two reasons; they are affected by both the nature of the C—H bond broken and the size of the transition state ring involved.

## Reactions of Alkyl Radicals with Oxygen at 550°K.

$K$ , Cc. Molecule <sup>-1</sup>	$K$ (Dimensionless)	$E$ , Kcal. Mole <sup>-1</sup>	$A$ , Cc. Molecule <sup>-1</sup> Sec. <sup>-1</sup>	$k$ , Cc. Molecule <sup>-1</sup> Sec. <sup>-1</sup>
10 <sup>-15.3</sup>	—	0	10 <sup>-11.5</sup>	10 <sup>-11.5</sup>
—	10 <sup>5</sup>	6	10 <sup>-12.2</sup>	10 <sup>-14.6</sup>
—	10 <sup>2.9</sup>	8	10 <sup>-12.2</sup>	10 <sup>-16.2</sup>
—	10 <sup>5</sup>	6	10 <sup>-12.2</sup>	10 <sup>-14.6</sup>
—	10 <sup>2.6</sup>	8	10 <sup>-12.2</sup>	10 <sup>-16.2</sup>
—	10 <sup>3</sup>	7	10 <sup>-12.2</sup>	10 <sup>-15.4</sup>



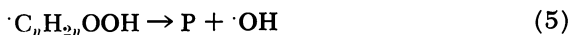
e.g.,



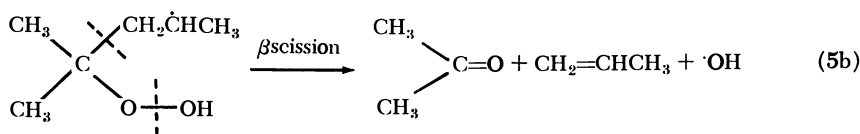
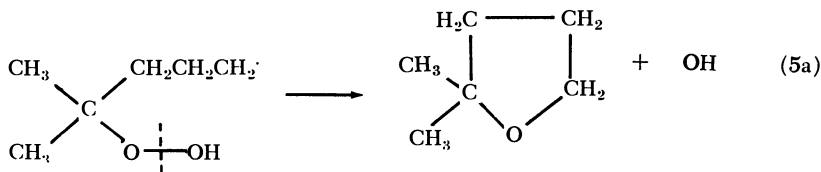
During the oxidation of 2-methylpentane, five radicals  $C_6H_{13}OO\cdot$  will be formed; the rearrangement by hydrogen transfer of these can, in theory, produce a total of 21 radicals  $\cdot C_6H_{12}OOH$  (24).

Hydroperoxyalkyl radicals can react in several ways. First, of course, alkylperoxy radical isomerization is reversible (Reaction —4). Secondly, several modes of decomposition (Reaction 5) occur, giving *O*-heterocycles, alkenes, and saturated and unsaturated aldehydes and ketones. (Alcohols can also be formed by the decomposition of the alkylperoxyalkyl radicals which result from isomerization by group transfer in alkylperoxy radicals.) These modes of decomposition have been enumerated (24, 25); only examples need be given here. Each mode of decomposition gives one or more product molecules plus one free radical, acting, therefore, as a propagation step. Moreover, the radical produced

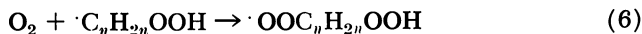
is usually (but not invariably)  $\cdot\text{OH}$ .



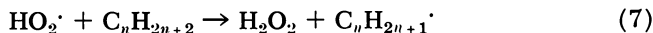
*e.g.*,



The third important mode of reaction of hydroperoxyalkyl radicals is addition to molecular oxygen (Reaction 6).



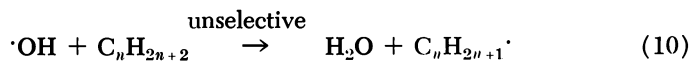
**Addition of  $\text{HO}_2\cdot$  to Alkenes.** Although Reaction 7 is frequently postulated as a reaction which, with Reaction 2, constitutes the primary chain-propagation process during the oxidation of alkanes at temperatures  $>450^\circ\text{C}$ ., at lower temperatures competing reactions of  $\text{HO}_2\cdot$  may render Reaction 7 ineffective (33). These competing reactions are the addition of  $\text{HO}_2\cdot$  to an alkene to give a hydroperoxyalkyl radical (Reaction 8) and its bimolecular self-destruction (Reaction 9).



Reaction 8 may, therefore, be the major chain-propagating reaction of  $\text{HO}_2\cdot$  between  $250^\circ$  and  $400^\circ\text{C}$ . The radicals produced will, of course, undergo the same fates as those produced in Reaction 4, regenerating (eventually) alkyl radicals. The main difference between the "alkene- $\text{HO}_2$  addition" route and the "alkylperoxy radical isomerization" route is that in the former case the hydroperoxyalkyl radicals formed are necessarily  $\alpha$ -radicals—*i.e.*, radicals in which the unpaired electron is borne by a carbon atom adjacent to that bearing the hydroperoxy group, such as 1-hydroperoxy-2-alkyl radicals—whereas isomerization can lead to  $\alpha$ -—*e.g.*, Reactions 4a and 4b— $\beta$ -—*e.g.*, Reaction 4c—and  $\gamma$ -—*e.g.*, Reaction 4d—hydroperoxyalkyl radicals.

**Indirect Regeneration of Alkyl Radicals (Step D)**

The hydroxyl radical will be the predominant entity which attacks the alkane to regenerate an alkyl radical (Reaction 10) under conditions where isomerization and decomposition are the usual fate of alkylperoxy radicals. The activation energy for attack on an alkane molecule by  $\cdot\text{OH}$ , although difficult to determine accurately (30), is low (1, 3) (1-2 kcal. per mole). This has an important consequence. The reaction will be unselective, being insensitive to C—H bond strength. Each and every alkyl radical derived from the alkane skeleton will therefore be formed. To describe the chain-propagation steps under conditions where isomerization is a frequent fate of alkylperoxy radicals it is necessary, then, to consider each and every alkylperoxy radical derived from the alkane and not just the tertiary radicals.



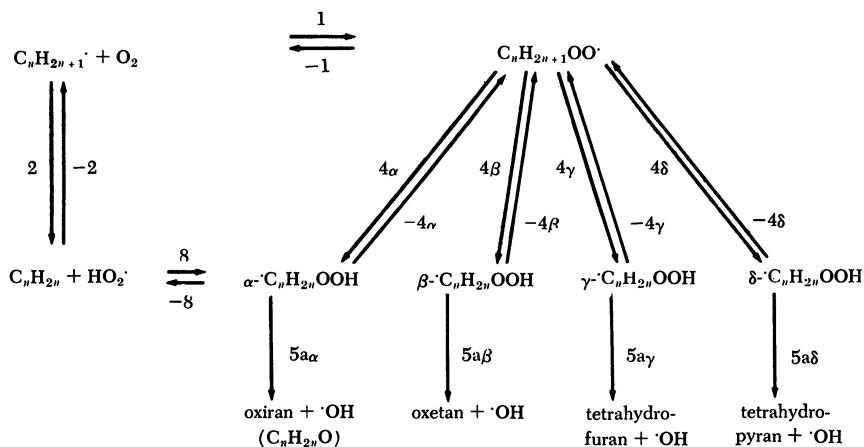
Hydroperoxyalkylperoxy radicals will also be potential abstracters of hydrogen from  $\text{C}_n\text{H}_{2n+2}$ , giving a dihydroperoxide and regenerating an alkyl radical in a Reaction 11 analogous to Reaction 3.

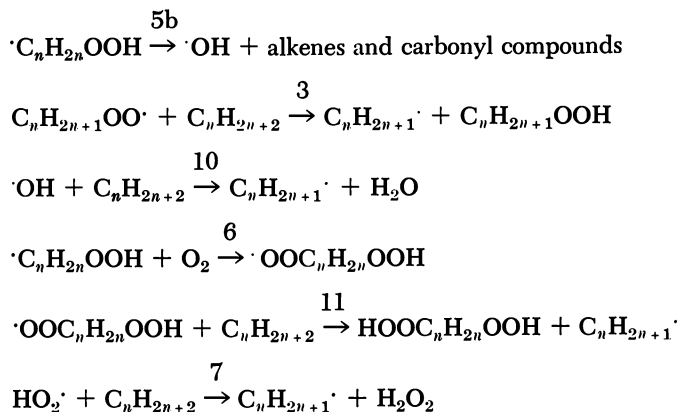


They may also abstract hydrogen from other species; in particular, reaction with  $\text{HO}_2\cdot$  may be important (33), giving a dihydroperoxide and oxygen and terminating the chain.

**Predominant Steps in Chain Propagation**

**General Scheme for Chain Propagation.** The reactions which have been discussed may be combined into a system of chain propagation which should be a general one during the thermal oxidation of alkanes.





This scheme (in which the reversible arrows are not meant to imply that equilibrium is attained) provides an excellent qualitative, and reasonably semiquantitative, description of the formation of products during the cool-flame oxidation at 523° to 580°K. of 2-methylpentane (24). Also, because of the different energy requirements for the various modes of Reactions 4 and 5, the scheme is capable of explaining, at least in principle, the complex dependence of rate on temperature during cool-flame oxidation (24, 51).

Since Reactions 4 and 8 have a common product, the scheme also incorporates, and hence in principle reconciles, the apparently contradictory "alkylperoxy radical isomerization" and "alkene-hydroperoxy radical addition" schemes for propagating chains during the oxidation of alkyl radicals. If this reconciliation is to hold in practice as well as in principle, however, two conditions are necessary.

First, hydroperoxy radicals must react predominantly *via* Reaction 8 and not *via* Reaction 7. It is difficult to assess this competition because of the uncertain energetics of these reactions. Assuming that  $k_7 = k_8$ , Reaction 8 is faster than Reaction 7 when the hydrogen abstracted in 7 is primary, the rate constants are approximately equal when it is secondary, and 7 predominates when it is tertiary. Only under conditions where the yields of alkenes are considerable and the alkane has no tertiary C—H bonds will Reaction 8 be important. Even then, abstraction of allylic hydrogen from the alkene by  $\text{HO}_2\cdot$  will compete strongly with Reaction 8.

Second, alkylperoxy radicals must react predominantly *via* Reaction 4 and not *via* Reaction 3. The ratio of the rates of intermolecular and intramolecular hydrogen abstraction by  $\text{C}_n\text{H}_{2n+1}\text{OO}\cdot$  is  $k_3[\text{C}_n\text{H}_{2n+2}]/k_4$ . When  $[\text{C}_n\text{H}_{2n+2}] = 200$  mm. of Hg =  $10^{18.5}$  molecules per cc.,  $k_3[\text{C}_n\text{H}_{2n+2}]$  has values between  $10^{2.8}$  and  $10^{0.1}$  sec.<sup>-1</sup> (see Table II). For intramolecular abstraction, the corresponding range of values of  $k_4$

is  $10^{7.7}$  to  $10^{1.5}$  sec.<sup>-1</sup>. For every alkylperoxy radical derived from 2-methylpentane, 2-methylpropane, or ethane the condition  $k_3[\text{C}_n\text{H}_{2n+2}]/k_4 \ll 1$  holds. At temperatures and pressures characteristic of the passage of cool flames, intramolecular abstraction predominates, in agreement with the experimental results.

It appears, then, that alkylperoxy radical isomerization is capable of producing hydroperoxyalkyl radicals during the oxidation of all alkanes and that alkene-hydroperoxy radical addition will serve a similar function during the oxidation of those alkanes which contain a high proportion of primary C—H bonds. It remains to determine the proportion of hydroperoxy alkyl radicals arriving by each route as equilibrium is approached.

**Table II. Likely Values for Rate Constant of Reaction  $\text{RO}_2' + \text{RH} \rightarrow \text{ROOH} + \text{R}'$**

<i>Fuel</i>	<i>Nature of H Abstracted</i>	<i>k<sub>3</sub>, Assuming Free Rotation, Cc. Molecule<sup>-1</sup> Sec.<sup>-1</sup></i>
Ethane	<i>p</i>	$10^{-17.7}$
2-Methylpropane	<i>p</i>	$10^{-18.1}$
	<i>t</i>	$10^{-15.7}$
2-Methylpentane	<i>t</i>	$10^{-16.0}$
	<i>s</i>	$10^{-17.1}$
	<i>p</i>	$10^{-18.4}$

**Nature of Reaction of Alkyl Radicals with Oxygen as Equilibrium Is Approached.** When the concentration of  $\text{C}_n\text{H}_{2n+1}\text{OO}'$  is small, alkyl radicals react with oxygen at *ca.* 550°K. predominantly to give alkylperoxy radicals. As  $k_4$  is small, however, the concentration of  $\text{C}_n\text{H}_{2n+1}\text{OO}'$  will gradually increase, and the effect of the reverse Reaction —1 will become appreciable. Eventually, an equilibrium will be approached, a constant proportion of  $\alpha\text{-C}_n\text{H}_{2n}\text{OOH}$  being formed by each route. If, as a first approximation, it is assumed that  $k_{-4\alpha}$  and  $k_{-8}$  are small compared with  $(\Sigma k_5 + k_6[\text{O}_2])$  (an assumption not fully justified in the former case), then at equilibrium the proportion of  $\alpha\text{-C}_n\text{H}_{2n}\text{OOH}$  which arises via  $\text{C}_n\text{H}_{2n} + \text{HO}_2'$  is  $k_8K_2/(k_{4\alpha}K_1 + k_8K_2)$ .

Calculation of this proportion, from the values of rate constants and equilibrium constants given in the Appendix, shows that it is always of the order of 1%. The route to hydroperoxyalkyl radicals *via* alkenes is therefore a minor one at temperatures of *ca.* 550°K. This is especially true with respect to the oxidation of large alkanes such as 2-methylpentane.

The calculation given above compares the rates of formation of  $\alpha$ -hydroperoxyalkyl radicals by the two routes; to compare the relative importance of the additive and abstractive modes of reaction of alkyl radicals with oxygen, it is necessary to consider also the formation of  $\beta$ -,  $\gamma$ -, and  $\delta$ -hydroperoxyalkyl radicals—*i.e.*, to compare  $k_8K_2$  with  $K_1\Sigma k_{4\alpha,\beta,\gamma,\delta}$ . These radicals can result only from alkylperoxy radicals. In large alkylperoxy radicals, such as 2-methylpentylperoxy radicals, hydrogen bearing  $\beta$ - and  $\gamma$ - (and in the case of terminal radicals  $\delta$ -) carbon atoms are available; 1,5, 1,6, and 1,7 H-transfer—*i.e.*, Reactions 4 $\beta$ , 4 $\gamma$ , and 4 $\delta$ —will compete therefore, with 1,4 H-transfer (Reaction 4 $\alpha$ ) and, as is evident from Table III, 1,5 H-transfer, and to a lesser extent 1:6 H-transfer, will compete successfully. The importance of the alkene route compared with the sum of the alkylperoxy radical routes will be very small, therefore. The total yields of oxygenated products such as dimethyltetrahydrofurans and carbonyl compounds from the oxidation of 2-methylpentane will therefore be large compared with the yields of hexenes, in agreement with experiment (24).

**Table III. Thermodynamic and Kinetic Parameters of Alkylperoxy Radical Rearrangement (Reaction 4)**

Nature of C—H Bond Broken	Position of C Atom from Which H Is Transferred	Transition State		$\Delta H$ , Kcal. Mole <sup>-1</sup>	$E$ , Kcal. Mole <sup>-1</sup>	$\log_{10}k_t$ ( $k$ in Sec. <sup>-1</sup> )	$\log_{10}K_t$	$\log_{10}k_{-t}$
		Ring Size (Including H)	$\Delta H$ , Kcal. Mole <sup>-1</sup>					
Primary	$\left\{ \begin{array}{l} \alpha, \gamma \\ \beta \\ \delta \end{array} \right.$	5 or 7	8	20.5	2.9	-3.2	6.1	
		6	8	14.6	5.2	-3.2	8.4	
		8	8	24.0	1.5	-3.2	4.7	
Secondary	$\left\{ \begin{array}{l} \alpha, \gamma \\ \beta \end{array} \right.$	5 or 7	4.5	17.0	4.3	-1.8	6.1	
		6	4.5	11.1	6.6	-1.8	8.4	
Tertiary	$\left\{ \begin{array}{l} \alpha, \gamma \\ \beta \end{array} \right.$	5 or 7	1.7	14.2	5.4	-0.7	6.1	
		6	1.7	8.3	7.7	-0.7	8.4	

With smaller alkylperoxy radicals, however, fewer  $\beta$ -,  $\gamma$ -, and  $\delta$ -carbon atoms are available. Thus, for example, the 2-methylprop-1-ylperoxy radical,  $\text{OOCH}_2\text{CH}(\text{CH}_3)_2$ , has no  $\gamma$ - or  $\delta$ -C atoms, and the  $\beta$ -C atoms carry primary hydrogen only. Isomerization of this alkylperoxy radical by 1,5 transfer of primary H competes only moderately successfully with isomerization by 1,4 transfer of tertiary H (Table III). In the ethylperoxy radical, only 1,4 H-transfer is possible. For these cases, then, hydrogen abstraction will be a more frequent mode of oxidation of the alkyl radical than for larger radicals, but the calculation suggests that it will account

for only 1% of the products. This is not true experimentally; alkenes are formed in considerable yields from small alkanes (28, 34, 36, 54).

The probable reason for this is that the assumption that  $k_{-4\alpha}$  and  $k_8$  are small compared with  $(\Sigma k_{5\gamma} + k_6[\text{O}_2])$  (see above) is not valid. For large alkyl radicals, this will have little effect on the course of chain propagation, and hence on the product spectrum, as addition of oxygen to such radicals gives alkylperoxy radicals in which both isomerization by hydrogen shift (Reaction 4) and decomposition of the resulting hydroperoxyalkyl radical (Reaction 5a) can occur by routes which involve cyclic transition states whose rings have numbers of members not greatly different from 6—*i.e.*, have low strain energies. In other words, the proper criterion is that  $k_{-4\gamma} < (\Sigma k_{5\gamma} + k_6[\text{O}_2])$ , and this is true. The formation of derivatives of tetrahydrofuran as the major *O*-heterocyclic species during the oxidation of hexanes (3, 19, 24), is a result of the availability of such a path, a seven-membered ring being involved in the isomerization step and a five-membered ring in the decomposition step.

Small radicals such as *tert*-butylperoxy and ethylperoxy can, however, react *via* 1,4 H-transfer only; the strain energy involved in *O*-heterocycle formation is 28 kcal. per mole. In this case,  $k_{-4\alpha} \approx 10^6 \text{ sec.}^{-1}$ ; whereas  $k_{5\alpha} = 10^{5.4} \text{ sec.}^{-1}$  and when  $[\text{O}_2] = 200 \text{ mm. of Hg}$ ,  $k_6[\text{O}_2] = 10^{5.5} \text{ sec.}^{-1}$ , so that  $k_{-4\alpha} < (\Sigma k_{5\alpha} + k_6[\text{O}_2])$ . The result is that in the oxidation of small alkyl radicals, the route *via* alkylperoxy radicals will be “blocked” because reverse Reaction -4 competes successfully with Reaction 5. Reaction 2 will thus be a more effective mode of reaction of alkyl radicals with oxygen and the conjugate alkene will be a major product.

Furthermore, it is possible that the estimate of  $k_8$  given here is too low and that reverse Reaction -8 competes successfully with Reaction 5a. In this event, alkene could be formed by the sequence of Reactions 1, 4a, and reverse -8 even if the rate of Reaction 2 were negligibly small compared with the rate of Reaction 1. Again, this would affect the oxidation of small alkenes much more than that of large ones.

### Conclusions

The “alkylperoxy radical isomerization” and “alkene-hydroperoxy radical addition” theories of chain propagation in the oxidation of alkyl radicals at *ca.* 300°C. have been combined into a single comprehensive reaction scheme.

Large alkyl radicals are oxidized to alkylperoxy radicals which isomerize to hydroperoxyalkyl radicals; the decomposition of these gives molecular products and hydroxyl radicals which attack alkanes unselectively to regenerate alkyl radicals. The alkene-HO<sub>2</sub> addition route is unimportant.

Small alkyl radicals, such as ethyl, are oxidized predominantly to the corresponding alkene because the isomerization of an  $\alpha$ -hydroperoxy-alkyl radical to the corresponding alkylperoxy radical competes successfully with its decomposition to an oxiran and a hydroxyl radical. The formation of alkenes *via*  $\alpha$ -hydroperoxyalkyl radicals (and not vice-versa) cannot be excluded, however.

## Appendix

### *Thermodynamic and Kinetic Parameters of Reactions 1 to 11*

**Reactions 1 and 6.** For alkyl radicals containing three or more carbon atoms, Reaction 1 is second-order, no third body being involved (23).  $\Delta H_1 = -28$  kcal. per mole [from  $D(R-OO\cdot)$ ] and  $\Delta S_1 = -32$  cal. per mole  $^\circ K.$  (10). The equilibrium constant,  $K_1$ , is given by  $K_1 = \exp(-\Delta H/RT) \exp(\Delta S/R) = 10^{4.1} \text{ atm.}^{-1} = 10^{-15.3 \pm 1} \text{ cc. molecule}^{-1}$  at  $550^\circ K.$  The rate constant,  $k_1 = A_1 \exp(-E_1/RT)$ , where  $E_1 = 0$  (8, 15). From transition state theory (22), at  $550^\circ K.$ ,  $A_1 = 1.1 \times 10^{-13} \text{ cc. molecule}^{-1} \text{ sec.}^{-1}$ , giving  $k_1 = 10^{-13.0} \text{ cc. molecule}^{-1} \text{ sec.}^{-1}$ . This result may be compared with the experimental values of  $10^{-12.8} \text{ cc. molecule}^{-1} \text{ sec.}^{-1}$  for propyl and butyl radicals (33) and  $10^{-11.7}$  to  $10^{-11.2} \text{ cc. molecule}^{-1} \text{ sec.}^{-1}$  for ethyl radicals (2, 23).

Knox (32) and Benson (12) consider that values of  $10^{-13} \text{ cc. molecule}^{-1} \text{ sec.}^{-1}$  are too low, even for large radicals, preferring values of *ca.*  $10^{-11.5} \text{ cc. molecule}^{-1} \text{ sec.}^{-1}$ . In this paper, this value has been used for all alkyl radicals.

The greater bulk of the radical reactant in Reaction 6 ensures that  $k_6 < k_1$ . A value of  $k_6 = 10^{-12} \text{ cc. molecule}^{-1} \text{ sec.}^{-1}$  has been used.

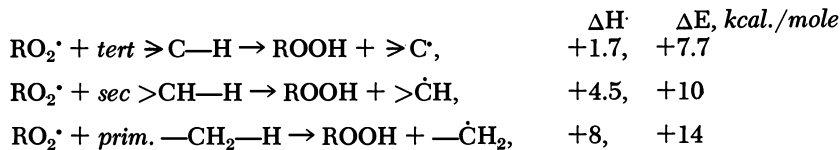
**Reaction 2.** The thermodynamic and kinetic quantities characterizing this reaction depend on the nature of the C—H bond broken.  $\Delta H$  has been calculated, for each of the reactions having the general Equation 2, using data from Refs. 10, 33, 40, 50. The value of  $\Delta S_2$  has been estimated by the method of partial group contributions (9).  $K_2$  has thus been calculated.

The activation energy,  $E_2$ , is not known. The empirical Semenov-Polanyi equation (46) ( $E = 11.5 + 0.25 \Delta H$ ) gives  $8 \leq E \leq 10$  kcal. per mole, depending on the nature of the C—H bond broken. Heicklen (29) prefers  $E = 5$  kcal. per mole. Values of 6 to 8 kcal. per mole (Table I) have therefore been assumed. Benson (12) estimates that  $A_2 \simeq 10^{-12.2} \text{ cc. molecule}^{-1} \text{ sec.}^{-1}$ ; hence,  $k_2$  has been calculated (Table I).

**Reactions 3, 7, and 11.** For endothermic intermolecular abstraction reactions several estimates of the relationship of  $E$  to  $\Delta H$  have been made.

Szabo (48) gives  $E = 3.6 + \Delta H$ , Otozai (42) gives  $E = 8 + 0.3 \Delta H$ , and Benson (10) suggests that, for abstraction by alkylperoxy radicals,  $E = \Delta H + 6$ . Values obtained from this equation are similar to those suggested by Knox (32); Benson's equation has therefore been used.

Since the strengths of tertiary, secondary, and primary C—H bonds are respectively (10, 40, 50) 91.7, 94.5, and 98.0 kcal. per mole and  $D(\text{RO}_2\text{—H}) = 90$  kcal. per mole, the enthalpy changes and activation energies are



The pre-exponential factor  $A_3$  has been discussed (for  $\text{RH} \equiv$  methane and cyclohexane) previously (22). For 2-methylpentane at  $550^\circ\text{K}$ .,  $A_3 \approx 10^{-12.9}$  cc. molecule<sup>-1</sup> sec.<sup>-1</sup>, assuming free rotation in the transition state. Corresponding values for 2-methylpropane and ethane are  $10^{-12.6}$  and  $10^{-12.2}$  cc. molecule<sup>-1</sup> sec.<sup>-1</sup>. The corresponding rate constants are given in Table II.

Reactions 7 and 11 will be characterized by approximately the same energetics as Reaction 3. The pre-exponential factors will increase in the order  $A_{11} < A_3 < A_7$  because of the bulks of the radical reactants.  $E_7$  is not known accurately but probably lies (18, 33, 42) in the range 6 to 15 kcal. per mole.

**Reaction 4.** Intramolecular abstraction of hydrogen involves a cyclic transition state and, although this does not affect the enthalpy change, account must be taken of the strain energy involved in calculating the probable activation energy. Saturated cycloalkane rings have the following strain energies (kcal. per mole): eight-membered, 10; seven-membered, 6.5; six-membered, 0.6; five-membered, 6.5; four-membered, 26; three-membered, 28 (11). In the absence of data for more closely related rings, it is assumed that the strain energies of the transition state rings of Reactions 4 and 5a are similar to these. This assumption is fair for Cope rearrangements (12); it probably holds also for alkylperoxy radical rearrangements. (For the present calculations, these results need be only relatively correct).  $E_4$  has therefore been determined by adding to  $E_3$  (the activation energy for the corresponding intermolecular reaction) the strain energy involved in forming the transition state ring.

Although an entropy of activation of about  $-15$  cal. mole<sup>-1</sup> °K.<sup>-1</sup> is involved in forming the transition state ring in reactions such as 4, the over-all entropy change accompanying intramolecular hydrogen abstraction is small, and the pre-exponential factor for a unimolecular reaction involving a cyclic transition state has been estimated (10) as  $10^{11}$

sec.<sup>-1</sup>. Rate constants  $k_4$  have thus been calculated. From  $\Delta H_4$  ( $= \Delta H_3$ ),  $K_4$  has been calculated, and hence  $k_{-4}$ . The values of these constants are given in Table III.

**Reaction 5.** Several kinds of decomposition of  $\cdot C_n H_{2n} OOH$  to a product (or products) +  $\cdot OH$  are possible. For simplicity, these calculations have been performed only for the case in which a single product P is formed, and that is an *O*-heterocycle. This mode of decomposition is a major one, particularly at temperatures characteristic of cool flames (3, 19, 20, 24, 45).



The pre-exponential factor of this irreversible unimolecular reaction is expected (10) to be about  $10^{11}$  per second. Although no activation energies for the formation of epoxide rings are known, the activation energy of the thermoneutral cyclization of the 3-iodopropyl radical, which is analogous (provided that it does not occur *via* a four-membered ring involving bonding by the *d*-electrons of iodine), is (11) *ca.* 17 kcal. per mole; the activation energies of the exothermic Reactions 5 will be smaller. The enthalpy changes for the formation of three-membered, four-membered, five-membered, and six-membered *O*-heterocycles are -13, -15, -35, and -40 kcal. per mole, respectively. From these values, activation energies are estimated, from the Semenov-Polanyi equation with allowance being made for the strain energies involved in ring formation by comparison with cyclopropane, as 14, 13, 4, and 2 kcal. per mole, respectively. At 550°K., therefore,  $k_{5,oxiran} = 10^{5.4}$  per second,  $k_{5,oxetan} = 10^{5.8}$  per second,  $k_{5,tetrahydrofuran} = 10^{9.4}$  per second, and  $k_{5,tetrahydropyran} = 10^{10.2}$  per second.

**Reaction 8.** The energetics of the addition to alkenes of  $RO_2\cdot$  and of  $HO_2\cdot$  will be reasonably similar. For the former reactions (10),  $\Delta H = -12$  kcal. per mole; the Semenov-Polanyi equation suggests then that  $E \simeq 8.5$  kcal. per mole. As, however, the activation energy for addition of  $RO_2\cdot$  to styrene (31) is 8.4 kcal. per mole whereas  $\Delta H = -25$  kcal. per mole, it is likely that for monoalkenes  $E$  is higher than 8.5. A value of  $E_8 = 11.5$  kcal. per mole would seem reasonable. Benson (12) estimates that  $A_8 \simeq 10^{-12.8}$  cc. molecule<sup>-1</sup> sec.<sup>-1</sup>. Thus,  $k_8 = 10^{-17.3}$  cc. molecule<sup>-1</sup> sec.<sup>-1</sup>. Knox (33) has calculated that  $K_8 = 10^{-20.8}$  cc. molecule<sup>-1</sup>, from which  $k_{-8} = 10^{3.5}$  per second.

### Literature Cited

- (1) Allara, D. L., Mill, T., Hendry, D. G., Mayo, F. R., *ADVAN. CHEM. SER.* **76**, 40 (1968).
- (2) Avramenko, L. I., Kolesnikova, T. V., *Izv. Akad. Nauk. SSSR, Otd. Khim. Nauk.* **1960**, 806, 989.

- (3) Bailey, H. C., Norrish, R. G. W., *Proc. Roy. Soc. (London)* **A212**, 311 (1952).
- (4) Bardwell, J., Hinshelwood, Cyril, *Proc. Roy. Soc. (London)* **A205**, 375 (1951).
- (5) Barnard, J. A., Ibberson, V. J., *Combust. Flame* **9**, 81, 149 (1965).
- (6) Batten, J. J., Gardner, H. J., Ridge, M. J., *J. Chem. Soc. (London)* **1955**, 3029.
- (7) Bell, K. H., McDowell, C. A., *Can. J. Chem.* **39**, 1424 (1961).
- (8) Bennett, J. E., Mile, B., Thomas, A., Eleventh Symposium (International) on Combustion, p. 853, Combustion Institute, Pittsburgh, Pa., 1967.
- (9) Benson, S. W., "Foundations of Chemical Kinetics," p. 665, McGraw-Hill, New York, 1960.
- (10) Benson, S. W., *J. Am. Chem. Soc.* **87**, 972 (1965).
- (11) Benson, S. W., *J. Chem. Phys.* **34**, 521 (1961).
- (12) Benson, S. W., private communication.
- (13) Berces, T., Trotman-Dickenson, A. F., *J. Chem. Soc. (London)* **1961**, 4281.
- (14) Cartledge, J., Tipper, C. F. H., *Proc. Roy. Soc. (London)* **A261**, 388 (1961).
- (15) Christie, M. I., *Proc. Roy. Soc. (London)* **A244**, 411 (1958).
- (16) Cullis, C. F., Fersht, E., *Combust. Flame* **7**, 353 (1963).
- (17) Cullis, C. F., Fish, A., Gibson, J. F., *Proc. Roy. Soc. (London)* **A284**, 108 (1965); **A292**, 575 (1966).
- (18) Cullis, C. F., Fish, A., Gibson, J. F., Tenth Symposium (International) on Combustion, p. 411, Combustion Institute, Pittsburgh, Pa., 1965.
- (19) Cullis, C. F., Fish, A., Saeed, M., Trimm, D. L., *Proc. Roy. Soc. (London)* **A289**, 402 (1966).
- (20) Cullis, C. F., Fish, A., Trimm, D. L., *Proc. Roy. Soc. (London)* **A273**, 427 (1963).
- (21) Cullis, C. F., Hardy, F. R. F., Turner, D. W., *Proc. Roy. Soc. (London)* **A251**, 265 (1959).
- (22) Denisov, E. T., Kosarev, V. P., *Russ. J. Phys. Chem.* **38**, 1565 (1964).
- (23) Dingeldy, D. P., Calvert, J. G., *J. Am. Chem. Soc.* **85**, 856 (1963).
- (24) Fish, A., *Proc. Roy. Soc. (London)* **A298**, 204 (1967).
- (25) Fish, A., *Quart. Rev. Chem. Soc. (London)* **18**, 243 (1964).
- (26) Fisher, I. P., Tipper, C. F. H., *Nature* **195**, 489 (1962); *Trans. Faraday Soc.* **59**, 1163, 1174 (1963).
- (27) Gray, J. A., *J. Chem. Soc. (London)* **1952**, 3150.
- (28) Hay, J., Knox, J. H., Turner, J. M. C., Tenth Symposium (International) on Combustion, p. 331, Combustion Institute, Pittsburgh, Pa. 1965.
- (29) Heicklen, J., *ADVAN. CHEM. SER.* **76**, 23 (1968).
- (30) Hoare, D. E., *Proc. Roy. Soc. (London)* **A291**, 73 (1966).
- (31) Howard, J. A., Ingold, K. U., *Can. J. Chem.* **44**, 1119 (1966).
- (32) Knox, J. H., *ADVAN. CHEM. SER.* **76**, 1 (1968).
- (33) Knox, J. H., *Combust. Flame* **9**, 297 (1965).
- (34) Knox, J. H., *Trans. Faraday Soc.* **55**, 1362 (1959); **56**, 1225 (1960).
- (35) Knox, J. H., Norrish, R. G. W., *Proc. Roy. Soc. (London)* **A221**, 151 (1954).
- (36) Knox, J. H., Wells, C. H. J., *Trans. Faraday Soc.* **59**, 2786, 2801 (1963).
- (37) Kyryacos, G., Menapace, H. R., Boord, C. E., *Anal. Chem.* **31**, 222 (1959).
- (38) Nalbandyan, A. B., International Oxidation Symposium, "Preprint," Vol. II, p. 397, 1967.
- (39) Nalbandyan, A. B., *Dokl. Akad. Nauk. SSSR* **86**, 589 (1952).
- (40) Nangia, P., Benson, S. W., *J. Am. Chem. Soc.* **86**, 2770 (1964).
- (41) Norrish, R. G. W., *Proc. Roy. Soc. (London)* **A150**, 36 (1935); *Discussions Faraday Soc.* **10**, 269 (1951).
- (42) Otozai, K., *Bull. Soc. Chem. Japan.* **24**, 218 (1951).

- (43) Robertson, A., Waters, W. A., *J. Chem. Soc. (London)* **1948**, 1574, 1578, 1585.
- (44) Salooja, K. C., *Combust. Flame*, **9**, 219 (1965).
- (45) Schroeder, V. E., Ohlmann, G., Leibnitz, E., *Z. Phys. Chem. (Leipzig)* **225**, 175 (1964).
- (46) Semenov, N. N., "Some Problems of Chemical Kinetics and Reactivity," Vol. 1, p. 27, Pergamon Press, London, 1958.
- (47) Shanin, M., Kutschke, K. O., *J. Phys. Chem.* **65**, 189 (1961); *Can. J. Chem.* **39**, 73 (1961).
- (48) Szabo, Z. G., *Chem. Soc., London, Spec. Publ.* **16**, 113.
- (49) Taylor, G. W., *Can. J. Chem.* **36**, 1213 (1958).
- (50) Teranishi, H., Benson, S. W., *J. Am. Chem. Soc.* **85**, 2887 (1963).
- (51) Walsh, A. D., Ninth Symposium (International) on Combustion, p. 1046, Academic Press, New York, 1963.
- (52) Walsh, A. D. *Trans. Faraday Soc.* **43**, 305 (1947)
- (53) Watson, J. S., Darwent, B. de. B., *J. Phys. Chem.* **61**, 577 (1957).
- (54) Zeelenberg, A. P., Bickel, A. F., *J. Chem. Soc. (London)* **1961**, 4014.
- (55) Zeelenberg, A. P., de Bruijn, H. W., *Combust. Flame* **9**, 281 (1965).

RECEIVED November 13, 1967.

## Discussion

**D. L. Trimm** (Imperial College, London): On the assumption that initial attack on the hydrocarbon involves molecular oxygen and that chain propagation involves selective radicals such as  $\text{RO}_2\cdot$ , products formed during the early stages of the reaction would be expected to reflect the increased chances of attack at the secondary and tertiary hydrogen atoms of the substrate. If, as you suggest, the radical  $\text{OH}\cdot$  is responsible for chain propagation during the cool flame, the products of reaction should be less selective, and considerable amounts of water should be associated with the production of *O*-heterocycles. Are you aware of any evidence that indicates that the selectivity of attack changes as a cool flame passes, or that water is produced together with *O*-heterocycles during the cool flame oxidation?

**C. Walling**: Rearrangements particularly of peroxy radicals have been mentioned recurrently in today's discussion of high temperature gas-phase autoxidations, and I will summarize briefly what is known about such processes in liquid-phase reactions run near room temperature.

Simple 1,2-shifts analogous to carbonium ion rearrangements occur with vinyl and phenyl groups and with halogens above fluorine, but there

are no authenticated shifts of hydrogen or alkyl groups in simple monoradicals.

Double bond additions occur most readily with double bonds in the 3,4- or 5,6 positions, the former providing the path for vinyl migration and the latter yielding five- or six-membered rings depending upon molecular structure.

Intramolecular hydrogen abstractions occur most readily through six-membered cyclic transition states and thus involve 1,5-shifts; 1,6-shifts occur about 1/10 as readily, and 1,4-shifts less than 1/100, since they are rarely detected.

Intramolecular displacements—*e.g.*, on peroxide oxygen—show rather less restriction as to ring size and apparently occur readily to yield three- to six-membered rings.

Viewed in this way, reactions yielding cyclic ethers should be thought of as two-step processes, epoxides probably arising from peroxy radical additions to olefins followed by 1,3-displacements, and larger rings arising *via* intramolecular hydrogen abstraction by peroxy radicals followed by 1,4- or 1,5-displacements. In all such reactions it is probably the first step which is slow and which determines the yield of product observed.

**A. Fish:** Water is certainly produced during cool flame oxidation. In my own work, I have not analyzed quantitatively for water because it is not a good diagnostic test of reaction mechanism. The assumption that, in the cool flame regime, chains are propagated by  $\text{RO}_2\cdot$  in the early stages of reaction is one which I would question. Certainly there is no evidence that the selectivity of attack changes with time; it appears that  $\cdot\text{OH}$  is responsible for propagation of the primary chain throughout the reaction.

In reply to Dr. Walling, I agree that oxirans can arise by addition to olefins of peroxy radicals followed by 1,3-displacements, but that larger rings must result *via* intramolecular hydrogen abstraction, followed by displacement. It is to be expected that rearrangement will occur more frequently in the gas phase at elevated temperatures than in the liquid phase near room temperature since it is favored relative to intermolecular hydrogen abstraction by high temperature and low hydrocarbon concentration. Although I agree that there are few authenticated cases in the liquid phase, there is a rapidly increasing amount of experimental evidence for chain propagation by alkylperoxy radical rearrangement in the gas phase.

**H. C. Bailey (B. P. Chemicals Ltd., England):** When we showed in 1952 that the hexane cool flame could give 17% of oxygen heterocycles, we suggested direct elimination of OH from ROO. Prior isomerization to R-HOOH should lead to more difunctionals than are observed.

## Formation of *O*-Heterocycles as Major Products of the Gaseous Oxidation of *n*-Alkanes

T. BERRY, C. F. CULLIS, M. SAEED, and D. L. TRIMM

Department of Chemical Engineering and Chemical Technology, Imperial College, Prince Consort Rd., London, S.W.7, England

*The gaseous oxidation of n-alkanes can, in suitable circumstances, yield substantial amounts of O-heterocycles of the same carbon number as the initial hydrocarbon. A comparative study has been carried out of the formation of O-heterocyclic products during the combustion of n-butane, n-pentane, and n-hexane. The way in which the yields of such compounds vary with reaction conditions has been investigated. As a result of the optimization of the amounts of O-heterocycles it has been possible to obtain maximum yields of these compounds of up to 30% from n-pentane but only about 10% from n-butane and n-hexane. An attempt is made to account for the observed differences in the amounts and nature of the O-heterocyclic products formed from the three n-alkanes.*

Previous studies have shown that both straight-chain and branched-chain hydrocarbons may, on gaseous oxidation, yield appreciable amounts of *O*-heterocyclic products (1, 2, 11). These compounds, which are predominantly of the same carbon number as the original hydrocarbon molecule, apparently arise by a mechanism involving the intramolecular rearrangement of initially formed alkylperoxy radicals (7). This isomerization reaction appears to be important mainly during certain combustion regimes. Under conditions where slow oxidation takes place, the yields of *O*-heterocycles characteristic of radical isomerization are generally small (18, 19), but under cool-flame conditions the yields may be greatly increased (4, 8, 15). The gaseous oxidation of hydrocarbons

in the cool-flame region might thus provide an economically viable method of preparing certain *O*-heterocycles.

The successful isolation of substantial amounts of *O*-heterocycles will depend to a considerable extent on the design of the reaction vessel. Thus, for example, high yields of such compounds are produced in the "falling cloud" reactor under conditions corresponding to cool-flame combustion (10, 11). Comparatively little information is available, however, as to the variation in yield with molecular structure of the initial hydrocarbon.

In the present work, therefore, a comparative study of the production of *O*-heterocycles during the cool-flame combustion of three consecutive *n*-alkanes—*viz.*, *n*-butane, *n*-pentane, and *n*-hexane—was carried out under a wide range of reaction conditions in a static system. The importance of carbon chain length, mixture composition, pressure, temperature, and time of reaction was assessed. In addition, the optimum conditions for the formation of *O*-heterocycles and the maximum yields of these products were determined. The results are discussed in the light of currently accepted oxidation mechanisms.

### **Experimental**

The apparatus and general procedure have been described (4). *n*-Butane, 99.9% pure, was obtained from the Matheson Co. and *n*-pentane, better than 99.5% pure, from Fluka A.G. A pure sample of *n*-hexane was kindly provided by Shell Research, Ltd. Many of the *O*-heterocycles required for calibrating the gas-liquid chromatography equipment were obtained commercially, and the remainder were synthesized from commercially available precursors. 2-*n*-Butyloxiran, 2-methyl-3-*n*-propyloxiran, 2,3-diethyloxiran, 2-*n*-propyloxiran and 2-methyl-3-ethyloxiran were prepared by oxidizing the corresponding alkenes with monoperphthalic acid (16). 2-Methyloxetan was prepared by dehydrating butane-1,3-diol with 30% sulfuric acid. 2,4-Dimethyloxetan was prepared from pentan-2,4-diol by the procedure recommended by Schmoyer and Case (13, 14). 2-Ethyl-4-methyloxetan was prepared from acetaldo by a reaction sequence described previously (4).

The condensable products were analyzed by gas-liquid chromatography using columns containing either 1,2,3-tris(2-cyanoethoxy)-propane or di-2-cyanoethyl ether supported on Embacel. Hydrocarbons were determined on columns containing either dimethylsulfolene or a combination of propylene carbonate, squalene, and silicone oil on Embacel (3).

### **Results**

The production of *O*-heterocycles from each of the three hydrocarbons was examined according to a standard procedure. Yields of *O*-heterocycles were expressed as percentages of the hydrocarbon introduced

into the reaction vessel. In all runs, except those involving the variation of yields with reaction time, the products were withdrawn from the reaction vessel immediately after passage of the final cool flame, the number of cool flames passing under given conditions having previously been determined in control experiments.

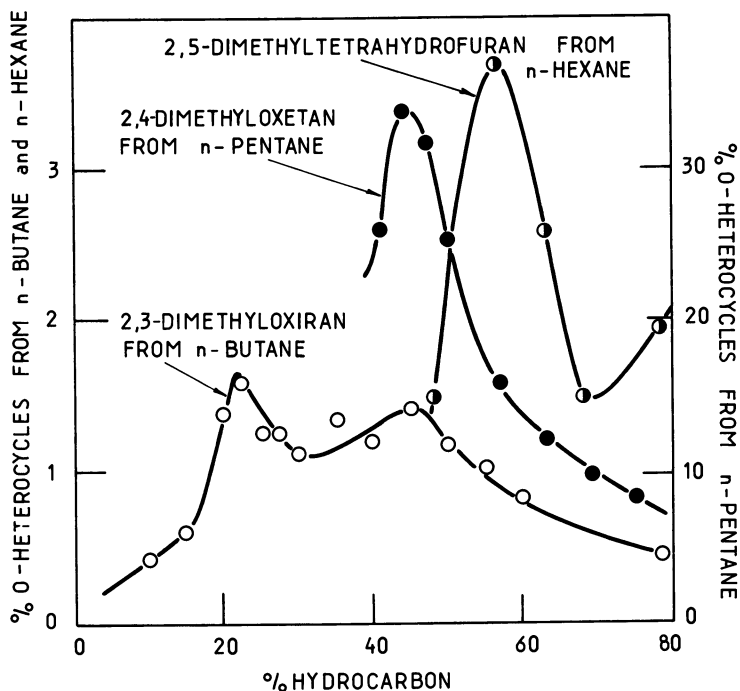


Figure 1. Optimum mixture compositions for production of O-heterocycles

In preliminary experiments, 1 to 1 hydrocarbon-oxygen mixtures were used to construct rough ignition diagrams and to allow product identification. After selecting temperature and pressure conditions corresponding to points in the center of the cool-flame regions, determinations were made of the optimum hydrocarbon-oxygen ratios for producing O-heterocycles. Figure 1 shows some typical results. *n*-Butane shows two peaks, and a further optimization carried out at a higher temperature showed that the first peak was more significant; the corresponding mixture composition was therefore subsequently taken as the optimum value. Table I lists these optimum compositions and the O-heterocycles identified among the oxidation products of each hydrocarbon.

**Table I. Yields of O-Heterocycles Obtained during Combustion of Different Alkanes under Optimum Conditions**

	<i>n-Butane</i>	<i>n-Pentane</i>	<i>n-Hexane</i>
Pressure, mm. Hg	240	141	135
Temperature, °C.	318	300	245
Hydrocarbon/ Oxygen	0.29	0.75	1.25
Yields of	2,3-Dimethyl-	2-Ethyl-3-	2-Methyl-3-
O-heterocycles	oxiran	methyl-	n-propyl-
as % of alkane	1.8(3.5 <sup>a</sup> )	oxiran	oxiran
introduced	0.5(1.0 <sup>a</sup> )	14	1.2
	2-Methyl-	2,4-Dimethyl-	2-Methyl-4-
	oxetan	oxetan	ethyl-
	0.4(0.2 <sup>a</sup> )	14	oxetan
	Tetrahydro-		4.0
	furan		2,5-Di-
	0.4(0.2 <sup>a</sup> )		methyl-
			tetrahy-
			drofuran
			5.6
	Total		10.8
	3.1(4.9)	28	
Total yields of O-heterocycles, % of alkane consumed	5.2(8.3)	43	11.8

<sup>a</sup> Figures in parentheses refer to yields at time when total yield is maximum.

Accurate ignition diagrams were then constructed, and their cool-flame regions are compared in Figure 2. The maximum numbers of cool flames observed for *n*-butane, *n*-pentane, and *n*-hexane were 6, 2, and 2, respectively. Typical results for the variation of the yields of *O*-heterocycles with pressure and temperature are given in Figures 3 and 4, respectively; the *O*-heterocycles not shown followed similar variations. Comparison of Figures 2, 3, and 4 shows that the yields of *O*-heterocycles obtained from all these hydrocarbons pass through maximum values in the cool-flame regions.

If it is assumed that the pressure optimizations shown in Figure 3 are valid at all temperatures, the maxima in Figure 4 represent the conditions for producing maximum amounts of *O*-heterocycles in the cool-flame regions. The peak in the amount of 2-methyl-3-ethyloxiran produced at low pressures (Figure 3) has been neglected since the quantities of reactants and products are both small. The yields of all the *O*-heterocycles formed under conditions corresponding to the maxima shown in Figure 4 are recorded in Table I.

Finally the yields of typical *O*-heterocycles as a function of time are given in Figure 5, where the time of the passage of the final cool flame is shown on the abscissa. With *n*-hexane and *n*-pentane, the yields of all

the *O*-heterocycles exhibited their maximum values immediately following the cool-flame pressure peaks. With *n*-butane this was not the case. After passage of the final cool flame, the yields of 2,3-dimethyloxiran and 2-ethyloxiran increased by a factor of about 2, while the yields of 2-methyloxetan and tetrahydrofuran decreased steadily. Thus, for *n*-butane a greater total yield of *O*-heterocycles, combined with a greater selectivity, can be obtained by withdrawing the products some time after passage of the final cool flame. The figures given in parentheses in Table I represent yields calculated on the assumption that these always vary with time in the way shown in Figure 5. Table I also shows the total yields of *O*-heterocycles calculated as percentages of the hydrocarbon consumed.

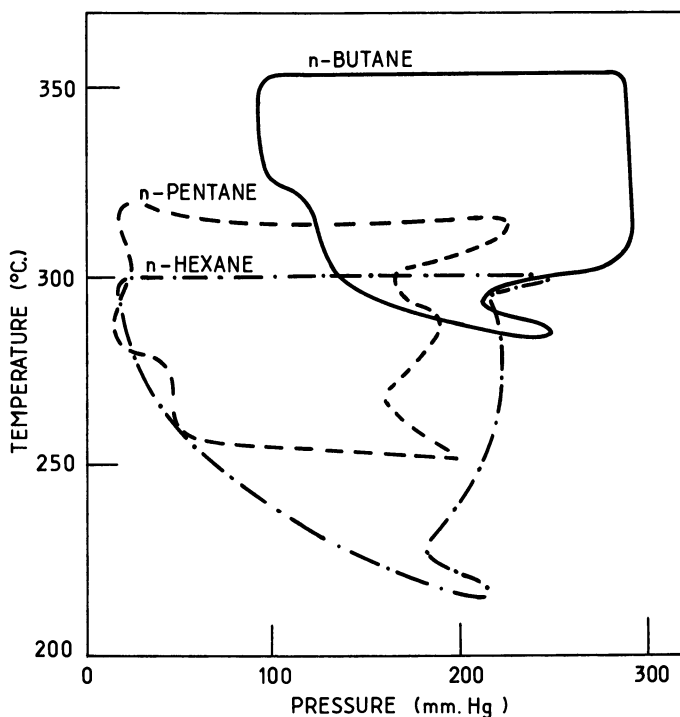


Figure 2. Cool-flame regions for hydrocarbon-oxygen mixtures giving optimum *O*-heterocycle production

### Discussion

One of the most striking observations during the present investigation is the existence of a well-defined maximum in the total yields of *O*-heterocycles formed from *n*-pentane (Table I). Although control experiments on the thermal decomposition and oxidation of *O*-heterocycles

(17) show that most of these compounds undergo some further reaction under the experimental conditions used, the extent of such reactions is not sufficient to invalidate the observed order of decreasing tendency to *O*-heterocycle formation—*viz.*, *n*-pentane > *n*-hexane > *n*-butane. In any case, the amounts of *O*-heterocyclic products detected represent lower limits to the amounts formed.

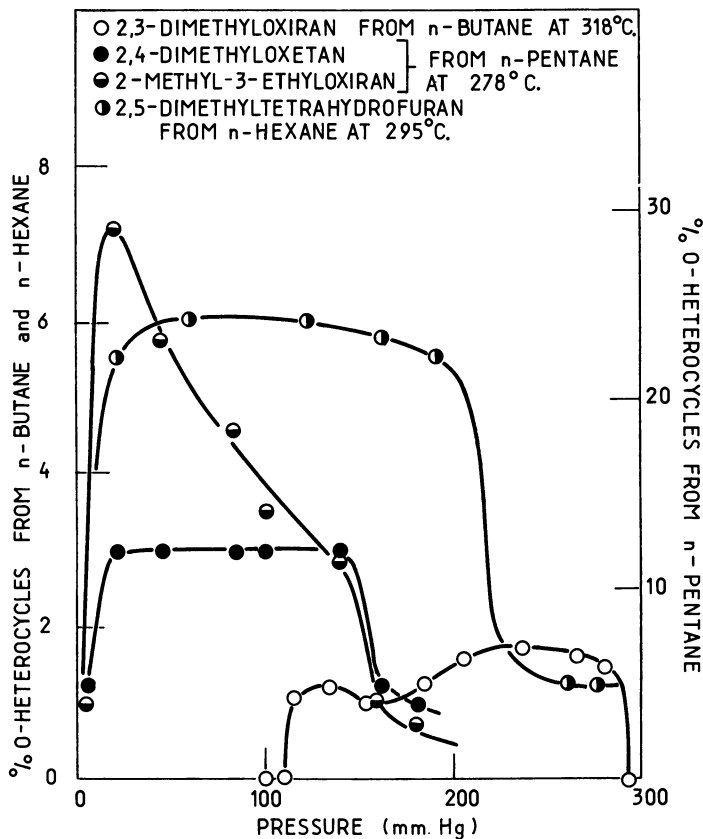
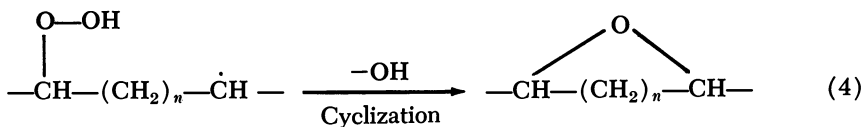
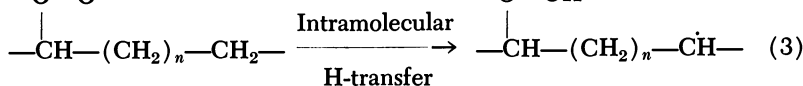
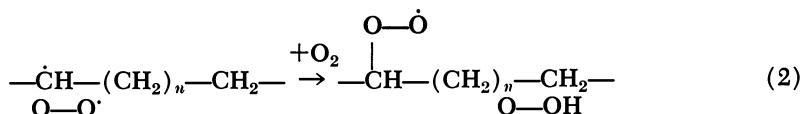


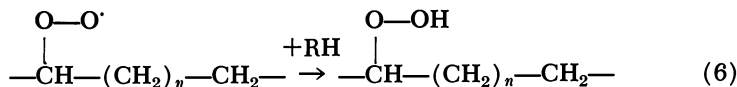
Figure 3. Yields of *O*-heterocycles as a function of pressure

Possible reasons for the observed sequence of *O*-heterocycle formation can best be discussed in terms of the generally accepted mechanism for the formation of such compounds during combustion processes (7).





The rates of Reactions 1 and 2 would be expected to be relatively insensitive to carbon chain length. Once alkylperoxy radicals are formed, however, they and other species subsequently derived from them may well suffer fates other than those shown. The observed sequence of total *O*-heterocycle yields may be explained in terms of the occurrence, in particular, of the two alternative reactions (Reactions 5 and 6).



Reaction 5 represents the decomposition or further oxidation of all the intermediate radicals taking part in Reactions 3 and 4, and Reaction 6 is the intermolecular abstraction by alkylperoxy radicals of hydrogen from another molecule.

It seems probable that the extents to which Reactions 5 and 6 take place will depend on carbon chain length. Thus, in general, Reaction 5 would be expected to become more important as the carbon chain length is increased, partly because of the greater number of available sites for oxidative attack, and partly because of the increasing number of modes of breakdown of large radicals. Reaction 6, on the other hand, may well decrease in importance as the carbon chain is lengthened owing to increased steric hindrance. The substantial contribution of Reaction 5 during the oxidation of *n*-hexane and of Reaction 6 during the oxidation of *n*-butane might thus lead to a maximum in the yield of *O*-heterocyclic compounds obtained with *n*-pentane. It is perhaps significant that similar high yields of *O*-heterocycles are obtained during the oxidation of 2-methylpentane, which also has a  $\text{C}_5$  chain (9).

Further supporting evidence for this explanation of the relatively low yields of *O*-heterocycles obtained with *n*-butane and *n*-hexane is provided by the optimum reactant mixture compositions found for the

different hydrocarbons (Table I). Thus, with *n*-butane, maximum amounts of C<sub>4</sub> *O*-heterocycles are obtained with low hydrocarbon-oxygen ratios and hence low hydrocarbon pressures at constant total pressure. This minimizes the occurrence of Reaction 6. Similarly, the highest yields of C<sub>6</sub> *O*-heterocycles are obtained during the oxidation of mixtures containing a relatively high *n*-hexane-oxygen ratio, under which conditions Reaction 5 would be likely to occur to only a small extent.

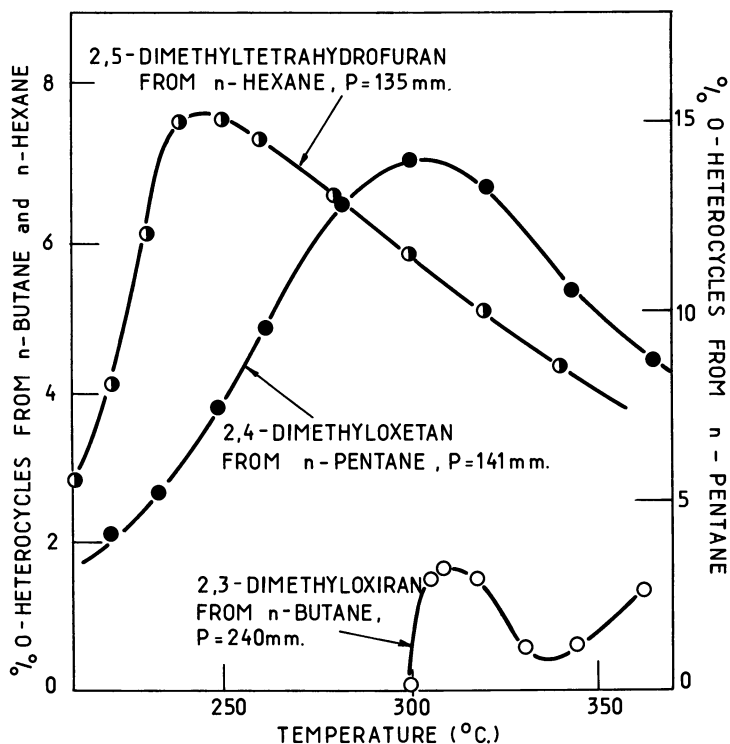


Figure 4. Yields of *O*-heterocycles as a function of temperature

Table I shows also the yields of individual *O*-heterocycles formed among the oxidation products of the different alkanes studied. Since it is known that abstraction of hydrogen by free radicals takes place more readily from a CH<sub>2</sub> group than from a CH<sub>3</sub> group (5, 6, 12), a marked tendency for the *O*-heterocycles not to include in the ring the terminal carbon atoms of the original hydrocarbons might be expected. With *n*-pentane and *n*-hexane, no such *O*-heterocycles are in fact found. On the other hand, *n*-butane on oxidation gives rise to several *O*-heterocycles with one or both terminal carbon atoms incorporated in the ring. This

qualitative difference in the nature of the products may be connected largely with the higher ratio of  $\text{CH}_3$  to  $\text{CH}_2$  groups in the  $\text{C}_4$  hydrocarbon. Another contributory factor may be the somewhat higher temperature used for the oxidation of *n*-butane; this would tend to make abstraction of hydrogen from the hydrocarbon less selective.

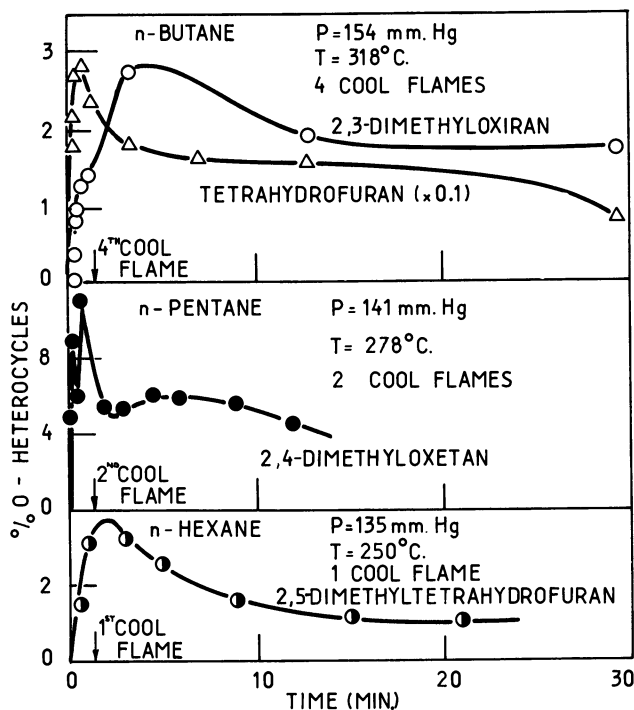


Figure 5. Yields of *O*-heterocycles as a function of time

Although the yields of *O*-heterocycles pass through maximum values in the cool flame regions (Figures 3 and 4), some of the results indicate that significant amounts of such compounds may also be formed during slow combustion at higher temperatures. This suggests that the production of *O*-heterocycles in the cool-flame region may be connected with the rise in temperature accompanying the passage of the cool flame. That this temperature rise may be as high as  $250^\circ\text{C}$ . has been demonstrated during studies of the oxidation of 2-methylpentane (8). Equally, however, the chemical processes which give rise to cool flames may become important during slow combustion at higher temperatures.

This work has thus shown that considerable quantities of *O*-heterocycles may be formed during the cool-flame combustion of *n*-alkanes

under appropriate experimental conditions. The results illustrate clearly, however, that to obtain good yields, the reaction conditions, in particular mixture composition and temperature, must be carefully optimized for each individual hydrocarbon.

### **Acknowledgment**

The authors thank the Science Research Council for its valuable financial support of this work.

### **Literature Cited**

- (1) Bailey, H. C., Norrish, R. G. W., *Proc. Roy. Soc.* **A212**, 311 (1952).
- (2) Chung, Y. H., Sandler, S., *Combust. Flame* **6**, 295 (1962).
- (3) Cullis, C. F., Fish, A., Pollard, R. T., *Proc. Roy. Soc. (London)* **A298**, 64 (1967).
- (4) Cullis, C. F., Fish, A., Saeed, M., Trimm, D. L., *Ibid.* **A289**, 402 (1966).
- (5) Cullis, C. F., Hardy, F. R. F., Turner, D. W., *Ibid.* **A244**, 573 (1958).
- (6) Cullis, C. F., Hardy, F. R. F., Turner, D. W., *Ibid.* **A251**, 265 (1959).
- (7) Fish, A., *Quart. Rev. (London)* **18**, 243 (1964).
- (8) Fish, A., *Proc. Roy. Soc. (London)* **A293**, 378 (1967).
- (9) Fish, A., *Ibid.* **A298**, 204 (1967).
- (10) Jones, J. H., Allendorf, H. D., Hutton, D. G., Fenske, M. R., *J. Chem. Eng. Data* **6**, 620 (1961).
- (11) Jones, J. H., Fenske, M. R., *Ind. Eng. Chem.* **51**, 262 (1959).
- (12) Knox, J. H., Smith, R. V., Trotman-Dickenson, A. F., *Trans. Faraday Soc.* **54**, 1509 (1958).
- (13) Schmoyer, L. F., Case, L. C., *Nature* **183**, 389 (1959).
- (14) Schmoyer, L. F., Case, L. C., *Ibid.* **187**, 592 (1960).
- (15) Schröder, V. E., Uhlmann, G., Leibnitz, E., *Z. Phys. Chem. (Leipzig)* **225**, 175 (1964).
- (16) Swern, D., "Organic Reactions," Vol. 7, p. 378, Wiley, New York, 1953.
- (17) Trimm, D. L., Saeed, M., *Combust. Flame* **10**, 311 (1966).
- (18) Zeelenberg, A. P., *Rec. Trav. Chim.* **81**, 720 (1962).
- (19) Zeelenberg, A. P., Bickel, A. F., *J. Chem. Soc.* **1961**, 4014.

RECEIVED November 8, 1967.

## Discussion

**D. L. Trimm:** Dr. Mayo has suggested that the formation of epoxides *via* alkenes may well be important and that, in particular, most of the 2,3-dimethyloxiran formed during the oxidation of *n*-butane is probably



0.43; *n*-pentane:  $f = 0$ ,  $r = 0.5$ ; *n*-butane:  $f = 0.42$ ,  $r = 0.6$ ; 2-methylpentane:  $f = 0.94$ ,  $r = 0.64$ ; isooctane:  $f = 1$ ,  $r = 0.84$ ; 2,2-dimethylbutane:  $f = 1$ ,  $r = 0.86$ ; isobutane:  $f = 1$ ,  $r = 0.9$ ; neopentane:  $f = 1$ ,  $r = 1$ ), but it is difficult to see why  $f$  should increase so rapidly in the range  $0.5 < r < 0.65$ .

### *Literature Cited*

- (1) Chung, Y. H., Sandler, S., *Combust. Flame* **6**, 295 (1962).
- (2) Fish, A., *Proc. Roy. Soc. (London)* **A298**, 204 (1967).
- (3) Kyriacos, G., Menapace, H. R., Boord, C. E., *Anal. Chem.* **31**, 222 (1959).
- (4) Maynard, J. B., Legate, C. E., Graiff, L. B., *Combust. Flame* **11**, 155 (1967).
- (5) Rust, F. F., Collamer, D. O., *J. Am. Chem. Soc.* **76**, 1055 (1954).
- (6) Zeelenberg, A. P., *Rec. Trav. Chim. Pays-Bas* **81**, 720 (1962).
- (7) Zeelenberg, A. P., Bickel, A. F., *J. Chem. Soc.* **1961**, 4014.

## Slow Combustion of Ketones

J. A. BARNARD

Department of Chemical Engineering, University College, London, England

*The slow combustion reactions of acetone, methyl ethyl ketone, and diethyl ketone possess most of the features of hydrocarbon oxidation, but their mechanisms are simpler since the confusing effects of olefin formation are unimportant. Specifically, the low temperature combustion of acetone is simpler than that of propane, and the intermediate responsible for degenerate chain branching is methyl hydroperoxide. The Arrhenius parameters for its unimolecular decomposition can be derived by the theory previously developed by Knox. Analytical studies of the slow combustion of methyl ethyl ketone and diethyl ketone show many similarities to that of acetone. The reactions of methyl radicals with oxygen are considered in relation to their thermochemistry. Competition between them provides a simple explanation of the negative temperature coefficient and of cool flames.*

Although the combustion of many substituted hydrocarbons—*e.g.*, alcohols and aldehydes—has been thoroughly investigated (25), the combustion of ketones has been strangely neglected, even though these compounds are frequently produced in the partial combustion of hydrocarbons, and acetone has been used as a fuel in high performance internal combustion engines. The only previous studies devoted specifically to the combustion of ketones are by Steacie (32) and by Bardwell and Hinshelwood (4, 5, 6, 7), although there are a few passing references to ketone combustion elsewhere (3, 24, 26). Finally, during this work a paper on the cool flames of some ketones (and esters) was presented by Hoare *et al.* (18).

### **Experimental**

Our investigations have been concerned with acetone (8), methyl ethyl ketone, and diethyl ketone, and have been conducted in a static

system following the reaction by pressure change and by detailed chemical analysis. The principal analytical methods have been described (8).

### *Results and Discussion*

The three compounds exhibit the major superficial features of hydrocarbon combustion; the pressure-time curves are sigmoidal, and the rate of reaction, as given by  $(d\Delta p/dt)_{\max}$ , exhibits a region of negative temperature coefficient.

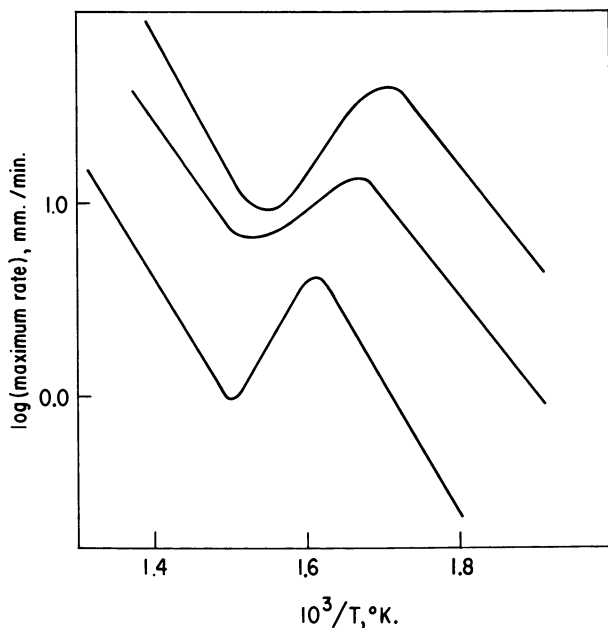


*Figure 1. Variation of maximum rate of reaction with temperature*

*Upper, 40 mm. of diethyl ketone + 40 mm. of oxygen  
Center, 50 mm. of methyl ethyl ketone + 50 mm. of oxygen  
Lower, 100 mm. of acetone + 100 mm. of oxygen*

The increasing reactivity as the homologous series ascends is illustrated in Figure 1. All three ketones show cool flames; the cool-flame limits (35) of acetone are shown in Figure 2.

The cool flames of acetone and of methyl ethyl ketone show some interesting differences (Figure 3). The successive cool flames of acetone are of similar character, but decreasing amplitude; the cool flames of methyl ethyl ketone are of two distinct types. In the example illustrated

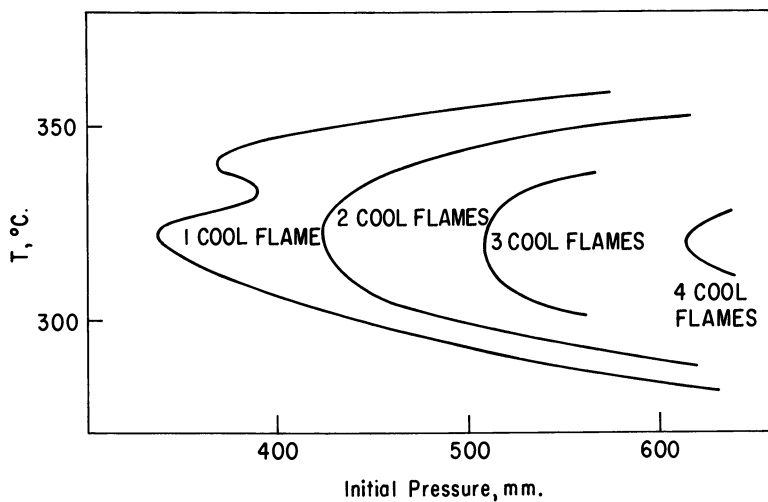


Figure 2. Cool flame limits for an equimolar acetone-oxygen mixture (35)

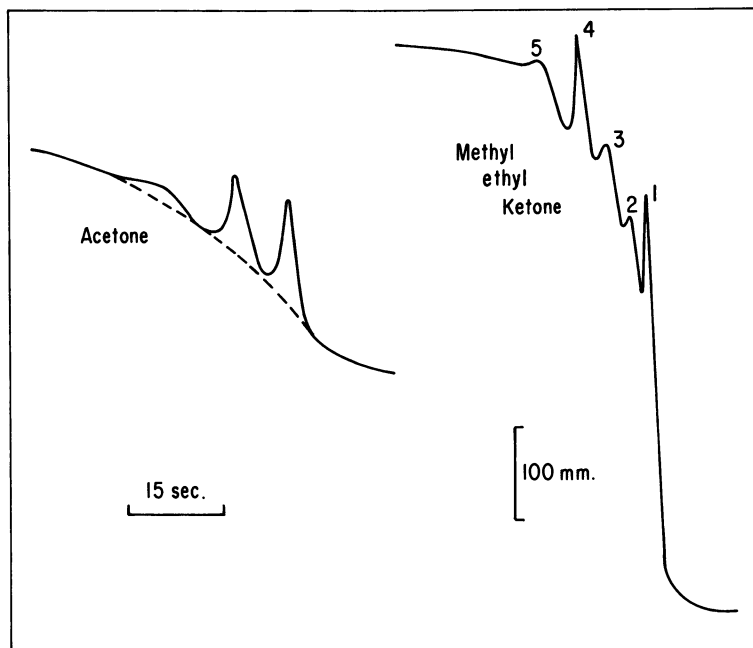


Figure 3. Cool flames of acetone and methyl ethyl ketone (35)

Left, 300 mm. of acetone + 300 mm. of oxygen at 320°C.

Right, 250 mm. of methyl ethyl ketone + 250 mm. of oxygen at 308°C.

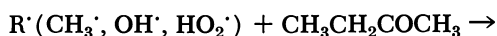
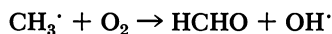
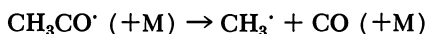
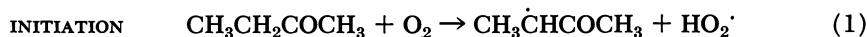
in Figure 3, flames 1 and 4 are sharp and intense, whereas flames 2, 3, and 5 are less intense and slow.

In a discussion of the mechanism it is convenient to consider three combustion regimes, one operating above about 400°C., another below 320°C., and the third between these temperatures, and within which under appropriate conditions cool flames may occur.

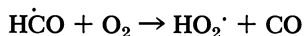
**High Temperature Reaction.** Reaction in the high temperature regime produces carbon monoxide, water, methane, formaldehyde, and methanol (8); the two higher ketones also form ethylene (1). The intermediate responsible for chain branching appears to be formaldehyde. The concentration of formaldehyde and the rate of reaction run parallel over the whole of the reaction, as shown in Figure 4 for diethyl ketone.

Adding formaldehyde reduces the induction period without effect on the rate, until the induction period is zero; further additions increase the rate (*see* Figure 5).

A mechanism which explains these main experimental facts is the following. Methyl ethyl ketone is taken as the typical example.



The hydroxyl radical is typically nonselective, and will give  $\dot{\text{C}}\text{H}_2\text{CH}_2\text{COCH}_3$  and  $\text{CH}_3\text{CH}_2\text{CO}\dot{\text{C}}\text{H}_2$ , in addition to  $\text{CH}_3\dot{\text{C}}\text{HCOCH}_3$ . The first of these yields ethylene readily, but there was no evidence of ketene formation by pyrolysis of the second, which therefore probably disappears by another path.



Allowance must also be made for some oxidation of the 3-keto-2-butyl radicals since the yield of ethylene is less than expected if the thermal decomposition (Reaction 2) were the only fate of the 3-keto-2-butyl radicals.

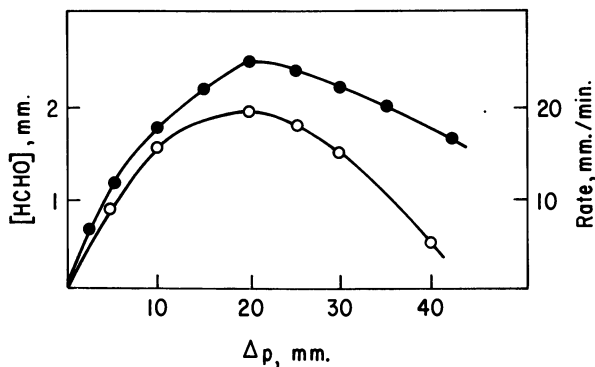


Figure 4. Variation of formaldehyde and rate of reaction throughout the reaction of 40 mm. of diethyl ketone + 40 mm. of oxygen at 400°C. (1)

- Formaldehyde, left axis
- $(d\Delta p/dt)_{\text{max}}$ , right axis

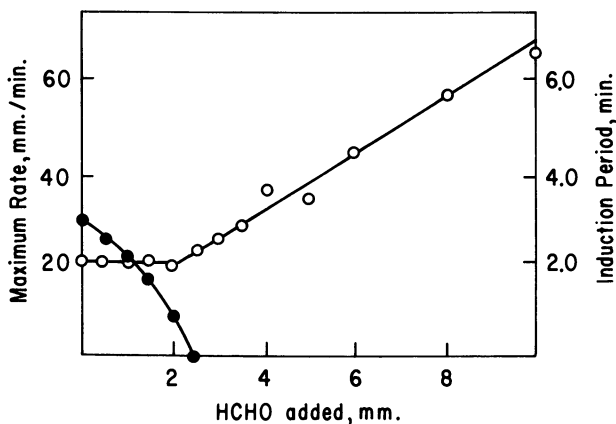
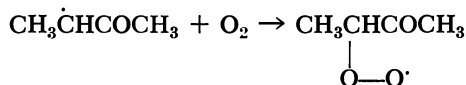


Figure 5. Effect of addition of formaldehyde on slow combustion of 40 mm. of diethyl ketone and 40 mm. of oxygen at 400°C. (1)

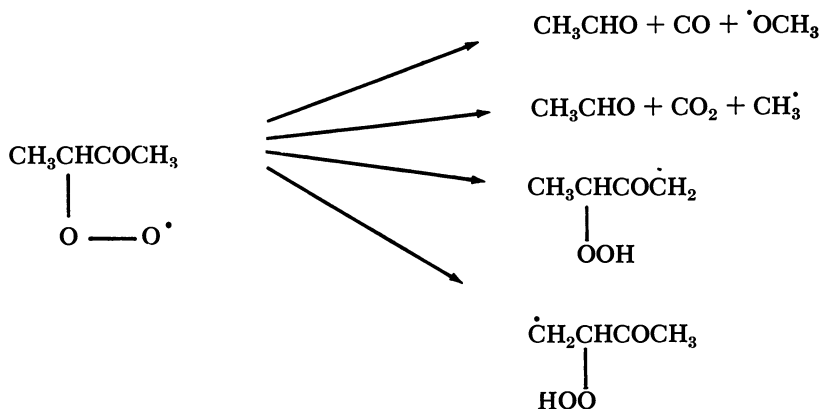
- $(d\Delta p/dt)_{\text{max}}$ , left axis
- Induction period, right axis

The primary oxidation step must be, in the case of the 3-keto-2-butyl radical,

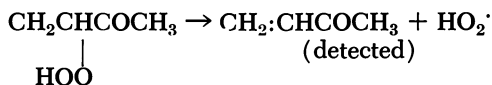
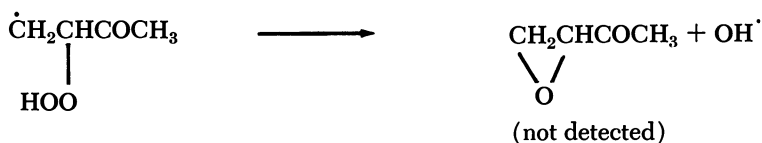
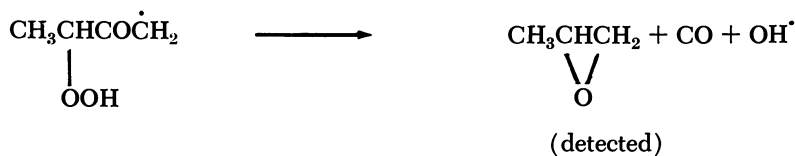
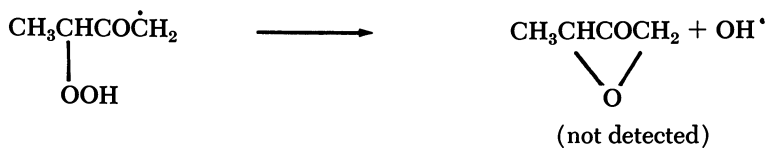
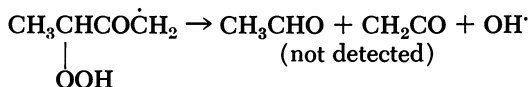


followed by isomerization or decomposition of the 3-keto-2-butylperoxy radical.

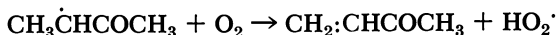
Possible reactions include (14, 15, 16, 34):



followed by pyrolysis of the hydroperoxy radicals.



Methyl vinyl ketone may also arise by:



The detection of 1,2-propylene oxide in the products from methyl ethyl ketone combustion is particularly interesting. It parallels the formation of ethylene oxide in acetone combustion (8) and of 1,2-butylene oxide in the combustion of diethyl ketone. Thus, there is apparently a group of isomerization reactions in which carbon monoxide is ejected from the transition state with subsequent closing of the C—C bond. Examination of scale molecular models shows that reactions of this type are, at any rate, plausible geometrically.

The products which can only arise by  $\text{RO}_2$  isomerization are nonetheless formed, but only in small amounts. Under typical conditions, about 2% of the ketone reacts to form the corresponding epoxide.

**Low Temperature Reaction.** Reaction in the low temperature regime below  $320^\circ\text{C}$ . is of a different character. The products include carbon dioxide and significant quantities of peroxy compounds, as well as carbon monoxide, water, formaldehyde, and methanol, but methane and ethylene are formed only in traces. The peroxy compounds comprise hydrogen peroxide from all three ketones, methyl hydroperoxide from acetone (8) and methyl ethyl ketone (1), and ethyl hydroperoxide from diethyl ketone (1). Methyl ethyl ketone also gives large amounts of peracetic acid (1).

Methyl ethyl ketone is unique, in that long and irreproducible induction periods were observed; on occasion, reaction ensued only after 7 hours and then was completed within 10 minutes. During the long induction period the only detectable product was methanol. No convincing reason can be advanced to account for this anomalous behavior. The virtual absence of ethylene from the products of the low temperature slow combustion of methyl ethyl ketone strongly suggests that the low-temperature mechanism proceeds almost exclusively by further oxidation of the radicals produced by hydrogen abstraction from the parent ketone.

For acetone we believe that the reactions involved in the low temperature regime are (8):

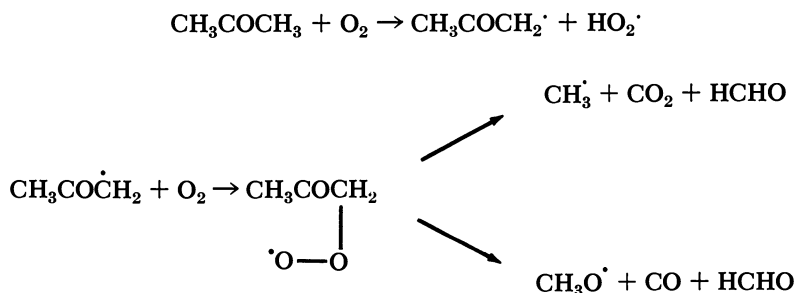


Figure 6 shows the variation of peroxide concentration in methyl ethyl ketone slow combustion, and similar results, but with no peracid formed, have been found for acetone and diethyl ketone. The concentrations of the organic peroxy compounds run parallel to the rate of reaction, but the hydrogen peroxide concentration increases to a steady value. There thus seems little doubt that the degenerate branching intermediates at low temperatures are the alkyl hydroperoxides, and with methyl ethyl ketone, peracetic acid also. The two types of cool flames given by methyl ethyl ketone may arise from the twin branching intermediates (1) observed in its combustion.

There is further evidence for the role played by methyl hydroperoxide in the low temperature combustion of acetone. Knox (23) showed that if one assumes a simple basic chain mechanism for oxidation, then the acceleration constant,  $\phi$ , which characterizes the exponential acceleration to maximum rate, is given by

$$\phi = n\alpha k_b k_p [\text{RH}] / k_t - (k_b + k_d)$$

where  $n$  = number of new chain-propagating radicals produced in the branching step

$\alpha$  = fraction of the main chain steps leading to the formation of the degenerate branching intermediate, I

$k_b$  = rate constant of the branching reaction

$k_p$  = rate constant of the propagating step

$k_t$  = rate constant of the termination reaction

$k_d$  = rate constant of the nonbranching destruction of I

Now values of  $\phi$  are already obtained from plots of  $\log \Delta p$  vs. time, and if we assume that  $k_d$  is negligible and that all the main chain steps yield the branching intermediate, and hence that  $\alpha = 1$  and is independent of [RH], then a plot of  $\phi$  vs. [RH] should yield a straight line with an intercept equal to  $k_b$ .

For the low temperature slow combustion of acetone (21),  $k_b$  has been obtained by this method at four temperatures. The corresponding Arrhenius plot is a good straight line with the equation:

$$k_b = 10^{12.63} \exp(-38,500/RT) \text{ sec.}^{-1}$$

If the branching reaction is



the activation energy should be close to the dissociation energy of the O—O bond. Benson (13) has estimated  $\Delta H_f^\circ(\text{CH}_3\text{OOH})$  to be  $-32.1$  kcal. per mole, and  $\Delta H_f^\circ(\text{OH}\cdot)$  is 8.0 kcal. per mole. Some uncertainty surrounds the value for  $\Delta H_f^\circ(\text{CH}_3\text{O}\cdot)$ , Gray and Williams (17) giving

−0.5 kcal. per mole, while Benson (11) prefers 2.0 kcal. per mole. These figures combine to place the O—O bond dissociation energy in methyl hydroperoxide in the range 39.6 to 42.1 kcal. per mole. Our experimental value is in satisfactory agreement with this.

Little can be said about the pre-exponential factor. It is lower than that reported by Kirk and Knox (20) for the decomposition of ethyl and *tert*-butyl hydroperoxide, but it is still in the expected range for a unimolecular fragmentation into two radicals (9).

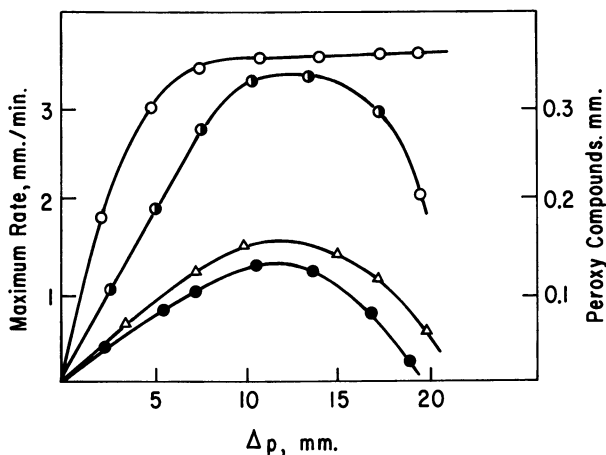


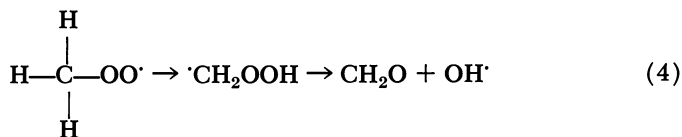
Figure 6. Concentration of peroxy compounds and rate of reaction throughout reaction of 50 mm. of methyl ethyl ketone and 50 mm. of oxygen at 250°C. (1)

- $\Delta$   $d(\Delta p)/dt_{max}$ , left axis  
 $\bullet$   $CH_3OOH$ , right axis  
 $\circ$   $H_2O_2$ , right axis  
 $\ominus$   $CH_3COOOH$ , right axis

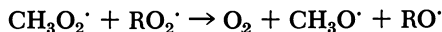
**Intermediate Temperature Reaction and Negative Temperature Coefficient.** The change-over in the mechanism in the slow combustion of acetone between the low and high temperature regimes can be understood in terms of a change in the products of methyl radical oxidation. Below 350°C., methylperoxy radicals will be present in large concentrations relative to methyl, as shown by the independent calculations of Benson (12) and Knox (22). They can disappear by two paths, either by hydrogen abstraction if there is a donor with a sufficiently labile hydrogen,



or decomposition, for which the most likely route is Reaction 4.



Radical-radical reactions such as



which are, of course, well known in the liquid phase (2), can be shown to be unimportant at  $[\text{RO}_2] < 10^{-6}M$ . At  $300^\circ\text{C}$ . this corresponds to a pressure of  $\text{RO}_2$  radicals of between 0.01 and 0.1 mm., which seems implausibly high. Consequently such radical-radical reactions are not of major significance in the main chain steps.

Now the ability of  $\text{HO}_2$  to abstract hydrogen from alkanes such as ethane, and thus propagate a chain reaction at temperatures around  $300^\circ\text{C}$ ., has recently been questioned, it being convincingly argued that once the reaction rate has become appreciable, mutual reaction of  $\text{HO}_2\cdot$  radicals will be faster than abstraction, which possesses a substantial energy barrier. Since the thermochemistries of abstraction reactions by  $\text{HO}_2\cdot$  and  $\text{CH}_3\text{O}_2\cdot$  are quite similar, it may be doubted whether hydrogen abstraction by  $\text{CH}_3\text{O}_2$  will be sufficiently fast to compete effectively with other reactions of this radical.

However, with tertiary C—H bonds whose strength is about 91.5 kcal. per mole (33) and with fuels containing resonance-weakened C—H bonds, abstraction can take place readily.

The C—H bond strength in acetone has not been measured, but a reasonable estimate (8), based on the empirical rule of Semenov (30), leads to a value of about 92 kcal. per mole. Benson (10) and Kerr (19) have independently suggested a similar value, which they regard as an upper limit.

In the light of these estimates, Reaction 3 does not seem unreasonable; it would be about 2 kcal. per mole endothermic, and might therefore be expected to have an activation energy of about 8 kcal. per mole, and a pre-exponential factor of around  $2 \times 10^{12}$  cc. molecule<sup>-1</sup> sec.<sup>-1</sup> (12).

The competing decomposition Reaction 4 is about 26 kcal. per mole exothermic but is likely to possess a fairly large activation energy. There is no reliable way of estimating this, but Semenov (31) has inferred a value of around 20 kcal. per mole, which seems reasonable but is perhaps on the low side. The transition state is a strained four-membered ring, and we may justifiably expect a low pre-exponential factor, say  $10^{12}$  per second.

If  $k_3 = 2 \times 10^{12} \exp[-8000/RT]$  molecules cc. sec.<sup>-1</sup> and  $k_4 = 10^{12} \exp[-25000/RT]$  sec.<sup>-1</sup>, then at 100 mm. of acetone pressure Reactions 3

and 4 proceed at equal rates at about 375°C. Below this temperature methyl hydroperoxide is the predominant product from methyl radical oxidation, and its formation leads to chain branching in acetone slow combustion. The same is true for diethyl ketone, but with ethyl hydroperoxide ethyl peroxy is less stable than methyl peroxy, and consequently the region of negative temperature coefficient begins at a lower temperature for diethyl ketone than for acetone. For methyl ethyl ketone, there is the further complication that peracetic acid may also act as a branching agent. Its formation may be linked with the production of large quantities of acetyl radicals at fairly low temperatures.



Reverting now to acetone combustion, no methane could be detected at 284°C., whereas at 498°C. about 0.7 mm. was formed per millimeter of acetone consumed. The explanation of this can be seen in the shift of the equilibrium in Reaction 5

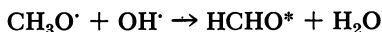


to the left as the temperature is raised. Hence, methyl radicals do not necessarily disappear solely by oxidation but may themselves abstract hydrogen. Furthermore, the decomposition path (Reaction 4) becomes increasingly important, and the main product of methyl radical oxidation becomes formaldehyde. Since formaldehyde cannot bring about branching by



until moderately high temperatures (400°C. and above) are reached, the reaction rate falls in the region just below 400°C. In this connection it may be significant that upward swings of all the Arrhenius curves in Figure 1 commence at roughly the same temperature.

**Cool Flames.** Cool flames are confined, roughly speaking, to the temperature regime which exhibits the negative temperature coefficient of the rate. The flames are clearly nonisothermal, and the light emission which is most intense at the end of the maximum rate period is probably caused by radical-radical reactions (27, 28) such as



and



which are sufficiently exothermic to give formaldehyde in its first excited electronic level, which lies some 77 kcal. above its ground state.

As a tentative explanation [which follows the ideas of Salnikov (29), and others (4, 5, 6, 7, 27)] we may suggest the following. Imagine a

situation where the slow combustion is proceeding quickly—*e.g.*, acetone at 320°C. and 350 mm. pressure. The reaction is exothermic, and the temperature rises (35).

The increased temperature results in an increased rate of destruction of the branching intermediate (methyl hydroperoxide) with a consequent further increase of the rate, but also a decreased rate of formation of fresh hydroperoxide since Equilibrium 5 is displaced to the left, and the alternative reactions of methylperoxy increase in rate faster than that leading to formation of hydroperoxide. Consequently the quasi-stationary concentration of methyl hydroperoxide falls, and the rate of reaction declines since the new product of methyl oxidation—formaldehyde—cannot bring about branching at these temperatures. The temperature of the reaction mixture falls (because the rate has fallen), and when it has fallen sufficiently, provided sufficient of the reactants remain, the whole process may be repeated, and several further flames may be observed.

This explanation is supported by the work of Bardwell and Hinshelwood (6), who found that the peroxide concentration built up exponentially just before the passage of each cool flame and that immediately after the cool flame the peroxide concentration had fallen sharply.

The complicated situation in which methyl radicals participate in the equilibrium with oxygen and methylperoxy and the methylperoxy radicals can react further by at least two alternative routes, is capable of explaining many of the features of acetone slow combustion. Similar arguments, with appropriate modifications, can be developed for the combustion of other fuels.

### *Acknowledgment*

The author acknowledges the collaboration of T. W. Honeyman, E. Kirschner, A. Cohen, M. Akbar, and A. Watts in some of this work and thanks them for permission to quote from their unpublished results.

### *Literature Cited*

- (1) Akbar, M., Ph.D. Thesis, London, 1966.
- (2) Allara, D. L., Mill, T., Hendry, D. G., Mayo, F. R., *ADVAN. CHEM. SER.* **76**, 40 (1968).
- (3) Avramenko, V. A., Neimann, M. B., *Acta Physicochim. URSS* **10**, 601 (1939).
- (4) Bardwell, J., *Proc. Roy. Soc.* **207**, 470 (1951).
- (5) Bardwell, J., Hinshelwood, Cyril, *Ibid.* **A201**, 26 (1950).
- (6) Bardwell, J., Hinshelwood, C., *Ibid.* **205**, 375 (1951).
- (7) Bardwell, J., Hinshelwood, C., *Ibid.* **207**, 461 (1951).
- (8) Barnard, J. A., Honeyman, T. W., *Ibid.* **A279**, 236, 248 (1964).

- (9) Benson, S. W., "Foundations of Chemical Kinetics," p. 262, McGraw-Hill, New York, 1960.
- (10) Benson, S. W., *Ibid.*, p. 377.
- (11) Benson, S. W., *Ibid.*, p. 390.
- (12) Benson, S. W., *J. Am. Chem. Soc.* **87**, 972 (1965).
- (13) Benson, S. W., Buss, J. H., *J. Chem. Phys.* **29**, 546 (1958).
- (14) Cullis, C. F., Fish, A., Saeed, M., Trimm, D. L., *Proc. Roy. Soc.* **A289**, 402 (1966).
- (15) Fish, A., *Ibid.* **A293**, 378 (1966).
- (16) Fish, A., *Ibid.* **298**, 204 (1967).
- (17) Gray, P., Williams, A., *Chem. Rev.* **59**, 239 (1959).
- (18) Hoare, D. E., Li, Ting-Man, Walsh, A. D., Eleventh Combustion Symposium, p. 879, The Combustion Institute, Pittsburgh, 1967.
- (19) Kerr, J. A., *Chem. Rev.* **66**, 465 (1966).
- (20) Kirk, A. D., Knox, J. H., *Trans. Faraday Soc.* **56**, 1296 (1960).
- (21) Kirschner, E., Ph.D. Thesis, London, 1965.
- (22) Knox, J. H., *Combust. Flame* **9**, 297 (1965).
- (23) Knox, J. H., *Trans. Faraday Soc.* **55**, 1362 (1959).
- (24) MacCormac, M., Townsend, D. T. A., *J. Chem. Soc.* **1938**, 238.
- (25) Minkoff, G. J., Tipper, C. F. H., "Chemistry of Combustion Reactions," Butterworth & Co., London, 1962.
- (26) Mulcahy, M. F. R., *Trans. Faraday Soc.* **45**, 537 (1949).
- (27) Norrish, R. G. W., Knox, J. H., *Proc. Roy. Soc.* **A221**, 151 (1954).
- (28) Postnikov, L. M., Shlyapintokh, V. Ya, *Doklady Akad. Nauk SSR* **150**, 340 (1963).
- (29) Salinkov, I. E., *Compt. Rev. Acad. Sci. URSS* **60**, 405 (1948).
- (30) Semenov, N. N., "Some Problems in Chemical Kinetics," Vol. 1, p. 29, Princeton University Press, Princeton, N. J., 1958.
- (31) Semenov, N. N., *Ibid.*, Vol. 2, p. 230.
- (32) Steacie, E. W. R., *Can. J. Res.* **6**, 265 (1932).
- (33) Teranishi, H., Benson, S. W., *J. Am. Chem. Soc.* **85**, 2887 (1965).
- (34) Walsh, A., "Ninth Combustion Symposium," p. 1046, Academic Press, New York, 1963.
- (35) Watts, A., unpublished work.

RECEIVED October 9, 1967.

## Radical Reactions in the Last Stages of Gas-Phase Hydrocarbon Oxidation

L. R. SOCHET, J. P. SAWERYSYN, and M. LUCQUIN

Laboratoire de Chimie de la Combustion, Faculte des Sciences de Lille, Université de Lille, France

*In the last stages of hydrocarbon oxidation, by both the low and high temperature mechanism, when the oxygen concentration is low, a new phenomenon appears—the pic d'arrêt. The methodical study of the reaction of propane and oxygen at various pressures, temperatures, and concentrations indicates three different aspects of the slow oxidation. When the pic d'arrêt occurs, the analysis of some reaction products indicates an increase in the amounts of methane, ethane, acetaldehyde, ethyl alcohol, propyl alcohol, and especially isopropyl alcohol, and a decrease in the formation of hydrogen peroxide and olefin. All these results are explained by radical reactions such as:  $R' + RO_2' \text{ (or } HO_2') \rightarrow ROOR \rightarrow 2 RO' \rightarrow \text{oxygenated products and } R' + R' \rightarrow RR.$*

The systematic use of new physical methods to study gas-phase hydrocarbon oxidations [light emission (6, 8), gauge pressure transducer, and more recently the reaction rate *vs.* time (15, 16), or *vs.* pressure (16, 18)] has revealed a new phenomenon—the *pic d'arrêt*—in the final stages of the reaction between 250° and 400° C. (6, 8, 15, 16).

The *pic d'arrêt* is characterized by a sharp increase in light intensity emitted by the reaction and by a sudden but temporary acceleration of the reaction. At high temperatures it is possible to observe the *pic d'arrêt* for methane, ethane, propane, butane, and pentane, with distinguishing features for each (17).

We investigated the oxidation of only propane at the high temperature (430°C.) *pic d'arrêt*—first with factors affecting the type of reaction, then with analyses for some reaction products (aldehydes, hydrogen peroxide, alcohols, and hydrocarbons). All experimental data can be explained by a radical reaction mechanism which is discussed.

### Experimental

Oxidations were carried out under static conditions in a thermostatted 30-cc. silica vessel mounted in a furnace. Hydrocarbon-oxygen mixtures, prepared in a storage bulb at room temperature, were admitted to the reaction vessel by momentarily opening a tap.

The development of the reaction was followed by measuring pressure change ( $\Delta p$ ), light emission ( $I$ ), reaction rate ( $d\Delta p/dt$ ), and by chemical analysis. Pressure rise was recorded by a pressure transducer (A.C.B. 504H). Reaction rate ( $d\Delta p/dt = W$ ) was obtained by using a resistance-capacity circuit of suitable time constant,  $\theta = RC$  (16, 18), appropriate to the branching factor of the reaction,  $\phi$ . It was possible to record simultaneously pressure rise *vs.* time and rate *vs.* time or rate *vs.* pressure rise.

Light emission was recorded with an IP 21 R.C.A. photomultiplier tube in the range 3000–7000 Å. Interference filters (spectral bandwidth  $\Delta\lambda = 100\text{--}140$  Å.) showed that the light emission of the *pic d'arrêt* arises from the same emitter as that from the slow reaction—probably excited formaldehyde (16). The *pic d'arrêt* appears as a clear pulse on the record of light intensity *vs.* time (Figure 1).

The reaction was stopped at convenient stages for analysis by withdrawing the mixture rapidly. The products were analyzed in three separate series of runs (aldehydes and peroxides, alcohols, hydrocarbons). Each arrow in Figures 1, 2, and 3 indicates the moment at which the products were analyzed.

Formaldehyde, total aldehydes, and hydrogen peroxide were analyzed in aqueous solution by a polarographic method (17) similar to that of Mac Nevin and Sandler (9, 10, 12).

Methanol, ethanol, *n*- and isopropyl alcohol and allyl alcohol were determined by gas chromatography on a 3-meter column packed with 15% Hallcomid on 60-80 mesh acid-washed Chromosorb. Methane, ethane, ethylene, and propylene were also determined by gas chromatography using a 3-meter column packed with 60-80 mesh activated alumina. Products were identified by comparing their retention times with those of pure standards.

### Results

**Reaction Zones.** Pressure-temperature (Figure 4) for a 1 to 1 propane-oxygen mixture or pressure-concentration curves (Figure 5) at 429°C. show three regions for both the low and high temperature combustions.

Low Temperature Zone 250°–350°C.	{	Region 4: slow reaction Region 5: slow reaction with <i>pic d'arrêt</i> Region 6: cool flames
High Temperature Zone 400°–600°C.	{	Region 1: slow reaction Region 2: slow reaction with <i>pic d'arrêt</i> Region 3: normal flames

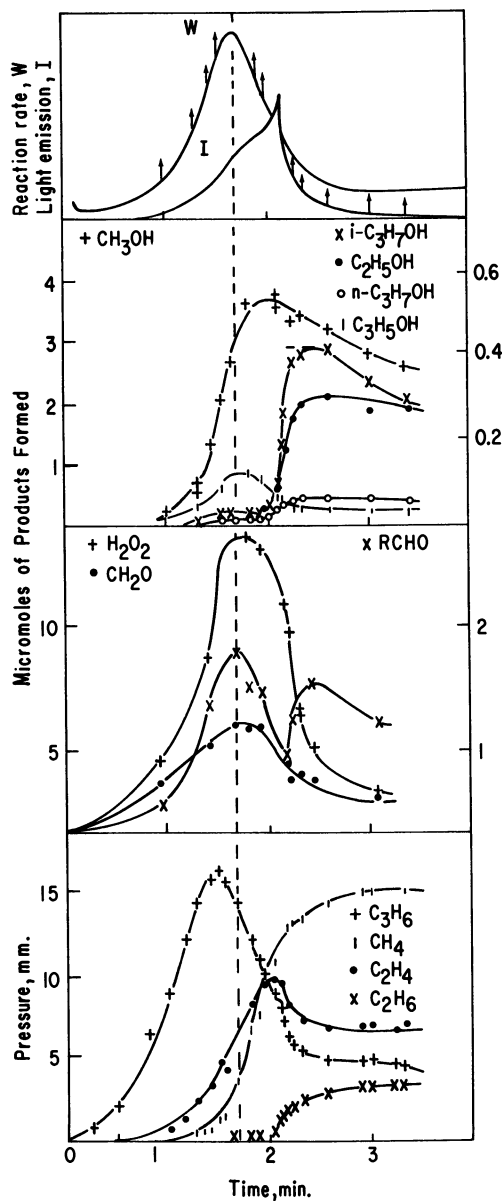


Figure 1. Kinetics of the formation of different products during propane oxidation at  $430^\circ\text{C}$ . Propane concentration = 30%. Mixture: 90 mm.  $\text{C}_3\text{H}_8$  and 210 mm.  $\text{O}_2$

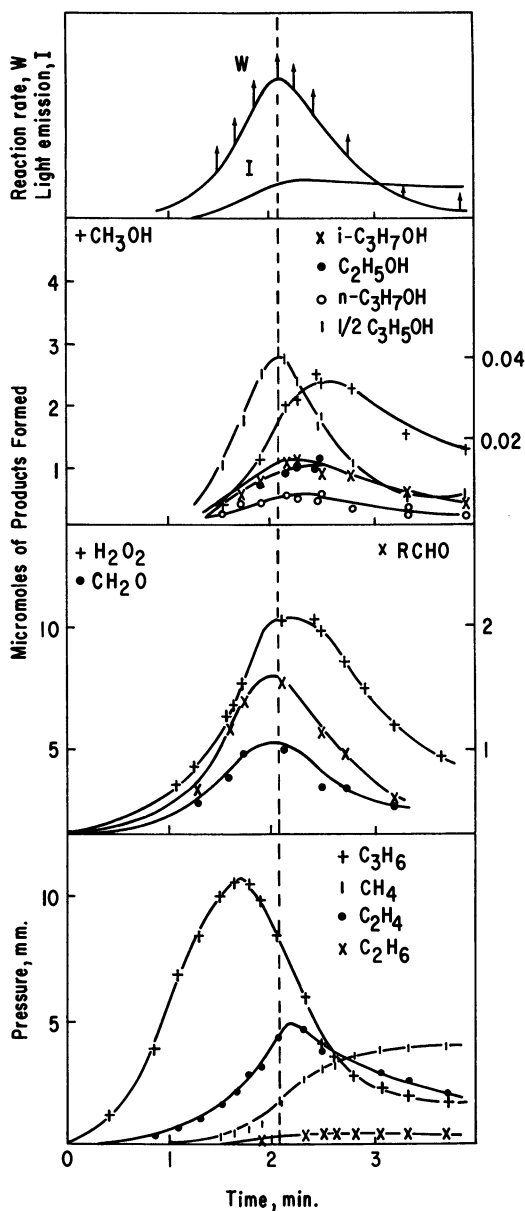


Figure 2. Kinetics of the formation of different products during propane oxidation at 430°C. Propane concentration = 20%. Mixture: 60 mm. C<sub>3</sub>H<sub>8</sub> and 240 mm. O<sub>2</sub>

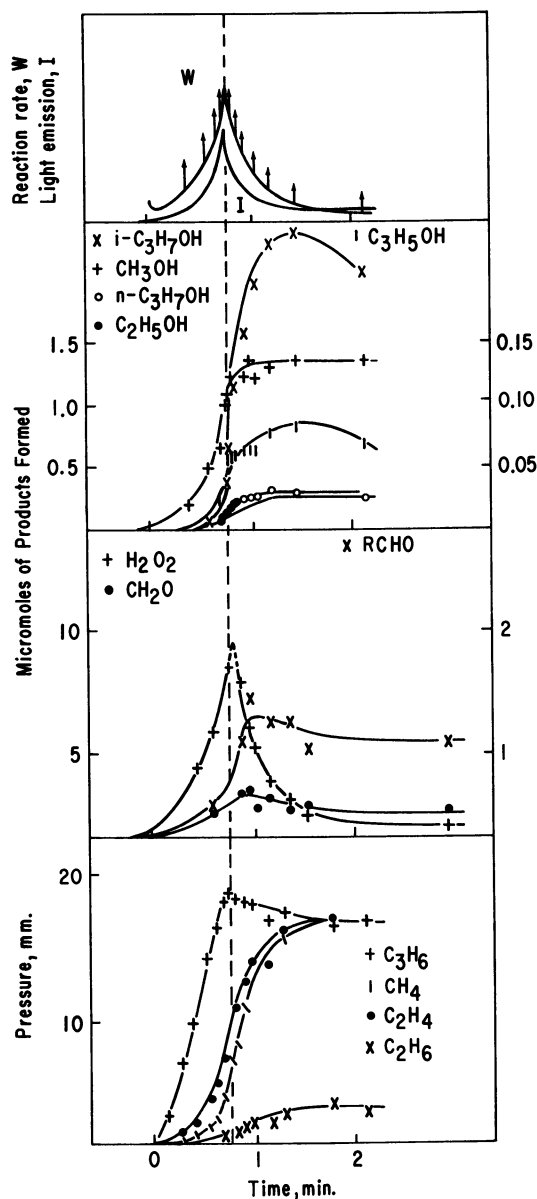


Figure 3. Kinetics of the formation of different products during propane oxidation at 430°C. Propane concentration = 85%. Mixture: 255 mm.  $\text{C}_3\text{H}_8$  and 45 mm.  $\text{O}_2$

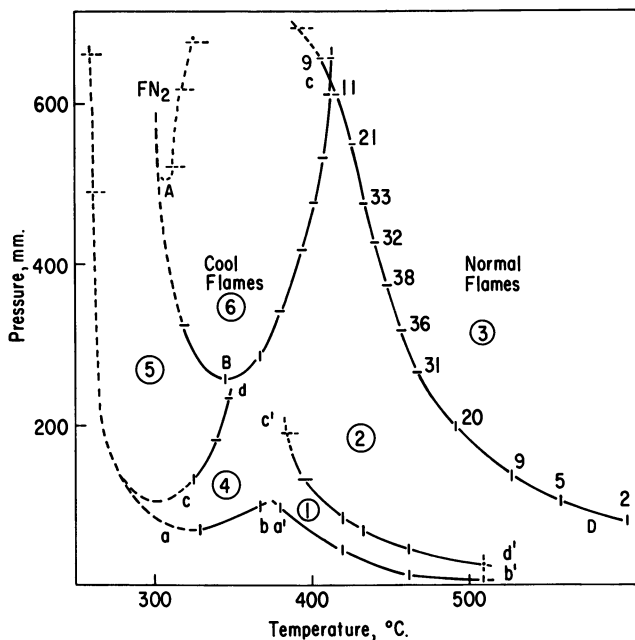


Figure 4. Regions of ignition, cool flames, slow oxidation with and without the pic d'arrêt in an equimolar propane-oxygen mixture. Bars on the boundaries represent experimental points, and numbers on these curves signify the duration of induction periods (in seconds). Numbered regions are defined in the text

Between 350° and 400°C. the two major regimes interact. Considering the 429°C. isotherm (Figure 5), Regions 1, 2, and 3 are observed. Region 2 may be subdivided further into two subregions: Region 2' and Region 2''. Therefore, there are three regions of slow reaction:

- (1) Slow reaction without *pic d'arrêt* (Region 1)
- (2) Slow reaction with *pic d'arrêt* after the maximum rate (Region 2')
- (3) Slow reaction where the maximum rate and the *pic d'arrêt* are superimposed (Region 2'')

Locating the isobar at 300 mm Hg (Figure 5) we can successively traverse these three regions, and the reaction rate ( $W$ ) and light emission ( $I$ ) are similar for each region to those in Figures 1, 2, and 3. As the hydrocarbon concentration increases, the *pic d'arrêt* occurs nearer the maximum rate of reaction, and when the mole fraction of the hydrocarbon exceeds 75%, the two coincide. How do the reaction products change at the *pic d'arrêt*?

**Analysis.** The results of the polarographic and chromatographic (16) analyses of the reaction products in the three regions described above are discussed below.

**REGION 1 (MOLE FRACTION OF PROPANE < 25%).** Figure 2 (%  $C_3H_8 = 20$ ) shows that the yields of aldehydes, and hydrogen peroxide follow the reaction rate approximately. Yields of alcohols and olefins pass through maxima. Methane is formed according to a sigmoid curve, the maximum rate of formation occurring simultaneously with the maximum reaction rate. The yield of ethane is always small.

**REGION 2' (MOLE FRACTION OF PROPANE BETWEEN 25 AND 75%).** Figure 1 (%  $C_3H_8 = 30$ ) shows that the formation of products in the early stages is similar to that observed in Region 1. However, when the *pic d'arrêt* appears, notable differences occur. The yields of acetaldehyde,

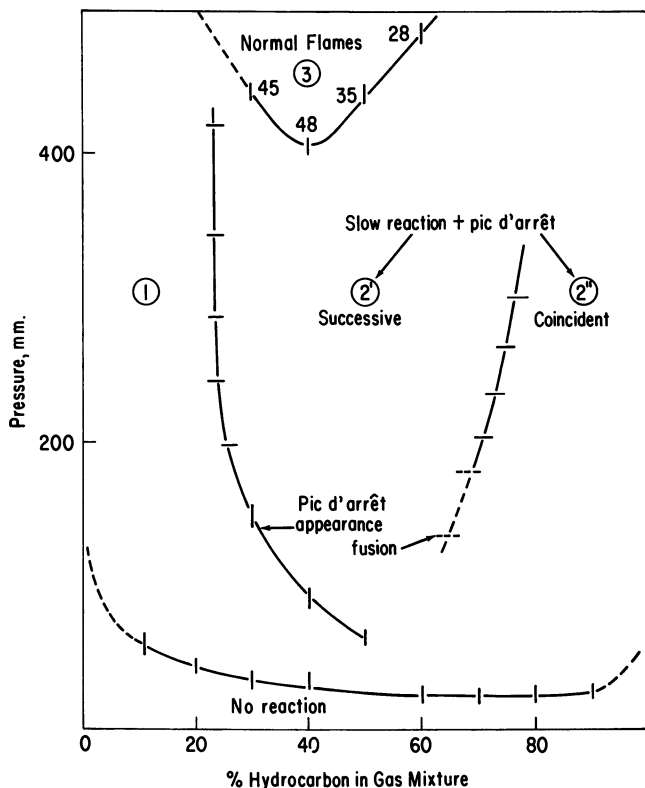


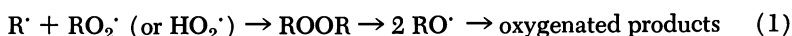
Figure 5. Regions of ignition, slow reaction with and, without the *pic d'arrêt* in propane oxidation at 429°C. Bars on the normal flames boundary represent experimental points and numbers on this curve signify duration of induction periods (in seconds). Numbered regions are defined in the text

ethanol, propyl alcohol, and especially isopropyl alcohol and ethane increase, and the maximum rate of methane formation occurs not at the maximum reaction rate but during the *pic d'arrêt*. Yields of hydrogen peroxide and olefin decrease.

REGION 2'' (MOLE FRACTION OF PROPANE > 75%). Figure 3 (% C<sub>3</sub>H<sub>8</sub> = 85) shows that the effect of *pic d'arrêt* on the formation of main products is similar to that for Region 2' but less clear-cut.

### Discussion

As the mole fraction of propane in the mixture increases, the *pic d'arrêt* occurs closer to the maximum reaction rate. Further, the pressure rise between the start of the reaction and the *pic d'arrêt* is independent of the initial hydrocarbon pressure and depends only on the oxygen pressure at a given temperature (16, 18). These observations combined with the rapid quenching of luminescence after the *pic d'arrêt* are consistent with the complete exhaustion of oxygen at about this point in the reaction (2, 4, 11) and may be analogous to that of the "oxygen cut-off" observed during liquid-phase oxidations (7, 19). At low temperatures we believe that the *pic d'arrêt* arises when previously formed peroxy radicals disappear by reactions with the alkyl radicals, favored by low oxygen concentration, leading to oxygenated products and hydrocarbons.



**Oxygenated Products.** The formation of peroxy radicals at higher temperature depends on the competition between the reactions (1, 3, 13, 14):

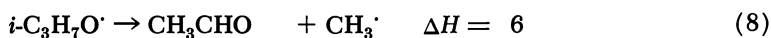
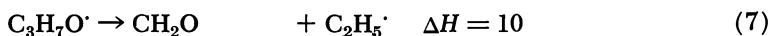
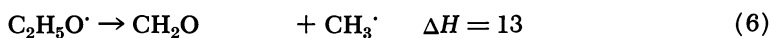


It is possible that HO<sub>2</sub>' reacts with alkyl radicals, but it cannot be the sole reaction responsible for the formation of oxygenated products during the *pic d'arrêt* since the HO<sub>2</sub>' radical concentration becomes very high at 450°–500°C., while the *pic d'arrêt* disappears (Figure 4).

We therefore believe that the *pic d'arrêt* always arises from reactions of alkylperoxy radicals rather than of HO<sub>2</sub>' radicals, and indeed that it can act as a "peroxy radical tracer" occurring when a critical peroxy radical concentration is achieved. Its disappearance at a certain temperature and reappearance at a higher temperature (*see* 250-mm. Hg isobar in Figure 4) after the region of negative temperature coefficient is in agreement with this view.

At the end of reaction the initial hydrocarbon concentration is still important, but there are also many other hydrogen donors. Thus, in the absence of oxygen, reactions of alkoxy radicals will lead to aldehydes by pyrolysis and to alcohols by abstraction. Let us examine these two possible reactions for each alkoxy radical.

Aldehydes are obtained by cleavage of the C—C bond in the  $\alpha$  position of C—O bond according to the following reactions:



All these reactions are endothermic and have high activation energies. The observation that acetaldehyde concentration rises during the *pic d'arrêt* while that of formaldehyde decreases suggests that only the last reaction is important and that formaldehyde is formed by oxidation (*e.g.*, of  $\text{CH}_3$ ) rather than by pyrolysis.

Since the burst of illumination is caused by excited formaldehyde, as we have previously shown (15, 16), we should observe an increase in formaldehyde unless it is formed in small amounts in a very energetic reaction such as:



These reactions become all the more important when the oxygen concentration is low and the concentrations of alkoxy and particularly methoxy radicals increase. Thus, the sudden onset of the final stage of the reaction is explained by the conversion of peroxy radicals in the absence of oxygen to the much more reactive alkoxy radicals (5).

Alcohols are formed by hydrogen abstraction:

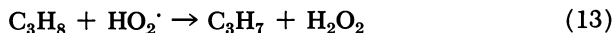


The explanation for the slow decrease in methanol is the same as for formaldehyde. The dramatic increase in the yields of ethyl and propyl alcohols at the *pic d'arrêt* clearly indicate the importance of abstraction reactions of the type above and of the appearance of alkoxy radicals at this point in the reaction.

The predominance of isopropyl alcohol over *n*-propyl alcohol is readily explained since abstraction of the secondary H atoms in propane by free radicals will be easier than abstraction of the primary H atoms,

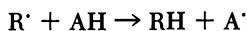
thus leading predominantly to secondary propylperoxy radicals and secondary peroxy radicals.

The behavior of hydrogen peroxide is determined by the reactions:



The faster disappearance of hydrogen peroxide at the *pic d'arrêt* can be explained by the failure of Reaction 3, owing to the exhaustion of oxygen while Reaction 14 continues.

**Hydrocarbon Formation.** Biradical or abstraction reactions such as:



lead to ethane and methane. The decrease in olefin formation is caused by the complete oxygen consumption and consequently by the disappearance of Reaction 3.

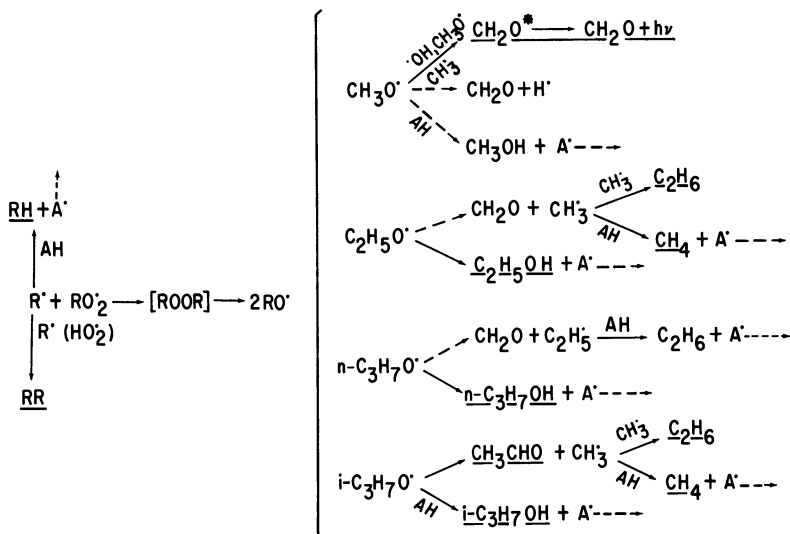


Figure 6. Mechanism of *pic d'arrêt*

### Conclusion

The mechanism of the *pic d'arrêt* is shown in Figure 6. All underlined compounds have been found in the reaction products. The suggested mechanism seems justified; it leads to alkoxy radicals, which are

characterized by light emission, aldehydes, and alcohols. A secondary outcome is the formation of methane and ethane (owing to oxygen deficiency) as well as a more rapid disappearance of hydrogen peroxide and olefin. For each zone, the reaction's behavior is different. Hence, each reaction should be analyzed after these zones have been studied carefully.

### Literature Cited

- (1) Benson, S. W., *J. Am. Chem. Soc.* **87**, 972 (1965).
- (2) Dechaux, J. C., Lucquin, M., *J. Chim. Phys.*, in press.
- (3) Falconer, J. W., Knox, J. H., *Proc. Roy. Soc.* **250A**, 493 (1959).
- (4) Knox, J. H., Wells, C. H. J., *Trans. Faraday Soc.* **59**, 2786 (1963).
- (5) Knox, J. H., *Journées d'études sur la Combustion*, Nice, France, March 1967.
- (6) Lefebvre, M., Ph.D. Thesis, Paris, 1964.
- (7) Lloyd, R. A., *Trans. Faraday Soc.* **61**, 2173, 2182 (1965).
- (8) Lucquin, M., *J. Chim. Phys.* **55**, 827 (1958).
- (9) Mac Nevin, V. M., Urone, P. F., *Anal. Chem.* **25**, 1760 (1953).
- (10) Mac Nevin, V. M., Urone, P. F., Omietanski, M. L., Dunton, M. L., *Symp. Combust., 5th, Pittsburgh, 1954*, p. 402 (1955).
- (11) Postnikov, L. M., Shlyapintokh, V. Ya., Shumilina, M. N., *Kinetics Catalysis (USSR)* **6**, 161 (1965).
- (12) Sandler, S., Chung, Yu Ho, *Anal. Chem.* **30**, 1252 (1958).
- (13) Satterfield, C. N., Reid, R. C., *J. Phys. Chem.* **59**, 283 (1955).
- (14) Satterfield, C. N., Wilson, R. E., *Ind. Eng. Chem.* **46**, 1001 (1954).
- (15) Sochet, L. R., Lucquin, M., *J. Chim. Phys.* **62**, 796 (1965).
- (16) Sochet, L. R., Ph.D. Thesis, Centre de Documentation C.N.R.S. AO.1398, Lille, France, 1967.
- (17) Sochet, L. R., Egret, J., Lucquin, M., *J. Chim. Phys.* **63**, 1555 (1966).
- (18) Sochet, L. R., Lucquin, M., *J. Chim. Phys.* in press.
- (19) Vasiliev, R. F., Karpukhine, O. N., Shlyapintokh, V. Ya., *Dokl. Akad. Nauk SSSR* **125**, 106 (1959).

RECEIVED January 23, 1968.

## Discussion

**Frank R. Mayo:** Although Dr. Sochet and his co-workers have made a persuasive case for associating the *pic d'arrêt* with the nonterminating interactions of alkyl and alkylperoxy radicals, I have some comments on their scheme. First, the work of Knox (1, 2) also shows that the oxidation of propane gives propylene as the principal primary product. That the concentration of propylene goes through a maximum shows that it is oxidized further, and preferentially, as the chain carrier changes. Acetaldehyde and formaldehyde are expected major products, but their high

reactivities permit only very low steady state concentrations. These considerations suggest that the alkyl radicals of Dr. Sochet may be coming from decarbonylation of aldehydes and of acyl radicals and decarboxylation of acyloxy radicals as well as from alkoxy radicals. Even at the *pic d'arrêt*, there are probably more alkylperoxy than alkoxy radicals (from reactivity considerations), and thus aldehydes are more likely to arise from interaction of one radical of each type than from two alkoxy radicals.

The apparent absence of acetone is surprising. It should be an important product of chain termination by two isopropylperoxy radicals and it should survive further oxidation as well as isopropyl alcohol. I wonder if the authors looked for acetone, and if they could find it if they added it to the feed. Its changing concentration could clarify the changing termination mechanisms.

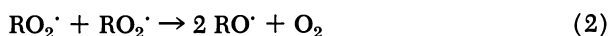
An increase in rate of oxidation (at steady rate of initiation) as the oxygen pressure approaches zero would be unprecedented in liquid-phase oxidations at and below 100°C. However, Dr. Sochet's work suggests that a maximum in the steady rate of a liquid-phase oxidation might appear at a low oxygen pressure at some temperature above 150°C. This phenomenon might be investigated for its bearing on practical oxidations.

### Literature Cited

- (1) Falconer, J. W., Knox, J. H., *Proc. Roy. Soc.* **A250**, 493 (1959).
- (2) Knox, J. H., *Trans. Faraday Soc.* **56**, 1225 (1960).

**L. R. Sochet:** The term used by Dr. Mayo—"the maximum rate of pressure change"—leads to ambiguity. It is better to talk of the sudden but temporary increase in the over-all rate of reaction which occurs at the same time as an increase in light emission, *after* the maximum rate of reaction (Figure 1).

Effectively, we must compare the symmetrical and crossed terminating or nonterminating reactions of alkyl radicals with alkylperoxy radicals.



Reaction 1 is a terminating one, which accounts for the formation of ethane and probably methane connected with the appearance of the *pic d'arrêt* (Figure 1).

Heicklen (1) gives for the two last reactions  $k_2 = 10^{9.4}$  mole<sup>-1</sup> l. sec.<sup>-1</sup> and  $k_3 = 10^{8.8}$  mole<sup>-1</sup> l. sec.<sup>-1</sup>. The ratio of the corresponding rates will

be  $W_2/W_3 = 10^{0.6} [\text{RO}_2\cdot]/[\text{R}\cdot]$ . As a first approximation if we assume that the reaction  $\text{R}\cdot + \text{O}_2 \rightleftharpoons \text{RO}_2\cdot$  is an equilibrium, we have  $W_2/W_3 = 10^{0.6} [\text{O}_2] K_{\text{eq.}}$ . Benson (2) proposes  $K_{\text{eq.}} = 10^{3.61} \text{ mole}^{-1} \text{ l.}$  for the isopropyl radical at 430°C. It is possible to calculate the ratio  $W_b/W_c$  for different oxygen pressures.

$P_{\text{O}_2}$ , mm. Hg:	150	15	1.5	0.15
$W_b/W_c$ :	55	5.5	0.5	0.05

This clearly shows that Reaction 3 becomes more important when the oxygen concentration in the mixture is low. Our measurements (3) of oxygen concentration, just before the *pic d'arrêt* occurs, indicates that this concentration is sufficiently low.

During the reaction, propylene concentration goes through a maximum followed by maxima in aldehyde concentration. However, with the *pic d'arrêt* there is *simultaneously* an increase of aldehydes and alcohols (ethanol, *n*- and isopropyl alcohol). Consequently, alcohols are not formed by aldehyde oxidation, and we must find a new source of alkoxy radicals to explain the experimental facts. It is likely that Reaction 3 would be the right one. This reaction becomes important only when oxygen concentration in the mixture is low and accounts for the sudden increase in the rate of reaction. The subsequently decreasing rate is caused by the complete consumption of oxygen (3, 4) [analogy with oxygen cut-off (5) or oxygen drop (6) in liquid phase] and the disappearance of Reaction 3 which is replaced by the terminating Reaction 1.

We also must remark that there is no increase in methanol concentration with the *pic d'arrêt*, and the mechanism proposed by Dr. Mayo does not account for the formation of *n*- and isopropyl alcohol even if we consider propionaldehyde.

### Literature Cited

- (1) Hecklen, J., *ADVAN. CHEM. SER.* **76**, 23 (1968).
- (2) *See Ref. (1).*
- (3) *See Ref. (2).*
- (4) *See Ref. (11).*
- (5) *See Ref. (7).*
- (6) Vasiliev, R. F., *Progr. Reaction Kinetics* **4** (1967).

## Reactions of Hydrocarbons in Slowly Reacting Hydrogen–Oxygen Mixtures

R. R. BALDWIN, C. J. EVERETT,<sup>1</sup> D. E. HOPKINS, and R. W. WALKER

The University, Hull, England

*Traces of hydrocarbons have been added to slowly reacting H<sub>2</sub> + O<sub>2</sub> mixtures in aged boric-acid-coated vessels at 480°–500°C. Measurements of hydrocarbon loss and H<sub>2</sub>O formation have enabled relative velocity constants for the attack of the radicals H, O, OH, and HO<sub>2</sub> on the additive to be assessed for CH<sub>4</sub> and C<sub>2</sub>H<sub>6</sub>. With CH<sub>4</sub>, the results also show that CH<sub>3</sub> radicals react at almost equal rates with H<sub>2</sub> and O<sub>2</sub> at 500 mm. Hg pressure, and that the reaction with O<sub>2</sub> appears to have both second- and third-order components. Detailed analyses of the reaction products obtained with ethane and neopentane enable the reactions of the radical produced in the primary attack to be elucidated, and mechanisms to account for the various products are given.*

Much valuable information, particularly of a qualitative nature, on the mechanism of hydrocarbon oxidation has been obtained by studying the reaction between the hydrocarbon and oxygen (17) directly. This approach does have the disadvantage for quantitative studies, however, that both the nature and relative concentrations of the radicals involved are controlled by the hydrocarbon and its oxidation products, and these usually vary during the course of the reaction (13, 14); moreover, reproducible results are not easy to obtain, presumably because the surface often acts as an erratic source of chain initiation, chain termination, or both. This paper describes a useful and complementary technique, in which small amounts of hydrocarbons and related compounds are added to slowly reacting H<sub>2</sub> + O<sub>2</sub> mixtures in aged boric-acid-coated vessels at temperatures of about 500°C.; under these conditions the reaction is highly reproducible.

<sup>1</sup> Present address: National Research Council, Ottawa, Ontario, Canada.

Two types of investigation can be made:

(a) By examining the relative rates of consumption of additive and formation of water, the relative rates of attack of H, O, OH, and HO<sub>2</sub> on the additive can be obtained.

(b) By analyzing the products at various stages in the reaction, the fate of the radicals produced in the primary attack can be examined.

Provided that the concentration of the additive is kept sufficiently low, both types of investigation have the advantage that the concentrations of the radicals H, O, OH, and HO<sub>2</sub> do not alter significantly from their values in the absence of hydrocarbon and remain relatively unaltered as the hydrocarbon is consumed. Although quantitative information can also be obtained by studying the inhibition of the second limit by hydrocarbons (2), the present studies are complementary since the relative concentrations of H, O, and OH differ considerably from those present at the second limit. Compared with second-limit inhibition studies, quantitative investigation (a) above has the following advantages:

(a) The results are simpler to obtain.

(b) The interpretation depends much less on knowing the subsequent reactions of the radical produced in the primary attack.

(c) The method can be applied to a much wider range of compounds.

With second-limit studies, product analysis normally serves little purpose since there is little detectable reaction outside the boundary, and reaction is effectively complete if explosion occurs. With the slow reaction this limitation does not arise, and the second aspect of the addition studies has involved analyzing the oxidation products to obtain detailed information on subsequent reactions of the radicals formed in the primary process which removes the hydrocarbon.

A program involving a wide range of additives is planned, and this paper aims to illustrate the scope of the method rather than to present full and final details of the results obtained with individual additives.

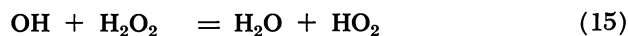
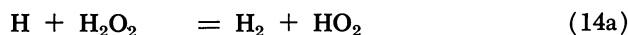
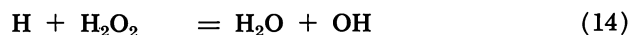
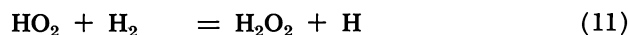
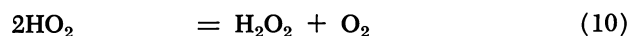
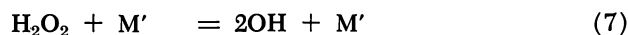
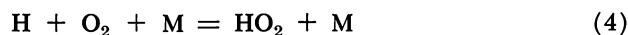
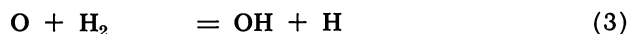
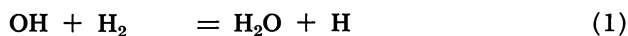
### *Experimental*

The general procedure has already been described (3). As in previous studies, a standard mixture was selected containing 0.28, 0.14 mole fractions of H<sub>2</sub>, O<sub>2</sub>, respectively, the remainder being N<sub>2</sub>. Independent variation of the H<sub>2</sub> and O<sub>2</sub> mole fractions could thus be achieved by interchange with N<sub>2</sub>. To avoid explosion on entry, one gas (normally H<sub>2</sub>) was placed in the reaction vessel, and the remaining premixed gases were admitted from the mixing bulb. The pressure change was followed 2 seconds after admission of the gases by using a pressure transducer. The induction period of about 60 seconds which exists at 500°C. proved convenient in enabling the base line of the transducer record to be established accurately. A Langham-Thomson UP-4 pressure transducer gave

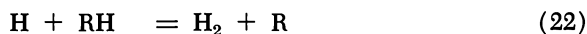
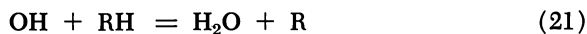
full-scale recorder deflections for about 30 mm. Hg, while using the S.E. Laboratories SE 1150 permitted full-scale deflection with 4 mm. Hg or less. After a suitable time or pressure change, a sample was analyzed. All carbon-containing compounds were estimated by gas chromatographic methods, except for HCHO, which was estimated colorimetrically with chromotropic acid. The concentrations of the major products are probably accurate to about 2% of their concentration. Greater accuracy was possible in measuring hydrocarbon consumption by using a sample taken from the mixing bulb to calibrate the gas chromatographic equipment immediately before running the test sample. A temperature of 500°C. was used for CH<sub>4</sub>, C<sub>2</sub>H<sub>4</sub>, and C<sub>2</sub>H<sub>6</sub>, while neopentane was studied at 480°C.

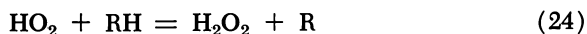
### *Quantitative Kinetic Results*

The full mechanism for the H<sub>2</sub> + O<sub>2</sub> reaction in aged boric-acid-coated vessels involves Reactions 1-4, 7, 8, 10, 11, 14, 14a, and 15, given below:



Although this scheme can be treated analytically (4) by making reasonable approximations, it is more satisfactory to use computer programs. By suitably selecting the velocity constant ratios involved, the second limit, the induction period preceding slow reaction, and the maximum rate of the slow reaction can be predicted over a wide range of mixture composition with root mean square deviations of 1.5, 4, and 4%, respectively (5). These programs can be modified to include the Reactions 21-24 given below:





Although the subsequent reactions of the radical R should be known, this is not essential if the concentration of added RH is kept sufficiently low so that the concentrations of the radicals H, O, OH, and HO<sub>2</sub> are hardly altered from their values in the uninhibited reaction. This can be checked easily by measuring the reaction rate in the presence and absence of the additive, and Table I gives typical results for adding methane and ethane to the standard mixture (0.28, 0.14 mole fractions of H<sub>2</sub>, O<sub>2</sub>, respectively) at 500 mm. Hg and 500°C. Similar results have been obtained for other H<sub>2</sub> + O<sub>2</sub> mixtures.

**Table I. Effect of Adding Hydrocarbon on Reaction Rate**

<i>Hydrocarbon Added</i>	<i>Maximum Rate, dP/dt (mm. Hg/min.)</i>	<i>Induction Period to Half Max. Rate (sec.)</i>
none	6.10	47
1% CH <sub>4</sub>	6.20	47
3% CH <sub>4</sub>	6.40	45
0.1% C <sub>2</sub> H <sub>6</sub>	6.25	50
1.0% C <sub>2</sub> H <sub>6</sub>	8.5	67

Methane loss was usually small (5–20%) for reasonable amounts of water formation ( $\Delta P = 5\text{--}20$  mm. Hg), so that the initial ratio  $-d[\text{RH}]/d[\text{H}_2\text{O}]$  could be taken as  $\Delta[\text{RH}]/\Delta[\text{H}_2\text{O}]$  with sufficient accuracy for the analytical treatment discussed below. With computer interpretation, increased accuracy is possible if the initial concentrations of the various reactants are replaced by their mean concentrations during the reaction period. Because it was not considered sufficiently accurate to measure small differences by gas chromatography, the extent of oxidation was determined by oxidizing all the products to carbon dioxide, which was then measured (6). Because of the absence of any significant effect of methane on the rate, concentrations of methane up to 3% were sometimes used instead of the normal 1%.

As Table I shows, adding 1% ethane has a marked effect on the rate, so that 0.1% was used for the kinetic studies. With ethane, the rate of hydrocarbon consumption is much greater, as shown in Figure 1, which gives the percentage of ethane remaining in the reaction vessel as a function of  $\Delta P$  for three mixtures. For a preliminary interpretation, initial ratios can be obtained either by taking the initial tangent, or, more accurately, by using the tangent to the  $\log [C_2H_6]_0/[C_2H_6]$  vs.  $\Delta P$  plot, which is more nearly linear. For more accurate interpretation, numerical integration can be used to allow for changes in reactant concentration, while allowance for pressure changes owing to RH oxidation and H<sub>2</sub>O<sub>2</sub>

formation, marginally necessary with methane, become more important with ethane. Since ethane is significantly consumed before maximum rate, allowance for the changing  $\text{H}_2\text{O}_2$  and radical concentration is also necessary.

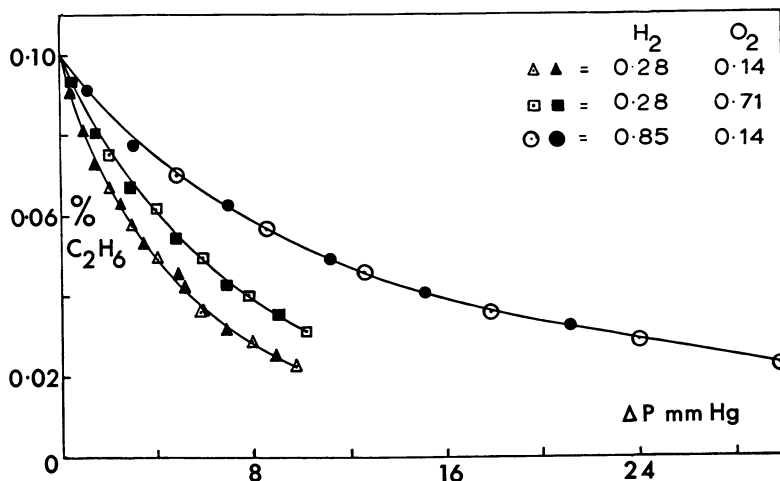


Figure 1. Plot of  $\text{C}_2\text{H}_6$  concentration as a function of pressure change; 51-mm. vessel, 500 mm. Hg,  $500^\circ\text{C}$ . The open and closed symbols represent experiments separated by an interval of 3 months

Although computer treatment is ultimately the most convenient way to interpret the results accurately, a preliminary analytical treatment is useful in defining both the reactions involved and the approximate velocity constant ratios to use in the computer treatment. The analytical treatment also emphasizes the essential simplicity of the method—*i.e.*, despite the apparent complexity of the  $\text{H}_2 + \text{O}_2$  mechanism, the predominant reactions of the radicals H, O, OH, and  $\text{HO}_2$  are Reactions 4, 3, 1, and 10, respectively. The relative rates of additive consumption and water formation are determined effectively by the competition between these reactions and the reactions of the corresponding radical with the additive, the remaining reactions of the  $\text{H}_2 + \text{O}_2$  system merely affecting slightly the relative radical concentrations and the rate of water formation. Thus, with suitable approximations, relatively simple expressions for  $-d[\text{RH}]/d[\text{H}_2\text{O}]$  can be obtained for attack of H, O, and OH on the hydrocarbon, and the expression for  $\text{HO}_2$  attack is more complex only because the competition between Reactions 10 and 24 depends on the  $\text{HO}_2$  concentration.

An analytical treatment is possible if Reactions 8 and 14a, which are of minor importance, and Reactions 11 and 15 are neglected. Reaction

11 increases the stationary  $\text{H}_2\text{O}_2$  concentration, particularly at high  $\text{H}_2$  concentrations, while Reaction 15 reduces the  $\text{H}_2\text{O}_2$  concentration, particularly at low  $\text{H}_2$  concentrations. However, computer calculations show that the relative concentrations of H, O, and OH are almost unaffected by the occurrence of these reactions, the absolute concentrations increasing almost proportionally to the  $\text{H}_2\text{O}_2$  concentration. The  $\text{HO}_2$  concentration increases almost with the half-power of the  $\text{H}_2\text{O}_2$  concentration since the main reaction of  $\text{HO}_2$  is Reaction 10. Thus, unless the reaction  $\text{HO}_2 + \text{RH}$  plays a major role, the simple analysis given below is valid.

Adding each of the Reactions 21–24 in turn to the simplified  $\text{H}_2 + \text{O}_2$  mechanism gives, after reasonable approximations which have been discussed elsewhere (6), the following expressions:

$$\text{OH} + \text{RH} \quad \frac{-d[\text{RH}]}{d[\text{H}_2\text{O}]} = \frac{k_{21}[\text{RH}]}{k_1[\text{H}_2]} \quad (\text{a})$$

Since Reaction 1 is the main source of  $\text{H}_2\text{O}$ , this simplified expression can be derived directly from

$$\begin{aligned} d[\text{H}_2\text{O}]/dt &= k_1[\text{OH}][\text{H}_2] \\ -d[\text{RH}]/dt &= k_{21}[\text{OH}][\text{RH}] \end{aligned}$$

$$\text{O} + \text{RH} \quad \frac{-d[\text{RH}]}{d[\text{H}_2\text{O}]} = \frac{k_2 k_{23}[\text{RH}]}{k_3 k_4 [\text{H}_2] M} \quad (\text{b})$$

$$\text{H} + \text{RH} \quad \frac{-d[\text{RH}]}{d[\text{H}_2\text{O}]} = \frac{k_{22}[\text{RH}]}{k_4 [\text{O}_2] M} \quad (\text{c})$$

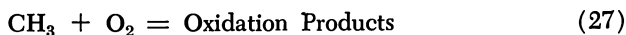
$$\text{HO}_2 + \text{RH} \quad \frac{-d[\text{RH}]}{d[\text{H}_2\text{O}]} = \frac{k_{24}[\text{RH}]}{(4k_2 k_7 k_{10} [\text{O}_2] M' / k_{14})^{1/2}} \quad (\text{d})$$

All these derivations assume that radical R is converted to oxidation products and that it does not reform the hydrocarbon. The relations are summarized in Table II, which also includes the experimental results for methane and ethane.

Table II allows for the increase in M and M' with increasing  $\text{H}_2$  mole fraction, which is equivalent to an apparent order of 0.3 with respect to  $\text{H}_2$ .

With methane, the marked dependence of  $-d[\text{RH}]/d[\text{H}_2\text{O}]$  on  $\text{H}_2$  concentration suggests that O or OH is the dominant attacking radical. The small effect of total pressure, as well as other evidence (6), rules out attack by O. The marked positive power in  $\text{O}_2$  cannot, however, be explained by the existing reactions since introducing either Reaction 22 or 24 would create a negative power in  $\text{O}_2$ . The only feasible explanation is competition between the reactions:





This competition was omitted from the initial analysis since second-limit inhibition studies with higher hydrocarbons had suggested that reaction of the alkyl radical with  $\text{O}_2$ , to give an olefin and  $\text{HO}_2$ , is much faster than reaction with  $\text{H}_2$ . The importance of Reaction 26 with methane suggests that the reaction of  $\text{CH}_3$  with  $\text{O}_2$  is more difficult than for higher alkyl radicals.

**Table II. Summary of Analytical Treatment**

Assumed Inhibition Reaction	Order With Respect To			
	$\text{H}_2$	$\text{O}_2$	RH	$P_{\text{total}}$
OH + RH (21)	-1	0	+1	0
H + RH (22)	-0.3	-1	+1	-1
O + RH (23)	-1.3	0	+1	-1
$\text{HO}_2$ + RH (24)	-0.1	-0.5	+1	0
Exp., RH = $\text{CH}_4$	-1.3	+0.4	+1	small
Exp., RH = $\text{C}_2\text{H}_6$	-0.8	-0.3	+1	small

Introducing Reactions 26 and 27 with 21 gives the relation:

$$R = \frac{-d[\text{RH}]}{d[\text{H}_2\text{O}]} = \frac{k_{21}[\text{CH}_4]}{k_1[\text{H}_2]} \times \frac{k_{27}[\text{O}_2]}{k_{26}[\text{H}_2] + k_{27}[\text{O}_2]} \quad (e)$$

This can be re-arranged to:

$$y/x + k_{26}/k_{27} = (k_{21}/k_1)(iy/Rx^2) \quad (f)$$

where  $x$ ,  $y$ ,  $i$ , are the mole fractions of  $\text{H}_2$ ,  $\text{O}_2$  and  $\text{CH}_4$  respectively. For most mixtures, the plot of  $y/x$  vs.  $iy/Rx^2$  is a good straight line, but the points at low  $y/x$  lie systematically above the line (Figure 2). Under these conditions, Reaction 22 becomes important, and assuming that the presence of methane does not alter the relative concentrations of H and OH significantly, the corresponding equation becomes:

$$y/x - (k_{22}/k_4)(i/RxM) + k_{26}/k_{27} = (k_{21}/k_1)(iy/Rx^2) \quad (g)$$

With three unknown parameters, simple graphical solution is no longer possible, but a computer treatment enables the optimum values of  $k_{22}/k_4$ ,  $k_{26}/k_{27}$ , and  $k_{21}/k_1$  to be obtained. Table II shows that the occurrence of Reaction 22 introduces a pressure dependence, and the value of  $k_{22}/k_4$  required to explain the effect of pressure is much lower than that required to explain the behavior at low  $\text{O}_2$  concentration where Reaction 22 becomes important. An alternative method of introducing a pressure dependence is to write Reaction 27 in the termolecular form (Reaction 27a):



If Reaction 27a alone is used, the predicted effect of total pressure on  $-d[\text{RH}]/d[\text{H}_2\text{O}]$  is now in the wrong direction if parameters are used which give the best interpretation of the effect of mixture composition at constant pressure. Since Reaction 27 alone gives too great an effect of pressure but in the right direction, a combination of Reactions 27 and 27a obviously will improve the agreement, and with the full computer treatment the root mean square deviation between observed and calculated values of  $-d[\text{RH}]/d[\text{H}_2\text{O}]$  can be reduced to 4% for a wide range of mixture composition. Evidence is thus obtained either for the bimolecular and termolecular forms of  $\text{CH}_3 + \text{O}_2$  or for the occurrence of Reaction 27a in the range between second and third order. A more elaborate computer treatment, which makes some allowance for reactant consumption as the reaction proceeds, is being developed, but preliminary values for the parameters at 500°C. are given below:

$$\begin{aligned} k_{21}/k_1 &= 1.1 \pm 0.1, & k_{22}/k_2 &= 7.0 \pm 3.0^a \\ k_{26}/k_{27} &= 7.0 \pm 3.0, & k_{27a}/k_{27} &= 0.008 \pm 0.004 \\ & & & \text{mm. Hg}^{-1} \text{ (M = H}_2\text{)} \end{aligned}$$

<sup>a</sup> Using  $k_2/k_4 = 18.5$  mm. Hg (M = H<sub>2</sub>)

The values for  $k_{21}/k_1$ ,  $k_{22}/k_2$  have been used elsewhere (6, 7, 19) to obtain Arrhenius parameters for Reactions 21 and 22. Using the value of

$$k_{26} = 3.2 \times 10^8 e^{-10,000/RT} \text{ liter mole}^{-1} \text{ sec.}^{-1}$$

given by Whittle and Steacie (18), we obtain

$$k_{27} = 1.4 \times 10^5 \text{ and } k_{27a} = 2.6 \times 10^7$$

A recent review by McMillen and Calvert (16) quotes values of  $k_{27}$  ranging from  $4.8 \times 10^5$  to  $1.3 \times 10^9$  liter mole<sup>-1</sup> sec.<sup>-1</sup> near room temperature; the high values are quite inconsistent with the present estimate. Using acetone as third body, several workers (16) give

$$k_{27a} = 3 \times 10^{10} \text{ liter}^2 \text{ mole}^{-2} \text{ sec.}^{-1}$$

near 200°C. Comparison with the present work is confused by uncertainty as to the relative efficiencies of acetone and H<sub>2</sub>, but unless the value is much greater than 100, Reaction 27a would appear to have a significant negative activation energy.

The above analysis indicates clearly that contrary to views expressed by many workers on methane oxidation, the termolecular reaction of  $\text{CH}_3 + \text{O}_2$  must be of major importance at these temperatures. Benson (10) has expressed the view that the bimolecular reaction is unimportant even at high temperature and has suggested that the  $\text{CH}_3\text{O}_2$  radical forms  $\text{CH}_3\text{O}_2\text{H}$  by hydrogen abstraction from  $\text{HO}_2$ ,  $\text{H}_2\text{O}_2$ , or possibly H<sub>2</sub>. Preliminary analysis suggests that even if this were the case, a second-order

contribution cannot necessarily be eliminated, but detailed analysis is in progress.

With ethane, the absence of any positive power in  $O_2$  (Table II) suggests that reactions of  $C_2H_5$  with  $O_2$  predominate over the reaction:



Independent studies, including the addition of ethane to  $D_2 + O_2$  mixtures, are planned to evaluate any small occurrence of Reaction 26e, but in the meantime the results for ethane have been interpreted using Equation h which can be derived from Equation g by assuming all  $C_2H_5$  radicals are converted to oxidation products.

$$R[O_2]M/[C_2H_6] = k_{22}/k_4 + (k_{21}/k_1)[O_2]M/H_2 \quad (h)$$

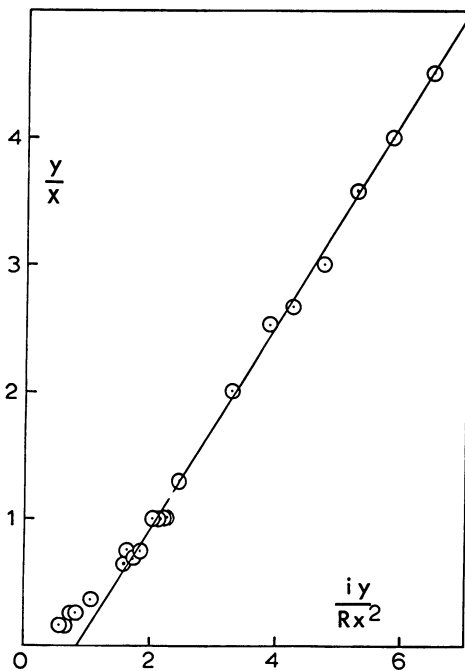


Figure 2. Plot of  $y/x$  vs.  $iy/Rx^2$  for  $CH_4$  addition; 51-mm. vessel, 500 mm. Hg,  $500^\circ C$ .

Figure 3 shows the plot of  $R[O_2]M/[C_2H_6]$  vs.  $[O_2]M/[H_2]$ , in which  $H_2$ ,  $O_2$ , and  $C_2H_6$  have each been varied by a factor of 10, the total pressure by a factor of 2.5. From the gradient and intercept of the straight line, preliminary values of  $k_{21e}/k_1 = 8.5$ ,  $k_{22e}/k_2 = 30$  are obtained.

These ratios are reasonably consistent with those obtained from second-limit inhibition studies (2), but detailed comparison is premature because (a) the present analysis needs refinement as indicated earlier, and (b) the values from second-limit studies are based on the assumption that all  $C_2H_5$  radicals give chain termination and also give the combined effect of  $OH + RH$  and  $O + RH$ .

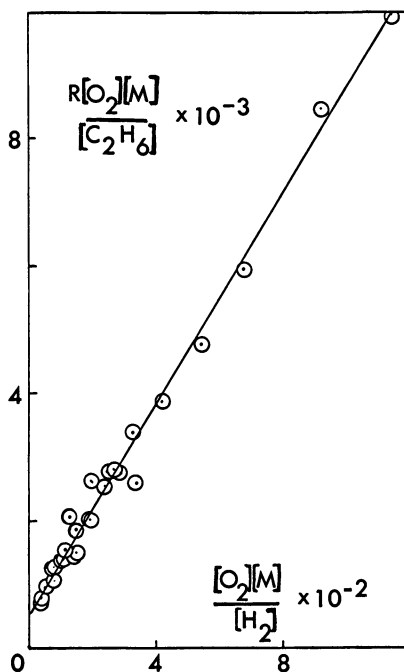


Figure 3. Plot of  $R[O_2]M/[C_2H_6]$  vs.  $[O_2]M/[H_2]$  for  $C_2H_6$ ; 51-mm. vessel,  $500^\circ C$ .

### Analytical Studies

Except for methane, the kinetic studies have been carried out using 0.1% mole of hydrocarbon, so that the relative concentrations of H, O, OH, and  $HO_2$  were not disturbed. However, in the analytical work 1% of the additive has been used to allow accurate measurement of the minor products. By presenting the concentration of product as a function of either hydrocarbon loss or pressure change, it is possible to distinguish primary, secondary, and tertiary products.

**Addition of Ethane.** Figure 4 shows the product concentrations as a function of ethane loss for the mixture  $x = 0.28$ ,  $y = 0.14$ . The carbon

balance is  $100 \pm 2\%$  over the entire range and is largely accounted for by  $C_2H_4$ ,  $CH_4$  and  $CO$ , with smaller amounts of  $C_2H_4O$ ,  $CH_3CHO$ ,  $HCHO$ , and  $CO_2$ . It is apparent that at least 90% of the  $C_2H_5$  radicals are oxidized to  $C_2H_4$ , and thus Reaction 28e is the main process removing  $C_2H_5$  radicals at  $500^\circ C$ .



The kinetic studies with ethane have established that reaction of  $C_2H_5$  radicals with  $H_2$  can occur only to a minor extent; the only other possible reactions of  $C_2H_5$  are with  $O_2$  to form either ethylene oxide or acetaldehyde, and these can occur only to a small extent.

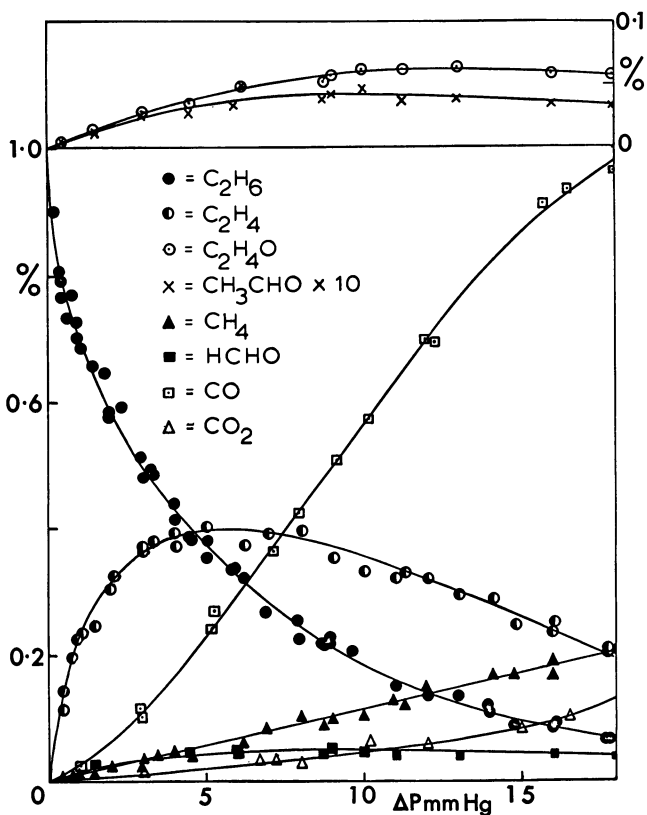
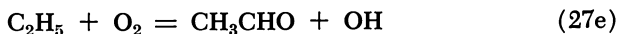
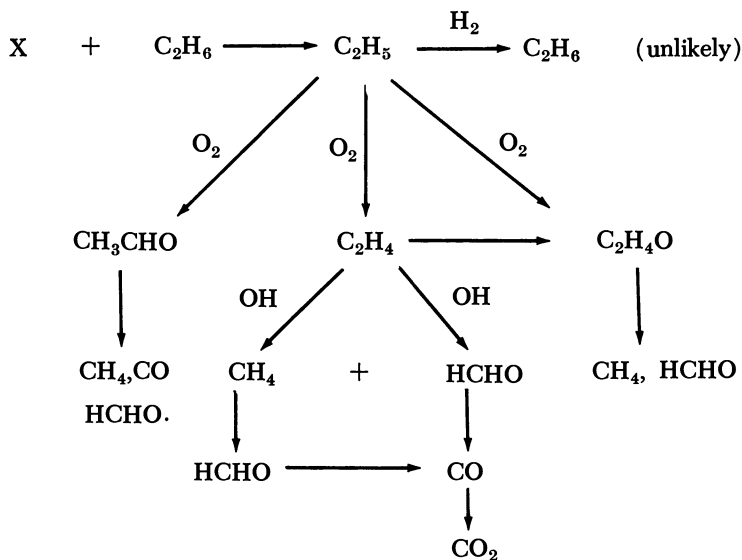


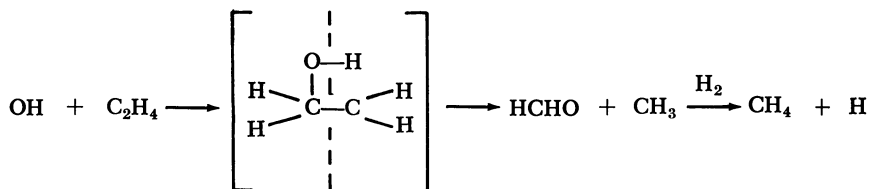
Figure 4. Variation of products with pressure change for  $C_2H_6$ ; 51-mm. vessel,  $500^\circ C$ .,  $H_2 = 140$  mm. Hg,  $O_2 = 70$  mm. Hg, total pressure = 500 mm. Hg

It seems likely that the major proportion of  $C_2H_4O$  is formed from  $C_2H_4$  rather than  $C_2H_5$  radicals, and this view is confirmed from studies where  $C_2H_4$  has been used as the additive and from analysis data for propionaldehyde oxidation at  $440^\circ C$ . where  $C_2H_4$  and  $CH_3CHO$  are primary products, but the concentration profile for  $C_2H_4O$  is distinctly autocatalytic in character (8). The same conclusion has been reached by Knöx and Wells (15).

Products arising from mutual reactions between radicals are unlikely because of the low level of concentrations involved and the rapid alternative reactions with  $H_2$  and  $O_2$ .  $CH_4$ ,  $CO$ ,  $HCHO$ , and  $CO_2$  are undoubtedly secondary products and are probably formed by the following reactions.



**Addition of  $C_2H_4$  and  $C_2H_4O$ .** Evidence for the formation of  $CH_4$  from  $C_2H_4O$  and  $C_2H_4$ , as indicated above, has been obtained by adding  $C_2H_4O$  and  $C_2H_4$  to reacting  $H_2 + O_2$  mixtures. The  $CH_4$  from  $C_2H_4$  is probably formed in the following way:



Similar reactions have been observed with isobutene and propylene and will be discussed later.

**Addition of Neopentane.** With neopentane, the primary products are 2-butene, 3,3-dimethyloxetane, HCHO, and CH<sub>4</sub>. (Recent studies using mixtures of high O<sub>2</sub> content suggest that acetone may also be a primary product.) No pivalaldehyde, (CH<sub>3</sub>)<sub>3</sub>CCHO, was found even in trace amounts. Adding pivalaldehyde to the H<sub>2</sub> + O<sub>2</sub> reaction showed that although it was removed rapidly, detection would have been easy if it had been formed in significant amounts in neopentane studies. The secondary products are propylene, acetone, CO, and isobutyraldehyde, and at an even later stage C<sub>2</sub>H<sub>4</sub> and CO<sub>2</sub> are formed. In addition acetaldehyde, C<sub>2</sub>H<sub>5</sub>CHO, C<sub>2</sub>H<sub>6</sub> and 2-butanol have been detected in trace amounts. Figure 5, which gives concentration profiles for some of the products, shows how it is possible to distinguish clearly between primary, secondary, and tertiary products. Thus,  $d[\text{product}]/d[\text{neopentane}]$  is a maximum initially for the primary products, 3,3-dimethyloxetane and 2-butene, but the other curves show a definite autocatalytic character. Further, the secondary products, acetone and propylene, are formed at a maximum rate when the primary products are at maximum concentration. A similar relationship also exists between the concentrations of the tertiary product, C<sub>2</sub>H<sub>4</sub>, and the secondary product, propylene. A reaction scheme accounting for the major products can be written as shown opposite.

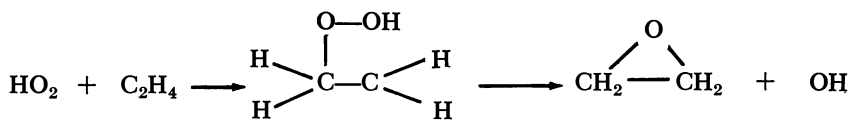
The reaction paths can be confirmed simply by adding intermediates to reacting mixtures of H<sub>2</sub> + O<sub>2</sub>. Thus, when 2-butene is added, the primary products are propylene, acetone, isobutyraldehyde, CH<sub>4</sub>, and HCHO. Propylene gives C<sub>2</sub>H<sub>4</sub>, C<sub>2</sub>H<sub>5</sub>CHO, HCHO, CH<sub>3</sub>CHO, and CH<sub>4</sub> as primary products. 3,3-Dimethyloxetane has not been added to date, and its oxidation products are thus not clear. Its structure would be consistent with acetone and isobutyraldehyde as major oxidation fragments.

### Discussion

In a number of cases, an addition reaction of OH radicals to olefins has been required to explain several of the major products. Although OH abstracting from olefins and HO<sub>2</sub> reactions with olefins can also explain some of the products, only the addition reaction is uniquely satisfactory. Thus, it is difficult to see how CH<sub>3</sub> radicals, required to explain the presence of methane, can be obtained from C<sub>2</sub>H<sub>3</sub> radicals which would be formed in an abstraction reaction of OH with C<sub>2</sub>H<sub>4</sub>. Similarly, while acetone and propylene can be plausibly formed if HO<sub>2</sub> attack is mainly responsible for the removal of 2-butene, it is not easy to see how the large quantities of methane are produced. It is not possible, of course,



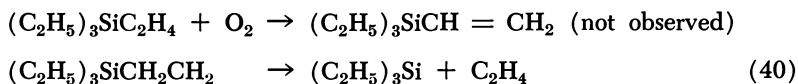
to rule out OH abstraction and  $\text{HO}_2$  reactions completely. Indeed, OH abstraction reactions are probably sufficiently fast to play a major part in the product sequence. Further, it is likely that  $\text{C}_2\text{H}_4\text{O}$  is formed by  $\text{HO}_2$  attack on  $\text{C}_2\text{H}_4$ , perhaps as follows.



It is interesting to compare the reactions of the different species of alkyl radical in the  $\text{H}_2 + \text{O}_2$  environment at  $480^\circ\text{--}500^\circ\text{C}$ .  $\text{CH}_3$  radicals react at almost the same rates with  $\text{H}_2$  and  $\text{O}_2$  at pressures of 500 mm. Hg. The only detectable oxidation product is  $\text{HCHO}$  but the molecularity of the reaction is uncertain as discussed earlier.  $\text{C}_2\text{H}_5$  radicals appear to react almost uniquely with  $\text{O}_2$  to give  $\text{C}_2\text{H}_4$  and  $\text{HO}_2$ . Small quantities of  $\text{CH}_3\text{CHO}$  are formed, either directly or possibly through the intermediate formation of  $\text{C}_2\text{H}_5\text{OO}$ , which may then give  $\text{CH}_3\text{CHO}$  at the surface.

Neopentyl radicals either decompose to give 2-butene and  $\text{CH}_3$  radicals or react with  $\text{O}_2$  to form 3,3-dimethyloxetane. No pivalaldehyde is detected, and the variation of  $\Delta(\text{neopentane})/\Delta(\text{H}_2\text{O})$  with mixture composition rules out any significant reaction of neopentyl radicals with  $\text{H}_2$ . The formation of the dioxetane in large quantities suggests that  $\text{RO}_2$  radicals have a definite existence at  $500^\circ\text{C}$ . and are stable enough to allow ring closure and elimination of the OH radical. The absence of pivalaldehyde even in trace amounts indicates that aldehydes are not easily formed from reactions of alkyl radicals with  $\text{O}_2$  and suggests that the reactions of  $\text{CH}_3$  and  $\text{C}_2\text{H}_5$  with  $\text{O}_2$  to give  $\text{HCHO}$  and  $\text{CH}_3\text{CHO}$  respectively are probably complex.

A further type of reaction of alkyl radicals has been found by studying the addition of tetraethylsilane to the  $\text{H}_2 + \text{O}_2$  reaction. Here the only primary carbon-containing products were  $\text{CH}_3\text{CHO}$  and  $\text{C}_2\text{H}_4$ , with no trace of triethylvinyl silane, the anticipated product by analogy with the behavior of simple alkyl radicals. Furthermore, the carbon balance in the early stages of reaction was virtually accounted for by  $\text{CH}_3\text{CHO}$  and  $\text{C}_2\text{H}_4$  alone. If triethylvinyl silane had been formed in significant amounts, it would have been detected since it proved to be no more reactive than tetraethylsilane when added to the  $\text{H}_2 + \text{O}_2$  reaction. The products can be explained by the following reaction sequence.





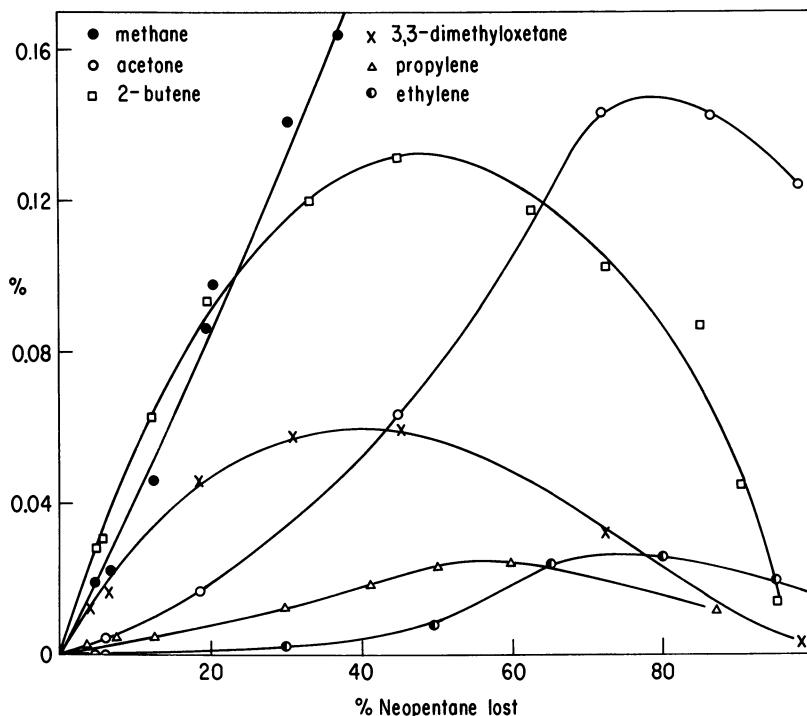
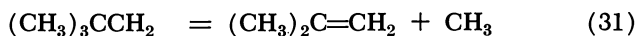
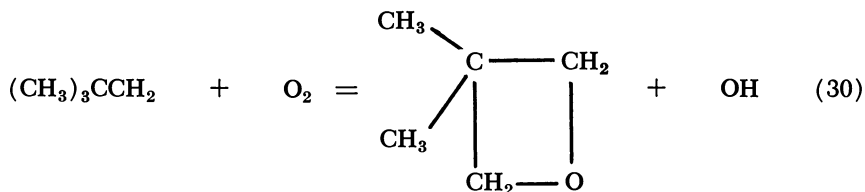
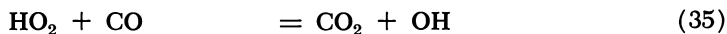


Figure 5. Variation of products with neopentane loss; 51-mm. vessel, 480°C.,  $H_2 = 140$  mm. Hg,  $O_2 = 70$  mm. Hg, total pressure = 500 mm. Hg

similar, and the percent of each lost must be about the same. Likewise, if acetone and propylene are formed only from the attack of 2-butene by OH radicals, then using the acetone to propylene ratio at 20% loss of neopentane,  $k_{32}/k_{33} = 2.2$ ; this ratio will be modified if significant amounts of acetone are formed as primary products from 3,3-dimethyloxetane.





CO and CO<sub>2</sub> are major products, especially in the later stages when neopentane is used. If it is assumed that all the CO<sub>2</sub> is formed by the reaction of OH radicals with CO (Reaction 34) and that H<sub>2</sub>O is formed principally from OH + H<sub>2</sub> (Reaction 1), then  $k_{34}/k_1$  is given by

$$\frac{[\text{H}_2]d[\text{CO}_2]/dt}{[\text{CO}]d[\text{H}_2\text{O}]/dt}$$

Measuring CO<sub>2</sub> using gas chromatography and H<sub>2</sub>O as pressure change,  $k_{34}/k_1 = 0.7$ . Studies (2) of the CO/H<sub>2</sub>/O<sub>2</sub> system using 1% CO have given  $k_{34}/k_1 = 0.61$ , making similar assumptions to those above. A more precise treatment has shown that Reaction 35 as well as Reaction 34 is responsible for removing CO. Thus, the ratios really represent a combination of the effects of Reactions 34 and 35. However, the closeness of the results from the two studies is gratifying and suggests that most of the CO<sub>2</sub> in the neopentane system is formed from gas-phase reactions of CO.

### Conclusions

The preliminary results presented in the paper indicate the scope of the method both for studying the attack of the radicals H, O, OH, and HO<sub>2</sub> on the additive and for investigating the behavior of the radicals formed in the primary attack. The method can be applied to a wide range of additives, and the information that can be obtained is being extended further by using D<sub>2</sub> + O<sub>2</sub> mixtures.

### Acknowledgment

Part of this work has been supported by the United States Air Force under Grant No. AF EOAR 65-68 through the European Office of Aerospace Research (OAR). A grant to D. E. H. from the Science Research Council is also gratefully acknowledged.

### Literature Cited

- (1) Appleby, W. G., Avery, W. H., Meerbott, W. H., Sartor, A. F., *J. Am. Chem. Soc.* **75**, 1809 (1953).
- (2) Baldwin, R. R., Jackson, D., Walker, R. W., Webster, S. J., "10th International Combustion Symposium," p. 423, Combustion Institute, Pittsburgh, Pa., 1965.
- (3) Baldwin, R. R., Simmons, R. F., *Trans. Faraday Soc.* **51**, 680 (1955).
- (4) Baldwin, R. R., Mayor, L., *Trans. Faraday Soc.* **56**, 80, 103 (1960).
- (5) Baldwin, R. R., Jackson, D., Walker, R. W., Webster, S. J., *Trans. Faraday Soc.* **63**, 1665, 1676 (1967).

- (6) Baldwin, R. R., Norris, A. C., Walker, R. W., "11th International Combustion Symposium," p. 889, Combustion Institute, Pittsburgh, Pa., 1967.
- (7) Baldwin, R. R., Hopkins, D. E., Norris, A. C., Walker, R. W., unpublished work.
- (8) Baldwin, R. R., Langford, D., Walker, R. W., unpublished work.
- (9) Baldwin, R. R., Everett, C. J., Walker, R. W., submitted for publication.
- (10) Benson, S. W., private communication.
- (11) Eaborn, C., "Organo-Silicon Compounds," Butterworths and Co., London, 1965.
- (12) Kerr, J. A., *Chem. Rev.* **66**, 465 (1966).
- (13) Knox, J. H., Turner, J. M. C., *J. Chem. Soc.* **1965**, 3491.
- (14) Knox, J. H., *Combust. Flame* **9**, 297 (1965).
- (15) Knox, J. H., Wells, C. H. J., *Trans. Faraday Soc.* **59**, 2861 (1963).
- (16) McMillan, G. R., Calvert, J. G., "Oxidation and Combustion Reviews," C. F. H. Tipper, ed., Vol. 1, p. 93, Elsevier, Amsterdam, 1965.
- (17) Minkoff, G. J., Tipper, C. F. H., "Chemistry of Combustion Reactions," Butterworths and Co., London, 1962.
- (18) Whittle, E., Steacie, E. W. R., *J. Chem. Phys.* **21**, 993 (1953).
- (19) Wilson, W. E., Westenberg, A. A., "11th International Combustion Symposium," p. 1143, Combustion Institute, Pittsburgh, Pa., 1967.

RECEIVED February 5, 1968.

## Some Current Views of the Mechanism of Free Radical Oxidations

SIDNEY W. BENSON

Department of Thermochemistry and Chemical Kinetics, Stanford Research Institute, Menlo Park, California 94025

*The low and high temperature mechanisms for hydrocarbon oxidation are reviewed. The mechanism of olefin formation above 250°C. is considered in detail, and it is concluded that it occurs via a bimolecular H atom transfer rather than as a rearrangement of an RO<sub>2</sub>' radical. This latter conclusion devolves upon a high activation energy (> 12 kcal.) for RO<sub>2</sub>' + SH → RO<sub>2</sub>H + S when SH has a tertiary H atom. The interaction of two RO<sub>2</sub>' to form 2RO· + O<sub>2</sub> is considered with reference to some of the high activation energies reported for this step and the possibility of H atom abstraction to form RO<sub>2</sub>H plus the Criegee zwitterion. >C=O → O. Some new wall effects are discussed briefly.*

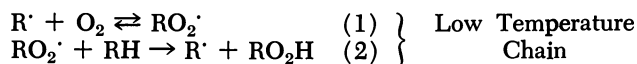
**A**t this type of meeting one becomes keenly aware of the controversial and unsolved problems that exist in the field under discussion. To put these problems in better perspective, I should like to spend some time discussing three points: (1) areas of agreement which have been reached in the field of free radical oxidation; (2) problems which are definitely unsettled at the moment, and about which there appears to be appreciable controversy; (3) and finally, some of the unknown features of oxidations whose parameters are still not resolved.

Within the last 15 years, the field of chemical kinetics, particularly gas phase kinetics, has undergone considerable change. One might almost be tempted to term this revolutionary. The nature of this change is that a large body of quantitative data has been accumulated about elementary unimolecular reactions and bimolecular reactions involving radicals,

atoms, and molecules. This quantitative data takes the form of specific rate constants at specified temperatures, and for many of these rate constants we know also the Arrhenius parameters—*i.e.*, the Arrhenius *A* factor and the activation energy.

Another result which has emerged during this period is that radical reactions in the gas phase, and in not strongly polar solvents, do not differ appreciably in their kinetic parameters. Differences which appear to exist can be traced back to fairly well understood kinetic phenomena.

Organic oxidations can be divided roughly into low temperature and high temperature regimes. The papers we have heard in this session seem to show general agreement on what has been termed the low temperature chain. This is indicated by Reactions 1 and 2 below.



The major product of this chain is the alkyl hydroperoxide. The secondary products which are observed are the results of the reactions of alkyl radicals in the system with the hydroperoxide or of the secondary spontaneous breakdown of the hydroperoxide if the temperature is sufficiently high. This chain mechanism predominates in the temperature regime from about 30° to about 250°C., for the gas phase or in relatively inert solvents.

Above 250°C. we approach, in the gas phase, what is known as the cool flame regime. This is characterized by induction periods and by the appearance of pressure peaks and luminescent phenomena in the oxygen-hydrocarbon system. The consensus of present data seems to support the contention that these cool flames arise from the secondary decomposition of the hydroperoxides produced by the low temperature chain. The unimolecular decomposition of the hydroperoxide yields active alkoxy and hydroxyl radicals:



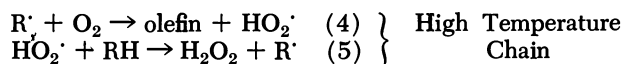
The bond strength for the hydroperoxide scission is about 43 kcal., and the *A* factors are expected to be around  $10^{15}$  sec.<sup>-1</sup>.

With these parameters, the half-life of a typical hydroperoxide is about 1 second at 330°C. and about 10 seconds at 290°C. These short lifetimes permit the hydroperoxides to act as secondary initiation sources to increase the rate of hydrocarbon decomposition. This is the effect that has been described by Semenov and his co-workers as degenerate chain branching.

In about the same temperature region—*i.e.*, of the cool flame phenomena—one begins to see also a negative temperature coefficient in the

rate of chain oxidation. Several papers in the last three years have shown that the absolute rate of oxidation of a 1:1 hydrocarbon-oxygen mixture, for example, at fixed contact times, decreases with increasing temperature from about 300° to about 350°C. From about 350° to 400°C. the rate begins to accelerate again until finally at temperatures above 420°C., one reaches the normal explosion limit (9, 14, 15, 16, 17).

This region of negative temperature coefficient can be quantitatively ascribed to the failure of the system to produce alkyl hydroperoxide as a product at the higher temperatures. Instead, with increasing temperature because of the reversibility of Reaction 1, the equilibrium concentration of alkyl peroxy radicals decreases in favor of alkyl radicals, and the high temperature mechanism supersedes the low temperature mechanism (Reactions 4 and 5).



The result of this change in mechanism is that the major products at high temperatures are olefins and hydrogen peroxide and their secondary decomposition products, which of course include water. The relatively unstable alkyl hydroperoxide produced by the low temperature chain is replaced by the much more stable hydrogen peroxide. The result is that the secondary initiation, responsible for the cool flames, is replaced by a much slower initiation—the second-order decomposition of hydrogen peroxide (Reaction 6).

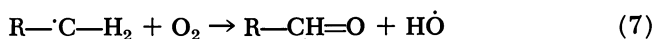


This second-order decomposition of hydrogen peroxide has been studied independently, and its rate parameters are known. The activation energy is *ca.* 48 kcal., and its lifetime is about 1 second at about 900°K. At temperatures of *ca.* 450° to 550°C., it proceeds at a sufficiently rapid rate to be responsible for initiating the normal explosion limit, which one finds for stoichiometric hydrocarbon-oxygen mixtures.

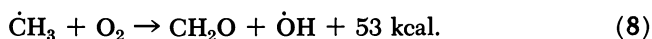
There appears to be a general agreement about the over-all nature of these chain systems and the secondary initiations which occur in them. There is, however, not so widespread an agreement about the details of how some of these step reactions occur.

In particular, the question has been raised about whether Reaction 4 occurs as a simple atom transfer in a bimolecular collision between the radical  $R\cdot$  and  $O_2$ , or whether it goes thru the same type of peroxy radical structure as Reaction 1. This problem has its roots deep in the history of oxidation kinetics, and early examples occur during the 1930's. At that time several authors, inspired more by the need to explain products than by the constraints of any detailed transition state theory, were

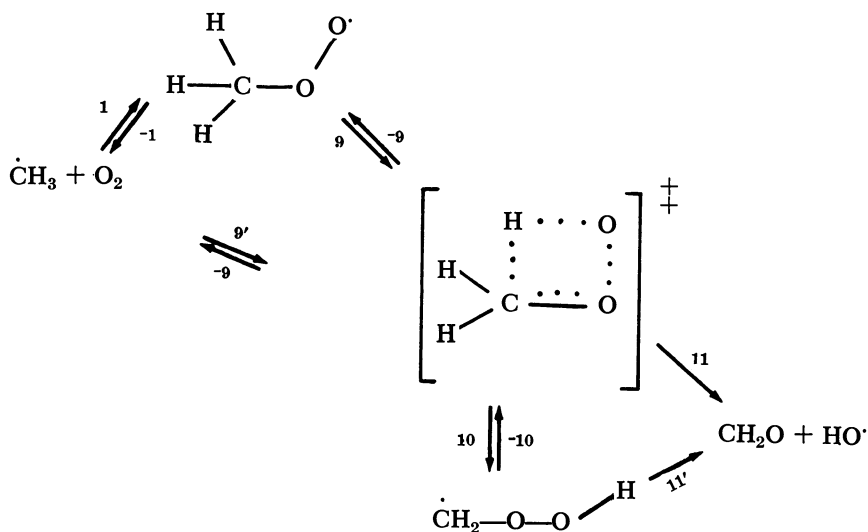
inclined to write as a propagation step, the reaction of  $R\cdot + O_2$  to give carbonyl compounds plus hydroxyl radicals (Reaction 7).



I have spent some time trying to explore the experimental basis for such a reaction, and at the moment I feel that there is no good experimental foundation for writing it. From a structural point of view, it appears to be a highly unlikely reaction. The simplest example of such a reaction would be the reaction of methyl radicals with oxygen to produce formaldehyde, plus hydroxyl radical (Reaction 8)



This reaction is exothermic by 53 kcal., and a number of authors have felt that this large exothermicity can provide the reaction's driving force. However, if one begins to examine the details of such a reaction, then one must consider that it must occur either thru a precursor alkylperoxy radical in competition with Reaction 1, or else that it occurs as a four-center reaction. This is illustrated below.



However, we must recognize that the large driving force for this reaction comes from two sources: (1) the formation of the carbon-oxygen single bond—Reaction 1—which is exothermic by about 28 kcal. This initially

forms the hot alkylperoxy radical; (2) the second stage of the reaction is the formation of the C=O  $\pi$ -bond, and the over-all change here is exothermic by only 28 kcal. However, the  $\pi$ -bond is 75 kcal. in formaldehyde, for example, and no fraction of this is expected to appear until a considerable amount of double bond character is already present between carbon and oxygen. This would be described by Reaction 11 in the above scheme.

In either case, one has to proceed through a four-centered complex for which there is no appreciable driving force and for which all evidence indicates an order of 20 to 26 kcal. of strain energy. In addition, the A factor for such a reaction, because it involves a tight transition state with loss of internal rotation, is expected to be low by about a factor of 10. The over-all result is that one expects a four-centered transition state, a relatively high activation energy, and a relatively low A factor.

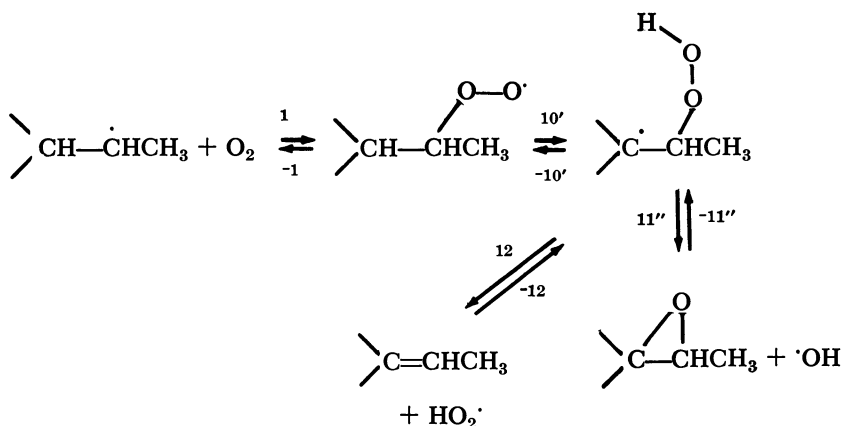
Neil Spokes and I, in this laboratory (SRI), have studied some of the reactions of radicals with oxygen from 500°K., for the methyl radical, to 1500°K. (7). The technique is the method of very low pressure pyrolysis (VLPP), which has been described recently (6). For methyl radicals we found that there is no measurable reaction over this entire temperature range after 10,000 collisions of methyl with oxygen. From these results, we can assign a lower limit to the activation energy for Reaction 8, of 24 kcal.

If this is correct, it means that no basis exists in any of the systems reported for this reaction since competing reactions are always several powers of 10 faster.

The last argument which has been raised favoring this reaction is that the 28 kcal. of bond energy liberated in forming the methylperoxy radical produce a hot species, which in the next step then can use these 28 kcal. to abstract internally the hydrogen atom and isomerize to the hydroperoxy alkyl radical, shown in the diagram above as Step 10. However, such a step is very slow compared with the back reaction of dissociation, Step -1, or the more probable thermalization of the hot methylperoxy radical by collisions with other molecules.

It should also be noted that Step 10 is thermodynamically uphill by about 3 to 4 kcal., so that if it did occur, the back reaction (-10) should be very rapid. In any case, anyone who seriously employs a reaction of this type should think carefully about the experimental evidence in favor of it.

Let us now return to the question of the mechanism of Reaction 4. It has been suggested that olefins may arise from the internal isomerizations of alkylperoxy radicals. The path for such a reaction is shown as follows.



The maximum fraction of conversion of alkylperoxy to olefin by such a mechanism is given by the ratio  $k_{10}'/[k_{10}' + k_{-1} + k_2(\text{RH})] = [1 + k_{-1}/k_{10}' + k_2(\text{RH})/k_{10}']^{-1}$ . From transition state theory (4) we can estimate the A factor for Step 10' as  $10^{11.5 \pm 0.3} \text{ sec}^{-1}$ , while  $k_1$  has been measured at  $10^{9.6} \text{ liter/mole sec.}$  (8). Using the estimated  $\Delta S_1$  (4) we calculate  $A_{-1} = 10^{15.3} \text{ liter/mole-sec.}$  The activation energy for Reaction -1 is equal to the endothermicity of 27 kcal. (5).

The activation energy of 10' can be estimated as the sum of its endothermicity—4.5 kcal.; the strain energy of the five-membered transition state ring—6.3 kcal. (4)—and the normal activation energy for hydrogen atom abstraction. Some results in this volume favor a value for the latter of from 16 to 18 kcal. for abstraction by  $\text{RO}_2\cdot$  from a tertiary C—H bond (1). If the value is high, then  $E_{10}' \sim 27 \text{ kcal.}$ , and the fractional conversion is  $\lesssim k_{10}'/k_{-1} = 10^{-3.8}$ . The competing path to produce olefin is the exothermic metathesis, Reaction 4. We can estimate  $A_4 \geq 10^{8.7} \text{ liter/mole-sec.}$  and can only guess at an activation energy of about 3 kcal. However, even if the activation energy were 6 kcal., the rate of production of olefin *via* Reaction 4 at  $300^\circ\text{C.}$  would still be about eight times faster than the maximum rate *via* the intramolecular rearrangement mechanism.

There is related evidence from the studies by Rust (13) on the oxidations of neat 2,3- and 2,4-dimethylpentanes that the strain energy in the five-membered ring is higher than 6.3 kcal. Rust found mainly diperoxy compound from the oxidation of the 2,4-isomer, showing that the internal hydrogen atom abstraction from the  $\gamma$ -carbon atom competes favorably ( $\sim 19$ -fold faster) with external abstraction of a similar hydrogen atom. With estimated A-factors of  $10^{10.8} \text{ sec}^{-1}$  and  $10^{8.3} \text{ liter/mole-sec.}$ , respectively for the internal and external abstractions and an effective liquid phase concentration of tertiary C—H bonds of  $\sim 10M$ , we predict a ratio

of 30:1 for the ratio of di- to monosubstituted products, in reasonable agreement with the observed ratio of 19:1. The close agreement suggests that activation energies for internal and external abstraction cannot differ by more than 1 kcal.

Experiments with the 2,3-dimethylpentane gave no measurable di-substitution. If we assume that it is less than  $10^{-2}$ , and use  $A$  factors of  $10^{11.5}$  sec.<sup>-1</sup> and  $10^{8.3}$  liters/mole-sec. for the internal ( $\beta$ -abstraction) and external abstraction, respectively, then we conclude that the activation energy for internal abstraction is at least 8.0 kcal. larger than that for external abstraction. This is significantly higher than the 6.3 kcal. strain energy of a five-membered ring used in the preceding calculation.

If the activation energy for tertiary hydrogen atom abstraction by an  $RO_2'$  radical is only 12 kcal., then the  $\beta$  internal abstraction from a secondary  $CH_2$  will have an activation energy of only 24.5 kcal. (using 8 kcal. strain), and it is possible for the internal and external olefin production to be competitive at 300°C. if  $E_4 = 6$  kcal., but not if  $E_4 = 3$  kcal.

There is one last experimental result arguing for a high activation energy for internal  $\beta$ -C—H abstraction. When Steps 11'' and 12 compete, epoxidation (Step 11'') always seems to be faster than olefin formation (Step 12). This is true in the HCl catalyzed, chain decomposition of *tert*-Bu<sub>2</sub>O<sub>2</sub> which produces isobutylene oxide and negligible isobutene (2) *via* a peroxyalkyl radical. Similar behavior is observed from the addition of HO<sub>2</sub>' and RO<sub>2</sub>' to olefins, which produce mainly ethers or epoxides at rapid rates (12). Note that although we estimate  $A_{12} \sim 10^{13.4}$  sec.<sup>-1</sup> and  $A_{11''} \sim 10^{11.5}$  sec.<sup>-1</sup>, Step 12 is endothermic by  $\sim 11$  to 13 kcal., while Step 11'' is exothermic by 10 to 17 kcal. A reasonable estimate for  $E_{12}$  is 20 kcal., while  $E_{11''}$  has an upper limit of 16 kcal., and some data (12) point to a value closer to 10 kcal.

Detailed studies of the quantitative kinetic reactions of radicals have shown that the transition states which involve either pentavalent carbon or trivalent oxygen generally require high activation energies. At the moment I can think of only one example of a gas phase reaction which involves pentavalent carbon for which an authentic experimental basis has been presented—*i.e.*, the thermoneutral attack of I atoms on cyclopropane to form  $\cdot CH_2CH_2CH_2I$  radical. The activation energy is *ca.* 18 kcal. (3). Even trivalent oxygen, which seems a little more reasonable, has relatively few examples. The only class for which there seems to be fairly strong evidence is the epoxidation reaction of hydroperoxyalkyl radicals. The activation energies appear to be in the neighborhood of 15 kcal., although the reactions are appreciably exothermic (*see*, however, Ref. 11).



disproportionation of primary and secondary alkylperoxy radicals is possible with the production of the well-known zwitterion (Reaction 15).



This reaction is certainly exothermic and by analogy with similar hydrogen abstraction reactions might be expected to have an activation energy of anywhere from zero to 8 kcal. If it should be proved that this is the terminating interaction or a possible terminating interaction of primary and secondary alkylperoxy radicals, then we must begin to think anew about the entire mechanism for the over-all chain decomposition and oxidation of hydrocarbons. I believe it would also require us to review seriously our interpretation of the spin resonance work on alkylperoxy radicals at low temperatures.

In this unknown area, we can place the question of the nature and composition of oxygenated species which occur in these systems. Considerable dispute surrounds the origin of the epoxides. There is even further question about the nature of the processes responsible for the destruction of the epoxides.

In this regard, it is well to remember the role which the wall plays on the nature of the products obtained from gas phase oxidation. There is certainly common agreement that walls and wall reactions are important in this respect. For example, Hay *et al.* (11) have shown the importance of the walls in determining the nature and composition of the oxygenated products from 2-butane + O<sub>2</sub> at 270°C. Cohen's study on the photo-oxidation of acetone also illustrates this point (10). He found that if acetone is photolyzed by itself in a quartz vessel, the normal products—methane, ethane, carbon monoxide, and methyl ethyl ketone—are produced.

However, if the photochemical reaction is run in the presence of oxygen, then of course, the methyl radicals are oxidized, and one obtains instead methanol, formaldehyde, and their decomposition products. Now, if the vessel is pumped out after a photo-oxidation and once again a normal photolysis of acetone is run, the products in the first 10 or 15 minutes are still oxidation products rather than hydrocarbon products. It takes from 15 to 30 minutes to remove whatever it is that is attached to the wall before the normal photochemical decomposition of pure acetone products are produced. These results should remind us that oxidation systems do produce species, some of which are not known or understood.

In conclusion, if one is to work in the field of radical oxidation of hydrocarbons or organic compounds, he must remember that there are strong constraints on the mechanisms which we may write. Arrhenius parameters are no longer mysterious numbers but can be related with

reasonable precision to molecular structure. Similarly, activation energies for many reactions can be inferred from analogous reactions with reasonable precision. These constraints should limit greatly the diversity of schemes which may be constructed to account for given sets of products. In particular, it should constrain appreciably some of the more fanciful imaginative efforts which have appeared in the past literature.

This meeting has been extremely successful in bringing together workers from different fields, who in the past have generally tended to ignore each others' work. I hope that this meeting will bring about a closer collaboration among these groups in the future.

### Literature Cited

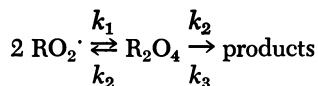
- (1) Allara, D., Hendry, D. G., Mayo, F. R., Mill, T., *ADVAN. CHEM. SER.* **76**, 40 (1968).
- (2) Batt, L., Benson, S. W., Flowers, M., *J. Chem. Phys.* **37**, 2662 (1962).
- (3) Benson, S. W., *J. Chem. Phys.* **34**, 521 (1961).
- (4) Benson, S. W., "Thermochemical Kinetics," Chap. III, Wiley, New York, 1968.
- (5) Benson, S. W., Shaw, R., *ADVAN. CHEM. SER.* **75**, 288 (1968).
- (6) Benson, S. W., Spokes, G. N., *J. Am. Chem. Soc.* **89**, 2525 (1967).
- (7) Benson, S. W., Spokes, G. N., unpublished results.
- (8) Calvert, J. G., Dingley, D. P., *J. Am. Chem. Soc.* **85**, 856 (1963).
- (9) Chung, Y. H., Sandler, S., *Combust. Flame* **6**, 295 (1962).
- (10) Cohen, A., *J. Chem. Phys.* **47**, 3828 (1967).
- (11) Hay, J., Knox, J. H., Turner, J. M. C., *10th Symp. Combust.* 331 (1965).
- (12) Hendry, D., personal communication.
- (13) Rust, F. F., *J. Am. Chem. Soc.* **79**, 4000 (1957).
- (14) Salooja, K. C., *Combust. Flame* **6**, 275 (1962).
- (15) *Ibid.*, **8**, 311 (1964).
- (16) *Ibid.*, **9**, 219 (1965).
- (17) *Ibid.*, p. 373.

RECEIVED February 2, 1968.

## Discussion

**C. Walling:** In the discussion at this session an interesting contradiction has arisen which needs to be resolved. Extensive data on liquid phase autoxidations near room temperature indicate that bimolecular interactions of peroxy radicals (particularly tertiary peroxy radicals) are slow processes with appreciable activation energies. In contrast, analysis of high temperature gas-phase processes indicate fast interactions occurring at almost every collision.

A possible reconciliation is the recognition that these reactions are composite processes:



where step 1 is slightly exothermic. If  $E_3 > E_2 > E_1$ , the decomposition of the tetroxide (3) could be rate controlling at low temperatures, and the initial low activation energy, Step 1, could be rate controlling at high temperatures. Bartlett and Guaraldi [*J. Am. Chem. Soc.* **89**, 4799 (1967)] have recently reported convincing evidence for tetroxide formation and stability at low temperatures ( $-100^\circ\text{C}$ .), but my proposal does require a peculiar and unexpected relation between pre-exponential factors,  $A_3 \gg A_2$ .

## The Influence of Environmental Factors on the Activity of Homogeneous Oxidation Catalysts

C. F. CULLIS

The City University, St. John Street, London, E.C.1, England

This brief introduction will emphasize the connecting theme which runs through the five main chapters in the section on the homogeneous catalysis of oxidation processes. It is well known that the reaction of organic compounds with oxygen, both in the gas and liquid phase, generally takes place by a free radical chain mechanism. The observed over-all influence of a catalyst is therefore the sum of its separate effects on the various constituent stages. Thus, a given additive may exert quite distinct influences on the initiation, propagation, and termination steps, and the magnitudes of these separate influences—and hence the balance between them—will in general depend on various factors. In many systems, the opposing influences of a particular catalyst on the various reaction stages may be quite delicately balanced. However, this balance may change sharply with experimental conditions, and sometimes an additive, which in one set of circumstances acts as a catalyst, may under only slightly different conditions inhibit oxidation. All subsequent papers in this section deal with the oxidation of organic compounds in the presence of additives which may, according to the prevailing conditions, act either as catalysts or as inhibitors of the over-all reactions concerned. These studies shed valuable light on the interplay between the initiation, propagation, and termination steps and yield useful information about these separate processes.

The chapter by K. C. Salooja is the only one which deals specifically with the homogeneous catalysis of the gaseous oxidation of organic compounds, and it is concerned in particular with the influence of temperature on the catalytic activity of additives. In general, halogen compounds exert a dual effect on gaseous oxidation reactions, according to the experimental conditions. Thus, the predominant mode of action at relatively low temperatures of a compound such as hydrogen bromide is to promote oxidation by enhancing chain initiation (5) or chain branching

(1). In flames, on the other hand, this compound exerts a well-defined inhibiting effect, mainly as a result of the replacement of highly reactive radicals by much less active bromine atoms (7, 10). The present systematic investigation of the influence of a wide variety of halogen compounds shows that the action of these additives arises principally from the halogen atoms and hydrogen halides formed on oxidative degradation (5). Special attention has been paid to the temperature range 700° to 1000°C. where, with a wide variety of organic fuels and halogen compounds, the promoting influence of the additive gradually changes to an inhibiting effect. This transition is ascribed to the replacement, as the temperature is increased, of large relatively unreactive chain carriers such as HO<sub>2</sub> and RO<sub>2</sub> by smaller more active radicals such as H and OH. Halogen atoms are more effective chain-propagating entities than HO<sub>2</sub> and RO<sub>2</sub>, but they are not as reactive as H and OH which they replace when these species react with hydrogen halides. Thus, as the nature of the propagating radicals alters with increasing temperature, so the overall promoting effect of halogen compounds changes into an over-all inhibiting influence.

A somewhat similar dual effect of certain halogen compounds has recently been observed during studies of the gaseous oxidation of some olefinic polymers. Thus, hydrogen bromide inhibits the oxidation at *ca.* 400°C. of polyethylene (4), but it promotes the oxidation of polypropylene under otherwise identical experimental conditions (3). A similar contrast between the behavior of the two polymers is found when bromine is incorporated chemically into them (3). A possible explanation is that with polypropylene there is a net increase in the rate of chain propagation as a result of the relatively rapid attack of bromine atoms at the tertiary C—H bonds. The lower rate of abstraction of the somewhat less labile hydrogen atoms in polyethylene is, however, perhaps insufficient to counterbalance the enhanced chain-termination with the result that hydrogen bromide here exerts an over-all inhibiting influence. This is then a good example of how a relatively simple change in reactant structure may cause a given additive to change from a catalyst to an inhibitor.

The four remaining papers all deal with the catalysis of liquid-phase oxidation processes by transition metal ions (6). A. T. Betts and N. Uri show in particular how metal complexes can either catalyze or inhibit oxidation according to their concentration. In this investigation, various hydrocarbons (especially 2,6,10,14-tetramethylpentadecane) were used as substrates, and metal ions were present either as salicylaldimine or diisopropylsalicylate chelates. These compounds are considerably soluble in non-polar media, and this makes it possible to examine their effect over a much wider range of concentration than is usually accessible in this type of work. These studies show that catalyst-inhibitor conversion is always

observed with increasing catalyst concentration when there is direct competition only between first-order initiation, involving the metal chelate and molecular oxygen, and second-order termination, involving the reaction of alkylperoxy radicals with the metal chelate to form an inactive bidentate ligand. If, however, significant amounts of hydroperoxide have accumulated or are added at the start of the reaction, initiation involving the metal chelate and hydroperoxide is so efficient that the inhibiting influence is no longer observed.

Y. Kamiya illustrates the influence on catalytic activity of the form of the catalyst. Thus, in the cobalt-catalyzed oxidation of hydrocarbons in acetic acid solution, introduction of bromide ions increases the activity of the catalyst, especially when the metal ion concentration is fairly high. The presence of bromides also results in a marked increase in the proportion of carbonyl compounds among the products and it is believed that these are formed as a result of a propagation step in which bromine-containing cobaltous ions react with alkylperoxy radicals.

The chapter by C. J. Swan and D. L. Trimm, which also emphasizes the effect on catalytic activity of the precise form of a metal complex, shows too that, depending on the metal with which it is associated, the same ligand can act either as a catalyst or inhibitor. The model reaction studied was the liquid-phase oxidation of ethanethiol in alkaline solution, catalyzed by various metal complexes. The rate-determining step appears to be the transfer of electrons from the thiyl anion to the metal cation, and it is shown that some kind of coordination between the metal and the thiol must occur as a prerequisite to the electron transfer reaction (8, 9). In systems where thiyl entities replace the original ligands, quantitative yields of disulfide are obtained. Where no such displacement occurs, however, the oxidation rates vary widely for different metal complexes, and the reaction results in the production not only of disulfide but also of "overoxidation" and hydrolysis products of the disulfide.

Finally, J. F. Ford, R. C. Pitkethly, and V. O. Young show how, as a result of the chemical changes which the catalyst may undergo during the reaction, the delicate balance between chain initiation and chain termination can alter with time and hence give rise to complex and unusual kinetic relationships. Thus, in certain circumstances, the co-oxidation of indene and thiophenol, which is catalyzed by iron complexes, may exhibit behavior in which the reaction virtually ceases and then subsequently restarts spontaneously. In the early stages of reaction, initiation seems to occur by a redox chain cycle involving thiophenol, indene hydroperoxide, and the iron complex. As the reaction proceeds, however, the rate of initiation changes since the structure of the complex is altered as a result either of oxidative degradation or of the simple

replacement of the ligands therein. A detailed mechanism has been proposed which accounts satisfactorily for the rates of oxidation observed over the first 90% of the reaction.

All the work described in this section thus has a common theme inasmuch as it deals with the influence of various environmental factors on the activity of homogeneous oxidation catalysts. In particular, the results shed valuable light on the ways in which temperature, the structure of the organic substrate, the concentration and the form of the catalyst, and reaction time may all affect the nature and kinetics of the various competing stages involved in the reaction of organic compounds with molecular oxygen.

### *Literature Cited*

- (1) Allen, E. R., Tipper, C. F. H., *Proc. Roy. Soc.* **A258**, 251 (1960).
- (2) Bacon, R. G. R., *Chem. Ind.* **1962**, 19.
- (3) Carabine, M. D., Cullis, C. F., Groome, I. J., *Proc. Roy. Soc. (London)*, in press.
- (4) Cullis, C. F., Smith, D. J., *Trans. J. Plastics Inst.* **1967**, 39.
- (5) Cullis, C. F., Fish, A., Ward, R. B., *Proc. Roy. Soc.* **A276**, 527 (1963).
- (6) Denisov, E. T., Emanuel, N. M., *Russian Chem. Rev.* **29**, 645 (1960).
- (7) Fish, A., *Combust. Flame* **8**, 84 (1964).
- (8) Fraser, R. T. M., *Rev. Pure Appl. Chem.* **11**, 64 (1961).
- (9) Jones, M. M., Connor, W. A., *Ind. Eng. Chem.* **55** (9), 15 (1963).
- (10) Rosser, W. A., Wise, H., Miller, J., "Seventh Symposium on Combustion," p. 175, Butterworth and Co., London, 1959.

RECEIVED February 5, 1968.

## Catalyst-Inhibitor Conversion in Autoxidation Reactions

A. T. BETTS and N. URI

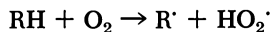
Ministry of Technology, Explosives Research and Development Establishment, Waltham Abbey, Essex, England

*Metal catalysis, which is claimed to have an important role in initiating autoxidation, appears to be so complex that in some systems catalysts are converted to inhibitors when their concentrations are increased. The additives examined include the N-butylsalicylaldimino and N-phenylsalicylaldimino chelates of cobalt(II), copper(II), nickel(II), and zinc as well as a number of 3,5-diisopropylsalicylato metal chelates. Some were autoxidation catalysts, some were inhibitors, and some exhibited catalyst-inhibitor conversion. Reaction mechanisms which account for most of the observed phenomena are proposed. The scope for developing metal chelates as antioxidants and the implications concerning the critical antioxidant concentration are outlined.*

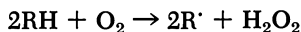
The major objective of this work was to understand better the effect of heavy metals in autoxidation reactions in view of the importance of trace metals in oils, fats, rubber, plastics, and other materials. Because of our interest in the stability of polyolefins such as polyethylene and polypropylene the major model substance used was 2,6,10,14-tetramethylpentadecane. With its four tertiary C—H bonds it is a suitable model for either polypropylene or branched polyethylene. Hexadec-1-ene was also used since its mono-olefinic character could be typical of some residual unsaturation in polyethylene. *N*-alkylamides served as model substances for polyamides, and a few experiments were also carried out with methyl linoleate. While studying the causes of initiation of the autoxidation of these substances we observed that certain compounds were catalysts at low concentrations but became inhibitors at higher concentrations. The phenomenon was called “catalyst-inhibitor conversion.”

### *Initiation of Autoxidation*

While it is generally accepted that autoxidation is a chain reaction involving  $R\cdot$  and  $RO_2\cdot$  radicals, the mechanism of initial free radical formation is both controversial and incompletely understood. To overcome the difficulties inherent in postulating the initiation step:



because of its large activation energy, the idea of termolecular initiation,



recently gained ground (3, 5, 7). Denisov demonstrated that in a significant number of autoxidation reactions the observed activation energy for initiation agreed well with the calculated value, but there appear to be important exceptions. Carlsson and Robb (3) presented evidence to support Denisov's mechanism but could not reconcile the observed activation energies for the initiation of Tetralin and indene autoxidation and those calculated using

$$E = (2D(R-H) - 138) \text{ kcal.}$$

where  $D(R-H)$  is the bond dissociation energy of the weakest C—H bond. This discrepancy could, however, be caused by the prior formation of hydrocarbon-oxygen complexes, an assumption which has been confirmed recently by a more detailed investigation (2). However, to obtain reproducible results and eliminate metal impurities it was necessary not only to purify the substrates by chromatography but also to coat reaction vessels with dimethyldichlorosilane. It is also interesting that Carlsson and Robb (3) ascribe large differences between the reaction rates for the initiation of indene autoxidation which they observed and those previously reported by Russell (17) to impurities under his experimental conditions. Further, Pitkethly (16) recently found that chromatography can introduce as much iron into hydrocarbons as it removes. The evidence of Carlsson and Robb would be more conclusive if it could be supported by analytical data concerning the trace metal content, which could be derived from neutron activation analysis for copper and cobalt and possibly from atomic absorption spectra for iron. While a direct reaction with molecular oxygen is feasible, evidence for the participation of trace metals was discussed in detail elsewhere (22). The *raison d'être* of this work was our interest in the initiation of autoxidation, and notwithstanding unexpected results at higher concentrations, the apparently essential even if relatively inefficient initiation step involving cobalt(II) chelates and molecular oxygen forms part of the basic explanation of the observed phenomena.

### Experimental

**Reagents.** Purification of 2,6,10,14-tetramethylpentadecane and hexadec-1-ene was described previously (1). Two different methods were used to prepare salicylaldimine chelates varying with the central metal atom. Bis(*N*-butylsalicylaldimino)nickel, bis(*N*-phenylsalicylaldimino)nickel, bis(*N*-butylsalicylaldimino)zinc (the phenyl complex could not be made), bis(*N*-butylsalicylaldimino)oxyvanadium(IV), and tris(*N*-butylsalicylaldimino)cobalt(III) were all prepared according to the method of Charles (4) for the copper(II) and nickel *N*-alkyl complexes. This method is based on the interaction of the amine, salicylaldehyde, and metal salt, usually the acetate. The method we used for preparing the copper(II) and cobalt(II) *N*-butylsalicylaldimines involves prior preparation of the salicylaldehyde metal complex (18). While this is optional for the copper chelates, it is essential for the bis(*N*-butylsalicylaldimino)cobalt(II). It is necessary to prepare the cobalt(II) chelate in an atmosphere of oxygen-free nitrogen, purified *e.g.*, according to Heaton and Uri (9). The purity of the compound was ascertained by microanalysis for C, H, N, and metal. This is usually sufficient for all the other salicylaldimines we prepared, but for the cobalt(II) chelate it was necessary to ascertain absence of cobalt(III) by thin-layer chromatography and by measuring the visible and near ultraviolet absorption spectrum using a freshly made ethyl alcohol solution. The spectra of the Co(II) and Co(III) chelates in ethyl alcohol are shown in Figure 1. The freshly made Co(II) solution has a light absorption peak at 360  $m\mu$  with a molar extinction coefficient of 8800. For a pure Co(II) chelate solution the ratio of extinction coefficients measured at 360 and 390  $m\mu$  (where the Co(III) chelate peak is situated) is 1.72. This ratio would decrease sharply as a result of Co(III) contamination.

Most diisopropylsalicylates were received as gift samples from E. W. Duck; some were prepared according to a method he suggested (6). Di(*n*-butylphosphonium)cobalt(II)dimethylglyoxime ( $C_{32}H_{64}N_4O_4P_2Co$ ) was a side product obtained by R. Simkins during the synthesis of  $CoR(D_2H_2)B$ , where  $R = C_6H_5$ ,  $B = P(n-C_4H_9)_3$  and  $DH =$  dimethylglyoxime (20). Zinc acetylacetonate was prepared according to Lappert and Truter (13).

**Procedures.** Oxygen uptake was measured with conventional Warburg apparatus at temperatures up to 60°C. Apiezon T grease was used because of its resistance to hot water. It was desirable to have silica gel with a moisture indicator in one of the sidearms for all hydrocarbon autoxidation experiments although this was optional with amides. When a significant amount of oxygen was taken up, the original pressure was restored so that any dependence of oxygen partial pressure on the rate of oxygen uptake would have been unlikely to produce any deviation greater than experimental error. The sensitivity of the apparatus allowed us to measure reaction rates between 1 and 500  $\mu$ liters/ml. substrate/hour.

Induction periods at temperatures over 60°C. were measured in a larger, modified version of the apparatus described by Martin (14). Boiling water was replaced as heating fluid by suitably thermostatted silicone oil (MS-550). The reaction flasks (25 or 50 ml. capacity) usually contained 1 gram of the sample, and where necessary built-in magnetic

stirrers were used. The flasks were connected to U-tube mercury manometers; the mercury level in the open manometer arm was followed by a hollow glass float connected to a balanced lever system so as to produce a trace parallel to the direction of chart movement, whose speed could be varied. The end of the induction period was marked by a change in the direction of the trace, whose slope can also be used to estimate the rate of oxygen consumption. Peroxide determinations were carried out according to Heaton and Uri (9).

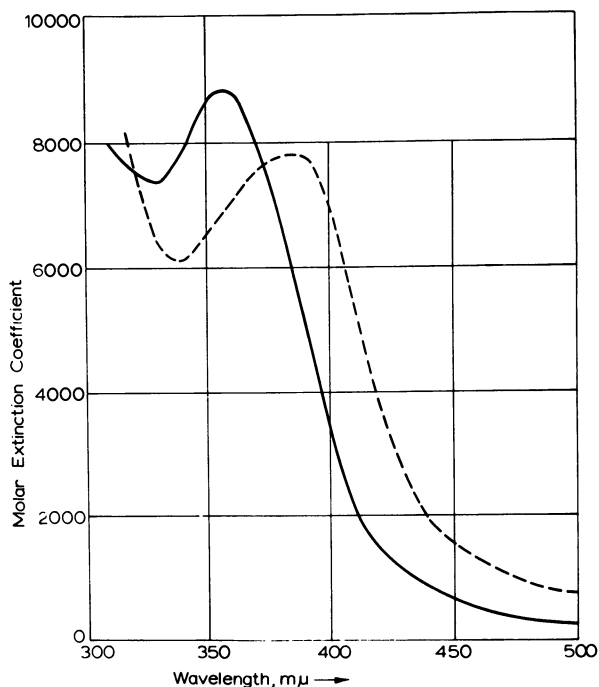


Figure 1. Absorption spectra of purified cobalt *N*-butylsalicylaldimines in ethyl alcohol

— *bis*(*N*-butylsalicylaldimino)cobalt(II)  
- - - *tris*(*N*-butylsalicylaldimino)cobalt(III)

## Results

**Catalyst-Inhibitor Conversion.** The system 2,6,10,14-tetramethylpentadecane-*bis*(*N*-butylsalicylaldimino)cobalt(II) at 50°C. illustrates well the observed catalyst-inhibitor conversion (Figure 2). At low concentrations up to  $M/20,000$  the metal chelate is a conventional catalyst; no induction period is observed, and the reproducible initial autoxidation rates are proportional to the square root of catalyst concentration. From the curves shown in Figure 2 catalyst deactivation becomes apparent at

a relatively early stage of the autoxidation reaction (11). The first indication of prolonged induction periods occurs at a cobalt concentration of  $M/10,000$  which becomes reproducible with carefully purified peroxide-free hydrocarbon when the cobalt concentration is increased to  $M/5000$ . This induction period increases to over 700 hours when the cobalt chelate concentration is increased to  $M/200$ , so that for all practical purposes it would be regarded as an efficient inhibitor. In this case, which generally applies to hydrocarbon autoxidation, inhibition is not carried beyond the induction period. This subsequent inhibition, however, applied in the system cobaltous acetate/*N*-butylacetamide at 50° and 60°C. (1). The latter is therefore a different type of catalyst-inhibitor conversion; this interesting difference can be explained fully on the basis of the postulated reaction mechanism.

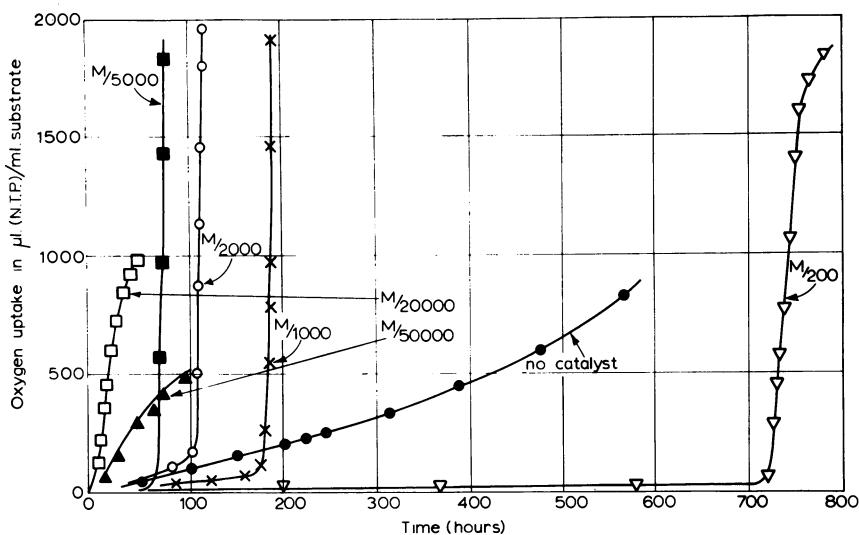


Figure 2. Autoxidation of 2,6,10,14-tetramethylpentadecane at 50°C. in the presence of bis(*N*-butylsalicylaldimino)cobalt(II)

**Effects of Different Metal Salicylaldimine Chelates.** Varying the central metal profoundly affected catalytic and inhibitory properties. There were only small quantitative variations, however, between *N*-phenyl- and *N*-butylsalicylaldimines having the same central metal atom. The only other salicylaldimines where catalyst-inhibitor conversion could be demonstrated were those of copper(II). With copper(II) both the catalytic and the inhibitory effects are much less pronounced than for cobalt(II). Surprisingly nickel(II) complexes behaved like conventional catalysts for hydrocarbon autoxidation—*i.e.*, the rate is proportional to

the square root of catalyst concentration. It is a weak catalyst compared with the corresponding cobalt(II) complex at concentrations where only catalytic effects exist, although it is noteworthy that at  $M/200$  bis(*N*-butylsalicylaldimino)nickel in TMPD at  $50^{\circ}\text{C}$ . the maximum rate of autoxidation approached  $50 \mu\text{liters/ml. substrate/hour}$ . The different behavior of nickel and copper complexes is illustrated in Figure 3.

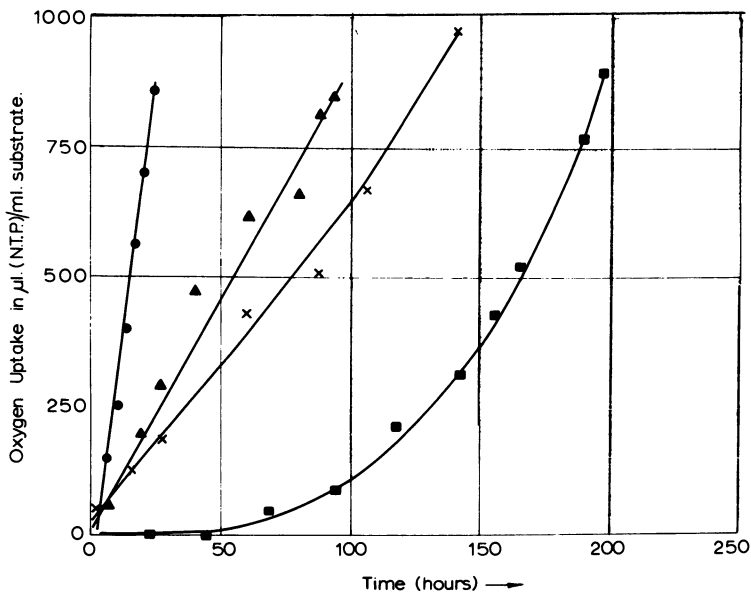


Figure 3. Autoxidation of 2,6,10,14-tetramethylpentadecane at  $50^{\circ}\text{C}$ . in the presence of nickel(II)- and copper(II) salicylaldimines

Catalyst: bis(*N,n*-butylsalicylaldimino)nickel(II)

▲ containing  $M/2000$  catalyst

● containing  $M/200$  catalyst

Catalyst: bis(*N,n*-butylsalicylaldimino)copper(II)

+ containing  $M/2000$  catalyst

■ containing  $M/200$  catalyst

In the autoxidation of *N*-butylacetamide all the salicylaldimine chelates showed only inhibitory effects. We also found that two salicylaldimine chelates showed no significant catalytic properties and exhibited only inhibitory effects even in hydrocarbon autoxidation—*viz.*, bis(*N*-butylsalicylaldimino)zinc and bis(*N*-butylsalicylaldimino)oxyvanadium(IV). While there are some well known antioxidants containing zinc (*e.g.*, zinc dialkylthiophosphates or zinc dithiocarbamates), this is not a general property for zinc compounds. Zinc acetylacetonate, for example, had no inhibitory effect in the autoxidation of hydrocarbons or amides.

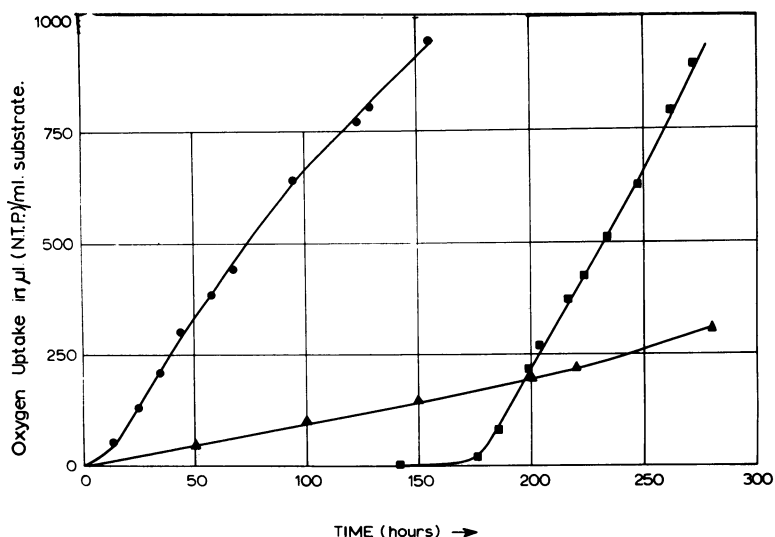


Figure 4. Autoxidation of 2,6,10,14-tetramethylpentadecane at 50°C. in the presence of bis(3,5-diisopropylsalicylato)cobalt(II)

Catalyst: bis(3,5-diisopropylsalicylato)cobalt(II)

- ▲ containing no catalyst
- containing M/20000 catalyst
- containing M/2000 catalyst

**Diisopropyl Salicylates and Other Chelates.** A variety of chelates with 3,5-diisopropyl-2-hydroxybenzoic acid as the ligand were examined to compare catalytic and inhibitory effects with those of the salicylaldimino chelates. There were remarkable similarities in the behavior of the cobalt and copper chelates, although there are some important qualitative and quantitative differences. Bis(diisopropylsalicylato)cobalt(II) was an efficient catalyst at  $M/20,000$  in the autoxidation of 2,6,10,14-tetramethylpentadecane and became an inhibitor as regards the lengthening of the induction period, when its concentration in the same substrate was increased in a manner analogous to that for bis(*N*-butylsalicylaldimino)cobalt(II). However, the autoxidation rates were well below those observed with cobalt salicylaldimine chelate in the higher concentration range. The inhibitory effect on the rate of autoxidation at the end of the induction period is not of the order of magnitude found in the system *N*-butylacetamide-cobaltous acetate; instead of a conventional square-root relationship for catalyst concentration the rate obtained at  $M/20,000$  appears to be a maximum. This is illustrated in Figure 4, where the previously reported effect of catalyst deactivation is just noticeable in the experiment containing the cobalt chelate at  $M/20,000$  when total oxygen

uptake exceeded 600  $\mu$ liters/ml. substrate. 3,5-Diisopropylsalicylatocopper(II) also produced the same phenomenon as the corresponding salicylaldimine chelate. At  $M/20,000$  the copper compound is a catalyst showing no significant induction period while at  $M/2,000$  (all in TMPD at  $50^\circ\text{C}.$ ) the induction period was approximately 120 hours. In contrast to the cobalt complexes there was no significant depression in the rate of autoxidation at higher copper concentrations at the end of the induction period. The nickel complexes show a considerable discrepancy: whereas the salicylaldimines behaved like conventional catalysts, bis(3,5-diisopropylsalicylato)nickel produced inhibitory properties only. Other chelates were examined; many, such as cobaltic, ferric, and nickel acetyl acetates, behaved like conventional catalysts. On the other hand di-(*n*-butylphosphonium)cobalt(II)dimethylglyoxime inhibited hydrocarbon and amide autoxidation without revealing any catalytic properties even at the lowest concentrations.

The inhibitory properties of the diisopropyl salicylate chelates were quite marked even at elevated temperatures. This applied particularly to the nickel(II) and chromium(III) complexes when tested as inhibitors in TMPD at a temperature as high as  $120^\circ\text{C}.$  These experiments were carried out at least in duplicate but frequently were repeated four times; once reasonable reproducibility was established, the induction period given in Table I was taken as the average of the experimental observations.

**Table I. 3,5-Diisopropyl Salicylato Metal Chelates as Inhibitors of Hydrocarbon Autoxidation<sup>a</sup>**

Chelate	Induction Period, Hours	
	TMPD	Hexadec-1-ene
DIPS Co(II)	509	392
DIPS Cu(II)	27	153
DIPS Ni(II)	>1,200	350
DIPS Cr(III)	>1,200	114

<sup>a</sup>  $T = 120^\circ\text{C}.$ , chelate concentration =  $M/200$ .

The inhibitory properties of the diisopropyl salicylato chelates were confirmed in high pressure polyethylene at elevated temperatures. A more detailed study of this application to polyethylene and other polymers is in progress.

**Catalysis and Inhibition.** The varied behavior of most of the metal chelates we studied is summarized in Tables II and III. Table II indicates which chelates exhibited catalyst-inhibitor conversion in TMPD at  $50^\circ\text{C}.$ , and generally, analogous observations were made with hexadec-1-ene. *N*-butyl- and *N*-phenylsalicylaldimino ligands are presented in Tables II and III as BuSal and PhSal, respectively; in addition the metal and its

valence are also given. The metal-free *N*-phenylsalicylaldimine base had neither catalytic nor inhibitory properties. DIPS stands for the 3,5-diisopropylsalicylato ligand. Table III gives a survey of inhibitory effects at elevated temperatures.

**Table II. Catalyst-Inhibitor Conversion in the Autoxidation of 2,6,10,14-Tetramethylpentadecane at 50°C.<sup>a</sup>**

Complex	M/20,000	M/2,000	M/200
(BuSal) <sub>2</sub> Co(II)	+	-	-
(BuSal) <sub>2</sub> Cu(II)	+	-	-
(BuSal) <sub>2</sub> Ni(II)	+	+	+
PhSalH	0	0	0
(PhSal) <sub>2</sub> Co(II)	+	-	Not sol.
(PhSal) <sub>2</sub> Cu(II)	+	-	-
(PhSal) <sub>2</sub> Ni(II)	+	+	Not sol.
(DIPS) <sub>2</sub> Co(II)	+	-	
(DIPS) <sub>2</sub> Cu(II)	+	-	
(DIPS) <sub>2</sub> Ni(II)	0	-	
(DIPS) <sub>3</sub> Cr(III)	0	-	

<sup>a</sup> Symbols: + = catalyst; - = inhibitor; 0 = no effect; no entry = not examined.

**Table III. Inhibition at 100° and 120°C. by M/200 Metal Chelate<sup>a</sup>**

Complex	TMPD at 100°C.	C <sub>16</sub> H <sub>32</sub> at 100°C.	C <sub>16</sub> H <sub>32</sub> at 120°C.	N-Butylacetamide at 120°C.
(BuSal) <sub>2</sub> Co(II)	0	-	0	-
(BuSal) <sub>2</sub> Cu(II)	0	-	0	-
(BuSal) <sub>2</sub> Zn	-	-	-	-
(PhSal) <sub>2</sub> Co(II)	-	-	-	-
(DIPS) <sub>2</sub> Co(II)	-	-	-	-
(DIPS) <sub>2</sub> Cu(II)	-	-	-	-
(DIPS) <sub>2</sub> Ni(II)	-	-	-	-
(DIPS) <sub>3</sub> Cr(III)	-	-	-	-
BuPCo(II)DG <sup>b</sup>	-			-

<sup>a</sup> Symbols: - = active inhibitor; 0 = no measurable inhibition; no entry = not examined.

<sup>b</sup> BuPCo(II)DG = Di(*n*-butylphosphonium)cobalt(II)dimethylglyoxime.

As the data in Table I show, some of the metal chelates can be regarded as outstanding inhibitors. While in general diisopropylsalicylates were more powerful inhibitors than the corresponding salicylaldimines, some of the latter were by no means insignificant in their inhibitory properties, particularly regarding *N*-butylacetamide. The quantitative data concerning *N*-butylacetamide will be published separately. It is noteworthy that a cobalt(II) complex—*i.e.*, di(*n*-butylphosphonium)-

cobalt(II)dimethylglyoxime was an efficient inhibitor even at elevated temperatures and significantly superior in this respect to the corresponding salicylaldimines. It exhibited an induction period of 860 hours in the autoxidation of TMPD at 100°C. compared with approximately 1 hour for the substrate itself and 12 hours for the substrate containing bis(*N*-phenylsalicylaldimino)cobalt(II) at the same concentration—*i.e.*, *M*/200; bis(*N*-butylsalicylaldimino)cobalt(II) is a catalyst under these conditions. These examples are quoted to indicate the scope in the development of new metal chelates as inhibitors of autoxidation.

**Changes in Absorption Spectra.** When the metal chelate exhibited only catalytic properties in hydrocarbon autoxidation—*e.g.*, for bis(*N*-butylsalicylaldimino)nickel or bis(*N*-phenylsalicylaldimino)nickel, noticeable changes in the absorption spectra were observed only when oxygen uptake reached the levels where catalyst deactivation and ultimately catalyst destruction made itself apparent. In most cases this was not observed before the total amount of oxygen uptake exceeded 500  $\mu$ liters (NTP)/ml. substrate. By contrast, interesting changes were observed during the induction period where catalyst-inhibitor conversion was applicable, and we concentrated our attention on the autoxidation of TMPD in the presence of bis(*N*-butylsalicylaldimino)-cobalt(II) at 60°C. The experiments were carried out in specially constructed silica Warburg vessels which allowed, on the one hand, normal measurement of oxygen uptake and, on the other hand, light absorption determination after tipping the solution either into a 1-cm. or a 2-mm. spectrophotometric cell. Each Warburg flask was fitted with a double joint connecting it with the manometer so there was no need to open the flasks when taken out of the bath for tipping and spectrophotometric measurements; the advantage of opening only the manometer tube to the atmosphere—necessary to avoid the suck-back of manometer fluid—is that problems arising from moisture penetration, the temperature dependence of oxygen solubility, and the subsequent need to re-establish the gas-liquid equilibrium at the higher temperature do not arise. It is thus possible to continuously compare oxygen uptake with changes in absorption spectra. Figure 5 shows these spectral changes relative to oxygen uptake. The implications of the data presented in Figure 5 are interesting; they indicate that during the induction period (the first 26 hours are regarded as such—*i.e.*, the time taken for oxygen uptake to reach 100  $\mu$ liters/ml. substrate) the absorption spectrum changes in two stages. There is a significant change during the first 4 hours and a second phase (the next 22 hours), in which above 400  $m\mu$  the change in the absorption spectrum is much less marked. The spectra taken after 10 and 26 hours, respectively, were so similar that they are presented as one curve. This applied also to additional spectra taken between 10 and 26 hours where changes

in absorption spectra were regarded as negligible. The absorption between 400 and 450  $m\mu$  is at its maximum during this stationary period. Subsequently the absorption begins to drop over the range 350 and 450  $m\mu$ , but at least initially the general shape of the curve is maintained. When autoxidation is allowed to proceed to more advanced stages—*e.g.*, the spectrum of Figure 5 after 34 hours—catalyst destruction has reached a stage where there is only a minor resemblance with the absorption spectrum ascertained in the earlier stages.

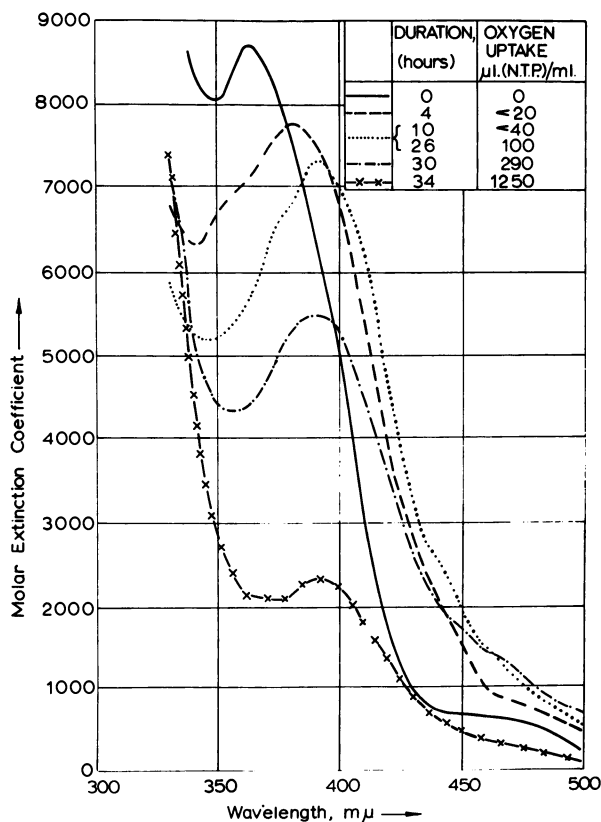


Figure 5. Changes in the absorption spectrum during the autoxidation of 2,6,10,14-tetramethylpentadecane at 60°C. in the presence of M/1000 bis(*n*-butylsalicylaldimino)cobalt(II)

**Isolation of Intermediary Complex.** We believe that we were successful in isolating the intermediary complex formed during the induction period. Again we concentrated our attention on the system TMPD–bis(*N*-butylsalicylaldimino)cobalt(II) and for this isolation 40°C. was found

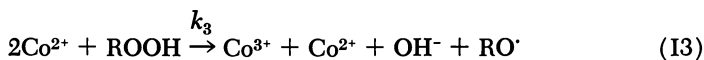
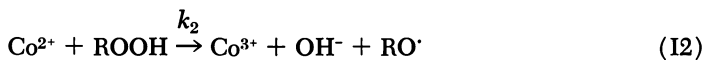
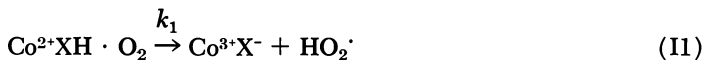
to be the most suitable autoxidation temperature. A sample of 82 mg. of the chelate was dissolved in 100 ml. TMPD and allowed to stand for 100 hours at 40°C. when the absorption in the range of 400–450  $m\mu$  has reached its peak—*i.e.*, it is comparable with the dotted curve of Figure 5 obtained after 26 hours—just before the end of the induction period. TMPD was then diluted five times with petroleum ether (30–40°C., free of aromatic hydrocarbons) and chromatographed through a column of neutral alumina (Brockman Grade 1). Residual hydrocarbon was eluted with excess petroleum ether solvent. Two layers remained near the top of the column; first, a predominant nonfluorescent green layer, and secondly, a nearly colorless layer which fluoresced when submitted to 365  $m\mu$  radiation. The second layer was small and appeared to have the same characteristics as the one normally obtained when the starting chelate was chromatographed under the same conditions. The two layers were separated mechanically, and the green layer was extracted with *ca.* 50 ml. ethyl alcohol; it was again chromatographed through alumina without subsequent elution. In that way the remaining, not insignificant, quantity of the starting chelate is retained by the alumina. The intermediary complex was more strongly adsorbed on alumina than the starting chelate from a petroleum ether solution but much more weakly adsorbed on the same adsorbens from ethyl alcohol solution. The solution in ethyl alcohol after being subjected to the chromatographic separation of the remaining cobalt(II) complex, was evaporated at room temperature *in vacuo* at the highest possible speed (to avoid decomposition of the complex), and 26 mg. of a microcrystalline green solid residue was obtained. Unlike bis(*N*-butylsalicylaldimino)-cobalt(II) and tris(*N*-butylsalicylaldimino)cobalt(III) the green intermediary complex thus isolated did not exhibit fluorescence when subjected to thin layer chromatography on silica. Microanalytical results were as follows: C = 60.9%; H = 7.25%; N = 5.5%; Co = 12.1%. If one assumes that the intermediary complex has the formula:  $2CoX_2 \cdot 2RO_2$ , where X = *N*-butylsalicylaldimino ligand, and  $RO_2 = C_3H_7O_2$  (presumably resulting from chain transfer and not unlikely, bearing in mind the structure of TMPD), the calculated results for  $C_{50}H_{70}N_4O_8Co_2$  are: C = 61.7%; H = 7.25%; N = 5.76%; Co = 12.1%. By contrast the starting chelate, bis(*N*-butylsalicylaldimino)cobalt(II) ( $= C_{22}H_{28}N_2O_2Co$ ) would produce: C = 64.2%; H = 6.86%; N = 6.81%; Co = 14.35%, and tris(*N*-butylsalicylaldimino)cobalt(III) ( $= C_{33}H_{42}N_3O_3Co$ ) would produce: C = 67.5%; H = 7.21%; N = 7.15%; Co = 10.05%. The melting point of the intermediary complex, notwithstanding its completely different composition, was practically the same as that of the cobalt(III) chelate—*i.e.*, 170°C. (that of the cobalt(II) chelate was 148°C.).

Bis(*N*-butylsalicylaldimino)cobalt(II) and tris(*N*-butylsalicylaldimino)cobalt(III) and the unknown intermediary complex were heated *in vacuo* at 195°C. for 3 hours, and the gas-phase products were examined in a MS/2H mass spectrograph. There was evidence of decomposition products for the intermediary complex only. The major peaks, apart from the largest which could be attributed to CO<sub>2</sub>, (there was quantitative agreement for the 44, 22, and 16 peaks for identification) there were major peaks at 43, 41, 39, 30, 29, 28, and 27, indicating various hydrocarbon fragments. While a quantitative interpretation of the mass spectrum was not possible, it was not inconsistent with our assumptions concerning the basic structure of the complex. In particular it was proved that the intermediary complex contains a significant amount of oxygen not present in the starting chelate. The purity of the intermediary complex was confirmed not only by its sharp melting point but also by means of thin-layer chromatography, indicating for all practical purposes a single substance.

### Discussion

The phenomenon of catalyst-inhibitor conversion involves a concentration effect which we believe is best explained by the following assumptions. As long as the concentration of hydroperoxide is very low, a relatively inefficient initiation reaction (I1), involving molecular oxygen, which is first order with regard to cobalt competes with a termination reaction T(2a,b) which is second order with regard to cobalt (we use cobalt as an illustration since most of the work was concentrated on this metal). At a certain cobalt concentration inhibition is therefore bound to overtake initiation, but the situation would change abruptly if hydroperoxides were present since initiation involving metal and hydroperoxide according to Reaction I2 and I3 is much more efficient than the reaction involving metal and molecular oxygen. Steady-state kinetics could be used to explain satisfactorily all the observed phenomena. The postulated scheme is:

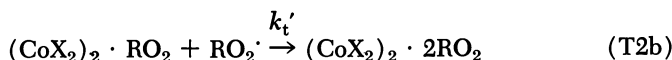
#### INITIATION REACTIONS



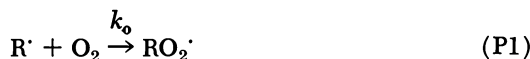
## TERMINATION REACTIONS



This rapidly established equilibrium is followed by the rate-determining step,



## PROPAGATION REACTIONS



and the rate-determining step



The rate of initiation may be expressed by

$$r_i = k_1[\text{Co}] + [\text{ROOH}](k_2[\text{Co}] + k_3[\text{Co}]^2)$$

Assuming that

$$\frac{d[\text{R}\cdot]}{dt} = r_i - k_o[\text{R}\cdot][\text{O}_2] + k_p[\text{RO}_2\cdot][\text{RH}] = 0$$

and

$$\frac{d[\text{RO}_2\cdot]}{dt} = k_o[\text{R}\cdot][\text{O}_2] - k_p[\text{RO}_2\cdot][\text{RH}] - [\text{RO}_2\cdot]^2(k_t + k_t'[\text{Co}]^2) = 0$$

it follows that

$$[\text{RO}_2\cdot] = \sqrt{\frac{r_i}{(k_t + k_t'[\text{Co}]^2)}}$$

In hydrocarbon autoxidation when Reaction I3 predominates over I2, the rate equation for oxygen uptake becomes:

$$\frac{-d[\text{O}_2]}{dt} = k_p[\text{RH}] \frac{\sqrt{[\text{Co}]} \sqrt{(k_1 + k_3[\text{Co}][\text{ROOH}])}}{\sqrt{(k_t + k_t'[\text{Co}]^2)}}$$

A reaction of the metal catalyst and hydroperoxide, second order with regard to metal, has been previously postulated (15), and our experience suggests that this is not infrequent in hydrocarbons. In the presence of phenolic antioxidants T1 is correctly neglected for most practical purposes. With the metal chelates which we have been studying this would not be justifiable at relatively low concentrations such as  $M/20,000$ .

As long as the hydroperoxide concentration can be neglected, simplification leads to three ranges of cobalt concentrations:

(1) The higher range where cobalt is an inhibitor and  $k_t \ll k_t'[\text{Co}]^2$  is postulated. The rate equation then becomes:

$$\frac{-d[\text{O}_2]}{dt} = k_p[\text{RH}] \frac{\sqrt{k_1}}{\sqrt{k_t'}\sqrt{[\text{Co}]}}$$

This is basically similar to the equation proposed by Hammond *et al.* (8) for weak phenolic antioxidants.

(2) The lower range where cobalt is a conventional catalyst and  $k_t \gg k_t'[\text{Co}]^2$  is postulated. The rate equation for oxygen uptake becomes:

$$\frac{-d[\text{O}_2]}{dt} = k_p[\text{RH}] \frac{\sqrt{k_1}\sqrt{[\text{Co}]}}{\sqrt{k_t}}$$

(3) The intermediate range where the sensitivity to traces of hydroperoxidic contamination is such that despite considerable care reproducible results were not possible and where the complex rate equation does not lend itself to simplification. The fact that this range usually covered less than an order of magnitude (*e.g.*, a concentration range of  $M/20,000$  to  $M/5000$ ) is not so surprising when one takes into account a termination reaction which is second order with regard to cobalt concentration.

When hydroperoxide concentration becomes significant, Reaction II will be negligible, and for hydrocarbons where Reaction I3 predominates over I2, the rate equation becomes:

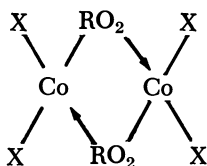
$$\frac{-d[\text{O}_2]}{dt} = k_p[\text{RH}] \frac{\sqrt{k_3[\text{ROOH}]}}{\sqrt{k_t'}}$$

This rate equation agrees with the findings that soon after the end of the induction period the rate of oxygen uptake becomes independent of metal concentration with many catalysts (*e.g.*, both cobalt and copper salicylaldehydes or diisopropyl salicylates). By contrast cobaltous acetate had a lasting inhibitory effect in the autoxidation of *N*-butylacetamide and similar *N*-alkylamides (1). This can, however, be explained by assuming that Reaction I2 predominates over I3 in amide autoxidation since in this case the rate equation becomes:

$$\frac{-d[\text{O}_2]}{dt} = k_p[\text{RH}] \frac{\sqrt{k_2}\sqrt{[\text{ROOH}]}}{\sqrt{k_t'}[\text{Co}]}$$

The intermediary complex in the system TMPD/bis(*N*-butylsalicylaldehyde)cobalt(II) is assumed to be an inactive bidentate chelate

$(\text{CoX}_2)_2 \cdot 2\text{RO}_2$  in which  $\text{RO}_2$  radicals act as bridges, such as



The changes in absorption spectra (Figure 5) support the kinetic assumption that the formation of the intermediary complex occurs in two stages—*viz.*, a fast equilibrium followed by a second rate-determining step. It is also noteworthy that the spectrum of the intermediary complex is more closely related to a Co(III) than a Co(II) salicylaldimine chelate which would agree with the proposed structure. As pointed out in the results, microanalytical data for the isolated intermediary complex and mass spectrographic analysis of its thermal decomposition products were reasonably consistent with the proposed formula provided that it is assumed that  $\text{R} = \text{C}_3\text{H}_7$ . Dimerization was previously postulated for metal salicylaldimines—*i.e.*, by Holm (10) in the case of the nickel chelate, and peroxy bridges should facilitate it. Since we do not know the mechanism by which the hydrocarbon is split into fragments of lower molecular weight, the proposed formula for the intermediary complex should be regarded as hypothetical. There is also the possibility that the microanalytical data presents averages covering a number of homologs.

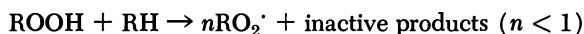
It is interesting to compare the cobalt(II) salicylaldimines with the corresponding nickel and copper chelates. It cannot be said that all the observed phenomena are yet fully understood although we believe we have gained some new insight into the complexities of the behavior of these metal chelates. In the concentration range we examined the nickel salicylaldimines exhibited only catalytic properties, and this seems to indicate that a reaction with molecular oxygen or hydroperoxide leads to an unstable Ni(III) chelate or, as assumed by Gray and co-workers (23) or Schrauzer and Mayweg (19), there are nickel chelates which can change their charge by electron transfer without involving a change in the valence state of nickel itself. Such a change of charge would be produced by the reaction with the hydroperoxide or molecular oxygen, in both cases be accompanied by free radical formation. Stilbene dithiolates and similar complexes where this charge transfer was observed are being studied in these laboratories as autoxidation catalysts and inhibitors. Since for nickel salicylaldimines there were no complications as a result of catalyst-inhibitor conversion, it was relatively easy to estimate the activation energy for the initiation reaction, which corresponds to  $\sim 20$  kcal. By contrast the Arrhenius equation could not be applied for the

cobalt chelates because of the discontinuities or so-called "critical phenomena."

The fact that the nickel salicylaldimine chelates had no pronounced inhibitory effect could be attributed to prior dimerization as postulated by Holm (10) even in the absence of  $\text{RO}_2'$  bridging ligands. This might severely impair the ability to consume  $\text{RO}_2'$  radicals, and hence the chelate would have no significant inhibitory properties. This is likely to be a specific feature for nickel salicylaldimines for among the diisopropylsalicylate metal complexes the nickel chelate was the most efficient inhibitor in hydrocarbon autoxidation and was also successfully applied to polyethylene. For diisopropylsalicylato nickel it must be assumed that dimerization occurs only with bridging  $\text{RO}_2'$  radicals, and furthermore there can be no electron transfer leading to free radical formation in view of the fact that experimental evidence does not indicate even the slightest catalytic properties.

One of the most surprising findings is the observed catalyst-inhibitor conversion with copper complexes. Since a copper(III) chelate is not regarded as feasible, a possible explanation might be that copper(I) formed by reducing impurities is the active species at least as far as catalysis is concerned.

In recent years Emanuel, Neiman, and their respective schools have greatly contributed to the theory of antioxidant action by studying the phenomenon of the critical antioxidant concentration in terms of a degenerate branched chain reaction. The critical antioxidant concentration, a well-established feature of phenolic antioxidants, is one below which autoxidation is autocatalytic and above which it proceeds at a slow and steady rate. Since the theory allowed not only a satisfactory explanation of the critical antioxidant concentration itself but elucidation of many refinements, such as the greater than expected activity of multifunctional phenolic antioxidants (21), we wondered whether catalyst-inhibitor conversion could be fitted into its framework. If degenerate chain branching is assumed to be the result of



the critical inhibitor concentration  $[\text{A}]_{\text{cr}}$  would be given by

$$[\text{A}]_{\text{cr}} = \frac{n}{1-n} \frac{k_p[\text{RH}]}{k_a}$$

where the only hitherto undefined rate constant  $k_a$  applies to the consumption of  $\text{RO}_2'$  radicals by the antioxidant A. If RH is replaced by a metal catalyst,  $n$  would be unity for all practical purposes; hence, the above equation is not applicable, and it is doubtful whether the concept of critical concentration could be applied as usefully to metal catalysts

as to phenolic antioxidants. Nevertheless, Knorre *et al.* (12) postulated this hypothesis to apply in the system cupric stearate/*n*-decane at 140°C. where 0.06 mole % was determined as the critical cupric stearate concentration. We do not think that metal stearates are suitable for demonstrating catalyst-inhibitor conversion in the same manner as metal salicylaldimines or diisopropylsalicylates since at room or slightly elevated temperatures (50° or 60°C.) the metal stearates are, as Knorre *et al.* observed, almost insoluble in hydrocarbons. At higher temperatures quantitative and reproducible observations are more difficult because thermal hydroperoxide formation and decomposition become increasingly complicating factors. Even under these severe conditions cupric stearate still exhibits inhibitory properties. In agreement with our assumptions the authors found that some of the copper present was in the cuprous state even in the early stages of autoxidation. Apart from the difficulty arising out of  $n = 1$ , there may be some doubt whether the reaction of cupric stearate with  $RO_2^{\cdot}$  radicals could be so efficient that the recombination of radicals can be neglected; at first sight the sharpness of the transition observed by Knorre *et al.* (12) could suggest a termination reaction which is second order with regard to cupric stearate, perhaps similar to the one which we postulate for salicylaldimines. Phenolic antioxidants are consumed and oxidized to inactive oxidation products during the induction period. Since in many cases there is evidence that the inhibiting metal chelate remains predominantly in the same valence state (this applies particularly to active copper and nickel chelates), it is difficult to see how it can be inactivated during the induction period by a mechanism substantially different from the one we postulated. Knorre *et al.* (12) have not suggested any specific mechanism for the reaction of copper stearate with  $RO_2^{\cdot}$  radicals.

### Summary

With well-defined metal chelates which are soluble in hydrocarbons there are certain concentrations at which a transition from catalysis to inhibition occurs. The effect is particularly pronounced with cobalt(II) chelates but was also observed with others. The type of ligand has a profound effect—*e.g.*, nickel salicylaldimines were for all practical purposes conventional autoxidation catalysts while the nickel diisopropylsalicylate complex was among the outstanding inhibitors. While we have gained new insight, the phenomenon is not yet fully understood; even from an experimental point of view one may sometimes fail to observe it because solubility limits the concentration range which can be investigated. This study would seem to indicate that there is significant scope in the development of metal chelates as autoxidation inhibitors.

### Acknowledgments

We thank A. J. Owen for carrying out the thermal decomposition of the intermediary complex. The technical assistance of Jean M. Burgess, D. Thompson, and the late P. Flood in various parts of the work is gratefully acknowledged.

### Literature Cited

- (1) Betts, A. T., Uri, N., *Makromol. Chem.* **95**, 22 (1966).
- (2) Betts, J., Robb, J. C., private communication.
- (3) Carlsson, D. J., Robb, J. C., *Trans. Faraday Soc.* **62**, 3403 (1966).
- (4) Charles, R. G., *J. Org. Chem.* **22**, 677 (1957).
- (5) Denisov, E. T., *Russ. J. Phys. Chem.* **38**, 1 (1964).
- (6) Duck, E. W., private communication.
- (7) Dulog, L., *Makromol. Chem.* **77**, 206 (1964).
- (8) Hammond, G. S., Boozer, C. E., Hamilton, C. E., Sen, N., *J. Am. Chem. Soc.* **77**, 3238 (1955).
- (9) Heaton, F. W., Uri, N., *J. Sci. Food Agr.* **9**, 781 (1958).
- (10) Holm, R. H., "Advances in the Chemistry of Coordination Compounds," S. Kirschner, Ed., Macmillan, New York, 1961.
- (11) Kamiya, Y., Beaton, S., Lafortune, A., Ingold, K. U., *Can. J. Chem.* **41**, 2034 (1963).
- (12) Knorre, D. G., Chuchukina, L. G., Emanuel, N. M., "The Oxidation of Hydrocarbons in the Liquid Phase," N. M. Emanuel, Ed., p. 164, Pergamon, London, 1965.
- (13) Lappert, E. L., Truter, M. R., *J. Chem. Soc.* **1960**, 4996.
- (14) Martin, H. F., *Chem. Ind.* **1961**, 364.
- (15) Mesrobian, R. B., Tobolsky, A. V., "Autoxidation and Antioxidants," W. C. Lundberg, Ed., Vol. I, Chap. 3, Interscience, New York, 1961.
- (16) Pitkethly, R. C., *Chem. Ind.* **1967**, 2067.
- (17) Russell, G. A., *J. Am. Chem. Soc.* **78**, 1041 (1956).
- (18) Sacconi, L., Ciampolini, M., Maggio, F., Cavasino, F. P., *J. Am. Chem. Soc.* **84**, 3246 (1962).
- (19) Schrauzer, G. N., Mayweg, V. P., *J. Am. Chem. Soc.* **87**, 3585 (1965).
- (20) Schrauzer, G. N., Kohnle, J., *Ber.* **97**, 3056 (1964).
- (21) Shlyapnikov, Y. A., Miller, V. B., Neiman, M. B., Torsueva, E. S., *Dokl. Akad. Nauk. SSSR* **151**, 148 (1963).
- (22) Uri, N., "Autoxidation and Antioxidants," W. C. Lundberg, Ed., Vol. I, Chap. 2, Interscience, New York, 1961.
- (23) Werden, B. G., Billig, E., Gray, H. B., *Inorg. Chem.* **5**, 78 (1966).

RECEIVED February 5, 1968.

## Discussion

**Dale G. Hendry:** Qualitative aspects of inhibition by metal complexes of the type presented here have been known for some time and have been reported by several research groups. To obtain quantitative information we have compared the length of the induction period with known rates of initiation and find that generally more than one metal ion is required to terminate each initiated chain; only in special cases have we found the number of metal ions to be one per initiated chain. Where Betts and Uri propose that one metal ion terminates each chain for the complex bis(*N,n*-butylsalicylaldimino)cobalt, we have found the actual value to be 2 rather than unity. This value is independent of inhibitor concentration, hydrocarbon concentration, and the rate of initiation. However, we have found that changing the ligands may alter the required number of metal ions per initiated chain from 1 to about 4. Thus, in general more chemistry is involved than a simple interaction of the peroxy radical with the metal ion, and Betts and Uri's suggestions for the structure of intermediate complex and the mechanism are inadequate. We will publish a more complete report of our research later, which will include data for the effect of several complexes containing various ligands and metal ions on the oxidation of several hydrocarbons.

**N. Uri:** I am interested to learn that our work has stimulated Dr. Hendry to investigate the question of the number of metal atoms required to react with one  $\text{RO}_2\cdot$ . Without knowing the precise experimental conditions and indeed the type of hydrocarbon used (we could not, for example, observe inhibition with bis(*N*-butylsalicylaldimino)cobalt(II) in Tetralin autoxidation), I find it difficult to formulate my own views at this stage. It is worth drawing attention, however, to the fact that the basic feature of our mechanism is that two metal atoms react with one peroxy radical and that this reaction competes with first-order initiation involving molecular oxygen. Our experimental results suggest that the first  $\text{RO}_2\cdot$  radical absorption is rapidly established whereas the second step is very slow. The number of  $\text{RO}_2\cdot$  consumed per atom of cobalt will, therefore, depend on the timing of the measurements. It is interesting that Dr. Hendry finds that under certain conditions as many as four metal atoms consume one  $\text{RO}_2\cdot$ . I certainly do not think that the suggested formula of the intermediate complex is well established, and it should merely be regarded as a hypothesis which at this juncture fits our experimental results better than any other.

**H. Berger:** The derivation of the expression for the critical inhibitor concentration given by Shlyapnikov ("Preprint," International Oxidation

Symposium, Vol. I, p. 549, 1967) is as follows, with  $x = 1$ :

$$\frac{d([\text{R}\cdot] + [\text{RO}_2\cdot])}{dt} = 2w_o - xk_3[\text{RO}_2\cdot][\text{IH}] + \delta k_4[\text{ROOH}][\text{RH}]$$

$$\frac{d[\text{ROOH}]}{dt} = k_2[\text{RO}_2\cdot][\text{RH}] + k_3[\text{RO}_2\cdot][\text{IH}] - k_4[\text{ROOH}][\text{RH}]$$

from which:

$$[\text{IH}]_{\text{cr}} = \frac{\delta k_2 [\text{RH}]}{(x - \delta) k_3}$$

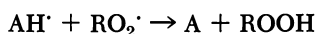
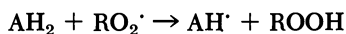
In my opinion, since the interaction of a phenolic inhibitor with  $\text{RO}_2\cdot$  will consume two  $\text{RO}_2\cdot$  but produce one  $\text{ROOH}$ ,  $x$  should be 2; if this is the case, Dr. Uri's criticism of the attempt of Knorre *et al.* to explain the effect of cupric stearate is not valid unless  $\delta(n)$  becomes  $> 2$ , which is improbable at the low  $\text{ROOH}$  concentration involved.

**Dr. Uri:** I cannot agree entirely with Dr. Berger's view that the equation for the critical antioxidant concentration, which was developed by the schools of N. M. Emanuel and M. B. Neiman, should be revised by introducing  $x$  for the following reason.

Using Dr. Berger's nomenclature it seems that where  $x = 2$ , which is the case for most phenolic antioxidants, the number of  $\text{ROOH}$  ultimately produced for every molecule of antioxidant consumed, will also equal 2; therefore, the middle term in his second equation would be

$$+ xk_3[\text{RO}_2\cdot][\text{IH}].$$

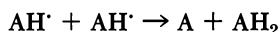
Dr. Berger omitted the  $x$  in this term. If there is an  $x$  in the first equation there should also be an  $x$  in the second equation. If we refer to a phenolic antioxidant (on which Dr. Berger concentrates his arguments), such as hydroquinone, as  $\text{AH}_2$  (with  $\text{AH}\cdot$  being the semiquinone radical), then the two equations would be



While the first step is rate determining, the stoichiometry of

$$\frac{-\Delta\text{RO}_2}{\Delta\text{ROOH}} = 1$$

is not affected even if the second step is something like,



and the formula will not contain the term

$\frac{\delta}{(x - \delta)}$  but  $\frac{\delta}{x(1 - \delta)}$  (and specifically  $\frac{\delta}{2(1 - \delta)}$  for phenolic antioxidant) so that  $x$  merely affects the magnitude of the constant.

Apart from this mathematical aspect I think that the useful concept of critical antioxidant concentration is valid for degenerate chain branching where the effect of the presence of antioxidant on hydroperoxide decomposition is relatively minor but not when it is the predominant initiation reaction. For metals reacting with hydroperoxides the number of radicals formed may even exceed unity. Kolthoff and Medalia [*J. Am. Chem. Soc.* 71, 3777 (1949)] demonstrated that for the reaction of ferrous ion with hydrogen peroxide as many as six ferrous atoms can be oxidized by one molecule of hydrogen peroxide as a result of this effect. I do not think, therefore, that the "critical antioxidant concentration" should be applied to those cases in which the so-called antioxidant is the catalyst.

**Frank R. Mayo:** At its present stage I think that the isolation and discussion of the "intermediary complex" is more of a diversion than a useful contribution to the paper of Betts and Uri. First, I am unable to see any plausible route by which propylperoxy radicals might be formed in quantity in the low temperature oxidation of their hydrocarbon. Second, the product which they isolated contains 0.8% less carbon and 1.1% more oxygen (by difference) than the structure which they propose. Third, their supposed intermediate,  $2\text{CoX}_2 \cdot 2\text{PrO}_2$ , containing two peroxy radicals, survived chromatography over alumina in several solvents at room temperature and also thin layer chromatography on silica. Fourth, our own experience suggests that their (possibly) pure product is some inactive by-product from their catalyst and some bifunctional oxygen compound such as a dibasic acid.

**N. Uri:** When experimental work reveals unusual phenomena, the investigator should offer his reasonable interpretation. Hence, I cannot agree that the efforts to isolate the intermediary complex and proposals concerning its structure are a "diversion." The analytical results obtained were approximately halfway between  $2\text{CoX}_2 \cdot 2\text{PrO}_2$  and  $2\text{CoX}_2 \cdot 2\text{BuO}_2$ . We were aware that they do not entirely agree with  $2\text{PrO}_2$ , but they were closer to the  $2\text{PrO}_2$  formula than to the  $2\text{BuO}_2$  formula, and I have not excluded the possibility of a mixture of homologs difficult to distinguish by thin layer chromatography. In my opinion a dibasic acid is less likely to survive chromatography than the proposed complex. In any case I look forward to the publication of the results obtained by Mayo and Hendry.

# Influence of Solubility and Structure on the Activity of Metal Complex Oxidation Catalysts

C. J. SWAN and D. L. TRIMM

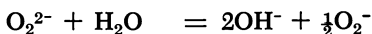
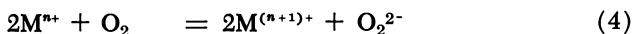
Department of Chemical Engineering and Chemical Technology,  
Imperial College, London, England

*The effects of adding various metal ions and metal complexes on the rate of a model oxidation reaction have been studied in some detail. The model reaction chosen—the oxidation of ethanethiol in aqueous alkaline solution in the presence of metal-containing catalysts—involves the transfer of an electron from the thiol anion to the metal. The catalytic activity of additives depends upon the solubility of the particular metal complex and varies according to the nature of the ligand attached to the metal ion. In conjunction with different metals, the same ligand can act either as a catalyst or as an inhibitor. The results are discussed in the light of proposed reaction mechanisms.*

Interpreting the mechanism of the liquid-phase oxidation of organic compounds in the presence of metal complexes is complicated by the ambiguity as to the exact nature of the oxidants. Metal complexes may act as either heterogeneous (16) or homogeneous oxidants. In the latter case, the multiplicity of complexes which may be produced under reaction conditions can complicate the over-all reaction (18). The present investigation has been devised to study the importance of solubility of metal complexes and to assess the effect of coordinated ligands in determining the kinetics and mechanism of a model reaction.

The model reaction chosen, the metal-catalyzed oxidation of ethanethiol to diethyl disulfide by molecular oxygen, is of considerable academic (13, 21) and industrial (11) interest. The over-all reaction may be represented by the scheme





Further oxidation and hydrolysis of diethyl disulfide to sulfonic and sulfinic acids do not occur when the reaction proceeds in aqueous solvents (13, 22).

In general, the electron transfer reaction (Reaction 2) controls the over-all rate of reaction, and the nature of the catalyst has a profound effect on the kinetics of oxidation (23). Thus Wallace *et al.* (23) have compared the catalytic efficiencies of metal phthalocyanines with metal pyrophosphates, phosphates, phosphomolybdates, and phosphotungstates. The activity of metal pyrophosphates was ascribed to the ease of electron transfer through the metal coordination shell, the reaction being suggested to occur at the solid pyrophosphate-liquid interface. On the other hand, the catalytic effectiveness of a series of metals, added to solution as simple salts, has been explained in terms of their ability to form soluble complexes containing thiols (13). It was not clear whether the high rates of oxidation were caused by the solubility of metal complexes or by the peculiar nature of the thiol complexes.

### Experimental

**Materials.** Ethanethiol, obtained from the Eastman Kodak Co., was distilled under nitrogen at atmospheric pressure. The middle fraction collected had a boiling range of less than 0.1°C. and was stored under nitrogen at 0°C. in a vessel fitted with a rubber serum cap. Alkaline solutions were prepared from AnalaR sodium hydroxide (Hopkin and Williams) and deionized distilled water and were stored in steam-cleaned screw-capped polyethylene bottles.

Metal catalysts were prepared as follows: Solutions of the sulfates of Cu, Co, Ni, Fe, and Mg were prepared from AnalaR reagents (Hopkin and Williams) in deionized distilled water. Conventional techniques were used to prepare  $\text{Coen}_3\text{Cl}_3$  (8), *cis*- $[\text{Coen}_2\text{Cl}_2]\text{Cl}$  (9),  $\text{K}_3\text{Co}(\text{CN})_6$  (10), *cis*- $[\text{Co}(\text{NH}_3)_4(\text{H}_2\text{O})(\text{Cl})]\text{Cl}_2$  (17), and  $[\text{Co}(\text{NH}_3)_5\text{CO}_3]\text{NO}_3$  (1). Pyrophosphates were prepared by mixing aqueous solutions containing stoichiometric amounts of the appropriate metal sulfate and of tetrasodium pyrophosphate, respectively (20). Phthalocyanines were prepared by the method of Linstead *et al.* (2, 6), using phthalonitrile and anhydrous metal chlorides. AnalaR grade metal salts were used throughout these preparations. Hemin and chlorophyll (British Drug Houses, Ltd.), vitamin B<sub>12</sub> (Halewood Chemicals, Ltd.), and Na<sub>2</sub>CoEDTA (Koch Light Laboratories, Ltd.) were used without further purification.

Oxygen (British Oxygen Co., Ltd.) was obtained from cylinders and purified by fractionation from traps cooled to -196°C.

Since the oxidation of thiols is known to be strongly catalyzed by traces of metal ions, all experimental techniques were designed to prevent the introduction of extraneous metal ions. Control experiments involving the uncatalyzed oxidation of ethanethiol (5) were used to confirm that contamination was negligible.

**Apparatus.** The course of the reaction was followed by periodically measuring the volume of oxygen absorbed at constant pressure, the apparatus used being in principle similar to that of Bolland (3). The reactant solution was shaken in a reaction vessel which was connected to a gas buret and to one arm of a pressure-sensing cell, such that consumption of oxygen in the reaction vessel caused a current to pass through an electrolytic cell connected to the free side of the gas buret. By this means the pressure of oxygen in the working side of the gas buret could easily be controlled to  $\pm 0.4$  mm. at 760 mm. A detailed description of the apparatus has been published (5).

For any given experiment the catalyst and alkaline solutions were first pipetted into the reaction vessel, which was then closed with a rubber serum cap and purged with oxygen. The thiol was then injected from a graduated hypodermic syringe, and the reaction vessel connected to the gas buret and to a mechanical shaker. Readings of the volume of oxygen in the gas buret were taken as often as necessary, generally every 5 minutes.

### Results and Discussion

All results reported refer to the oxidation of 0.5M ethanethiol in 2M sodium hydroxide solutions (50 ml.) under a constant pressure of 750 mm.

**Table I. Comparison of Porphyrin Ligands with Simple**

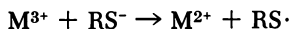
	<i>Added as</i>	<i>Added Concn., M</i>	<i>Solubility of Metal, Mg./Ml.</i>
None	—	—	—
Fe	FeSO <sub>4</sub> ·7H <sub>2</sub> O	10 <sup>-3</sup>	8.4 × 10 <sup>-4</sup>
	Hemin	10 <sup>-3</sup>	2.2
Co	CoSO <sub>4</sub> ·7H <sub>2</sub> O	10 <sup>-3</sup>	4.1 × 10 <sup>-4</sup>
	Vitamin B <sub>12</sub>	10 <sup>-3</sup>	3.1
Mg	MgSO <sub>4</sub> ·7H <sub>2</sub> O	10 <sup>-3</sup>	1.3 × 10 <sup>-2</sup>
	Chlorophyll	10 <sup>-3</sup>	0.6
Ni	NiSO <sub>4</sub> + aq.	10 <sup>-3</sup>	6.3 × 10 <sup>-4</sup>
Cu	CuSO <sub>4</sub> ·5H <sub>2</sub> O	10 <sup>-5</sup>	6.0 × 10 <sup>-3</sup>

<sup>a</sup> Based on oxygen uptake.



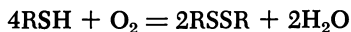
as would be the case if the formation of metal-thiol complexes were sterically hindered.

On the other hand, if it were possible to block the coordination sites of a metal by using a strongly attached ligand such as cyanide, then "outer-sphere" electron transfer reactions should become more important (12).



Under these circumstances, thiyl radicals should be produced which will either dimerize or react in some other way. Diethyl disulfide should, then, be only one of a range of products.

Striking confirmation of this can be seen by inspecting results reported in Table I. The oxidation of ethanethiol by simple metal salts in the presence of 0.25M cyanide occurs slowly and proceeds to a final oxygen uptake of 300% when compared with the theoretical amounts calculated in terms of the reaction



No disulfide could be detected among the products of reaction.

Further evidence has been obtained to support the contention that the active catalysts are metal complexes dissolved in solution. With experiments reported in Table II, the kinetics of oxidation under standard conditions in the presence of various metal salts are compared with the rates of reaction when solid residues have been filtered from solution. The agreement between the rates in Cases 1 and 3 of Table II (where the amount of metal available is dictated by the solubility of metal complexes) shows that solid precipitates play little or no part in catalysis in all the systems studied. The amount of metal in solution has been measured in Cases 2 and 3; metal hydroxide complexes (Case 2) are not as soluble as metal-thiol complexes, and neither is as soluble as metal phthalocyanines (19). The results of experiments involving metal pyrophosphates are particularly interesting, in that it has previously been suggested that cobalt pyrophosphates act as heterogeneous catalysts. The results in Table II show that this is not true in the present system.

In the light of the above discussion, it is necessary to redefine the criteria useful for describing catalytic activity. The coordination atmosphere of any given metal may be expected to affect the catalytic activity by influencing the solubility of the metal. If the metal complex, added to the reactant solution, can be replaced by thiyl entities, colored metal-thiol complexes may be produced, and the rate of reaction in all cases should correspond to Case 3 for adding simple metal salts (Table II). If the metal complex cannot be replaced, the rate of reaction may be quite different and will depend on the ease with which an electron

**Table II. Effect of Filtration on Rate of Reaction Using Whatman No. 42 Papers (pore size 1.1 microns)**

<i>Metal</i>	<i>Added as</i>	<i>Added Concn., M</i>	<i>Rate of Oxidation (<math>\times 10^{-6}</math>) <math>\frac{-d[O_2]}{dt}</math> Mole L.<sup>-1</sup> Sec.<sup>-1</sup></i>	<i>Condi- tions<sup>a</sup></i>	<i>Measured Metal Concentration in Solution, M</i>
Cu	CuSO <sub>4</sub> ·5H <sub>2</sub> O	10 <sup>-3</sup>	32.6	1	1.0 × 10 <sup>-3</sup>
		10 <sup>-3</sup>	27.0	2	N.m. <sup>b</sup>
		10 <sup>-3</sup>	24.4	3	N.m.
		10 <sup>-5</sup>	13.2	1	1.0 × 10 <sup>-5</sup> <sup>c</sup>
		10 <sup>-5</sup>	13.2	2	1.0 × 10 <sup>-5</sup>
		10 <sup>-5</sup>	13.2	3	1.0 × 10 <sup>-5</sup>
	Cu <sub>2</sub> P <sub>2</sub> O <sub>7</sub>	1.3 × 10 <sup>-2</sup>	22.2	1	N.m. <sup>d</sup>
		1.3 × 10 <sup>-2</sup>	21.2	3	N.m.
	Cu phthalocyanine	3.5 × 10 <sup>-3</sup>	5.4	1	N.m.
		3.5 × 10 <sup>-3</sup>	5.4	2	N.m.
Co	CoSO <sub>4</sub> ·7H <sub>2</sub> O	10 <sup>-3</sup>	10.3	1	1.0 × 10 <sup>-3</sup>
		10 <sup>-3</sup>	7.6	2	8.9 × 10 <sup>-5</sup>
		10 <sup>-3</sup>	9.9	3	6.4 × 10 <sup>-4</sup>
	Co <sub>2</sub> P <sub>2</sub> O <sub>7</sub>	1.3 × 10 <sup>-2</sup>	18.6	1	N.m. <sup>e</sup>
		1.3 × 10 <sup>-2</sup>	18.0	3	N.m.
	Vitamin B <sub>12</sub>	10 <sup>-3</sup>	80.4	1	1.0 × 10 <sup>-3</sup>
		10 <sup>-3</sup>	80.4	2	1.0 × 10 <sup>-3</sup>
	Co phthalocyanine	3.5 × 10 <sup>-3</sup>	47.6	1	N.m.
		3.5 × 10 <sup>-3</sup>	47.6	2	N.m.
	Ni	NiSO <sub>4</sub> + aq.	10 <sup>-3</sup>	15.2	1
10 <sup>-3</sup>			3.4	2	1.3 × 10 <sup>-5</sup>
10 <sup>-3</sup>			14.6	3	5.3 × 10 <sup>-4</sup>
Ni <sub>2</sub> P <sub>2</sub> O <sub>7</sub>		1.3 × 10 <sup>-2</sup>	8.5	1	N.m. <sup>f</sup>
		1.3 × 10 <sup>-2</sup>	8.2	3	N.m.

<sup>a</sup> 1. No filtration.

2. Reaction solution filtered before addition of thiol.

3. Reaction solution filtered after addition of thiol.

N.m. = not measured.

<sup>b</sup> Rate of reaction diffusion-controlled.

<sup>c</sup> No solid material could be filtered from solutions.

<sup>d</sup> Catalyst appeared unchanged at end of reaction; no dissolution evident.

<sup>e</sup> Red Co-thiol complex produced.

<sup>f</sup> Brown Ni-thiol complex produced.

can be transferred across the coordination system to the metal ion. All these types of behavior have been observed, using various complexes of one metal. The results are reported in Tables I, III, and IV.

When cyanide was added to the solutions, complete coordination of metal ions occurred, and the reaction rate and product spectrum

changed markedly (Table I). On the other hand, although cobalt phthalocyanine and vitamin B<sub>12</sub> did not disproportionate to form cobalt-thiol complexes, the rates of reaction in these cases were accelerated above the rate of diffusion of oxygen into solution under normal conditions (Table II, measured by adding copper sulfate at 10<sup>-3</sup>M). This increase above the value dictated by diffusion control is probably caused by uptake of oxygen by metal complexes at the liquid-gas interface, metal phthalocyanines acting as oxygen "carriers" (7, 14). With the exception of complexes containing ethylenediamine, all other complexes added to solution appeared to disproportionate completely, and metal-thiol complexes were formed (Table III), the rates of reaction being similar to

**Table III. Effect of Ligand Environment on Catalytic Activity of Cobalt Complexes**

<i>Complex</i> (10 <sup>-3</sup> M Co, unless Otherwise Stated)	<i>Rate of Oxidation</i> ( $\times 10^{-6}$ ) $\frac{-d[O_2]}{dt}$ Mole L. <sup>-1</sup> Sec. <sup>-1</sup>	<i>Formation of</i> <i>Co-thiol</i> <i>Complexes</i> <sup>a</sup>
CoSO <sub>4</sub> ·7H <sub>2</sub> O	10.3	+
<i>cis</i> -[Co(NH <sub>3</sub> ) <sub>4</sub> (H <sub>2</sub> O)Cl]Cl <sub>2</sub>	10.7	+
[Co(NH <sub>3</sub> ) <sub>5</sub> Co <sub>3</sub> ]NO <sub>3</sub>	9.8	+
<i>cis</i> -[Coen <sub>2</sub> Cl <sub>2</sub> ]Cl	8.0	+
Co en <sub>3</sub> Cl <sub>3</sub> ·3H <sub>2</sub> O	6.2	+ <sup>(1)</sup>
K <sub>3</sub> Co(CN) <sub>6</sub>	2.1	-
Na <sub>2</sub> Co(EDTA)	8.1	+
Co <sub>2</sub> P <sub>2</sub> O <sub>7</sub>	9.6	+
Co <sub>3</sub> (PO <sub>4</sub> ) <sub>2</sub>	12.0	+
Co phthalocyanine (3.5 × 10 <sup>-3</sup> M)	47.6	-
Vitamin B <sub>12</sub>	80.4	-
Copy <sub>2</sub> Cl <sub>2</sub>	11.9	+

<sup>a</sup> + Complex formed.

- Complex not formed.

+<sup>(1)</sup> Complex formed in small amount only.

the rate measured on adding the same amount of metal sulfate. Ethylenediamine could not be displaced completely from coordination with cobalt (4); only small amounts of colored complex were formed, and the rate of oxidation was intermediate between normal rates and the rates in the presence of cyanide complexes. Although it is not possible to calculate the stability and solubility of any metal thiol complex, it would appear from the above results that the stability constant of the cobalt thiol complex lies somewhere between that of Coen<sub>3</sub><sup>3+</sup> (10<sup>49</sup>) and that of Co(CN)<sub>6</sub><sup>3-</sup> (10<sup>84</sup>) (4).

It is also possible to compare the catalytic efficiencies of various metals surrounded by the same ligand (Table IV). In all cases, metal

pyrophosphates appear to disproportionate to some extent to give metal-thiol complexes. Metal phthalocyanines act both to increase reaction rate (cobalt, iron) and to decrease it (copper) since the complex itself is a poor catalyst by comparison with the behavior of simple metal salts. The phthalocyanine structure should allow the easy passage of an electron between thiol anions and the metal in all cases. The inhibition of reaction in the presence of copper phthalocyanine is apparently caused by the fact that this complex is relatively insoluble in the alkaline solutions (Table II). Naturally occurring complexes containing similar tetrapyrrolic macrocyclic ligands have been found to be efficient catalysts in all cases (Table I). No metal-thiol complexes could be identified in solution, and the complexes were completely soluble.

**Table IV. Comparison of Phthalocyanines and Pyrophosphates with Simple Metal Salts**

<i>Metal</i>	<i>Added as</i>	<i>Added Concn., M</i>	<i>Rate of Oxidation (<math>\times 10^{-6}</math>) <math>\frac{-d[O_2]}{dt}</math> Mole L.<sup>-1</sup> Sec.<sup>-1</sup></i>	<i>% Conversion in 1 Hour<sup>a</sup></i>
Fe	FeSO <sub>4</sub> ·7H <sub>2</sub> O	10 <sup>-3</sup>	4.0 × 10 <sup>-6</sup>	10
	Fe <sub>2</sub> P <sub>2</sub> O <sub>7</sub>	10 <sup>-3</sup>	3.8 × 10 <sup>-6</sup>	10
	Fe <sup>II</sup> phthalocyanine	3.5 × 10 <sup>-3</sup>	14.7 × 10 <sup>-6</sup>	13
Co	CoSO <sub>4</sub> ·7H <sub>2</sub> O	10 <sup>-3</sup>	10.3 × 10 <sup>-6</sup>	32
	Co <sub>2</sub> P <sub>2</sub> O <sub>7</sub>	10 <sup>-3</sup>	9.6 × 10 <sup>-6</sup>	26
	Co <sub>3</sub> (PO <sub>4</sub> ) <sub>2</sub>	1.3 × 10 <sup>-2</sup>	18.6 × 10 <sup>-6</sup>	41
		5.0 × 10 <sup>-3</sup>	15.2 × 10 <sup>-6</sup>	40
	Co phthalocyanine	3.5 × 10 <sup>-3</sup>	47.6 × 10 <sup>-6</sup>	100
Cu	CuSO <sub>4</sub> ·5H <sub>2</sub> O	10 <sup>-3</sup>	32.6 × 10 <sup>-6</sup>	100
	Cu <sub>2</sub> P <sub>2</sub> O <sub>7</sub>	10 <sup>-3</sup>	12.8 × 10 <sup>-6</sup>	36
		1.3 × 10 <sup>-2</sup>	22.2 × 10 <sup>-6</sup>	56
	Cu phthalocyanine	3.5 × 10 <sup>-3</sup>	5.4 × 10 <sup>-6</sup>	20
Ni	NiSO <sub>4</sub> + aq.	10 <sup>-3</sup>	15.1 × 10 <sup>-6</sup>	29
	Ni <sub>2</sub> P <sub>2</sub> O <sub>7</sub>	10 <sup>-3</sup>	8.6 × 10 <sup>-6</sup>	25
		1.3 × 10 <sup>-2</sup>	8.6 × 10 <sup>-6</sup>	25
None	—	—	1.0 × 10 <sup>-6</sup>	3

<sup>a</sup> Based on oxygen uptake.

In the presence of 0.25M cyanide (Table I), the rate of reaction was found to decrease markedly, except in the case of hemin. With that exception, the close correlation between rates of reaction in the presence of cyanide for simple salts and for metal porphyrins shows that

cyanide is replacing porphyrin ligands. One possible explanation of the hemin results is that although the cyanide cannot displace the macrocyclic ligand, it can substitute into the porphyrin structure and affect the speed of transfer of an electron through that structure to some small extent.

The catalytic action of a metal complex thus depends on the stability and solubility of the complex present in the reactant solutions. Provided that the coordination atmosphere of a metal ion is not displaced by thiol entities, the nature of the ligand affects the rate of electron transfer and the kinetics of the over-all oxidation.

### **Acknowledgment**

The authors express their gratitude to the British Petroleum Co. for the award of a Research Bursary to one of them (C.J.S.).

### **Literature Cited**

- (1) Bailar, J. C., ed., "Inorganic Synthesis," Vol. 4, p. 171, McGraw-Hill, New York, 1953.
- (2) Barrett, P. A., Dent, C. E., Linstead, R. P., *J. Chem. Soc.* **1936**, 1719.
- (3) Bolland, J. L., *Proc. Roy. Soc.* **A186**, 218, 1946.
- (4) *Chem. Soc. Spec. Publ.* No. 17 (1964).
- (5) Cullis, C. F., Hopton, J. D., Trimm, D. L., in preparation.
- (6) Dent, C. E., Linstead, R. P., *J. Chem. Soc.* **1934**, 1027.
- (7) Eley, D. D., *Research* **12**, 292 (1959).
- (8) Fernelius, W. C., ed., "Inorganic Syntheses," Vol. 2, p. 221, McGraw-Hill, New York, 1946.
- (9) *Ibid.*, p. 222.
- (10) *Ibid.*, p. 225.
- (11) Gleim, W. K. T., Urban, P., U. S. Patent **2,853,432** (1958).
- (12) Halpern, J., *Quart. Rev.* **15**, 207 (1961).
- (13) Hopton, J. D., Swan, C. J., Trimm, D. L., *ADVAN. CHEM. SER.* **75**, 216 (1968).
- (14) Jirgensons, B., "Natural Organic Macromolecules," Pergamon, New York, 1962.
- (15) Jones, M. M., Connor, W. A., *Ind. Eng. Chem.* **55**, 15, September (1963).
- (16) Ladbury, J. W., Cullis, C. F., *Chem. Revs.* **58**, 403 (1958).
- (17) Rochaw, E. G., ed., "Inorganic Syntheses," Vol. 6, p. 178, McGraw-Hill, New York, 1960.
- (18) Stewart, R., "Oxidation Mechanisms. Applications to Organic Chemistry," W. A. Benjamin, New York, 1964.
- (19) Swan, C. J., unpublished work.
- (20) Van Wazer, J. R., "Phosphorus and Its Compounds," Vol. 16, Interscience, New York, 1958.
- (21) Wallace, T. J., Schriesheim, A., *J. Org. Chem.* **27**, 1514 (1962).
- (22) Wallace, T. J., Schriesheim, A., *Tetrahedron Letters* **17**, 1131 (1963).

- (23) Wallace, T. J., Schriesheim, A., Hurwitz, H., Glaser, M. B., *Ind. Eng. Chem. Process Design Develop.* **3**, 237 (1964).
- (24) Walling, C., "Free Radicals in Solution," Wiley, New York, 1957.

RECEIVED December 21, 1967.

## Discussion

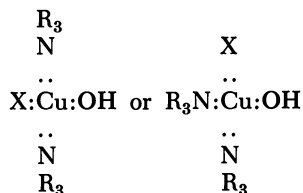
**H. Berger** (Koninklijke/Shell Laboratorium, Amsterdam): Concerning the effect of cyanides on metal catalysis (deactivation and formation of oxygenated products), what are your arguments against the explanation that the metal ion becomes completely inactive, while the products arise from a mechanism analogous to that proposed by Berger [*Rec. Trav. Chim.* **82**, 733 (1963)] for the oxidation in *tert*-butyl alcohol with excess mercaptan relative to base, Did you check that no hydrolysis of disulfide occurs in the presence of cyanide?

**D. L. Trimm**: Although the mechanism suggested by Berger would appear to be unimportant in the presence of metal ions dissolved in aqueous solution, it may well be important when metal ions are complexed with cyanide ions. Qualitative tests for products expected on the basis of this mechanism were attempted on reaction solutions and on test samples, but these were not successful in the presence of cyanide. If thiyl-free radicals are produced, as suggested above, these would be expected to react either with oxygen or with organic impurities, or to dimerize. Traces of disulfide could be identified among the reaction solutions in some cases, but tests for other products were unsuccessful in the presence of cyanide. Both of these reaction mechanisms are possible, then. No hydrolysis of diethyldisulfide was detected in the presence of cyanide, using test solutions over a week.

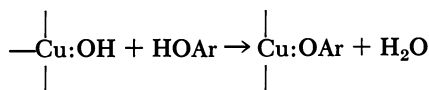
**Frank Mayo**: Is there any evidence in this system of attack on disulfides by hydroxyl ions, as suggested by Daneby and Hunter [*J. Org. Chem.* **32**, 2047 (1967)]?

**D. L. Trimm**: We have found no evidence of such attack on the alkyl and aryl disulfides produced in our study, even at a sodium hydroxide concentration of 5*M*. Such reactions would be expected to occur more easily, however, with substituted disulfides such as 3,3'-dithiodipropionic acid or 2,2'-dithiodiethylamine.

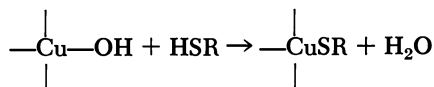
**Allan S. Hay:** In the oxidative coupling of phenols with copper-amine catalysts and oxygen the evidence is quite compelling that the active catalyst has the structure



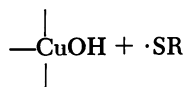
where X is preferably chloride or bromide. The first step in the reaction is



Catalysts of this type are also extraordinarily reactive for the oxidative coupling of thiols to disulfides, and the reaction is quantitative in a wide variety of organic solvents. In this case, the analogous first step would be



Electron transfer from sulfur to copper would now give a copper(I) complex, and the mercapto radical which is uncharged could now be readily displaced by another ligand, or the complex could be oxidized further by oxygen to give



Subsequent dimerization of the radicals would give the disulfide.

# Autoxidation of Hydrocarbons Catalyzed by Cobalt and Bromide Ions

YOSHIO KAMIYA

Faculty of Engineering, University of Tokyo, Hongo, Tokyo, Japan

*The autoxidation of hydrocarbons catalyzed by cobalt salts of carboxylic acid and bromide ions was kinetically studied. The rate of hydrocarbon oxidation with secondary hydrogen is exactly first order with respect to both hydrocarbon and cobalt concentration. For toluene the rate is second order with respect to cobalt and first order with respect to hydrocarbon concentration, but it is independent of hydrocarbon concentration for a long time during the oxidation. The oxidation rate increases as the carbon number of fatty acid solvent as well as of cobalt anion salt are decreased. It was suggested that the cobalt salt not only initiates the oxidation by decomposing hydroperoxide but also is responsible for the propagation step in the presence of bromide ion.*

The rate of metal salt-catalyzed autoxidation of hydrocarbons reaches a maximum at a certain catalyst concentration (1, 7, 13), and any further increases in this concentration do not accelerate the rate. However, when bromide ion is added to the solution of hydrocarbon and fatty acid with metal salts, the oxidation rate increases over the maximum value of  $k_3^2(\text{RH})^2/2k_6$  as a function of metal concentration.

Although cobalt and bromide ion catalysis have been studied by Ravens (11) and recently by Hay and Blanchard (4), there are many important aspects yet to be elucidated.

In this paper we hope to clarify the features of cobalt bromide catalysis using various hydrocarbons and a neutral bromide as sodium bromide at low temperatures and at moderate concentrations of cobalt.

## *Experimental*

The experimental technique has been described (6). Hydrocarbons were oxidized at temperatures from 35° to 95°C. in a 1:1 mixture by

volume of fatty acid and hydrocarbon unless otherwise stated. The oxidation products were analyzed by gas-liquid chromatography. Isotactic polypropylene (powdered, MW,  $2.5 \times 10^5$ ), atactic polypropylene (MW,  $6 \times 10^4$ ), and polystyrene (MW,  $2 \times 10^5$ ) were the polymers used. To analyze the oxidation products in a long run, a 50-ml. cylindrical flask with condenser, oxygen inlet, and sample outlet was used under vigorous agitation.

### Results

When the cobalt salt of carboxylic acid and bromide ion are dissolved in acetic acid, a cobalt bromide complex is formed instantaneously. For cobalt dibromide a pronounced induction period was observed, but adding sodium acetate eliminates entirely the induction period, suggesting that cobalt monobromide is responsible for the catalysis.

Typical oxygen absorption curves (Figure 1) show a short induction period and steady rate even after considerable absorption of oxygen at NaBr/cobalt ratio above 1/1.

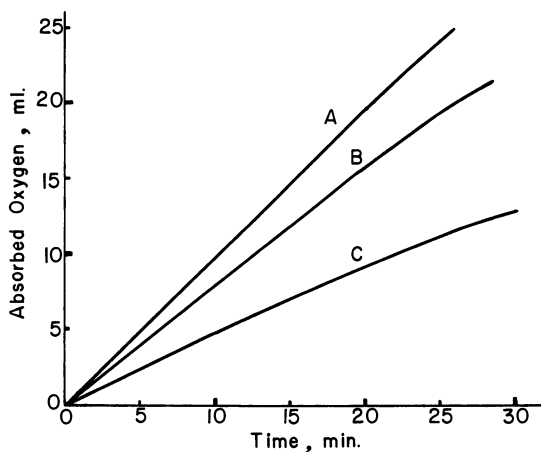


Figure 1. Oxygen absorption curves in the autoxidation of 4.07M ethylbenzene catalyzed by  $2 \times 10^{-2}$ M CoAc and NaBr in acetic acid

- A: NaBr,  $8 \times 10^{-3}$ M  
 B: NaBr,  $2 \times 10^{-2}$ M  
 C: NaBr,  $1 \times 10^{-2}$ M

**Cobalt Concentration.** The effect of bromide ion becomes appreciable at cobalt concentrations above 0.001M and quite remarkable above 0.01M. The ratio of  $\rho_{Br}$  (oxidation rate in the presence of 0.1M NaBr) to  $\rho_0$  (oxidation rate in the absence of NaBr) at cobalt concentration

0.05M is shown in Table I. The effect of bromide ion on the cobalt-catalyzed oxidation of methylbenzenes is quite large.

**Table I. Effect of NaBr on Oxidation Rate of Hydrocarbons Catalyzed by  $5 \times 10^{-2}M$  Cobalt Acetate in Acetic Acid**

Hydrocarbon	Temperature, °C.	$\rho_{Br}/\rho_0$
Tetralin	50	4
Cumene	60	4
Ethylbenzene	80	30
<i>n</i> -Dodecane	80	86
<i>p</i> -Xylene	80	400

The activation energy of over-all oxidation catalyzed by 0.02M cobalt acetate and 0.04M NaBr is very small—8.3 kcal./mole for ethylbenzene, 8.7 for *p*-xylene, and 14.9 for *n*-dodecane.

The broken line in Figure 2 shows that the steady rate of oxidation of 4.07M ethylbenzene in acetic acid, catalyzed by cobalt acetate, reaches a limiting rate of  $2.2 \times 10^{-5}$  mole liter<sup>-1</sup> sec.<sup>-1</sup> (after correcting for the dielectric effect (5, 9),  $1.8 \times 10^{-5}$ ), which is in excellent agreement with the theoretical limiting rate of  $1.85 \times 10^{-5}$  mole liter<sup>-1</sup> sec.<sup>-1</sup> as calculated by  $k_3^2(\text{RH})^2/2k_6$ .

However, the rate of oxidation in the presence of bromide ion (Figure 2) is exactly first order with respect to cobalt. The autoxidation of hydrocarbons catalyzed by cobalt and bromide ion is characterized by the fact that the rate increases with increasing cobalt concentration, while the rate at high cobalt concentrations reaches a limiting value in the absence of bromide ion.

Similar first-order correlation between cobalt and the rate was obtained for *n*-dodecane. The oxidation rate of *n*-dodecane decreases as cobalt concentration is increased to more than 0.05M, probably owing to chain termination by cobalt as reported for Tetralin (8). The oxidation rate of toluene is nearly second order with respect to cobalt (Figure 3).

**Hydrocarbon Concentration.** The steady rate of hydrocarbon oxidation is exactly first order with respect to hydrocarbon concentration, but it tends to be independent of this concentration below 1.0M (Figure 4). The cobalt-catalyzed autoxidation of Tetralin (6) and ethylbenzene at 0.05M cobalt in the absence of bromide is exactly second order with respect to hydrocarbon concentration.

In reactions catalyzed by cobalt and bromide the oxidation rates of ethylbenzene, cumene, and Tetralin start to decrease after several percent conversion and are roughly proportional to the hydrocarbon concentration during the oxidation.

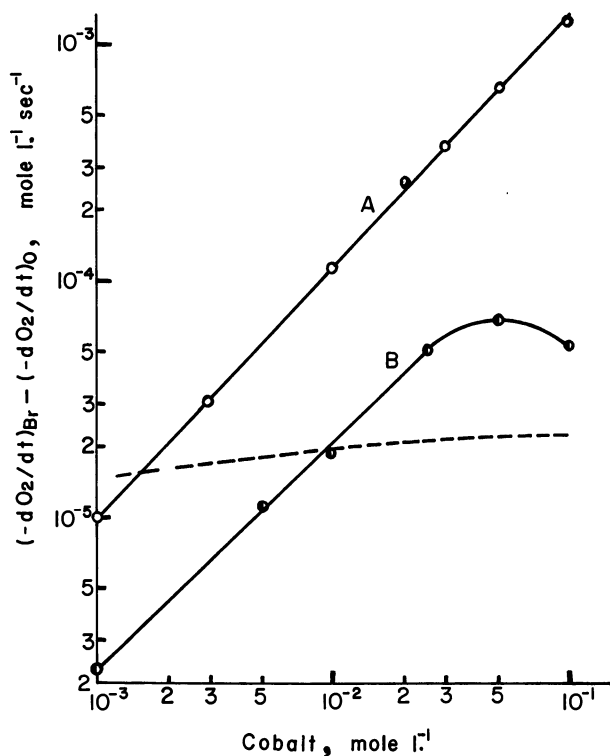


Figure 2. Steady rate of hydrocarbon oxidation as a function of cobalt concentration at  $\text{NaBr}/\text{Co} = 2/1$  at  $80^\circ\text{C}$ .

A: 4.07M ethylbenzene in acetic acid

B: 2.20 n-dodecane in n-butyric acid

Broken line: oxidation rate of ethylbenzene in absence of NaBr

However, for toluene and *p*-xylene, the rates are constant up to 70% conversion as the NaBr/cobalt ratio increases (Figure 5). The rate seems independent of hydrocarbon concentration during the oxidation, although the steady oxidation rate is exactly proportional to initial hydrocarbon concentration. Separate experiments showed that the rate increases if benzaldehyde is added but decreases as hydrocarbon and bromide ion are consumed or water is added.

According to visible spectra (Figure 6) and potentiometric titration, the concentration of bromide ion decreases gradually as toluene oxidation proceeds, but the total amount of bromide ion after treating the solution with alkali remains constant (Figure 7). The bromide ion converted to organic bromides (benzyl bromide) during the oxidation can be hardly

regenerated at temperatures below 80°C. About 25 toluene molecules were oxidized per bromine atom at 80°C.

**Ratio of Bromide Ion to Cobalt.** As the NaBr/cobalt molar ratio is increased, the oxidation rate increases and becomes constant at NaBr/cobalt = 1/1 or 2/1. A NaBr effect similar to that in Figure 8 was observed independent of cobalt and hydrocarbon concentrations at temperatures from 35° to 80°C.

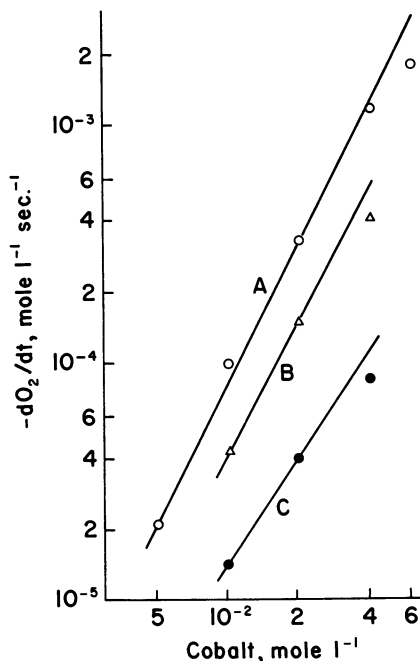


Figure 3. Steady rate of oxidation of 4.7M toluene in acetic acid as a function of cobalt concentration at NaBr/Co = 2/1

A: 80°C.  
B: 65°C.  
C: 50°C.

However, when a strong bromide such as calcium bromide is used, the oxidation rate reaches a maximum (Figure 8) and decreases as the ratio is increased, probably owing to the formation of inactive cobalt dibromide.

**Effect of Acid Strength.** When a higher fatty acid is used instead of acetic acid, the oxidation rate is lower as the carbon number of the

fatty acid is increased and is of the order of acid strength given in Table II. The equilibrium constant may be affected by the anion of cobalt salts since the oxidation rates of ethylbenzene and *n*-dodecane in propionic or butyric acids increase 15% by using cobalt acetate instead of cobalt decanoate. In a stronger acidic solution decanoate anion will be substituted by solvent acid anion. A weaker acid anion will result in a smaller equilibrium constant—*i.e.*, smaller cobalt bromide concentration.



The solvent acid also affects the oxidation rate since the rate with cobalt acetate (Table II) is reduced in propionic or butyric acids in contrast to the increase in the hydroperoxide decomposition rate.

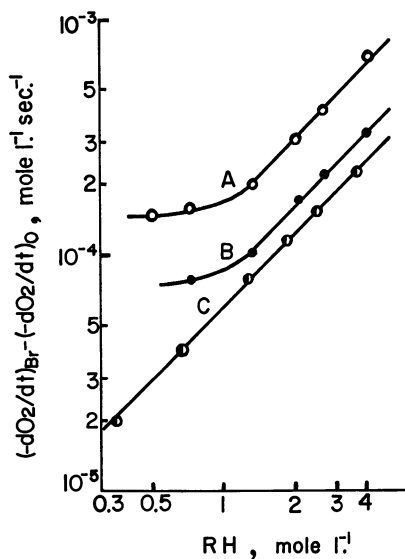


Figure 4. Steady rate of hydrocarbon oxidation as a function of hydrocarbon concentration with  $5 \times 10^{-2} \text{M}$  CoAc and  $1 \times 10^{-1} \text{M}$  NaBr in acetic acid

A: Ethylbenzene at 80°C.  
 B: *p*-Xylene at 80°C.  
 C: Tetralin at 35°C.

**Oxidation Products.** Although the ratio of hydroxyl to carbonyl products is 1/1 or nearly so in the ordinary metal salt-catalyzed autoxidation of hydrocarbons, higher proportions of carbonyl compounds are obtained in autoxidations catalyzed by cobalt and bromide ion—*e.g.*,

acetophenone from ethylbenzene, dodecanone from dodecane, and benzaldehyde from toluene. This change in alcohol-to-carbonyl ratio establishes the presence of different chain carriers in the presence of bromide.

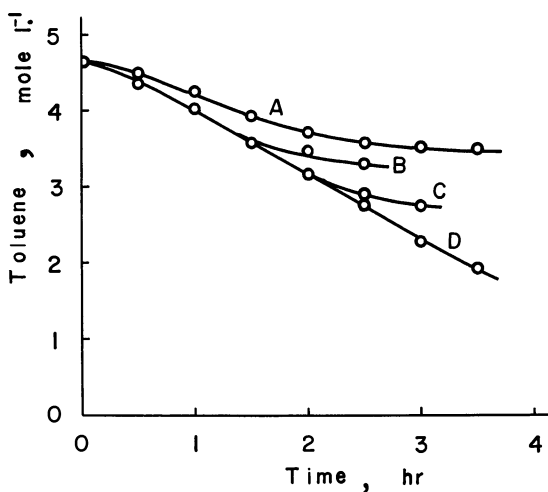


Figure 5. Consumption of toluene during the oxidation catalyzed by  $2 \times 10^{-2}$  M CoAc and NaBr in acetic acid

NaBr concentrations:

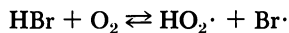
A:  $2 \times 10^{-2}$  M

B:  $4 \times 10^{-2}$  M

C:  $8 \times 10^{-2}$  M

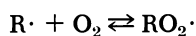
D:  $1.6 \times 10^{-1}$  M

**Partial Pressure of Oxygen.** It was reported that the oxidation rate of *p*-toluic acid catalyzed by cobalt and bromide ion at 130°C. is half order with respect to the partial pressure of oxygen, and the initiating reaction is suggested to be the following.



Therefore, the effect of partial pressure on the oxidation rate of ethylbenzene, Tetralin and *p*-xylene was examined carefully. However, at temperatures below 80°C. the rate was independent of the partial pressure of oxygen at pressures of 400–760 mm. Hg.

The dependence of the rate on the oxygen pressure (II) at higher temperature may be ascribed to the rate at which oxygen dissolves in the solution or to the following equilibrium (I).



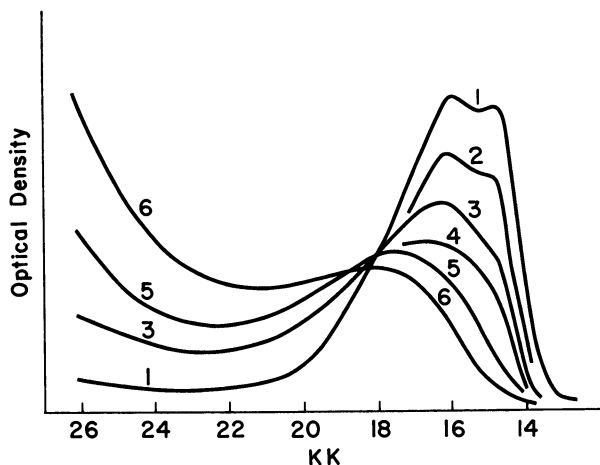


Figure 6. Visible spectra of 4.7M toluene in acetic acid with  $5 \times 10^{-3}M$  cobalt and  $1 \times 10^{-2}M$  NaBr at  $80^{\circ}C$ . during oxidation

*Minutes:*

- (1): 0
- (2): 25
- (3): 65
- (4): 85
- (5): 105
- (6): 120

**Synergistic Effect of Metal Salts.** When 20% of the cobalt is replaced by manganese, approximately a sixfold increase in the oxidation rate of *p*-xylene (Figure 9) was observed, showing that the metals are strongly synergistic. Similar synergistic results are obtained in the oxidation of ethylbenzene and cumene (Figure 9).

In contrast to the effect of manganese, cupric salt strongly retards the oxidation, reducing the rate of *p*-xylene by a factor of more than 10 when 20% of cobalt is replaced by cupric acetate.

**Effect on the Oxidation of Polymers.** In the cobalt bromide catalysis, the steric hindrance to the intramolecular hydrogen abstraction in the autoxidation of polymers is expected to be reduced remarkably.

The oxidation rate of 0.5 gram atactic polypropylene with 0.02M cobalt acetate in 10 ml. of a 1/1 mixture by volume of chlorobenzene and acetic acid increases from  $2.7 \times 10^{-4}$  to  $2.76 \times 10^{-3}$  mole  $kg^{-1}$   $sec^{-1}$  in the presence of 0.04M sodium bromide. The rate of powdered isotactic polypropylene under the same conditions increases only from  $2.05 \times 10^{-3}$  to  $2.45 \times 10^{-3}$  mole  $kg^{-1}$   $sec^{-1}$  in the presence of sodium bromide.

The effect of bromide ion was more pronounced in polystyrene oxidation. Although polystyrene in a 1/1 mixture by volume of chlorobenzene and acetic acid is barely autoxidized at 100°C. in the presence of cobalt salt or initiators, the oxidation catalyzed by cobalt is so strongly accelerated by bromide ion that it proceeds rapidly even at temperatures as low as 45°C. (Figure 10).

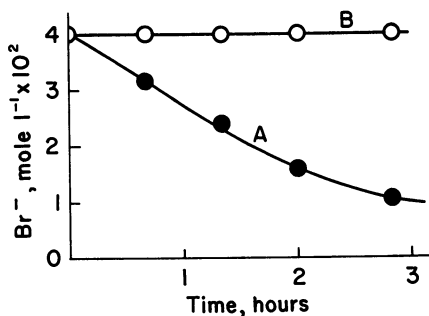


Figure 7. Concentration of bromide ion during the oxidation of 4.7M toluene in acetic acid with  $2 \times 10^{-2}$ M cobalt and  $4 \times 10^{-2}$ M NaBr at 80°C.

A: Before alkali treatment  
B: After alkali treatment

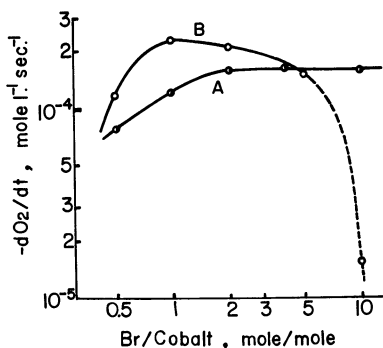
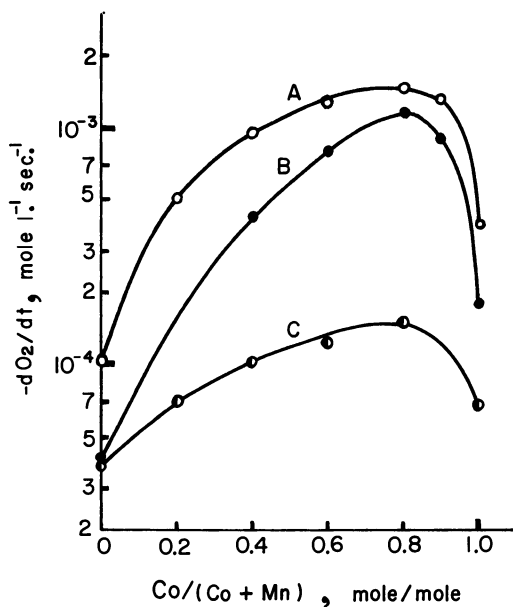


Figure 8. Steady rate of oxidation of 4.07M ethylbenzene catalyzed by CoAc and bromide ion in acetic acid as a function of the Br/Co molar ratio

A: CoAc,  $2 \times 10^{-2}$ M, NaBr at 65°C.  
B: CoAc,  $1 \times 10^{-2}$ M, CaBr₂ at 80°C.

**Table II. Effect of Cobalt Anion and of Solvent Acid on Oxidation Rate of 4.07M Ethylbenzene with  $2 \times 10^{-2}$ M Cobalt and  $4 \times 10^{-2}$ M NaBr in Acetic Acid at 65°C.**

Cobalt Salt	Solvent	$-dO_2/dt \times 10^4$ , mole/liter/sec.
Cobalt acetate	Acetic acid	1.55
	Propionic acid	1.37
	<i>n</i> -Butyric acid	1.18
Cobalt decanoate	Acetic acid	1.55
	Propionic acid	1.21
	<i>n</i> -Butyric acid	0.99



*Figure 9. Mixing effect of cobalt with manganese on the oxidation of hydrocarbons at NaBr/metal = 2/1 in acetic acid*

- A: Ethylbenzene, 4.07M at 80°C.; total metal concentration,  $3 \times 10^{-2}$ M  
 B: *p*-Xylene, 4.06M at 80°C.; total metal,  $2 \times 10^{-2}$ M  
 C: Cumene, 3.58M at 50°C.; total metal,  $2 \times 10^{-2}$ M

### Discussion

Ravens (11) proposed that hydrogen bromide initiates chains by reacting with molecular oxygen to produce bromine atom which initiates

the peroxide chain. Hay and Blanchard (4) concluded that hydrogen bromide does not initiate chains but accelerates chain propagation by reacting with peroxy radicals so that hydrocarbon is attacked by bromine atom rather than peroxide radicals, and hydrogen bromide is regenerated from organic bromide by cobalt.

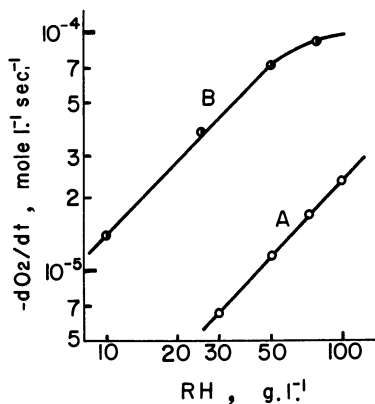


Figure 10. Steady rate of polystyrene oxidation as a function of hydrocarbon concentration catalyzed by  $2 \times 10^{-2}M$  CoAc in  $1 \times 10^{-2}M$  NaBr in a 1:1 mixture by volume of chlorobenzene and acetic acid

A: at 45°C.

B: at 60°C.

However, our fast oxidations were obtained under conditions where the concentration of free hydrogen bromide was extremely low. The following observations suggest that free hydrogen bromide is probably not responsible for chain propagation.

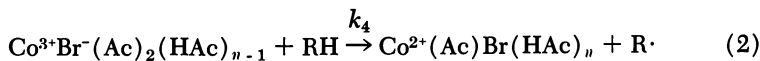
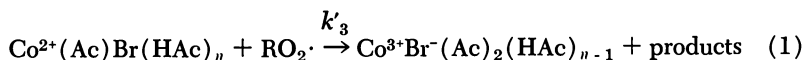
(a) The steady concentration of Tetralin hydroperoxide (10) is only slightly affected by adding sodium bromide.

(b) Even at temperatures where organic bromide is stable, the catalyst retains its activity for a long time. For example, the number of hydrocarbon molecules oxidized per bromine atom was only 1–2 in the oxidation by hydrogen bromide and AIBN but 25 in the oxidation by cobalt and sodium bromide.

(c) Carbonyl compounds are formed in greater yields than alcohols.

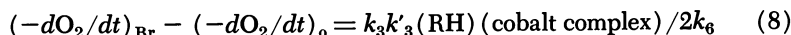
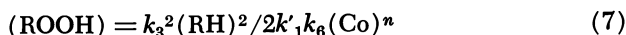
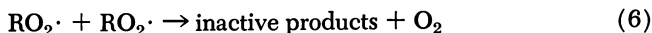
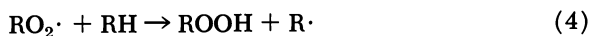
(d) The rate of oxidation is first order in hydrocarbon concentrations at high cobalt concentrations.

To explain the above results, we suggest that a cobalt bromide rather than hydrogen bromide complex is responsible for the propagation step. A hydrogen-bonded cobalt bromide complex may be considered.



It is known that olefins are oxidized easily by cobaltic sulfate (2) and toluene by  $\text{Co}^{3+}(\text{H}_2\text{O})_6$  (3). We found that various hydrocarbons (12) such as toluene, ethylbenzene, and cumene can be oxidized rapidly by cobaltic acetate in the absence of oxygen.

Assuming that the propagation reaction proceeds by Reactions 1 and 2 and that  $k_4 > k'_3$ , the steady-state treatment, including well-established elementary reactions (3 to 6), gives Reactions 7 and 8 when the rate of hydroperoxide decomposition equals its rate of formation.



The kinetic results on the oxidation of secondary hydrogen (Figures 2 and 4) show good agreement with Reaction 8.

The induction period in the oxidation of ethylbenzene catalyzed by cobalt and sodium bromide in the presence of 2,6-di-*tert*-butyl-*p*-cresol indicates that the direct initiation is negligible compared with the rate of initiation by the cobalt-catalyzed decomposition of hydroperoxide.

### Literature Cited

- (1) Benson, S. W., *J. Am. Chem. Soc.* **87**, 972 (1965).
- (2) Bawn, C. E. H., Sharp, J. A., *J. Chem. Soc.* **1957**, 1854.
- (3) Cooper, T. A., Clifford, A. A., Mills, D. J., Waters, W. A., *J. Chem. Soc.* **1966** (B) 793.
- (4) Hay, A. S., Blanchard, H. S., *Can. J. Chem.* **43**, 1306 (1965).
- (5) Howard, J. A., Ingold, K. U., *Can. J. Chem.* **42**, 1044 (1964).
- (6) Kamiya, Y., Beaton, S., Lafortune, A., Ingold, K. U., *Can. J. Chem.* **41**, 2020 (1963).
- (7) Kamiya, Y., Beaton, S., Lafortune, A., Ingold, K. U., *Can. J. Chem.* **41**, 2034 (1963).
- (8) Kamiya, Y., Ingold, K. U., *Can. J. Chem.* **42**, 2424 (1964).
- (9) Kamiya, Y., *Bull. Chem. Soc. Japan* **38**, 2156 (1965).

- (10) Kamiya, Y., *Tetrahedron* **22**, 2029 (1966).
- (11) Ravens, D. A. S., *Trans. Faraday Soc.* **55**, 1768 (1959).
- (12) Sakota, K., Kamiya, Y., Ohta, N., unpublished work.
- (13) Woodward, A. E., Mesrobian, R. B., *J. Am. Chem. Soc.* **75**, 6189 (1953).

RECEIVED October 9, 1967.

## Discussion

**P. de Radzitzky:** Dr. Kamiya has observed a synergistic effect when manganese is added to the catalytic system Br/Co during the oxidations of *p*-xylene, cumene, and ethylbenzene, but no effect was observed for Tetralin or dodecane. Although the mechanism advanced by the author has possibly some validity, I think that the explanation is much simpler.

When using the catalytic system Br/Co the oxidation of ethylbenzene stops at acetophenone and that of *p*-xylene at an aldehyde. Oxidizing ethylbenzene in acetic acid and using only cobalt as catalyst we have noticed that a reaction which has stopped when a good part of ethylbenzene has been transformed chiefly into acetophenone can be restarted with extreme vigor by adding manganese, which oxidizes acetophenone almost quantitatively and quickly to benzoic acid. Similarly cumene is oxidized to acetophenone and then to benzoic acid as shown by a study of the synthesis of terephthalic acid from *p*-diisopropylbenzene [Van Helden, R., Kooyman, E. C., *Rec. Trav. Chim.* **80**, 57 (1961)]. Undoubtedly *p*-tolualdehyde will also be oxidized to *p*-toluic acid in the presence of manganese.

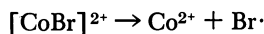
On the other hand, Tetralin which does not contain acetyl groups and dodecanone which contains only a minor amount of unactivated acetyl groups do not oxidize further under the same conditions when one adds manganese.

Therefore, I think that the higher rate of oxygen absorption observed when manganese is added to the Br/Co system is well explained for *p*-xylene, cumene, and ethylbenzene by the simultaneous oxidation of the acetyl or aldehyde groups originally formed. The fact that dodecane and Tetralin are not oxidized at a higher rate when manganese is added also supports this hypothesis.

**Allan S. Hay:** It has been amply and repeatedly demonstrated in this conference that many of the steps in autoxidation reactions are not adequately understood. When one adds a catalyst to an already complex

reaction (in this case one consisting of cobalt and bromide ions), the number of discrete steps or reaction intermediates that one can write is overwhelming.

Dr. Kamiya has attempted to explain the role of the catalyst according to Reactions 13–15, and he has attempted to differentiate between these proposed reaction steps and the simplified Reactions 3 and 4. It is not clear to me what types of structures he is trying to portray by using the empirical formulae  $\text{Co}^{2+}\text{BrH}$  and  $\text{Co}^{3+}\text{Br}^-$ . There does not seem to be any evidence for any unusual complexes in these solutions, and there does not seem to be any need to postulate them. It really becomes a matter of semantics because nobody believes that in solution  $\text{Br}\cdot$ , for example, exists as such, but it must be solvated by or coordinated with other species. Dr. Kamiya also implies that the initiation step is a direct reaction of the hydrocarbon with  $\text{Co(III)}$  ion. To my knowledge, a reaction such as this in acetic acid solution has never been demonstrated. We have shown that the reaction between cobalt(III) acetate in acetic acid and toluene is negligibly slow. It would be more likely to consider the reaction



and the  $\text{Br}\cdot$  formed could act as the initiator.

In considering the equilibrium depicted in Reaction 2 the author states essentially that at higher and higher dilution since the equilibrium would be displaced more to the right, the rate of the reaction should increase if this rate depends on  $\text{HBr}$  concentration. It is true that the equilibrium would be displaced to the right, but the absolute concentration of  $\text{HBr}$  in solution obviously decreases as the concentration of cobalt acetate bromide decreases; hence, the rate should, of course, decrease as  $\text{CoAcBr}$  concentration decreases.

# Homogeneous Catalysis of a Multistep Chain Oxidation

J. F. FORD and V. O. YOUNG

British Petroleum Co., Ltd., Sunbury-on-Thames, Middlesex, England

R. C. PITKETHLY

British Petroleum Co., Ltd., Sunbury-on-Thames, Middlesex, England, and  
The City University, London, England

*Co-oxidation of indene and thiophenol in benzene solution is a free-radical chain reaction involving a three-step propagation cycle. Autocatalysis is associated with decomposition of the primary hydroperoxide product, but the system exhibits extreme sensitivity to catalysis by impurities, particularly iron. The powerful catalytic activity of N,N'-di-sec-butyl-p-phenylenediamine is attributed on ESR evidence to the production of radicals, probably  $>NO\cdot$ , and replacement of the three-step propagation by a faster four-step cycle involving  $R\cdot$ ,  $RO_2\cdot$ ,  $>NO\cdot$ , and  $RS\cdot$  radicals. Added iron complexes produce various effects depending on their composition. Some cause a fast initial reaction followed by a strong retardation, then re-acceleration and final decay as reactants are consumed. Kinetic schemes that demonstrate this behavior but are not entirely satisfactory in detail are discussed.*

Co-oxidation of indene and thiophenol takes place readily if the reactants in benzene solution are shaken with oxygen at temperatures in the range 20° to 40°C. (7). The major primary product has been shown to be *trans*-2-phenylmercapto-1-indanyl hydroperoxide, I, which rearranges spontaneously to the two racemes of *trans*-2-phenylsulfinyl-1-indanol, II (8), and a tentative reaction scheme involving a three-step radical chain based on the suggestion of Kharasch, Nudenberg, and Mantell (11) was proposed for the formation of I. These three products accounted for 86% of the oxygen absorbed.

Concurrently with our work, Oswald and co-workers published a series of papers that greatly extended the knowledge of the scope of co-oxidation of unsaturated compounds with thiols (15). The results of their work were also consistent with the tentative reaction mechanism of co-oxidation.

The spontaneous rearrangement of I has been the subject of a detailed kinetic study (6) which showed that a synchronous hydrogen exchange took place in a dimeric complex.

The rate of rearrangement, although sufficient to reduce the yield of hydroperoxide (typically to 75 weight %), is not great enough to affect the kinetics of co-oxidation significantly. However, the rearrangement is accompanied by a side reaction, also second-order, which is probably another mode of decomposition of the dimeric complex. This side reaction is catalyzed by iron complexes and is believed to be the chain branching step and source of radicals which gives rise to the autocatalytic progress of co-oxidation in aromatic solvents.

This paper discusses three aspects of our extensive but as yet incomplete studies of the reaction: oxygen uptake in rigorously purified materials, the effects of added iron complexes, and the influence of a well-known radical capture agent. An interesting feature of the last, anticipated from the work of Rosenwald (19) on inhibitor sweetening, was the large accelerating effect of *N,N'*-di-*sec*-butyl-*p*-phenylenediamine on the co-oxidation reaction.

Attention is drawn to the complex kinetics which can result from delicately balanced catalysis of initiation and termination reactions and changes in the sequence of propagation reactions.

### **Experimental**

**Purification of Reactants and Solvents.** Indene and thiophenol of the origin and purity already described (8) were further purified as follows. Indene was percolated under oxygen-free nitrogen through a column containing half its volume of acid-free alumina (obtained from British Drug Houses). Portions of about 10 volume % of the eluate were discarded at the beginning and end. The heart cut was washed four times with equal volumes of 15 weight % NaOH, with 15% iron-free hydrochloric acid (BDH electronic grade), and finally with water (distilled water percolated through Permutit Biodeminrolit). The material thus obtained after drying over anhydrous analytical reagent grade magnesium sulfate had a boiling point of 67°C./13 mm.,  $n_D^{20}$  1.5765, freezing point 1.549°, and purity determined by freezing point not less than 99.5%. Examination by gas-liquid chromatography and infrared failed to detect any impurities. Immediately before use, this material was percolated under nitrogen through silica gel which had been freed from iron by washing with iron-free HCl until the washings showed no color change

with ammonium thiocyanate and freed from acid by washing with iron-free water. Use of quartz or borosilicate glass vessels for the final operation, providing both were first washed with iron-free HCl and water, made no significant difference in the co-oxidation. The total iron content of indene thus obtained was about 0.7 p.p.m. compared with about 5 p.p.m. before treatment.

Thiophenol was percolated through iron-free silica gel. The total iron content of the thiophenol thus obtained was about 0.5 p.p.m. Benzene (AnalaR grade) was distilled over sodium and percolated through iron-free silica gel. The total iron content of benzene thus obtained was about 0.14 p.p.m. Isooctane was redistilled and similarly treated. Curves A,A' and B,B' of Figure 1 were duplicate runs on two separate batches of components prepared by this procedure.

Anhydrous ferric chloride was used as received from British Drug Houses. 1,2-Bis(salicylidene amino)ethane iron(III) chloride [ $\text{Fe}(\text{bissalen})\text{Cl}$ ] was prepared in the usual way from ferric chloride and 1,2-bis(salicylidene amino)ethane. Found: C, 53.26; H, 4.12; N, 7.44; Fe, 15.6; Cl, 9.84. Calculated for  $\text{C}_{16}\text{H}_{14}\text{N}_2\text{O}_2\text{ClFe}$ : C, 53.7; H, 3.91; N, 7.83; Fe, 15.6; Cl, 9.93 weight %. This was a high melting (above  $300^\circ\text{C}$ .), nonrecrystallizable brown solid.

Ferric acetylacetonate was prepared in the usual way from freshly precipitated ferric hydroxide (m.p.,  $183.5^\circ\text{C}$ . (d.) (corr). Found: C, 50.8; H, 5.98; Fe, 15.48. Calculated for  $\text{C}_{15}\text{H}_{21}\text{O}_6\text{Fe}$ : C, 50.9; H, 5.95; Fe, 15.8 weight %). *N,N'*-Di-*sec*-butyl-*p*-phenylenediamine (DSBPD) was commercially available material (ICI Topanol M) redistilled (b.p.,  $105^\circ\text{C}/0.05\text{ mm}$ .). Examination by infrared failed to detect any impurities. The first fraction obtained from the distillation contained *p*-phenylenediamine (2 weight % on total DSBPD).

**Examination of Co-Oxidation Products.** Co-oxidation products were identified and hydroperoxide and sulfoxide yields were measured as previously described (7, 8). The observed stoichiometric ratio of indene, thiophenol, and oxygen consumed in the whole reaction is 1:1.06:1 (8).

**Oxygen Uptake-Time Measurements.** These were carried out, usually at  $20^\circ \pm 0.1^\circ\text{C}$ . and at  $760 \pm 5\text{ mm}$ . total pressure (680 mm. partial pressure of oxygen) on 5-ml. samples using the apparatus described by Bolland (2). Reactants dissolved in the appropriate amounts of solvent were introduced into a 15-ml. borosilicate glass flask (previously in contact with iron-free HCl for 24 hours and washed with iron-free water) cooled in dry ice-acetone using calibrated pipetes (similarly treated). Co-oxidations were usually carried out at  $[\text{indene}]_0 = [\text{PhSH}]_0 = 0.15M$  in benzene. Replacing washed borosilicate glassware with quartz or by plastic (polyethylene) made no significant difference in the oxygen-uptake vs. time curves.

**Iron Estimations.** These were carried out by extracting the iron with "iron-free" HCl ( $\sim 0.2\text{ p.p.m.}$ ), followed by measurement using a square wave polarograph. Reproducibility and accuracy on samples in which known amounts of ferric acetylacetonate had been placed were poor ( $\pm 50\%$ ). Wet combustion techniques followed by estimations using the square wave polarograph gave worse results than the procedure described.

**Addition of DSBPD during Co-Oxidation at 20°C.** A co-oxidation in the absence of DSBPD (5 ml. solution, 0.15M in thiophenol and indene) was allowed to proceed until 0.08 mole of O<sub>2</sub> per mole of PhSH had been absorbed; the reaction mixture was then frozen. A solution of 5 ml. of benzene containing  $9 \times 10^{-4}$  gram of DSBPD was added, and the co-oxidation was restarted. The subsequent rate obtained was 0.0086 compared with an initial rate of 0.015 mole of O<sub>2</sub> per mole of PhSH per minute obtained when a similar solution of DSBPD was added at the start of a co-oxidation.

### Results and Discussion

**Co-Oxidation in absence of Added Catalysts or Inhibitors.** Figure 1 (curves A,A', B,B') shows typical oxygen uptake vs. time curves obtained after using the procedures for purifying indene, thiophenol, and benzene and cleaning the reaction vessel as described above. On the experience of several hundred runs, the reproducibility expected was such that the time for uptake of 0.5 mole of O<sub>2</sub> per mole of PhSH would be in the range 150 to 200 minutes. Despite all efforts, it was estimated that iron

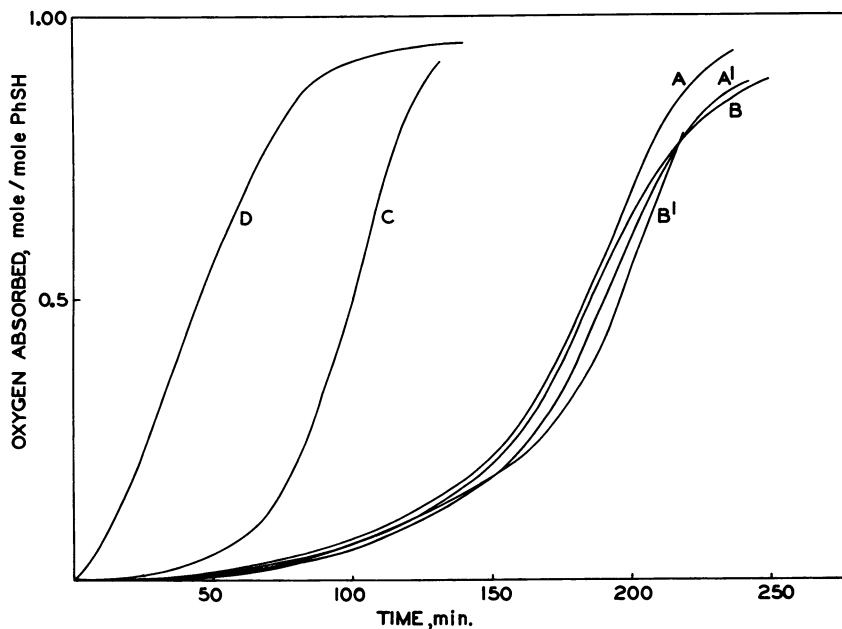


Figure 1. Co-oxidation of indene and 0.15M thiophenol in benzene at 20°C.

A,A', B,B': Purified reagents, no additives

C: 0.0075M (PhCOO)<sub>2</sub>

D: 0.015M (PhCOO)<sub>2</sub> + 0.0075M PhNMe<sub>3</sub>

was still present in the reactants and solvent, giving the curves of Figure 1, to a total concentration in the reaction mixture of about 0.2 p.p.m. If these procedures were not used, curves like those obtained with added iron (Figure 2) were sometimes obtained, and generally, in the presence of added iron complexes, greater variability was found—*e.g.*, curves 375R to 377R in Figure 2. Neither the indene nor the thiophenol, alone, absorbed measurable amounts of oxygen under the conditions of a co-oxidation run.

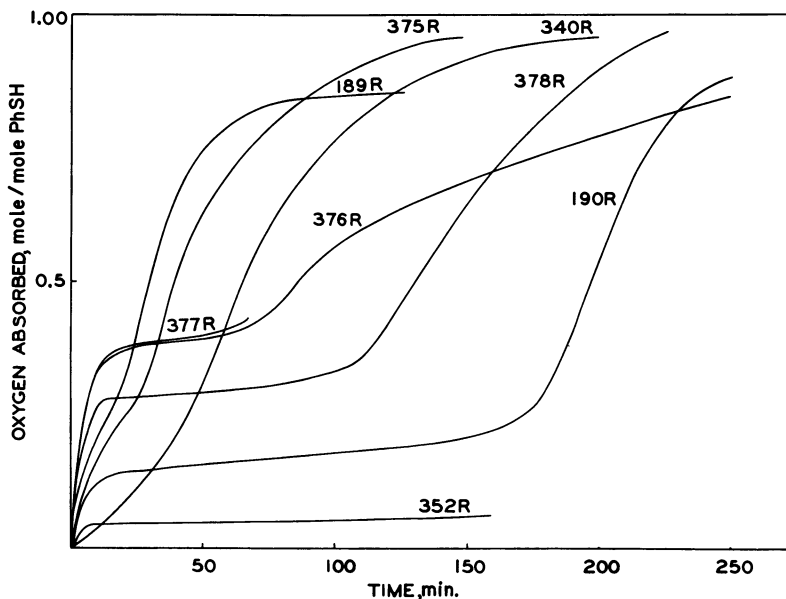


Figure 2. Effect of iron complexes on co-oxidation of indene and thiophenol in benzene at 20°C.

*FeCl<sub>3</sub>*

189R,  $3.14 \times 10^{-4}$ M

190R,  $3.14 \times 10^{-5}$ M

*Fe(acac)<sub>3</sub>*

352R,  $1.26 \times 10^{-5}$ M

378R,  $1.48 \times 10^{-5}$ M

375R,  $5.89 \times 10^{-5}$ M

376R,  $5.89 \times 10^{-5}$ M

377R,  $5.89 \times 10^{-5}$ M

*Fe(bissalen)Cl*

340R,  $3.0 \times 10^{-5}$ M

Benzoyl peroxide (Figure 1, curve C) or even more effectively, benzoyl peroxide plus dimethylaniline (Figure 1, curve D), accelerated the reaction to varying degrees. Strong bases altered the course of the

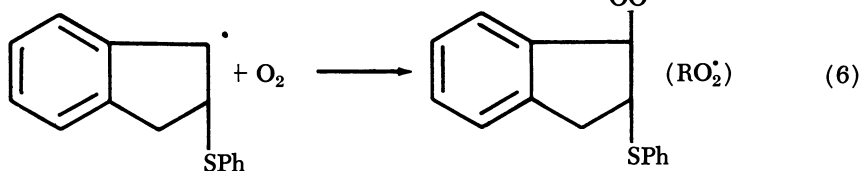
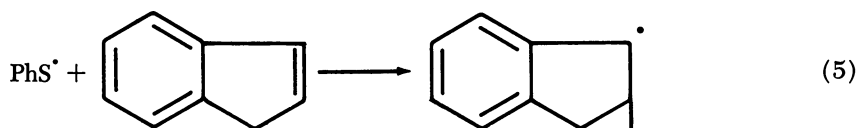
reaction by accelerating the direct oxidation of thiophenol to diphenyl disulfide.

It was initially assumed as in other autoxidation systems, that auto-catalysis arose from first- or second-order radical-producing decompositions of the hydroperoxide product of the reaction, and this led to Reaction Scheme 1 (shown below).

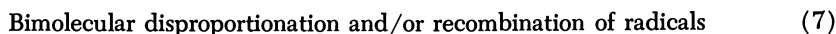
#### Initiation



#### Propagation



#### Termination



#### Reaction Scheme 1

The greater speed of the co-oxidation compared with autoxidation of the indene alone was accounted for by assuming that Reactions 4 and 5 are faster than addition of  $\text{RO}_2^\cdot$  to indene.

Analyzing the kinetics of this system (18) showed that linear combination of the three initiating reactions could account for long accelerating periods but could not explain a constant or slightly falling rate which was sometimes observed in the early stages of co-oxidation. The kinetic analysis also suggested that the slow rise and general shape of the oxygen-uptake curves could be accounted for if the radical buildup were slow and nonstationary. This explanation was rejected after several experiments in which a rapidly progressing co-oxidation was quenched in liquid air, and the mixture was allowed to warm to  $20^\circ\text{C}$ . under nitrogen

and stand for a time. After subsequent refreezing, replacement of nitrogen by oxygen, and rewarming, the reaction proceeded at exactly the rate observed just before the interruption. Thus, unless the free radicals were startlingly long-lived, the initiation must come from stable products, and the reaction is in a pseudo-steady state—*i.e.*, the main propagation chain responds rapidly to changes in initiation and termination rates.

The influence of the products of the reaction on the kinetics was then examined. First, the stable products, isolated from the reaction mixture after rearrangement of hydroperoxide was complete (8), were added (5 weight % on PhSH) in separate experiments to the indene-thiophenol reaction mixture. The racemic sulfoxides, II, the corresponding *trans*-hydroxysulfide, a ketosulfoxide concentrate, and freshly recrystallized diphenyl disulfide, had no significant effect on the oxygen uptake *vs.* time curves. Second, portions of the whole co-oxidation mixture after oxygen absorption ceased, and containing about 0.11 mole per liter of hydroperoxide, I, when added to a fresh reaction mixture greatly increased the oxidation rate. However, varying the amounts of added fresh co-oxidation products showed a complex and rather irreproducible concentration dependence. The effect of partly decayed co-oxidation products was also unexpectedly complex, and completely decayed products containing no hydroperoxide could vigorously accelerate co-oxidation. This confirmed that simple first- or second-order radical-producing decompositions of peroxide could not adequately explain the catalytic behavior of the products, although the peroxide undoubtedly played an essential role in the autocatalysis of the main reaction itself.

Peroxide in solution is necessary to produce fast co-oxidation. When isooctane was used as solvent instead of benzene, a slow and linear oxygen uptake was observed (0.5 mole per mole of indene in 100 hours at 20°C.). This behavior was the result of low solubility in the paraffin of the hydroperoxide, I, which precipitated out and rapidly rearranged to inactive sulfoxides.

We conclude that although Scheme 1 represents a basic mechanism for co-oxidation of indene and thiophenol, the system is so sensitive to the effects of catalysts and inhibitors that interpreting its behavior necessitates studying the initiation and termination mechanisms.

**Co-Oxidation in Presence of Added *N,N'*-di-*sec*-butyl-*p*-phenylene-diamine.** Figure 3 shows typical oxygen uptake curves obtained if DSBPD is added at concentrations around  $10^{-2}$  to  $10^{-4}M$  to the indene-thiophenol reaction mixture. The reproducibility was good. The products after oxygen absorption was complete and the hydroperoxide had been allowed to decay were substantially the same as those obtained in the absence of DSBPD. Uptake of oxygen was extremely slow when either of the main reactants was omitted.

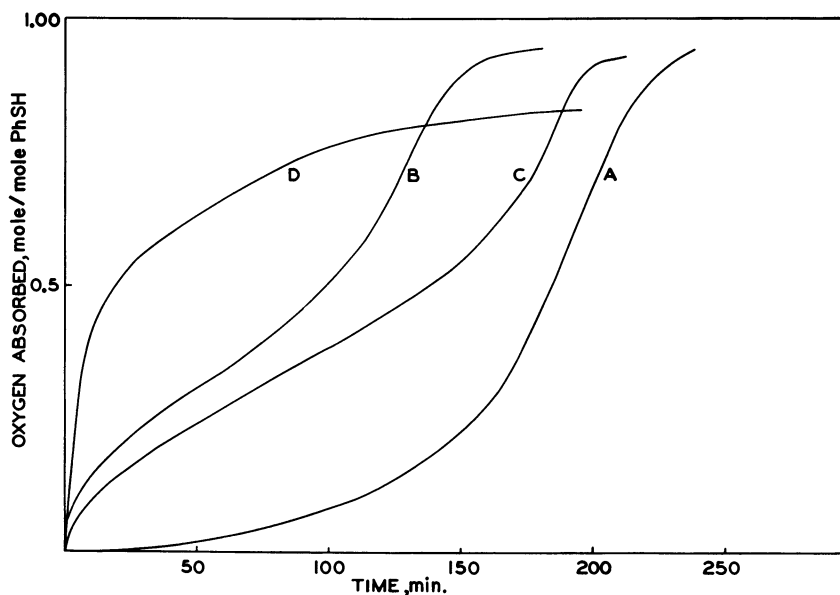


Figure 3. Effect of *N,N'*-di-*sec*-butyl-*p*-phenylenediamine on co-oxidation of indene and 0.15M thiophenol in benzene at 20°C.

- A: no additive  
 B:  $7.5 \times 10^{-5}$ M DSBPD  
 C:  $7.5 \times 10^{-5}$ M preoxidized DSBPD  
 D:  $7.5 \times 10^{-3}$ M DSBPD

It is reasonably well established that aromatic amines act as inhibitors of hydrocarbon autoxidation by capturing the chain-propagating radical ( $\text{RO}_2\cdot$ ) to form, eventually, species which do not propagate the chain. Thus, in competition for  $\text{RO}_2\cdot$  with a hydrocarbon, the amine is successful. In the co-oxidation reaction, since PhSH is known to be an efficient radical scavenger or polymerizing chain transfer agent, RSH might be expected to compete successfully with the amine for  $\text{RO}_2\cdot$ . This would explain a lack of inhibiting action of DSBPD in the co-oxidation but not the large accelerations it can produce, nor the high initial rates observed with no significant induction period.

Rosenwald (19) attributed the acceleration of the reactions involved in inhibitor sweetening to the reaction of an unidentified oxidation product of the amine with thiol to produce mercaptyl radicals. However, the oxidation of neat DSBPD is slow at 20°C. ( $3.3 \times 10^{-5}$  mole of  $\text{O}_2$  per mole of amine per second) and partial pre-oxidation of the DSBPD until 0.26 mole of  $\text{O}_2$  was absorbed per mole of amine did not enhance the activity of the amine (compare curves B and C in Figure 3). Furthermore, allowing the co-oxidation to proceed for a time before adding the

DSBPD did not significantly alter the accelerated rate of co-oxidation. It must, therefore, be concluded that the initiation arises from interaction of the amine with a reactant and not with a product such as hydroperoxide. In addition, Rosenwald's "oxidized state" of the amine cannot be among the stable oxidation products of the amine.

The reactions of DSBPD were therefore examined. DSBPD did not appear to react with thiophenol under nitrogen, but it did react slowly with oxygen. Pure DSBPD showed no ESR spectrum, but bubbling oxygen through the sample tube was followed by the appearance of a red color and a three-line spectrum (Figure 4), with  $g = 2.003$  and splitting  $a_N = 11.9$  gauss and partly resolved fine structure ( $a_H = ca., 2.3$  gauss). After the oxygen was pumped off, the three-line spectrum faded.

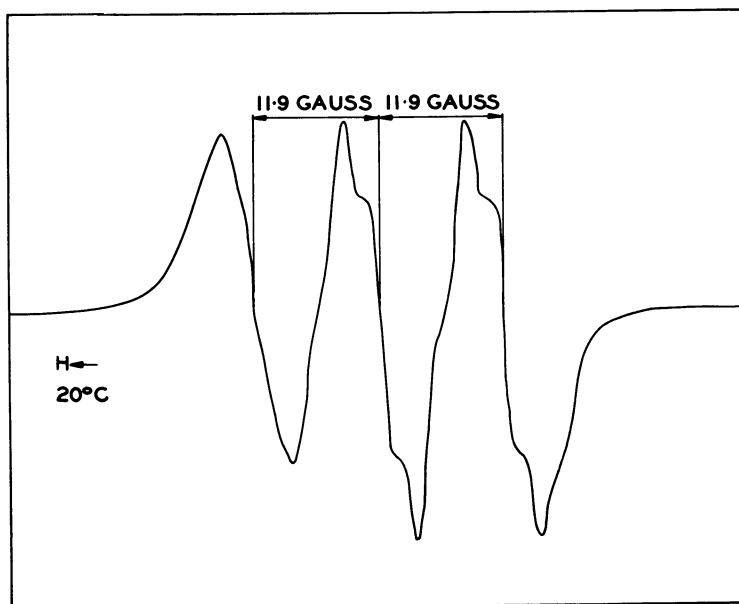


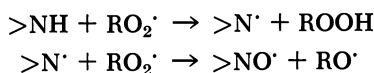
Figure 4. *N,N'*-Di-sec-butyl-*p*-phenylenediamine plus oxygen at 20°C.

This behavior is not consistent with the formation of Wurster ions, which have been postulated as intermediates and in fact demonstrated to occur in polar solvents (3) but indicates the formation of a nitroxyl radical intermediate in the presence of oxygen and its decay when the oxygen is removed. [Sullivan (23) gives a number of references to nitroxyl radicals.] The possibility that  $R_2N'$  radicals are formed as a

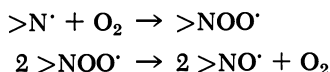
result of hydrogen abstraction by radicals and the problem of distinguishing the ESR spectra of  $R_2N^{\cdot}$  and  $R_2NO^{\cdot}$  radicals are discussed by Copinger and Swalen (5). They favor decomposition mechanisms involving oxidation-reduction chains between  $>NO^{\cdot}$  and  $>NOH$ . Hydrogen abstraction reactions involving diphenylnitroxyl- and diphenylhydroxylamine have been postulated to account for catalysis of benzoyl peroxide decomposition (4).

Admitting thiophenol to an oxidizing sample of DSBPD immediately quenched the three-line ESR spectrum. Also DSBPD containing thiophenol absorbed oxygen much more rapidly than the amine itself and formed diphenyl disulfide and water, but no color appeared. However, thiophenol does not discharge the color of an oxidized sample of the amine. Thus, although the nitroxyl radical may be red, the color of the oxidized amine is mostly associated with the products of further oxidation. It is evident that the  $>NO^{\cdot}$  radical from DSBPD reacts readily with thiophenol, presumably abstracting hydrogen and producing  $PhS^{\cdot}$  radicals. Other more stable  $>NO^{\cdot}$  radicals have been reported to behave similarly (9).

Baird and Thomas (1) have shown that radical initiators—*e.g.*, AZDN in the presence of oxygen—produce  $>NO^{\cdot}$  radicals from primary and secondary amines and Thomas (24) proposed a mechanism for amine attack by  $RO_2^{\cdot}$  radicals:

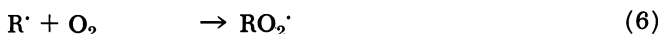
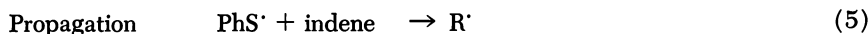
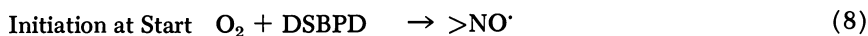


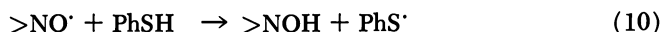
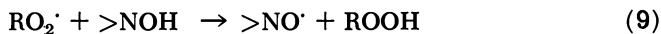
An alternative mechanism for nitroxyl radical production analogous to one of the higher temperature modes of  $RO_2^{\cdot}$  destruction is:



These reactions are probably fast, and a plausible modification of Reaction Scheme 1 gives Scheme 2, which fits the observed facts.

If the  $>N^{\cdot}$  radicals are more active than  $>NO^{\cdot}$ , they could play a more important role in the chain propagation; however, the rate of reaction of  $Ph_2N^{\cdot}$  with thiols is relatively slow and even at  $100^{\circ}C$ . is incomplete after more than 100 hours (26). Only the radical which has been identified is included in Scheme 2.





Termination      Disproportionation and/or combination of radicals      (7)



*Reaction Scheme 2*

In Reaction Scheme 2 the acceleration of co-oxidation by DSBPD arises from  $>\text{NO}'$  radical production by direct interaction of the amine with oxygen in Reaction 8, together with the introduction of a pair of fast steps (Reactions 9 and 10) which bypass the rate-determining step of the main propagation chain (Reaction 4 of Scheme 1). The main propagation chain has now become a four-step chain consisting of Reactions 5, 6, 9, and 10.

Consumption of the DSBPD results from further oxidation of the  $>\text{NO}'$  radical (Reaction 12) but may also occur by hydrogen abstraction from the alkyl group leading to imine formation (5) or by disproportionation reactions yielding quinonoid structures (9). The existence of this reaction system may therefore be transitory. However, the main chain is long, and the effect of  $7.5 \times 10^{-3}M$  DSBPD lasts almost throughout the oxidation of  $0.15M$  indene-thiophenol (*see* Figure 3).

**Co-Oxidation in Presence of Added Iron Complexes.** Our study of the influence of added iron on the co-oxidation is not yet complete, and we have encountered experimental difficulties (not yet overcome) in recognizing changes in the coordination shells or complexing species and in measuring concentrations of  $\text{Fe}^{3+}$  and  $\text{Fe}^{2+}$  at p.p.m. concentrations in hydrocarbon solvents during the co-oxidation. However, several interesting observations have been made, and several possible reaction schemes have been examined.

A wide range of iron compounds catalyze the indene-thiophenol co-oxidation reaction—*e.g.*,  $\text{FeCl}_3$  and a variety of complexes formed by chelation. Differences in their behavior are believed to be correlated approximately with the ease of displacement of ligands by thiols or with their susceptibility to attack by peroxide, but the lack of reproducibility which has made much of this work extremely tedious makes quantitative deductions difficult.

Figure 2 shows typical oxygen-uptake curves obtained after adding ferric complexes or ferric chloride (at about  $10^{-4}M$ ) to indene-thiophenol reaction mixtures in benzene solution. The three consecutive runs (375-377R) made under apparently identical conditions reasonably represent the variability found.

The products of co-oxidation examined after oxygen absorption has ceased and after the hydroperoxide had rearranged were substantially the same as those obtained in absence of added iron, although some changes in the yields of minor products resulted from the effects of the iron complexes on the decomposition of the hydroperoxide.

The reactions when ferric chloride or ferric acetylacetonate is present occur in three stages: (1) an initial fast reaction decreasing in rate, (2) an arrest during which the oxidation rate may be very low, and (3) a "sigmoid" phase in which an autocatalytic reaction is finally overtaken by reactant consumption. With the ferric (bisäalen) chloride complex, the reaction was accelerated but Stages 1 and 2 did not appear (curve 340R, Figure 2).

In examining the kinetics of this type of chain reaction (18), it was found that the major characteristics of all the curves of Figure 2 could be reproduced by assuming:

(a) Radicals were produced in two reactions, the rate of one being independent of the extent of reaction and that of the other being proportional to the square of the extent—*e.g.*, the latter might be a second-order decomposition of the main peroxide product and might be catalyzed by iron.

(b) Radicals were removed in two ways, by bimolecular termination processes and by a reaction, whose rate is proportional to the extent of reaction.

Such a system was delicately balanced, and small changes in the arbitrary constants could greatly alter the shapes of the reaction curves. However, before claiming that this system represents the reactions which are occurring, a plausible explanation must be found for the termination reaction, which had a rate proportional to the extent of reaction. Two possible assumptions have been considered, but neither fully stands up to experimental test, and it is evident that the system is one of subtle balance and complexity.

It was first assumed that an inhibitor was produced as a by-product. However, the accuracy with which the initiation rates had to be balanced seemed to demand too great a coincidence if the inhibitor production occurred in a side reaction independent of the initiation reactions. Thus, although possible products which were demonstrably powerful inhibitors of the co-oxidation reaction—*e.g.*, thiolsulfonates—could be postulated, this mechanism was unsatisfactory and did not fully explain the role of iron. Furthermore, diphenyl disulfide, which is a precursor of thiolsulfonate in the presence of hydroperoxide, did not inhibit the reaction. The possibility that the negative term represented a diminishing contribution from a radical-producing process was then studied.

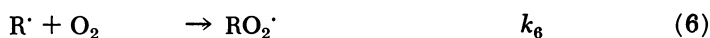
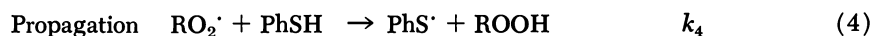
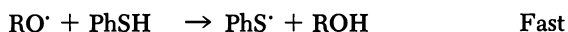
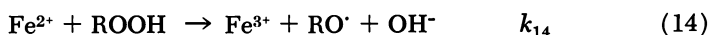
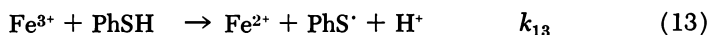
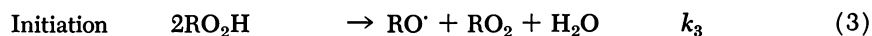
Careful examination of the oxygen-uptake curves with ferric acetylacetonate or ferric chloride present, failed to reveal an induction period

or initial accelerating phase which, if it occurred, must have lasted less than a minute. In view of the rigorous purification procedures used, the occurrence of a high initial rate in Stage 1 does not support the proposition that the iron accelerates the initial stages of co-oxidation by the usual redox interactions with a hydroperoxide product, whether this arises from direct oxidation of indene (20) or from the co-oxidation reaction. Furthermore, ferric acetylacetonate is not an effective catalyst for the autoxidation of indene, as we have found, nor of 1-octene (10), and a concentration of  $1.8 \times 10^{-4}M$  gives only a fivefold increase in the rate of decomposition of hydroperoxide I to products other than II at 20°C.

In order to produce a high initial rate we suggest that the iron complex must produce radicals by attacking a reactant, and the thiol is the most likely one. This proposal is supported by the recent demonstration by Wallace (25) that ferric octanoate readily reacts with thiols at ambient temperature to give  $RS\cdot$  radicals which are effectively captured by an olefin, provided the ratio of thiol to iron concentrations is not greater than 10.

Ferric ions and complexes in aqueous media react readily with cysteine (13, 21) or thioglycollic acid (14, 22) to form purple complexes which rapidly change to the ferrous form with accompanying formation of disulfides. It was not unreasonable, therefore, to assume that such a reaction provided rapid production of  $RS\cdot$  radicals in the initial stages of co-oxidation and that this rate should decrease as reduction to ferrous occurred. Eventually reoxidation of ferrous to ferric by peroxide would assert itself, and the rate could rise again.

The system including all these assumptions has not yet been calculated, but the slightly simplified Reaction Scheme 3 has been examined. Although it was also found inadequate, it has some interesting kinetic properties.



*Reaction Scheme 3*

Assuming a pseudo-steady state in which initiation and termination rates may change but remain equal and that Reaction 6 is fast compared with 4 and 5:

Rate of radical production

$$r = k_7 (\text{RO}_2\cdot)^2$$

and

$$(\text{RO}_2\cdot) = \sqrt{\frac{r}{k_7}}$$

If the main chain is long,

$$\begin{aligned} \frac{-d[\text{O}_2]}{dt} &= k_6 [\text{O}_2] [\text{R}\cdot] \simeq k_4 [\text{PhSH}] [\text{RO}_2\cdot] \\ &= k_4 [\text{PhSH}] \sqrt{\frac{r}{k_7}} \end{aligned}$$

Let  $w = k_{14}[\text{RO}_2\text{H}]/k_{13}[\text{PhSH}]_0$

and with long chains

$$[\text{PhSH}]/[\text{PhSH}]_0 = 1 - \frac{k_{13}}{k_{14}} w = 1 - x$$

where  $x =$  fractional extent of reaction

$$\begin{aligned} y &= [\text{Fe}^{2+}]/[\text{Fe}]_0 = 1 - [\text{Fe}^{3+}]/[\text{Fe}]_0 \\ z &= r/k_{13} [\text{PhSH}]_0 [\text{Fe}]_0 \\ \tau &= k_{13} [\text{PhSH}]_0 t \\ \alpha &= k_{14} [\text{Fe}]_0 / k_{13} [\text{PhSH}]_0 \\ \beta^2 &= k_4^2 [\text{PhSH}]_0 / k_{13} k_7 [\text{Fe}]_0 \\ \gamma &= k_3 / k_{14} \alpha = k_3 k_{13} [\text{PhSH}]_0 / k_{14}^2 [\text{Fe}]_0 \end{aligned}$$

Then

$$\begin{aligned} \frac{dy}{dt} &= k_{13} [\text{Fe}^{3+}] [\text{PhSH}] / [\text{Fe}]_0 - k_{14} [\text{Fe}^{2+}] [\text{ROOH}] / [\text{Fe}]_0 \\ \frac{dy}{d\tau} &= (1 - y) \left( 1 - \frac{k_{13} w}{k_{14}} \right) - wy \\ z &= \{ k_3 [\text{RO}_2\text{H}]^2 + k_{13} [\text{Fe}^{3+}] [\text{PhSH}] + k_{14} [\text{Fe}^{2+}] [\text{RO}_2\text{H}] / \\ &\quad k_{13} [\text{PhSH}]_0 [\text{Fe}]_0 \\ &= \left\{ \gamma w^2 + (1 - y) \left( 1 - \frac{k_{13} w}{k_{14}} \right) + wy \right\} \\ \frac{d[\text{RO}_2\text{H}]}{dt} &= k_4 [\text{RO}_2\cdot] [\text{PhSH}] - k_3 [\text{RO}_2\text{H}]^2 - k_{14} [\text{Fe}]^{2+} [\text{RO}_2\text{H}] \\ \frac{dw}{d\tau} &= \alpha \left\{ \beta \sqrt{z} \left( 1 - \frac{k_{13} w}{k_{14}} \right) - \gamma w^2 - wy \right\} \end{aligned}$$

If  $y$  is small—*i.e.*, when extent of reaction,  $x$ , is small—

$$\frac{dw}{d\tau} = \alpha \{ \beta \sqrt{z} - w^2 - wy \}$$

$$\frac{dy}{d\tau} = 1 - y - wy$$

$$z = (1 - y + wy + \gamma w^2)$$

This system of equations was solved by a predictor-corrector method for several values of  $\alpha$ ,  $\beta$ , and  $\gamma$  using a digital computer. It was not possible to examine values of  $\beta$  above 50 ( $\alpha = 0.001$ ,  $\gamma = 0$ ) as the method broke down because of accumulated errors. Up to these values, although a step is formed in the extent of reaction *vs.* time curve, the rate of acceleration in the third phase of the reaction was much slower than observed in the experiments.

The stopping and restarting type of reaction can be accounted for by a mechanism in which initiation rates change as the  $[\text{Fe}^{3+}]/[\text{Fe}^{2+}]$  ratio is altered by the increasing  $[\text{ROOH}]$  and decreasing  $[\text{PhSH}]$ . However, this mechanism is inadequate, as further experiments showed.

If the deceleration in Stage 1 of the co-oxidation were in fact caused by removal of ferric iron by Reaction 13 of Scheme 3, then premixing the iron complex and thiol should have a profound effect. In the strict absence of oxygen it was expected that all the ferric complex would be reduced to ferrous, and no reaction, or at most a slow buildup, would be predicted from Scheme 3 on adding indene and oxygen. However, as comparison of Curves B and A of Figure 5 shows, there is little effect on the behavior of the system. The explanation cannot be that admission of oxygen promptly restores the ferrous to ferric because premixing of iron and thiol and standing in air would then lead to catalytic oxidation of thiol to disulfide. This did not happen, since Curves C, D and E (Figure 5) showed final oxygen consumptions approaching those obtained without premixing in air or in the absence of added iron.

The effect of oxygen on the reaction of the iron complex with thiol was to reduce the effectiveness of the iron as a catalyst in the initial stage of co-oxidation and made Curves D and E (Figure 5) similar to that produced by the  $\text{Fe}(\text{bissalen})\text{Cl}$  complex (Curve 340R, Figure 3). It is evident that the mechanism of the iron-catalyzed co-oxidation is more complex than the schemes postulated so far. That oxygen has an effect on the thiol-iron reaction is not surprising and was presumably foreseen by Wallace (25), who worked in nitrogen, but this reaction also is more complex in aromatic hydrocarbon solvents than was previously assumed. Michaelis and Schubert (13, 14, 21, 22) showed that ferric ion in aqueous solution readily forms with thiols purple ferric complexes which decay to

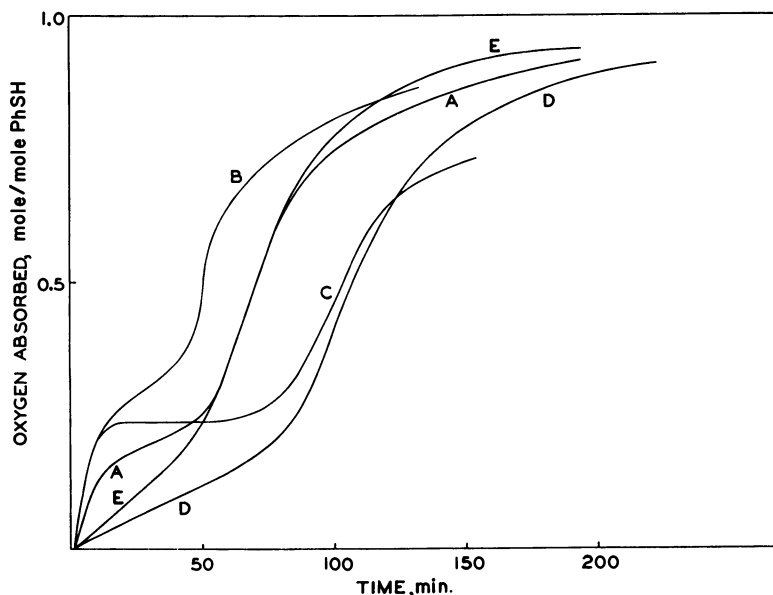


Figure 5. Effect of premixing iron complex and thiophenol

- A: Normal procedure  
 All reactants mixed in cold; premixed  $\text{Fe}(\text{acac})_3$  + PhSH solutions allowed to stand before adding indene:  
 B: 150 min. under nitrogen  
 C: 150 min. under nitrogen and trace of oxygen  
 D: 180 min. in air  
 E: 150 min. in air

colorless ferrous, compounds and the latter can be re-oxidized with oxygen. We have found that in benzene or toluene solutions thiophenol does not decolorize  $\text{Fe}(\text{acac})_3$ , even in air, although changes in the visible (but not infrared) spectra occur. It seems clear that exchange of ligands can occur—*i.e.*, thiol could enter the complex—electron transfer from sulfur to  $\text{Fe}^{\text{III}}$  may then follow with release of  $\text{RS}^\cdot$  radicals. However, nothing is known of the relative stabilities of the various series of complexes which could be formed or of the stabilities with respect to electron transfer to or from the metal. If we add to these variables the possibility of radical attack on the ligands (12, 16, 17) and the largely unknown field of electron transfer reactions between metal complexes and free radicals, the complexity of the problem becomes formidable indeed. It is unwise to argue by analogy from aqueous systems and almost impossible to follow such reactions at present in the p.p.m. concentration range in oxidizing systems. But this is where future work must be concentrated to solve the problems of homogeneous catalysis by metals in such systems. Use of spectroscopic and fast reaction techniques

in examining carefully selected separate reaction steps will undoubtedly throw light on this problem.

### **Conclusions**

The co-oxidation of indene and thiophenol in benzene proceeds by a three-step cyclic free radical chain reaction. Autocatalysis associated with the hydroperoxide which is the main primary product occurs, but the effect is complicated by other trace components. The reaction is extremely sensitive to catalysts and inhibitors, and its kinetic features are determined by the initiation and termination processes.

The well known amine antioxidant, *N,N'*-di-*sec*-butyl-*p*-phenylenediamine, is a powerful catalyst for the co-oxidation reaction and acts in two ways: by producing, in direct reaction with oxygen,  $>\text{NO}'$  radicals which are capable of reacting with thiophenol to produce  $\text{PhS}'$  radicals, thus initiating the reaction, and by replacing the rate-determining propagation step by a pair of faster reactions involving  $>\text{NO}'$  (or  $>\dot{\text{N}}$ ) radicals, thus converting the three-step chain into a four-step chain.

Iron complexes have profound effects, depending on their stabilities. Many markedly accelerate the initial stages of the co-oxidation reaction but retard and even stop the reaction in the middle stages. The kinetic features can be accounted for largely by a balance among several initiation and termination reactions, but discrepancies suggest that changes occur in the composition of the complexes as a result of ligand exchange or displacement, attack on ligands by free radicals, and changes in oxidation state of the metal during oxidation, and that these are accompanied by changes in reactivity and therefore in catalytic activity.

Systematic study of the stability of metal complexes in nonaqueous systems and their reactivity with thiols, free radicals, etc., is required for a fuller understanding of their complex effects on the co-oxidation reaction.

### **Acknowledgment**

The authors thank the British Petroleum Co., Ltd., for permission to publish this paper. They are indebted to J. C. Blackburn for the ESR measurements and interpretation and to R. C. Palmer for developing the system of equations and for programming and arranging the computations by digital computer.

### **Literature Cited**

- (1) Baird, J. C., Thomas, J. R., *J. Chem. Phys.* **35**, 1507 (1961).
- (2) Bolland, J. L., *Proc. Roy. Soc. (London)* **186A**, 218 (1946).

- (3) Boozer, C. E., Hammond, G. S., *J. Am. Chem. Soc.* **26**, 3861 (1954).
- (4) Chalfont, G. R., Hey, D. H., Liang, C. S. Y., Perkins, M. J., *Chem. Commun.* No. 8, 367 (1967).
- (5) Coppinger, G. M., Swalen, J. D., *J. Am. Chem. Soc.* **83**, 4900 (1961).
- (6) Ford, J. F., Pitkethly, R. C., Young, V. O., National Bureau of Mines Conference on Low Temperature Oxidation, Bartlesville, Okla., May 1961.
- (7) Ford, J. F., Pitkethly, R. C., Young, V. O., "Preprints of Papers," Division of Petroleum Chemistry, ACS Meeting, Miami, Fla., **2** (1), 111 (April 1957).
- (8) Ford, J. F., Pitkethly, R. C., Young, V. O., *Tetrahedron* **4**, 325 (1958).
- (9) Forrester, A. R., Thomson, R. H., *Nature* **203**, 74 (1964).
- (10) Indictor, N., Jochsberger, T., *J. Org. Chem.* **31**, 4271 (1966).
- (11) Kharasch, M. S., Nudenberg, W., Mantell, G. J., *J. Org. Chem.* **16**, 524 (1951).
- (12) Mendelsohn, M., Arnett, E. M., Freiser, H., *J. Phys. Chem.* **64**, 660 (1960).
- (13) Michaelis, L., Barron, E. S. G., *J. Biol. Chem.* **83**, 191, 367 (1929); **84**, 777 (1930).
- (14) Michaelis, L., Schubert, M., *J. Am. Chem. Soc.* **52**, 4418 (1930).
- (15) Oswald, A. A., Wallace, T. J., in "Chemistry of Organic Sulfur Compounds," Vol. 2, Chap. 8, p. 217, N. Kharasch and C. Y. Meyers, eds., Pergamon Press, 1966.
- (16) Patmore, E. L., Ph.D. thesis, University of Connecticut, 1963; University Microfilms Inc., Ann Arbor, Mich., 1966.
- (17) Patmore, E. L., Gritter, R. J., *Proc. Chem. Soc.* **1962**, 328.
- (18) Pitkethly, R. C., unpublished manuscript.
- (19) Rosenwald, R. H., *Petrol. Processing* **6** (9), 969 (1951); **11** (10), 91 (1956).
- (20) Russell, G. A., *J. Am. Chem. Soc.* **79**, 3871 (1957).
- (21) Schubert, M., *J. Am. Chem. Soc.* **53**, 3851 (1931).
- (22) *Ibid.* **54**, 4077 (1932).
- (23) Sullivan, A. B., *J. Org. Chem.* **31**, 2811 (1966).
- (24) Thomas, J. R., *J. Am. Chem. Soc.* **82**, 5955 (1960).
- (25) Wallace, T. J., *J. Org. Chem.* **21**, 3071 (1966).
- (26) Wallace, T. J., Mahon, J. J., Kelliher, J. M., *Nature* **206**, 709 (1965).

RECEIVED November 13, 1967.

## Discussion

**H. Berger:** Do you think that the fact that strong bases do not lead to co-oxidation but to disulfide, is an indication that no  $RS\cdot$  radicals are involved in this side reaction?

**R. C. Pitkethly:** Yes, our experience and that of others (1, 2, 3) would indicate that the oxidation of disulfides in alkaline media involves

formation and reaction of metal complexes and that free  $RS\cdot$  radicals are not formed in any appreciable concentration.

***Literature Cited***

- (1) Hill, J., McAuley, A., Chemical Society Autumn Meeting, Sept. 20, 21, 1967, Paper B4.
- (2) Overberger, C. G., Burg, K. H., Baly, W. H., *J. Am. Chem. Soc.* **87**, 4125 (1965).
- (3) Swan, C. J., Trimm, D. L., *Chem. Ind.* **1967**, 1363.

## The Influence of Halogen Compounds on Combustion Processes

K. C. SALOOJA<sup>1</sup>

Shell Research, Ltd., Thornton Research Centre, P.O. Box 1, Chester, England

*Studies of the effects of chlorine, bromine, and iodine compounds on hydrocarbon combustion show that in general these compounds (1) promote preflame oxidation at almost all stages, (2) promote ignition near minimum ignition temperatures but inhibit it at temperatures approaching those in flames, and (3) inhibit flame processes, though with notable exceptions. Different halogen compounds vary markedly in the magnitude of their effects. Mechanisms are advanced to explain the observations.*

Halogen compounds promote slow combustion (1, 5, 11, 16, 17), and yet they strongly inhibit flame processes (4, 6, 7, 8, 10, 18). These effects have intrigued many investigators, but it is still not clear at what stage and how the effect changes from promotion to inhibition.

We have systematically studied the influence of halogen compounds on all oxidation stages that lead to ignition. This was followed by studies on the ignition process at temperatures ranging from just above the minimum ignition points to temperatures approaching those in flames. Finally, we studied the effect of halogen compounds on flames.

The halogen compounds used were methylene dichloride, chloroform, carbon tetrachloride, ethylene dichloride, ethyl bromide, ethylene dibromide, bromoform, methyl iodide, and ethyl iodide. The hydrocarbons selected for their interesting combustion properties were hexane, 2-methylpentane, 2,2-dimethylbutane, hex-1-ene, heptane, methylcyclohexane, isooctane, diisobutylene, benzene, toluene, *m*-xylene, and ethylbenzene.

<sup>1</sup>Present address: Esso Research, Ltd., Abingdon, Berkshire, England.

### **Experimental**

The experimental conditions used to study oxidation reactions leading to ignition and to study ignition over a wide range of temperature have been described previously (12, 13).

Briefly, the studies of oxidation processes leading to ignition were carried out in a flow system at atmospheric pressure. A homogenous mixture of fuel vapor and air was passed through a quartz reaction chamber held at a uniform temperature inside a furnace. The temperature of the furnace was raised gradually till ignition occurred. The product gases were continuously passed through infrared analyzers to estimate carbon monoxide and carbon dioxide, and through a paramagnetic analyzer to estimate oxygen. The patterns of behavior in terms of the formation of carbon monoxide or carbon dioxide or in terms of the consumption of oxygen were similar with each fuel; the results, therefore, are presented in terms of only one measurement—namely, the formation of carbon monoxide.

Ignition studies over a wide range of temperature were done in a different quartz chamber to which oxygen and fuel vapor in nitrogen were supplied through separate preheating tubes to prevent their interaction before reaching the ignition chamber. The reactants mixed in a small narrow section of the chamber, where their residence time was barely 2% of that in the reaction tube. The composition of the gases and their flow through the tube was kept so uniform that the flame always passed through the tube as a flat disc. To determine the ignition lag, the rate of flow of the gases, which had been kept too fast for ignition to occur, was reduced till ignition took place. The limiting ignition pressure was measured, and then the ignition lag (the residence time of the fuel-air mixture at the instant of ignition) was calculated. Although the limiting ignition pressures were different for different fuels, comparisons in all cases were made under identical mass-flow conditions.

Flame speeds were measured on a nozzle burner. Fuel and air were metered and mixed in the same manner as in the preflame studies. The entire gas supply line and burner assembly were electrically heated to avoid condensation of fuels and additives. The burner was surrounded by a wider tube to prevent ambient air from influencing the flame. The flame speed was determined from the height of the flame cone.

All hydrocarbons and halogen compounds used were virtually pure; no impurities could be detected by gas-liquid chromatography.

### **Results**

**Preflame and Ignition Studies.** The studies were carried out with twice stoichiometric fuel-air mixtures. When a halogen compound was present in a fuel, the flow rate of the fuel stream was adjusted to maintain the hydrocarbon-to-air ratio at twice stoichiometric.

As experienced by previous investigators (5, 17), the reproducibility of results was poor unless successive runs on pure hydrocarbons (in the absence of halogen compounds) were carried out before examining the

effect of each halogen compound. All results reported, with and without the halogen additives, are the means of at least three separate runs (Figures 1 to 9).

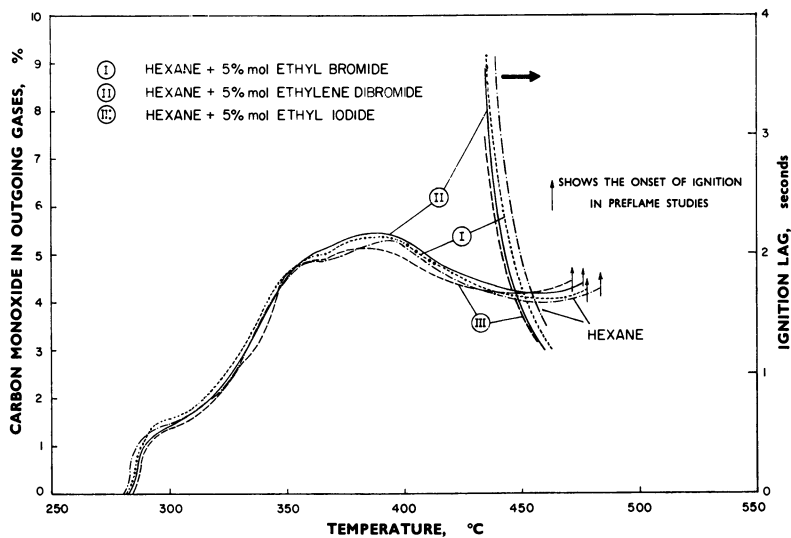


Figure 1. Effect of ethyl bromide, ethylene dibromide, and ethyl iodide on the preflame and ignition characteristics of hexane

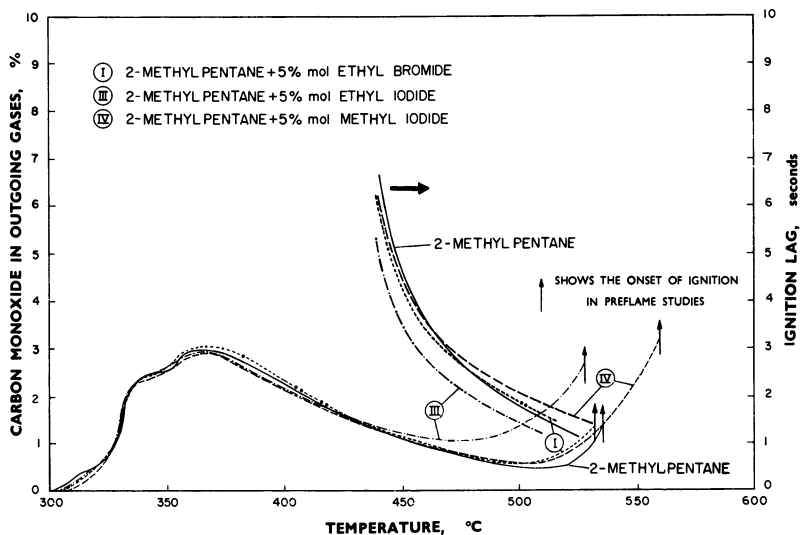


Figure 2. Effect of methyl iodide, ethyl iodide, and ethyl bromide on the preflame and ignition characteristics of 2-methylpentane

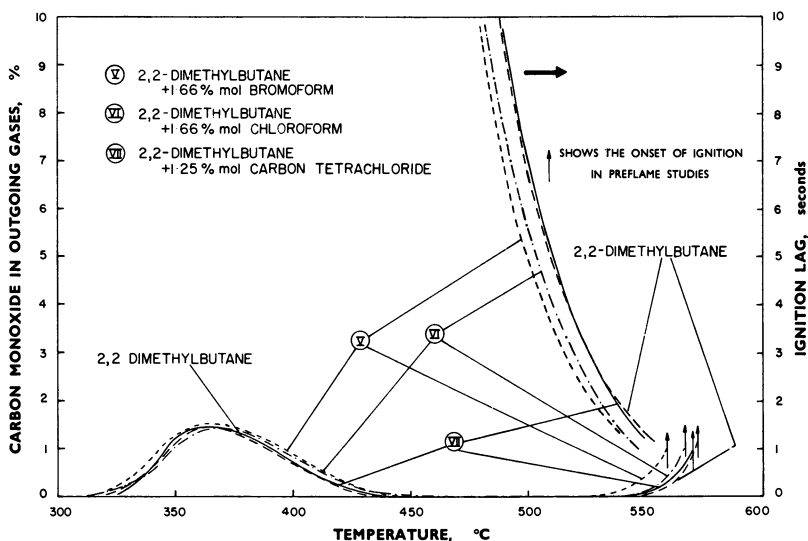


Figure 3. Effect of bromoform, chloroform, and carbon tetrachloride on the preflame and ignition characteristics of 2,2-dimethylbutane

With hydrocarbons which begin to oxidize in the "low temperature" region—*i.e.*, hexane (Figure 1), 2-methylpentane (Figure 2), 2,2-dimethylbutane (Figure 3) and hex-1-ene (the results are not shown since they were similar to those for hexane)—the halogen compounds exercised an appreciable influence, mainly above the "low temperature" region. Thereafter, their effect increased with temperature. All the halogen compounds promoted oxidation, and except for methyl iodide, they also promoted the onset of ignition.

Promotion of ignition is particularly interesting since these halogen compounds are known to inhibit flame processes. The results on ignition-lag/temperature relationships, also presented in each figure, clearly show the considerable promoting effect of halogen compounds. Even with methyl iodide, which inhibited ignition in the flow experiments (at the shortest residence time studied), the magnitude of inhibition decreased on increasing the residence time, and eventually the effect changed to one of promotion.

Further, the effectiveness of a halogen compound was not entirely caused by its halogen content. For example, ethyl iodide promoted combustion more than methyl iodide, and chloroform more than carbon tetrachloride.

The next group of hydrocarbons on which the effect of halogen compounds may be considered includes isooctane (Figure 4), diisobutylene

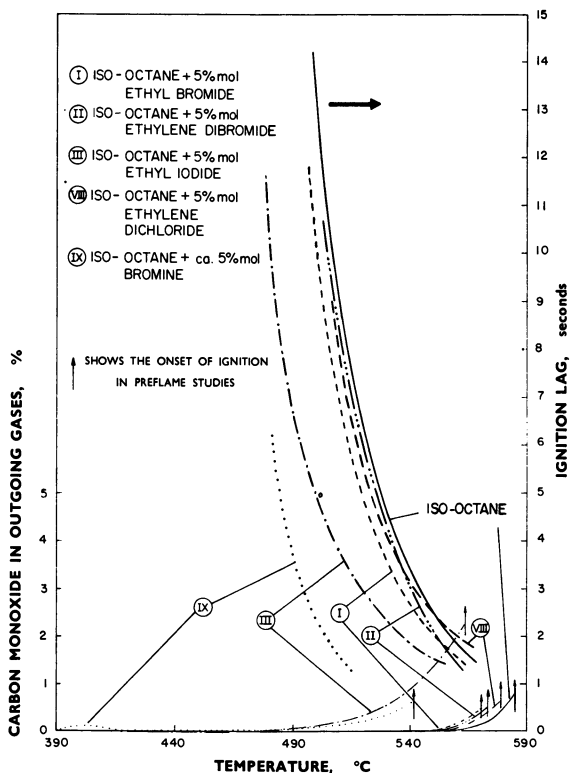


Figure 4. Effect of bromine, ethyl bromide, ethyl iodide, ethylene dibromide, and ethylene dichloride on the preflame and ignition characteristics of iso-octane

(the results are not presented since they were similar to those for iso-octane), ethylbenzene (Figure 5), and toluene (Figure 6), all of which oxidize only in the "high temperature" region. In general the halogen compounds promoted the oxidation and ignition of these hydrocarbons more than they did those of the previous group. Altogether the results clearly establish that the effect of halogen compounds increases with temperature; the promoting effect was greatest for toluene, which oxidizes at higher temperatures than the other hydrocarbons.

The nature of the base fuel also influenced the response to halogen compounds. For instance, although isooctane and ethylbenzene both oxidize and ignite within almost the same temperature range, ethyl iodide markedly promoted the oxidation and ignition of isooctane, but with ethylbenzene it only promoted oxidation, while inhibiting ignition.

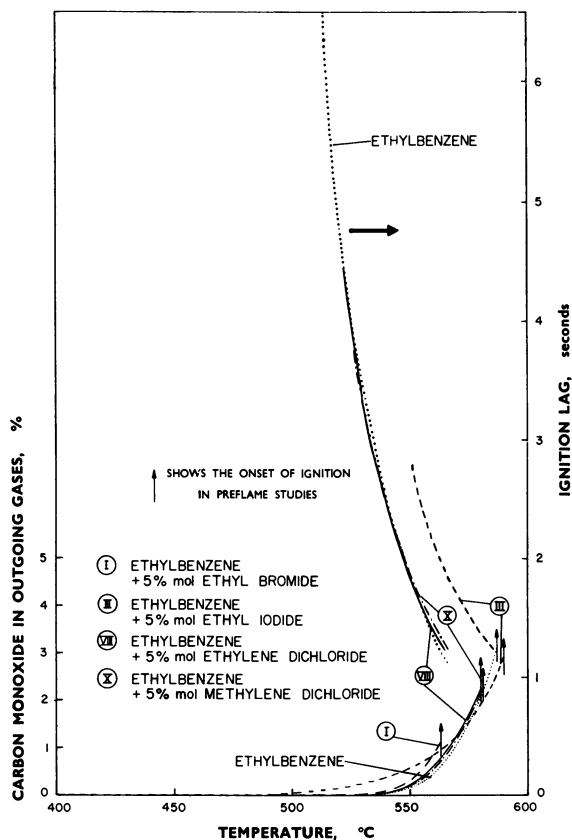


Figure 5. Effect of ethyl bromide, ethyl iodide, methylene dichloride, and ethylene dichloride on the preflame and ignition characteristics of ethylbenzene

The effectiveness of the halogen compounds depended on the particular halogen concerned; the promoting effect on oxidation increased in the order: chlorine compounds < bromine compounds < iodine compounds. Although iodine compounds were the most effective in promoting oxidation, their effect on ignition was often less than that of bromine compounds, and as mentioned earlier, they sometimes inhibited ignition.

There can be little doubt that the effect of halogen compounds arises primarily from their halogen content. In experiments with bromine, rather than with bromine compounds, the promoting effect of the halogen was quite marked; with isooctane the effect was so marked that some reaction occurred in the "low temperature" region.

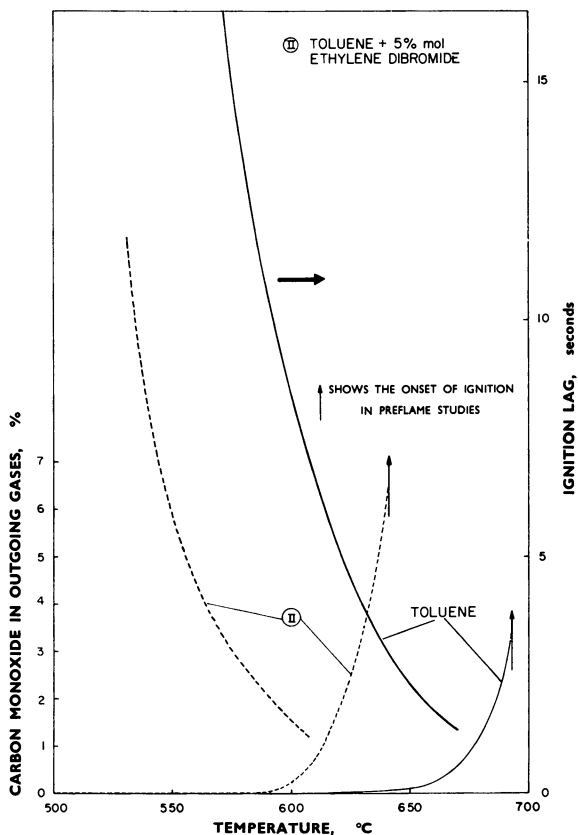


Figure 6. Effect of ethylene dibromide on the pre-flame and ignition characteristics of toluene

Cullis, Fish, and Ward (5) have suggested that the halogen compounds exercise their effect only when they release their halogen atoms or form halogen acids. The validity of this suggestion can be checked readily from our results with benzene. This is because benzene has such a high resistance to oxidation that the reaction observed in the presence of halogen compounds, particularly in the earliest stages, can be regarded as being largely caused by the breakdown of the halogen compounds. The information thus obtained may be compared with the results for the other hydrocarbons because it has been obtained under identical conditions.

Comparison does show that in general the relative effectiveness of different halogen compounds agrees with the ease of their oxidative degradation.

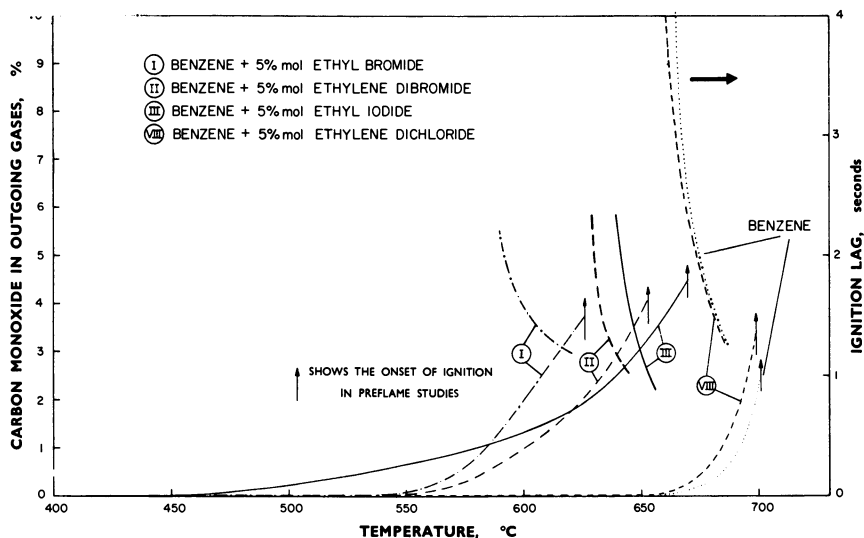


Figure 7. Effect of ethyl bromide, ethyl iodide, ethylene dichloride, and ethylene dibromide on the preflame and ignition characteristics of benzene

The more detailed conclusions that can be drawn from the studies of halogen compounds with benzene (Figures 7-9) are:

(a) Oxidative degradation occurs more readily with ethyl iodide than with ethyl bromide. With increasing temperature, however, the increase in degradation is greater with ethyl bromide.

(b) Ethylene dibromide is more stable than ethyl bromide.

(c) Ethyl dichloride is considerably more stable than ethylene dibromide, and chloroform more so than bromoform.

(d) Chloroform is slightly less stable than carbon tetrachloride, but methylene dichloride is much more stable.

**Ignition Studies at High Temperatures.** In view of the observed promoting effect of halogen compounds on ignition near the minimum promoting temperatures and their generally known inhibiting effect on flames, their effect on ignition in the intervening temperature range was studied. The results of the effect of ethylene dibromide, in 5% molar concentration, on the ignition lags of isooctane, benzene, toluene, and *m*-xylene at temperatures ranging between 700° and 900°C. are shown in Figure 10.

The effects, in general, were (a) ignition was promoted at 700°C.; (b) the magnitude of promotion decreased with temperature till eventually inhibition set in; (c) the magnitude of inhibition increased with temperature. With benzene inhibition set in below 750°C., with toluene

at about 875°C., and with *m*-xylene at about 890°C. With isoctane inhibition had not commenced by 900°C.

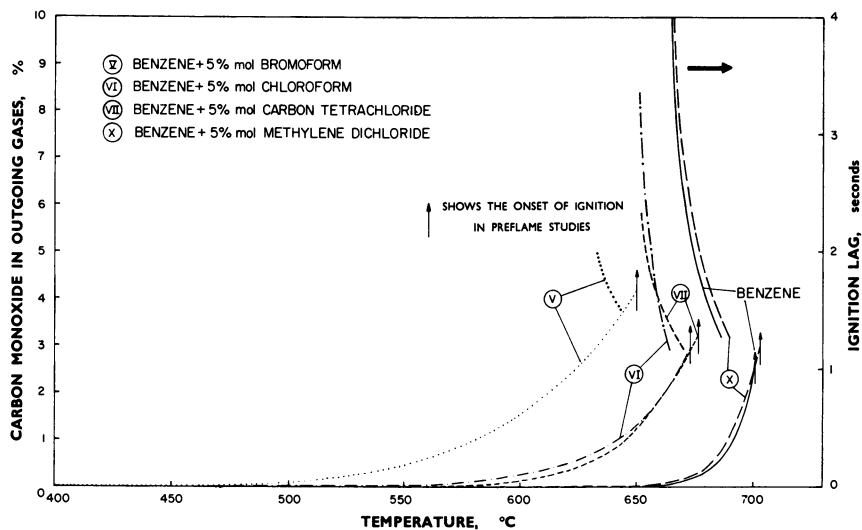


Figure 8. Effect of methylene dichloride, chloroform, carbon tetrachloride, and bromoform on the preflame and ignition characteristics of benzene

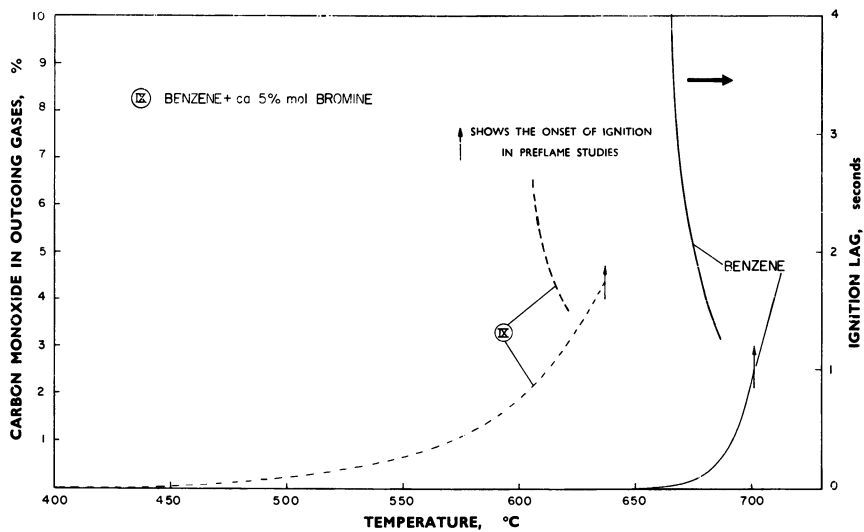


Figure 9. Effect of bromine on the preflame and ignition characteristics of benzene

**Flame Studies.** The effects of ethylene dibromide, bromoform, and chloroform on flame speeds of several hydrocarbons were examined. These studies were carried out with 5% molar concentration of the halogen compounds in each hydrocarbon. All the experiments were carried out under identical conditions, and the results reported in Table I are the mean of at least three separate determinations.

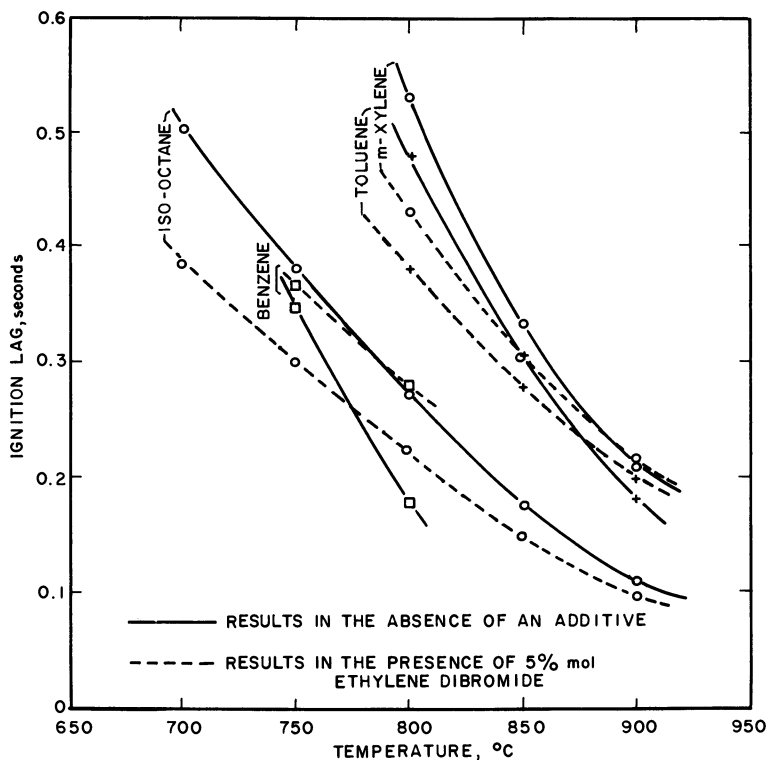


Figure 10. Effect of ethylene dibromide on the ignition lags of hydrocarbons at temperatures ranging from 700° to 900°C.

Bromine compounds reduced flame speeds in all cases, but chloroform increased them in most cases. Although the promoting effect of chloroform has not been reported before and the view generally is that chlorine compounds reduce flame speeds, a close examination of previous data (4, 6, 7, 9) reveals that under certain conditions, chlorine and methyl chloride had increased flame speeds.

**Table I. Effect of Halogen Compounds on Flame Speeds of Hydrocarbons**

Hydrocarbon	Fuel-to-Air Ratio, Times Stoichiometric	Change in Flame Speed, % (-, Inhibition; +, Promotion)		
		Ethylene Dibromide <sup>a</sup>	Bromoform <sup>a</sup>	Chloroform <sup>a</sup>
Hexane	1.28	-12.8	-17.5	+9.5
Heptane	1.40	-12.6	-15.0	+2.2
Methylcyclohexane	1.43	-13.3	-9.4	-0.5
Isooctane	1.31	-10.5	-6.6	+5.3
Diisobutylene	1.35	-7.7	-7.7	+5.6
Benzene	1.35	-26.7	-14.7	+9.2
Toluene	1.15	-13.8	-20.8	-3.0
<i>m</i> -Xylene	1.32	-4.6	-3.7	+0.8
Ethylbenzene	1.17	-12.2	-16.1	-5.5

<sup>a</sup> Molar concentration, 5%.

### Discussion

These studies provide comprehensive information on the effects of many halogen compounds on the combustion behavior of various hydrocarbons. The combustion behavior included preflame oxidation, ignition over a wide range of temperature, and the flame process. The effect of iodine compounds on preflame combustion, which had not been previously investigated, is now reported.

The results enable us to deduce a general mechanism for the reactions underlying (a) the change which often occurs in the nature of the effect of halogen compounds in going from one combustion stage to another and (b) the relative differences in the effectiveness of different halogen compounds.

**Mechanism of Action of Halogen Compounds.** The action of halogen compounds is generally considered to arise primarily from the free halogen atoms and hydrogen halides they form on oxidative degradation. Our results support this point of view, although in a few cases, at low temperatures, they do not entirely agree with it.

**Preflame Oxidation.** The principal reactions responsible for promoting preflame oxidation are considered to be the following, where X represents a halogen atom:





Promotion occurs because these reactions provide an extra mode of chain propagation and chain branching.

Reactions 1, 2, and 3 would constitute promoting steps when their activation energies are lower than those of the corresponding reactions:



This is likely when  $\text{HX} = \text{HBr}$ , and even more so when  $\text{HX} = \text{HI}$ . Cullis, Fish, and Ward (5) give  $E_{1(\text{HX})} = 39.5 \text{ kcal. mole}^{-1}$  when  $\text{HX} = \text{HBr}$ , and  $E_{1'(\text{RH})} = 55 \text{ kcal. mole}^{-1}$  when  $\text{RH} = \text{CH}_4$ . It is probable that  $E_{1(\text{HBr})}$  is also lower than  $E_{1'}$  for several hydrocarbons. The values deduced for  $E_{1(\text{HI})}$  and  $E_{1(\text{HCl})}$  are 23.5 and 55 kcal. mole<sup>-1</sup>, respectively. Thus, HI would be expected to exercise a much greater promoting effect than HBr, and HCl to exercise hardly any at all.

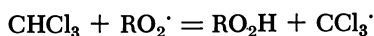
Reaction 4 was proposed by Allen and Tipper (1) as a result of studying the kinetics of the HBr-induced oxidation of 2-butane. The exact scheme of this reaction has not been proposed.

The promoting effect of Reaction 5 should be strongest with chlorine and weakest with iodine atoms since the activation energy of this reaction with respect to the different halogen atoms is (2):

$$E_{5(\text{Cl})} : E_{5(\text{Br})} : E_{5(\text{I})} = 5 : 18 : 33$$

Of Reactions 1 to 5, Reactions 2, 3, and 4 probably play the more important role because they favor the formation of the kinetically important peroxides and enhance their contribution to chain branching. Their ease of reaction is expected to decrease in the order  $\text{HI} > \text{HBr} > \text{HCl}$ , and this accounts for the fact that the order of effectiveness of the halogen compounds in promoting preflame oxidation is: iodine > bromine > chlorine.

Seakins (16) has reported that the "low temperature" oxidation of propane is promoted by chloroform but not by carbon tetrachloride. Our studies, however, show that chloroform and carbon tetrachloride have generally similar effects on all preflame stages (Figure 3) and that their patterns of oxidative degradation are also similar (Figure 8). Under the conditions of Seakins' experiments the following reaction, which he suggested, probably initiates the sequence of reactions responsible for promotion.



The differences observed between the susceptibilities of different hydrocarbons to the promoter action of halogen compounds are generally similar to those observed between their susceptibilities to the promoter action of nitrates (15). The explanation previously proposed for the different effects of nitrates (15) probably holds in this case also.

**Ignition.** Our previous studies on ignition at high temperatures (14) have shown that while only lower concentrations of organic peroxides are formed at temperatures approaching ignition, hydrogen peroxide continues to form up to at least 800°C. The absence of organic peroxides agrees with the views of Walsh (19) that RO<sub>2</sub> radicals are probably unstable at temperatures above the cool flame region. Hence, of Reactions 1 to 5, only Reactions 1, 2, and 5 are likely to be involved in promotion at ignition temperatures.

Since reactive species such as H', OH', and R' would be formed in greater concentrations at ignition temperatures than at lower temperatures, their reactions with hydrogen halides (shown below) would be important in ignition.



Reaction 8 reverses the promoting effect of Reaction 5, while Reactions 6 and 7 result in inhibition because they replace the highly reactive H' and OH' by a less reactive X'.

Since the bond dissociation energy of hydrogen iodide is less than that of hydrogen bromide [ $D_{\text{H-I}}$ , 70.5 kcal.;  $D_{\text{H-Br}}$ , 86.5 kcal. (3)], Reactions 6, 7, and 8 should occur more readily with hydrogen iodide. This would account for the fact that the promoting effect of iodine compounds on ignition is less than that of bromine compounds.

The fact that increasing temperature causes the effect of halogen compounds on ignition to change gradually from promotion to inhibition may be associated with the increasing influence of Reactions 6, 7, and 8 at higher temperatures. That this occurs most markedly with benzene could be attributed to benzene's having the lowest H:C ratio of the hydrocarbons used. The concentrations of H' and OH' would be the lowest, and they would suffer the maximum proportionate decrease on adding a halogen compound. On similar grounds, the effect on other hydrocarbons should be, as observed, in the following decreasing order: benzene > toluene > *m*-xylene > isooctane.

**Flames.** Reactions 6 and 7 must be largely responsible for inhibition in flames. They replace the highly reactive H' and OH' by a less reactive X'. The loss in the concentration of H' and OH' would decrease the

relative importance of the chain-branching reaction,  $H\cdot + O_2 = OH\cdot + O\cdot$ , and the exothermic reaction,  $OH\cdot + CO \rightarrow CO_2 + H\cdot$ . These factors and others which could contribute to the inhibiting effect of halogen compounds have been elaborated (10).

The halogen atoms generated in Reactions 6, 7, and 8 would react with fuel fragments, giving the promoting step:



As discussed, the promoting effect of halogens on this reaction would decrease markedly in the order: chlorine > bromine > iodine.

The over-all effect of halogen compounds would depend on the relative ease of occurrence of the inhibiting reaction (involving  $HX$ ) and the promoting reaction (involving  $X\cdot$ ). As discussed earlier, the inhibiting reaction would occur less readily with chlorine compounds than with bromine compounds, and the promoting reaction less readily with bromine compounds than with chlorine compounds. As observed, the over-all effect could be one of strong inhibition with bromine compounds and that of moderate promotion with chloroform.

### *Acknowledgment*

The author thanks D. T. S. Cuthbertson for his able assistance in experimental work, and T. M. Sugden, F. R. S. for helpful comments.

### *Literature Cited*

- (1) Allen, E. R., Tipper, C. F. H., *Proc. Roy. Soc. A* **258**, 251 (1960).
- (2) Benson, S. W., "The Foundation of Chemical Kinetics," McGraw-Hill, New York, 1960.
- (3) Cottrell, T. L., "The Strengths of Chemical Bond," Butterworths Scientific Publications, London, 1954.
- (4) Creitz, E. C., *J. Res. Natl. Bur. Std.* **65 A**, 389 (1961).
- (5) Cullis, C. F., Fish, A., Ward, R. B., *Proc. Roy. Soc. A* **276**, 527 (1963).
- (6) Garner, F. H., Long, R., Graham, A. J., Badakhashan, A., "Sixth Symposium on Combustion," p. 802, Reinhold, New York, 1957.
- (7) Lask, G., Wagner, H. Gg., "Eighth Symposium on Combustion," p. 432, Williams and Wilkins, Baltimore, 1962.
- (8) Miller, D. R., Evers, R. L., Skinner, G. B., *Combust. Flame* **7**, 137 (1963).
- (9) Palmer, H. B., Seery, D. J., *Combust. Flame* **4**, 213 (1960).
- (10) Rosser, W. A., Wise, H., Miller, J., "Seventh Symposium on Combustion," p. 175, Butterworths Scientific Publications, London, 1959.
- (11) Rust, F. E., Vaughn, W. E., *Ind. Eng. Chem.* **41**, 2595 (1949).
- (12) Salooja, K. C., *Combust. Flame* **4**, 117 (1960).
- (13) *Ibid.*, **5**, 243 (1961).
- (14) *Ibid.*, **9**, 219 (1965).

- (15) Salooja, K. C., *J. Inst. Petrol.* **48**, 119 (1962).
- (16) Seakins, M., *Proc. Roy. Soc. A* **274**, 413 (1963).
- (17) *Ibid.*, **A 277**, 279 (1964).
- (18) Simmons, R. F., Wolfhard, W. G., *Trans. Faraday Soc.* **51**, 1211 (1955).
- (19) Walsh, A. D., *Trans. Faraday Soc.* **43**, 305 (1947).

RECEIVED October 9, 1967.

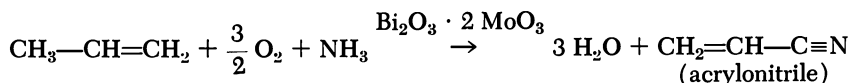
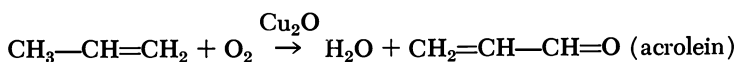
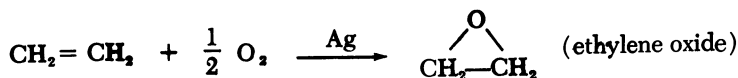
# Problems in Heterogeneous Catalytic Oxidation

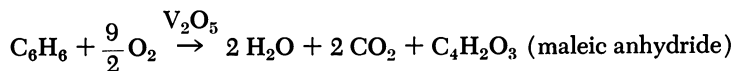
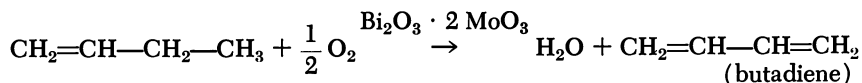
HERVEY H. VOGEL

Shell Development Co., Emeryville, Calif.

*Current problems in understanding the oxidation of hydrocarbons are outlined and illustrated by data for the reactions of ethylene and propylene over suitable catalysts. Difficulty arises because the structures and energies of the intermediates on the catalytic surface are not known and reaction steps are often obscure. In oxidizing ethylene to ethylene oxide over silver there are many ways in which oxygen can be adsorbed on the surface. A scheme of coupled reactions involving two mechanisms explains the limiting selectivity of 80%. In oxidizing propylene to acrolein over cuprous oxide or bismuth molybdate the mechanism involves, with both catalysts, initial removal of a methyl hydrogen to form an allylic species. Kinetics are different for the two catalysts, however.*

**H**eterogeneous catalytic oxidation of hydrocarbons can produce many compounds containing oxygen, as well as olefins and diolefins. Similar oxidations may be used to transform one oxygen-containing compound into another or to oxidize organic materials completely to carbon dioxide. Some of these reactions are of challenging industrial importance, and all hold much scientific interest. Examples of commercially significant reactions are:





Closely related are many oxidations of nonhydrocarbons and oxidations carried out in fuel cells.

Basic understanding of such reactions lags far behind technological applications. Most of these reactions were discovered accidentally, and our knowledge of how to carry them out and to control them is largely empirical. There is no rational basis, beyond the rough guidelines of the periodic table, for selecting new or improved catalysts. The mechanisms proposed for these reactions are woefully lacking in detail, and there is little possibility of quantitative calculation of reaction improvement or new syntheses.

A proper description of heterogeneously catalyzed oxidation reactions must treat several difficult problems simultaneously. First is the characterization of the solid surface in its reactive state. What oxygen species exist on this surface and what reactions does each species undergo? What other sites for adsorption are present? Second is the problem of reaction path. What steps are involved in the reaction? What are the structures and relative energy contents of the intermediates? Third is the problem of reaction velocity, a general and difficult problem in all chemistry. What are transition states, activation energies, and reaction probabilities for the various steps?

Judging by the progress being made in homogeneous catalysis, the most important goals of further study of heterogeneous reactions must be determining reaction steps in considerable detail and ascertaining structures and relative energies of the intermediates involved in these steps. Simple solutions are hardly expected. The recent efforts to relate catalysis to electronic properties of the solid have shown that electrons are involved in oxidation reactions, but this is hardly new. The role of the electron in oxidation-reduction reactions has been known for about 50 years. Unfortunately, bulk electrical measurements on solids supply little detail about individual reaction sites. Margolis, Krylova, and Aleksandrova (12) concluded after studying electronic properties of complex hydrocarbon oxidation catalysts that catalysts cannot be chosen for selectivity on the basis of electrophysical properties alone. The semiconductor theory of catalysis has been disappointing, largely because too much was expected from it.

### Solid Surfaces

A simple example of a catalytic solid is metallic silver. It is the best known catalyst for oxidizing ethylene to ethylene oxide. Under the conditions of use, oxidizing silver to silver oxide is not thermodynamically possible, but oxygen is rapidly and strongly adsorbed to form up to a monolayer on the surface. There is considerable evidence of both adsorbed oxygen atoms and oxygen molecules. Thus, some of the conceivable simple structures on the three low-index planes are as shown in Table I, where M denotes a silver (or metal) atom in a surface plane.

The molecular oxygen species are named according to Cornaz *et al.* (4), who also give a qualitative discussion of the electron orbitals for

Table I. Types of Oxygen Bonding on Silver

Species	No. of M Atoms; Form	Plan	Elevation
Atomic	One		$\begin{array}{c} \text{O} \\   \\ \text{M} \end{array}$
	Two	$\text{M}-\text{O}-\text{M}$	$\begin{array}{c} \text{O} \\ / \quad \backslash \\ \text{M} \quad \text{M} \end{array}$
	Three	$\begin{array}{c} \text{M} \\   \\ \text{O} \\ / \quad \backslash \\ \text{M} \quad \text{M} \end{array}$	
	Four	$\begin{array}{c} \text{M} \quad \text{M} \\ \backslash \quad / \\ \text{O} \\ / \quad \backslash \\ \text{M} \quad \text{M} \end{array}$	
Molecular	One; linear		$\begin{array}{c} \text{O} \\   \\ \text{O} \\   \\ \text{M} \end{array}$
	One; perpendicular		$\begin{array}{c} \text{O}=\text{O} \\   \\ \text{M} \end{array}$
	One; angular		$\begin{array}{c} \text{O} \quad \text{O} \\ \backslash \quad / \\ \text{O} \\   \\ \text{M} \end{array}$
	Two; angular	$\text{M}-\text{O}-\text{O}-\text{M}$	$\begin{array}{c} \text{O} \quad \text{O} \\ / \quad \backslash \\ \text{M} \quad \text{M} \end{array}$

these forms. Still further structures are possible by bonding linear molecules to two or more metal atoms. Furthermore, on the three low-index planes (100, 110, 111) of a face-centered cubic metal four different types of M—M pairs are available. Totalling the combinations, but without considering edges, steps, or defects, at least 37 adsorbed oxygen species are conceivable. Different degrees of charge ( $O^-$ ,  $O^{2-}$ , etc.) can increase the numbers, as can interaction between species.

Clearly all these species are not equally stable. But which actually participate in the oxidation reaction? How rapidly are the species interconverted? What effects do impurities (adsorbed chloride or sulfide) have on the relative populations? We cannot answer these questions. Some ideas are advanced below that require several species to be simultaneously involved in ethylene oxidation.

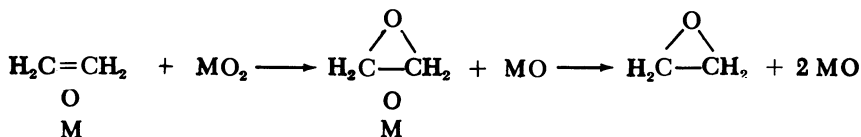
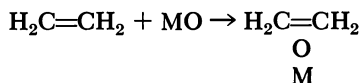
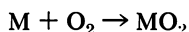
In attempting to characterize the surface of an oxidation catalyst, it is essential to study the catalyst in its operating condition. The result of passing oxygen and a reducing agent together over a solid is often a steady-state condition of the surface at an intermediate oxidation state. For ethylene oxidation over silver the fractional coverage with oxygen,  $\theta$ , is estimated at 0.2 to 0.5 during operation, whereas standing in  $O_2$  alone gives  $\theta$  close to 1.0. With a copper catalyst for oxidizing propylene to acrolein under normal operating conditions the surface steady state leads to a bulk state of cuprous oxide,  $Cu_2O$ . This does not mean that the active surface is identical to that of  $Cu_2O$  in an inert atmosphere, but it does say that the surface cannot be covered entirely with either oxygen or propylene since these conditions are known to lead to bulk states of  $CuO$  or  $Cu$ , respectively. Thus, in this example the bulk composition supplies some evidence about the surface steady state.

### **Reaction Path**

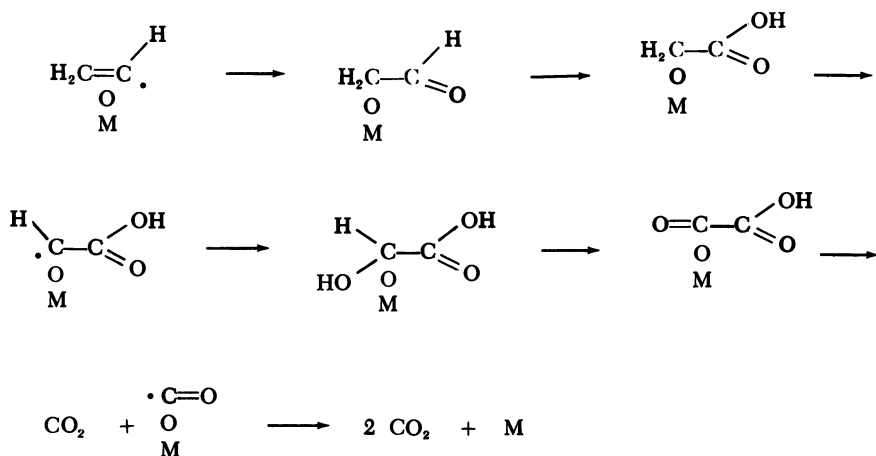
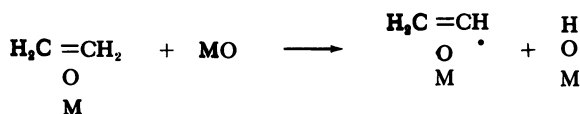
A reaction involving significant changes in molecular structure must proceed along a path (or paths) constituted of several steps, which are usually relatively simple, according to the principle of "least atomic motion." Oxidations of hydrocarbons may easily involve six to 20 steps, or more. Complete knowledge of the reaction will include the structures and energies of the intermediates and the rates of the steps connecting them. This is a formidable assignment, especially since intermediates may consist of short-lived species on rare types of surface sites. Such intermediates are not easily studied by the usual techniques of molecular physics.

As an example consider the oxidation of ethylene over metallic silver at 200 to 300°C. Let M represent the site of adsorption on the metal surface; it can be a single Ag atom or a group of two, three, or four Ag

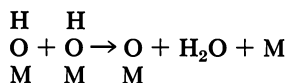
atoms. Reaction steps can be written as follows, where MO and MO<sub>2</sub> represent surface species:



Thus, five steps lead to ethylene oxide. Remaining steps that produce CO<sub>2</sub> as a parallel product may proceed by successive reaction with the MO species.



There will also be reactions such as



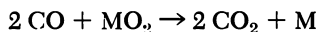
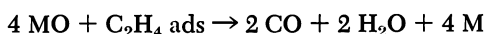
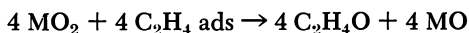
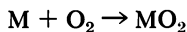
The above species are admittedly speculative, but clearly several steps are necessary to get from ethylene to CO<sub>2</sub>. Many of the intermedi-

ates are "bound" radicals, somewhat analogous to the free radicals of homogeneous systems. Since only ethylene oxide and  $\text{CO}_2$  are observed in appreciable quantities in the gas phase, the intermediates en route to  $\text{CO}_2$  evidently remain on the surface at all times. Migration on the surface is not precluded, however.

An interesting question concerns the dissipation of the energy released in oxidation. To what extent does energy remain in an intermediate or at a catalyst site and thus promote subsequent reaction steps? Energy dissipation steps must be rapid at a solid surface, but reaction steps may also be fast. Sakharov (14) has proposed energy chains on solid catalysts as an explanation of the limiting conversions—short of equilibrium—that are sometimes observed. He supposes that at low reactant concentration the rate of energy supply to the active sites is too low, and reaction ceases. Such energy chains are conceivable in oxidations.

Some features of ethylene oxidation may be explained by a chemical coupling of reactions of the type well known in homogeneous systems. In particular, the conversion to  $\text{CO}_2$  may be coupled with the oxidation to ethylene oxide. This is suggested by the limiting selectivity to ethylene oxide of 75 to 80 moles per 100 moles of  $\text{C}_2\text{H}_4$  converted over silver catalysts. An 80% selectivity has not been exceeded by any variation in process conditions or catalyst. Furthermore, selectivity varies little with temperature; in these laboratories only a small decline (from 75 to 68%) was noted in going from a reaction temperature of  $190^\circ$  to  $320^\circ\text{C}$ . under well controlled conditions at atmospheric pressure with excess air. Also, selectivity under these conditions varied little with conversion when a slightly different catalyst was used at 200 to  $260^\circ\text{C}$ ., and with space velocity varied by a factor of 4, selectivity declined from 71 to 68% as conversion increased from 20 to 80%. The following coupling scheme can explain a near-constant selectivity.

If the initial reaction of ethylene is with a peroxidic-adsorbed  $\text{O}_2$  to form ethylene oxide and  $\text{MO}$ , as indicated above, the  $\text{MO}$  may be consumed in a separate series of steps that lead to  $\text{CO}_2$ .



This will give a limiting selectivity of 4/5, or 80%. The idea of coupled reactions in the ethylene oxide synthesis goes back to at least 1942, when it was published by Worbs (19). Other combinations can be devised, as listed in Table II. In each case the complex  $\text{MO}_2$  is the starting species, and one oxygen atom of this complex is assumed to react with

**American Chemical Society**

**Library**

**1155 16th St., N.W.  
Washington D.C. 20036**

ethylene to form ethylene oxide. Further reactions of the second O atom (MO oxygen) follow.

**Table II. Coupled Ethylene Oxidation**

Case	Assumption	Selectivity, %
I	Second O atoms are used by reaction with $C_2H_4$ to form $CO + H_2O$	80
II	Second O atoms are used up by reaction with $C_2H_4$ to form $CO_2 + H_2O$	85.7
III	Second O atoms are used up by reaction with $C_2H_4O$ to form $CO + H_2O$	66.7
IV	Second O atoms are used up by reaction with $C_2H_4O$ to form $CO_2 + H_2O$	80
V	Second O atom reacts with $C_2H_4$ to start a chain using any $O_2$ that gives $CO_2 + H_2O$	50

In Cases I and III the CO is assumed to be oxidized to  $CO_2$  by means of gas-phase  $O_2$ , or by equal amounts of oxygen atoms of the first and second type. Still other cases can be imagined, with selectivities of 0 to 100%, but in view of observed results, one or more of the above five cases seems most likely.

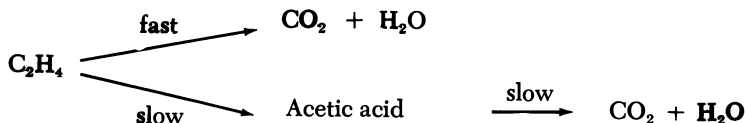
Oxidizing ethylene over a clean silver surface gives a selectivity of 45 to 50%, but by suitably moderating the surface with traces of adsorbed chloride the selectivity rises to 75 to 80% (16). The mechanism of this improvement is obscure, but a shift from Case V to Case I coupling can explain it. Undoubtedly the presence of chloride ions on the surface can change the types or relative amounts of adsorbed oxygen species.

The coupling theory for ethylene oxidation requires only that each adsorbed  $O_2$  molecule form two types of reactive O atoms. Many such pairs are conceivable. It will be of great interest to determine what types are participating in the reactions. The adsorption rate measurements of Czanderna (5, 6) were interpreted as indicating charged  $O_2$  molecules and charged O atoms on a silver surface at about 200°C.

If there are indeed two types of reactive oxygen present on a surface, it may be possible to remove one or the other preferentially by adding another reactant. This effect has not been demonstrated as far as we know.

Another problem in mechanistic steps is posed by the oxidation of hydrocarbons over platinum metals, where the small amounts of aldehydes or acids observed appear not to be intermediates from the main sequence of steps. For example, Kemball and Patterson (11), in oxidizing  $C_2H_4$  over palladium at 50° to 140°C., found acetic acid in amounts up to 3% accompanying the main product,  $CO_2$ . It might be thought that the

acetic acid represents an intermediate, but experiments showed that acetic acid is very slowly oxidized to  $\text{CO}_2$  under the same conditions. Thus, the rough mechanistic path is:



In each branch many individual steps must be involved. What differentiates one branch from the other? Why doesn't acetic acid return to the fast branch, where the intermediates are presumably very similar?

### Reaction Rates

The problem of calculating reaction rate is as yet unsolved for almost all chemical reactions. The problem is harder for heterogeneous reactions, where so little is known of the structures and energies of intermediates. Advances in this area will come slowly, but at least the partial knowledge that exists is of value. Rates, if free from diffusion or adsorption effects, are governed by the Arrhenius equation. Rates for a particular catalyst composition are proportional to surface area. Empirical kinetic equations often describe effects of concentrations, pressure, and conversion level in a manner which is valuable for technical applications.

Kinetics of reaction must be considered when attempting to postulate mechanisms, but kinetic equations alone are unreliable in fixing mechanism. For example, in the oxidation of propylene to acrolein, cuprous oxide and bismuth molybdate have very different kinetics, yet the studies of Vogé, Wagner, and Stevenson (18), and especially of Adams and Jennings (1, 2) show that in both cases the mechanism is removal of an H atom from the  $\text{CH}_3$  group to form an allylic intermediate, from which a second H atom is removed before the O atom is added. The orders of the reactions and the apparent optimum catalysts (16) are as follows:

	$\text{Cu}_2\text{O}$	$\text{Bi}_2\text{O}_3 \cdot 2\text{MoO}_3$
Approximate order in $\text{O}_2$	1	0
Approximate order in $\text{C}_3\text{H}_6$	0	1

The different orders can be explained by the relative coverages of the surfaces with oxygen and propylene at the steady state, but these orders have little to do with the mechanism.

Kinetic equations are of value in interpreting results of integral flow reactors. Work in our laboratories has supplied data on propylene oxida-

tion over  $\text{Cu}_2\text{O}$ , where the reaction rate appears to be limited by oxygen adsorption. The reaction scheme is, mainly,



For the kinetics we suppose that propylene reacts with adsorbed oxygen, and that a certain amount of adsorbed but unreactive propylene interferes with oxygen adsorption. Thus, propylene appears in the numerator for the primary reaction, and in the denominator for both primary and secondary reactions. If  $B$  stands for the fraction of  $\text{C}_3\text{H}_6$  that is oxidized, and  $D$  for the fraction oxidized to  $\text{CO}_2$ , the kinetic equations for the system may be written:

$$dB/dt = k_1(\text{O}_2)(\text{C}_3\text{H}_6)/(\text{C}_3\text{H}_6)$$

$$dD/dt = k_2(\text{O}_2)(\text{C}_3\text{H}_4\text{O})/(\text{C}_3\text{H}_6)$$

and

$$dD/dB = n(B - D)/(1 - B)$$

where  $n = k_2/k_1$ . Solving the differential equation gives  $D = [nB - 1 + (1 - B)^n]/(n - 1)$ , and acrolein selectivity in percent, is  $100(B - D)/B$ . The percentage conversion of oxygen is  $100r(B + 3.5D)$ , where  $r$  is the initial ratio of  $\text{C}_3\text{H}_6/\text{O}_2$ . This scheme gives a reaction which is first order

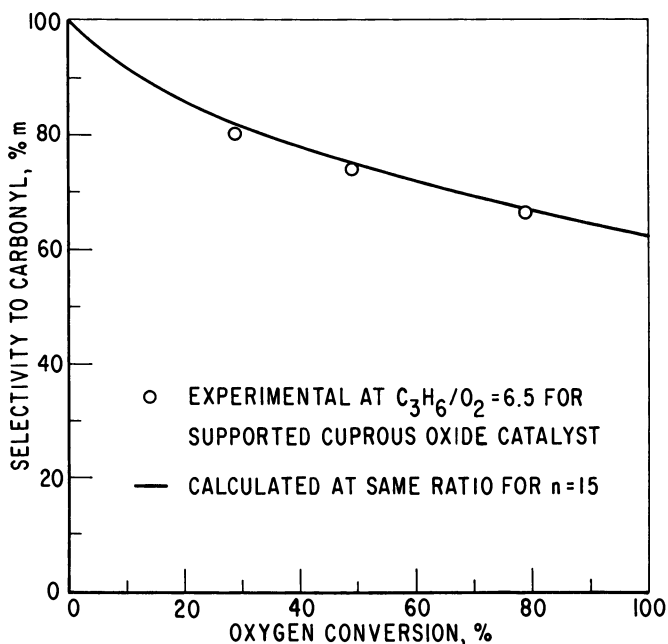


Figure 1. Selectivity for propylene oxidation over cuprous oxide

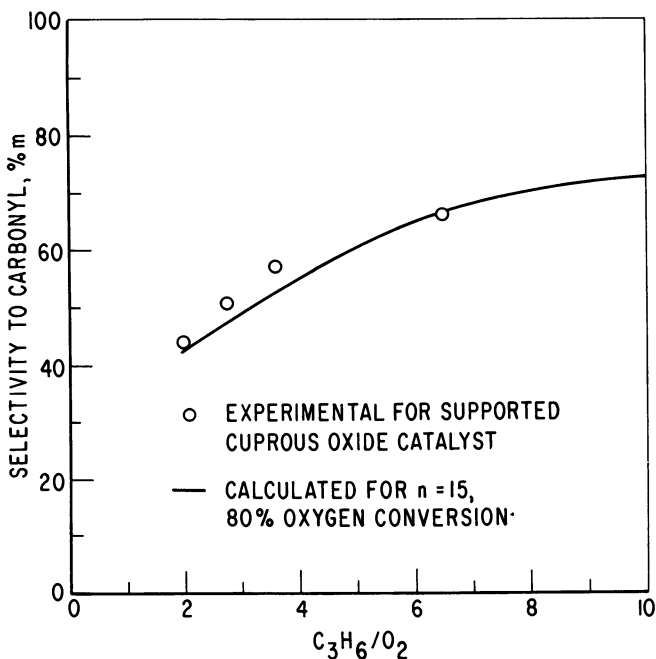


Figure 2. *Effect of propylene-oxygen ratio on selectivity*

in oxygen and independent of propylene. The  $C_3H_6/O_2$  ratio strongly influences selectivity, as shown by the experimental points and calculated curves of Figures 1 and 2. The selectivity at a given ratio and conversion is independent of total pressure, as observed, but we cannot presume that these kinetics tell us much of the mechanism or of the critical factors which make the catalyst selective for a given product.

### **Catalyst Selection**

Moderately good correlations are being established for the relative activities of transition metals for the total oxidation of hydrocarbons to  $CO_2$ . Moro-Oka, Morikawa, and Ozaki (13) show a fair relationship between oxidation rate of 2- $C_4H_8$ ,  $C_2H_2$ , or  $C_2H_4$  and the heat of formation of the oxide per oxygen atom contained therein. Maximum activity is observed at the lowest values of heat of formation.

The matter of selectivity to a particular product is more subtle. Roughly, one needs a catalyst-oxygen bond that is neither too strong nor too weak. But among materials of this class, some are selective and others are not. An average bulk bond strength may not be the same as that holding the reactive oxygen atoms on a surface. In the past, highly selective catalysts seem to have been discovered accidentally or to have

come from an extensive empirical search. Once discovered, of course, a catalyst can be optimized by systematically varying its preparation and composition.

Examples of selective catalysts for oxidizing propylene to acrolein show a wide variation. Effective catalysts include  $\text{Cu}_2\text{O}$  (8),  $\text{Bi}_2\text{O}_3 \cdot 2\text{MoO}_3$  (15),  $\text{TeO}_2 \cdot 6\text{MoO}_3$  (17),  $\text{Sb}_2\text{O}_3 \cdot 6\text{SnO}_2$  (3),  $1.4\text{As}_2\text{O}_3 \cdot \text{Fe}_2\text{O}_3$  (9, 10), and  $4\text{MnO}_2 \cdot 5\text{TeO}_2 \cdot 2\text{P}_2\text{O}_5 \cdot 10\text{MoO}_3$  (7). Though all these can be used to oxidize propylene to acrolein with good selectivity, they are by no means equivalent. The optimum conditions and the by-products are somewhat different for each. Furthermore, characterization by means of other reactions shows wide differences, as illustrated by the comparison of cuprous oxide and bismuth molybdate in Table III, taken from data obtained in our laboratory.

**Table III. Comparison of Cuprous Oxide and Bismuth Molybdate**

<i>Catalyst</i>	$\text{Cu}_2\text{O}$	$\text{Bi}_2\text{O}_3 \cdot 2\text{MoO}_3$
Propylene Oxidation		
Chief product	Acrolein	Acrolein
Temp. range, °C.	300–400	400–525
Order in $\text{O}_2$	1	0
Order in $\text{C}_3\text{H}_6$	0	1
Press. effect on rate	Increases	Increases
Press. effect on select.	None	Decreases
Oxidations of other materials		
Hydrogen	Fast to $\text{H}_2\text{O}$	No reaction
Ethylene	Fast to $\text{CO}_2$	Little reaction
Acetaldehyde	Fast to $\text{CO}_2$	Fast to $\text{CO}_2$ and acid
Ethane	Moderate to $\text{CO}_2$	No reaction
Isopropyl alcohol	Fast to acetone	Fast to propylene
Propionaldehyde	Slow to $\text{CO}_2$	Moderate to $\text{CO}_2$ and acids
Acrolein	Moderate to $\text{CO}_2$	Slow to $\text{CO}_2$
1-Butene	Moderate to methyl vinyl ketone + others	Fast to butadiene

### Conclusions

The main problems in understanding heterogeneous catalytic oxidation reactions are determining detailed mechanisms and the structures and energies of the intermediates, and explaining the rates of the major and side reactions and of catalytic activity in terms of surface properties.

Approaches to these problems that are likely to prove successful include continued intensive study of known reaction systems, checking mechanisms and intermediates by using tracers, further attention to the minor products, and attempts to trap reactive species by adding suitable competitive reactants. More can be done in following reactions

of fractional monolayers on catalyst surfaces with sensitive analytical methods. Energies of bonding to the surface must be used for correlations rather than average energies of bulk solids. Evidence for surface migrations as well as for propagation into the vapor phase should be sought. The newer physical tools such as ESR, nuclear magnetic resonance, infrared, LEED, and field emission microscopes will help in learning the structures of surface compounds. Catalyst characterization will include—but not be limited to—electrical measurements. Visible and ultraviolet reflectance of catalysts may help since electronic transitions are vital. Catalyst evaluations in carefully planned chemical experiments, with actual reactions, will remain essential.

### *Literature Cited*

- (1) Adams, C. R., Jennings, T. J., *J. Catalysis* **2**, 63 (1963).
- (2) *Ibid.*, **3**, 549 (1964).
- (3) Bethell, J., Hadley, D. J., U. S. Patent **3,094,565** (1963).
- (4) Cornaz, P. F., Van Hooff, J. H. C., Pluijm, F. J., Schuit, G. C. A., *Discussions Faraday Soc.* **41**, 290 (1966).
- (5) Czanderna, A. W., *J. Phys. Chem.* **68**, 2765 (1964).
- (6) Czanderna, A. W., *J. Colloid Interface Sci.* **22**, 482 (1966).
- (7) Eden, J. S., U. S. Patent **3,228,890** (1966).
- (8) Hearne, G. W., Adams, M. L., U. S. Patent **2,451,485** (1948).
- (9) Ishikawa, T., Kamio, T., *Kogyo Kagaku Zasshi* **67**, 1015, 1018 (1964).
- (10) Ishikawa, T., Tezuka, T., Sato, K., *Kogyo Kagaku Zasshi* **67**, 1021 (1964).
- (11) Kembell, C., Patterson, W. R., *Proc. Roy. Soc.* **A270**, 219 (1962).
- (12) Margolis, L. Ya., Krylova, A. V., Aleksandrova, E. S., *Kinetika i Kataliz* **7**, 69 (1966).
- (13) Moro-Oka, Y., Morikawa, Y., Ozaki, A., *J. Catalysis* **7**, 23 (1967).
- (14) Sakharov, G. D., *Dokl. Akad. Nauk SSSR* **167**, 863 (1966).
- (15) Veatch, F., Callahan, J. L., Milberger, E. C., Forman, R. W., "Proceedings of 2nd International Congress on Catalysis," Vol. II, p. 2647, Editions Technip, Paris, 1960.
- (16) Vogé, H. H., Adams, C. R., *Advan. Catalysis* **17**, 151 (1967).
- (17) Vogé, H. H., Armstrong, W. E., U. S. Patent **3,168,572** (1965).
- (18) Vogé, H. H., Wagner, C. D., Stevenson, D. P., *J. Catalysis* **2**, 58 (1963).
- (19) Worbs, H., dissertation, Technischen Hochschule Breslau, 1942; U. S. Office of Technical Services, PB Rept. **98705**.

RECEIVED October 11, 1967.

## Some Techniques for Studying the Surface of Solid Oxidation Catalysts

S. W. WELLER

Department of Chemical Engineering, State University of New York at Buffalo, Buffalo, N. Y.

*Selected techniques are discussed for characterizing transition metal oxide and metal catalysts for organic oxidations. Chromia is considered a representative transition metal oxide, platinum and silver as representative metals. The importance of catalyst characterization under reaction conditions is emphasized since the chemical state of the catalyst surface depends on the competitive rates of adsorption, surface reaction, and desorption of several gaseous constituents in the redox atmosphere existing during oxidation. Moreover, cyclic changes in surface chemistry during cyclic processes may significantly affect reaction stoichiometry as well as catalytic activity.*

A major objective of heterogeneous catalysis is interpreting catalytic behavior in terms of the structure, texture, and chemistry of the catalyst surface. Achieving this objective requires detailed knowledge of the surface at an atomic level.

The solid catalysts useful in organic reactions may be categorized loosely into three groups: acid catalysts, catalysts for hydrogenation reactions, and catalysts for oxidation reactions. The structure and action of solid acid catalysts are relatively well understood, thanks in large part to the extensive pre-existing knowledge of carbonium ion chemistry and of the nature of an acid. Even here it is chastening to note the current controversy on the nature of acid catalysts based on synthetic zeolites.

Hydrogenation catalysts, particularly metals, are also relatively well characterized because of extensive study. This has occurred partly for commercial reasons; catalyzed organic reactions of great industrial importance—e.g., hydrogenation and reforming—involve reducing conditions. In part, however, this has occurred because of the esthetic attrac-

tiveness of studying clean metal surfaces with elegant experimental tools such as field ion microscopy and low energy electron diffraction.

A considerable spectrum of techniques also exists for studying the surfaces of solid oxidation catalysts. Several of these are discussed below. No attempt has been made here to be comprehensive. For example, the powerful tool of optical absorption spectroscopy (particularly infrared) is now so well-known and widely used that there is no need here to emphasize its importance.

Before proceeding a word of caution is in order. There is much ambiguity in the loose characterization of catalysts given above. First, in a general sense the same nominal catalyst may be effective for both hydrogenative and oxidative reactions—*e.g.*, platinum and chromia. On a finer scale, however, profound differences in the surface chemistry of a given catalyst may exist in oxidizing and reducing atmospheres, even though the same crystallographic bulk phase is present. This is true of both chromia and platinum at elevated temperatures. The active catalytic surface will then be quite different in the two environments. This situation is further confounded in organic oxidation reactions because both reducing and oxidizing gaseous constituents are present. The actual state of the catalyst surface depends on the competitive rates of adsorption, surface reaction, and desorption of the several gaseous constituents. At the present state of knowledge, our best recourse is to the experimental characterization of the catalyst surface under reaction conditions.

### *Selected Techniques for Studying Catalyst Surfaces*

The following discussion of techniques is eclectic. Two points are clear:

- (1) The various techniques are complementary, and as many of them as possible should be applied to the same catalysts;
- (2) Most of the reported work has been on catalysts studied after arbitrary pretreatment rather than under reaction conditions.

For focus, the discussion is centered on two nominal classes of oxidation catalysts—transition metal oxides, exemplified by chromia, and metals, exemplified by platinum and silver.

### *Transition Metal Oxides (Chromia)*

The complexity of the situation may be illustrated by tracing the development of our knowledge of chromia catalysts. It is now clear that Cr ions on the surface may occur in valence states from Cr<sup>II</sup> to Cr<sup>VI</sup>; all intermediate valence states have been shown to occur, and all are possible in a regime of temperature and gas composition where the thermodynamically stable bulk phase is Cr<sub>2</sub>O<sub>3</sub>.

A landmark in characterizing chromia-alumina catalysts at the molecular level was the pioneering work of Eischens and Selwood (9, 10) on magnetic susceptibility-composition isotherms. The change in susceptibility of the chromium, as the chromia content was varied, was found to be associated with an almost constant magnetic moment but a varying Weiss constant. The data were consistent with a model in which the chromia occurred as small crystallites on the surface of the alumina, the crystallite size decreasing with decreasing chromia concentration to the limit of a two-dimensional dispersion of chromium ions on the alumina surface. This model has proved useful in all subsequent work.

The electrical conductivity of chromia decreases with decreasing oxygen pressure and becomes still lower in hydrogen (4). This result led to classifying chromia as an oxygen excess, *p*-type semiconductor. However, by observing that the sign of the thermoelectric potential changes in going from an oxidizing to a reducing atmosphere, Chapman *et al.* (6) deduced that chromia becomes an *n*-type semiconductor in pure hydrogen.

Voltz and Weller largely confirmed the results both of Bevan *et al.*, and of Chapman *et al.* (21, 24). New facts were added, however, by studying the chemisorption of both oxygen and hydrogen in cycling experiments and by attempts to measure, by direct iodometric titration, the extent to which surface  $\text{Cr}^{\text{III}}$  ions were oxidized to higher valent forms by oxygen (22, 23). It appeared that the bulk of the surface ions are oxidized to higher valent forms in 1 atm. oxygen at 500°C. and reduced in 1 atm. hydrogen.

Matsunaga (15) applied the magnetic techniques of Eischens and Selwood and the chemisorption and chemical techniques of Voltz and Weller to a series of chromia-alumina catalysts. He found that in the limit of low chromia contents, where Eischens and Selwood deduced a two-dimensional distribution of chromium ions, treatment with oxygen at 450°C. resulted in an average valence number of six for all of the chromium ions in the sample.

ESR techniques, introduced about 10 years ago, added an extraordinarily powerful tool for characterizing in detail the individual paramagnetic species which might be present in the catalyst under varying conditions.  $\text{Cr}^{2+}$ ,  $\text{Cr}^{3+}$ ,  $\text{Cr}^{4+}$ , and  $\text{Cr}^{5+}$  are paramagnetic, although  $\text{Cr}^{6+}$  is not. With their co-workers, MacIver, Cossee, and Voevodsky (7, 17, 18) found that catalysts prepared by progressive reduction of  $\text{CrO}_3\text{-Al}_2\text{O}_3$  contained substantial quantities of  $\text{Cr}^{5+}$  and  $\text{Cr}^{4+}$  ions. Cossee and Van Reijen (7) state that hydrogen reduction above 300°C. gives the trivalent state as the stable final product. Pecherskaya *et al.* (81), however, observe that "rigorous reduction" with hydrogen results in a disappearance

of the narrow line associated with  $\text{Cr}^{3+}$ , possibly by reduction to  $\text{Cr}^{2+}$  to give the spinel  $\text{CrAl}_2\text{O}_4$ .

How much information concerning the surface can be obtained from thermodynamic considerations? There are some relevant data available for the thermodynamics of the bulk phases but few for the surface (two-dimensional) phases.

Bulk  $\text{CrO}_3$  loses oxygen at fairly low temperatures to form a host of reported intermediate oxides.  $\text{CrO}_2$ , the best defined of these, decomposes to  $\text{Cr}_2\text{O}_3$  with a decomposition pressure of 1 atm. at about  $430^\circ\text{C}$ . (5). At temperatures of  $450^\circ\text{--}500^\circ\text{C}$ ., therefore,  $\text{Cr}_2\text{O}_3$  is the stable bulk phase in oxygen pressures up to 1 atm. Bulk  $\text{Cr}_2\text{O}_3$  is also resistant to reduction by hydrogen in this temperature range. At  $500^\circ\text{C}$ . the equilibrium constant for the reaction  $\text{Cr}_2\text{O}_3(\text{s}) + \text{H}_2(\text{g}) = 2\text{CrO}(\text{s}) + \text{H}_2\text{O}(\text{g})$  is  $2.2 \times 10^{-5}$  (12). For any reduction of the bulk phase to occur at  $500^\circ\text{C}$ . and a hydrogen partial pressure of 1 atm., therefore, the water partial pressure must be maintained below  $1.7 \times 10^{-2}$  mm. Hg.

These results are useful but far from definitive in establishing the nature of the catalyst surface in contrast to the bulk. In oxygen, Matsunaga's data show, surprisingly, that all of the surface chromium ions are  $\text{Cr}^{6+}$  under conditions where  $\text{Cr}_2\text{O}_3$  is the stable bulk phase (15). In 1 atm. dry hydrogen Weller and Voltz observed that the hydrogen chemisorption at  $500^\circ\text{C}$ . corresponded to almost one atom of hydrogen for each surface oxide ion (23). Clearly one must be concerned with a large swing in valence number of the surface chromium ions from  $\text{Cr}^{6+}$  to  $\text{Cr}^{2+}$ , including all possible intermediates, in different atmospheres. Furthermore, in the complicated atmosphere occurring during organic oxidations, one is not able *a priori* to predict even whether the net environment at the surface is oxidizing or reducing in character.

A particularly interesting situation occurs in reactions, such as butane dehydrogenation over chromia, which are normally operated cyclically without reaching steady state. The deposition of coke and drop in catalyst temperature during the dehydrogenation period necessitate frequent catalyst regeneration by air. The surface chromium ions therefore vary regularly in valence number between  $3+$  and  $6+$ , on about a 15-minute cycle. Under these conditions, about 20% of the butane dehydrogenation to butadiene may be attributable to oxidation of the butane by the  $\text{Cr}^{6+}$  (or equivalently, by the chemisorbed oxygen) in the freshly regenerated catalyst [10 minute on-stream period, feed rate = 0.6 gram  $\text{C}_4\text{H}_{10}$ /gram catalyst-hr. (LHSV = 1),  $1.4 \times 10^{-4}$  moles chemisorbed  $\text{O}_2$ /gram of regenerated catalyst]. The question, "what is the catalyst?" here becomes difficult to answer.

### *Metals (Platinum, Silver)*

Physical methods for characterizing clean surfaces of metals are generally well known and do not require elaboration here. One property of the solid deserves mention, however, because it has been investigated mostly by metallurgists and has not yet been studied adequately in catalysis. This property is the microstructure, in the sense of grain boundaries in a polycrystalline material, and probably more importantly, in the sense of the density of emergent dislocations (edge and screw) which are present at the surface even in a single crystal. These represent high energy sites, where the catalytic activity may be expected to be atypical. A particularly useful technique for characterizing the microstructure of metal foils is transmission electron microscopy, which can be extended to studying all surfaces by using carbon extraction replicas (19).

As yet no catalytic studies seem to have been published on samples in which dislocation density was determined directly. A provocative study has been published recently, however, on silver ribbon which was annealed to various degrees after initial cold-working (20). The dislocation density was indirectly characterized by measuring hardness and thermoelectric potential, both of which decreased as the annealing temperature was increased. Uhara *et al.* found that the catalytic activity for three reactions—decomposition of  $\text{H}_2\text{O}_2$ , oxidation of  $\text{C}_2\text{H}_5\text{OH}$ , and decomposition of  $\text{HCOOH}$ —decreased with increasing annealing temperature in a manner paralleling the decrease in hardness and thermoelectric potential. These results are not definitive, but they suggest that further direct study of the role of dislocations in catalysis will prove rewarding.

A fundamental problem in characterizing metal surfaces in oxidation catalysis is that, as with transition metal oxides, the chemistry of the surface is shaped by the reaction conditions. Margolis has taken the plausible position that most metal surfaces in oxygen are covered with oxygen and behave like metal oxides (13, 14). This is true even of platinum, a classical example of a "metal" catalyst, and here again predictions from bulk thermodynamics are unreliable with respect to the surface.

The thermodynamic data for the platinum oxides are not well established. However, a reasonable value for the free energy of formation of the lower oxide,  $\text{PtO}$ , at  $527^\circ\text{C}$ . is  $-1$  kcal./mole (5, 25). This corresponds to an oxygen dissociation pressure at  $527^\circ\text{C}$ . of 0.28 atm.—*i.e.*, bulk  $\text{PtO}$  is unstable toward decomposition to bulk  $\text{Pt}$  for oxygen pressures below 0.28 atm. Bulk  $\text{PtO}_2$  is, of course, even less stable. Nevertheless, it has been reported that at this temperature and an oxygen pressure

of 10 cm. (0.13 atm.), platinum on alumina chemisorbs oxygen in amount sufficient to convert 80% of the platinum completely to  $\text{PtO}_2$  (16).

If one is to achieve better understanding of the catalytic behavior of metals in oxidation reactions, more attention should be given to measuring surface thermodynamics and to establishing the surface chemistry under reaction conditions. There are striking elements of difference between metal behavior in reducing and oxidizing conditions. As an interesting example, platinum is notoriously sensitive toward sulfur poisoning in hydrogenation, presumably because of the stability (and relative inactivity) of PtS. By contrast, platinum catalysts appear to be quite suitable for oxidizing sulfur-containing organic compounds (25). [Among the few literature references on this matter is an observation by Davy (8) that sulfur does not act on platinum in the presence of air.] This insensitivity to sulfur poisoning probably arises from the fact that the reactions  $\text{PtS} + 3/2 \text{O}_2 = \text{PtO} + \text{SO}_2$  and  $\text{PtS} + \text{O}_2 = \text{Pt} + \text{SO}_2$  are favorable by some 55–60 kcal./mole.

Almquist and Black and Emmett and Shultz 40 years ago pointed out how measurements of surface equilibria, as in the surface reaction  $3/4 \text{Fe} + \text{H}_2\text{O} = 1/4 \text{Fe}_3\text{O}_4 + \text{H}_2$ , can yield values for the excess surface free energy of surface atoms (I, 2, 11). For a single gaseous constituent (as for oxygen on platinum), the method reduces to determining chemisorption isotherms. In any case the free energy of formation of the surface phases will be a function of the surface coverage (or gas composition), in contrast to the thermodynamics for bulk phases. A particularly elegant application of this approach has been reported by Bénard (3). In this work the surface reaction  $\text{Ag} + \text{H}_2\text{S} = \text{AgS} + \text{H}_2$  at 400°C. was studied over silver single crystals, and the extent of surface sulfiding as a function of the  $P_{\text{H}_2\text{S}}/P_{\text{H}_2}$  ratio in gas phase was established separately for the (100), (110), and (111) faces by using radioactive sulfur in the  $\text{H}_2\text{S}$ . The extent of surface coverage by sulfur at a given  $P_{\text{H}_2\text{S}}/P_{\text{H}_2}$  ratio varied greatly with surface face, decreasing in the order (110) > (100) > (111).

It is clear that equilibrium measurements of surface thermodynamics cannot predict surface composition under the dynamic conditions of catalytic oxidation. Nevertheless, such measurements will provide a sounder base than bulk thermodynamics for understanding the surface chemistry and permit working backward, from direct measurements of surface chemistry during reaction, to predictions concerning the micro-environment at the surface under reaction conditions.

#### *Literature Cited*

- (1) Almquist, J. A., Black, C. A., *J. Am. Chem. Soc.* **48**, 2814 (1926).
- (2) Almquist, J. A., *J. Am. Chem. Soc.* **48**, 2820 (1926).

- (3) Bénard, J., "Coloquio sobre Quimica Fisica de Proceso in Superficies Solidas," p. 375, Consejo Superior de Investigaciones Cientificas, Madrid, 1965.
- (4) Bevan, D. J. M., Shelton, J. P., Anderson, J. S., *J. Chem. Soc.* **1948** (1729).
- (5) Brewer, L., *Chem. Rev.* **52**, 1 (1953).
- (6) Chapman, P. R., Griffith, R. H., Marsh, J. D. F., *Proc. Roy. Soc. (London)* **A 224**, 419 (1954).
- (7) Cossee, P., Van Reijen, L. L., *Proc. Intern. Congr. Catalysis, Paris*, **2**, 1679 (1960).
- (8) Davy, E., *Phil. Mag.* **40**, 31 (1812).
- (9) Eischens, R. P., Selwood, J. *Am. Chem. Soc.* **69**, 1590, 2698 (1947).
- (10) *Ibid.*, **70**, 2271 (1948).
- (11) Emmett, P. H., Shultz, J. F., *J. Am. Chem. Soc.* **51**, 3249 (1929).
- (12) Maier, C. G., *U. S. Bur. Mines Bull.* **436** (1942).
- (13) Margolis, L. Ya., *Izv. Akad. Nauk, S.S.S.R., Otd. Khim. Nauk* **1958**, 1175.
- (14) *Ibid.*, **1959**, 225.
- (15) Matsunaga, Y., *Bull. Chem. Soc. Japan* **30**, 868 (1957).
- (16) Mills, F. A., Weller, S. W., Cornelius, E. B., *Proc. Intern. Congr. Catalysis, Paris*, **2**, 2221 (1960).
- (17) O'Reilly, D. E., MacIver, D. S., *J. Phys. Chem.* **66**, 276 (1962).
- (18) Pecherskaya, Y. I., Kazansky, V. B., Veovodsky, V. V., *Proc. Intern. Congr. Catalysis, Paris*, **2**, 1694 (1960).
- (19) Thomas, G., "Transmission Electron Microscopy of Metals," Wiley, New York, 1962.
- (20) Uhara, I., Kishimoto, S., Yoshida, Y., Hikino, T., *J. Phys. Chem.* **69**, 880 (1965).
- (21) Voltz, S. E., Weller, S. W., *J. Am. Chem. Soc.* **75**, 5227 (1953).
- (22) *Ibid.*, **76**, 4701 (1954).
- (23) *Ibid.*, p. 4695.
- (24) Weller, S. W., Voltz, S. E., *Z. Physik. Chem. (N.F.)* **5**, 100 (1955).
- (25) Weller, S. W., unpublished results.

RECEIVED April 8, 1968.

## Oxidation on Metal Oxide Surfaces

TH. G. J. SIMONS, E. J. M. VERHEIJEN, PH. A. BATIST, and  
G. C. A. SCHUIT

Technical University, Eindhoven, Netherlands

*The reduction of transition metal oxides and of  $\text{SnO}_2 + \text{Sb}_2\text{O}_3$  by 1-butene and butadiene were investigated. A single parameter  $Q_o$ , defined as the heat necessary to dissociate  $1/2 \text{ O}_2$  from the oxide, determined the type of reaction. Starting from  $Q_o = 17$  ( $\text{MnO}_2$ ) and proceeding to  $Q_o = 70$  ( $\text{SnO}_2$ ), the reduction produces:*



*Maximum production of butadiene occurs around  $Q_o = 50$ . In some cases such as  $\text{SnO}_2$  the reoxidation by  $\text{O}_2$  of the reduced surface causes the surface to become more strongly oxidizing. This is ascribed to the formation of peroxide radical ions.*

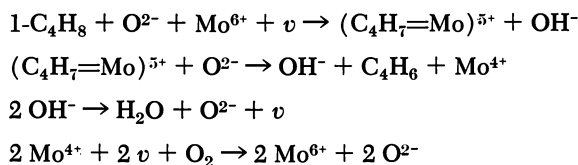
**W**e are concerned here with a class of oxidation reactions sharing the following characteristics:

- (a) The substances that are oxidized are unsaturated organic compounds, such as olefins or aromatics.
- (b) The oxidation is catalyzed by inorganic oxides, such as transition metal oxides ( $\text{V}_2\text{O}_5$ ,  $\text{MoO}_3$ ) or oxides of metals with a filled *d*-shell ( $\text{SnO}_2$ ) or a combination of both types ( $\text{Bi}_2\text{O}_3$ – $\text{MoO}_3$ ).
- (c) The oxidation occurs in the range  $300^\circ$ – $600^\circ\text{C}$ .

For specific cases such as olefin oxidation over Bi–Mo oxide combinations some information concerning the oxidation mechanism is available. The work of Adams and Jennings (2), of Sachtler (16), and of Adams (1) has led to the general acceptance of an allylic intermediate. The discoverers of the Bi–Mo catalyst system (21) showed that propene is converted to acrolein, while Hearne and Furman (9) proved that butene forms butadiene. The allylic intermediate therefore can in principle react in two different ways: (1) formation of a conjugated diene

under further scission of a H atom; (2) formation of a C=C—C=O system by H scission and simultaneous O addition.

Conversion of 1-butene is accompanied by double-bond isomerization, and the experimental observation that the cis/trans ratio of the 2-butene is close to 1 led Batist *et al.* (4) to postulate the allylic intermediate to be  $\pi$ -bonded presumably to an exposed Mo cation. Experiments on reducing Bi<sub>2</sub>O<sub>3</sub>, MoO<sub>3</sub>, and Bi<sub>2</sub>O<sub>3</sub>—MoO<sub>3</sub> by 1-butene in the temperature range of the oxidative dehydrogenation were interpreted by Batist *et al.* (5) as showing that the oxidation proceeds *via* reduction of the oxide system, followed by dehydration and reoxidation. The reaction scheme proposed was:



Here  $v$  represents an anionic vacancy on the surface near a Mo<sup>6+</sup> ion, and (C<sub>4</sub>H<sub>7</sub> = Mo)<sup>5+</sup> stands for the  $\pi$ -bonded allylic complex, while O<sup>2-</sup> and OH<sup>-</sup> are anions belonging to the oxide. The subordinate role of gaseous oxygen in this mechanism, although supported by experimental evidence, is surprising. Dowden (8) has postulated from general principles that surface peroxides—*i.e.*, a form of adsorbed oxygen—are necessary intermediates in oxidation reactions. Indeed, the presence of peroxides has been demonstrated by ESR measurements on some but not all oxide systems. Khazansky and Pariiski (12) found peroxidic radical ions on TiO<sub>2</sub>, and their structures have been discussed at length (7, 11). Kokes (14) observed a peroxide radical ion on ZnO, and this has been investigated further by Sancier (18). Recently van Hooff and van Helden (10) in our laboratory demonstrated similar ESR signals on SnO<sub>2</sub> as given by TiO<sub>2</sub> and showed that one of these signals disappeared after introducing 1-butene. No such signals were observed on MoO<sub>3</sub> or Bi<sub>2</sub>O<sub>3</sub>—MoO<sub>3</sub> catalysts, however, showing that no peroxidic radical cations need be introduced in the reaction mechanism for this catalyst.

This brings us to the problem of selective oxide catalysts. It is well known that the Bi<sub>2</sub>O<sub>3</sub>—MoO<sub>3</sub> catalyst is exceptional in its catalytic activity, there being only small amounts of more extensive oxidation of the hydrocarbons investigated. However, V<sub>2</sub>O<sub>5</sub> is a more powerful oxidizing catalyst, producing considerable amounts of CO<sub>2</sub>. Sachtler and de Boer (17) postulated that activity and selectivity should depend, as generally predicted by Balandin (3), on the strength of the metal-oxygen bond. Strong bonds make inactive catalysts, weak bonds make catalysts that produce complete oxidation, while intermediate cases should lead to

selective oxidation. Klier (13) also postulated that activity for CO oxidation should go through a maximum with the strength of the metal-oxygen bond. There is some experimental evidence for these proposals, especially from the work of Sachtler and de Boer, but the representative points in the Balandin "volcano" plots show considerable scatter. An intrinsic difficulty arises from uncertainty as to the influence of oxygen. If it is assumed that O<sub>2</sub> must be "adsorbed" on the surface before oxidation can occur, it also must be taken into account that the surface layers of the catalyst may be in a higher oxidation state than the bulk. For instance, Cr<sub>2</sub>O<sub>3</sub> may react at its surface to form Cr<sup>5+</sup> cations (15). The relevant bond strength M-O is then different for this oxidized state than would arise from the consideration that reduction comes first and oxidation only serves to re-establish the original oxidation state. Experiments on the influence of metal bond strengths on the catalytic activities of metal oxides in the oxidation of propylene (20) are difficult to interpret since heat and mass transport phenomena may have been considerably important in the over-all process.

To arrive at a better understanding of oxide activities, it seems advantageous to study separately the various processes that are now supposed to form a part of the over-all oxidations. This paper reports on two aspects:

(a) Reduction of a series of transition metal oxides by 1-butene—speed of reduction and products of the reaction. The oxides chosen were TiO<sub>2</sub>, V<sub>2</sub>O<sub>5</sub>, Cr<sub>2</sub>O<sub>3</sub>, MnO<sub>2</sub>, Fe<sub>2</sub>O<sub>3</sub>, Co<sub>3</sub>O<sub>4</sub>, NiO, CuO, and ZnO.

(b) Comparison of 1-butene conversion over SnO<sub>2</sub> (with or without Sb<sub>2</sub>O<sub>3</sub> promotor) in the absence or presence of O<sub>2</sub>.

### *Interaction Between 1-Butene and Butadiene with Some Metal Oxides*

Small amounts (1.1 ml.) of 1-butene or butadiene were pulsed over *ca.* 1 gram of the oxide heated in a microreactor, the continuous gas current being He. The reaction products were separated by gas chromatography (8 meters; 15% demethylsulfolane on Chromosorb 30/60). This was repeated for various temperatures of the microreactor. The oxides used (*see* Appendix) and their surface areas are given in Table I, which also summarizes the information derived from the runs. The following parameters were used:

$T_{50}$ : temperature at which 50% of the feed is converted to CO<sub>2</sub>.

Maximum % diene: maximum conversion to butadiene (usually at temperature  $T_{50}$ ).

Maximum isomerization %: maximum conversion to 2-butene.

cis/trans: cis/trans ratio in the 2-butenes formed.

loss: conversion to products not accounted for.

Table I. Reduction of

Name	Oxide		Conversion of		
	Surface area sq. meters/gram	$Q_0$ Kcal. <sup>-1</sup>	$T_{50}$	Max. % diene	Max. isom. %
TiO <sub>2</sub>	2.1	69	>>500	6	53
V <sub>2</sub> O <sub>5</sub>	2.8	29	340	2	61
Cr <sub>2</sub> O <sub>3</sub>	8.8	?	>>500	13	76
MnO <sub>2</sub>	1.7	17	245	3	0
Fe <sub>2</sub> O <sub>3</sub>	121.1	56	345	50	20
Co <sub>3</sub> O <sub>4</sub>	2.6	38	365	10	1
NiO	6.1	58	440	22	50
CuO	0.35	34	350	2	5
ZnO	17.3	83	>>500	3	80
SnO <sub>2</sub>	4	70	610	11	15

"Loss" is of a varied nature. For the butadiene conversion on V<sub>2</sub>O<sub>5</sub>, where it is particularly high, it was mainly maleic anhydride. On ZnO and Cr<sub>2</sub>O<sub>3</sub> considerable amounts of cracking were observed. There is, moreover, often some material retained by the oxide that can be separated from it only by pulsing O<sub>2</sub> over it; it then appears as CO<sub>2</sub>. Any successive run over one and the same amount of oxide was therefore always preceded by O<sub>2</sub> pulses until no more CO<sub>2</sub> was observed.

Finally, in Table I, Column  $Q_0$  refers to the heat of dissociation of O<sub>2</sub> from the oxide to the next lower oxidation state, calculated per half mole O<sub>2</sub>. The necessary data for the enthalpies of formation ( $H_f$ ) were derived from "Handbook of Chemistry and Physics" (45th ed., 1964–1965).

Figures 1 and 2 show the data obtained for an oxide with low (MnO<sub>2</sub>,  $Q_0 = 17$ ), intermediate Fe<sub>2</sub>O<sub>3</sub> ( $Q_0 = 56$ ), and high  $Q_0$  (SnO<sub>2</sub> = 70 and ZnO = 83).

If  $T_{50}$  for the oxidation of 1-butene to CO<sub>2</sub> and of butadiene to CO<sub>2</sub> is plotted *vs.*  $Q_0$  (Figure 3), it increases with increasing  $Q_0$ . That the plots show considerable scatter is not surprising; the surface areas of the various samples differ by a factor 400. Indeed, those samples having the highest surface areas (Fe<sub>2</sub>O<sub>3</sub>) show the greatest deviation from the general trend and in the direction expected.

If these data are accepted as relevant, at least for the reduction process one of Sachtler and de Boer's conclusions (*i.e.*, that activity should decrease with increasing metal oxygen bond strength) appears confirmed.

Their second conclusion (*i.e.*, that there should be maximum selectivity for intermediate bond strengths) also seem confirmed by our experiments. If the maximum production of butadiene is accepted as a measure

**Metal Oxides by 1-Butene**

<i>1-Butene</i>		<i>Conversion of Butadiene</i>		<i>Remarks</i>
<i>Cis/trans at max.</i>	<i>Loss max.</i>	$T_{50}$	<i>Loss max.</i>	
1.15	2	370	3	Loss is maleic anhydride
4-0.9	20	>>500	57	Loss is cracking
0.8	10	—	—	
	14	285	2	
1	23	410	17	
1	5	400	5	
0.8	4	410	2	
3	0	370	4	
0.8	42	—	—	Loss is cracking
2-1	20	>600	4	

for this selectivity, Figure 3 shows that there is indeed a maximum around  $Q_o = 50-60$ . This value appears more significant in view of the fact that  $Q_o$  values for  $\text{MoO}_3$  and  $\text{Bi}_2\text{O}_3$  are 50 and 45 and therefore in the range of maximum selectivity.

It is interesting to speculate on what would happen if oxide reduction became more substantial—*e.g.*, by repeating the injection of pulses of 1-butene without intermediate reoxidation. Clearly, the substances investigated this way should belong to those easily reduced specimens such as  $\text{MnO}_2$  or  $\text{Co}_3\text{O}_4$ . The immediate consequence would be oxygen depletion of the surface layers and hence a decrease in the concentration of  $\text{O}^{2-}$  ions. Moreover,  $Q_o$  is expected to rise. For instance,  $Q_o$  for  $\text{MnO}_2$  to  $\text{Mn}_2\text{O}_3$  is 17, but from  $\text{Mn}_2\text{O}_3$  to  $\text{Mn}_3\text{O}_4$  increases to 34. Likewise,  $Q_o$  ( $\text{Co}_3\text{O}_4 \rightarrow \text{CoO}$ ) = 38 but  $Q_o$  ( $\text{CoO} \rightarrow \text{Co}$ ) = 57. This would entail a shift of the reaction in the direction of strongly suppressed total oxidation since both factors work in the same direction. However, for the production of butadiene a decrease in  $\text{O}^{2-}$  concentration should decrease, an increase in  $Q_o$  should increase the butadiene production, and the two factors would tend to cancel. The results of experiments of this type in which a series of 1-butene pulses was fed to the oxide are given in Figure 4. Calculating the degree of reduction at the end of the experiment shows that  $\text{MnO}_2$  must have been reduced to  $\text{Mn}_2\text{O}_{3.2}$  and  $\text{Co}_3\text{O}_4$  to  $\text{Co}_3\text{O}_{3.2}$ .

For  $\text{MnO}_2$  we observe a decrease in 1-butene consumption (60–40%) a stronger decrease in  $\text{CO}_2$  formation (calculated on 1-butene 50–20%), an increase in butadiene formation (4–10%) and a slight increase in isomerization (1–3%). There is, moreover, a considerable increase in percentage “loss” (0–12%, not shown in figure).

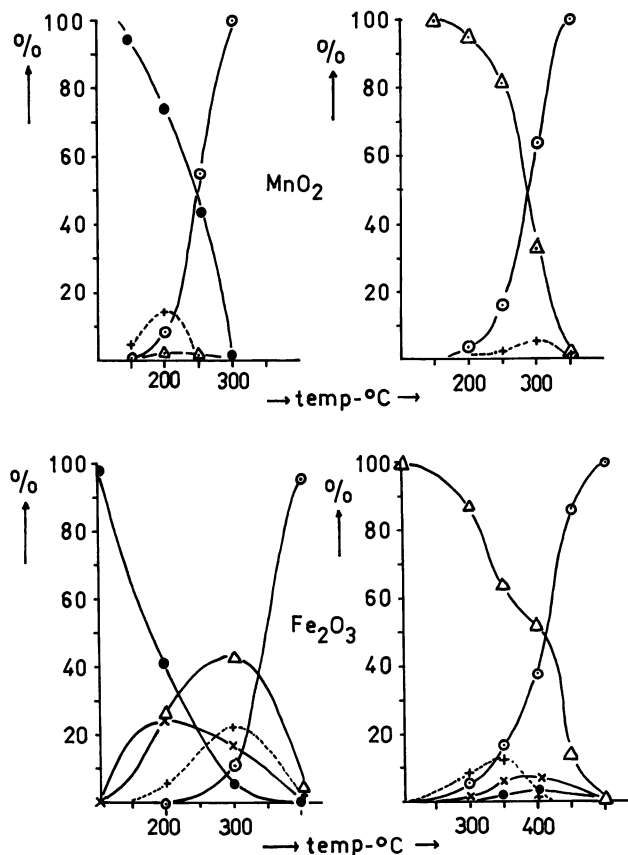


Figure 1. Reaction of 1-butene (left) and butadiene (right) with  $MnO_2$  and  $Fe_2O_3$

- 1-butene
- △ butadiene
- $CO_2$  divided by 4
- × 2-butene
- + "loss"

The  $Co_3O_4$  results are somewhat different. Both  $CO_2$  formation and butadiene production decrease in roughly constant ratios. However, isomerization increases strongly. "Loss" remains small, of the order of 1–2%.

It seems that the order of shifts in the various reactions going from strongly oxidizing to a more moderate activity is  $CO_2 \rightarrow$  "loss"  $\rightarrow$  butadiene  $\rightarrow$  isomerization. If "loss" is identified with oxygen-containing substances, this would conform to expectations. This sequence is also in line with the results of Table I with one notable exception:  $V_2O_5$  is

strongly oxidizing, but at the same time it is a strong isomerization catalyst.

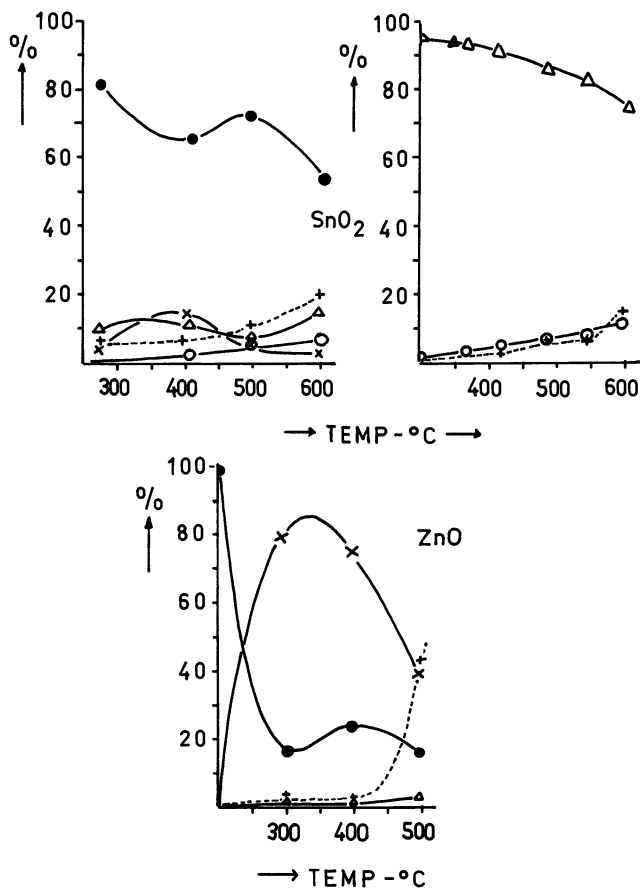


Figure 2. Reaction of 1-butene (left) with SnO<sub>2</sub> and ZnO and of butadiene with SnO<sub>2</sub>. For symbols see Figure 1

### *The Actions of O<sub>2</sub> and Lattice Oxygen*

For one catalyst, SnO<sub>2</sub>, a comparison was made between the activities of gaseous oxygen and lattice oxygen. Since this study involved the activity of the SnO<sub>2</sub>-Sb<sub>2</sub>O<sub>3</sub> combination (6), it seems appropriate to discuss the structural properties of this combination. Various mixtures (Sn/Sb ratio 9/4, 6/4, 3/4, and 1/4) were prepared by firing at 900°C. for 24 hours. X-ray data and infrared KBr wafer measurements showed the presence of only SnO<sub>2</sub>, Sb<sub>2</sub>O<sub>4</sub> and Sb<sub>2</sub>O<sub>3</sub> if this substance had been

in excess. The combination, however, possessed a bluish-grey color, whose origin is obscure.  $\text{Sb}_2\text{O}_3$ , if fired at  $900^\circ\text{C}$ . in oxygen also showed an x-ray diagram that resembled that of  $\text{Sb}_2\text{O}_4$ .

The sample of  $\text{SbO}_2$  we prepared showed no activity toward 1-butene, which is somewhat surprising, since from Skinner's data (19) one deduces a  $Q_o$  value of 46 and therefore a stronger tendency to reduction than  $\text{SnO}_2$ , for example.

Although the x-ray data indicate that no formation of compounds or of solid solutions occurs between  $\text{SnO}_2$  and  $\text{SbO}_2$ , there is a strong influence of  $\text{SbO}_2$  addition on the catalytic properties.

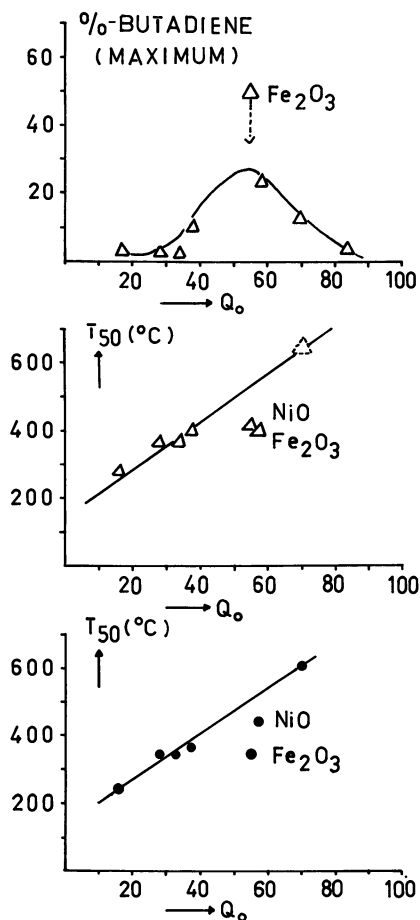


Figure 3.  $T_{50}$  values and maximum butadiene formation as function  $Q_o$  (see Table I and text)

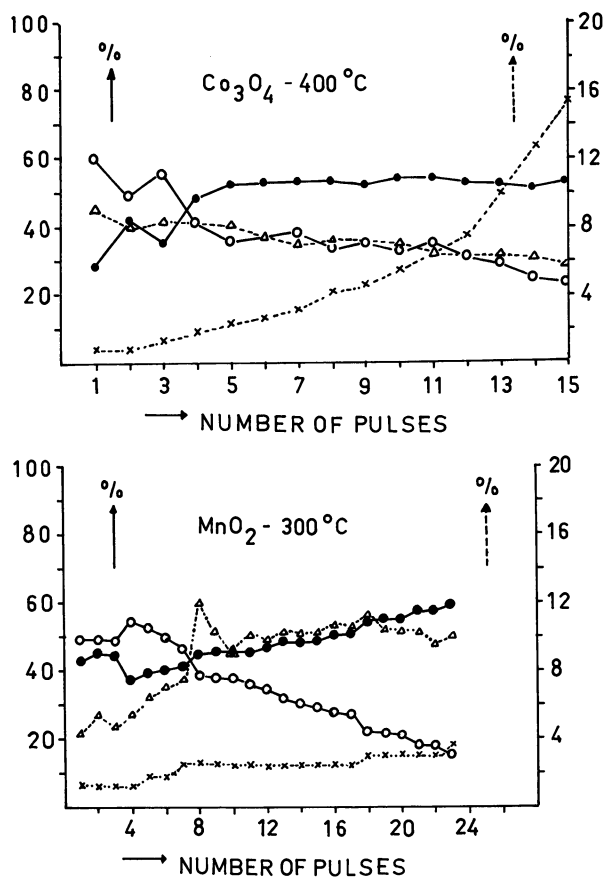


Figure 4. Reduction of  $\text{MnO}_2$  and  $\text{Co}_3\text{O}_4$  as function of reduction (number of pulses 1-butene). For symbols, see Figure 7

To show this influence, consider Figure 5-A where the degree of conversion of 1-butene and butadiene over  $\text{SnO}_2$  have been plotted as function of the temperature for pulses consisting of mixtures of  $\text{O}_2$  and hydrocarbon. The conversion has been plotted as a fraction of the pulse volume, and since this initially consisted of 0.40 parts hydrocarbon, the conversion for 1-butene is nearly complete at  $400^\circ\text{C}$ . Further, the conversion to butadiene drops at higher temperatures, and the reason is immediately obvious from Figure 5-B which shows that butadiene is very reactive if  $\text{O}_2$  is present, again contrary to its behavior if the pulse contained only butadiene. Now, adding  $\text{Sb}_2\text{O}_3$  to  $\text{SnO}_2$  decreases the conversion of 1-butene and almost eliminates that of butadiene. Moreover, both "loss" and isomerization are eliminated.

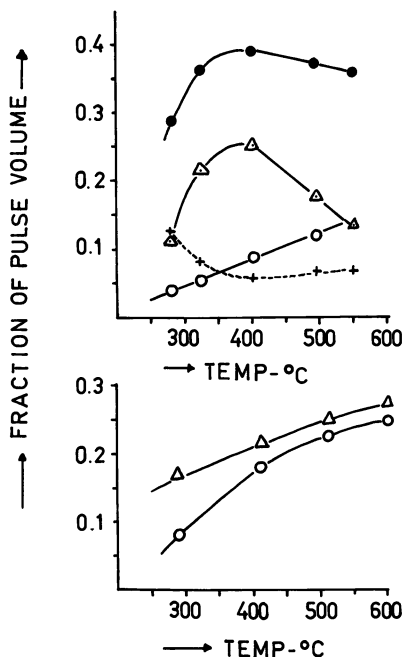


Figure 5. Products of reaction from 1-butene (top) and butadiene (bottom) if pulsed in volume ratio 0.6 O<sub>2</sub> and 0.4 hydrocarbon over SnO<sub>2</sub> (500 mg., preheated 24 hours at 850°C.). Reaction temperatures 400° and 430°C. For symbols see Figure 1

To investigate further this influence of O<sub>2</sub>, pulses of mixtures of hydrocarbon and oxygen of variable composition were fed to the catalyst. The catalysts studied were SnO<sub>2</sub>, 9 SnO<sub>2</sub> + 2 Sb<sub>2</sub>O<sub>3</sub> and—for comparison—a Bi<sub>2</sub>O<sub>3</sub> + 2 MoO<sub>3</sub> catalyst. The results are given in Figures 6 and 7. Those for the Bi/Mo catalyst agree completely with earlier results. The conversion of butene increases linearly with its partial pressure, and the fraction converted to butadiene remains constant over the whole range of compositions (90%). Isomerization, always in the ratio cis/trans = 1 also increases linearly with the partial pressure of butene. The conversion of O<sub>2</sub> is fast; it is equivalent to the amount of butene converted if O<sub>2</sub> is in excess.

The picture is familiar: reduction of the oxide by 1-butene in a reaction that is first order in the hydrocarbon followed by a fast reoxidation of the oxygen-depleted surface to a state that is equal to the initial one.

Different but still comparatively easy to understand is the reaction over the Sn/Sb catalyst. If it is in excess, the conversion of butene—90% to butadiene—is constant and independent of the composition indicating that reduction is fast and limited by the amount of oxygen available on the surface. Isomerization is absent, further proof of the speed of the reduction. At lower hydrocarbon pressures the rate is proportional to butene pressure. Consumption of  $O_2$  is never complete, showing that the reoxidation is slow, and it is only when  $O_2$  is in excess that oxygen consumption manages to keep pace with reduction. Here we encounter a situation where the surface reduction is fast, as it should be according to

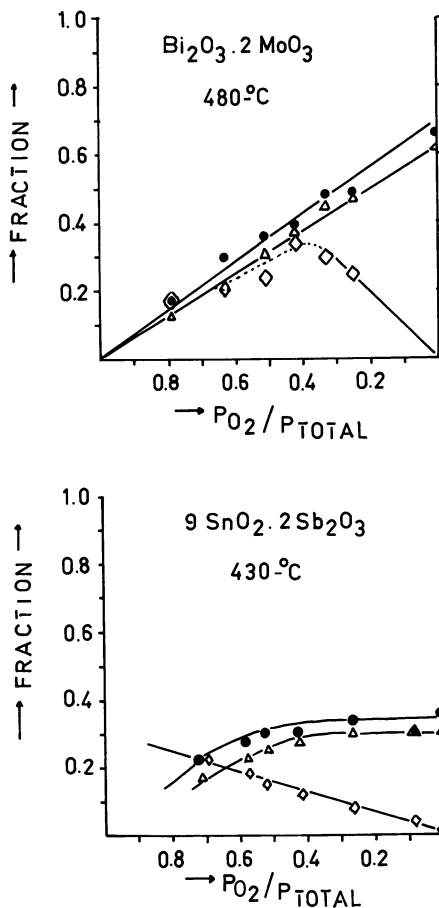


Figure 6. Products of reaction as function of pulse composition. Feed, 1-butene. For symbols see Figure 1.  $\diamond$ ,  $O_2$

the  $Q_0$  value but where reoxidation is slow. The surface therefore remains depleted but always comparable in its reactivity to the original one.

The situation for  $\text{SnO}_2$  is more complex. With the pure hydrocarbon there is only partial reaction, about 50% to butadiene, a small amount to  $\text{CO}_2$  and the rest unaccounted for. There is considerable isomerization ( $\text{cis/trans} = 2$ ). Adding  $\text{O}_2$  increases the amount converted with a product distribution that is different since most of the butene now converted goes to butadiene. The amount of butene converted passes through a maximum and then decreases in accordance with its partial pressure; at lower hydrocarbon pressures the total combustion is pronounced. Oxygen consumption is fast. Clearly the surface which in its original state reacts only slowly with the hydrocarbon is quickly reoxidized, but in this reoxidation it acquires a more potent oxidizing capacity. Therefore, the reoxidized surface contains peroxide groups. The superior reactivity of the surface is reflected in a marked decrease of the isomerization that in its reduced form now shows a  $\text{cis/trans}$  ratio of 1. A new phenomenon is encountered in which the reducing properties of the surface no longer indicate the catalyzed reaction proper. Dowden's reaction mechanism is clearly better suited to explain the reaction encountered here.

### Discussion

To a certain extent reasonable agreement exists between theoretical and experimental results; for a number of oxides the rate of reduction by 1-butene parallels a decrease in the strength of the metal-oxygen bond as given by the dissociation energy  $Q_0$ . This is true even though the present data, although admittedly less convincing than desired, allow for the possibility that intermediate metal-O bond strengths are favorable for selectively oxidizing the hydrocarbon. However, for the actual catalysis it seems necessary to add a new detail to the model; it is evidently not always true that catalysis consists of reduction of the oxide followed by reoxidation of the catalyst to its original state (*see* the  $\text{SnO}_2$  catalyst). Therefore, we introduced a new feature—*viz.*, reoxidation of the oxygen-depleted oxide under the formation of surface peroxides (Figure 8). If  $Q_0$  is small, the mobility of the oxygen ions, even at a low temperature might be sufficient to maintain a constant and fast supply of oxygen ions to the allyl intermediate, enabling complete combustion of this allyl radical. Increasing  $Q_0$  causes a decreased mobility of the  $\text{O}^{2-}$  and therefore a higher temperature for the reactions to occur. The average residence time of the adsorbed state of the hydrocarbon as the allyl intermediate, however, is reduced at the higher temperature, and the chances for complete combustion become smaller; partial oxidation,

therefore, is indicated. At still higher  $Q_0$  the reduction is slow, but now peroxides seem to take over in the oxidation catalysis. This introduces the question: why are peroxides only encountered for these oxides that are reduced with difficulty? To answer this question, assume that bond strength of metal-O<sup>2-</sup> is  $a$ , and that of metal-O<sub>2</sub><sup>2-</sup> is  $b$  kcal./mole. It seems reasonable to assume that  $b$  increases as  $a$  since the type of bonding may be considered similar. If O<sub>2</sub> dissociates from the surface, the energy necessary is  $2a - c$ , where  $c$  is the strength of the O=O bond:  $Q_0 = \frac{1}{2}(2a - c)$ .

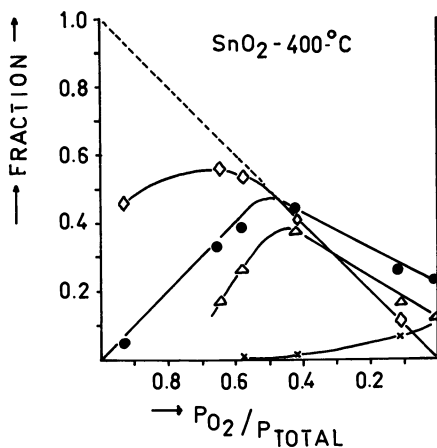


Figure 7. Products of reaction as function of pulse composition. Feed, 1-butene. For symbols see Figure 1.  $\diamond$ , O<sub>2</sub> converted

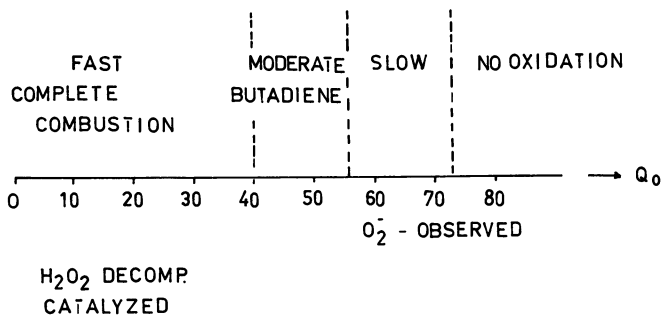


Figure 8. Summary of catalytic reactions depending on metal-oxygen bond strength  $Q_0$

The heat necessary to effect dissociation of the peroxide is  $b - d$ , where  $d$  is the heat accompanying the conversion of a single O—O bond present in the peroxide to a double bond; estimates from bond strengths in peroxides indicate that  $d$  is large and only about 30 kcal. smaller than  $c$ . The heat needed to dissociate  $O_2$  from the oxide ( $2a - c$ ) therefore is considerably greater than to dissociate  $O_2$  from the peroxidic state. If, as we have assumed,  $a$  and  $b$  show parallel changes with a change of the metal-ion, those oxides that easily lose O by reduction cannot form surface peroxides; they should then be effective peroxide decomposition catalysts as is the case. Conversely, for surface peroxides to be formed one should seek oxides with relatively large  $Q_0$  values; so far this seems to agree with experimental results. A similar qualitative conclusion would apply for the  $O_2^-$  radical ion. The present experimental data therefore appear at least qualitatively understood.

However, closer inspection shows that we are still far from a satisfactory theory. By far the greatest unknown is the lack of an adequate description of the hydrocarbon residue, originally the allyl intermediate but in later stages of the combustion of an as yet completely obscure type. Consequently we do not know whether the bond strengths of organic residues on the surface do not change with the metal ion as was tacitly assumed above. The present knowledge is even too limited to ascertain whether the allylic intermediate is  $\sigma$ - or  $\pi$ -bonded, and of the following intermediates we know next to nothing. Although the theoretical consideration given above might be considered, the present understanding of oxidation catalysis cannot be considered satisfactory, and there is an urgent need for more information regarding the structures of oxygenated intermediates and the way in which they are bonded to the surface.

## Appendix

### *Preparation of Oxides*

**TiO<sub>2</sub>.** TiCl<sub>4</sub> distilled over Cu, hydrolyzed in water (0°C.), treated with conc. NH<sub>4</sub>OH, filtered, washed Cl-free, dried at 120°C., preheated 4 hrs. 500°C., followed by 4 hrs. 800°C. in air (x-ray pattern of rutile).

**V<sub>2</sub>O<sub>5</sub>.** Firing of NH<sub>4</sub>VO<sub>3</sub> at 500°–500°C., followed by 28 hrs. heating in wet air current at 530°–570°C.

**Cr<sub>2</sub>O<sub>3</sub>.** Evaporation of solution of Cr(NO<sub>3</sub>)<sub>3</sub> · 9H<sub>2</sub>O heated 16 hrs. at 500°C.

**MnO<sub>2</sub>.** Decompose Mn(NO<sub>3</sub>)<sub>2</sub> · 6H<sub>2</sub>O in air at 190°C. Powdering, treating in boiling HNO<sub>3</sub> (1:1), and preheating in air at 450°–500°C.

**Fe<sub>2</sub>O<sub>3</sub>.** Precipitation from ferric nitrate solution by ammonia. Filtering and washing till NO<sub>3</sub>-free. Drying at 50°C., powdering, followed by heating in dry air at 180°–220°C. and finally 500°C., amorphous.

**Co<sub>3</sub>O<sub>4</sub>.** Heating of Co(NO<sub>3</sub>)<sub>2</sub> · 6H<sub>2</sub>O for 1 hr. at 700°C.

**NiO.** Heating of Ni(NO<sub>3</sub>)<sub>2</sub> · 6H<sub>2</sub>O for 4 hrs. at 400°C.

**CuO.** Slow heating of copper nitrate to 400°C., powdering, heating to 850°C. for 1 hr. Powdering and repeated heating at 700°C.

**ZnO.** Precipitation of ZnOH by adding solutions of ZnCl<sub>2</sub> and NH<sub>4</sub>-oxalate at 70°C. Washing of precipitate, drying by heating at 240°C. (6 hrs.) and finally 4 hrs. 400°C.

### *Literature Cited*

- (1) Adams, C. R., *Proc. Intern. Congr. Catalysis, Amsterdam* **3**, 240 (1964).
- (2) Adams, C. R., Jennings, T. T., *J. Catalysis* **2**, 63 (1963).
- (3) Balandin, A. A., *Advan. Catalysis* **10**, 120 (1958).
- (4) Batist, Ph. A., Lippens, B. C., Schuit, G. C. A., *J. Catalysis* **5**, 55 (1966).
- (5) Batist, Ph. A., Kapteijns, C. J., Lippens, B. C., Schuit, G. C. A., *J. Catalysis* **7**, 33 (1967).
- (6) Bethell, T., Hadley, D. J., U. S. Patent **3,094,565** (1963).
- (7) Cornaz, P. F., van Hooff, J. H. C., Pluijm, F. J., Schuit, G. C. A., *Discussions Faraday Soc.* **41**, 290 (1966).
- (8) Dowden, D. A., *Col. Quimica Fisica Proc. Superficies Solidas Madrid*, 1965, p. 177.
- (9) Hearne, G. W., Furman, K. E., U. S. Patent **2,995,320** (July 4, 1961).
- (10) van Hooff, J. H. C., van Helden, J. F., *J. Catalysis*, to be published.
- (11) Iyengar, D., Codell, M., Karra, J., Turkevich, J., *Discussions Faraday Soc.* **41**, 323 (1966).
- (12) Khazansky, V. B., Pariisky, G. B., *Proc. Intern. Congr. Catalysis, Amsterdam* **3**, 367 (1964).
- (13) Klier, K., *J. Catalysis*, to be published.
- (14) Kokes, R. J., *Proc. Intern. Congr. Catalysis, Amsterdam* **3**, 484 (1964).
- (15) van Reyen, L. L., Ph.D. Thesis, Eindhoven, 1964.
- (16) Sachtler, W. M. H., *Rec. Trav. Chim.* **82**, 243 (1963).
- (17) Sachtler, W. M. H., de Boer, N. H., *Proc. Intern. Congr. Catalysis, Amsterdam* **3**, 252 (1964).
- (18) Sancier, K. M., *J. Catalysis* **5**, 314 (1966).
- (19) Skinner, H. A., *Symp. Thermodynamics Thermochemistry Lund*, 1963, 115 (1964).
- (20) Takeuchi, T., Honma, M., Takeda, H., *Bull. Chem Soc. (Japan)* **39**, 2101 (1966).
- (21) Veatch, F., Callahan, J. L., Milberger, E. C., Forman, R. W., *Actes Congr. Intern. Catalyse, 2e Paris*, 1960 **2**, 2647 (1961).

RECEIVED October 20, 1967.

## Oxidation of 2-Methylpropene over Copper Oxide Catalysts in the Presence of Selenium Dioxide

R. S. MANN and K. C. YAO

Department of Chemical Engineering, University of Ottawa, Ottawa, Canada

*The air oxidation of 2-methylpropene to methacrolein was investigated at atmospheric pressure and temperatures ranging between 200° and 460°C. over pumice-supported copper oxide catalyst in the presence of selenium dioxide in an integral isothermal flow reactor. The reaction products were analyzed quantitatively by gas chromatography, and the effects of several process variables on conversion and yield were determined. The experimental results are explained by the electron theory of catalysis on semiconductors, and a reaction mechanism is proposed. It is postulated that while at low selenium-copper ratios, the rate-determining step in the oxidation of 2-methylpropene to methacrolein is a p-type, it is n-type at higher ratios.*

The selective air oxidation of 2-methylpropene (isobutene) to methacrolein (methacryl aldehyde) is of considerable importance. Though several patents (1, 2, 4, 6, 17) have appeared during the last 20 years describing the use of various metal oxides in the partial oxidation of 2-methylpropene, kinetic studies have been reported only recently by Mann and Rouleau (14, 15) and Shapovalova (18). Kruzhalov *et al.* (13) and Kominami *et al.* (12) studied the air oxidation of propylene to acrolein over  $\text{CuSeO}_3$ , supported on activated alumina and silica gel. They suggested that selenium assisted the rupture of the chain reaction for the decomposition of the allyl hydroperoxide radical or as a promoter for the active centers of the catalyst during the catalytic reaction. Margolis *et al.* (16) studied the effects of several additives upon the catalytic activity and selectivity of metals and semiconductors on the oxidation of

propylene and ethylene. They found that the additives having an electro-negative value,  $E$ , greater than that of the catalyst decreased the activity of the catalyst and increased the work function and selectivity of the catalyst for the oxidation of ethylene and propylene. Hadley (7-10) also claimed that adding selenium to an oxidation catalyst increased its life and selectivity in the oxidation of olefins to unsaturated aldehydes. However, no mention is made in the literature of the selectivity and optimal amounts of selenium dioxide that can be used to oxidize 2-methylpropene to methacrolein under different operating conditions.

This paper reports the effect of various amounts of selenium dioxide under different operating conditions on the conversion of 2-methylpropene to methacrolein and proposes a hypothesis for the hydrocarbon oxidation, which explains particularly the reactivity and selectivity of selenium-copper oxide catalysts in oxidizing 2-methylpropene.

### Experimental

The partial air oxidation of 2-methylpropene to methacrolein in a constant and continuous supply of selenium dioxide was investigated in an isothermal integral flow reactor, constructed of 316 stainless steel. The schematic diagram of the apparatus used to study the reaction is shown in Figure 1.

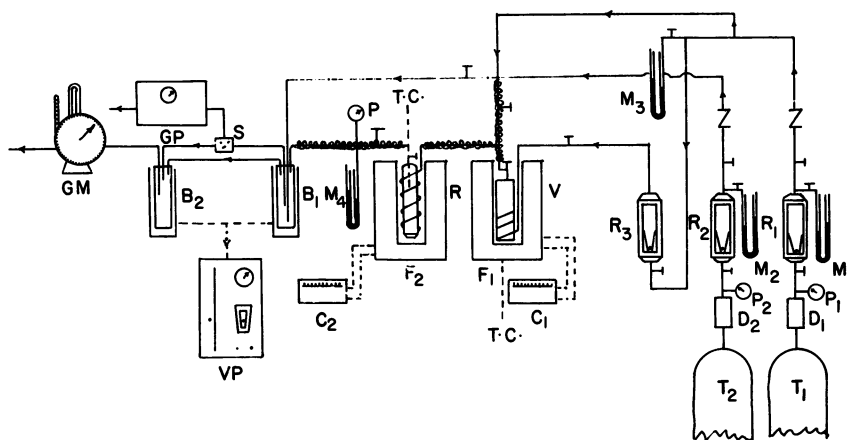


Figure 1. Schematic of the apparatus

$B_1$ , ice trap  
 $B_2$ , liquid nitrogen trap  
 $C_1, C_2$ , temperature controllers  
 $D_1, D_2$ , drying tubes  
 $F_1, F_2$ , furnaces  
 $GP$ , gas partitioner  
 $GM$ , wet-gas meter  
 $M_1, M_2, M_3, M_4$ , manometers

$P_1, P_2, P_3$ , pressure gages  
 $R$ , reactor  
 $R_1, R_2, R_3$ , rotameters  
 $S$ , sampling valve  
 $T_1$ , air tank  
 $T_2$ , 2-methylpropene tank  
 $V$ , selenium dioxide vaporizer  
 $VP$ , vapor fractometer

The flow rates of the reactants, air, and 2-methylpropene, were measured by Brooks rotameters. The reactants were mixed well before they entered the preheating section. Two streams of air were used. While one stream passed through the selenium dioxide vaporizer and carried a certain amount of selenium dioxide vapor with it, the other stream bypassed it. The reactor was made of stainless steel tubing 6 inches long and 0.5 inch in outside diameter. The gases entered the reactor at the bottom through a porous stainless steel plate, which served as a support for the catalyst. The preheating section was made of tubing 6 feet long and 1/8 inch in outside diameter, long enough to preheat the gases entering the reactor to the desired reaction temperature. The reactor with the preheating section was immersed in a constant temperature liquid metal bath, consisting of a mixture of 50% bismuth and 50% lead by weight. The metal mixture was heated by an electric furnace, the temperature of which was controlled to within  $\pm 3^\circ\text{C}$ . by a Honeywell Pyrovane temperature controller.

The flow rate of the inlet air to the selenium vaporizer was kept constant, and different amounts of selenium dioxide vapor carried by air were obtained by adjusting the temperature of the vaporizer. Thus, selenium and its compounds (oxides) were uniformly distributed over the thin layer of catalyst bed. Since the catalyst was present in small amounts, selenium retained by the catalyst could not be determined accurately. However, most of it was recovered from the product stream by condensation. An air condenser was installed in the exit line of the reactor to remove the condensed selenium, thereby ensuring that selenium did not pollute the air.

The exit gases from the reactor were first led to an air condenser to remove condensed selenium dioxide and then through an ice-cooled trap, where acids, water, and a small portion of the aldehyde condensed. The uncondensed gases were passed through a gas-sampling valve, leading to a Fisher gas partitioner, containing a hexamethylphosphoramide (HMPA) column and a  $13\times$  molecular sieve column connected in series, which could determine carbon dioxide, carbon monoxide, nitrogen, oxygen, and 2-methylpropene. The off-gases from the sampling valve passed through a liquid nitrogen trap, where the remainder of the aldehydes which did not condense at ice temperature were condensed. The condensate, mixed with a known amount of diethyl ether, was injected with a syringe into a Perkin-Elmer Vapor Fractometer Model 154D, containing a Carbowax 1500 on Teflon column, which could separate several saturated and unsaturated aldehydes and water.

The pumice-supported copper oxide catalyst containing 16 weight % of copper was prepared by impregnating 20 to 40-mesh crushed pumice stone with a copper nitrate solution and drying it at  $105^\circ\text{C}$ . for 6 hours. The dried catalyst was subsequently calcined at  $600^\circ\text{C}$ . for 6 hours and placed in the reactor. The catalyst was activated by passing air over it for 12 hours before any experimental run was made.

### *Results and Discussion*

The effect of various variables was investigated: weight ratio of selenium in feed to copper in the supported catalyst ( $Z = 0.0067$  to

0.0422), oxygen (in the air)-2-methylpropene ratio in the feed ( $\bar{R} = 0.7168$  to 1.6644), and operating temperature ( $T = 350^\circ$  to  $425^\circ\text{C}.$ ), on the conversion of 2-methylpropene ( $X$ ), rates of formation of various products, carbon dioxide, water, and methacrolein ( $Y$ ), and selectivity ( $S$ ) for methacrolein.

While conversion is referred to as the moles of 2-methylpropene reacting (or consumed) per hour to the moles of 2-methylpropene fed per hour, the rate of formation is referred to as the moles of various products formed per hour per gram of the catalyst. Yield of methacrolein is defined as the ratio of moles of methacrolein produced per hour to the total moles of product formed per hour, and the selectivity for methacrolein formation is referred to as the moles of methacrolein produced per mole of 2-methylpropene reacting.

The weights of the catalyst and 2-methylpropene charged into the feed were maintained constant during the runs. A different feed composition ratio was obtained by adjusting the rate of air flow.

Figure 2 shows the effect of  $Z$  on the conversion, rates of formation, and selectivity for a  $W/F$  (reciprocal of space velocity) ratio of 1.68 and oxygen-2-methylpropene ratio,  $\bar{R}$ , of 0.7168 at  $425^\circ\text{C}.$  The conversion of 2-methylpropene increased rapidly with the increased amounts of selenium dioxide up to  $Z = 0.0067$  and then decreased slightly with further increased amounts of selenium dioxide. Though the rate of carbon dioxide formation decreased slowly in the beginning, it decreased rapidly with the increased amounts of selenium dioxide up to  $Z = 0.020$ , beyond which there was no substantial decrease in the rate with increasing amounts of selenium dioxide. The rate of water formation increased slowly with increasing amounts of selenium dioxide up to  $Z = 0.0067$ , and then decreased. The rate of methacrolein formation increased steadily with increasing amounts of selenium dioxide up to  $Z = 0.020$ , then decreased slightly.

The selectivity for methacrolein first increased rapidly with increased amounts of selenium dioxide, and then decreased. The optimal amount of selenium dioxide giving the highest selectivity was about  $Z = 0.03$  (corresponding to about 0.7% by weight of the pumice-supported catalyst) under different operating conditions.

The effect of various oxygen-2-methylpropene ratios in the feed ( $\bar{R}$ ) on the conversion, rate of formation, and selectivity for  $Z = 0.02$  at  $425^\circ\text{C}.$  is shown in Figure 3. While the conversion of 2-methylpropene and rate of formation of methacrolein increased steadily with feed ratios, the rates of formation of water and carbon dioxide increased rapidly with increasing  $\bar{R}$ . However, the selectivity decreased with increased oxygen-2-methylpropene ratios in the feed.

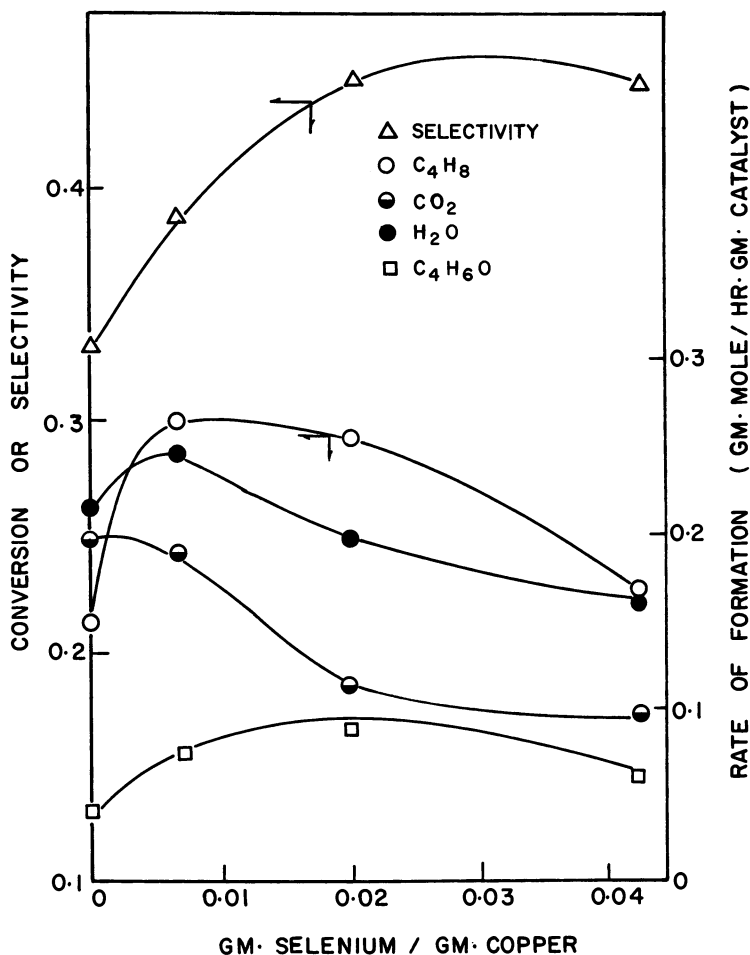


Figure 2. Effect of selenium dioxide on conversion, rate of formation, and selectivity

The effect of temperature on conversion and selectivity for  $\bar{R} = 0.9910$  and  $Z = 0.020$  is shown in Figure 4. With increase in temperature from 350° to 425°C., although the conversion increased, the selectivity remained nearly constant.

Bretton, Wan, and Dodge (3) and several other workers (19) have treated heterogeneous oxidation of hydrocarbons as a homogeneous reaction, neglecting the effect of solid catalysts. They suggest that the oxidation reaction involves a free radical mechanism (22) in which the first step is the removal of a hydrogen atom from the hydrocarbon, forming a free radical, which then can react with a molecule of oxygen

to form a peroxide radical. The radical then gains a hydrogen atom, becoming a peroxide, which later decomposes. This mechanism does not take into consideration the physical properties of the solids and the surface effects. We therefore prefer to use the electron theory of catalysis (21), and modify it accordingly to explain our results.

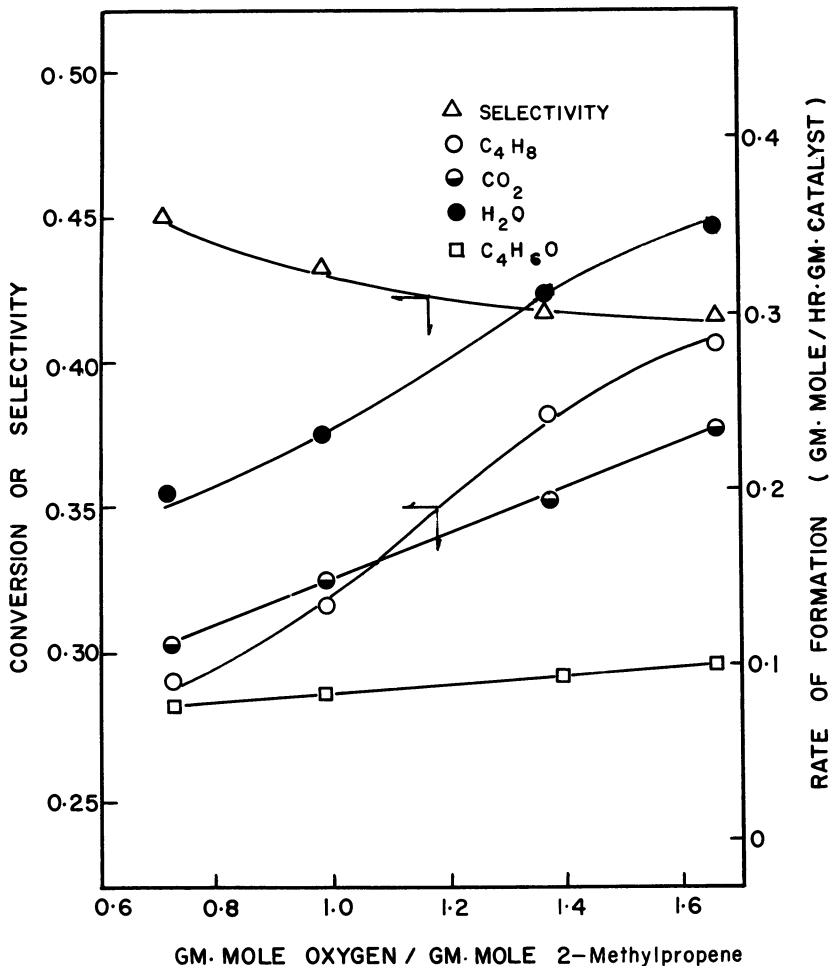


Figure 3. Effect of feed composition on conversion, rate of formation, and selectivity

We treat the free electrons or positive holes on the surface as one of the reactants or products and propose that a surface reaction between charged adsorbed particles, both reactants and products, is the essential

step, and that the heterogeneous catalytic reactions traditionally described as taking place:

- (1) diffusion (external and internal) of reactants and products.
- (2) adsorption and desorption of reactants and products (physical adsorption and weak chemisorption),
- (3) surface reaction

be modified to take place as follows:

- (1) electron transfer from or to the reactants (strong chemical band formation)
- (2) homogeneous reaction (formation of activated complex and rearrangement of the charged particles on the surface)
- (3) Electron transfer from or to the products.

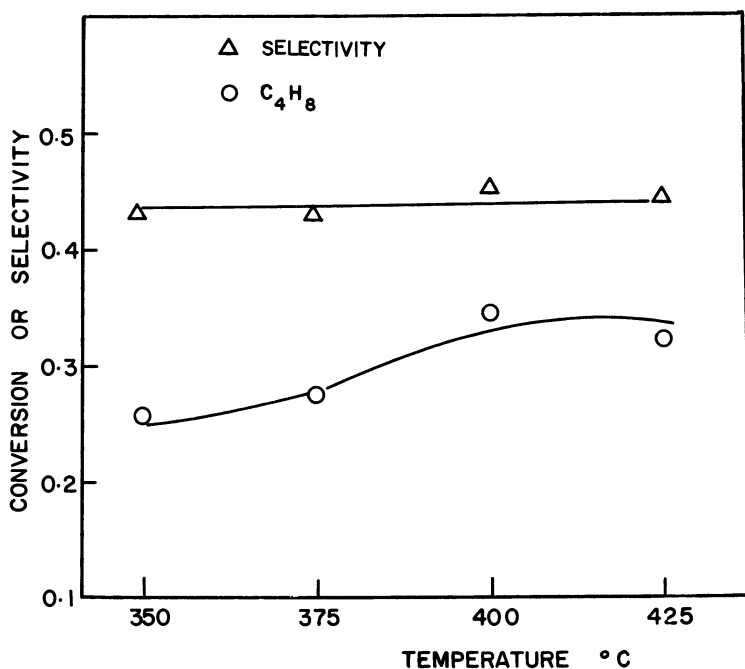
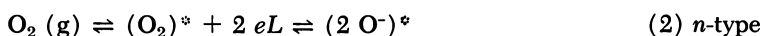
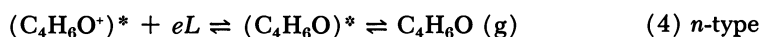
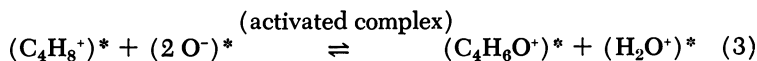


Figure 4. Effect of temperature on conversion and selectivity

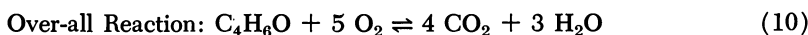
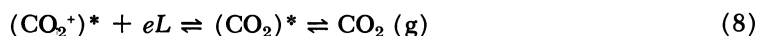
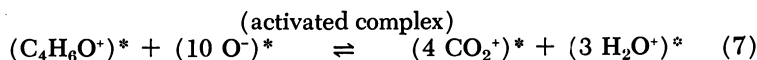
The formation of methacrolein by the partial oxidation of 2-methylpropene, based on the above modification, can be visualized to take place according to the following scheme.

Reaction I: Partial Oxidation

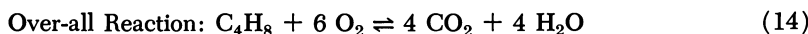
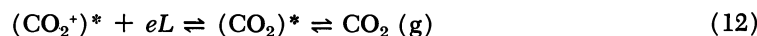
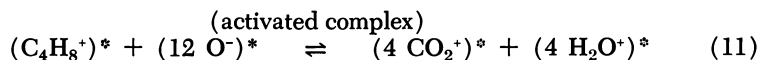




Reaction II: (Further Oxidation)



Reaction III: Complete Oxidation



Each step in the above reaction may contribute a certain resistance. The over-all rate is usually determined by the so-called rate-controlling step. The sign of electrical charge on each adsorbed particle is determined by measuring work function changes. Reactions I, II, and III can also be expressed in terms of the "power rate law" as follows:

$$r_1 = k_1 C_{C_4H_8^+}^{m_1} C_{O^-}^{n_1} - k_1' C_{C_4H_6O^+}^{m_1'} C_{H_2O^+}^{n_1'} \quad (15)$$

$$r_2 = k_2 C_{C_4H_6O^+}^{m_2} C_{O^-}^{n_2} - k_2' C_{CO_2^+}^{m_2'} C_{H_2O}^{n_2'} \quad (16)$$

$$r_3 = k_3 C_{C_4H_8^+}^{m_3} C_{O^-}^{n_3} - k_3' C_{CO_2^+}^{m_3'} C_{H_2O^+}^{n_3'} \quad (17)$$

Here the evaluation of the surface concentration of charged particles during the reaction is important for investigating the conversion and selectivity in the heterogeneous catalytic reaction. Using a treatment similar to Hauffe's (11), the concentration of charged particles on the surface can be evaluated at equilibrium as:

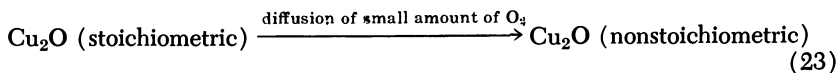
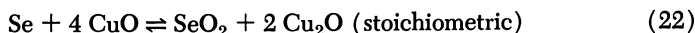
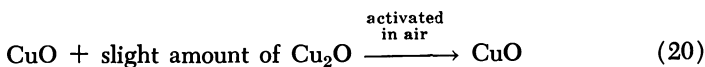
$$C_{C_4H_8^+} = K_{C_4H_8} \cdot P_{C_4H_8} \cdot \exp \left[ \frac{-2 \pi e^2}{\epsilon kT} \frac{(C_{C_4H_8^+})^2}{\eta_{(+)}^{(H)}} \right] \eta_{(+)}^{(H)} \quad (18)$$

and

$$C_{O^-} = K_{O_2} \cdot P_{O_2}^{1/2} \cdot \exp \left\{ 2 \sinh^{-1} \left[ \frac{2 \pi e^2}{\epsilon k T \eta_{(+)}^{(H)}} \frac{1}{2} \frac{C_{O^-}}{C_{O^-}} \right] \right\} \frac{1}{\eta_{(+)}^{(H)}} \quad (19)$$

The surface concentration of 2-methylpropene and oxygen ions is not a function of  $P_{C_4H_8}$  and  $P_{O_2}^{1/2}$  only but also depends on the positive hole concentration in the valence band of the bulk catalyst,  $\eta_{(+)}^{(H)}$ . An increase in the positive hole concentration  $[\eta_{(+)}^{(H)}]$  will therefore increase  $C_{C_4H_8^+}$  and decrease  $C_{O^-}$ .

Extending the definition of  $n$ -type and  $p$ -type reactions, as defined by Vol'kenshtein (21) to the electron transfer step, it would seem that the only reaction given by Equation 1 is a  $p$ -type reaction. This reaction would be accelerated by the increase in the value of free hole concentration. On the other hand, all other reactions besides the one given by Equation 1 are  $n$ -type and would be accelerated by the increase in free electron concentration. Hydrocarbon oxidation reactions catalyzed by solid oxides are accompanied by oxidation and reduction of the catalyst and the degree of the stoichiometric disturbance in the semiconductor changes. The catalytic process in the oxidation of 2-methylpropene over copper oxide catalyst in the presence of  $SeO_2$  can be visualized as:



A certain amount of selenium may be considered as an acceptor impurity to copper oxide since the Fermi level of copper oxide catalyst is lowered or its  $p$ -typeness is increased. This agrees with the observation of Margolis (16).

Mann and Rouleau (14) and Shapovalova *et al.* (18) studied the oxidation of 2-methylpropene to methacrolein in the absence of selenium dioxide, and they found that the oxidation of 2-methylpropene was a surface reaction controlling between adsorbed 2-methylpropene and weakly adsorbed oxygen. However, no theoretical explanation is given for this.

When 2-methylpropene (a donor-type gas) is adsorbed on the surface of cuprous oxide (a *p*-type semiconductor), because of the electropositive nature of 2-methylpropene, electrons from it flow to the catalyst surface, and pass through the acceptor level. Since the acceptance of these electrons is limited, an exhaustion boundary layer is formed, and the chemisorption of 2-methylpropene ceases at low coverage and far from equilibrium. On the other hand, when oxygen (an acceptor-type gas) is adsorbed on the surface, because of its electronegative nature, electrons flow from the catalyst to it and are removed from the valence band, creating free holes. Since the supply of these electrons from the valence band is great, the concentration of free holes is increased greatly, and an inundation boundary layer is formed. Chemisorption of oxygen on the surface is fast and proceeds easily, forming nearly a complete monolayer of it on the surface. The adsorption of oxygen on the surface of the catalyst is thus relatively much faster than the adsorption of 2-methylpropene on it. The adsorption of 2-methylpropene can, therefore, be considered as a next slower step than the surface reaction. Any increase in the adsorption rate of 2-methylpropene would, therefore, result in an increase in the over-all Reaction I (Equation 6). At this moment, the decrease in the available electrons in the valence band is still comparatively negligible in its effect on the concentration of holes, and the decreases in oxygen adsorption and product desorption rates are insignificant. Therefore, while 2-methylpropene conversion (Reaction I) increases rapidly at the beginning of the introduction of selenium dioxide ( $Z < 0.0067$ ), the rate of carbon dioxide formation is influenced slightly. This is in agreement with the findings of Voge *et al.* (20) and Enikeev *et al.* (5), who observed that in propylene oxidation, at temperatures higher than 350°C., carbon dioxide was mainly produced from Reaction II (Equation 10) and not from Reaction III (Equation 14).

Introducing a slightly larger amount of selenium dioxide ( $Z = 0.0067$  to 0.02) decreases the available electrons in the valence band appreciably, resulting in the slowing down of the rate of oxygen as the rate-determining step for Reaction II. The "power rate law" also indicates that the surface concentration of the charged adsorbed oxygen ion has a predominating influence on Reaction II. This results in the slowing down of the further oxidation reaction (Reaction II) much more rapidly than partial oxidation (Reaction I).

For higher amounts of selenium dioxide in the feed ( $Z > 0.02$ ), while the surface concentration of adsorbed oxygen ions gradually decreases, the surface concentration of adsorbed products becomes significant, and possibly results in the modifier's entering the catalyst lattice substitutionally, rather than interstitially,  $\text{Cu}^{2+}$ ,  $\text{Cu}^+$ , or  $\text{O}^-$  is replaced by selenium, forming a small unit of a covalent compound. Thus, both free

electrons and holes are annihilated, and active centers for 2-methylpropene and oxygen are blocked, decreasing the conversion and formation of carbon dioxide.

The rate of formation of water would increase with increased rates of conversion of 2-methylpropene and decrease with decreased rate formation. The yield of water, therefore, increased first and then decreased because of the combined effects of these two processes. On the other hand, if methacrolein is formed by Reaction I and subsequently further oxidized by Reaction II, its yield will depend on the extent of Reactions I and II, and an optimum will exist. In agreement with this, it was found that the optimal amount of selenium dioxide giving the highest selectivity under operating conditions was about 0.7% by weight of the catalyst.

The effect of the oxygen–2-methylpropene ratio,  $\bar{R}$ , on conversion, rate of formation and selectivity can be visualized easily from the fact that at a constant rate of 2-methylpropene flow, an increase in oxygen–2-methylpropene ratio would mean an increase in the partial pressure of oxygen ( $P_{O_2}$ ) or 2-methylpropene in the surface concentration of adsorbed oxygen ion ( $C_{O^-}$ ). Increased surface concentration of adsorbed oxygen ions would have a predominant influence on the course of the reaction, increasing the conversion and rates of formation and decreasing the selectivity with increased oxygen–2-methylpropene ratios in the feed.

### Nomenclature

- $C$  = surface concentration of charged adsorbed particles per sq. cm.  
 $e$  = unit electrical charge  
 $\epsilon$  = dielectric constant  
 $k$  = rate constant, forward reaction  
 $k'$  = rate constant, reverse reaction  
 $K_{(H)}$  = adsorption constant  
 $\eta_{(+)}$  = concentration of free holes in the bulk of catalyst/cc.  
 $m$  = reaction order  
 $n$  = reaction order  
 $p$  = partial pressure  
 $r$  = reaction rate, gram moles/hr. gram catalyst  
 $R$  = feed composition ratio (oxygen–2-methylpropene)  
 $S$  = selectivity  
 $T$  = absolute temperature  
 $W/F$  = reciprocal of space velocity  
 $X$  = percentage conversion of 2-methylpropene  
 $Y$  = rate of formation of products, g. moles/hr. g. catalyst  
 $Z$  = weight ratio of selenium in feed to copper in supported catalyst  
 $eL$  = free electrons  
 $pL$  = holes  
 $\psi$  = yield

### Acknowledgment

The authors are indebted to the Selenium-Tellurium Development Association, New York, for financial support of the project, and a fellowship to one of the authors (K. C. Y.).

### Literature Cited

- (1) Barclay, J. L., Bethell, J. R., Bream, J. M., Hadley, D. J., Jenkins, R. H., Stewart, D. G., Wood, B. W., British Patent **864,666** (April 6, 1961).
- (2) Barclay, J. L., Hadley, D. J., Stewart, D. G., British Patent **873,712** (July 26, 1961).
- (3) Bretton, R. H., Wan, S. U., Dodge, B. F., *Ind. Eng. Chem.* **44**, 594 (1952).
- (4) Dowden, D. A., Caldwell, A. M. U., British Patent **828,812** (Feb. 24, 1960).
- (5) Enikeev, É. Kh., Isaev, O. V., Margolis, L. Ya, *Kinetika i Kataliz* **1**, 431 (1960).
- (6) Farbenfabriken Bayer, A. G., British Patent **839,808** (June 29, 1960).
- (7) Hadley D. J., British Patent **694,354** (July 22, 1953).
- (8) *Ibid.* **727,318** (March 30, 1955).
- (9) Hadley, D. J., U. S. Patent **2,716,665** (Aug. 30, 1955).
- (10) *Ibid.* **2,810,763** (Oct. 22, 1957).
- (11) Hauffe, K., *Advan. Catalysis* **7**, 213 (1955).
- (12) Kominami, N., Shibata, A., Minekawa, S., *Kogyo Kagaku Zasshi* **65**, 1510 (1962).
- (13) Kruzhalov, B. D., Shestukhin, E. S., Garnish, A. M. *Kinetika i Kataliz* **3**, 247 (1962).
- (14) Mann, R. S., Rouleau, D., *ADVAN. CHEM. SER.* **51**, 40 (1965).
- (15) Mann, R. S., Rouleau, D., *Ind. Eng. Chem. Prod. Res. Develop.* **3**, 94 (1964).
- (16) Margolis, L. Ya, Enikeev, E. Kh., Isaev, O. V., Krijlova, A. V., *Kinetika i Kataliz* **3**, 181 (1962).
- (17) Montecatini, British Patent **847,564** (June 29, 1960).
- (18) Shapovalova, L. P., Gorokrovastiski, Ya B., Rufanik, M. Ya, *Kinetika i Kataliz* **5**, 330 (1964).
- (19) Tipper, C. F. H., "Oxidation and Combustion Reviews," Vol. 1, p. 225, Elsevier, New York, 1965.
- (20) Voge, H. H., Wagner, C. D., Stevenson, D. P., *J. Catalysis* **2**, 58, (1963).
- (21) Vol'kenshtein, F. F., "Electron Theory of Catalysis on Semiconductors," Macmillan, New York, 1963.
- (22) Waters, W. A., *Trans. Faraday Soc.* **42**, 184 (1946).

RECEIVED October 16, 1967.

# The Kinetics of Ammoxidation of Xylenes over Vanadium Catalysts

MASATOMO ITO, KENICHI SANO, and MICHITOSHI KITABATAKE

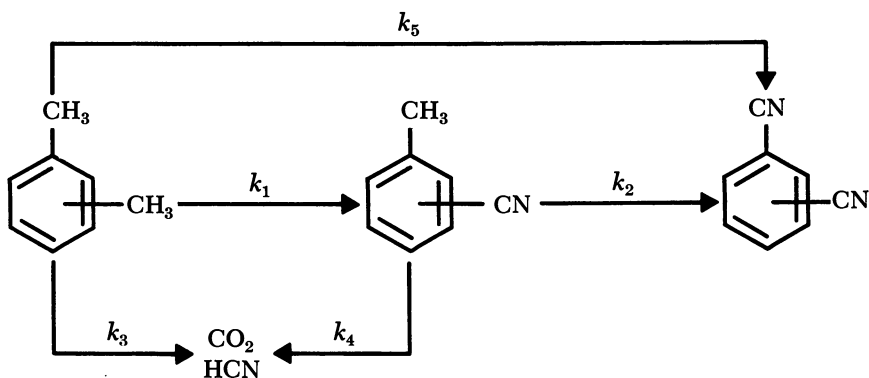
The Central Research Laboratory, Showa Denko Co., Ltd., Haramachi, Ohta-ku, Tokyo, Japan

*The kinetics of the ammoxidation of xylenes over a vanadium catalyst and mixed vanadium catalysts were studied. The reaction rate data obtained were correlated with the parallel consecutive reaction scheme by the rate equations based upon the Langmuir-Hinshelwood mechanism where the adsorption of xylenes was strong. The reaction rates of each path are remarkably affected by the kind of xylene and catalyst. The results of the physical measurement of catalysts indicated that the activity and the selectivity of reaction were affected by the nature and the distribution of metal ions and oxygen ion on catalyst surface.*

Recently, the kinetics of the ammoxidation of *m*-xylene (1) and xylene isomers (2) over vanadium catalyst, and of *m*-xylene over mixed vanadium catalysts (3) were reported. This paper summarizes the results concerning the specific rate constants for each reaction path obtained in the above studies and adds some data on physical properties of each catalyst.

## *Kinetic Studies*

The data on the rate of reaction of *o*-, *m*-, and *p*-xylene over vanadium oxide catalyst and of *m*-xylene over mixed vanadium oxide catalysts (chromium–vanadium and antimony–vanadium) were correlated with the reaction scheme below by the following rate expressions, which are based on the Langmuir-Hinshelwood mechanisms where the adsorption of *m*-xylene is strong.



where:

$$\begin{aligned} r_X &= k_X \\ r_M &= k_1 - k_M P_M / P_X \\ r_D &= k_5 + k_2 P_M / P_X \\ r_B &= k_3 + k_4 P_M / P_X \end{aligned}$$

The symbol  $r_X$  is the reaction rate of xylene,  $r_M$ ,  $r_D$ , and  $r_B$  are the formation rates of *m*-tolunitrile, dicyanobenzene, and other products ( $\text{CO}_2$ , HCN), respectively.  $P_M$  and  $P_X$  are the partial pressures of *m*-tolunitrile and xylene, respectively. The symbols  $k_X$ ,  $k_M$ ,  $k_1$ ,  $k_2$ ,  $k_3$ ,  $k_4$ , and  $k_5$  are the specific rate constants of the reaction paths of xylene, *m*-tolunitrile, respectively. The values of the specific rate constants for each reaction path are listed in Table I.

**Table I. Specific Rate Constants for Reactions of Xylenes over Vanadium Catalysts**

Xylene	Catalyst	Temperature °C.	Rate Constants					
			$k_X/k_M$	$k_1/k_X$	$k_3/k_X$	$k_5/k_X$	$k_2/k_M$	$k_4/k_M$
<i>m</i> -Xylene	V	420	4	0.55	0.20	0.25	0.81	0.19
<i>m</i> -Xylene	V	400	6	0.59	0.16	0.24	0.74	0.26
<i>o</i> -Xylene	V	400	4	0.56	0.12	0.32	0.77	0.23
<i>p</i> -Xylene	V	400	6	0.79	0.08	0.12	0.87	0.13
<i>p</i> -Xylene	V	380	8	0.80	0.06	0.11	0.84	0.16
<i>m</i> -Xylene	Cr-V	400	2	0.61	0.11	0.29	0.82	0.18
<i>m</i> -Xylene	Sb-V	400	1.2	0.72	0.08	0.20	0.83	0.17

When the vanadium oxide catalyst is used,  $k_M$  is much smaller than  $k_X$ , while the specific rate constant of the reaction of *m*-tolunitrile in the absence of xylene is larger than that of xylene. This seems to be caused by a strong adsorption of xylene on the catalyst surface.

The great variations in the reaction kinetics using a vanadium oxide catalyst for each xylene are shown by the relative ratios for the direct

formation of dicyanobenzenes from xylenes and for the formation of tolunitriles from xylenes—*i.e.*,  $k_5/k_X$  and  $k_1/k_X$ . The order  $k_5$  to  $k_X$ , for the direct formation of dicyanobenzenes, is ortho > meta > para.

Taking into account the steric effect, these results suggest that the adsorption of xylene on the catalyst surface occurs mainly by methyl groups. The ratio  $k_5/k_X$  therefore indicates the degree to which the two methyl groups of xylene adsorb simultaneously on the catalyst surface.

When a chromium–vanadium oxide and an antimony–vanadium oxide catalyst were used, the atomic ratio of chromium or antimony to vanadium was unity.

The ratios of  $k_X$  to  $k_M$  for both mixed vanadium catalysts were much smaller than that for a vanadium catalyst, while the selectivities for the formation of isophthalonitrile from *m*-tolunitrile,  $k_2/k_M$ , for mixed vanadium catalysts were higher than that for a vanadium catalyst.

In the absence of *m*-xylene, a higher selectivity for the formation of isophthalonitrile from *m*-tolunitrile was obtained for all catalysts. These results suggest that  $k_2/k_M$  decreases with a depression of the reaction rate of *m*-tolunitrile by *m*-xylene.

The relative ratios for the formation of *m*-tolunitrile from *m*-xylene,  $k_1/k_X$  was nearly the same for both a vanadium and a chromium–vanadium catalyst, but it was higher for an antimony–vanadium catalyst. The increase of  $k_1/k_X$ , which indicates an increase of the degree of single methyl group adsorption for *m*-xylene, seems to be ascribable to the strength of adsorption and the surface structure of an antimony–vanadium catalyst.

### *Physical Properties of Catalysts*

The fresh catalysts used for the ammoxidation of xylenes consisted essentially of  $V_2O_5$ ,  $SbVO_4$ , and  $\alpha$ -phase for a vanadium catalyst respectively. X-ray diffraction patterns for the catalysts showed that a vanadium catalyst consisted essentially of  $V_2O_4$ , while mixed catalysts retained the original composition even after prolonged use.

The infrared absorption spectrum of  $SbVO_4$  showed only weak absorption in the range 700–1200  $cm^{-1}$ .  $SbVO_4$  also gave a single broad ESR absorption spectrum with a *g* value of 1.98 and was difficult to reduce with ammonia at 400°C. This suggests that the nature of vanadium ion in  $SbVO_4$  is similar to that in  $V_2O_4$ .

The  $\alpha$ -phase in a chromium–vanadium system was quite different from  $CrVO_4$  with respect to the x-ray diffraction pattern, ESR absorption spectrum, and infrared absorption spectrum and could be reduced with ammonia at 400°C., thus differing from  $CrVO_4$ . Taking into account the infrared absorption spectra of a chromium–vanadium system, the

$\alpha$ -phase seems to have a transitional structure with the polyanion of  $\text{VO}_3^-$  and is reduced partially under reaction condition.

On the other hand, a catalyst in which the  $\text{CrVO}_4$  was one of major constituents had little catalytic activity for the ammoxidation of xylene. These observations indicate that the nature and the distribution of metal ions and oxygen ion on the catalyst surface affect the catalytic activity and selectivity. It is difficult to predict the relationship between the adsorptivity of reactants and the physical properties of catalyst, but it may be assumed that adding more electronegative metal ions affects the electronic properties of the vanadium ion, which functions as an adsorption center. Further details on the physical properties of catalysts for the ammoxidation of xylenes will be reported later.

### ***Acknowledgment***

The authors are grateful to Taijiro Oga, Hideo Ichinokawa, Hazime Tanaka, and Akira Matsumoto for their valuable discussions.

### ***Literature Cited***

- (1) Ito, M., Sano, K., *Bull. Chem. Soc. Japan* **40**, 1307 (1967).
- (2) *Ibid.*, p. 1315.
- (3) *Ibid.*, p. 1321.

RECEIVED October 16, 1967.

## Mechanisms of the Room Temperature Oxidation of Carbon Monoxide on Nickel Oxide

G. EL SHOBAKY, P. C. GRAVELLE, and S. J. TEICHNER

Université de Lyon, Institut de Recherches sur la Catalyse, Villeurbanne, France

*Nickel oxide, prepared by dehydration of nickel hydroxide under vacuum at 250°C. [NiO(250)], presents a greater activity in the room-temperature oxidation of carbon monoxide than nickel oxide prepared according to the same procedure at 200°C. [NiO(200)], although the electrical properties of both oxides are identical. The reaction mechanism was investigated by a microcalorimetric technique. On NiO(200) the slowest step of the mechanism is  $\text{CO}^-_{\text{(ads)}} + \text{CO}_{\text{(ads)}} + \text{Ni}^{3+} \rightarrow 2 \text{CO}_2(\text{g}) + \text{Ni}^{2+}$ , whereas on NiO(250) the rate-determining step is  $\text{O}^-_{\text{(ads)}} + \text{CO}_{\text{(ads)}} + \text{Ni}^{3+} \rightarrow \text{CO}_2(\text{g}) + \text{Ni}^{2+}$ . These reaction mechanisms on NiO(200) and NiO(250), which explain the differences in catalytic activity, are correlated with local surface defects whose nature and concentration vary with the nature of the catalyst.*

The oxidation of carbon monoxide on nickel oxide has often been investigated (4, 6, 8, 9, 11, 16, 17, 21, 22, 26, 27, 29, 32, 33, 36) with attempts to correlate the changes in the apparent activation energy with the modification of the electronic structure of the catalyst. Published results are not in agreement (6, 11, 21, 22, 26, 27, 32, 33). Some discrepancies would be caused by the different temperature ranges used (27). However, the preparation and the pretreatments of nickel oxide were, in many cases, different, and consequently the surface structure of the catalysts—*i.e.*, their composition and the nature and concentration of surface defects—were probably different. Therefore, an explanation of the disagreement may be that the surface structure of the semiconducting catalyst (and not only its surface or bulk electronic properties) influences its activity.

The catalytic activity of a given catalyst towards a given reaction combines two aspects, chemical and physical. The chemical aspect is related to the energy spectrum of species chemisorbed on a surface and involved in the reaction. The position of the energy levels of these species is determined primarily by the chemical nature of these species and the chemical nature of the surface.

For a given molecule on the catalyst surface, which is most often nonhomogeneous, the position of the energy levels depends on the nature of the adsorption centers: ions or lattice defects of thermal origin or resulting from the previous history of the catalyst.

Therefore, molecules of the same kind, chemisorbed on a nonhomogeneous surface, bring forth a spectrum of local levels of various nature and energy.

The physical aspect of the catalytic activity of a semiconducting oxide is related to the position of the Fermi level, which depends on the state of the system as a whole and is a collective property.

The Fermi level would remain the controlling factor in catalysis only as long as the local levels of the chemisorbed species involved in the reaction remain fixed. This means that the energy spectrum of the surface is defined and remains unchanged for a series of catalysts with different Fermi levels. The purpose of this paper is to show that in a comparison between two nickel oxide catalysts which differ in the energy spectrum of their surfaces, the Fermi level ceases to characterize the activity. In other words, the energy spectrum of the surface becomes the determining factor in catalytic activity. This is because after different treatments of the NiO catalyst, which are explained in detail, the energy of interaction with the solid of chemisorbed species varies greatly, whereas the Fermi level may or may not vary.

The influence of the surface structure upon the catalytic activity is likely to be particularly important in the case of finely divided nickel oxides, prepared at a moderate temperature, which present catalytic activity for this reaction at room temperature. In a previous work, we studied the room-temperature oxidation of carbon monoxide on nickel oxide prepared by dehydration of the hydroxide under vacuum ( $p = 10^{-6}$  torr) at 200°C., by means of a microcalorimetric technique (8, 20). The object of this work is to re-investigate, by the same method, the mechanism of the same reaction on a nickel oxide prepared at 250°C. [NiO(250)] instead of 200°C. [NiO(200)].

### *Experimental*

**Materials.** The nickel oxide was prepared by decomposition of a very pure nickel hydroxide (25) *in vacuo* ( $p = 10^{-6}$  torr) at 250°C. (24,

35). Composition, stoichiometry, electrical conductivity, apparent energy of activation of conductivity, surface area, and color of the oxide are presented in Table I together with the values for the oxide prepared at 200°C., according to the same procedure.

NiO(200) presents a small excess of oxygen, whereas NiO(250) contains metallic nickel (Table I). Magnetic measurements (15) have confirmed the chemical analysis (19). However, both oxides are *p*-type semiconductors, as shown by the Seebeck effect measurements. In the case of NiO(250), this result means that, although there is a total excess of nickel, the oxide phase still contains a small excess of oxygen (13). The electrical properties of both oxides are identical.

**Table I. Properties of Catalysts**

<i>Property</i>	<i>NiO(200)</i>	<i>NiO(250)</i>
Composition	NiO, 0.155 H <sub>2</sub> O (15)	NiO, 0.11 H <sub>2</sub> O (15)
Stoichiometry	0.016 at O <sub>exc.</sub> % NiO (19)	0.033 at Ni % NiO (19)
Electrical conductivity in vacuo, (ohm cm.) <sup>-1</sup>		
24°C.	10 <sup>-13</sup>	10 <sup>-13</sup>
200°C.	1.6 × 10 <sup>-10</sup>	2 × 10 <sup>-10</sup>
Apparent energy of activation of conductivity, kcal./mole	24	24
Surface area, sq. meters/gram	142 ± 7	156 ± 7
Color	Yellow-green	Yellow

**Methods.** The differential heats of adsorption of reagents and the differential heat of their interaction on the nickel oxide surface were measured in a Calvet microcalorimeter with a precision of 2 kcal. per mole. The apparatus has been described (18). For each adsorption of a single gas, small doses of gas are allowed to interact with a fresh nickel oxide sample (100 to 200 mg.) placed in the calorimeter cell maintained at 30°C. At the end of the adsorption of the last dose, the equilibrium pressure is, in all cases, 2 torr. Duplication of any adsorption experiment on a new sample gives the same results within 2 kcal. per mole of heat evolved and 0.02 cc. of gas adsorbed per gram. Electrical conductivities of the nickel oxide sample are measured in an electrical conductivity cell with platinum electrodes (1) by a d.c. bridge.

### **Results and Discussion**

**Adsorption of Reagents and Product of Reaction.** CHEMISORPTION OF OXYGEN. During the adsorption of the first doses of oxygen on NiO(250), the equilibrium pressure being of the order of 10<sup>-3</sup> torr, the

color of the oxide changes from yellow to black. At the same time, the electrical conductivity of the sample increases, and at the end of the adsorption (2 torr), reaches a value of  $1.8 \times 10^{-5}$  (ohm cm.)<sup>-1</sup>. This value does not change when the oxide, after the adsorption, is evacuated at 30°C. The same results were obtained for NiO(200) (23). Therefore, irreversible adsorption of oxygen produces ionic species on both oxides, the most probable structure for these ions being  $O^-_{(ads)}$  (14, 20, 23, 37). There is also, on both oxides, a reversible adsorption of oxygen which does not influence the electrical conductivity of the sample and which can be attributed to oxygen in a molecular form (23). Therefore, there is a close similarity between the processes of oxygen adsorption on both oxides. However, calorimetric measurements show that the reactivity of both surfaces, towards oxygen, is not identical. On NiO(250) the heat of adsorption of oxygen decreases rapidly with coverage (Figure 1). This has not been observed for NiO(200) (20), for which the initial heat of 60 kcal per mole (Figure 1) decreases to 10 kcal. per mole only at the end of the adsorption experiments. The NiO(250) surface presents active sites since the initial heat of adsorption is 80 kcal. per mole. These sites do not exist on NiO(200). Finally, NiO(250) chemisorbs less oxygen than NiO(200).

When nickel oxide is prepared under vacuum at 250°C., a small reduction of the solids occurs, giving some metallic nickel. It has been shown (35) and confirmed recently, that this reduction is not caused by grease vapors or adsorbed organic materials. The reduction is probably limited to the surface of NiO and is a consequence of the poor state of organization of the surface layers of the divided oxide, resulting from the low temperature of its preparation. The first step of the reduction is the departure of oxygen which leaves ionized vacancies in the surface lattice layers. Electrons from the vacancies are then trapped by nickel ions, and nickel atoms migrate and form nickel crystallites (13). Magnetic measurements (15) have shown that this metallic nickel (Table I) which exists in nickel oxide is not oxidized at 30°C.

The active sites for the oxygen adsorption, which are found on the surface of NiO(250) but not of NiO(200), are to be identified with anionic vacancies because this high heat of adsorption is not caused by the sorption of oxygen on the nickel phase (13). The decrease in the capacity for adsorption of oxygen at 30°C. when the temperature of oxide preparation is increased from 200° to 250°C. is explained by the reduction of surface nickel ions, sites for the adsorption only of oxygen, and the formation of nickel crystallites whose surface atoms may be active towards the adsorption of oxygen at 30°C. Recession of nickel ions below the surface for NiO(250) may also contribute to this decrease.

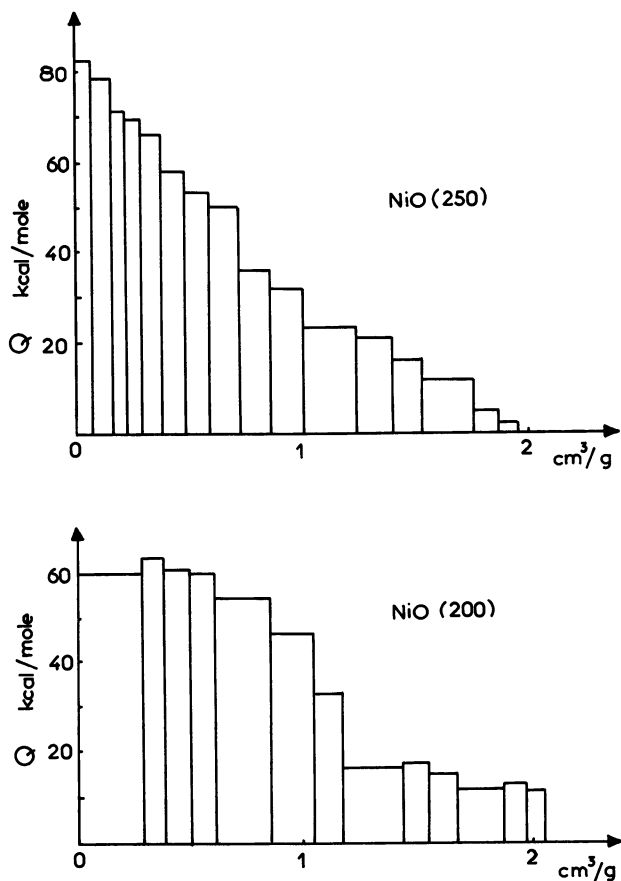


Figure 1. Adsorption of oxygen on NiO(250) and NiO(200)

**CHEMISORPTION OF CARBON MONOXIDE.** Chemisorption of carbon monoxide on NiO(250) does not change the electrical conductivity of the sample. The same result was obtained for NiO(200) (23). The curve of differential heats of adsorption of carbon monoxide on NiO(250) presents many similarities with the curve recorded in the case of NiO(200) (20). However, a few differences are noted. The heat of adsorption of the first dose (0.08 cc. per gram) of carbon monoxide on NiO(200) is high (42 kcal. per mole) (Table II). The adsorption of the next dose on the same oxide releases only 29 kcal. per mole. The initial high value of the heat adsorption was explained by the interaction of CO with excess surface oxygen (Table I), giving  $\text{CO}_{2(\text{ads})}$  (14). In the case of NiO(250), the initial heat of adsorption amounts to 29 kcal. per mole (Table II). It seems, therefore, that the surface excess oxygen

which reacts with CO in the case of NiO(200) does not exist on the surface of NiO(250). This oxygen cannot be identified with lattice anions, which do not react with CO at 30°C. to form CO<sub>2</sub>, but with strongly adsorbed species (14). It is probable that during oxide preparation under vacuum at 250°C., this excess oxygen is desorbed from the oxide surface.

**Table II. Heats of Adsorption of O<sub>2</sub>, CO, and CO<sub>2</sub> on Catalysts**

Gas	NiO(200)	NiO(250)
<b>Oxygen</b>		
Initial heat of adsorption, kcal./mole	60	80
Amount adsorbed at 2 torr, cc./gram	2.03	1.9
<b>Carbon monoxide</b>		
Initial heat of adsorption, kcal./mole	42 - 29	29
Amount adsorbed at 2 torr, cc./gram	4.5	5.5
<b>Carbon dioxide</b>		
Initial heat of adsorption, kcal./mole	46 - 31	29
Amount adsorbed at 2 torr, cc./gram	9.4	9.7

With the exception of the high initial heat of adsorption of CO on NiO(200), the differential heats of adsorption as a function of the amount of CO adsorbed are similar for both catalysts. Metallic nickel which exists in the sample prepared at 250°C. may chemisorb carbon monoxide (15). However, the metal content is small and cannot account for the heat released in these experiments on NiO(250), since the heat of chemisorption of CO on metallic nickel is still higher (42 kcal. per mole) than the heat registered during adsorption of the first dose (29 kcal. per mole).

**CHEMISORPTION OF CARBON DIOXIDE.** The curve of differential heats of adsorption of carbon dioxide on NiO(250) is similar to the curve which was obtained for the same adsorption on NiO(200) (20). The adsorbed amounts are almost identical (Table II), and the decrease in the heat of adsorption with coverage is the same for both oxides. Carbon dioxide is adsorbed at 30°C., on both oxides, in larger amounts than oxygen or carbon monoxide. It is therefore probable that the small differences which appear in the stoichiometry and the structure of the oxides when the temperature of their preparation is different do not have much influence on the fairly large number of adsorption sites for CO<sub>2</sub> which exist on both surfaces. However, the high heat, which is measured for the adsorption of the first dose of CO<sub>2</sub> on NiO(200) (Table II) (46 kcal. per mole) and which has been explained by the interaction between CO<sub>2</sub> and the surface excess oxygen giving CO<sub>3</sub><sup>-</sup><sub>(ads)</sub> ions (20), is not produced in the case of NiO(250). This difference, previously noted in the case of the adsorption of CO (Table II), is again explained by the departure of

surface excess oxygen when the temperature of NiO preparation is higher (250°C.). Nickel hydroxide does not adsorb the gases used in this work. Adsorption of a gas on a partially dehydrated nickel hydroxide is reduced proportionally to the water content in comparison with the amount adsorbed on a final sample of NiO(250). Therefore, no hydroxyl groups remaining on the surface seem to be involved in the chemisorption process.

As for NiO(200), the adsorption of CO<sub>2</sub> does not change the electrical conductivity of the sample. On both oxides, the adsorption of carbon dioxide is mostly irreversible.

**Interactions between Reagents on Oxide Surface.** When the catalyst is exposed to a reaction mixture, the adsorbed species formed may react between themselves and with the molecules from the gas phase. Any combination of interactions may represent possible steps of the mechanism of the reaction. In order to isolate elementary steps, the reagents are adsorbed in successive sequences (20, 23, 35). The amount of heat evolved for each sequence gives evidence of a specific interaction if different possible thermochemical equations are compared with the thermochemical data for the homogeneous reaction.

**SEQUENCE I: CO—O<sub>2</sub>—CO.** Nickel oxide, covered with carbon monoxide and placed at 30°C. under vacuum (amount of irreversibly adsorbed CO, 4.5 cc. per gram) is exposed in the calorimeter to gaseous oxygen. The differential heat registered as a function of coverage by oxygen is shown in Figure 2A. It is much higher than on pure NiO(250) (Figure 1). This gives evidence of an interaction between CO<sub>(ads)</sub> and oxygen. During the adsorption of oxygen, the electrical conductivity of the sample increases from  $\sim 10^{-13}$  to  $1.6 \times 10^{-7}$  (ohm cm.)<sup>-1</sup>. Therefore, ionic species are formed on the surface of the catalyst. These species cannot be identified with O<sup>-</sup><sub>(ads)</sub> because of their high heat of formation [120 kcal. per mole compared with 80 kcal. per mole for the adsorption of oxygen on pure NiO(250) (Table II)]. The stoichiometry of the interaction, determined by comparing the amounts of each adsorbed gas, indicates that one oxygen molecule is adsorbed for almost every pre-adsorbed CO molecule. Therefore, as for NiO(200) (34, 35), CO<sub>3</sub><sup>-</sup><sub>(ads)</sub> ions are formed by interaction of oxygen with carbon monoxide pre-adsorbed on NiO(250):



After the adsorption of oxygen, the sample is replaced under vacuum at 30°C. No desorption occurs, and no thermal effect is registered. Carbon monoxide may be adsorbed again, and its adsorption is followed by a decrease of the electrical conductivity of the sample from  $1.6 \times 10^{-7}$  to  $1.6 \times 10^{-10}$  (ohm cm.)<sup>-1</sup>. The differential heats measured during the

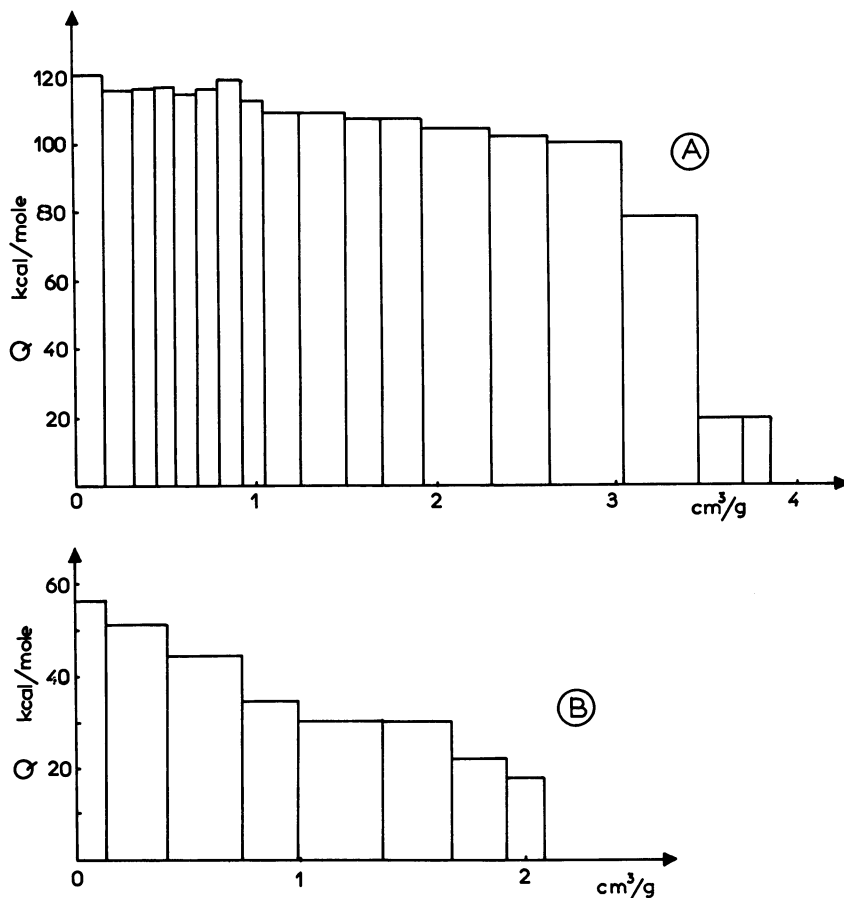
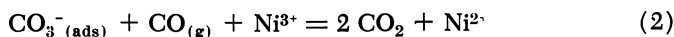


Figure 2. Differential heats

A: Adsorption of oxygen on  $\text{NiO}(250)$  containing preadsorbed carbon monoxide

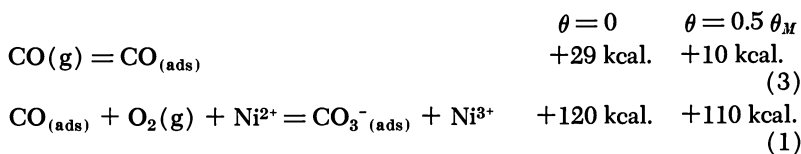
B: Adsorption of carbon monoxide on  $\text{NiO}(250)$  containing preadsorbed carbon monoxide and oxygen

second adsorption of carbon monoxide are reported in Figure 2B. They differ from the heats measured for the adsorption of CO on the pure  $\text{NiO}(250)$  (Table II). This must result from the interaction of carbon monoxide with preadsorbed species, and since this interaction decreases the electrical conductivity of the sample, it may be written as:

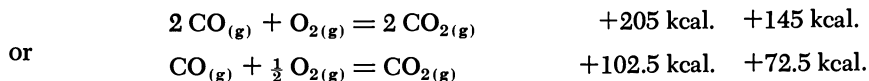
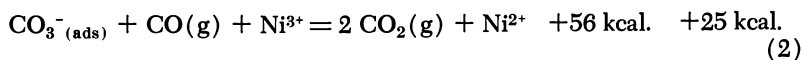


Direct evidence of this interaction is that carbon dioxide is condensed, at the end of sequence I, in the cold trap placed in the vicinity of the sample.

The following thermochemical cycle is in partial agreement with this result.

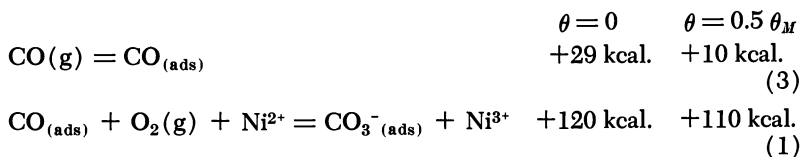


In the first hypothesis, it is assumed that  $\text{CO}_2$  is desorbed to the gas phase:

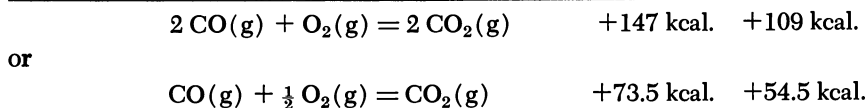
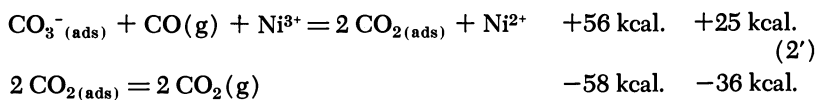


The heat of the homogeneous reaction being 68 kcal. per mole  $\text{CO}_2$  (31), the thermochemical cycle is balanced only for coverages ( $\theta$ ) of the oxide surface exceeding 50% of the initial coverage by CO ( $\theta_M$ ).

For CO and  $\text{CO}_2$  the coverage  $\theta = 1$  is obtained for an adsorption of 63 cc. of gas per gram of catalyst and for a half of this amount in the case of oxygen (34). According to the calorimetric data, carbon dioxide is therefore desorbed to the gas phase when the coverage of the surface by the reacting adsorbed species is high and when, consequently, their heat of formation and/or interaction is low. For low surface coverage ( $\theta = 0$ ), the following thermochemical cycle shows that the interaction between  $\text{CO}_3^-(\text{ads})$  and  $\text{CO}_{(\text{g})}$  yields carbon dioxide which remains adsorbed on the surface. The cycle is not balanced for high surface coverages.

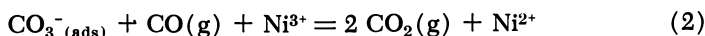
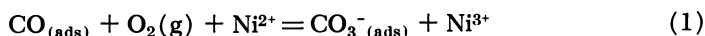


In the second hypothesis,  $\text{CO}_2$  remains adsorbed:

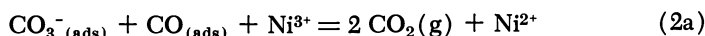


From the calorimetric study of the first sequence of adsorptions, it is possible to propose a mechanism (I) for the catalytic oxidation of carbon monoxide on NiO(250).

#### Mechanism I.



Calorimetric measurements do not allow discrimination between an interaction involving one adsorbed species and a gas or two adsorbed species. Step 2, for instance, may be written also:



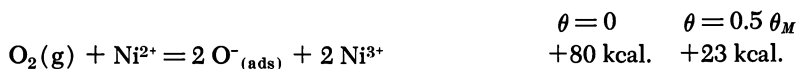
The calorimetric data show besides that a fraction of carbon dioxide remains adsorbed on the most active sites of the oxide. The reaction should be self-inhibiting. Finally, during the second adsorption of carbon monoxide, the electrical conductivity of the sample does not decrease to its low initial value. Ionic species, probably  $\text{CO}_3^-(\text{ads})$  ions, remain on the surface. The same conclusion is suggested by comparing Figure 2A and 2B. It appears that the quantity of CO which is adsorbed during the second adsorption of this gas (2 cc. per gram) is not large enough to transform all  $\text{CO}_3^-(\text{ads})$  ions (3.5 cc. per gram) into gaseous and adsorbed carbon dioxide. The nonreactivity of one fraction of  $\text{CO}_3^-(\text{ads})$  ions is not explained by calorimetric data but is related to the equilibrium of Reaction 2 or 2'. The transformation of  $\text{CO}_3^-(\text{ads})$  would be increased for an increased pressure of CO (30).

The same reaction mechanism (I) has been proposed for NiO(200) (8, 20). On this catalyst also a fraction of  $\text{CO}_3^-(\text{ions})$  does not react with carbon monoxide to form carbon dioxide. However, for NiO(200), the reason for the nonreactivity of some  $\text{CO}_3^-(\text{ads})$  ions has been deduced from the calorimetric measurements (8, 20).

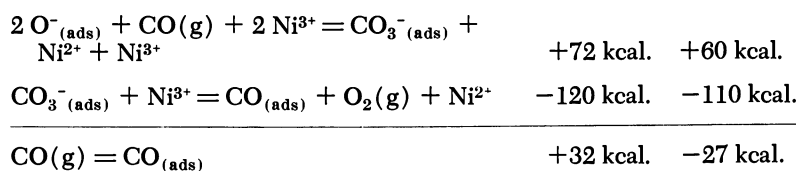
SEQUENCE II:  $\text{O}_2$ —CO. Oxygen is first adsorbed on NiO(250) at 30°C. The sample is then evacuated at 30°C. (amount of irreversibly adsorbed oxygen, 1.9 cc. per gram), and carbon monoxide is adsorbed at the same temperature (Figure 3). The electrical conductivity of nickel oxide containing preadsorbed oxygen  $1.8 \times 10^{-5}$  (ohm cm.)<sup>-1</sup> decreases during the adsorption of CO, and at the end of the adsorption, is identical to the conductivity of the pure oxide. Moreover, carbon dioxide is condensed in the cold trap. This shows that all ionized species are transformed into neutral species at the end of the interaction.

The possibility of the intermediate formation of  $\text{CO}_3^-$  (ads) ions and, finally, of  $\text{CO}_2$ (g) or  $\text{CO}_2$ (ads) may be examined by the use of the following thermochemical cycles:

Cycle 1, Formation of  $\text{CO}_3^-$  (ads)



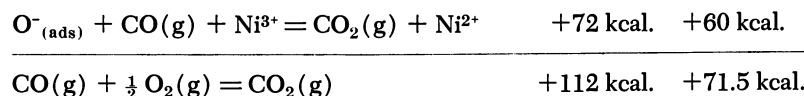
Hypothesis:



Cycle 2. Formation of  $\text{CO}_2$ (g)



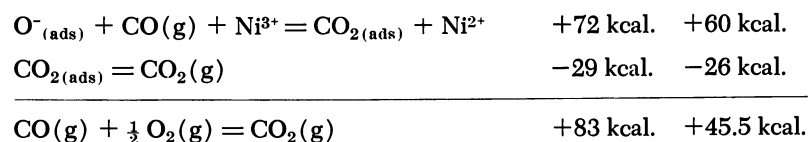
Hypothesis:



Cycle 3. Formation of  $\text{CO}_2$ (ads)



Hypothesis:



When the surface coverage is low ( $\theta = 0$ ), the formation of  $\text{CO}_3^-$  (ads) ions is possible, the heat of adsorption of carbon monoxide deduced from the cycle (32 kcal. per mole) being close to the value given by a direct experiment (29 kcal. per mole) (Table II). Moreover, this is the only possibility since Cycles 2 and 3 are not balanced for  $\theta = 0$ . Cycle 2, for gaseous  $\text{CO}_2$ , is balanced when the surface coverage is about half the maximum coverage by the oxygen, and this is the only cycle to be balanced for high surface coverages. Therefore, the formation of  $\text{CO}_2$ (g), from the interaction between adsorbed oxygen and carbon monoxide, is probable for high surface coverages, and indeed  $\text{CO}_2$  is found in the cold trap. Finally, Cycle 3, for adsorbed  $\text{CO}_2$ , is balanced for neither  $\theta =$

$0$  nor  $\theta = 0.5 \theta_M$ . However, Cycle 1 is balanced only for low coverages, when the heat of adsorption of oxygen is 75 to 80 kcal. per mole. When the heat of adsorption of oxygen is smaller—*i.e.*, for oxygen coverages  $0 < \theta < 0.5 \theta_M$ —Cycle 3 (and no other) becomes balanced.

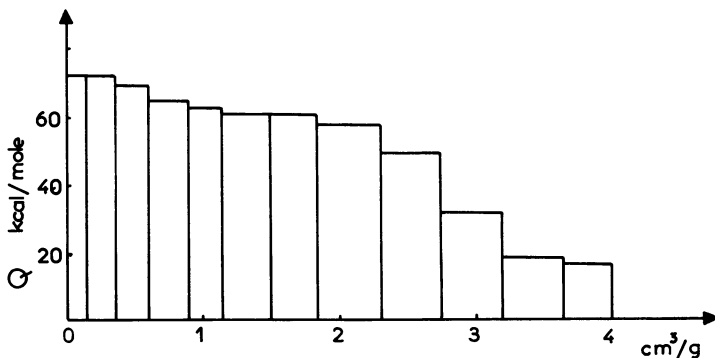
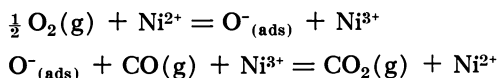


Figure 3. Adsorption of carbon monoxide on nickel oxide containing preadsorbed oxygen

It can be concluded from the calorimetric data that the interaction between adsorbed oxygen and carbon monoxide is a multiple process. For low surface coverages—*i.e.*, on the most active sites— $\text{CO}_3^-$  (ads) ions are formed. During the adsorption of the next doses of CO, these ions are converted into carbon dioxide, since the electrical conductivity of the sample finally returns to its initial value. When the coverage of the surface increases, a second type of interaction between adsorbed oxygen and carbon monoxide yields  $\text{CO}_2$  (ads) directly, and for a still increasing coverage—*i.e.*, on sites of a low activity—gaseous carbon dioxide is formed.

It would then appear that a second mechanism (II) is also probable for the catalytic oxidation of CO on NiO(250):

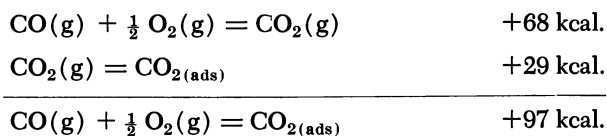
#### Mechanism II



The same sequence of adsorptions has been studied on NiO(200) (8, 20). The interaction between oxygen preadsorbed on NiO(200) and carbon monoxide yields only adsorbed carbon dioxide. Therefore, on NiO(200), gaseous carbon dioxide is produced during the catalytic reaction through Mechanism I (8, 20), whereas on NiO(250) two reaction paths are probable (Mechanisms I and II). These results show clearly

the influence that a modification in the catalyst preparation may have upon the catalytic reaction itself.

**Calorimetric Study of Catalytic Reaction.** Small doses of the stoichiometric mixture  $\text{CO} + \frac{1}{2} \text{O}_2$  are allowed to react with a sample of  $\text{NiO}(250)$  placed in the calorimeter. A cold trap is placed near the oxide sample. When the reaction of one dose is completed—when no more thermal effect is registered—the final pressure is in all cases low ( $p < 10^{-4}$  torr). The heat of reaction is plotted in Figure 4A as a function of the total volume of the reaction mixture introduced to the catalyst. During the reaction of the first doses, the heat of reaction is 78 kcal. per mole. It decreases progressively and, after the reaction of 15 cc. of gas mixture per gram of  $\text{NiO}(250)$ , it remains constant at a value of 69 kcal. per mole. The heat of the homogeneous reaction is 68 kcal. per mole (31). The higher values which are registered (Figure 4A) are explained by poisoning of the catalyst by adsorbed carbon dioxide



If all carbon dioxide had remained adsorbed on the surface, during the reaction of the first doses the registered heat of reaction should have been 97 kcal. per mole. The initial heats of reaction are lower (78 kcal. per mole). This means that gaseous carbon dioxide is produced during the reaction of the first doses. Therefore, inhibition of the most active sites of the catalyst surface proceeds, but progressively. Further evidence of the self-inhibition of the surface is obtained from the calorimetric results. In Figure 4B the percentage of the heat released during the reaction of doses A, B, and C (Figure 4A) is plotted as a function of time. The heat of reaction is produced more slowly for dose C than for B or A. Therefore, the catalytic activity decreases in the order  $A > B > C$ . The curve corresponding to dose C indicates a steady value of the activity, inhibition of the surface being then completed [heat of reaction, 69 kcal. per mole (Figure 4A) compared with 68 kcal. for the enthalpy of the homogeneous process]. These results demonstrate a progressive inhibition of the oxide surface by generated carbon dioxide remaining partially adsorbed. The same conclusion has already been deduced from the study of the surface interactions.

For  $\text{NiO}(200)$ , the initial heat of reaction is 90 kcal. per mole (20). Hence, a larger fraction of the carbon dioxide formed remains in the adsorbed state, and the catalytic activity decreases rapidly, after the conversion of increasing amounts of the stoichiometric mixture [Figure 4B: dose A' after conversion of 0.4 cc. per gram, dose B' after conversion

of 5.69 cc. per gram, dose C' after conversion of 22.68 cc. per gram. Compare with doses A, B, and C for NiO(250) in Figure 4A].

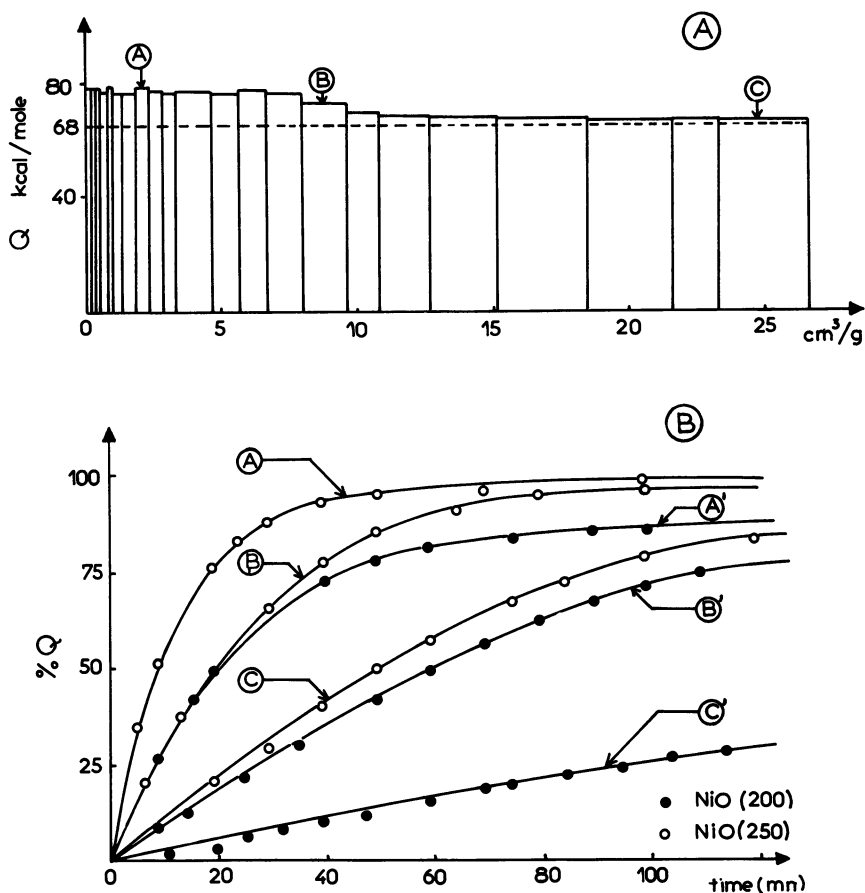


Figure 4. Heats of reaction

A: Calorimetric

B: Percentage evolved as a function of time for oxidation of carbon monoxide on NiO(250) for doses A, B, and C (Figure 4A) and A', B', and C' on NiO(200)

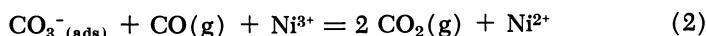
The catalytic activity, represented by the rate of evolution of the heat of reaction, is approximately the same for both catalysts when NiO(250) has converted 23.32 cc. per gram of the reaction mixture and NiO(200) has converted 5.69 cc. per gram (Figure 4B, curves C and B'). An even larger difference of activity is evident from curves C and C', both of which represent a steady value of the activity. The heat of reaction of doses C and C' on both catalysts is close to 68 kcal. per mole (20).

Carbon dioxide is then desorbed almost entirely to the gas phase, and the coverage of both surfaces by adsorbed  $\text{CO}_2$  must be close to its maximum value. Since the capacity of adsorption of both catalysts with respect to carbon dioxide is the same (Table II), the difference of their activities cannot be caused by a different coverage of their surfaces by carbon dioxide. A test carried out in a static reactor (catalyst weight 50 mg., initial pressure of the mixture  $\text{CO} + \frac{1}{2} \text{O}_2$  3 torr, liquid nitrogen trap to condense  $\text{CO}_2$ ) confirms that  $\text{NiO}(250)$  is more active than  $\text{NiO}(200)$  in the room-temperature oxidation of carbon monoxide (Figure 5).

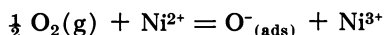
**Reaction Mechanism.** The rate of production of heat as a function of time gives indications of the velocity of the process taking place on the catalyst surface (Figure 4B). For instance, it has been shown (20) that, on  $\text{NiO}(200)$ , the adsorption of oxygen and the formation of  $\text{CO}_3^-_{(\text{ads})}$  ions are fast processes compared with the adsorption of carbon monoxide or the reaction between  $\text{CO}$  and  $\text{CO}_3^-_{(\text{ads})}$ . From calorimetric results and a kinetic study of the reaction, it has been concluded (8) that the decomposition of  $\text{CO}_3^-_{(\text{ads})}$  ions by adsorbed carbon monoxide to yield carbon dioxide is the slowest step of the reaction mechanism on  $\text{NiO}(200)$  (Mechanism I).

On the surface of  $\text{NiO}(250)$ , two simultaneous reaction paths are probable.

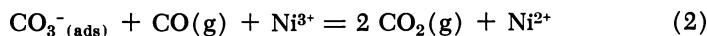
#### Mechanism I



#### Mechanism II



In order to determine which mechanism actually governs the catalytic reaction, it is necessary to compare the rates of the slowest steps of both mechanisms. As in the case of  $\text{NiO}(200)$ , calorimetric experiments show that adsorption of oxygen and formation of  $\text{CO}_3^-_{(\text{ads})}$  ions (Interaction 1) are fast processes also on the surface of  $\text{NiO}(250)$ . However, the following interactions are slower processes.



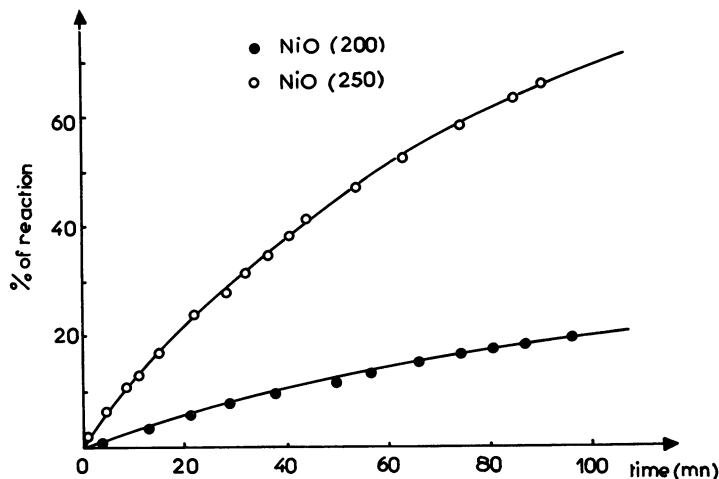
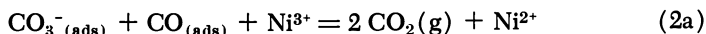


Figure 5. Kinetic curves for oxidation of carbon monoxide on NiO(200) and NiO(250)

Reactions 2 and 3 belong to Mechanism I, and Reaction 4 belongs to Mechanism II. Therefore, the slowest step of Mechanism II can only be Reaction 4.

As has been stated, the calorimetric method does not allow discrimination between the interactions involving two adsorbed species or one adsorbed species and a gas. Thus, the following interactions would also be proposed as possible slowest steps for Mechanisms I and II.



Interactions 2 and 4 represent a Rideal mechanism and Interactions 2a and 4a a Langmuir-Hinshelwood mechanism. However, to form  $\text{CO}_3^-(\text{ads})$ , by Interaction 1 in Mechanism I, CO must first be adsorbed; since Interaction 1 is a fast process, the adsorption of CO would be the slow step of Mechanism I, and the kinetics of the reaction would depend on  $p_{\text{CO}}$ . However, it has been shown (8, 28) that the reaction is zero order with respect to CO, and therefore the adsorption of CO and its conversion to  $\text{CO}_3^-(\text{ads})$  are faster processes than Interaction 2 which is the rate-limiting step and hence may be written in the form of 2a (Langmuir-Hinshelwood mechanism).

As for Mechanism II, for which a choice has to be made between rate-determining steps 4 and 4a, the kinetic results (7) show again that the reaction rate does not depend on  $p_{\text{CO}}$ . Here again step 4a has to be preferred (Langmuir-Hinshelwood mechanism) to step 4, (Rideal mechanism).

The rates of production of the heat evolved when a dose of carbon monoxide interacts with NiO(250) containing either  $O^-_{(ads)}$  ions (Reaction 4) or  $CO_3^-_{(ads)}$  ions (Reaction 2) are given as a function of time in Figure 6. In both cases, the same amount of carbon monoxide has been introduced previously to this particular dose. Thermochemical cycles and direct observation of the presence of carbon dioxide in the cold trap confirm that, during the interaction of this particular dose of CO, carbon dioxide is desorbed to the gas phase.

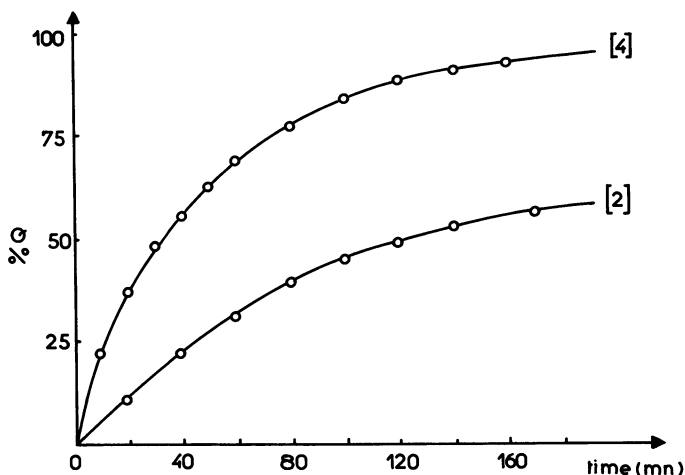


Figure 6. Percentage of heat as a function of time for Interactions 2 and 4

The rate of production of heat is greater for Interaction 4 (Mechanism II) than for Interaction 2 (Mechanism I).

Thus, again the limiting step of both Interactions 2 and 4 cannot be the adsorption of carbon monoxide (Equation 3) since the rates of adsorption of CO, without interaction with preadsorbed species, on nickel oxides containing nearly the same quantity of  $O^-_{(ads)}$  ions or  $CO_3^-_{(ads)}$  ions should be the same for the same coverage of the surface and the rate of production of heat would be the same.

Interaction 2a [in the case of NiO(200)] (8) is the slowest step of the reaction mechanism (I). In the case of NiO(250), this mechanism cannot control the reaction rate because Mechanism II is faster (Figure 6), and therefore it prevails. Hence, the most probable mechanism of the room-temperature oxidation of carbon monoxide on NiO(250) is Mechanism II. Finally, the difference between the catalytic activities of

NiO(200) and NiO(250) is explained by a change of the reaction Mechanism: Mechanism I on NiO(200) and Mechanism II on NiO(250).

**Nature of Active Sites.** There is no apparent correlation between the increase of catalytic activity and a modification of the electronic structure of nickel oxide, since the electrical properties of both catalysts are identical. It is probable that local modifications of the nickel oxide surface are responsible for the change of its activity and of the reaction mechanism. It should be possible to associate these structural modification with local modifications of the height of the Fermi level, but it would be difficult to explain the results by the electronic theory of catalysis which considers only collective electrons or holes. A discussion based only on the influence of surface defects seems, therefore, to be more straightforward.

The crystal field surrounding the surface ions suggest that the surface of a metallic oxide will be terminated preferentially by anions (10). However, when nickel oxide is prepared at a low temperature (200°C.), the surface mobility is not large enough to allow a complete reorganization of the surface, and exposed nickel ions may still exist. The increase of the temperature of preparation should result in a more regular structure of the outside lattice layer. The existence of a surface mobility in NiO at 250°C. is demonstrated by the annealing of surface defects induced at room temperature by neutron bombardment (5). For the nickel oxide used in this work, it has been shown (13) that foreign ions ( $\text{Li}^+$  and  $\text{Ga}^{3+}$ ) can be incorporated in the outside layers of the lattice, under vacuum, at 250°C., but not at 200°C. These results demonstrate that, at 250°C., the surface mobility may be large enough to facilitate a reorganization of the surface layers of the lattice and, consequently, the surface of the nickel oxide prepared at 250°C. should present a smaller number of defects such as exposed nickel ions than the surface of NiO(200). The increase of the temperature of preparation of nickel oxide from 200° to 250°C. therefore produces two types of surface modification, both connected with the increased ionic surface mobility—recession of nickel ions which are more exposed when the oxide is prepared at 200°C. and departure of oxygen with the resulting formation of anionic and cationic vacancies and nickel crystallites.

These surface modifications have little influence on the reactivity of the oxide towards the adsorption of CO and CO<sub>2</sub>. Both gases must be adsorbed at room temperature on Ni<sup>2+</sup> ions as has been shown through different experimental results (23, 34). However, participation of anions in the mechanism of adsorption of both gases is probable since oxygen from either CO or CO<sub>2</sub> is exchangeable with lattice anions at room temperature (2, 3).

In contrast with these results, the increase of the temperature of preparation of the catalyst and the resulting surface modifications influence the adsorption of oxygen. Oxygen is adsorbed on nickel ions, and the contributions of the anions to this adsorption may be only negative. The low surface coverage by adsorbed oxygen suggests that in both cases the adsorption sites are lattice defects with exposed nickel ions (5). Moreover, for a dissociative adsorption to occur, pairs of sites must exist. However, polarization of the oxygen molecule adsorbed on an active site may induce a second adsorption center for oxygen (5). This seems to be the case for the adsorption of oxygen on anionic vacancies which exist in NiO(250) since sequence  $O_2$ —CO has shown that the interaction between the most energetically adsorbed oxygen ions—*i.e.*, probably adsorbed on anionic vacancies—and carbon monoxide yields  $CO_3^-_{(ads)}$ , this species being formed by reaction of one carbon monoxide molecule with two oxygen ions adsorbed therefore on adjacent sites. This interaction is not registered on NiO(200) where only  $CO_{2(ads)}$  is formed.

On the less active sites of NiO(250) and on NiO(200), the interaction between oxygen adsorbed probably on exposed nickel ions and carbon monoxide yields carbon dioxide directly. Hence, the mean distance between such sites must be short enough to allow the adsorption of oxygen with dissociation of the molecule but long enough to restrict the interaction of CO to one oxygen ion. When the temperature of preparation of NiO is increased from 200° to 250°C., the number of these sites and their average activity decrease as a consequence of the recession of nickel ions. Desorption of carbon dioxide, formed by the interaction between oxygen ions adsorbed on this type of sites and carbon monoxide, is then possible on NiO(250) but not on NiO(200) and therefore gives a new path to the reaction mechanism (II). This desorption of  $CO_2$  must be a cooperative phenomenon with activation of the surface intermediate complex by the energy of interaction between  $O^-_{(ads)}$  and CO because direct adsorption of carbon dioxide on these sites is irreversible at room temperature (28, 30).

### Conclusions

The increase of the catalytic activity in the room-temperature oxidation of carbon monoxide, which results from the increase of the temperature of preparation of NiO from 200° to 250°C., is related to the difference in the reactivity of oxygen adsorbed on both surfaces. The interaction between adsorbed oxygen and carbon monoxide has roughly the same velocity on both oxides. But on NiO(200) this interaction yields only  $CO_{2(ads)}$ , whereas on NiO(250) the same interaction produces  $CO_3^-_{(ads)}$  on the most active sites (anionic vacancies) and  $CO_2(g)$  on the less

reactive sites (partially recessed nickel ions). Hence, the same interaction causes the inhibition of the surface sites on NiO(200) but yields the product of the catalytic reaction  $\text{CO}_2(\text{g})$  for NiO(250). Since this interaction is the limiting step of the reaction mechanism (Mechanism II) on NiO(250), whereas on NiO(200) the limiting step is the decomposition of  $\text{CO}_3^-_{(\text{ads})}$  by  $\text{CO}_{(\text{ads})}$  (Mechanism I), it is concluded that the catalytic activity may be governed by local chemical defects and not only by collective properties. Therefore, the activity may be correlated with the chemical structure of heterogeneous surfaces, and more specifically in this work, with the energy spectrum for the adsorption of oxygen.

### Literature Cited

- (1) Arghiroopoulos, B., Teichner, S. J., *J. Catalysis* **3**, 477 (1964).
- (2) Bailly, J. C., Gravelle, P. C., Teichner, S. J., *Bull. Soc. Chim.* **1967**, 1620.
- (3) Bailly, J. C., Teichner, S. J., *Bull. Soc. Chim.* **1967**, 2376.
- (4) Bielanski, A., Deren, J., Haber, J., Sloczynski, J., *Trans. Faraday Soc.* **58**, 166 (1962).
- (5) Charman, H. B., Dell, R. M., Teale, S. S., *Trans. Faraday Soc.* **59**, 469 (1963).
- (6) Cimino, A., Molinari, E., Romeo, G., *Z. Physik. Chem.* **16** (NF), 101 (1958).
- (7) Coue, J., Ph.D. Thesis 149, Lyon, 1963.
- (8) Coue, J., Gravelle, P. C., Ranc, R. E., Rue, P., Teichner, S. J., "Proceedings of 3rd International Congress on Catalysis," p. 748, North Holland Publishing Co., 1965.
- (9) Dell, R. M., Stone, F. S., *Trans. Faraday Soc.* **50**, 501 (1954).
- (10) Dowden, D. A., Wells, D., "2nd International Congress on Catalysis," p. 1499, Technip, Paris, 1961.
- (11) Dry, M. E., Stone, F. S., *Discussions Faraday Soc.* **28**, 192 (1959).
- (12) El Shobaky, G., Ph.D. Thesis 403, Lyon, 1966.
- (13) El Shobaky, G., Gravelle, P. C., Teichner, S. J., *Bull. Soc. Chim.* **1967**, 3244, 3251, 3670.
- (14) El Shobaky, G., Gravelle, P. C., Teichner, S. J., "International Congress on Calorimetry," p. 175, CNRS, Marseille, 1965.
- (15) El Shobaky, G., Gravelle, P. C., Teichner, S. J., Trambouze, Y., Turlier, P., *J. Chim. Phys.* **64**, 310 (1967).
- (16) Garner, W. E., Stone, F. S., Tiley, P. F., *Proc. Roy. Soc. (London)* **A197**, 294 (1949).
- (17) *Ibid.*, **A211**, 472 (1952).
- (18) Gravelle, P. C., *J. Chim. Phys.* **61**, 455 (1964).
- (19) Gravelle, P. C., El Shobaky, G., Urbain, H., *Compt. Rend.* **262**, 549 (1966).
- (20) Gravelle, P. C., Teichner, S. J., *J. Chim. Phys.* **61**, 527, 533, 625, 1089 (1964).
- (21) Keier, N. P., Roginsky, S. Z., Sazonova, I. S., *Dokl. Akad. Nauk USSR* **106**, 859 (1956).
- (22) Keier, N. P., Roginsky, S. Z., Sazonova, I. S., *Izvest. Akad. Nauk USSR Ser. Fiz.* **21**, 183 (1957).
- (23) Marcellini, R. P., Ranc, R. E., Teichner, S. J., "2nd International Congress on Catalysis," p. 289, Technip, Paris, 1961.
- (24) Marcellini, R. P., Teichner, S. J., *J. Chim. Phys.* **58**, 625 (1961).

- (25) Merlin, A., Teichner, S. J., *Compt. Rend.* **236**, 1892 (1953).
- (26) Parravano, G., *J. Am. Chem. Soc.* **75**, 1448, 1452 (1953).
- (27) Parravano, G., Boudart, M., *Advan. Catalysis* **7**, 47 (1955).
- (28) Ranc, R. E., Teichner, S. J., *Bull. Soc. Chim.* **1967**, 1717, 1730.
- (29) Roginsky, S. Z., Tselinskaya, T. F., *Zh. Fiz. Khim. USSR* **22**, 1360 (1948).
- (30) Rue, P., Teichner, S. J., *Bull. Soc. Chim.* **1964**, 2791.
- (31) "Selected Values of Chemical Thermodynamic Properties," *Nat. Bur. Std. Bull.* **500** (1952).
- (32) Schwab, G. M., Block, J. Z. *Physik. Chem.* **1** (NF), 42 (1954).
- (33) Schwab, G. M., Block, J., *J. Chim. Phys.* **51**, 664 (1954).
- (34) Teichner, S. J., Marcellini, R. P., Rue, P., *Advan. Catalysis* **9**, 458 (1957).
- (35) Teichner, S. J., Morrison, J. A., *Trans. Faraday Soc.* **51**, 961 (1955).
- (36) Wagner, C., Hauffe, K., *Z. Elektrochem.* **44**, 72 (1938).
- (37) Winter, E. R. S., *J. Catalysis* **6**, 35 (1966).

RECEIVED October 9, 1967.

# Ionization from the Heterogeneous Catalytic Oxidation of Hydrocarbons in the Vapor Phase

J. ENOCH JOHNSON, FOSTER J. WOODS, and MERLE E. UMSTEAD

Fuels Branch, Chemistry Division, Naval Research Laboratory,  
Washington, D. C. 20390

*The profound effect of molecular structure on ionization which occurs during platinum-catalyzed oxidation of hydrocarbons has been confirmed. Highly branched alkanes gave a much greater yield of ions than n-alkanes. The effect of oxygen concentration in the gas mixture on extent of oxidation and ionization varied with the hydrocarbon used. In general, increase in oxygen content considerably enhanced ion yield. However, with some hydrocarbons the fraction oxidized decreased markedly with increased oxygen concentration. The data seem consistent with an explanation based on lower temperature oxidation occurring only on the platinum surface, whereas at higher temperatures the catalytic process extends to some degree into the vapor phase. It is suggested further that dissociative adsorption of oxygen at higher temperatures is involved in the ion-producing process.*

Measurable ions are formed when hydrocarbons in an air stream are oxidized in the presence of a heated platinum filament (3, 10). The experimental evidence suggests that these ions are produced by the chemical oxidation reactions catalyzed by the platinum surface (10). That this process is one of chemionization is supported by the fact that the extent of ionization observed depended greatly on the molecular structure of the particular hydrocarbon being oxidized. This is in contrast to the ionization measured in flames, where the extent of ionization for saturated hydrocarbons, for example, does not appear to depend in any way on the molecular structure but only on the number of carbon atoms (9).

The marked influence of hydrocarbon structure on the ionization from catalytic oxidation prompted extension of this study to other selected hydrocarbons. In addition, the effect of the oxygen content of the gas mixture has been explored. The results have led to certain suggestions in regard to the processes involved in these examples of catalytic oxidation.

### **Methods**

The apparatus and procedures for studying the ionization related to catalytic combustion have been described (10). A potential of 300 volts d.c. was maintained between the cylindrical collector and the heated filament, with the collector being negative. After the filaments had been conditioned at 1000°C. for a few minutes, the background current was less than  $0.01 \times 10^{-9}$  amp., even at the highest filament temperatures used (900°C.).

The mixtures of gases and liquids were prepared by injecting a measured amount of the selected liquid or gaseous hydrocarbon into an evacuated stainless steel bottle, 1.7-liter capacity and then pressurizing with a gas mixture containing the desired concentration of oxygen to higher pressure, usually 10 atm. The hydrocarbon concentrations were usually about 4.0 mg. per liter. The prepared gas mixtures were passed through the combustion cell at a metered rate, usually 50 cc. per minute, and the ionization current was measured with a Keithley Model 220 electrometer. Carbon dioxide and carbon monoxide were determined using Beckman L/B Model 15A nondispersive infrared analyzers. Hydrocarbons were determined by gas chromatography using a DC-550 silicone column and a Beckman GC-2A hydrogen flame detector.

The hydrogen, carbon monoxide, and methane were obtained from the Matheson Co. The hydrocarbons used were Phillips Petroleum Co. pure grade (99+ mole %). The liquid hydrocarbons were percolated through silica gel before use.

### **Results and Discussion**

All of the data reported in this paper were obtained using a platinum filament as the catalyst. Under the experimental conditions used, a maximum of about 35 to 60% of the hydrocarbon in each case was oxidized. Although the ion yields can be expressed in several ways, for the most part they are presented as coulombs per mole of hydrocarbon oxidized.

**Effect of Hydrocarbon Molecular Structure on Ionization from Catalytic Oxidation in Air.** Figure 1 shows the data for the ion yields obtained for several hydrocarbons during oxidation in air over a platinum filament in the approximate temperature range of 400° to 900°C. The hydrocarbons fall into two broad categories: those which produced about 0.04 coulomb per mole of hydrocarbon oxidized, and those which produced about 1.0 coulomb or more per mole. The latter yield is similar to that obtained during combustion of hydrocarbons in a hydrogen flame

(9). Table I summarizes the data shown in Figure 1 in terms of maximum ion yields, plus data on a few other hydrocarbons (10).

In the series of compounds containing the *tert*-butyl group, when oxidized in air, the tendency was to produce a higher ion yield as the molecular weight decreased, with 2,2-dimethylpropane (neopentane) having the highest ion yield per mole of hydrocarbon oxidized. The facility with which the compounds such as 2,2-dimethylpropane produced ions compared with the other hydrocarbons investigated indicates that the *tert*-butyl group plays an important role in the ion-producing process. The relative stability of the trimethylcarbonium ion may be an important factor in this regard. However, 2-methylpropane itself yielded relatively few ions. These results suggest that the scission of a C—C bond to yield the *tert*-butyl group may be important to ion formation.

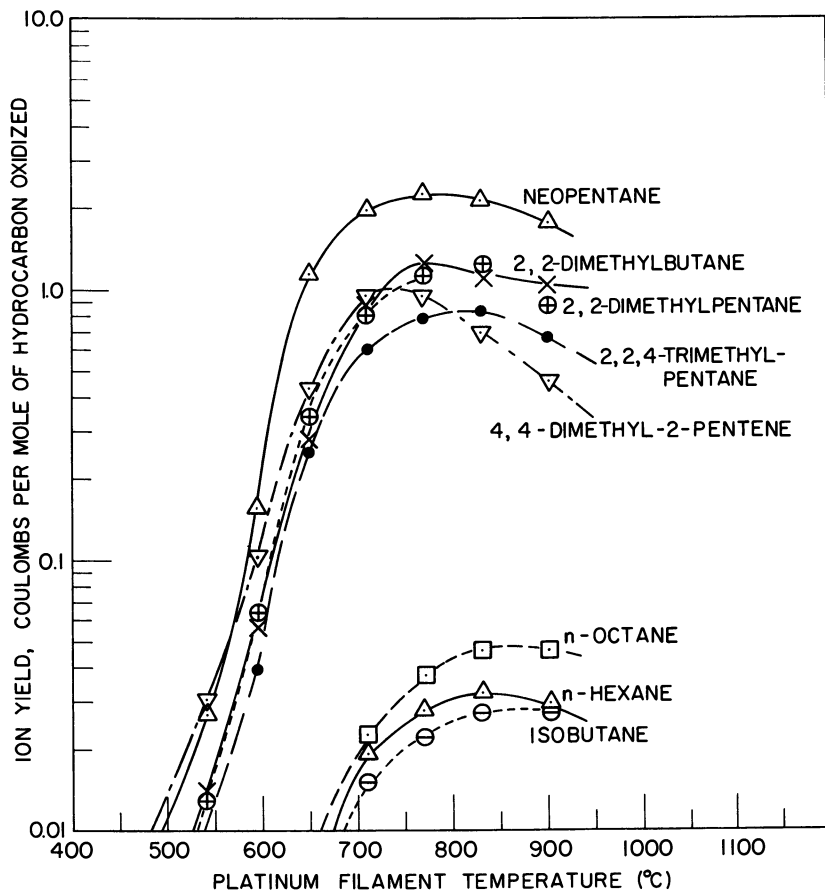


Figure 1. Effect of filament temperature on ion yield in air

**Table I. Maximum Ion Yield  
(Coulombs per Mole of Hydrocarbon Burned)**

Hydrocarbon	In Air	In 60% O <sub>2</sub> /40% N <sub>2</sub>
2,2-Dimethylpropane	2.28	2.47
2,2-Dimethylbutane	1.26	3.43
2,2-Dimethylpentane	1.21	2.21
4,4-Dimethyl-2-pentene	0.93	2.22
2,2,4-Trimethylpentane	0.83	1.77
2,3-Dimethylbutane <sup>a</sup>	0.14	—
<i>tert</i> -Butylbenzene <sup>a</sup>	0.13	—
3-Methylpentane <sup>a</sup>	0.12	—
2-Methylpentane <sup>a</sup>	0.09	—
<i>n</i> -Octane	0.05	0.10
<i>n</i> -Hexane	0.03	0.09
2-Methylpropane	0.03	0.05
Benzene <sup>a</sup>	0.002	—
Methane	<0.002	—

<sup>a</sup> Taken from Umstead *et al.* (10).

It was observed that 4,4-dimethyl-2-pentene was more readily oxidized than the saturated hydrocarbon—2,2-dimethylpentane—although the latter gave a significantly larger ion yield. In the case of this olefin, which was used as the stereoisomeric mixture, the *cis* and *trans* isomers were equally attacked in terms of hydrocarbon oxidized.

**Catalytic Oxidation of Mixtures Containing Carbon Monoxide.** Neither hydrogen (5) nor carbon monoxide (9) contributes to the ionization in flames, nor does a mixture of hydrogen and carbon monoxide in flames produce ionization (2). Analogously, it was shown (10) that neither hydrogen nor carbon monoxide produced ions when oxidized catalytically under conditions such as those prevailing in the present work. In further experiments with mixtures in air containing 0.5% CO and 0.5% H<sub>2</sub>, although as much as 75% of the CO in the mixture was oxidized to CO<sub>2</sub>, there was no measurable ion current ( $<0.01 \times 10^{-9}$  amp.). This is an additional example of the similarity between the ionization phenomena in catalytic oxidation and in flames.

Because carbon monoxide is strongly adsorbed on platinum, a mixture containing 3.8 mg. per liter of 2,2-dimethylbutane (2,2-DMB) and 0.5% CO in air was passed over the platinum filament at temperatures ranging from 400° to 900°C. The CO did not appear to interfere significantly with the oxidation of 2,2-DMB—for example, at 830°C. 35.4% of the 2,2-DMB was oxidized in the presence of CO, and 34.1% without CO added. At the same time the ion current was  $6.5 \times 10^{-9}$  amp. with CO and  $11.7 \times 10^{-9}$  amp. without CO, indicating a marked inhibiting effect of CO on the ion yield.

**Halogenated Hydrocarbons.** A few halogenated hydrocarbons were studied by the usual procedure, using mixtures in air over the platinum filament. Neither dichlorodifluoromethane ( $\text{CCl}_2\text{F}_2$ ) nor 1,1-dichloroethene yielded a measurable ion current at temperatures up to  $900^\circ\text{C}$ . 1,1,1-Trichloroethane yielded a modest ion current, but the results were erratic and not reproducible. There was some indication that the halogen compounds changed the behavior of the filament. Consequently, no further experiments with halogenated compounds were conducted. This erratic behavior was in contrast with the very reproducible results with hydrocarbons.

**Effect of Oxygen Concentration on Catalytic Oxidation and Ionization.** A number of the hydrocarbons studied were oxidized over platinum by the usual procedure using a mixture of 60% oxygen and 40% nitrogen

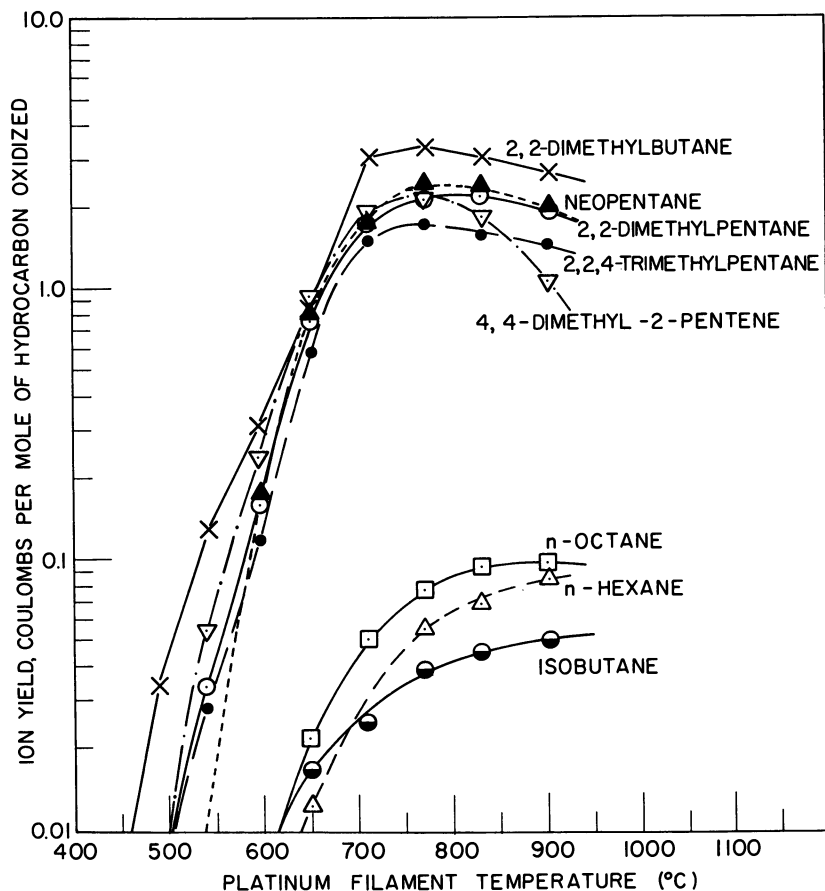


Figure 2. Effect of filament temperature on ion yield in 60%  $\text{O}_2$ , 40%  $\text{N}_2$

instead of air (Figure 2). In all cases the increased oxygen content resulted in increased ion yields. In many instances, the maximum ion yield was about twice that in air (Table I). The relative position of each hydrocarbon in terms of ion yield remains about the same as in air, with the principal exception that 2,2-DMB had the highest ion yield at 60% O<sub>2</sub>. The temperature at which maximum ion yield was obtained was about the same for air and 60% oxygen, except for the group which had the low yields. In these cases, it appeared that the peak ionization had not yet been reached at 900°C.

During these experiments, it was observed that at temperatures below 600° to 700°C., the percentage of hydrocarbon oxidized was less at 60% than at 21% oxygen. In some cases this difference was substantial. Reyerson and Swearingen (8) showed earlier that platinized gel catalyst was much less efficient for oxidizing methane when the oxygen content of the gas was increased from 28% to 73% in the temperature range of 250° to 400°C. In the present work several additional experiments were performed to study the effect of oxygen concentration on both ionization and oxidation of hydrocarbons.

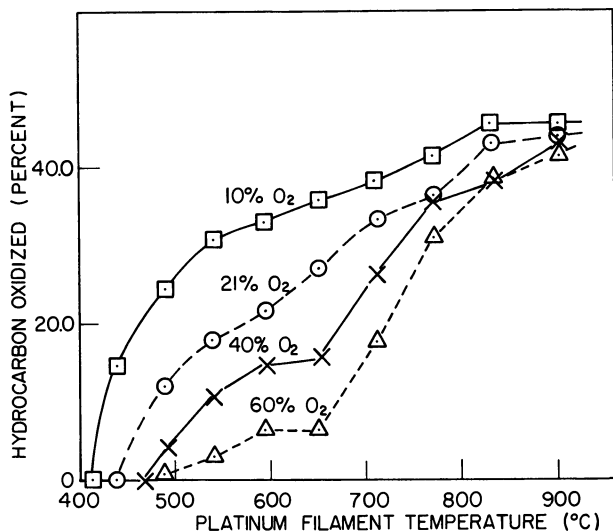


Figure 3. Effect of oxygen concentration on catalytic oxidation of 2,2-dimethylbutane

For example, gas mixtures were prepared containing 3.8 mg. per liter of 2,2-DMB in oxygen-nitrogen mixtures ranging from 10 to 60% O<sub>2</sub>. The percentage of the hydrocarbon which was oxidized was determined over a catalyst surface temperature range of 400° to 900°C. (Figure 3).

At the lower temperatures, it is evident that the increased oxygen content results in a markedly lesser attack on the hydrocarbon. Essentially all of the 2,2-DMB which was attacked was converted to carbon dioxide, especially at temperatures below about 750°C. This high conversion to carbon dioxide has been generally true of all hydrocarbons. It has been shown in earlier experiments that during the oxidation of hydrocarbons a small yield of CO occurs, which increases to several per cent at higher temperatures.

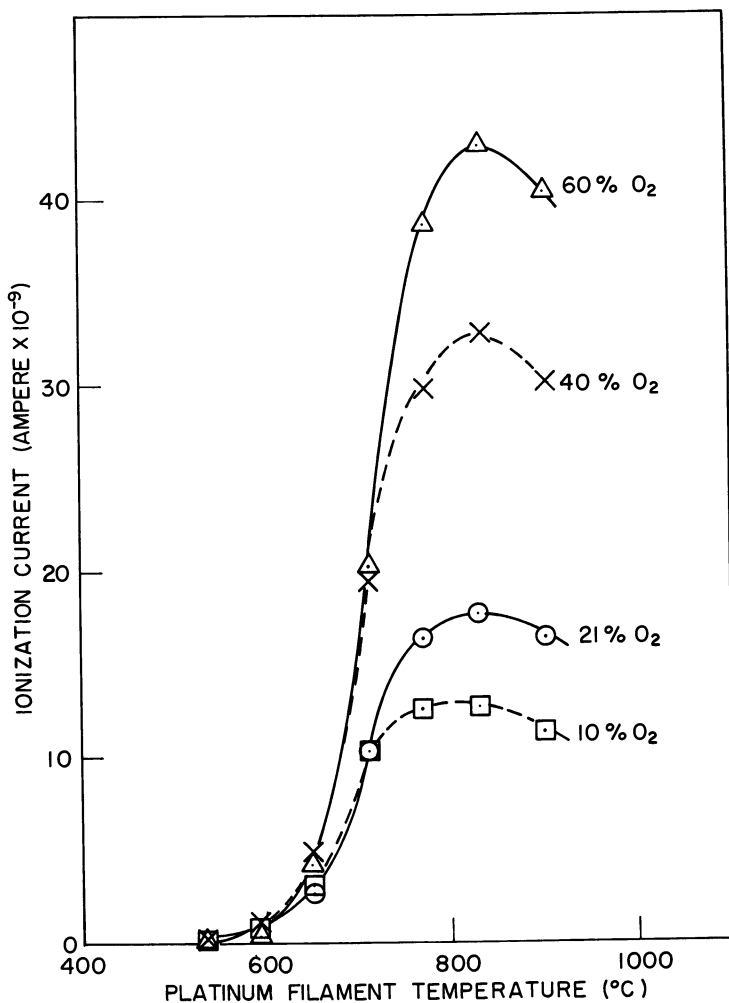


Figure 4. Effect of oxygen concentration on ionization during oxidation of 2,2-dimethylbutane

The ionization current measured during the oxidation of 2,2-DMB as a function of oxygen concentration is plotted in Figure 4. The ion current increases significantly as the oxygen content is increased, despite the fact that at lower temperatures the hydrocarbon oxidation yield is less with increased oxygen. The temperature at which significant ions are collected is nearly the same regardless of oxygen concentration (Figure 4). In Figure 3 a knee in the hydrocarbon oxidation curve appears and becomes more pronounced as oxygen concentration is increased. The temperature range at which this knee occurs is about the same as where the ion current increases markedly.

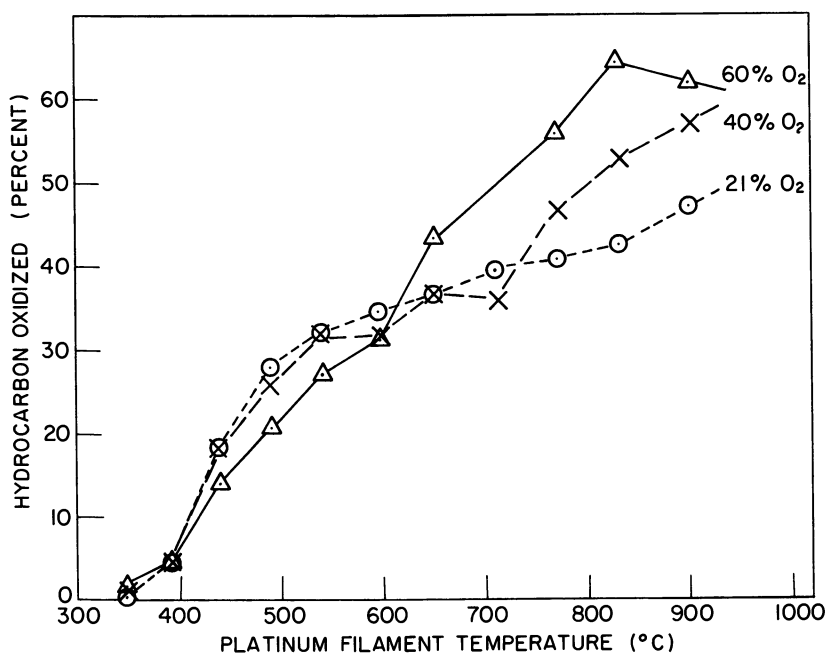


Figure 5. Effect of oxygen concentration on catalytic oxidation of *n*-hexane

Additional data relative to these oxidation phenomena were obtained for *n*-hexane. In similar experiments, *n*-hexane was oxidized in 21, 40, and 60% oxygen in nitrogen mixtures. The per cent hydrocarbon oxidized over the temperature range of 300° to 900°C. is shown in Figure 5. Only a slight decrease in *n*-hexane conversion with increased oxygen content at lower temperatures was observed, and above about 600° to 700°C., higher oxygen resulted in more oxidation of *n*-hexane. The ionization current increased as oxygen concentration increased (Figure 6). The ionization current increased markedly in the temperature range

where the oxidation curves exhibit an apparent change in reaction mode. Data for the oxidation of *n*-octane at 21 and 60% oxygen result in curves similar to *n*-hexane.

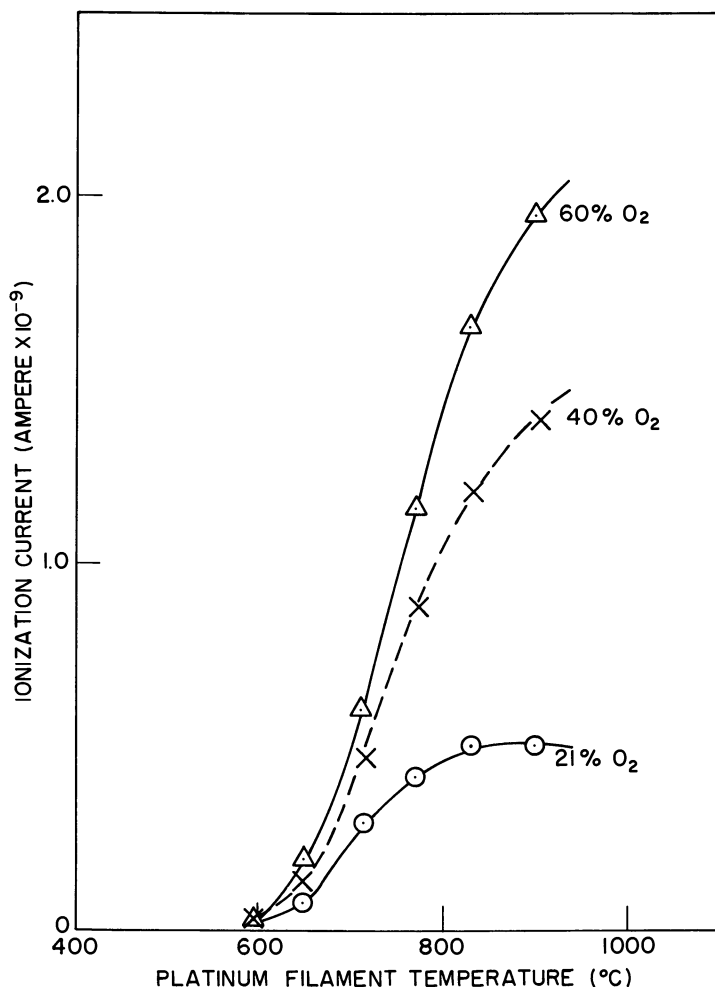


Figure 6. Effect of oxygen concentration on ionization during oxidation of *n*-hexane

Data for 2,2-dimethylpropane are plotted in Figure 7 for comparison with *n*-hexane and 2,2-DMB because 2,2-dimethylpropane gave the highest ion yield of the hydrocarbons studied. Little oxidation of 2,2-dimethylpropane in 60%  $\text{O}_2$  occurred until the platinum surface temperature

exceeded 600°C. The oxidation curve showed a strong increase in conversion of hydrocarbon at about the same temperatures at which the ion yield increased markedly. At 21% O<sub>2</sub>, the ion yield curve showed a break at *ca.* 600°C. also. However, the hydrocarbon oxidation curve was different from that at 60% O<sub>2</sub>, in that substantial oxidation occurred below 600°C. with a pronounced knee in the curve at about 650°C.

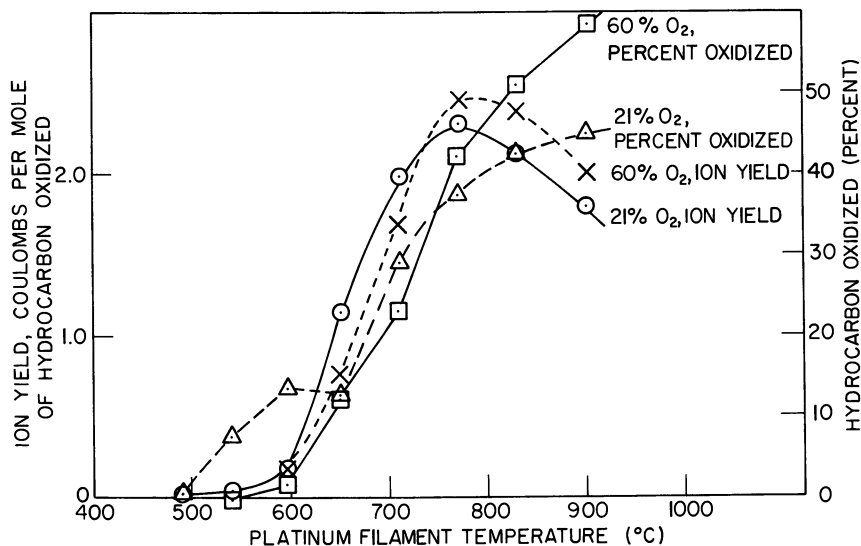


Figure 7. Effect of oxygen concentration on oxidation and ionization of 2,2-dimethylpropane

These data suggest that as the concentration of oxygen in the gas stream increases, the strong adsorption of oxygen molecules (1) interferes with adsorption of the hydrocarbon molecules. The result is that at lower temperatures fewer hydrocarbon molecules are oxidized as the oxygen concentration increases. This implies that both oxygen and hydrocarbon molecules must be adsorbed for reaction to occur, in accord with the Langmuir-Hinshelwood mechanism (6). The lesser effect of increased oxygen content on the oxidation at lower temperatures for *n*-hexane may be caused by a stronger adsorption of *n*-hexane compared with the branched hydrocarbons, particularly 2,2-dimethylpropane. No confirmatory data in this regard have been found, however.

It appears from Figure 3 that at about 650° to 700°C. a change occurs in the oxidation phenomena—*e.g.*, at 60% O<sub>2</sub>, further temperature increase results in a pronounced increase in oxidation yield, until at 850° to 900°C., the conversion of hydrocarbon is nearly the same at 10 and

60% O<sub>2</sub>. Several explanations of this effect can be offered. First, the adsorption of oxygen relative to hydrocarbon may change to permit a higher percentage of hydrocarbon to be adsorbed and oxidized, with no real change in mechanism. Second, an increase in the rate of oxidation at higher temperatures may decrease the length of time of residence of adsorbed molecules on a given site. This permits more hydrocarbon molecules to be adsorbed and oxidized. Third, mode of reaction may have changed to permit more and more oxidation of the hydrocarbon by the Rideal mechanism—*i.e.*, reaction between oxygen on the surface with hydrocarbon molecules in the gas phase (6). The latter explanation seems favored by the abrupt change in the hydrocarbon oxidation curves in Figure 3, rather than a more gradual change which might be expected for either of the other two explanations. However, the absence of products other than CO<sub>2</sub> and CO seems to speak against the Rideal mechanism. Partially oxidized products would be expected to become significant.

It is further apparent that the onset of ionization is closely related to the break in the oxidation curve at 600° to 700°C. These combined observations may be explained by suggesting a relationship to the dissociation of O<sub>2</sub> on the platinum surface, yielding adsorbed O atoms. Margolis (7) gives evidence for the dissociative adsorption of oxygen on platinum beginning at temperatures above 400°C. and becoming significant at higher temperatures. Such atoms may be quite reactive and may attack hydrocarbon molecules or radicals readily. It has been postulated in flame chemistry (5), for example, that ions are produced primarily from the reaction of two free radicals, CH and O, because such a system has the high energies required to produce ionization. Also chemions have been produced at room temperature by the vapor-phase reaction of oxygen atoms and hydrocarbon molecules (4). Here again the CH radical is proposed as the most likely reactant with the O atom. It is suggested, therefore, that in the present situation an adsorbed oxygen atom may react with a free radical from the hydrocarbon source to yield an ion. Whether this hydrocarbon-derived radical reacts in the adsorbed or vapor state is an open question. The suggestion that the dissociative adsorption of O<sub>2</sub> on the platinum surface is a controlling factor would also explain the similarities in temperature dependence of the oxidation and ionization phenomena from one hydrocarbon to another.

### *Literature Cited*

- (1) Bond, G. C., "Catalysis by Metals," p. 63, Academic Press, New York, 1962.
- (2) Bulewicz, E. M., Padley, P. J., "Ninth Symposium (International) on Combustion," p. 638, Academic Press, New York, 1963.

- (3) Folmer, O. F., Jr., Yang, K., Perkins, G., Jr., *Anal. Chem.* **35**, 454 (1963).
- (4) Fontijn, A., Miller, W. J., Hogan, J. M., "Tenth Symposium (International) on Combustion," p. 545, Combustion Institute, Pittsburgh, Pa., 1965.
- (5) Green, J. A., Sugden, T. M., "Ninth Symposium (International) on Combustion," p. 607, Academic Press, New York, 1963.
- (6) Laidler, K. J., "Catalysis," Vol. I, p. 151, Reinhold, New York, 1954.
- (7) Margolis, L. Ya., *Advan. Catalysis* **14**, 443 (1963).
- (8) Reyerson, L. H., Swearingen, L. E., *J. Phys. Chem.* **32**, 192 (1928).
- (9) Sternberg, J. C., Gallaway, W. S., Jones, D. T. L., "Gas Chromatography," pp. 231-267, Academic Press, New York, 1962.
- (10) Umstead, M. E., Woods, F. J., Johnson, J. E., *J. Catalysis* **5**, 293 (1966).

RECEIVED October 9, 1967.

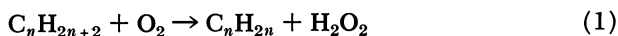
# Kinetic Study of the Formation of Hydrogen Peroxide by the Vapor-Phase Noncatalytic Oxidative Dehydrogenation of Propane

TAISEKI KUNUGI, MASASHI IKEDA, TOYOHARU MIYAKO, and  
TAKESHI MATSUURA

Department of Synthetic Chemistry, Faculty of Engineering, University of  
Tokyo, Hongo, Tokyo, Japan

*The applied kinetics for synthesizing hydrogen peroxide by the noncatalytic oxidative dehydrogenation of propane was studied using a conventional flow apparatus. Dehydrogenation was carried out successfully at temperatures ranging from 430° to 450°C. at atmospheric pressure and with residence time 6–10 sec. Besides the main products—hydrogen peroxide and propylene—appreciable amounts of formaldehyde, acetaldehyde, and methanol were obtained. Pretreatment of the inner reactor wall, with HF for the quartz reactor and with H<sub>3</sub>PO<sub>4</sub> for the stainless steel reactor, was effective in increasing remarkably the selectivity of the reaction producing hydrogen peroxide and propylene. The highest selectivity of ca. 60% was obtained at ca. 18% propane conversion using HF-treated quartz reactor.*

**D**uring studies on the noncatalytic oxidative dehydrogenation of hydrocarbons, we observed that hydrogen peroxide was obtained in fairly good yield under specific reaction conditions. The reaction can be described by the following stoichiometric equation:



where  $\text{C}_n\text{H}_{2n+2}$  represents ethane, propane, or butane.

Several papers have been published on the reaction mechanism (8, 9, 10, 11), and some patents (1, 2, 4) have also been issued. The process

has not yet been developed on a commercial scale, however, partly because of the difficulty in separating the oxygen-containing by-products such as formaldehyde, acetaldehyde, and methanol.

We have conducted experiments to improve the selectivity of the reaction for hydrogen peroxide formation, with a special attention to the influence of the reactor wall. These experimental results are interpreted by a simplified kinetic model, which is fairly well explained by knowledge of the rate of the free radical reaction.

### **Experimental**

A conventional flow apparatus shown in Figure 1 was used. It consisted of gas-flow controlling devices, tubular reactor in an electric furnace, Liebig condenser, liquid trap, etc. The temperature profile along the longitudinal axis of the reactor was measured by a thermocouple. The reaction zone is defined here as the part of the reactor above 350°C. The reaction temperature means the highest temperature in the reaction zone.

Propane was commercial 99.2% pure, the balance being ethane. Analysis was by gas chromatography in a column filled with a series combination of silica gel (3 meters, 80°C.) and molecular sieve (1 meter, 40°C.). Polarographic analysis of the liquid product (3) disclosed that the peroxide was composed of more than 99% hydrogen peroxide and less than 1% organic peroxides. Consequently, hydrogen peroxide content here is expressed as the total peroxide content determined by the sodium iodide method in 2-propanol (7), applicable to hydrogen peroxide analysis in the presence of aldehydes. The liquid product was analyzed also by gas chromatography. The column of triacetin supported on Celite-22 was 3 meters long, and it was kept at 130°C. Helium was used as a carrier gas at a flow rate of 15 ml./sec. The evaporator was heated to 200°C.

### **Results**

**Pretreatment of Quartz Reactor.** Hydrogen peroxide formed by dehydrogenative oxidation of hydrocarbons is known to decompose easily on the reactor wall. Several investigators have reported that alkaline reactor surfaces significantly accelerate the decomposition, and pretreatment of the reactor wall with acids effectively suppressed the decomposition reaction (5). We carried out the experiments by using the five quartz reactors, some pretreated with acids. Reactor I was fresh, neither pretreated nor aged; II was aged, not pretreated but used for the oxidation reaction for 60 days; III was treated with 30% aqueous solution of HF; IV was treated with 5% aqueous solution of H<sub>3</sub>PO<sub>4</sub>, and V was treated with 70% aqueous solution of HNO<sub>3</sub>. Pretreatment consisted of

immersing the reactors in the acidic solution for 12 hours at room temperature, followed by washing with distilled water until no acid was detected by litmus paper.

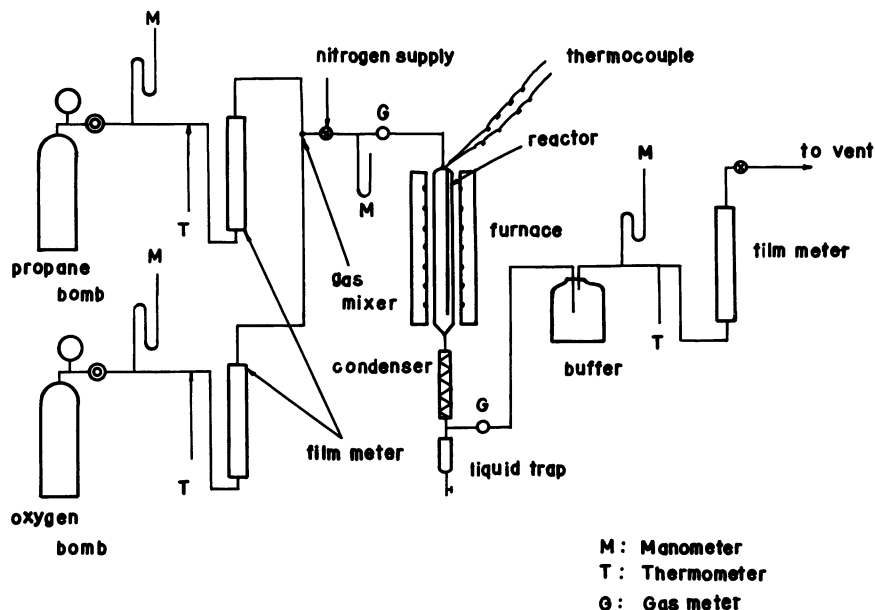
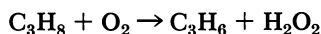


Figure 1. Schematic of experimental apparatus

The experimental results obtained with these reactors are summarized in Table I. Both reaction temperature and the molar ratio of propane to oxygen in the feed were kept constant at 430°C. and 3, respectively, while residence time was varied from 5 to 15 sec. Each experimental run was continued for about 4 hours. The hydrogen peroxide concentration in the liquid product sample was frequently checked by titration during the run. After the constant analytical value was attained, the products were subjected to the analytical procedure described before for obtaining the data given in the table.

For the experiment with Reactor III, hydrogen peroxide once formed by oxidative dehydrogenation seems hardly decomposed further. Since the hydrogen peroxide to propylene ratio is nearly equal to unity, Semenov's stoichiometry probably applies:



The results with Reactor I are notable for the rather high yields of methane and ethylene, in nearly equal molar ratio. These products might arise by the over-all equation:



Oxygen-containing by-products such as methanol, formaldehyde, and propylene oxide were also found. Although the ultimate products are water and carbon dioxide, here the amount of carbon dioxide was less than one-tenth that of carbon monoxide.

With respect to the untreated Reactor I, the hydrogen peroxide yield was very small, and that of methane, ethylene, carbon monoxide, and acetaldehyde was large. The small ratio of hydrogen peroxide to propylene is possibly caused by the successive decomposition of hydrogen peroxide once formed. With aged Reactor II, the yield of hydrogen peroxide and methanol increased, while that of methane, ethylene, and carbon monoxide decreased significantly.

Comparison of the experimental results with Reactors III, IV, and V (at oxygen consumption over 90%) indicates that Reactor III gave the highest selectivity (*ca.* 60%) as to hydrogen peroxide formation, and the lowest yield of by-products from pyrolysis and combustion. Reactor V gave poorer results than III or IV. The result with Reactor IV fell between those of Reactor III and V. Reactor II gave almost the same yield of hydrogen peroxide as Reactor III with somewhat lower selectivity for propylene formation. Therefore, the effect of reactor pretreatment on selectivity for hydrogen peroxide formation is:



**Pretreatment of Stainless Steel Reactor.** Since quartz is unsuitable for fabricating an industrial reactor, we tested stainless steel (SUS 27) reactors. One of these was treated with 30% phosphoric acid solution for 12 hours at room temperature and then washed thoroughly (Reactor VII); and other was untreated and unaged (Reactor VI). Oxidations were carried out at 430°C. with a propane/oxygen mole ratio of 3 and at various flow rates.

Results are shown in the last two columns of Table I. Hydrogen peroxide yield and its mole ratio to propylene were markedly larger with Reactor VII than with Reactor VI. Thus, the decomposition of the hydrogen peroxide formed is remarkably suppressed in Reactor VII. Yields of ethylene, carbon dioxide, and formaldehyde were larger in Reactor VI than VII, but yields of hydrogen peroxide and methanol were low.

The quartz reactor is more suitable for the hydrogen peroxide formation than the stainless steel reactor, the yield of hydrogen peroxide in

Reactor VII being only about 60% of that in Reactor III. Less methanol and formaldehyde were formed in Reactor VII, and yields of acetone and propylene oxide were insignificant. The selectivity in propylene was almost the same in the two reactors. Reactors I and VI showed some common features: less hydrogen peroxide and methanol were formed than in Reactors III and VII, while more ethylene and carbon dioxide were formed in Reactors I and VI.

**Aging of Reactor.** Although pretreated reactors give fairly good yields of hydrogen peroxide, aging is still indispensable in attaining

**Table I. Effect of**  
Reaction temperature, 430°C.;

Reactor	Run No.	Residence Time, sec.	Volume Expansion, out/in	Conversion, %	
				C <sub>3</sub> H <sub>8</sub>	O <sub>2</sub>
I <sup>a</sup> (untreated)	172	5.20	1.124	17.6	41.3
	170	6.80	1.228	33.8	96.5
	171	7.34	1.279	40.6	100
II (aged)	213	4.16	1.097	17.8	53.2
	212	9.95	1.157	26.9	95.5
	230	8.10	1.148	27.2	98.2
III (HF)	343	5.00	1.165	14.0	75.7
	342	6.23	1.133	20.1	90.9
	340	7.24	1.180	17.9	97.1
	334	8.58	1.11	20.8	96.4
IV (H <sub>3</sub> PO <sub>4</sub> )	248	3.52	1.095	17.2	58.0
	247	5.85	1.142	20.3	89.9
	224	7.42	1.12	22.8	93.5
	246	8.90	1.145	29.4	98.5
	245	14.70	1.174	36.9	98.5
V (HNO <sub>3</sub> )	253	4.93	1.160	20.7	80.0
	254	7.34	1.209	22.8	75.0
	250	9.7	1.179	33.4	76.0
	252	12.2	1.237	30.4	97.5
	251	14.2	1.237	35.2	91.8
VI <sup>b</sup> (untreated)	1,027	4.61	—	3.70	13.5
	1,028	6.04	—	10.2	34.5
	1,029	7.54	—	24.6	98.1
	1,030	9.10	—	23.2	99.8
VII (H <sub>3</sub> PO <sub>4</sub> )	1,051	3.45	—	2.5	32.2
	1,052	4.78	—	14.4	88.1
	1,053	5.61	—	17.9	88.4
	1,054	6.25	—	21.2	95.3
	1,055	7.13	—	20.2	98.0

maximum yield. Figure 2 shows that the yield of hydrogen peroxide increases with the reactor aging. For these experiments, the temperature was kept constant at 450°C., the propane to oxygen molar ratio was kept at 3, and the residence time was kept at *ca.* 3 sec. Each run was continued for more than 24 hours, and the liquid product, condensed at 2°C. for 30 minutes just before its sampling, was subjected to the hydrogen peroxide titration.

In quartz Reactor III, the hydrogen peroxide concentration reached 28 wt. % in 26 hours and thereafter remained constant. In untreated

### Pretreatment of Reactor Wall

mole ratio of propane to oxygen, 3

#### *Products, moles/100 moles of Propane Fed*

$C_3H_8$	$C_3H_6$	$C_2H_6$	$C_2H_4$	$CH_4$	CO	$CO_2$
82.4	6.7	0.15	1.41	2.40	9.7	1.33
66.2	13.1	0.86	6.71	5.94	24.1	2.32
59.4	13.4	1.47	9.97	9.34	27.4	2.63
82.2	10.2	0.77	2.08	0.64	11.9	1.10
73.1	11.7	0.88	2.94	2.15	18.8	1.64
72.8	12.0	0.72	2.22	1.58	18.2	1.69
86.0	9.76	1.31	1.68	0.76	9.1	0.60
79.9	10.0	0.27	1.84	1.35	11.0	0.64
82.1	10.6	0.24	2.19	1.93	12.4	0.84
79.0	9.50	0.20	1.86	1.65	12.1	0.91
82.8	9.67	0.62	1.88	0.64	10.7	1.14
79.7	11.32	0.73	2.63	1.52	15.3	1.57
77.2	9.59	0.75	2.53	1.91	15.1	1.57
70.6	11.09	0.81	2.99	3.41	18.2	1.86
63.1	8.50	0.74	2.50	2.74	15.2	1.42
79.3	8.20	0.61	2.42	1.38	14.3	1.21
77.2	9.30	0.14	2.09	0.84	12.4	1.14
66.6	9.85	0.55	2.01	0.85	13.9	1.32
69.6	12.1	0.61	2.96	2.10	18.3	1.68
64.9	12.2	0.67	3.09	2.08	18.0	1.57
96.3	2.65	—	0.40	trace	0.95	trace
89.8	5.26	—	2.31	1.10	3.50	trace
95.4	11.63	—	4.43	2.27	11.4	2.97
76.8	10.2	—	6.20	3.50	13.0	3.3
97.5	1.86	—	0.52	trace	1.69	trace
85.6	9.24	—	2.29	1.34	10.1	1.04
82.1	8.78	—	2.30	1.43	10.1	1.03
78.8	9.77	—	2.56	1.96	11.3	1.08
79.8	9.75	—	2.63	2.26	12.0	1.11

**Table I.**  
 Reaction temperature, 430°C.;  
 Products, moles/100 moles

Reactor	Run No.	O <sub>2</sub>	H <sub>2</sub> O <sub>2</sub>	H <sub>2</sub> O	CH <sub>3</sub> OH	HCHO
I <sup>a</sup> (untreated)	172	19.8	2.49	32.7	2.13	2.47
	170	0.15	0.68	52.6	0.66	2.88
	171	0	0.73	54.5	0.85	2.89
II (aged)	213	16.9	8.57	22.7	4.31	2.95
	212	1.34	10.01	35.3	4.02	1.94
	230	0.72	11.95	38.7	5.08	2.65
III (HF)	343	8.28	8.65	24.2	3.87	1.57
	342	3.09	9.93	26.1	4.30	1.51
	340	1.03	10.73	31.0	3.76	1.08
	334	1.27	9.48	28.6	3.68	1.99
IV (H <sub>3</sub> PO <sub>4</sub> )	248	13.7	6.52	33.5	4.72	2.81
	247	3.3	9.13	48.9	5.11	2.57
	224	1.98	9.18	47.6	4.07	2.20
	246	0.38	9.03	59.3	4.04	1.67
	245	0.56	6.04	69.1	3.72	1.98
V (HNO <sub>3</sub> )	253	6.19	4.46	37.5	2.91	2.36
	254	7.98	7.49	46.9	3.05	3.57
	250	8.12	8.30	52.6	3.24	2.14
	252	0.72	7.37	53.9	2.80	2.38
	251	2.60	6.51	57.6	3.69	2.08
VI <sup>b</sup> (untreated)	1,027	24.34	0.47	6.24	0.03	0.09
	1,028	21.80	0.76	15.92	0.08	0.41
	1,029	0.60	0.34	44.78	0.23	3.35
	1,030	0.10	0.1	45.2	0.31	2.02
VII (H <sub>3</sub> PO <sub>4</sub> )	1,051	22.3	1.88	9.80	0.95	0.36
	1,052	3.98	6.07	34.2	2.95	0.97
	1,053	3.86	5.60	33.4	2.96	1.11
	1,054	1.60	6.04	37.6	2.88	0.73
	1,055	0.68	6.36	43.1	3.26	0.45

<sup>a</sup> I–V: Transparent quartz reactors, i.d., 38 mm.; length 720 mm., surface by volume, 2.58 cm.<sup>-1</sup>.

quartz Reactor I, the hydrogen peroxide concentration was very low, never exceeding 3 wt. % in 28 hours. In the stainless steel Reactor VII, the concentration attained 28% in 16 hours, while with Reactor VI, the concentration was as small as 1 wt. % and constant. The aging of the reactor wall mentioned above seems most interesting, and the mechanism will be investigated further.

**Continued**

mole ratio of propane to oxygen, 3

*of Propane Fed*

$\text{CH}_3\text{CHO}$	$\text{CH}_3\text{COCH}_3$	$\text{CH}_3\text{CH} \begin{array}{c} \diagup \\ \text{O} \\ \diagdown \end{array} \text{CH}_2$	Selectivity <sup>c</sup> for Propylene, %	$\text{H}_2\text{O}_2/\text{C}_3\text{H}_6$ , mole ratio
3.75	2.13	2.88	37.9	0.372
3.96	0.66	2.19	38.8	0.052
3.77	0.86	0.31	33.0	0.054
2.81	1.72	1.85	57.3	0.84
2.84	1.81	0.39	43.5	0.86
4.68	3.41	0.52	44.1	0.996
1.68	0.16	1.10	69.7	0.80
1.53	0.28	1.29	49.7	0.993
1.35	0.37	1.22	59.2	1.013
1.15	0.59	1.34	45.7	0.998
2.21	2.00	1.39	56.2	0.674
2.20	1.75	2.12	55.9	0.806
1.80	0.64	2.52	42.0	0.959
1.73	0.62	2.50	37.7	0.815
1.74	0.48	2.44	23.0	0.710
1.77	0.96	1.27	39.6	0.545
2.32	0.50	2.10	40.8	0.806
2.05	1.09	2.97	29.5	0.843
2.08	0.38	2.42	39.8	0.609
2.26	0.34	2.91	34.7	0.534
0.08	—	—	71.6	0.178
0.23	—	—	51.5	0.145
3.02	—	—	47.3	0.029
1.26	—	—	44.0	0.009
0.64	—	—	74.4	1.010
1.94	—	—	64.1	0.657
2.66	—	—	49.0	0.638
1.89	—	—	46.1	0.618
1.78	—	—	48.3	0.652

<sup>b</sup> VI-VII: Stainless steel reactors, i.d., 28 mm.; length, 720 mm.; surface by volume, 2.22 cm.<sup>-1</sup>.

<sup>c</sup> Propylene formed/propane consumed.

**Effect of S/V Ratio.** The reactor wall plays two important roles in this oxidation. First, the reactor surface promotes the initiation of radical chain (12), but if it is exceedingly large, it adversely affects the total rate of the oxidation reaction (6, 12). Second, it accelerates heterogene-

ous decomposition of hydrogen peroxide. Accordingly, there could exist an optimum reactor surface-to-volume ratio ( $S/V$ ) to give the best yield of hydrogen peroxide. The effect of  $S/V$  was therefore investigated in the range of  $1\text{--}3\text{ cm.}^{-1}$ .

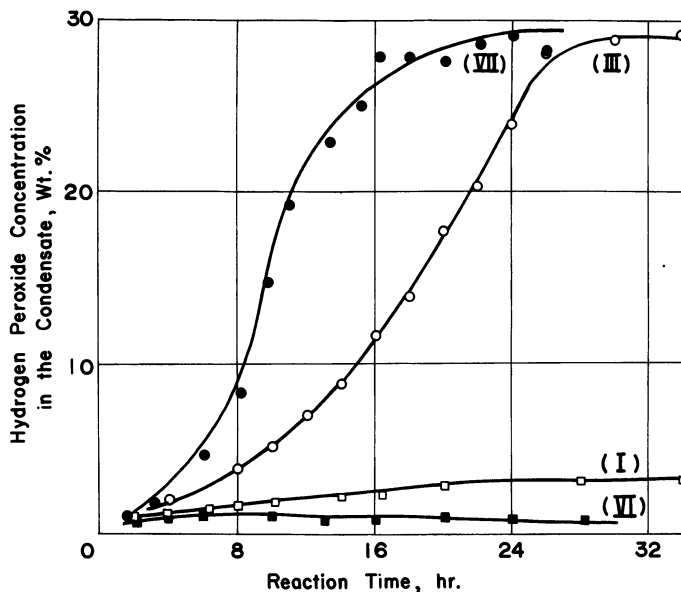


Figure 2. Aging of pretreated reactors

- (I) Quartz reactor untreated
- (II) Quartz reactor treated with HF
- (VI) SUS 27 reactor untreated
- (VII) SUS 27 reactor treated with  $H_3PO_4$

A quartz tube reactor (i.d. 38 mm., length 720 mm.) was used after 12 hours immersion in 30% HF solution at room temperature, followed by washing thoroughly with distilled water.

To change the wall surface area, quartz rods which had been subjected to the same pretreatment were inserted into the reactor in the axial direction. The results are presented in Table II, where the reaction temperature was  $430^\circ\text{C.}$ , and the propane to oxygen mole ratio was 3. Evidently the yield of hydrogen peroxide is the smallest at  $S/V$  of  $1.25\text{ cm.}^{-1}$  and the largest at  $2.58\text{ cm.}^{-1}$ .

As far as these experimental results are concerned,  $S/V$  of  $2.58\text{ cm.}^{-1}$  seemed optimum, but some further experiments should be done to cover smaller  $S/V$  ranges for designing industrial reactors.

**Table II. Effect of S/V of Reactor<sup>a</sup>**

Surface to Volume, cm. <sup>-1</sup>	1.25	1.93	2.58	3.00
Run No.	289	294	313	319
Residence time, sec.	8.20	10.70	8.95	12.6
Conversion, mole %				
C <sub>3</sub> H <sub>8</sub>	23.2	15.6	22.5	15.7
O <sub>2</sub>	100	98.5	92.0	84.4
Products, moles per 100 moles of propane fed				
C <sub>3</sub> H <sub>8</sub>	76.8	84.4	77.5	84.3
C <sub>3</sub> H <sub>6</sub>	8.23	9.98	12.9	9.37
C <sub>2</sub> H <sub>4</sub>	2.90	2.43	2.01	2.00
CH <sub>4</sub>	3.01	2.41	1.35	2.17
CO <sup>r</sup>	9.12	9.38	9.60	11.23
O <sub>2</sub>	trace	0.35	2.11	3.90
H <sub>2</sub> O <sub>2</sub>	6.01	9.50	12.57	8.94
H <sub>2</sub> O	26.0	24.9	33.9	21.2
CH <sub>3</sub> OH	3.81	3.86	4.42	5.02
HCHO	0.69	1.32	0.81	1.31
CH <sub>3</sub> CHO	1.51	1.91	1.37	1.83
CH <sub>3</sub> COCH <sub>3</sub>	0.59	0.60	1.08	1.14
CH <sub>3</sub> CH—CH <sub>2</sub>   O	1.64	1.62	0.98	0.92
Selectivity for propylene	35.5	63.0	57.4	59.7
H <sub>2</sub> O <sub>2</sub> /C <sub>3</sub> H <sub>6</sub> , mole ratio	0.730	0.952	0.975	0.954

<sup>a</sup> Reaction temperature, 430°C.; mole ratio of propane to oxygen, 3.

**Effect of Reaction Temperature.** The effect of the reaction temperature was investigated using Reactor III, which gives the highest hydrogen peroxide yield. A quartz tube reactor (i.d. 18 mm., length 600 mm.) was used after immersion in HF solution for 12 hours at room temperature, followed by washing with distilled water. The mole ratio of propane to oxygen was 2 at reaction temperatures 400, 430, and 450°C., and 4 at 480°C.

Table III gives the results for each reaction temperature. The experimental data are of the runs at the optimum residence time which give the maximum hydrogen peroxide yield at the respective temperature.

For Run 224 at a reaction temperature of 450°C. the residence time was shorter than that which would give the best result at this temperature. Probably a residence time of 6–7 sec. and a ratio of H<sub>2</sub>O<sub>2</sub>/C<sub>3</sub>H<sub>6</sub> of *ca.* 1 would be optimum.

Above 430°C., 10 mole % of hydrogen peroxide can be obtained. Accordingly, the optimum temperature for this reaction lies between 430–450°C. The selectivity for propylene is therefore 30–40% on the consumed propane with the mole ratio of hydrogen peroxide to propylene of nearly unity.

Table III. Effect of Reaction Temperature<sup>a</sup>

Reaction temperature, °C.	400	430	450	480 <sup>b</sup>
Run No.	226	221	224	269
Residence time, sec.	11.4	9.7	4.7	5.4
Conversion, mole %				
C <sub>3</sub> H <sub>8</sub>	30.8	32.7	36.4	20.4
O <sub>2</sub>	88.2	82.8	89.5	100
Products, moles per 100 moles of propane fed				
C <sub>3</sub> H <sub>8</sub>	69.2	67.3	63.6	79.7
C <sub>3</sub> H <sub>6</sub>	7.10	10.07	12.30	11.01
C <sub>2</sub> H <sub>4</sub>	1.98	2.41	1.44	2.33
CH <sub>4</sub>	1.68	1.88	2.57	1.44
CO	20.9	18.3	15.9	2.83
O <sub>2</sub>	3.88	5.49	3.33	0
H <sub>2</sub> O <sub>2</sub>	7.03	10.83	10.23	10.27
H <sub>2</sub> O	41.5	42.2	47.1	24.9
CH <sub>3</sub> OH	6.27	3.15	2.51	2.12
HCHO	3.11	1.80	1.16	0.85
CH <sub>3</sub> CHO	4.53	3.08	2.65	2.24
CH <sub>3</sub> COCH <sub>3</sub>	3.78	3.29	2.33	1.37
$\begin{array}{c} \text{CH}_3\text{CH} \\ \diagdown \quad \diagup \\ \text{O} \end{array}$ —CH <sub>2</sub>	0.75	0.57	0.27	4.32
Selectivity for propylene	23.0	30.8	33.8	54.1
H <sub>2</sub> O <sub>2</sub> /C <sub>3</sub> H <sub>6</sub> , mole ratio	0.99	1.08	0.83	0.93

<sup>a</sup> Opaque quartz reactor treated with HF, surface by volume 2.50 cm.<sup>-1</sup>, mole ratio of propane to oxygen, 2.

<sup>b</sup> Mole ratio of propane to oxygen, 4.

The optimum residence times are to be 11–12 sec. for 400°C., 8–10 sec. for 430°C., 6–7 sec. for 450°C. and 4–6 sec. for 480°C. Carbon monoxide, methanol, formaldehyde, and acetone are decreased with the increase in reaction temperature. At 480°C. the yield of carbon monoxide is a little less and that of propylene oxide is more than those at the other temperatures because of the smaller content of oxygen in the feed gas.

**Effect of Propane to Oxygen Mole Ratio in Feed.** Table IV gives the results for the propane and oxygen mole ratio ranging from 2 to 8. Stainless steel Reactor VII was used for these experiments after the phosphoric acid pretreatment; the reaction temperature was 430°C. The product gas was cooled in the Liebig condenser at 2°C., and the condensate was analyzed.

The main products were hydrogen peroxide, methanol, formaldehyde, acetaldehyde, and water. The change in mole ratio of propane and oxygen in feed from 2 to 8 had almost no influence upon the hydrogen peroxide formation. The yields of methanol, formaldehyde, and acetaldehyde increased and that of water decreased with decreasing mole ratio

of oxygen. For a mole ratio of 2, the residence time was so long that the experimental results did not agree with the general rule mentioned above.

In a quartz reactor both the amount of condensed liquid and the hydrogen peroxide concentration were larger than those with stainless steel reactor. For example the hydrogen peroxide yield of Run 340 was about 25% higher than that of Run 54.

A concentration of hydrogen peroxide as high as 28 wt. % was obtained by using Reactors III (quartz) and VII (SUS 27) (Figure 2). This is extremely high compared with those in Table IV, namely from 16–22 wt. %. This is caused by the general trend that the yield of water increases with an increase in oxygen consumption. The experiments in Figure 2 were carried out at the shorter residence time, while those in Table IV were conducted at the longer residence time where oxygen consumption was more than 90%.

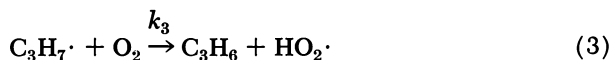
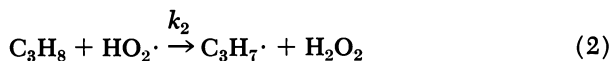
**Table IV. Effect of Feed Mole Ratio of Propane to Oxygen<sup>a</sup>**

Propane/oxygen, mole ratio	2	3	4	6	8	3 <sup>b</sup>
Run No.	62	54	88	92	99	340
Residence time, sec.	11.2	6.3	6.7	5.8	5.2	7.2
Conversion of oxygen, mole %	96.2	95.3	91.3	98.6	98.7	97.1
Condensate, grams/consumed						
O <sub>2</sub> mole	32.2	34.7	34.1	34.0	32.2	38.0
Composition of condensate, wt. %						
H <sub>2</sub> O <sub>2</sub>	19.8	19.0	16.1	18.0	18.7	22.0
CH <sub>3</sub> OH	9.35	8.55	10.3	12.4	17.4	10.0
HCHO	6.20	2.07	3.72	6.59	7.44	3.03
CH <sub>3</sub> CHO	8.03	7.73	9.87	14.03	16.11	4.35
H <sub>2</sub> O and others	56.6	62.7	58.3	47.6	38.7	60.6

<sup>a</sup> Stainless steel reactor treated with H<sub>3</sub>PO<sub>4</sub>, reaction temperature, 430°C., surface by volume, 2.22.

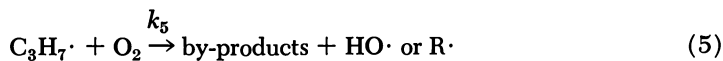
<sup>b</sup> Reactor III (transparent quartz reactor treated with HF) in Table I.

**Kinetic Studies.** The real reaction scheme would be so complicated that some simplification is desirable for discussion. First, the reactions which lead to the main products H<sub>2</sub>O<sub>2</sub> and C<sub>3</sub>H<sub>6</sub> are assumed to be:

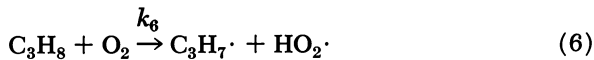


The by-products are formed by the following chain propagation:

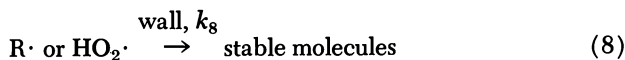




In addition to these chain propagation reactions the following chain initiation reactions are assumed.



The chain termination reactions are:



For the decomposition of hydrogen peroxide the following reaction is considered with Reaction 7:



The whole reaction scheme can be described by Figure 3.

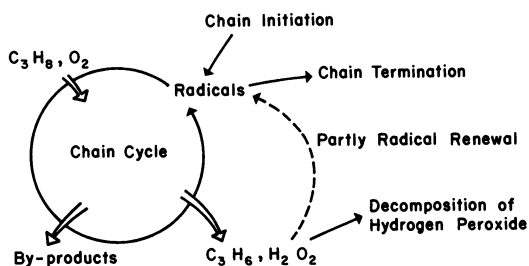


Figure 3. Reaction scheme

Reaction 7 means that hydrogen peroxide can be a radical source by decomposition—*i.e.*, one of the reaction products is the origin of radicals. Accordingly this oxidative dehydrogenation reaction has the feature of the degenerative branching. Naturally one may also assume that other peroxides or aldehydes could be origins of radicals. However, Reaction 7 is considered to be the sole source of radicals from the reaction products.

In the above all the radicals other than  $\text{HO}\cdot$  and  $\text{HO}_2\cdot$  were written by one symbol,  $\text{R}\cdot$ . For simplification, all the radicals which participate in this reaction are now expressed by  $\text{X}$ . The changes of radicals, oxygen,

hydrogen peroxide, and propylene with time can be described by the following equations based on the above reaction scheme:

$$\frac{d(X)}{dt} = k_8(C_3H_8)(O_2) + k_7(H_2O_2) - k_8(X) - k_9(X)^2 \quad (8)$$

$$- \frac{d(O_2)}{dt} = k_6(C_3H_8)(O_2) + (k_3 + k_5)(O_2)(X) \quad (9)$$

$$\frac{d(H_2O_2)}{dt} = k_2(C_3H_8)(X) - (k_7 + k_7')(H_2O_2) \quad (10)$$

$$- \frac{d(C_3H_8)}{dt} = (k_2 + k_4)(C_3H_8)(X) \quad (11)$$

If propylene is assumed to be formed along with hydrogen peroxide and allowed to react with the radical, the total rate of its formation is described by Equation 12.

$$\frac{d(C_3H_6)}{dt} = k_2(C_3H_8)(X) - k_{12}(C_3H_6)(X) \quad (12)$$

Now the stationary state assumption is applied to the Equation 8 to obtain:

$$(X) \doteq \left\{ \frac{k_8(C_3H_8)(O_2) + k_7(H_2O_2)}{k_9} \right\}^{1/2}$$

where  $k_8(C_3H_8)(O_2)$  is small enough compared with  $k_7(H_2O_2)$  outside the initial stage of the reaction. Then X is given by:

$$(X) \doteq (k_7/k_9)^{1/2}(H_2O_2)^{1/2}$$

By replacing (X) in Equations 9, 10, 11, and 12 with this equation, and by converting the concentrations of hydrogen peroxide, propane, and propylene into dimensionless concentrations, we obtain:

$$[H_2O_2] = \frac{100 \times (H_2O_2)}{(C_3H_8)_o}, \quad [C_3H_8] = \frac{100 \times (C_3H_8)}{(C_3H_8)_o},$$

$$[C_3H_6] = \frac{100 \times (C_3H_6)}{(C_3H_8)_o}, \quad [O_2] = \frac{100 \times (O_2)}{(O_2)_o},$$

we get:

$$- \frac{d[O_2]}{dt} = C_1[O_2][H_2O_2]^{1/2} \quad (9')$$

$$\frac{d[H_2O_2]}{dt} = \alpha C_2[C_3H_8][H_2O_2]^{1/2} - C_3[H_2O_2] \quad (10')$$

$$- \frac{d[C_3H_8]}{dt} = C_2[C_3H_8][H_2O_2]^{1/2} \quad (11')$$

$$\frac{d[\text{C}_3\text{H}_6]}{dt} = \alpha C_2 [\text{C}_3\text{H}_8] [\text{H}_2\text{O}_2]^{1/2} - C_4 [\text{C}_3\text{H}_6] [\text{H}_2\text{O}_2]^{1/2} \quad (12')$$

where  $C_1$ ,  $C_2$ ,  $C_3$ , and  $C_4$  are the reaction rate coefficients with the dimension  $t^{-1}$ , and  $\alpha$  is  $k_2/(k_2 + k_4)$ . For example

$$C_1 = (k_3 + k_5) (k_7/k_9)^{1/2} \frac{(\text{C}_3\text{H}_8)_0}{100}$$

These reaction rate coefficients are all computed using the experimental data. For example, both sides of Equation 9' are integrated into

$$-[\text{O}_2] \Big|_{t_0}^t = C_1 \int_{t_0}^t [\text{O}_2] [\text{H}_2\text{O}_2]^{1/2} dt$$

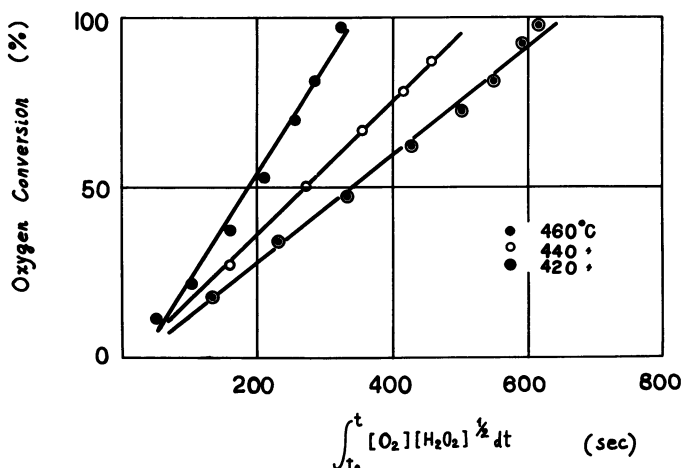


Figure 4. Oxygen conversion vs.  $\int_{t_0}^t [\text{O}_2] [\text{H}_2\text{O}_2]^{1/2} dt$   
Propane/oxygen = 3

The availability of Equation 9' will be assured if  $[\text{O}_2]$  and  $\int_{t_0}^t [\text{O}_2] [\text{H}_2\text{O}_2]^{1/2} dt$  are plotted to make a straight line, from the slope of which one can calculate the coefficient  $C_1$  (see Figure 4). By the same procedure  $C_2$  can be obtained from Equation 11'. Similarly, Equation 12' becomes

$$[\text{C}_3\text{H}_6] = \alpha \Delta [\text{C}_3\text{H}_8] - C_4 \int_{t_0}^t [\text{C}_3\text{H}_6] [\text{H}_2\text{O}_2]^{1/2} dt$$

and

$$\frac{[\text{C}_3\text{H}_6]}{\Delta [\text{C}_3\text{H}_8]} = \alpha - \frac{C_4}{\Delta [\text{C}_3\text{H}_8]} \int_{t_0}^t [\text{C}_3\text{H}_6] [\text{H}_2\text{O}_2]^{1/2} dt$$

by integration, where

$$\Delta[\text{C}_3\text{H}_8] = [\text{C}_3\text{H}_8]_0 - [\text{C}_3\text{H}_8]$$

Using this equation it is possible to obtain values of  $\alpha$  and  $C_4$ . Equation 10' can be used to calculate  $C_3$ . In Figure 5 the values of  $C_1$ ,  $C_2$ ,  $C_3$  as well as  $C_4$  and  $\alpha$  are shown, which were derived from experimental data.

At the reaction temperature 440°C. and feed gas composition  $\text{C}_3\text{H}_8/\text{O}_2 = 3$ , Equations 9', 10', and 11' become

$$\begin{aligned} \frac{d[\text{H}_2\text{O}_2]}{dt} &= 0.75 \times 3.2 \times 10^{-2} [\text{C}_3\text{H}_8] [\text{H}_2\text{O}_2]^{1/2} - 0.70 [\text{H}_2\text{O}_2] \\ &\quad - \frac{d[\text{O}_2]}{dt} = 2.0 \times 10^{-1} [\text{H}_2\text{O}_2]^{1/2} [\text{O}_2] \\ &\quad - \frac{d[\text{C}_3\text{H}_8]}{dt} = 3.2 \times 10^{-2} [\text{C}_3\text{H}_8] [\text{H}_2\text{O}_2]^{1/2} \end{aligned}$$

Applying the following initial condition

$$\begin{aligned} \text{at } t = 3 \quad & [\text{H}_2\text{O}_2] = 1 \\ & [\text{O}_2] = 90 \\ \text{and} \quad & [\text{C}_3\text{H}_8] = 98 \end{aligned}$$

the calculation was done with an analog-computer. As shown in Figure 6, calculated values agree well with the observed values within the range of experimental errors.

We now discuss the meaning of the reaction rate coefficients  $C_1$ ,  $C_2$ ,  $C_3$ , and  $C_4$ . In  $C_2 = (k_2 + k_4)(k_7/k_9)^{1/2} \frac{(\text{C}_3\text{H}_8)_0^{1/2}}{100}$ ,  $k_7$  is presumed from the literature to be about  $10^{15} e^{-45,000/RT}$  (M) where (M) is the inert gas concentration (mole/liter).  $k_9$  is the rate constant of the radical recombination and is about  $10^{11} e^{-O/RT}$ . The rate constant of hydrogen atom abstraction from propane molecule by a radical is assumed to be  $10^{11} e^{-10,000/RT}$ . The over-all rate constant  $(k_2 + k_4)(k_7/k_9)^{1/2}$  can then be estimated to be  $1.5 \times 10^{12} e^{-33,000/RT}$ , which corresponds to 0.7 (liter/mole)<sup>1/2</sup> sec.<sup>-1</sup> at 700°K.

One can also obtain the experimental value of  $C_2$  at this temperature from Figure 5. When conversion is made for the propane initial concentration in the feed gas, the over-all reaction rate of propane consumption becomes 1-2 (liter/mole)<sup>1/2</sup> sec.<sup>-1</sup> at 700°K. with an activation energy of 30 kcal. Therefore,  $C_2$  can be related reasonably to the calculated value of  $(k_2 + k_4)(k_7/k_9)^{1/2}$ .

From Figure 5 the activation energy of  $C_4$  is calculated to be about 25 kcal. which is acceptable.

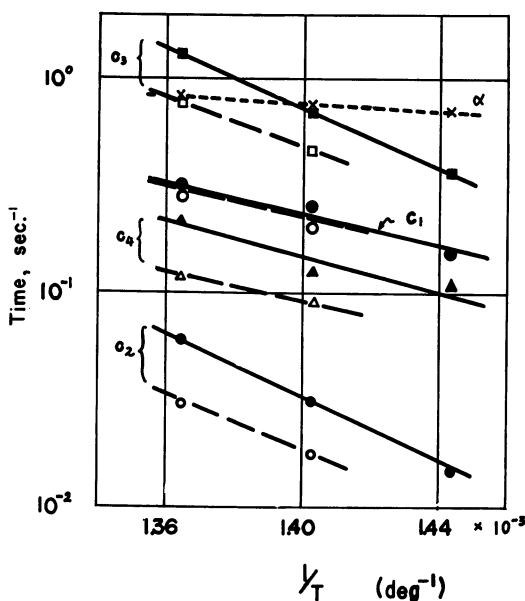


Figure 5. Values of various coefficients

— Propane/oxygen, 3  
 ---- Propane/oxygen, 4

For  $C_1$  the activation energy is 20 kcal. However, if this were really the activation energy of the over-all rate constant of oxygen consumption, then

$$\begin{aligned} E_{C_1} &\doteq E_{k_3, k_5} + \frac{1}{2}E_{k_7} - E_{k_9} \\ &= E_{k_3, k_5} + \frac{1}{2}(45) - \frac{1}{2}(0) \end{aligned}$$

$E_{k_3}$  or  $E_{k_5}$  is almost zero, and hence  $E_{C_1}$  is calculated to be 22.5 kcal./mole, in good agreement with the experimentally found value 20 kcal./mole. There could be another initiation reaction which has lower activation energy than Reaction 7.

It is clear that the reaction rate constants  $C_1$ ,  $C_2$ ,  $C_3$ ,  $C_4$ , and  $\alpha$  are available for illustrating the formation of various reaction products quantitatively, and these constants are quite reasonable from the theoretical viewpoint of radical reaction.

### Summary

The synthesis of hydrogen peroxide by noncatalytic oxidative dehydrogenation of propane was studied using the conventional flow reactor.

At the reaction temperatures ranging from 430° to 450°C. and residence time 6–8 sec. under atmospheric pressure the reaction proceeded with fairly high selectivity for hydrogen peroxide and propylene formation.

By suitable pretreatment of the reactor wall a hydrogen peroxide concentration of about 30% in the condensed reaction products was obtained, which is markedly higher than the previously reported values.

With regard to the influences of the reaction conditions, the following experimental results were obtained.

(1) By using a quartz reactor suitably pretreated the selectivity of the main reaction could be remarkably increased. The effect of pretreatment was in the following order of increasing selectivity.

treated with 30% HF > aged > treated with  $\text{H}_3\text{PO}_4$  >  
treated with  $\text{HNO}_3$  > untreated

(2) A good yield of hydrogen peroxide was also obtained in the stainless steel reactor by treating with phosphoric acid. The yield of hydrogen peroxide was, however, only 60% of those of the above quartz reactor.

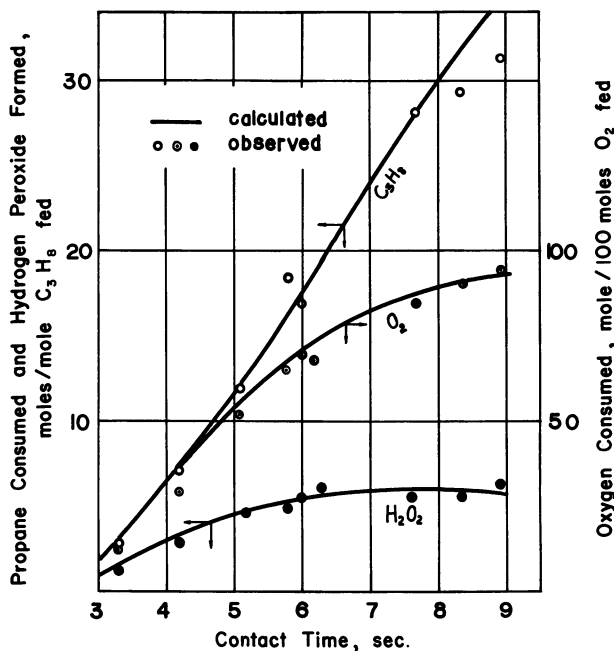


Figure 6. Comparison of calculated and observed values  
 $T = 440^\circ\text{C}$ .

Propane/oxygen = 3

(3) Even with the pretreated reactor, aging of 16–24 hours was necessary to obtain a high yield of hydrogen peroxide. While for the untreated reactor 10 days for pretreatment were required.

(4) The optimum condition for hydrogen peroxide formation was concluded to be a propane/oxygen mole ratio 3, temperature of 430°–450°C., and a residence time 6–10 sec.

Kinetic analysis of the experimental data was attempted using a simplified reaction scheme, although the actual reaction mechanism is rather complicated, as proposed by Semenov. We are convinced of the availability of such method for interpreting the reaction and for chemical plant design calculations.

### *Literature Cited*

- (1) Harris, C. R., U. S. Patent 2,533,581 (1950).
- (2) Kunugi, T., Japanese Patent 478,425 (1966).
- (3) Kuta, E. T., Quackenbush, F. W., *Anal. Chem.* **39**, 1069 (1960).
- (4) Lacomble, A. E., U. S. Patent 2,416,156 (1945).
- (5) Peace, R. N., Munro, P., *J. Am. Chem. Soc.* **57**, 2296 (1935).
- (6) Peace, R. N., *J. Am. Chem. Soc.* **51**, 1839 (1929).
- (7) Satterfield, C. N., *Anal. Chem.* **26**, 1792 (1954).
- (8) Satterfield, C. N., *Ind. Eng. Chem.* **46**, 1001 (1954).
- (9) *Ibid.*, **49**, 1173 (1957).
- (10) *Ibid.*, **41**, 2595 (1949).
- (11) Semenov, N. N., "Some Problems in Chemical Kinetics and Reactivity," Vol. 1, Princeton University, Princeton, N. J., 1958.
- (12) Steacie, E. W. R., *Proc. Roy. Soc.* **A146**, 583 (1934).

RECEIVED October 12, 1967.

# Oxidation of Olefins Catalyzed by Selenium

J. L. HUGUET

Celanese Chemical Co., Technical Center, P. O. Box 2768, Corpus Christi, Tex.

*The oxidation of 2-butene with selenium dioxide in acetic acid solution produces 1-acetoxy-2-butene as the oxidation product of the olefin and bis(1-methyl-2-acetoxypropyl)-selenide (I) as the final reduced state of the oxidant instead of elemental selenium. Further, (I) may act as a catalyst for the oxidation of 2-butene with peracetic acid or oxygen to 3-acetoxy-1-butene. A mechanism is proposed to explain the formation of selenides in the oxidation of olefins with selenium dioxide and their catalytic activity in the oxidation of olefins with other oxidants.*

The oxidation of olefins by selenium dioxide has received much attention because of the unique characteristics of the reaction that produces an allylic derivative of the olefin (ester, alcohol, or ether, depending upon the solvent) and elemental selenium as the final reduced state of the oxidant.

It has been reported occasionally that variable quantities of organo-selenium compounds are produced during the oxidation (3, 7). These compounds have been considered as side reaction products and have received little attention regarding their nature or possible role in the reaction. In this work we have studied the characteristics of these organoselenium compounds, their role in the mechanism of the oxidation of olefins with selenium dioxide, and their catalytic properties in the oxidation of olefins with other oxidants.

## **Experimental**

**Equipment and Materials.** The peracetic acid-acetic acid solution was obtained by distillation (100 mm. HgA, 40°C.) of Becco 40% solution in acetic acid, which had been dried with slight excess of acetic

anhydride. The olefins were from Phillips Petroleum Co. The 2-butene was a mixture of *cis* and *trans* isomers (45% *cis*).

The reaction system for the oxidation of the gaseous olefins consisted of a stirred glass reactor fitted with a gas buret, and it was operated at pressures up to 80 p.s.i.g. Reactions at higher pressures were conducted in a metal autoclave mounted in a rocker.

Vapor phase chromatography was used to analyze allylic oxidation products. The column,  $\frac{1}{4}$  inch  $\times$  35 feet, was packed with 20% UCON 5100 on Celite (50-70). NMR analyses were performed using a Varian A-60 instrument. Molecular weights were determined by cryoscopic methods (benzene and acetic acid solvents). Organoselenium compounds were analyzed for selenium by the method of Gould (2), which involves wet digestion of the sample, followed by iodometric titration of the selenium dioxide produced.

**Purification of the Organoselenium Compounds.** After the oxidation of 2-butene with selenium dioxide was completed, the acetic acid solvent and the volatile reaction products were distilled at reduced pressure (10 mm. HgA). The residue, a yellow oil, was purified by adsorption chromatography in a column packed with silica gel. *n*-Hexane and ethyl ether were used as eluents. The same procedure was applied to the fractionation and purification of the organoselenium compounds obtained from the oxidation of bis(1-methyl-2-acetoxypropyl) selenide with peracetic acid.

**Oxidation of Bis(1-methyl-2-acetoxypropyl)selenide with Peracetic Acid.** The oxidation of the selenide was conducted in a 10 wt. % solution in glacial acetic acid at 5°C. Peracetic acid was added dropwise as a 1M solution in acetic acid. To prevent any potential overoxidation of the selenide, only 0.3 mole of peracetic acid per mole of selenide was used.

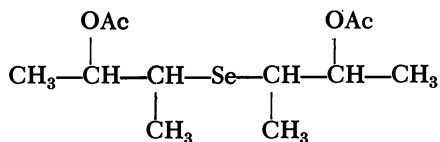
**Oxidation of Bis(1-methyl-2-acetoxypropyl)selenide in the Presence of 2-Butene.** The oxidation of the selenide was conducted at 5°C. in glacial acetic acid solution saturated with 2-butene. The initial reaction was discontinued after adding 0.3 mole of peracetic acid per mole of selenide. The temperature was raised to 45°C., and the reaction was allowed to proceed for 15 minutes under a 2-butene atmosphere. These steps were repeated several times until the addition of 7 moles of peracetic acid per mole of selenide was completed.

**Oxidation of 2-Butene with Oxygen, Catalyzed by Bis(1-methyl-2-acetoxypropyl)selenide.** This reaction was conducted at 120°C. and total pressures from 80 to 400 p.s.i.g. and oxygen partial pressures from 5 to 40 p.s.i.g.

## Results

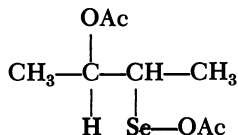
**Oxidation of 2-Butene with Selenium Dioxide.** The oxidation was conducted in glacial acetic acid at atmospheric pressure and temperatures from 56° to 80°C. Approximately 3 moles of olefin were absorbed per mole of selenium dioxide consumed. The reaction produced 0.85 mole of 1-acetoxy-2-butene, 0.03 mole of 3-acetoxy-1-butene, and 0.85

mole of bis(1-methyl-2-acetoxypropyl)selenide,



per mole of selenium dioxide consumed. Only trace amounts of elemental selenium could be observed occasionally. The structure of the organoselenium compound was determined by NMR analysis. The elemental analysis and the molecular weight determination were in agreement with the proposed structure.

**Oxidation of Bis(1-methyl-2-acetoxypropyl)selenide with Peracetic Acid.** The reaction produced 0.75 mole of 3-acetoxy-1-butene per mole of peracetic acid consumed, and a new organoselenium compound was isolated from the reaction solution. NMR analysis of this compound led us to suggest that it was a substituted alkylselenenyl acetate of the following structure:



1-methyl-2-acetoxypropylselenenyl acetate. Elemental analysis and molecular weight determination agreed with the proposed structure.

**Oxidation of Bis(1-methyl-2-acetoxypropyl)selenide in the Presence of 2-Butene.** The only product of the reaction was 3-acetoxy-1-butene. No epoxides and only traces of diols were detected in the reaction product. Approximately 0.85 mole of 3-acetoxy-1-butene was produced per mole of peracetic acid consumed, and approximately 90% of the original selenide was recovered unchanged.

**Oxidation of Bis(1-methyl-2-acetoxypropyl)selenide in the Presence of 2-Methyl-2-butene.** The analysis of the solution near the beginning of the reaction showed that 3-acetoxy-1-butene was the only initial product of the oxidation, but after adding 0.5 mole of peracetic acid per mole of selenide, increasing amounts of the oxidation products of 2-methyl-2-butene, such as 2-methyl-3-acetoxy-1-butene, and 3-methyl-3-acetoxy-1-butene were detected. After adding 4 moles of peracetic acid per mole of selenide, the allylic products from the oxidation of 2-methyl-2-butene appeared to be the only ones being formed in the reaction. The complex mixture of organoselenium compounds obtained at the end of the reaction was fractionated by adsorption chromatography. The NMR spectra of two of the fractions obtained indicated that they were relatively pure samples of bis(1,1-dimethyl-2-acetoxypropyl)selenide and

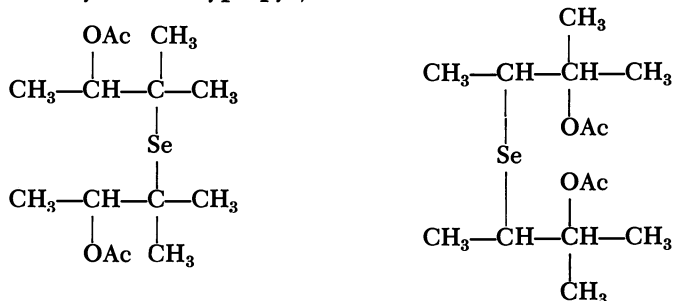
**American Chemical Society**

**Library**

**1155 16th St., N.W.**

**Washington, D.C. 20036**

bis(1,2-dimethyl-2-acetoxypropyl)selenide



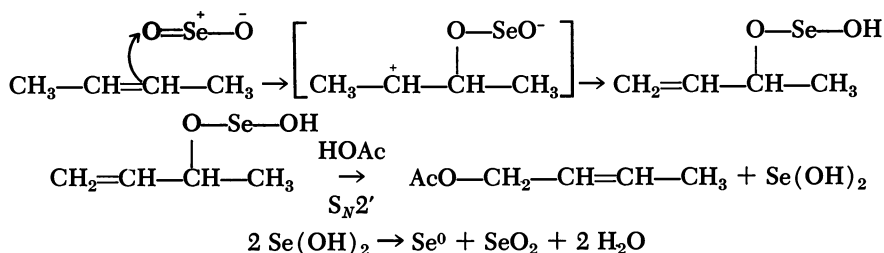
**Oxidation of 2-Butene with Oxygen, Catalyzed by Bis(1-methyl-2-acetoxypropyl)selenide.** The oxidation of the selenide by oxygen proceeded only when cupric chloride was added to the system. Since cupric chloride alone did not oxidize the selenide, we believe that the oxidation proceeds through interaction of oxygen with an intermediate complex formed by the selenide with the copper halide.

The product of the oxidation of 2-butene with oxygen in the presence of bis(1-methyl-2-acetoxypropyl)selenide was 3-acetoxy-1-butene in acetic acid as solvent and 3-hydroxy-1-butene ( $\alpha$ -methylallyl alcohol) in aqueous dioxane. The reaction rate depends on the selenide concentration.

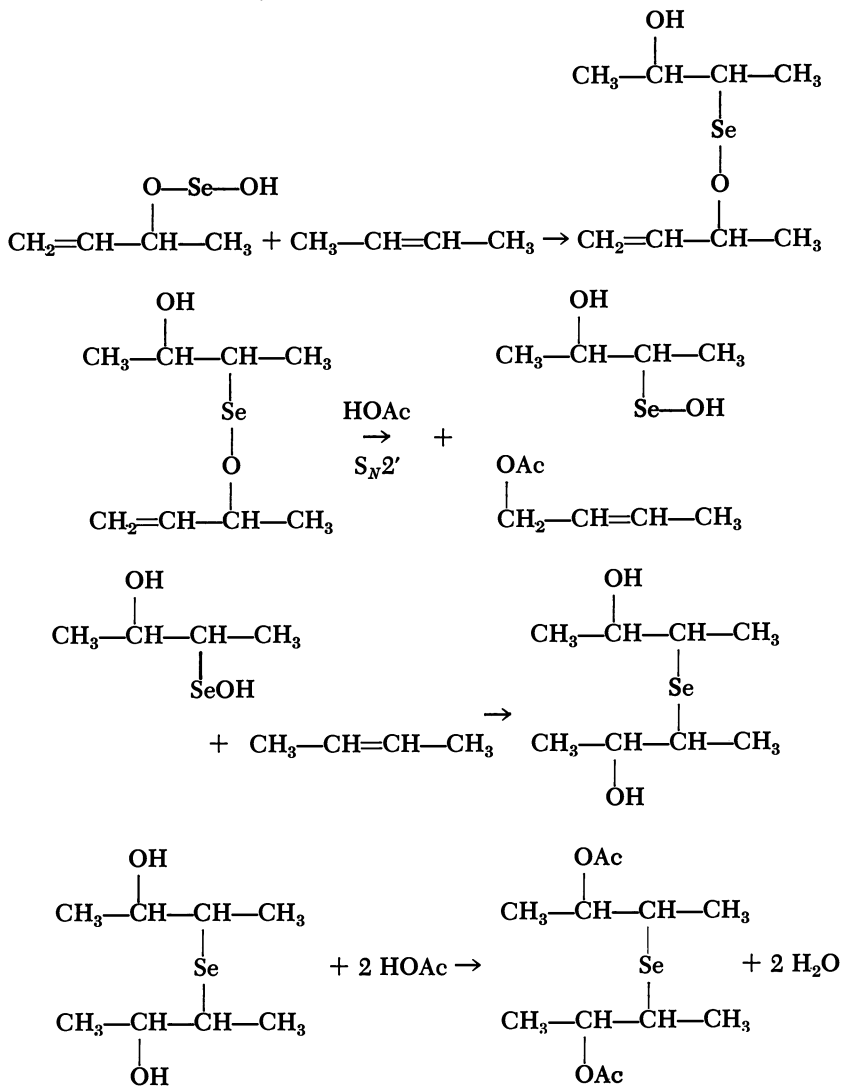
### Discussion

**Oxidation of 2-Butene with Selenium Dioxide.** The stoichiometry of the reaction of 2-butene with selenium dioxide shows that approximately 0.85 mole of 1-acetoxy-2-butene plus 0.85 mole of bis(1-methyl-2-acetoxypropyl)selenide are produced per mole of selenium dioxide consumed. This suggests that, at least for this particular group of olefins, in the mechanism of olefin oxidation with selenium dioxide the formation of selenides should be considered as the final reduced state of the oxidant rather than elemental selenium.

It has been generally accepted (5, 6) that the oxidation of olefins with selenium dioxide proceeds through attack on the olefinic double bond by selenium dioxide followed by rearrangement and solvolysis of the intermediate selenium(II) ester formed.

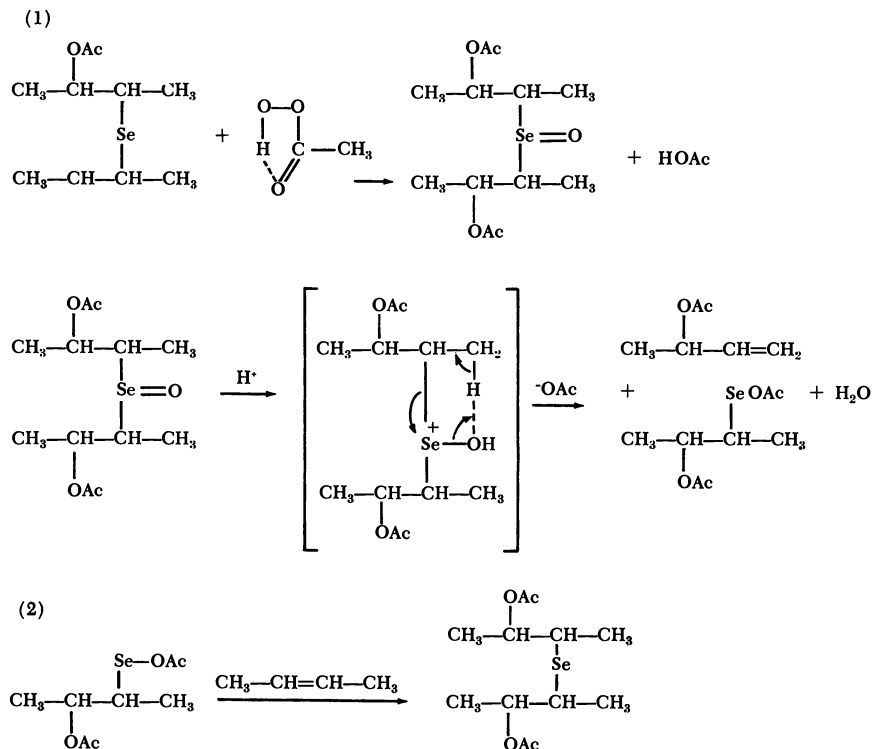


In the pathway that we are proposing for the formation of organoselenides, we also postulate the formation of a selenium(II) ester as the first step of the reaction. Further reaction of this ester with olefins followed by solvolysis will produce an intermediate alkylselenenic acid. Addition of this acid to an olefinic double bond will produce the type of selenide found in this system.



**Peracetic Acid Oxidation of 2-Butene Catalyzed by Bis(1-methyl-2-acetoxypropyl)selenide.** Based upon the identification of an alkylselenenyl acetate among the products of the oxidation of bis(1-methyl-2-

acetoxypropyl)selenide with peracetic acid (4) and based upon the reported addition of selenenyl acetates to olefinic (1) bonds, we postulate the following two-step mechanism for the oxidation of 2-butene catalyzed by bis(1-methyl-2-acetoxypropyl)selenide:

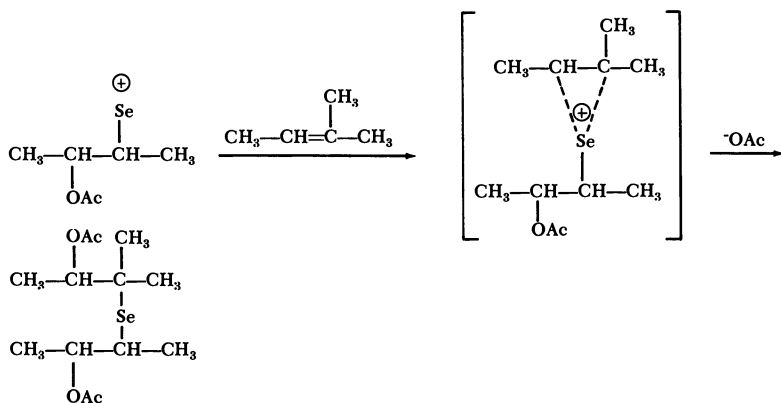
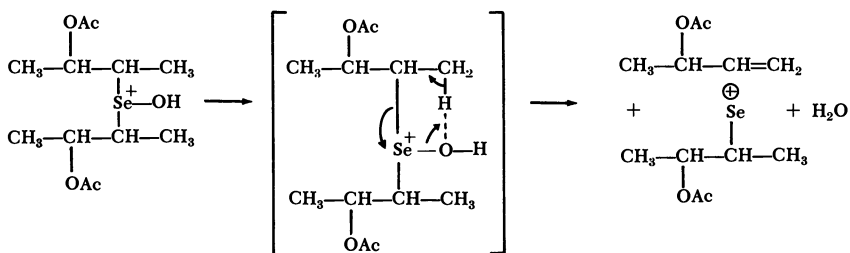


The fact that selenides with the selenium atom attached to the more highly substituted carbon of the double bond were identified among the products of the oxidation of bis(1-methyl-2-acetoxypropyl)selenide in the presence of 2-methyl-2-butene suggested that the reaction might proceed partially by the alternate mechanism shown opposite.

More experimental work involving the oxidation of selenides in the presence of substituted olefins is planned to elucidate this point further.

### Conclusions

(a) Organoselenium compounds play an important role in the oxidation of 2-butene with selenium dioxide. The organoselenides formed in the reaction should be considered as the final reduced state of selenium dioxide rather than elemental selenium.



(b) These organoselenides may function as catalysts in the oxidation of 2-butene with peracetic acid or oxygen, to 3-acetoxy-1-butene. (The oxidation of 2-butene with selenium dioxide under similar conditions produces 1-acetoxy-2-butene.)

(c) The mechanism of catalysis involves cleavage and regeneration of the selenide.

### Acknowledgments

The author thanks the Celanese Chemical Co. for permission to publish this work, Jack B. Causey for his valuable technical assistance, and L. W. Trevoy and L. Stautzenberger for their valuable suggestions.

### Literature Cited

- (1) Gosselck, J., *Angew. Chem. Intern. Ed. Engl.* **2**, 669 (1963).
- (2) Gould, E. S., *Anal. Chem.* **23**, 1502 (1951).
- (3) Guillemonat, A., *Ann. chim.* **11**, 193 (1939).
- (4) McCullough, J. D., Campbell, T. D., Gould, E. S., *J. Am. Chem. Soc.* **72**, 5753 (1950).
- (5) Nelson, C. H., Ph.D. Thesis, Clark University, 1965.
- (6) Schaefer, J. P., Horvath, B., *Tetrahedron Letters* **30**, 2023 (1964).
- (7) Wiberg, K. B., Nielsen, S. D., *J. Org. Chem.* **29**, 3353 (1964).

RECEIVED September 29, 1967.

## Autoxidation of Olefins Accompanying a Novel Hydrogen Transfer in a Silent Discharge

NOBORU SONODA, SHINJI YAMAMOTO, KENJI OKUMURA,  
SHUHEI NODA, and SHIGERU TSUTSUMI

Department of Chemical Technology, Faculty of Engineering, Osaka University,  
Yamadakami, Suita, Osaka, Japan

*The vapor-phase oxidation of olefins with oxygen or air has been carried out in a silent discharge. In the oxidation of cyclohexene, saturated products such as cyclohexanol and cyclohexanone were produced in comparable yields with corresponding  $\alpha,\beta$ -unsaturated derivatives. In the absence of oxygen, dimeric products such as bicyclohexyl, 3-cyclohexylcyclohexene, and 3,3'-bicyclohexenyl were formed; their relative product concentrations and the oxidation products described above demonstrate that allylic cyclohexenyl radical and cyclohexyl radical may be the main intermediates in these reaction systems. The formation of saturated products suggests that these oxidations may proceed accompanying a novel hydrogen transfer which may be occurring through some energetic process caused by the silent discharge.*

Although extensive studies have been done on the autoxidation of olefins, only a few reports have been published on these oxidations in a silent discharge. Fujimoto (7) and Sugino and co-workers (19) have reported the oxidation of ethylene and confirmed many of the reaction products. Inoue (13) reported that air oxidation of cyclohexane in the vapor phase at atmospheric pressure in a silent discharge led to the formation of cyclohexanol and cyclohexanone. He concluded that the first step of the reaction may be the formation of atomic oxygen through bond fission of the oxygen molecule by electron impact, followed by hydrogen

abstraction from cyclohexane by the atomic oxygen, and the rest of the reaction process may be similar to that of autoxidation.

In this paper, we report some observations on oxidation reactions of cyclohexene and propylene under silent discharge. A mixture of cyclohexene or propylene and air or oxygen under atmospheric pressure was allowed to react in a silent discharge tube at room temperature. Silent discharge was maintained under 60-cycle alternating current at 16 kvolts.

### *Experimental*

**Materials.** Cyclohexene, obtained by dehydration of reagent grade cyclohexanol (3), was heated at reflux over sodium metal, fractionated on a 60-cm. Helix packed column, stored over sodium, and filtered just before use. No impurity was found by gas chromatography (column, TCP and Si-550; carrier gas, helium). Propylene (Neriki Research Grade) used showed no impurity by gas chromatography (column, active carbon and acetylacetone).

**Procedure.** CYCLOHEXENE. All reactions were carried out in a flow apparatus. Air was stored in a 20-liter gas holder and was introduced under 60 cm. of water head. The flow rate was regulated and measured with a soap bubble flow meter. The metered air was passed through an anhydrous calcium chloride tube and then into a cyclohexene evaporator, dipping in a constant temperature bath. The composition of the gas mixture was controlled by regulating the bath temperature and was determined from the weight of cyclohexene vaporized and the volume of air passed. The gaseous mixture was transferred to a Siemens-type silent discharge tube: borosilicate glass, discharge length, 24 cm.; space gap, 3.5 mm.; discharge space volume, 50 ml. The secondary voltage applied to the discharge tube was fixed at 16 kvolts, and the secondary current was 1.0 ma.; 60-cycle alternating current was used. The circuit included a voltmeter and milliammeter. During the reactions, the temperature of the discharge tube was 40°–50°C. (Separate experiments confirmed that product distribution was hardly affected by the temperature in a range 25°–50°C.). The flow rate of the air was fixed at 1 ml./sec. for experimental Runs 1–4. Condensable products and unreacted cyclohexene were collected in traps at 0° and at –78°C. Gaseous products were collected in a gas holder at atmospheric pressure. Liquid products were analyzed quantitatively by gas chromatography using a 2-meter column of PEG-6000 and a 2-meter column of Si-500 at 160°C., carrier gas, helium. Gaseous products were also analyzed by gas chromatography; for hydrogen, methane, ethylene, ethane, and carbon dioxide using a 2-meter column of activated charcoal at 180°C., carrier gas, helium and nitrogen, and for all hydrocarbons using a 5-meter column of acetylacetone at 0°C., carrier gas, helium.

*Runs 1-4.* Unreacted cyclohexene was removed from the liquid products under reduced pressure at room temperature. The presence of small amount of hydroperoxides, confirmed by a positive lead tetraacetate test,

was found in the residual liquid, and the amount was determined iodometrically. The modified method of Wibaut titration (21), where the peroxides react with potassium iodide in 80% acetic acid at 35°C. in a carbon dioxide atmosphere, was used. Thin layer chromatograms of 2,4-dinitrophenylhydrazone derivative from the residual liquid showed strong spots of cyclohexanone and cyclohexenone derivatives, and the presence of formaldehyde which might interfere with the Wibaut titration (11) was not detected. The present method and the Hiatt method (11, 12), whose iodometry is not interfered with by some aldehydes, gave identical titers on the residual liquid. The amounts of peroxide were 6.5% for Runs 1 and 2, 5.0% for Run 3, and 3.5% for Run 4, calculated as 3-cyclohexenyl hydroperoxide in the residual liquid. Distillation of the residual liquid did not give the pure fraction of hydroperoxides owing to their lower contents; however, thermal decomposition by keeping the liquid at 130°C. caused a slight increase in the weight of 2,4-dinitrophenylhydrazone of the ketones. These facts indicate that these peroxides may be composed mainly of cyclohexyl hydroperoxide and 3-cyclohexenyl hydroperoxide, however, the ratio of the two peroxides was not determined. Gas chromatographic analyses of the residual liquid are shown in Table II; small amounts of these alcohols and carbonyl compounds may arise from pyrolysis of the hydroperoxides during the gas chromatography.

Three fractions were isolated from the residual liquid by preparative gas chromatography using a 3-meter column of PEG-6000 at 155°C., carrier gas, nitrogen.

Fraction 1 was found to have the same retention time as that of authentic cyclohexanone, and the infrared spectrum showed a strong absorption band at 1720  $\text{cm}^{-1}$  ( $\text{C}=\text{O}$ ). The 2,4-dinitrophenylhydrazone derivative was prepared, and a mixed melting point with an authentic sample was not depressed, m.p., 156°–157°C. [literature value 160.2°C. (5)].

Table I. Gas Chromatographic

Run	Gaseous Reactant, Composition, mole %		$\frac{\text{Cyclohexene}}{\text{Oxygen}}$ , mole ratio	Cyclohexene, Conversion ratio	Cyclo- hexanol
	Cyclohexene	Air			
1	11.4	88.6	0.61	21.3	13.8
2	15.8	84.2	0.89	18.1	17.3
3	28.8	71.2	1.91	11.3	16.3
4	59.8	40.2	7.00	3.6	14.6

Fraction 2 showed the same retention time as that of authentic cyclohexanol, and its infrared spectrum showed a strong absorption band at  $3350\text{ cm.}^{-1}$  ( $-\text{OH}$ ). The  $\alpha$ -naphthylurethane derivative was prepared, and a mixed melting point with an authentic sample was not depressed, m.p.,  $128^{\circ}$ – $129^{\circ}\text{C}$ . [literature value,  $128^{\circ}\text{C}$ . (17)].

Fraction 3 showed two retention times: (a) the same as that of cyclohexanol, and (b) the same as that of cyclohexenone; the infrared spectrum showed strong absorption bands at  $3350\text{ cm.}^{-1}$  ( $-\text{OH}$ ) and  $1680\text{ cm.}^{-1}$  ( $\text{C}=\text{O}$  conjugated). This was separated into two fractions by Girard's P reagent. The  $\alpha$ -naphthylurethane derivative of cyclohexanol was not depressed, m.p.,  $154.5^{\circ}$ – $155.5^{\circ}\text{C}$ . [literature value,  $156^{\circ}\text{C}$ . (22)].

The 2,4-dinitrophenylhydrazone derivative of Fraction 3b, ketonic part, was prepared, and a mixed melting point with an authentic derivative of cyclohexenone was not depressed, m.p.,  $167^{\circ}$ – $168^{\circ}\text{C}$ . [literature,  $163^{\circ}\text{C}$ . (1)].

To isolate acidic products which were not found by gas chromatographic analysis, the crude products were treated by ordinary methods, but only small amounts of viscous brownish red liquid products were obtained, and no adipic acid was isolated. Isolation of cyclohexene oxide was unsuccessful, however; gas chromatographic analysis based on the two columns showed clearly the presence of cyclohexene oxide. Gaseous products included ethylene, 1,3-butadiene, carbon dioxide, and an unidentified  $\text{C}_4$  hydrocarbon in the ratio of 12:6:3:1. Trace amounts of other gaseous hydrocarbons were also detected, and any gaseous peroxy compound was not detected. These hydrocarbons were considered to be decomposition products of activated cyclohexene.

*Run 5.* Commercial nitrogen used was purified by passing it through an alkaline solution of pyrogallol and a series of concentrated sulfuric acid, silica gel, and anhydrous calcium chloride tubes. The flow rate of nitrogen was fixed at 40 ml./min. Unreacted cyclohexene and low boiling products were removed from the collected products at reduced pressure.

### Analysis of Oxidation Products

Components, wt. %				<i>Cyclohexanol + Cyclohexanone</i>	<i>Ketones Alcohols</i> mole ratio
<i>Cyclo- hexanone</i>	<i>Cyclo- hexenol</i>	<i>Cyclo- hexenone</i>	<i>Cyclohexene oxide</i>	<i>Cyclohexenol + Cyclohexenone</i> mole ratio	
16.0	28.4	21.1	12.0	0.59	0.88
15.6	29.3	18.2	11.0	0.68	0.74
12.8	33.1	20.7	9.7	0.53	0.69
11.9	32.5	24.7	6.8	0.45	0.80

**Table II. Products from Discharge Reaction of Cyclohexene in the Absence of Oxygen (Run 5)<sup>a</sup>**

<i>Compound</i>	<i>mmole/hr.</i>	<i>Compound</i>	<i>mmole/hr.</i>
Bicyclohexyl	0.43	Hydrogen	0.45
3-Cyclohexylcyclohexene	0.95	Methane	trace
3,3'-Bicyclohexenyl	0.56	Ethylene	1.6
Unidentified C <sub>12</sub>	0.12	Ethane	trace
Cyclohexane	0.30	Acetylene	0.36
1,3-Cyclohexadiene	found <sup>b</sup>	Propylene	0.1
Unidentified and residue (C <sub>6</sub> unit)	0.98	Propane	0.51
		<i>n</i> -Butane	trace
		1-Butene	trace
		Butadiene	0.19
		Other C <sub>4</sub> -products	trace

<sup>a</sup> Composition of gaseous reactant: cyclohexene, 27.2%; nitrogen, 72.8%. Feed rate of cyclohexene, 40.2 mmoles/hr.

<sup>b</sup> Quantitative analysis was not done.

Gas-chromatographic analysis (column: PEG-6000, 2 meters, column temperature 180°C., carrier gas, He) of the residue showed that it consisted of three main products. The first peak was identified as bicyclohexyl, the second as 3-cyclohexylcyclohexene, and the third as 3,3'-bicyclohexenyl. The residue was distilled, and a fraction boiling at 90°–122°C./20 mm. Hg was collected. This fraction was poured into 10 times its volume of acetic acid. The solution was cooled to 0°C., and bromine was added. Colorless needle crystals and a red viscous oily liquid were obtained. The crystalline material was recrystallized from acetic acid and melted at 157.5°–160°C. (decomp.) [literature, 158°C. (6)]. A mixed melting point with an authentic tetrabromide of 3,3'-bicyclohexenyl was not depressed.

The oily liquid was purified by column chromatography (silica gel, 80 mesh; eluant, petroleum ether) and distilled. A colorless oily liquid (b.p., 123°–125°C./0.5 mm. Hg, *n*<sub>D</sub><sup>20</sup> 1.5530) was obtained. The infrared spectrum was that of 3-cyclohexylcyclohexene.

Analysis: calculated for C<sub>12</sub>H<sub>20</sub>Br<sub>2</sub>: C, 44.47; H, 6.22. Found: C, 44.48; H, 5.99.

The gas chromatogram of the remaining acetic acid solution showed that the two peaks identical with those of 3-cyclohexylcyclohexene and

**Table III. Oxidation Products of**

<i>Gaseous Reactant, Composition, mole %</i>		<i>Oxidation Products,</i>		
<i>Propylene</i>	<i>Oxygen</i>	<i>Methyl Alcohol</i>	<i>Acetaldehyde</i>	<i>Propylene Oxide</i>
99	1	0.20	trace	trace
95	5	0.60	0.35	trace
80	20	1.47	1.24	trace
70	30	1.68	1.62	trace

3,3'-bicyclohexenyl disappeared, and the peak identical with that of bicyclohexyl remained. The gas chromatogram of the fraction having b.p., 90°–122°C./20 mm. Hg showed that at least 13 peaks were present before the bicyclohexyl peak. These amounts were small, and since no further investigation was done, they were treated as unidentified products. A small peak was found close behind the peak of 3,3'-bicyclohexenyl. This seemed to be a C<sub>12</sub> product. The gas chromatogram of the low boiling fraction showed one peak identified as cyclohexane on two columns: TCP 2 meters, 80°C.; DNP 2 meters 70°C., carrier gas, He. The ultraviolet spectrum of this fraction showed  $\lambda_{\max}$  256 m $\mu$ , indicating the presence of 1,3-cyclohexadiene (9). This was also confirmed by treating (11) the fraction with maleic anhydride giving the Diels-Alder adduct, bicyclo-2,2,2-oct-5-ene-2,3-dicarboxylic anhydride; m.p., 145°–146.6°C., mixed melting point with an authentic sample (8) showed no depression.

*Autoxidation without Discharge.* To compare our results with normal autoxidation, the reaction was carried out using a reaction mixture similar to Run 4 without silent discharge. Low conversion of cyclohexene (0.051%) was observed at 60°C., indicating that the discharge oxidation was hardly affected by the normal autoxidation process under the present reaction conditions. The major product was 3-cyclohexenylhydroperoxide, and minor products were 3-cyclohexenol, 3-cyclohexenone, cyclohexene oxide, and trace amounts of residue; saturated materials such as cyclohexanol and cyclohexanone were not detected. The conversion of cyclohexene was raised to 0.15% when the reaction temperature was elevated to 140°C.; however, the kinds of product were not changed.

**PROPYLENE.** Propylene and oxygen were premixed in a fixed ratio, and the mixed gas was introduced to the discharge tube at the rate of 80 ml./min. The reaction was carried out at 0°C. in the same way as that of cyclohexene. All products were analyzed by gas chromatography using PEG-6000, TCP, and Si-DC550 columns for the oxygen-containing products listed in Table III, Golay U (90 meters), acetyl-acetone and active carbon columns for the liquid and gaseous hydrocarbon products.

### Propylene under Silent Discharge

*mmoles/200 mmoles Propylene*

<i>Propion- aldehyde</i>	<i>n-Propyl Alcohol</i>	<i>Acrolein</i>	<i>Allyl Alcohol</i>	<i>Acetone</i>	<i>Isopropyl Alcohol</i>
0.15	0.044	0.25	0.14	0.32	0.60
0.35	0.11	0.78	0.34	1.14	1.63
1.04	0.25	1.68	0.82	2.53	3.46
1.48	0.27	1.95	0.95	3.29	3.39

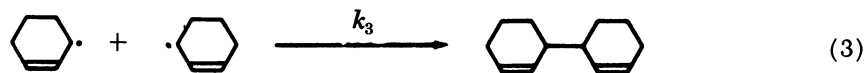
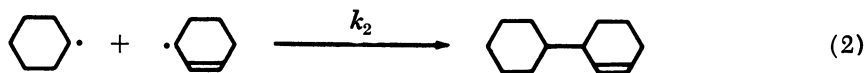
In the absence of oxygen, about 82 peaks of hydrocarbon products were observed in the gas chromatogram, which showed that the main products consisted of  $C_6$  hydrocarbons (Table IV), hydrogen, methane, acetylene, ethylene, ethane, methylacetylene, allene, propane, 1-butene, and butadiene.

**Table IV. Relative Amounts of  $C_6$  Products from Propylene in the Absence of Oxygen**

Products	Relative Amount, %
2,3-Dimethylbutane	28.0
2-Methylpentane	5.6
4-Methyl-1-pentene	40.1
1-Hexene	10.0
1,5-Hexadiene	12.6
Unidentified $C_6$	3.7

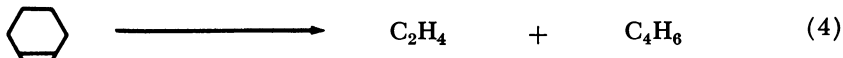
### Results and Discussion

An experiment in the absence of oxygen is summarized in Table II (Run 5). Bicyclohexyl, 3-cyclohexylcyclohexene, and 3,3'-bicyclohexenyl were the main products; small amounts of 1,3-cyclohexadiene and cyclohexane were also formed. The dimeric products may be formed by coupling reactions between cyclohexyl radicals and allylic cyclohexenyl radicals, in which ratio of rate constant  $\phi \left( = \frac{k_2}{(k_1 \cdot k_3)^{1/2}} \right)$  is 1.9 in agreement with statistical expectation ( $\phi = 2$ ) (16). Cyclohexane, cyclohexene, and 1,3-cyclohexadiene might be formed by hydrogen transfer reactions between these radicals.



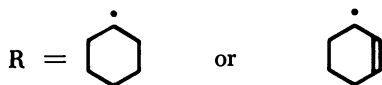
Although ion-molecule processes would be possible in some electron impact reactions, this process would not lead to the formation of dimeric products formed in the present experiments (20). Ethylene was the major gaseous product. Ethylene and butadiene may be produced from the reverse Diels-Alder reaction of cyclohexene (10) since they were also

produced in the presence of oxygen, and acetylene was probably formed by butadiene cleavage. It is not clear how hydrogen and propane are formed in this system.

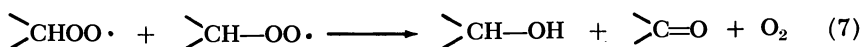


The results of the oxidation of cyclohexene are summarized in Table I. Cyclohexanol and cyclohexanone were obtained even at high oxygen concentration (Table I, Run 1) in yields comparable with that of 3-cyclohexenol, 3-cyclohexenone, and cyclohexene oxide. This indicates that the addition of a hydrogen atom to cyclohexene occurred fairly effectively in this reaction system despite the presence of oxygen molecules. Analysis of crude products showed the presence of small amounts of hydroperoxides, and they were decomposed during the gas chromatography; however, this decomposition did not cause the hydrogen addition. Jarvie and Cvetanovic (14) have reported the reaction of 1-butene with activated oxygen in microwave discharge, where 1-butene is not activated by the discharge; hence, the hydrogen addition reaction similar to the present case is not observed, and the kinds and distribution of the products are different from those of our experiments.

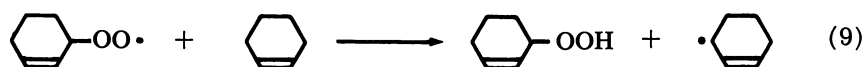
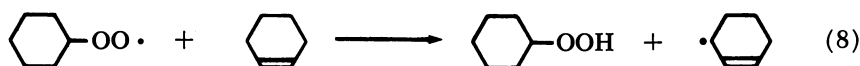
In the present oxidation, cyclohexyl radicals and cyclohexenyl radicals may react with oxygen molecules to form the corresponding peroxy radicals since oxygen molecules are effective scavengers of hydrocarbon free radicals. This was suggested by the fact that no coupling products were obtained in the presence of oxygen. Cyclohexyl peroxy radicals and cyclohexenyl peroxy radicals may be the most probable intermediates of the reaction in the presence of oxygen.



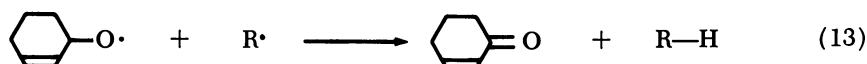
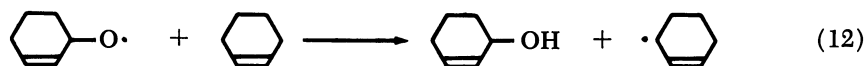
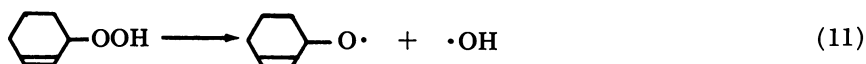
Then, a major part of these radicals would be consumed by chain termination to form corresponding alcohols and ketones. Yokohata and Tsuda (23, 24, 25) have suggested that the silent discharge reaction can well be interpreted in terms of radiolysis caused by the ionizing radiation of high LET (Linear Energy Transfer), and this would help explain the short chains of this oxidation.



However, the ratios of the unsaturated materials to the saturated materials and of the ketones to the alcohols (Table I) indicate that the yields of unsaturated materials are higher than those of saturated products, especially cyclohexenol. [The excess alcohol might come from  $2\text{ROO}\cdot \rightarrow 2\text{RO}\cdot + \text{O}_2$ ; however, its importance in the gas phase is unknown.] It was suggested from the above that some cyclohexenol and possibly cyclohexenone may be formed from cyclohexenyl hydroperoxide which is produced from chain reactions initiated by the cyclohexenyl peroxy radical and cyclohexenyl peroxy radical as shown below.



Decomposition of the hydroperoxides would be considered in terms of the following general scheme; for example, for cyclohexenyl hydroperoxide:



The formation of water, detected by the copper sulfate test, may be consistent with the above scheme. The decreasing yield of cyclohexene oxide with decreasing oxygen concentration suggests that cyclohexene oxide could be formed from the direct reaction of cyclohexene with



the second step is an ion-molecule reaction followed by neutralization. Oxidation products of propylene are shown in Table III. To discover the precursor of these products, C<sub>6</sub> components of the products, formed in the absence of oxygen, were analyzed (relative amounts are shown in Table IV).

These results suggest that isopropyl, *n*-propyl, and allyl radicals may be formed as the main intermediates in these reaction systems; however, further precise information was difficult to obtain because of the complex product distribution and instability of a mixture of the oxidation products owing to the presence of small amounts of acids and peroxidic components not analyzed.

The formation of the *n*-propyl radical from propylene suggests that this hydrogen transfer should proceed through some energetic process caused by silent discharge because a normal hydrogen atom addition to propylene proceeds almost exclusively to the terminal carbon (15). Thus, two molecular processes similar to those in the reactions of cyclohexene may be plausible to interpret the hydrogen transfer.

#### Literature Cited

- (1) Bartlett, P. D., Woods, G. F., *J. Am. Chem. Soc.* **62**, 2933 (1940).
- (2) Brill, W. F., *J. Am. Chem. Soc.* **85**, 141 (1963).
- (3) Coleman, G. H., Johnston, H. F., *Org. Syntheses, Coll.* **1**, 183 (1941).
- (4) Cvetanović, R. J., *J. Chem. Phys.* **25**, 376 (1956).
- (5) Farkas, A., Passaglia, E., *J. Am. Chem. Soc.* **72**, 3333 (1950).
- (6) Farmer, E. H., Michael, S. E., *J. Chem. Soc.* **1942**, 513.
- (7) Fujimoto, H., *Bull. Chem. Soc. Japan* **13**, 281 (1938).
- (8) Hammond, G. S., Warkentin, J., *J. Am. Chem. Soc.* **83**, 2554 (1961).
- (9) Henri, V., Pickett, L. W., *J. Chem. Phys.* **7**, 439 (1939).
- (10) Hershberg, E. B., Ruhoff, J. R., *Org. Syntheses, Coll.* **II**, 102 (1943).
- (11) Hiatt, R., Gould, C. W., Mayo, F. R., *J. Org. Chem.* **29**, 3461 (1964).
- (12) Hiatt, R., Strachan, W. M. J., *J. Org. Chem.* **28**, 1894 (1963).
- (13) Inoue, E., *Bull. Tokyo Inst. Technol., Ser. A*, **1957** (2) 1.
- (14) Jarvie, J. M. S., Cvetanović, R. J., *Can. J. Chem.* **37**, 529 (1959).
- (15) Moore, W. L., *J. Chem. Phys.* **16**, 916 (1948).
- (16) Pryor, W. A., "Free Radicals," p. 15, McGraw-Hill, New York, 1966.
- (17) Shriner, R. L., Fuson, R. C., Curtin, D. Y., "The Systematic Identification of Organic Compounds," 4th ed., p. 280, Wiley, New York, 1956.
- (18) Sickle, D. E. Van, Mayo, F. R., Arluck, R. M., *J. Am. Chem. Soc.* **87**, 4824 (1965).
- (19) Sugino, K., *et al.*, *J. Chem. Soc. Japan, Pure Chem. Sec.* **86**, 1200 (1965).
- (20) Wakeford, B. R., Freeman, G. R., *J. Phys. Chem.* **68**, 2635 (1964).
- (21) Wibaut, J. P., van Leeuwen, H. B., Van der Wal, B., *Rec. trav. chim.* **73**, 1033 (1954).
- (22) Willstater, R., Sonnenfeld, E., *Ber.* **46**, 2952 (1913).
- (23) Yokohata, A., Tsuda, S., *Bull. Chem. Soc. Japan* **39**, 53 (1966).
- (24) *Ibid.*, p. 1636.
- (25) *Ibid.*, **40**, 294 (1967).

RECEIVED September 29, 1967.

## Metal-Ion Catalyzed Oxidation of Acetaldehyde

G. C. ALLEN and A. AGUILÓ

Celanese Chemical Co. Technical Center, P. O. Box 2768, Corpus Christi, Tex.

*The oxidation of acetaldehyde with oxygen in the presence of manganese, cobalt, and copper acetates was studied. The results were correlated with  $^{14}\text{C}$ -tagged experiments and with the kinetics in acetic acid of (1) peracetic acid decomposition and (2) peracetic acid reaction with acetaldehyde. Both reactions are catalyzed by manganese and cobalt acetate but not by copper acetate. In the oxidation of acetaldehyde using any of the three metal acetates, the main path to acetic acid is via the reaction of peracetic acid with acetaldehyde. A complex of both of these substances with the metal ion in the  $3+$  state is proposed to explain the catalytic activity of cobalt or manganese. Although copper(II) acetate does not catalyze this reaction, the non-catalytic path proceeds through acetaldehyde monoperoacetate as an intermediate.*

The liquid-phase oxidation of acetaldehyde to acetic acid by air in the presence of metal salts is well known (24), and the kinetics and mechanism of this reaction have been studied widely (3, 4, 14, 17, 21, 24, 25). It is accepted that the oxidation is a chain reaction in which peracetic acid is produced and then either can decompose to acetic acid and oxygen or can react with acetaldehyde to produce acid *via* a postulated intermediate—acetaldehyde monoperoacetate. Although acetates of several metal ions have been mentioned as catalysts, those more generally used are the acetates of manganese, cobalt, copper, and mixtures of these last two. It is also generally accepted that manganese is the best catalyst for acetic acid production, and combinations of both cobalt and copper salts have been claimed to be superior in manufacturing acetic anhydride (24).

The present work was initiated as a consequence of an exploratory program on acetaldehyde oxidation in which copper(II), manganese(II), and cobalt(II) acetates were evaluated. The results indicate a significant difference both in acetaldehyde efficiency to acetic acid and in by-product distribution.

To understand the significant effect of catalyst nature, a better understanding of the main reactions, peracetic acid decomposition, and its reaction with acetaldehyde was needed. A literature survey showed that the kinetics were not well studied, most of the work being done at very low catalyst concentration ( $\sim 1$  p.p.m.), and there is disagreement with respect to the kinetic expressions reported by different authors. The emphasis has always been on the kinetics but not on the products obtained, which are frequently assumed to be only acetic acid and oxygen. Consequently, the effectiveness of a catalyst was measured only by the rates and not by the significant amount of by-products that can be produced. We have studied the kinetics of these reactions, supplemented by by-product studies and experiments with  $^{14}\text{C}$ -tagged acetaldehyde and acetic acid to arrive at a reaction scheme which allows us to explain the difference in behavior of the different metal ions.

### Experimental

**Materials.** Acetic acid and metal acetates were reagent grade and were used without purification. Commercial grade acetaldehyde (99+%) from the Celanese plant at Bishop, Tex., was used in the acetaldehyde oxidation experiments with oxygen. Acetaldehyde was distilled before use in the kinetic experiments. Carbon-14 labelled acetaldehyde and acetic acid were obtained from New England Nuclear Co. Anhydrous peracetic acid in acetic acid was prepared from Becco (FMC Corp.) 40% peracetic acid and acetic anhydride with sulfuric acid catalyst. Peracetic acid (*ca.* 4 moles/liter) was recovered by flashing under reduced pressure (25°–40°C. and 20–30 mm. Hg). This material contained less than  $10^{-4}$  mole/liter hydrogen peroxide ( $\text{KMnO}_4$  titration).

**Acetaldehyde Oxidation.** The acetaldehyde oxidation experiments were carried out in a continuous backmixed glass reactor (36 inches long  $\times$  1.5 inches i.d.) at 50 p.s.i.g. The volume of liquid in the reactor was about 550 ml. Acetaldehyde (*ca.* 800 grams/hr.) and catalyst solutions in acetic acid (*ca.* 25 ml./hr.) were fed by positive displacement pumps. The oxidizing gas, 90% oxygen and 10% nitrogen, was fed into the bottom of the reactor through a sparger. Mixing was effected by circulating the reactor contents with a centrifugal pump (350 liters/hr.). The temperature was controlled by water flow to a heat exchanger in the circulation line. Pressure was controlled by a spring-loaded valve. The desired acetaldehyde concentration was obtained by adjusting oxygen flow. Liquid product was removed at a rate sufficient to maintain a constant liquid level. The liquid product was analyzed for acetic acid by titration. By-products and acetaldehyde in the liquid product were determined by gas chromatography. Metal ion analyses were done using

a Perkin-Elmer atomic absorption spectrophotometer model 303. Gaseous products were analyzed by a mass spectrometer. Acetic acid efficiencies were calculated from material balance runs of about 3 hours duration and were corrected to 100% acetaldehyde accountability (usual accountability was 97–102%). In radioactive tracer studies,  $^{14}\text{C}_1$ -acetic acid dissolved in acetaldehyde was fed to the reactor. Carbon dioxide for counting was collected as barium carbonate by passing the vent gas into barium hydroxide solution. Counting was done on a Hyamine 10-X (Rohm and Haas) solution which was obtained by absorption of carbon dioxide which had been liberated from the washed barium carbonate by the action of sulfuric acid. Acetic acid for counting was obtained by separation by preparative gas chromatography from the reactor product. Counting was done on a Packard-Tricarb liquid scintillation counter.

**Studies of Products Formed in Peracetic Acid Reactions.** These experiments were carried out in a three-necked flask fitted with a stirrer, gas collecting tube, and dropping funnel. Peracetic acid (*ca.* 4 moles/liter) was added dropwise to the catalyst-acetic acid solution (with or without acetaldehyde) at such a rate that the temperature was maintained between 28° and 32°C. Occasional cooling with ice was necessary. The gaseous products were collected by displacement of a saturated acidic magnesium sulfate solution. Liquid product was analyzed by gas chromatography and gaseous product by mass spectrometry. In two of the experiments with cobalt acetate as catalyst  $^{14}\text{C}$ -acetaldehyde (equal labelling in each carbon atom) was used. The gas produced was scrubbed with sodium hydroxide solution, and the methane thus obtained was combusted to  $\text{CO}_2$  for absorption in Hyamine 10-X solution prior to counting.

**Kinetic Studies. PERACETIC ACID DECOMPOSITION.** Studies with manganese catalyst were conducted by the capacity-flow method described by Caldin (9). The "reactor" consisted of a glass tube (5 inches long  $\times$  2 inches o.d.), a small centrifugal pump (for stirring by circulation), and a coil for temperature control (usually  $\pm 1^\circ\text{C}$ .); total liquid volume was 550 ml. Standardized peracetic acid solutions in acetic acid (0.1–0.4M) and catalyst solutions also in acetic acid were metered into the reactor with separate positive displacement pumps. Samples were quenched with aqueous potassium iodide. The liberated iodine was titrated with thiosulfate. Peracetic acid decomposition rates were calculated from the feed rate and the difference between peracetic acid concentration in the feed and exit streams.

Peracetic acid decomposition kinetics in the presence of cobalt or copper acetates were studied in the same apparatus used for the manganese-catalyzed reaction. However, in these studies it was used as a batch reaction system. The reactor was charged with peracetic acid (*ca.* 0.5M in acetic acid) and allowed to reach the desired temperature. At this time the catalyst (in acetic acid) was added. Samples were withdrawn and quenched with potassium iodide at measured time intervals.

**PERACETIC ACID-ACETALDEHYDE REACTION.** The cobalt- and manganese-catalyzed reactions of peracetic acid with acetaldehyde were studied by a continuous flow technique (9). Peracetic acid (0.15M in acetic acid) and acetaldehyde-catalyst solutions were metered through rotameters to a mixing T (standard 0.25-inch stainless steel Swagelok T) and

then to a reaction tube (0.25-inch stainless steel). With sample valves attached to the reaction tubes with T's at different points, the reaction mixture was sampled at times from 0.032 to 0.500 min. after mixing. These times were calculated from the total flow and volume of the reactor to each point. The reaction was quenched by flowing the sample into a tared potassium iodide solution. Peracetic acid and total peroxide were determined by iodometric titrations (Methods III and IV below). Acetaldehyde was determined by gas chromatography.

The reaction between acetaldehyde and peracetic acid in the presence of copper or with no metal acetate present was studied by the method of Bawn and Williamson (4) using Methods I and II (*see below*) for determining peracetic acid and total peroxide, respectively.

**Peroxide Determinations.** Bawn and Williamson report two iodometric procedures for determining peracetic acid (Methods I and III below) and one method for determining total peroxide (4) (Method II). Bawn and Jolly report another method for total peroxide (5) (Method IV below). The difference between total peroxide and peracetic acid is assumed to be acetaldehyde monoperoxide (AMP). Each method was tested in our preliminary studies. Method III is preferred for peracetic acid because the results are more reproducible. In Method I a large blank titration was always observed, while in Method III the blank titration was very small. Method IV is preferred for total peroxide because it seems to be more sensitive to total peroxide and less sensitive to water content of the acetic acid solvent.

Method I (4). Sample was quenched with a solution of 50 ml. acetic acid and 2.5 ml. saturated aqueous potassium iodide.

Method II (4). Samples were quenched with a solution of 50 ml. acetic acid and 1–2 grams potassium iodide.

Method III (4). Samples were quenched with a solution of 50 ml. 1*N* sulfuric acid and 1–2 grams potassium iodide.

Method IV (5). Samples were quenched with a solution of 25 ml. acetic acid, 1.5 grams sodium bicarbonate, 1 ml. water, and 1–2 grams potassium iodide.

The liberated iodine was titrated after standing for 15 min. Blank determinations were done in each method. A carbon dioxide blanket, obtained by putting a small amount of dry ice in each flask, was used to reduce the amount of iodine produced by atmospheric oxygen.

## Results

**Acetaldehyde Oxidation.** In the oxidation of acetaldehyde with oxygen–nitrogen mixtures, at conditions under which the rate-limiting factor is oxygen transfer to the solution, manganese(II) acetate gives a better efficiency to acetic acid than copper(II) acetate, which in turn is better than cobalt(II) acetate. However, when either cobalt(II) or copper(II) acetate is used in the presence of manganese(II) acetate, the

results are similar to those obtained when manganese acetate is used alone. Table I presents typical experimental results, selected to compare catalysts at similar catalyst and acetaldehyde concentrations.

**Table I. Effect of Metal Ions on Efficiency of Acetic Acid Production by Acetaldehyde Oxidation**

	Mn	Cu	Co	Mn-Cu	Mn-Co
Concentration, p.p.m.	120	170	103	130-110	150-190
Acetaldehyde, wt. % <sup>a</sup>	2.0	2.0	2.0	1.7	2.4
Acetic acid efficiency, % <sup>b</sup>	94	88	76	95	96

<sup>a</sup> Steady-state concentration in reactor.

<sup>b</sup> Acetic acid, acetic anhydride, and acetate present as ester, moles/100 moles of acetaldehyde reacted. These efficiencies have been corrected for the acetic acid added with the catalyst solution.

**Table II. By-products from Methyl Group in Acetaldehyde Oxidation at 80°C.**

Catalyst	Catalyst Conc., p.p.m.	AcH wt. % <sup>a</sup>	By-products				
			CH <sub>4</sub> <sup>b</sup>	CH <sub>3</sub> -O- <sup>c</sup>	HCHO <sup>d</sup>	HCO <sub>2</sub> - <sup>e</sup>	CO <sub>2</sub> <sup>f</sup>
Mn	15	1.8	42	12	3	11	29
	15	5.4	54	14	4	12	17
	120	1.4	19	18	3	18	43
	124	4.5	31	16	5	7	43
Cu	56	1.2	12	28	1	26	35
	58	3.0	25	27	3	23	26
	430	1.2	9	30	1	15	45
	497	3.0	14	36	3	14	35
Co	103	2.0	63	14	1	7	15
	135	5.1	69	13	1	4	14
	997	1.8	63	15	2	6	15
	990	5.8	71	15	1	7	7
Mn-Cu	150-120	0.8	6	12	3	8	71
	130-110	1.7	8	24	3	10	55
Mn-Co	150-190	2.4	8	22	5	16	48
	154-138	9.3	20	18	5	23	35

<sup>a</sup> Steady-state concentration in reactor.

<sup>b</sup> Moles of methane/100 moles of acetaldehyde oxidized to by-products.

<sup>c</sup> Moles of methyl formate + moles of methyl acetate/100 moles of acetaldehyde oxidized to by-products.

<sup>d</sup> Moles of formaldehyde/100 moles of acetaldehyde oxidized to by-products.

<sup>e</sup> Moles of methyl formate + moles of formic acid/100 moles of acetaldehyde oxidized to by-products.

<sup>f</sup> Moles of CO<sub>2</sub>/100 moles of acetaldehyde methyl group oxidized to by-products. Calculated by difference. CO<sub>2</sub> = 100 - (CH<sub>4</sub> + CH<sub>3</sub>-O- + HCHO + HCO<sub>2</sub>-).

The degradation of acetic acid during the oxidation of acetaldehyde does not contribute significantly to the formation of by-products. This was established in experiments with cobalt and manganese acetates using  $^{14}\text{C}_1$ -acetic acid at the 100-p.p.m. catalyst level and with a 2% steady-state acetaldehyde concentration. Only 6.4 and 10.1% of the total carbon dioxide (for cobalt and manganese acetate, respectively) were produced from the carboxyl group of acetic acid.

The distribution of by-products originating from the methyl group in acetaldehyde oxidation is significantly different for each catalyst. Typical results are presented in Table II. Methane is the predominant by-product with cobalt acetate, while methane and carbon dioxide and methyl esters and carbon dioxide predominate with manganese and copper acetates, respectively.

Determination of the steady-state peroxide concentration during acetaldehyde oxidation experiments indicates that for manganese and cobalt acetates this concentration is below 0.01M while for copper(II) acetate values as high as 0.046M have been obtained.

**Peracetic Acid Decomposition.** Peracetic acid solutions in acetic acid are stable at 30°C. in the absence of catalyst. Addition of copper(II)

**Table III. By-products from Methyl Group and Acetic Acid Efficiency in Peracetic Acid Reactions**

Catalyst	Mn <sup>a</sup>	Cu <sup>a</sup>	Co <sup>a</sup>	Co <sup>b</sup>
Temperature, °C.	30	73	30	30
Catalyst concentration, p.p.m.	433	655	438	459
	<i>Moles per 100 Moles of Peracetic Acid Reacted</i>			
<i>Product Distribution</i>				
Methyl acetate <sup>c</sup>	1	5	<sup>a</sup>	<sup>a</sup>
Methyl formate <sup>c</sup>	1	<sup>a</sup>	1	<sup>a</sup>
Methyl alcohol	<sup>d</sup>	1	<sup>d</sup>	<sup>d</sup>
Formaldehyde	1	1	5	2
Formic acid <sup>e</sup>	1	12	6	2
Carbon monoxide	<sup>a</sup>	<sup>a</sup>	2	1
Carbon dioxide <sup>e</sup>	11	8	9	1
Methane	1	1	1	34
Acetic acid <sup>f</sup>	84	72	77	60

<sup>a</sup> Decomposition.

<sup>b</sup> Reaction with excess acetaldehyde.

<sup>c</sup> Contains alcohol moiety only.

<sup>d</sup> Formic acid plus formate in methyl formate.

<sup>e</sup> This is the CO<sub>2</sub> obtained from methyl group: 0.5 (moles CO<sub>2</sub>—moles other by-products) per 100 moles of peracetic acid reacted.

<sup>f</sup> Acetic acid values are by difference = 100 - Σ other products. In the reaction of peracetic acid with acetaldehyde the acetic acid efficiency is based only on peracetic acid reacted and assuming 100% efficiency of acetaldehyde.

<sup>g</sup> No analysis.

<sup>h</sup> Less than 0.5.

acetate does not produce any effect at this temperature, while the addition of manganese or cobalt acetate catalyzes the decomposition. The products of the decomposition of peracetic acid are presented in Table III. In each case acetic acid is the most important product, and the by-product distribution is similar. The most significant difference is the high proportion of formic acid produced by decomposition of peracetic acid in the presence of copper(II). This reaction was the only one that was studied at 73°C. owing to its much lower rate. In all these experiments we also found some oxygen in the vent (2.2–6.6 moles/100 moles of peracetic acid decomposed). The total amount of oxygen produced is not known since some of it could have reacted with free radicals formed in the reaction. The oxygen accountability is poor; if this arises from errors in the by-products analyses, the acetic acid efficiencies could be as low as 60%.

Since copper(II) does not significantly catalyze the peracetic acid decomposition, we have studied the kinetics of this reaction only in the presence of manganese and cobalt acetates.

With manganese as catalyst, plots of  $\log -d[\text{CH}_3\text{COOOH}]/dt$  vs.  $\log [\text{CH}_3\text{COOOH}]$  gave slopes close to 2. Accordingly, we have treated the data as a second-order reaction in peracetic acid as shown in Figure 1. The different values of the experimental second-order rate constant ( $k_1'$ ) were plotted as a function of total manganese ( $\text{Mn}_T$ ) concentration, and the plot indicates a first-order dependence on total manganese concentrations as shown in Figure 2. The experimental rate law for the manganese-catalyzed decomposition of peracetic acid is thus

$$-d[\text{CH}_3\text{COOOH}]/dt = k_1[\text{Mn}_T][\text{CH}_3\text{COOOH}]^2 \quad (1)$$

Values of  $k_1$  at different temperatures are given in Table IV. From an Arrhenius plot of these values the activation energy  $E_a$  was calculated to be 9.2 kcal./mole.

With cobalt as catalyst the plot of  $\log [\text{peracetic acid}]$  vs. time was linear for each cobalt acetate concentration. The first-order rate constants obtained at different cobalt concentrations ( $k_2'$ ) were plotted as a function of total cobalt ( $\text{Co}_T$ ) concentration, and the plot indicates a first-order dependence on total cobalt as shown in Figure 3. The experimental rate law for the cobalt-catalyzed decomposition is thus:

$$-d[\text{CH}_3\text{COOOH}]/dt = k_2[\text{Co}_T][\text{CH}_3\text{COOOH}] \quad (2)$$

Values of  $k_2$  at different temperatures are given in Table IV. From an Arrhenius plot of these values the activation energy  $E_a$  was calculated to be 20.1 kcal./mole.

**Reaction of Peracetic Acid with Acetaldehyde.** The reaction of peracetic acid with acetaldehyde was studied in the absence of metal ions

and in the presence of copper, manganese, and cobalt acetates. Table V shows that the efficiency to acetic acid, based on peracetic acid, is very high except for the cobalt-acetate catalyzed reaction, which produces significant amounts of methane (*see* Table III). We have shown by using  $^{14}\text{C}$ -acetaldehyde that only 1–3% of the methane comes from the methyl group of acetaldehyde. In some of the cobalt acetate experiments we have also determined ethane, acetone, and biacetyl and have found them to be present only in trace quantities in the product.

The kinetics of the noncatalytic reaction were studied by the method of Bawn and Williamson (4). They found 3.3–3.7 moles/liter for the equilibrium constant for the formation of the intermediate acetaldehyde monoperacetate (AMP) and a first-order rate constant for the decomposition of this intermediate to acetic acid of  $0.015 \text{ min}^{-1}$  at  $25^\circ\text{C}$ . We found difficulty in reproducing our results probably caused mainly by the high values of the blanks in the iodometric methods used. However, as an average of four determinations we obtained  $0.03 \text{ min}^{-1}$  at  $30^\circ\text{C}$ .

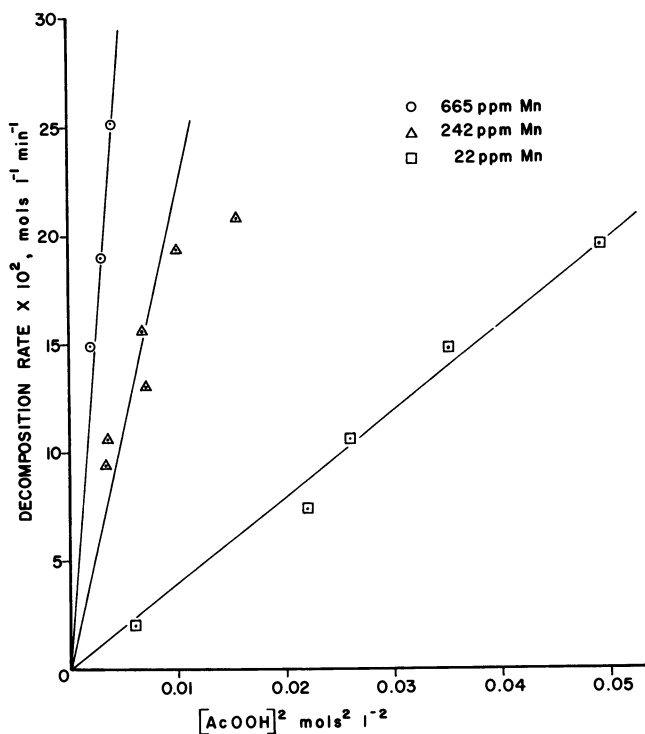


Figure 1. Manganese-catalyzed decomposition of peracetic acid at  $30^\circ\text{C}$ .

for the rate constant for AMP decomposition and 0.02 at 30°C. in the presence of copper(II) acetate (average of two determinations). We believe that these differences are within our experimental error and conclude that copper(II) acetate does not catalyze the formation or decomposition of the intermediate AMP and that this decomposition is relatively slow.

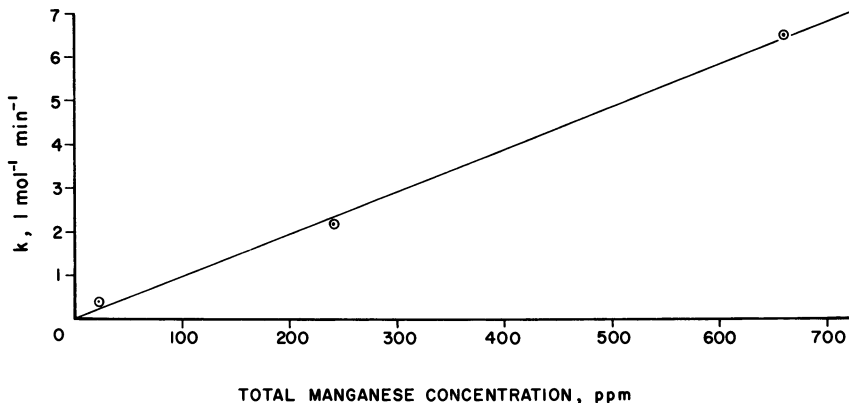


Figure 2. Effect of manganese acetate on peracetic acid decomposition at 30°C.

Table IV. Effect of Temperature on the Metal-Catalyzed Peracetic Acid Decomposition

Temperature, °C.	Cobalt Catalyst $k_1$ , liters mole <sup>-1</sup> min. <sup>-1</sup>	Manganese Catalyst $k_2$ , liters <sup>2</sup> mole <sup>-2</sup> min. <sup>-1</sup>
30	1.5	54.5
45	—	87.2
48	14.1	—
60	—	251
73	118	—

In the presence of manganese and cobalt acetates the reaction becomes very fast, and the intermediate AMP cannot be detected. The kinetics of these reactions were studied in a flow reactor, and the results gave a good second-order fit (first order in peracetic acid and first order in acetaldehyde) at different catalyst concentrations. The plot of [acetaldehyde] vs. [peracetic acid] was linear with a slope of 1, indicating that equimolar quantities of the two substances are reacting. A plot of the experimental second-order rate constants ( $k_3'_{Co}$ ) as a function of catalyst concentration gave a very good first-order fit for cobalt acetate

(Figure 4). The data for manganese acetate ( $k_{3'Mn}$ ) are much more scattered but can also correspond to a first-order fit (Figure 5). It is believed that the greater scattering of the data with manganese is caused by the difficulties encountered in measuring rates of such a fast reaction with our equipment.

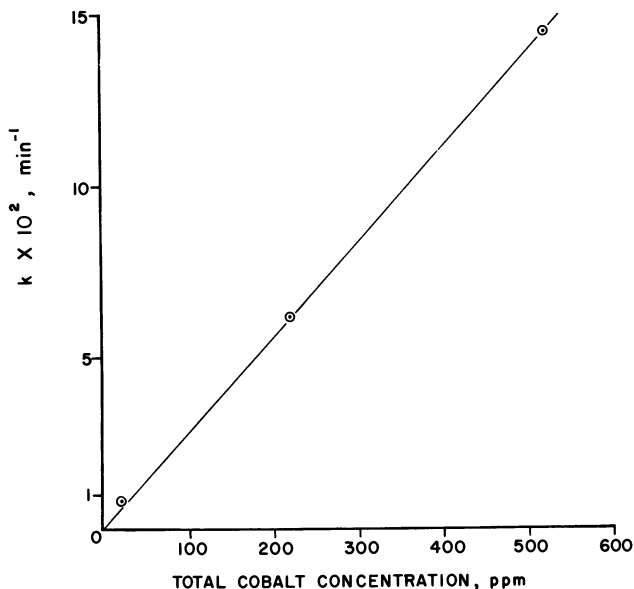


Figure 3. Effect of cobalt acetate on peracetic acid decomposition at 30°C.

The experimental kinetic expression for each of these metal acetates is thus:

$$-d[\text{CH}_3\text{COOOH}]/dt = -d[\text{CH}_3\text{CHO}]/dt = k_3[\text{total metal ion}][\text{CH}_3\text{—COOOH}][\text{CH}_3\text{CHO}] \quad (3)$$

$$\text{At } 30^\circ\text{C. } k_{3\text{Co}} = 290 \text{ liters}^2 \text{ mole}^{-2} \text{ min.}^{-1} \text{ and } k_{3\text{Mn}} = 1.8 \times 10^4 \text{ liters}^2 \text{ mole}^{-2} \text{ min.}^{-1}$$

Some experiments were conducted with *p*-toluenesulfonic acid and acetyl borate as catalysts, using the same concentration range as for the metal acetates, to test their catalytic action in the reaction of acetaldehyde with peracetic acid. The results, although they did not rule out some catalytic activity, clearly indicated that these acids are much less active catalysts than manganese and cobalt acetates.

**Table V. Acetic Acid Efficiency from the Reaction of Peracetic Acid with Acetaldehyde at 30°C.**

Catalyst	Mn	Cu	Co	None
Catalyst concentration, p.p.m.	429	428	459	—
Efficiency to acetic acid <sup>a</sup>	98	96	60	97

<sup>a</sup> Moles of acetic acid/100 moles of peracetic acid reacted. This efficiency has been calculated based on the analyses of by-products rather than the direct determination of acetic acid and assuming an acetaldehyde efficiency to acetic acid of 100%.

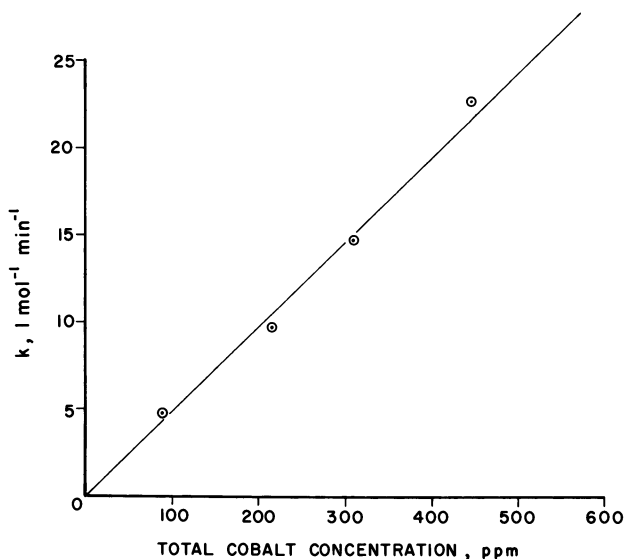


Figure 4. Effect of cobalt acetate on the reaction of peracetic acid with acetaldehyde at 30°C.

### Discussion

**Peracetic Acid Decomposition.** Although, by comparing the rate of peracetic acid decomposition with the rate of its reaction with acetaldehyde, we can rule out the decomposition as a major path in acetaldehyde oxidation (*see below*), we will discuss the possible mechanisms for the catalytic decomposition of peracetic acid.

Cobalt and manganese acetates, which are added in the 2+ oxidation state, are known to be oxidized in acetic acid solutions by peracetic acid through a fast and efficient over-all reaction (19):



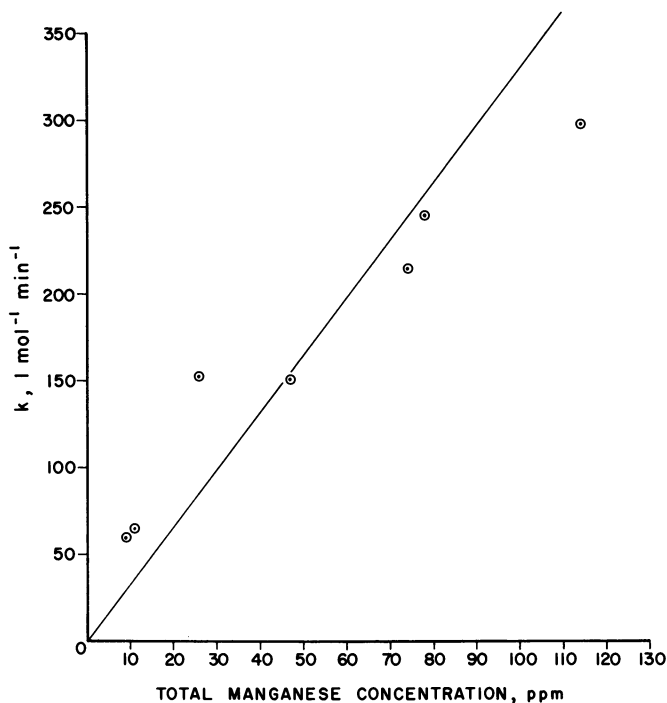
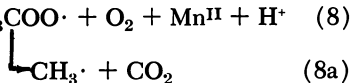
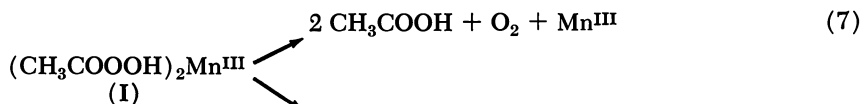


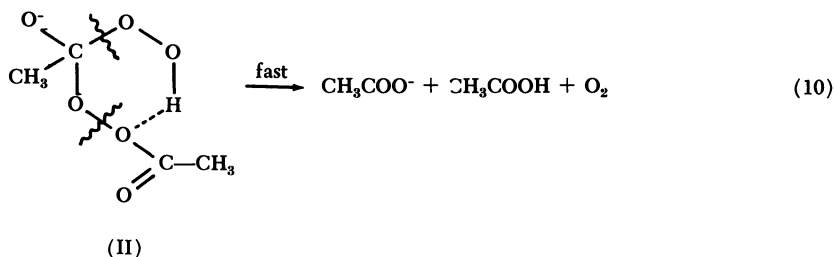
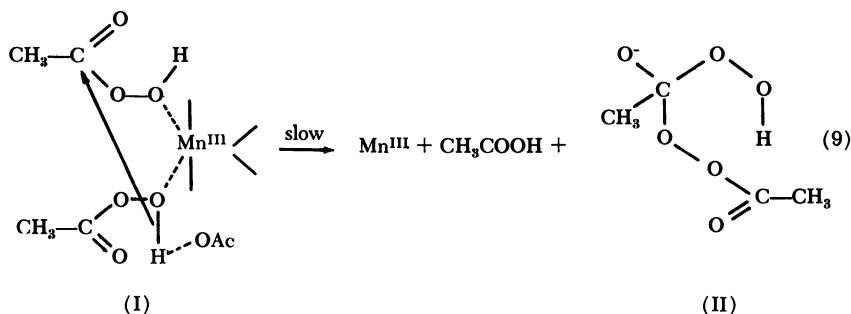
Figure 5. Effect of manganese acetate on the reaction of peracetic acid with acetaldehyde at 30°C.

Thus, in solutions of peracetic acid in acetic acid the predominant cationic species are probably in the 3+ oxidation state.

A possible mechanism for manganese(III) catalysis would be the stepwise formation of a manganese(III) complex with two peracetic acid molecules which then would decompose in the rate-determining step. The formation of this complex should be rapid since it is known that manganese(III) complexes are substitution labile (6, 23):



The nature of the predominant ionic species of manganese(III) or cobalt(III) in acetic acid solutions is not known, and consequently detailed formulation of complex I and its mode of decomposition cannot be made. In the decomposition of I to by-products (Equation 8) a net one-electron transfer from peracetic acid to manganese(III) occurs. In Reaction 7, however, there is no net electron transfer, although a series of successive oxidation-reduction steps within the complex cannot be ruled out. Another possibility could be that in Reaction 7 the manganese(III) ion is acting only as a superacid (7) in that it facilitates the approach of two peracetic acid molecules and, owing to the high positive charge of the cation, it induces a positive charge on the carbon of one of the peracetic acid molecules. This would facilitate nucleophilic attack by oxygen of the other peracetic molecule.



Intermediate II has been postulated by Koubek *et al.* (18) for the bimolecular decomposition of peracetic acid in aqueous solutions.

A drawback of the simple superacid mechanism is that it implies no particular specificity for manganese(III); any other tripositive cation which readily complexes with peracetic acid should be a good catalyst for the reaction. Preliminary experiments with chromium(III), aluminum(III), and boron(III) acetates indicate that none of these salts catalyzes

the decomposition of peracetic acid. Hence, the decomposition of Complex I may be more complicated, as suggested previously.

A mechanism represented by Equations 5, 6, 7, and 8 could be applied to cobalt(III), but the rate-limiting step would have to be the first substitution reaction to account for the experimental rate equation (Equation 2). It is known that cobalt(III) complexes are substitution inert (6, 23) unless significant amounts of cobalt(II) are present (1, 8, 23), and hence one could visualize the first and slow step as follows:



Reaction 11 involves hydrogen atom transfer as proposed by Halpern *et al.* (13) in the mechanism of formic acid oxidation by cobalt(III) in aqueous solutions. In this reaction one could consider that as peracetic acid approaches the coordination sphere of  $\text{Co}^{\text{III}}$  and transfers the hydrogen atom to the coordinated acetate, the  $\text{Co}^{\text{III}}$  atom is transformed into a  $\text{Co}^{\text{II}}$  complex of peracetoxy radical (or  $\text{Co}^{\text{III}}$  complex of peracetate anion). Complexes of free radicals with metal ions have been postulated by Kochi (16). The substitution rate in this complex could be intermediate between the rate of substitution of cobalt(III) and cobalt(II) complexes owing to the contribution of the resonance structures:



This would explain the rapid substitution rate of another peracetic acid molecule into the cobalt(III)–peracetate complex to form an intermediate similar to I.

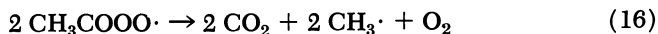
An alternate mechanism for the cobalt(III)-catalyzed peracetic acid decomposition with a sequence of oxidation-reduction reactions, could be as follows:



followed by the fast oxidation of cobalt(II) by peracetic acid. Here Reaction 13 is equivalent to Reaction 12—a hydrogen atom transfer—but with formation of a free peracetoxy radical. Since the peroxide–hydrogen bond is of high energy, a homolytic splitting of that bond could be produced in a relatively fast reaction only by powerful one-electron oxidizing agents such as  $\text{Co}^{\text{III}}$  and  $\text{Mn}^{\text{III}}$  but not by  $\text{Cu}^{\text{II}}$ . Reaction 14 has been proposed (19) in analogy with a similar reaction in the iron(II)–iron(III)-catalyzed decomposition of hydrogen peroxide. This mechanism could explain the experimental kinetics equation obtained for cobalt acetate (Equation 2) by assuming that Reaction 14 is rate limiting, but

it will not explain the experimental kinetic equation obtained for manganese acetate (Equation 1).

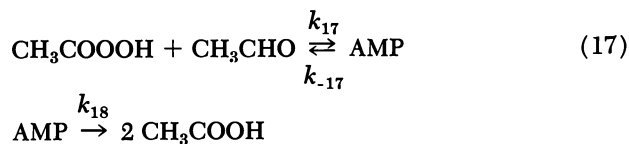
The by-products in both mechanisms will be produced by Reactions 8, 14, and 16:



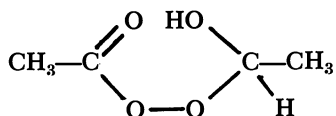
This reaction has been proposed to occur in the vapor phase by McDowell and Sifniedes (20). The peracetoxy radical in the first mechanism proposed will be produced by Reaction 13, which in this case is a secondary reaction. Reoxidation of the metal ion in the 2+ oxidation state could also lead to by-products at low metal ion-peracetic acid ratios (4, 19).

The methyl radicals produced in Reactions 2a, 15, and 16 could abstract hydrogen to produce the small amounts of methane found in the by-products or could be oxidized with oxygen and/or the metal ions in the 3+ oxidation state. Oxidation of alkyl radicals by metal ions has been studied extensively (11, 12). Also, the oxidation of the intermediates methanol, formaldehyde, and formic acid by cobalt(III) and manganese(III) has been reported (2, 13, 15).

**Reaction of Acetaldehyde with Peracetic Acid.** The reaction of peracetic acid with acetaldehyde in the absence of catalyst has been studied by several authors (4, 14). The reaction produces acetic acid through the intermediate AMP:



The equilibrium constant of Reaction 17 has been determined (4):  $K_{17} = k_{17}/k_{-17} = 3.5 \text{ mole}^{-1} \text{ liter}$  at 25°C., and  $k_{17}$  can be estimated to be of the order of  $1 \text{ liter mole}^{-1} \text{ min.}^{-1}$  at 30°C. from the work of Kagan and Lubarsky (14). Bawn and Williamson (4) determined  $k_{18}$  to be  $0.015 \text{ min.}^{-1}$  at 25°C. The structure of AMP has been established by infrared spectroscopy (22):



Since copper(II) does not catalyze the AMP decomposition, the mechanism for acetic acid formation in the presence of copper(II) acetate is indicated by Reactions 17 and 18.

In the reaction of peracetic acid with acetaldehyde we do not know that manganese and cobalt ions in the 3+ oxidation state are the predominant species. Based on the color of the solutions during reaction

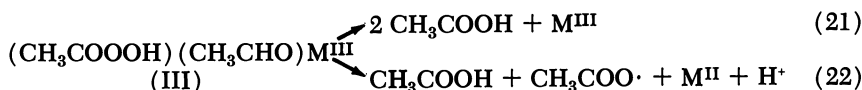
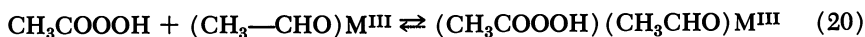
the predominant species are probably in the 3+ oxidation state. (The solutions are green when using cobalt and brown when using manganese, as also observed in the peracetic acid decomposition.) We cannot rule out, however, the presence of significant amounts of metal ion in the 2+ oxidation state.

With manganese and cobalt acetate the reaction of peracetic acid with acetaldehyde is very fast, and AMP is not detected. By comparing our rates with literature values of  $k_{17}$ ,  $k_{-17}$ , and  $k_{18}$  we cannot propose a mechanism in which the only role of the metal ion is to catalyze the decomposition of AMP. The experimental rates in the presence of either manganese or cobalt acetates are much faster than the noncatalytic rate of formation of AMP. Thus, AMP *per se* is probably not an intermediate in the presence of these catalysts.

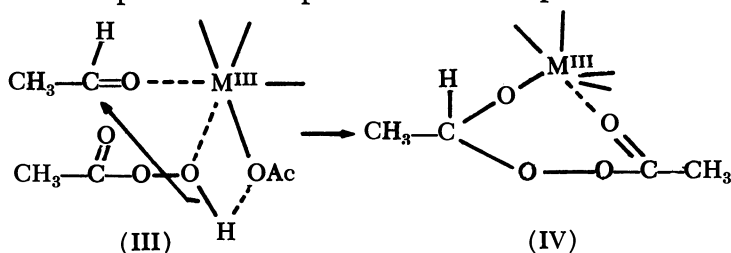
We believe that catalysis occurs by formation of a complex between acetaldehyde, peracetic acid, and the metal ion in the 3+ oxidation state. The metal ion could be acting as a superacid as for peracetic acid decomposition, although oxidation-reduction reactions within the complex cannot be ruled out. Here again, we have found a disturbing lack of catalytic activity of other trivalent metals (aluminum, iron, and chromium). Simple acid catalysis is not as effective as proved when using *p*-toluenesulfonic acid and acetyl borate. This indicates that at least more than one coordination position is needed to obtain a complex of the proper configuration.

The proposed mechanism will give the experimental kinetic equation (25) by assuming that the rate-determining step is the formation or decomposition of the complex and that the metal(III)-metal(II) ratio is approximately constant during reaction.

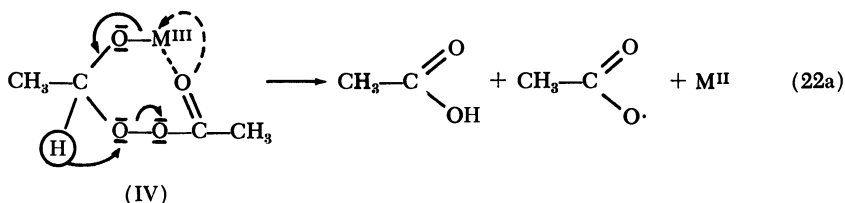
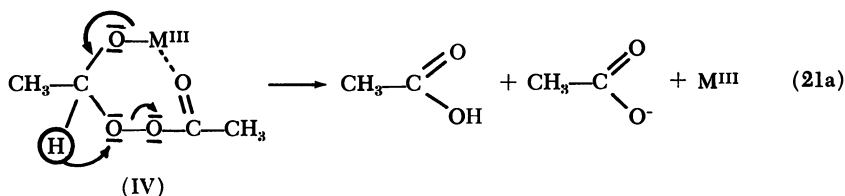
Thus, the proposed mechanism is as follows:



The decomposition of complex III could be represented as follows:



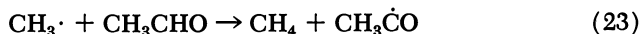
The intermediate (IV) could be decomposed by two pathways:



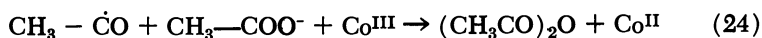
In Reaction 21a there is no net electron transfer to the metal, and the only product is acetic acid. In Reaction 22a, a one-electron transfer to the metal ion occurs, and the peracetic acid moiety of the complex is transformed into an acetoxy radical which will decompose rapidly to CH<sub>3</sub>· and CO<sub>2</sub>.

Reaction 22a is important only with cobalt acetate catalyst and accounts for the fast rate of methane formation during the reaction of peracetic with acetaldehyde. It can also explain how methane is produced only from the methyl group of peracetic acid. This reaction path is more important with cobalt probably because of the higher oxidation potential of the cobalt(III)–cobalt(II) couple relative to that of the manganese(III)–manganese(II) couple.

In the reaction of peracetic acid with acetaldehyde (in the absence of oxygen) the majority of the methyl radicals abstract hydrogen, preferentially from acetaldehyde, to form methane:



The acetyl radicals produced in this reaction must be oxidized by cobalt(III) to acetic acid and/or anhydride in a fast step since only traces of other possible by-products (biacetyl and acetone) were found.



Oxidation of acyl radicals by iron(III) has been postulated by Coffman *et al.* (10).

The sequence of Reactions 19, 20, and 21 indicates that substitution on the metal ion by at least one of the substrates is faster than the over-all reaction rate. This can be understood easily for manganese(III) complexes (substitution labile). It is, however, more difficult to rationalize for cobalt(III) unless the rate of cobalt(II)–cobalt(III) exchange is very fast in this system.

**Oxidation of Acetaldehyde.** When using cobalt or manganese acetate the main role of the metal ion (beside the initiation) is to catalyze the reaction of peracetic acid with acetaldehyde so effectively that it becomes the main route to acetic acid and can also account for the majority of by-products. Small discrepancies between acetic acid efficiencies in this reaction and those obtained in acetaldehyde oxidation can be attributed to the degradation of peracetoxy radicals—a peracetic acid precursor—by Reactions 14 and 16. The catalytic decomposition of peracetic acid is too slow (relative to the reaction of acetaldehyde with peracetic acid) to be significant. The oxidation of acetyl radical by the metal ion in the 3+ oxidation state as in Reaction 24 is a possible side reaction. Its importance will depend on the competition between the metal ion and oxygen for the acetyl radical.

When acetaldehyde is oxidized in the presence of copper(II), the noncatalytic reaction between acetaldehyde and peracetic acid may be the main route to acetic acid. Since this reaction is slow, one would expect the presence of a significant concentration of peroxide in the reactor product, and we have confirmed this experimentally. Acetic acid can also be produced by oxidizing acetyl radicals by copper(II); the copper(I) formed could be easily reoxidized by oxygen. The by-products when using copper(II) acetates must be produced mainly by degradation of peracetoxy radicals by Reaction 14 and 16 since peracetic acid decomposition is negligible and the reaction of acetaldehyde with peracetic acid produces essentially only acetic acid.

Comparing the reaction rates of peracetic acid and acetaldehyde in the presence of each of the metal ion acetates clearly indicates why mixtures of either cobalt or copper acetate with manganese acetate behave in a fashion similar to manganese acetate when used alone.

With any of the catalysts most of the by-products (except CO<sub>2</sub>) are produced from methyl radicals, and it is the fate of this radical which will determine the by-product distribution in the air oxidation of acetaldehyde.





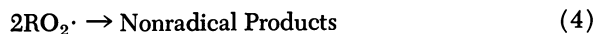
## Nitric Acid Catalysis in the Oxidation of Aromatic Hydrocarbons

K. L. OLIVIER and L. V. E. GOTHLICH

Union Oil Co. of California, Research Center, Brea, Calif.

*Oxidation of p-xylene to terephthalic acid in acetic acid containing cobalt or manganese salts and nitric acid gives yields of 70–80%. In the absence of these salts some p-toluic acid but no terephthalic acid is produced. In the absence of nitric acid, toluic and terephthalic acids are formed, but the reaction rate is considerably lower. About 5 wt. % of water leads to high yields and to low loss of nitric acid to inert species. Plots of the molar ratio of oxygen to p-xylene vs. acid yields showed a rapid increase in yield as the ratio increased to about 70% of that required for 100% conversion to terephthalic acid. At higher oxygen ratios, the yield remained constant, even though oxygen consumption increased. At higher ratios all organic species were degraded somewhat.*

**A**utoxidation of alkylaromatic hydrocarbons has been studied extensively in recent years (1, 2, 3, 11, 12 13), and the mechanism (Reactions 1–4) is now well understood.



In the presence of heavy metal salts this reaction scheme is modified principally by introducing Reactions 5 and 6, which increase the rate of free radical production (14).



The cyclic sequence of Reactions 5 and 6 can be accelerated by adding a species which promotes the formation of Co(III) from Co(II). In the oxidation of alkylaromatic hydrocarbons ozone (7), acetaldehyde (8), and methyl ethyl ketone (4) act as promoters in this way.

During other studies catalytic amounts of nitric acid accelerated the air oxidation of noble metals suspended in acetic acid. A similar effect might be anticipated in the oxidation of Co(II) to Co(III).

### *Experimental*

The experiments were run in a one-half gallon stainless-steel autoclave equipped with a mechanical stirrer. Hydrocarbon (*p*-xylene) and metal catalysts were charged in acetic acid solution. The system was flushed and pressurized with helium to 400 p.s.i.g. After heating the autoclave to the desired temperature (175°-220°C.) 70% aqueous nitric acid, diluted with acetic acid, was steadily injected by a piston pump, while oxygen was added in 10-20-p.s.i.g. installments. At the end of the reaction the autoclave was cooled to 65°C. The gas phase was collected in a previously helium-flushed and evacuated 35-liter tank and analyzed for oxygen, nitrogen, nitrous oxide, nitrogen dioxide, carbon monoxide, carbon dioxide, and methane by gas-liquid chromatography. The product mixture was drained from the autoclave and filtered. The residue was washed with acetic acid and ether to yield terephthalic acid. From aliquots of the filtrate the nitrate content was determined by the Kjeldahl method. A fraction boiling between 56° and 110°C. was removed by distillation and analyzed by gas-liquid chromatography. After removing most of the acetic acid, the distillation residue was dissolved in ammonia and reprecipitated with hydrochloric acid to give *p*-toluic acid.

### *Results and Discussion*

The heavy metal-catalyzed oxidation of *p*-xylene to terephthalic acid in stirred autoclaves was greatly accelerated by adding catalytic quantities of nitric acid to the acetic acid solvent (9). Reactions carried out for 2 hours at 200°C. afforded 60-80% yields of terephthalic and *p*-toluic acids in varying ratios; the highest yield of terephthalic acid was 70%. In the absence of either the heavy metal catalyst or nitric acid under otherwise identical conditions *p*-toluic acid was produced in 20-40% yields, but no terephthalic acid was formed.

Limited screening of heavy metals and variation in concentration indicated that an equimolar mixture of cobalt and manganese acetates was an efficient catalyst. Lead and vanadium salts were inactive. A metal ion concentration of about 0.02*M* was sufficient; little rate enhancement was observed at higher concentrations.

Higher nitric acid concentration also promoted the reaction, but the enhanced rate was offset by a lesser selectivity. A practical limit of 5

wt. % concentrated nitric acid was chosen. Buffering the reaction medium by a nitrate salt in lieu of the acid and by adding lithium acetate decreased the oxidation rate.

Figure 1 shows the yield of terephthalic and *p*-toluic acids plotted vs. the percent of the oxygen required by theory for 100% conversion to terephthalic acid. The rapid initial rise in *p*-toluic acid production is expected since this acid is undoubtedly the precursor of terephthalic acid. At low oxygen ratios *p*-tolualdehyde as well as unconverted *p*-xylene is present in the mixture. At higher oxygen values the *p*-toluic acid content decreases as terephthalic acid production increases. The fact that a constant yield is maintained even with further increases in oxygen concentration indicates that degradation of the product is slow relative to oxidative attack on solvent. Independent experiments in which the two product acids were exposed to the reaction conditions for prolonged times resulted in some degradation.

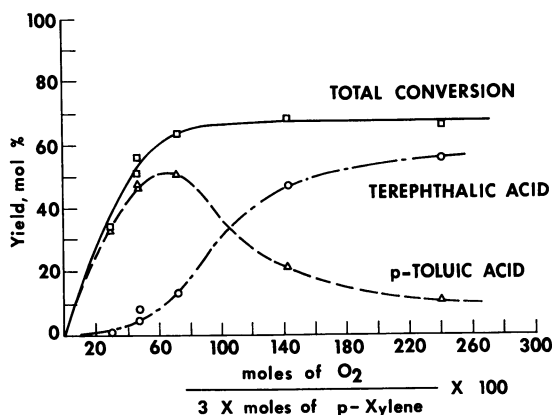


Figure 1. Product yields vs. oxygen ratio

Another effect of high oxygen concentrations was increased oxidative attack on the solvent. This is shown in Figure 2. Methane and methyl acetate were detected in most of the runs, and it is likely that these materials were formed by free-radical attack on acetic acid. Loss of nitric acid to the nonregenerable species nitrous oxide and nitrogen was reduced in the presence of high oxygen concentrations.

A series of experiments was carried out in which the concentration of water in the system was varied. Figure 3 shows a maximum in yield at about 5 wt. % water in the reaction mixture at the end of the run. This finding is apparently in disagreement with Fetterly (6), who claims that an anhydrous reaction medium is required.

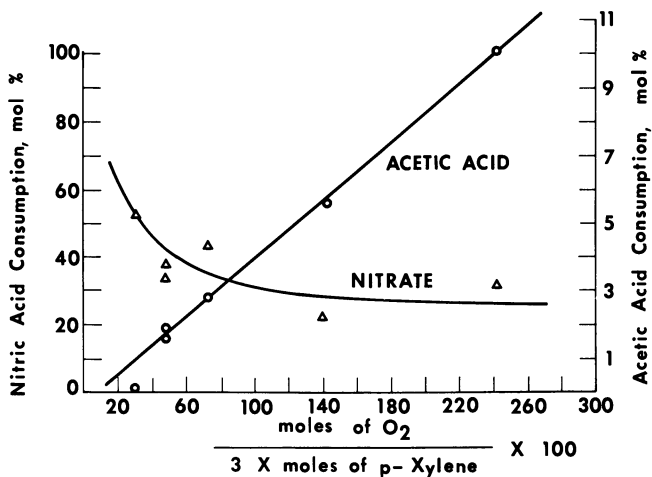


Figure 2. Nitric acid and acetic acid consumption vs. oxygen ratio

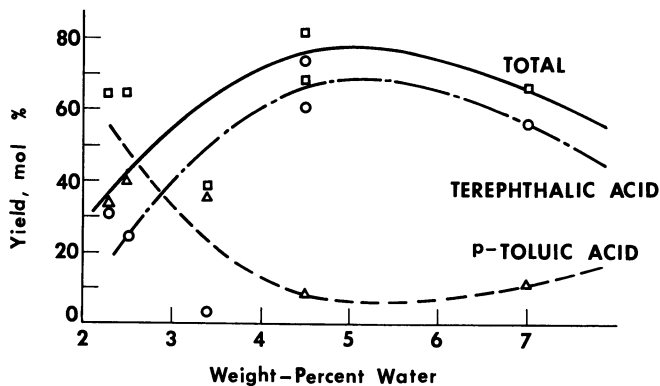


Figure 3. Product yields vs. water concentration

The consumption of nitric and acetic acids is plotted as a function of percent water in the system in Figure 4. The minimum in the nitric acid curve at the 5% level coincides with the maximum in yield (Figure 3). This is not surprising; it merely indicates that the yield depends on the activity of the cocatalyst.

The dependence of yield on temperature is shown in Figure 5. The maximum in yield of terephthalic acid occurs at 200°–210°C. Yields did not improve in experiments carried out in two temperature stages. Surprisingly, decomposition of acetic acid is remarkably independent of

temperature over the range 175°–220°C. (Figure 6). The maximum in nitric acid consumption coincides with the maximum in yield of terephthalic acid.

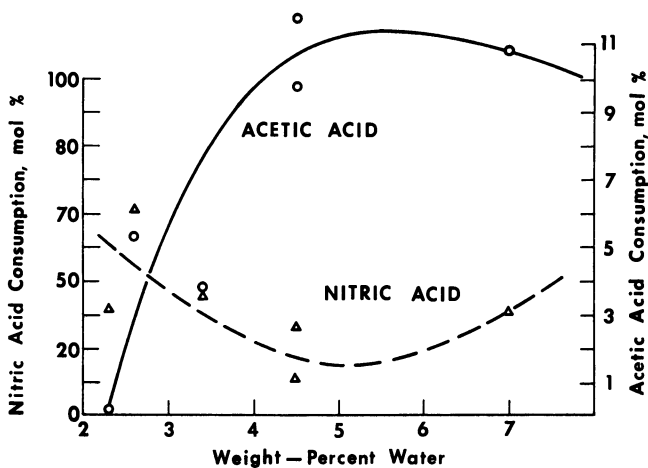


Figure 4. Nitric acid and acetic acid consumption vs. water concentration

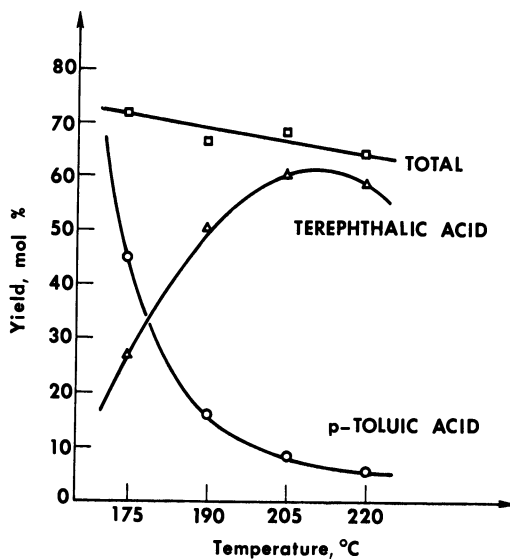


Figure 5. Temperature dependence of product yields

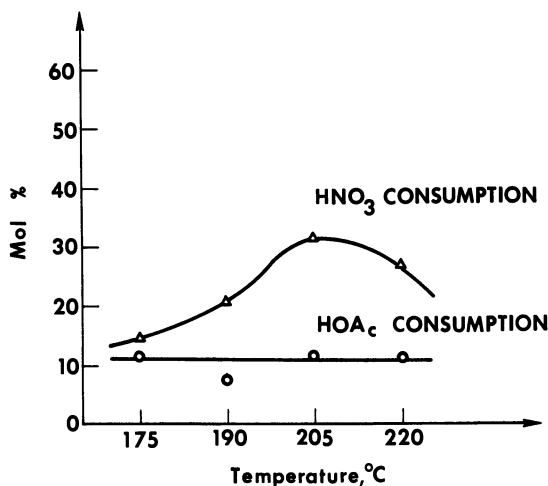
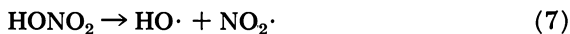


Figure 6. Temperature dependence of nitric acid and acetic acid consumption

The effectiveness of nitric acid as a cocatalyst is probably caused by two factors. One of these is the homolytic scission of the nitric acid molecule (Reaction 7) to produce free radicals which act as initiators (5) (Reaction 1).



Nitric acid can also catalyze the oxidation by oxidizing Co(II) to Co(III), thus facilitating the cyclic sequence of Reactions 5 and 6.

Table I. Oxidation of Other Hydrocarbons<sup>a</sup>

Hydrocarbon	Temp., °C.	Products, Mole % Yield
<i>m</i> -Xylene	200	Isophthalic acid, 61 <i>m</i> -Toluic acid, 19
<i>o</i> -Xylene	200	Phthalic anhydride, 37 <i>o</i> -Toluic acid, 8
Pseudocumene	200	Trimellitic acid, 23 Methylphthalic acid, 39 Dimethylbenzoic acid, 14
Toluene	200	Benzoic acid, 47
<i>p</i> -Cymene	200	Terephthalic acid, 48 <i>p</i> -Toluic acid, 14
2,6-Dimethylnaphthalene	175	2,6-Naphthalic acid, 20 6-Methyl-2-naphthoic acid, 10
Anthracene	90	Anthraquinone, 99

<sup>a</sup> Typical conditions: 1 mole of hydrocarbon in 400 grams of HOAc containing 1 wt. % each of cobalt and manganese acetate tetrahydrate; 1/3 mole of HNO<sub>3</sub> in HOAc added continuously during 2 hours; oxygen added in 10–20 p.s.i.g. increments at 400 p.s.i.g.

Although most of the experiments were carried out using *p*-xylene as substrate, several exploratory runs were made using other aromatic hydrocarbons. These are summarized in Table I. Maximum yields were not determined. Alkyl-naphthalenes gave highly colored oxidates, from which only small amounts of naphthoic and naphthalic acids could be isolated. Oxidation of anthracene gave virtually quantitative yields of anthraquinone under extremely mild conditions (10).

### *Acknowledgments*

The authors thank the management of the Union Oil Co. of California for permission to publish this work, W. D. Schaeffer for helpful discussions, E. J. Walker and L. C. Smith for assistance in the experimental work.

### *Literature Cited*

- (1) Bateman, L., *Quart. Rev. London* **8**, 147 (1954).
- (2) Blanchard, H. S., *J. Am. Chem. Soc.* **81**, 4548 (1959).
- (3) Bolland, J. L., *Quart. Rev. London* **3**, 1 (1949).
- (4) Brill, W. F., *Ind. Eng. Chem.* **52**, 837 (1960).
- (5) Duffin, H. C., Hughes, E. D., Ingold, C., *J. Chem. Soc.* **1959**, 2734.
- (6) Fetterly, L. C., U. S. Patent **2,839,575** (June 17, 1958).
- (7) Hay, A. S., Eustance, J. W., Blanchard, H. S., *J. Org. Chem.* **25**, 616 (1960).
- (8) Hull, D. C., U. S. Patent **2,673,217** (March 23, 1954).
- (9) Olivier, K. L., Schaeffer, W. D., U. S. Patent **3,227,752** (Jan. 4, 1966).
- (10) Peters, G., U. S. Patent **1,455,448** (1923).
- (11) Russell, G. A., *J. Am. Chem. Soc.* **79**, 3781 (1957).
- (12) *Ibid.*, **77**, 4583 (1955).
- (13) *Ibid.*, **78**, 1047 (1956).
- (14) Woodward, A. E., Mesrobian, R. B., *J. Am. Chem. Soc.* **75**, 6189 (1953).

RECEIVED April 1, 1968.

## Air Oxidation of Alcohols to Esters *via* Bromine–Nitric Acid Catalysis

E. F. LUTZ

Shell Development Co., Emeryville, Calif. 94608

*Primary aliphatic alcohols are air-oxidized to the corresponding esters in the presence of a bromine–nitric acid catalyst. Evidence supporting a mechanism, which is not a free radical chain process, is presented.*

The bromine oxidation of alcohols (1) was first reported in 1901 by Bugarszky, who found that ethanol formed ethyl acetate in concentrated aqueous alcohol (76% weight EtOH) and acetic acid in dilute solution (3, 4). The oxidation of acetaldehyde in aqueous solution, now known to proceed through the hydrate (6), gave acetic acid (5). Tri-bromide ions, formed during the reaction, do not oxidize ethanol and are responsible for a decrease in reaction rate with increasing time (6). Bromination becomes an important side reaction at low pH (6). Secondary alcohols oxidize to ketones (2).

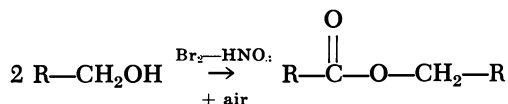


The application of bromine oxidation in a catalytic fashion attracted our attention as a useful route to acids and esters.

### **Results and Discussion**

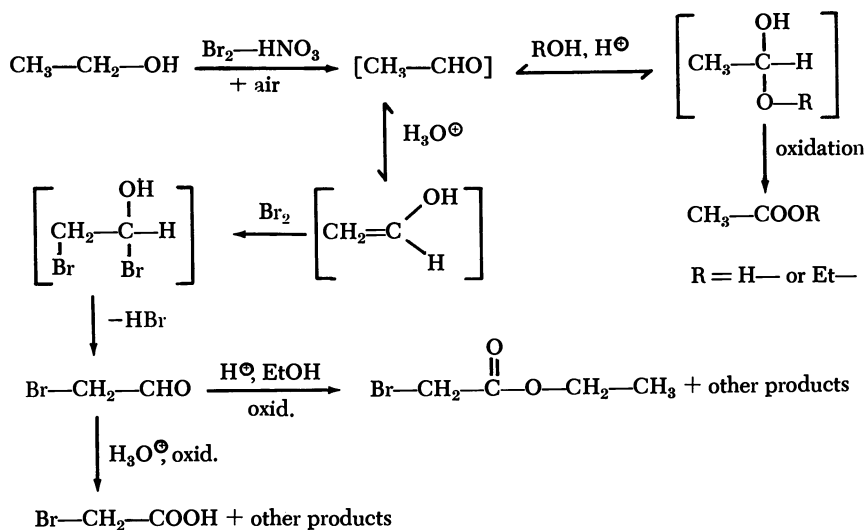
High valent ( $\bar{\text{N}} + 2$ ) nitrogen oxides catalyze the air oxidation of hydrogen bromide to bromine (9), and this led to the development of an alcohol air-oxidation catalyst based on bromine and nitric acid.

The higher aliphatic alcohols ( $\text{C}_8\text{—C}_{21}$ ), as summarized in Table I, are oxidized in high yield to the corresponding esters.



The oxidation is fast (even in a rocking autoclave), shows no induction period, and is essentially unaffected by the form in which the catalyst is added. No oxidation is obtained when either of the catalyst components is used independently or when chlorine is substituted for bromine. Free acid is not obtained with the water-insoluble alcohols.

In contrast, the alcohols of low molecular weight give poor yields and a mixture of products. This can be explained by the intermediate aldehydes' water solubility, which favors enolization and hydration in the acidic medium, leading to catalyst consumption and a distribution of products.



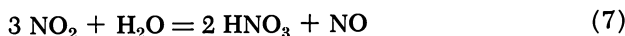
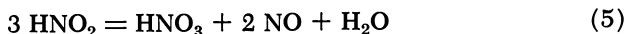
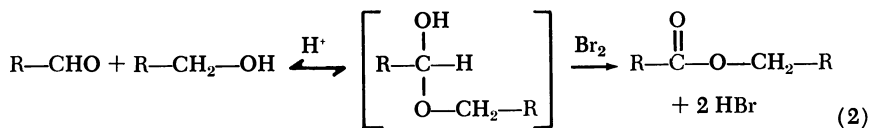
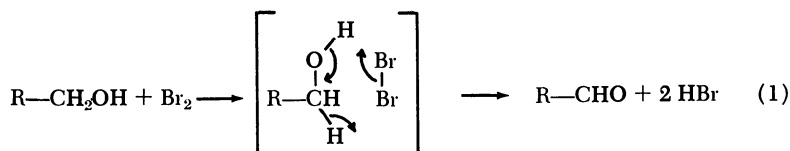
The alcohols of higher molecular weight brominate to a minor extent and this is probably caused, at least in part, by thermal bromination during the initial exotherm.

The oxidation of lauryl aldehyde gives lauric acid in 53.4% yield. This reaction is not exothermic and is much slower than that of the corresponding alcohol. Neopentyl glycol oxidizes to a low molecular weight polyester in 21% yield.

Upon completion of the oxidation, bromine was always found in the organic layer when phase separation occurred.

**Mechanism of Oxidation**

Our observations are summarized as follows: (1) no induction period, (2) fast alcohol oxidation in an oxygen-poor liquid phase, (3) no carboxylic acids from the higher alcohols, (4) slow oxidation of lauryl aldehyde to lauric acid in the presence of water, and (5) recovery of bromine in the organic phase on reaction completion. These data show that the reaction is not a radical chain process but rather a bromine oxidation in which the halogen is continuously regenerated, as shown in Reactions 1 through 7.



A cyclic transition state as proposed by Barker *et al.* (2) is most attractive for the initial bromine oxidation of the alcohol since the reaction probably takes place in the organic phase. Other transition states have also been proposed which are better suited to homogeneous oxidations in aqueous solution (8, 13). The regeneration of bromine from nitryl bromide and hydrogen bromide in the organic phase is analogous to the known formation of bromine from hydrogen bromide and *N*-bromosuccinimide (10, 11). (The physical properties of nitryl bromide have not been described because of its fleeting existence, and the assumption is made that its solubility in the organic phase will be similar to that of bromine.) Talbot and Thomas (14) have postulated that NOCl reacts with surface-adsorbed HCl at 25° to 55°C. to form Cl<sub>2</sub>.

Table I. Alcohol

<i>Alcohol, Mmoles</i>	<i>Solvent, Cc.</i>	<i>Catalyst, Mmoles</i>	<i>Temp., °C.</i>
Ethanol, 200	Benzene, 25 H <sub>2</sub> O, 6	48% aq. HBr, 50 NaNO <sub>2</sub> , 17	60
1-Butanol, 250	—	Br <sub>2</sub> , 25 Concd. HNO <sub>3</sub> , 12	60
2-Ethylhexanol, 100	H <sub>2</sub> O, 6.5	48% aq. HBr, 25 NaNO <sub>2</sub> , 9	55
1-Dodecanol, 100	H <sub>2</sub> O, 13	48% aq. HBr, 50 NaNO <sub>2</sub> , 17	(92) <sup>c</sup> 61
1-Dodecanol, 100	H <sub>2</sub> O, 18	Concd. HCl, 30 NaNO <sub>2</sub> , 17	59
1-Dodecanol, 100	H <sub>2</sub> O, 1	Br <sub>2</sub> , 17	65
Dodecanol, <sup>d</sup> 1400	—	Br <sub>2</sub> , 140 Concd. HNO <sub>3</sub> , 70	(121) 90
Dodecanol, 1400	—	Br <sub>2</sub> , 140 Concd. HNO <sub>3</sub> , 70	(131) 80–90
1-Dodecanal, 50	H <sub>2</sub> O, 4	Br <sub>2</sub> , 13 Concd. HNO <sub>3</sub> , 6	65
Heneicosanol, <sup>f</sup> 200	—	Br <sub>2</sub> , 20 Concd. HNO <sub>3</sub> , 10	86–90
Neopentyl glycol, 100	H <sub>2</sub> O, 9	Br <sub>2</sub> , 25 Concd. HNO <sub>3</sub> , 12	(86) 75

<sup>a</sup> Oxidations carried out in glass-lined rocking autoclave.

<sup>b</sup> Assumed, not rigorously established.

<sup>c</sup> Parentheses indicate peak temperature of initial exotherm.

<sup>d</sup> 81% *n*-C<sub>12</sub>OH, remainder other primary C<sub>12</sub> alcohols.

The estimated boiling points and the known critical temperatures of the inorganic compounds in the system show that all except NO (and possibly HBr to a limited extent) remain in the condensed phase throughout the reaction. [Boiling points, °C., at 60 atm. (critical temperatures, °C.) (12): Br<sub>2</sub>, 243.5 (302.2); HBr, 70.6 (90.0); NO, -94.9 (-92.9); N<sub>2</sub>O<sub>4</sub>, 132.2 (158).] Thus, NO, as formed, enters the gas phase, where it is rapidly oxidized to NO<sub>2</sub> (N<sub>2</sub>O<sub>4</sub>) which condenses, returning to the liquid phase for nitric acid regeneration. This represents an efficient use of nitric acid catalysis since as much as 18 moles of alcohol are oxidized per mole of nitric acid.



- (6) Farkas, L., Perlmutter, B., Schächter, O., *J. Am. Chem. Soc.* **71**, 2827-35 (1949).
- (7) Hay, A. S., Blanchard, H. S., *Can. J. Chem.* **43**, 1306 (1965).
- (8) Kaplan, L., *J. Am. Chem. Soc.* **80**, 2639 (1958).
- (9) Merton-Bingham, B. E., Posner, A. M., *J. Am. Chem. Soc.* **77**, 2634 (1955).
- (10) Russell, G. A., Desmond, K. M., *J. Am. Chem. Soc.* **85**, 3139 (1963).
- (11) Skell, P. S., Tulene, D. L., Readio, P. D., *J. Am. Chem. Soc.* **85**, 2850 (1963).
- (12) Stull, D. R., *Ind. Eng. Chem.* **39**, 546 (1947).
- (13) Swain, C. G., Wiles, R. A., Bader, R. F., *J. Am. Chem. Soc.* **83**, 1945 (1961).
- (14) Talbot, P. J., Thomas, H. J., *Trans. Faraday Soc.* **55**, 1884 (1959).

RECEIVED October 9, 1967.

# Oxidation of Aromatic Hydrocarbons to Alcohols and Aldehydes

ELLIS K. FIELDS and SEYMOUR MEYERSON

Research and Development Departments, Amoco Chemicals Corp. and American Oil Co., P. O. Box 431, Whiting, Ind. 46394

*Aromatic aldehydes and alcohols can be prepared in moderate yields by oxidizing aromatic hydrocarbons with oxygen at atmospheric pressure, using acetic acid as solvent and cobalt acetate and bromide as catalysts. Low voltage mass spectrometry is useful in following the course of the reaction and predicting, with considerable accuracy, the period for optimum conversions, as well as determining the nature of minor products. Oxidation of toluene- $\alpha$ -d<sub>3</sub> indicates radical abstraction of hydrogen from the aromatic ring as well as from the side chain.*

**A**lkylated aromatic hydrocarbons have been oxidized to alcohols, aldehydes, and acids by various oxidants such as potassium permanganate, sodium dichromate, nitric acid, and oxygen. A procedure involving the use of oxygen at atmospheric pressure, together with cobalt acetate and hydrobromic acid in refluxing acetic acid, was described by Hay and Blanchard (12); although they showed the formation of some alcohol and aldehyde, they stressed primarily the preparation of carboxylic acids. By using lower concentrations of catalysts, we hoped to convert aromatic hydrocarbons in appreciable yields to aromatic alcohols and aldehydes, as well as to find the products of coupling of hydrocarbon radicals.

The rate of formation of oxidation intermediates was followed by withdrawing aliquots during oxidation runs and determining intensities of the parent peaks in low voltage mass spectra as measures of the relative concentrations of starting hydrocarbon and products. Although sensitivity—*i.e.*, the proportionality factor between parent-peak intensity and concentration—differs from one compound to another, peak heights for any one compound in the spectra of samples of equal size ( $0.6\mu$ ) are

directly proportional to concentrations of that compound in the various samples. Closely related compounds have roughly equal sensitivities at the ionizing voltage employed in our work (10), and, in any case, the use of intensity ratios is perfectly valid for intercomparison of concentration ratios of identical components in separate samples (11, 23) within the limits of reproducibility of the low voltage data.

### Experimental

Hydrocarbons were purchased from Eastman and Aldrich and, where necessary, purified to 99+ % purity. Hemimellitene was furnished by M. C. Hoff, Amoco Chemicals Corp. Acetic acid was J. T. Baker ACS reagent grade; cobalt acetate and cobalt bromide were Fisher certified grade.

In a typical oxidation, a solution of 286 ml. (5 moles) of acetic acid, 3.26 grams (0.01 mole) cobalt bromide hexahydrate, 7.47 grams (0.03 mole) cobalt acetate tetrahydrate, and 61.5 ml. (0.5 mole) of *p*-xylene was refluxed in a Vibra-Mix apparatus (Chemische Apparat, Zurich) with oxygen passing in at the rate of 0.6 cu. foot per hour. Aliquots (25 ml.) were withdrawn after 30 minutes and 1 hour and hourly thereafter for 5 more hours. Each aliquot was treated with 100 ml. of water and 150 ml. of ether; the ether layer was washed with three 50-ml. portions of water and dried, and the ether was distilled. The ether-free residue was analyzed by low voltage (approximately 7.5 volts, uncorrected) mass spectrometry on a Consolidated model 21-103c instrument with the inlet system at 250°C. The repellers were maintained at an average potential of 3 volts, the exact values being selected to give maximum sensitivity. Conventional 70-volt spectra were also measured to help establish the identities of components where molecular weight alone was not adequate to remove all ambiguity. Total ion current at 70 volts, measured independently of the spectrum (24), was nearly constant for the samples in each series, confirming that essentially the same amount of sample was admitted in each case. Reproducibility on repeated oxidations was within 7%. Result of a typical analysis are shown in Table I for toluene oxidation.

Table I. Results of Typical Analysis

Compound	Time, Hours						
	0.5	1	2	3	4	5	6
	Relative Concentration, Scale Divisions of Peak Height						
Toluene	490	340	210	80	40	20	16
Benzaldehyde	20	40	60	40	8	0	0
Benzyl alcohol	36	40	30	20	10	1	0
Benzyl acetate	6	10	14	16	10	0	0
Benzoic acid	6	10	30	80	140	180	160
Bibenzyl	13	10	7	6	0	0	0

Table II. Products from Reaction of Indium and Benzylic Bromides

Mass	Relative Intensity	Suggested Identities
<i>Benzyl Bromide</i>		
168	53	Methylbiphenyl and isomers— $C_6H_5C_7H_7$
182	18	Bibenzyl and isomers— $(C_7H_7)_2$
258	100	$C_6H_4(C_7H_7)_2$
272	8	$(C_7H_6)(C_7H_7)_2$
348	68	$C_6H_4C_7H_6(C_7H_7)_2$
362	13	$C_7H_7C_7H_6C_7H_6C_7H_7$
438	26	$C_7H_7C_7H_6C_6H_4C_7H_6C_7H_7$
<i><math>\alpha</math>-Bromo-<i>o</i>-xylene</i>		
92	54	Toluene
106	29	Xylene
120	16	$C_9H_{12}$
134	61	$C_{10}H_{14}$
184–186	13	<i><math>\alpha</math>-Bromo-<i>o</i>-xylene</i>
196	100	$C_7H_7C_8H_9$
210	39	$(C_8H_9)_2$
224	8	$C_8H_9C_9H_{11}$
288–290	8	Bromobixylyl
300	95	$C_7H_6(C_8H_9)_2$
314	27	$(C_8H_8)(C_8H_9)_2$
392–394	6	Bromoterxylyl
404	45	$C_7H_6C_8H_8(C_8H_9)_2$
418	13	$C_8H_9C_8H_8C_8H_8C_8H_9$
508	4	$C_8H_9C_8H_8C_7H_6C_8H_8C_8H_9$

During the workup of the *o*-xylene oxidation run, a strong lachrymator made its presence felt. This was probably  *$\alpha$ -bromo-*o*-xylene*, although it was not detected in the low voltage mass spectrum. We suspected that a strong peak at mass 104, undoubtedly caused chiefly by a fragment ion derived from *o*-methylbenzyl alcohol by loss of  $H_2O$  (1), might also contain a contribution from benzocyclobutene from the interaction of  *$\alpha$ -bromo-*o*-xylene* with the indium tube used to introduce samples into the spectrometer. To test this possibility, benzyl bromide and  *$\alpha$ -bromo-*o*-xylene* were run separately under the same conditions.

When the benzyl and xylyl bromides were brought in contact with indium tubes for sampling, the indium was quickly discolored and pitted. The spectra of the material so taken up were recorded despite the clear evidence of reaction between the indium and the bromide. Relative intensities in the low voltage spectra and suggested identities of the compounds responsible for the peaks are shown in Table II. The chief result of indium attack on  *$\alpha$ -bromo-*o*-xylene* was expected to be removal of a bromine atom to produce a xylyl radical. If this were the case, the major stable products should be xylene polymers of molecular weight 210, 314,

etc. This series is present but it is vastly overshadowed by the series of molecular weight 196, 300, etc., which is presumably derived from one benzyl or tolyl group and one or more xylyl group. The component of molecular weight 134 also seems anomalous. The molecular weight and the 134:133:119 intensity distribution (70-volt spectrum) could be accounted for by tetramethylbenzene, but there seems no obvious reason why such a species should be more abundant than trimethylbenzene, toluene, or even xylene. The explanation may be that indium bromide, formed from indium and the benzylic bromides, acts as a strong Lewis acid. In addition to condensations to diarylmethanes and polyarylpoly-methanes, it brings about demethylation and transmethylation. These reactions are being investigated in solution on a larger scale.

Despite our failure to find any supporting spectral evidence, the suspected presence of  $\alpha$ -bromo-*o*-xylene and the absence of *o*-methylbenzyl acetate in the oxidation products from *o*-xylene suggest a solvolysis rate for this benzylic halide lower than for the isomeric methylbenzyl bromides.

### Discussion

The rates of appearance and disappearance of oxidation intermediates for nine hydrocarbons are shown in Figures 1 to 10. Ordinate values are peak heights, scaled to an original hydrocarbon concentration of 500; the summation of peak heights may vary considerably among aliquots in a series, reflecting differences in sensitivity among the components. Aldehyde builds up rapidly in toluene and the three xylenes and then is consumed; in contrast, acetophenone from ethylbenzene oxidation continues to increase in concentration over 6 hours. This behavior agrees with the findings that cobalt is far less effective than manganese in catalyzing the oxidation of acetophenone (30).

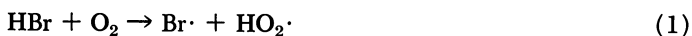
The rate of oxidation of *p*-xylene with the same concentration of cobalt ion with bromide ion (Figure 6) was six times as fast as without bromide (Figure 7).

We have not been able to unscramble the complex kinetics of *p*-xylene oxidation. Ravens studied the second stage of oxidation, that of *p*-toluic acid in acetic acid with cobalt and manganese acetates and sodium bromide (25), and established the rate equation

$$-d[\text{O}_2]/dt = k[\text{Co}^{2+}][\text{NaBr}]^{1/2}[\text{O}_2]^{1/2}$$

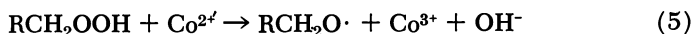
for the autoxidation scheme:

Initiation





Propagation

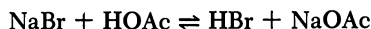


Termination



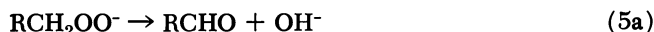
} nonradical products

Sodium bromide with acetic acid furnished hydrogen bromide:

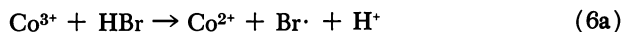


Hydrogen bromide is a weak acid in acetic acid solution and exists mainly in the unionized form (17).

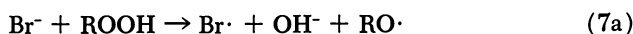
Reaction 1 has been postulated both in oxidations of alkanes in the vapor phase (29) and in the anti-Markovnikov addition of hydrogen bromide to olefins in the liquid phase (14). Reaction 2 involves the established mechanism for free-radical bromination of aromatic side chains (2). Reaction 4 as part of the propagation step, established in earlier work without bromine radicals (26), was not invoked by Ravens, because of the absence of  $[\text{RCH}_3]$  in the rate equation. Equations 4 to 6, in which Reaction 6 was rate-determining, were replaced by Ravens by the reaction of peroxy radical with  $\text{Co}^{2+}$ :



and by reduction of  $\text{Co}^{3+}$  by HBr, analogous to the reaction of cobaltic ion and water (5, 6):



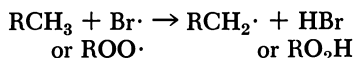
In our study, bromide ion was present in half the concentration of cobalt ion. If bromide ion were active only in a propagation step such as Reaction 6a proposed by Ravens (25) or, alternatively, Reactions 7a and 8a:



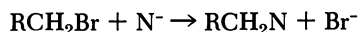
the rate enhancement should have been approximately 50% rather than 600% over the oxidation without bromine. The large rate increase by bromide ion strongly suggests that its major role is to initiate rather

than to propagate many radical chains; its behavior in the liquid phase thus parallels its behavior in the vapor phase (29).

Although an appreciable amount of *p*-tolualdehyde was formed in oxidations with and without bromide, relatively little *p*-methylbenzyl alcohol and acetate resulted in the absence of bromide (1/10 to 1/25 as much as with bromide ion). The contrasting results suggest that the benzyl alcohol is a minor product in the autoxidation chain, as previously postulated by Boland, Bateman, and others (4, 7, 8, 15, 27), and is formed in the presence of bromide by solvolysis:



or



Such rapid solvolysis has been demonstrated for benzyl bromide in acetic acid containing cobalt acetate (10).

Under conditions of high partial pressures of oxygen, the concentration of  $\text{Br}\cdot$  is much lower and that of  $\text{O}_2$  higher, so the benzyl radicals give peroxy radicals and hydroperoxides rather than benzyl alcohol and acetate. Evidence for this is the appreciable amount of benzyl dimer (dimethylbibenzyl) resulting in the presence of bromide in our oxidations at relatively low partial pressure of  $\text{O}_2$ . Benzyl radicals are formed so rapidly that they cannot be scavenged by oxygen and dimerize instead. In the much slower oxidation without bromide all benzyl radicals can find oxygen with which to react, and dimethylbibenzyl is totally absent.

Mass spectrometer analyses of the fractions taken at regular intervals indicate the optimum conversions of aromatic hydrocarbons directly to aldehydes and alcohols by oxidation, as shown in Table III. Semiquantitative yields derived from low voltage mass spectral intensities and values found by gas chromatography were generally in good agreement—for example, oxidations of toluene and *p*-xylene, worked up after 2 hours, gave the results shown in Table IV.

The ratio of alcohol to acetate depends upon workup procedure, which differed in the two cases. In addition, acetates of benzylic alcohols typically break down under electron impact by a low energy process to produce ketene and the corresponding alcohol ion. The peak at the parent mass of the alcohol, throughout this work, most likely contains a contribution so derived from the acetate. A careful distinction between the alcohol and acetate was not deemed important for our purposes, so

we have in many cases taken the sum of the two presumed parent peaks as a measure of the total concentration of the two components.

Although total conversion of hydrocarbon to aldehyde plus alcohol and acetate is not always high, the yields are sufficient to be attractive for the less common aromatic aldehydes and alcohols.

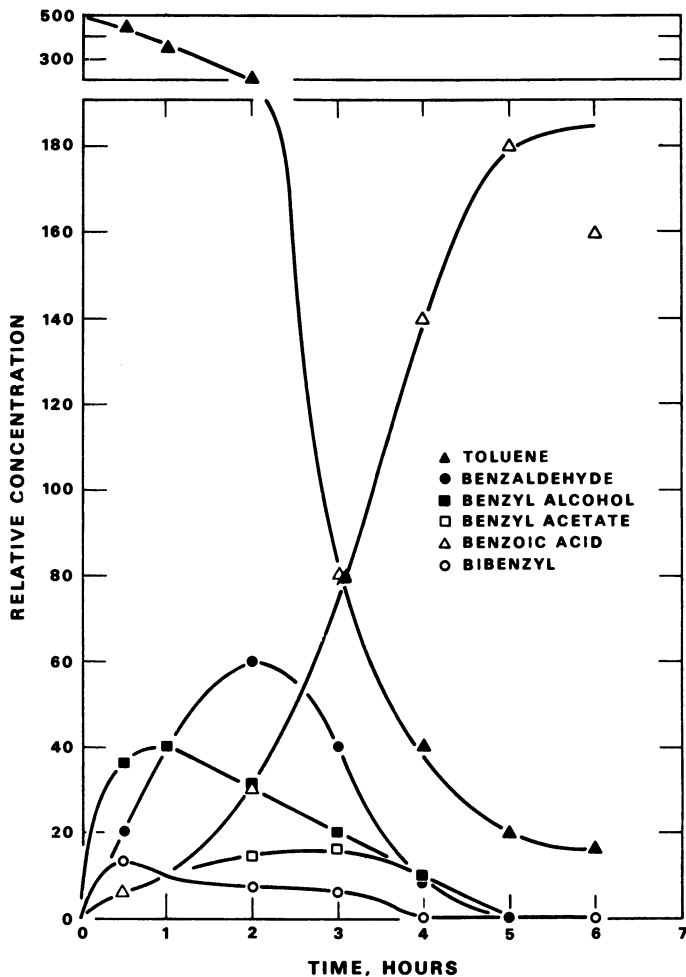
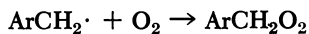


Figure 1. Oxidation of toluene

Comparing results for the three xylene isomers (Figures 4 to 6), we find *m*- and *p*-xylene are similar, whereas *o*-xylene differs sharply in one important respect from the other two. The concentration of 2,2'-dimethylbiphenyl exceeds or equals that of tolualdehyde for the first half of the

oxidation period, whereas tolualdehyde in the other two cases is greater by factors of 1.5 to 5 than the dimethylbibenzyl. The *o*-methylbenzyl radical thus appears to be substantially more stable than the *m*- and *p*-isomers, and prefers to dimerize rather than react with oxygen. The reaction:



supposedly has a zero energy of activation; this may not hold true for  $\text{Ar} = o\text{-methylbenzyl}$ .

Minor oxidation products are shown in Table V; the numbers are relative intensities in the low-voltage mass spectra. The trimeric products

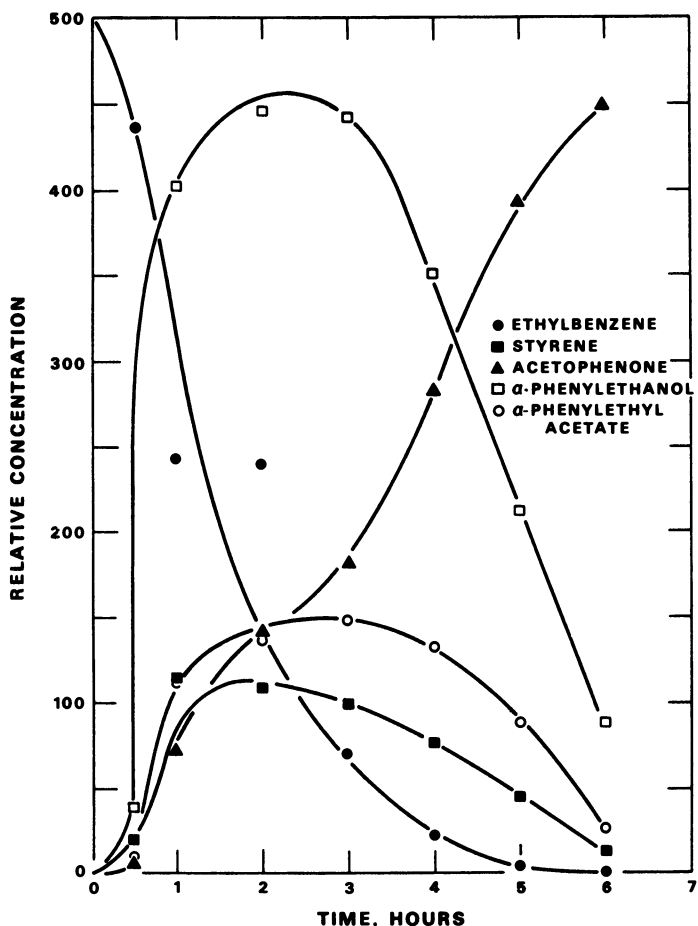
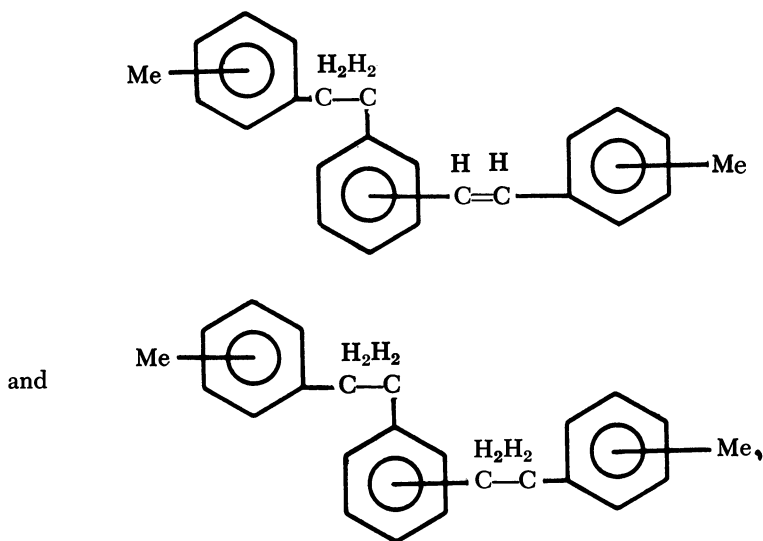


Figure 2. Oxidation of ethylbenzene

$C_{24}H_{24}$  and  $C_{24}H_{26}$  from the xylenes, presumably



are formed in greatest amount from *o*-xylene, providing further evidence for the stability of the *o*-methylbenzyl radical.

The rates of oxidation of aromatic hydrocarbons are shown in Table VI. The rates were determined by following disappearance of the original hydrocarbon rather than oxygen absorption—the technique used by most investigators.

*p*-Xylene oxidized most rapidly, followed by *o*- and *m*-xylene. This is the reverse of the basicities of the three xylenes (20) and would suggest a  $\pi$ -complex between the aromatic hydrocarbon and peroxy or other free radical, such as found by Russell for chlorine atoms (28). However, this order of base strength cannot be correlated with the rates of oxidation of other hydrocarbons; ethylbenzene and cumene are only slightly more basic than toluene, and the methylnaphthalenes are about as basic as *m*-xylene (19).

*p*-Xylene has twice as many benzylic hydrogens as toluene, and oxidizes about twice as fast. *o*-Xylene, also with six benzylic hydrogens, oxidizes only slightly faster, and *m*-xylene more slowly, than toluene. Further, on a purely statistical basis, hemimellitene has 1.5 times as many benzylic hydrogens as *p*-xylene and should therefore oxidize 1.5 times as rapidly. Its rate is less than 1/10 that of *p*-xylene; evidently, a steric, or perhaps polar, effect is far more important than the statistical factor. Co-oxidations are under way to confirm these differences.

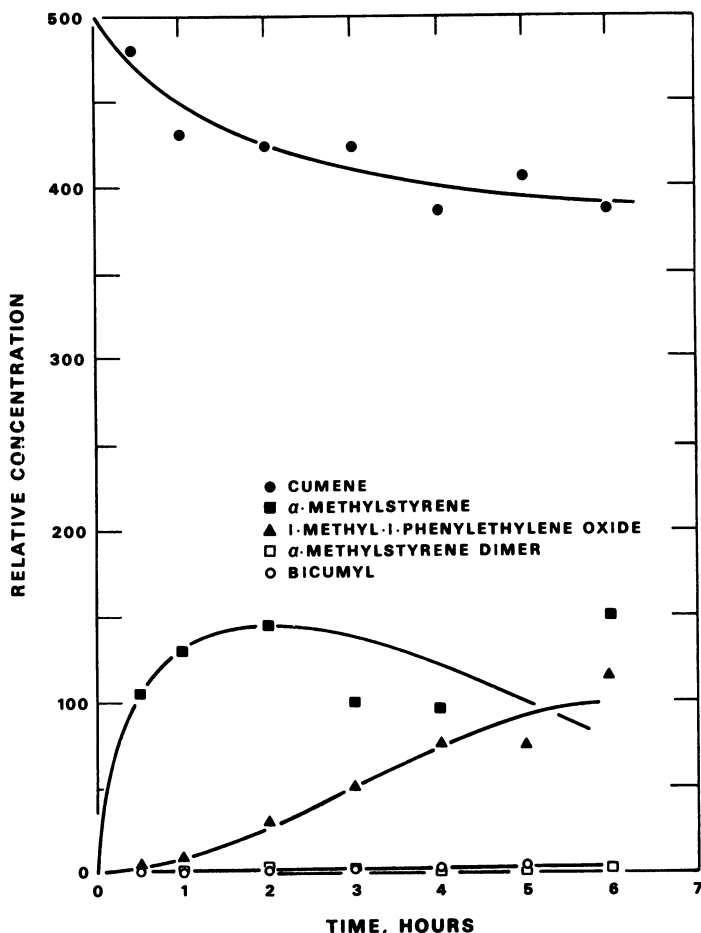
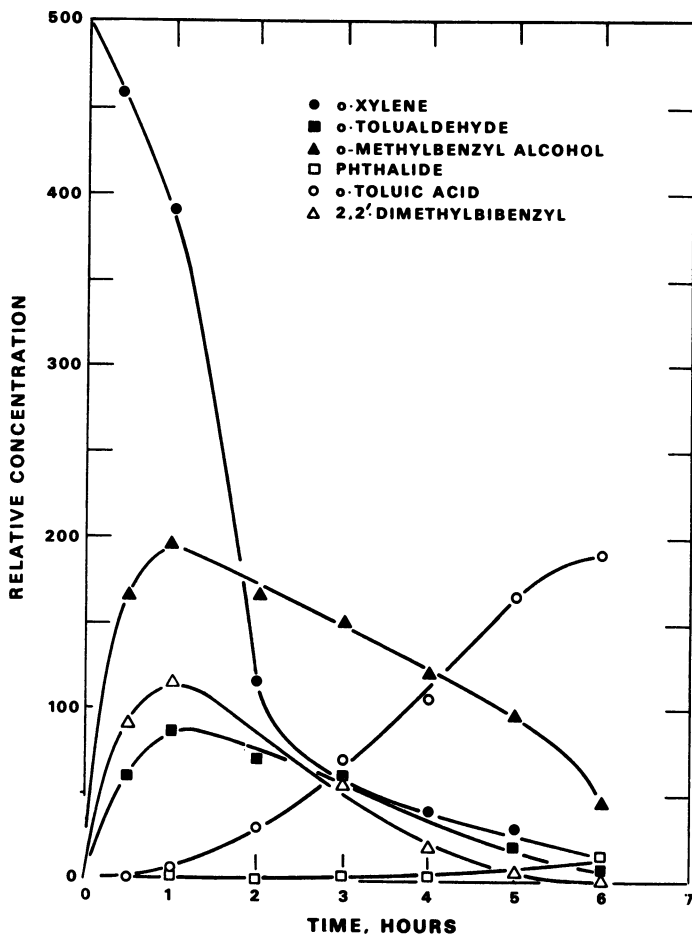
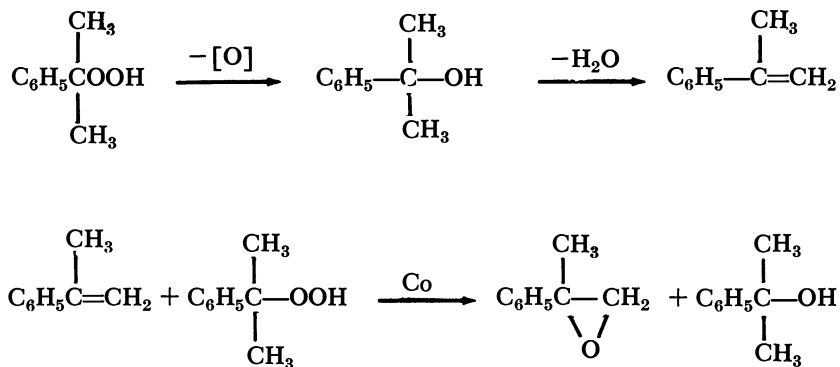


Figure 3. Oxidation of cumene

Cumene oxidized relatively slowly, at about 1/13 the rate of *p*-xylene. This was not caused by the formation of phenol, as might be expected by an acid-catalyzed rearrangement of cumene hydroperoxide. No phenol or product clearly derived from phenol, as by radical attack or by oxidation to a quinone, was detected at any time in the reaction mixture. The two major products were  $\alpha$ -methylstyrene and 2-phenylpropylene oxide; their concentrations increased with time. The group at Shell also observed the formation of  $\alpha$ -methylstyrene and 2-phenylpropylene oxide among the products of cumene oxidation in butyric acid at 140°C. with cobalt and manganese catalysts (30).

$\alpha$ -Methylstyrene rather than phenol might function as the retarder, consuming hydroperoxide by the following reactions.

Figure 4. Oxidation of *o*-xylene

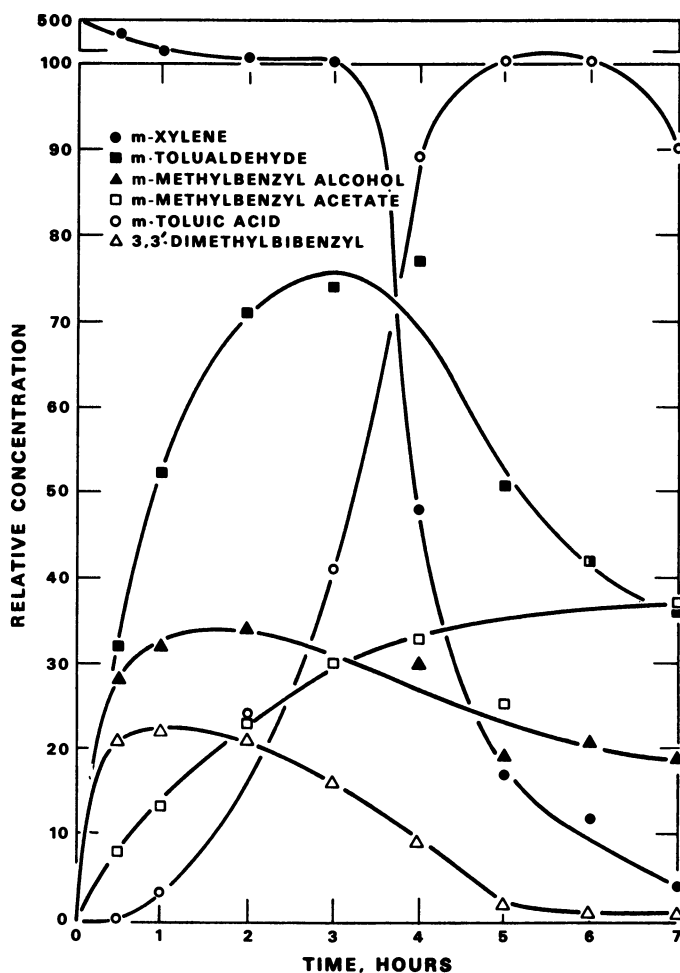


Figure 5. Oxidation of *m*-xylene

This is similar to the process in which ethylbenzene is oxidized by air to the hydroperoxide, then treated with propylene in the presence of transition metal oxides or salts to yield  $\alpha$ -phenylethanol and propylene oxide (18), although, as Mayo points out (21), Co is a poor catalyst in this reaction.

Phenylethylene oxide might be expected among the oxidation products from ethylbenzene by similar reactions. Its absence may be caused by the relative reluctance of styrene to react with peroxy radicals.  $\alpha$ -Methylstyrene, which can yield the more stable  $\beta$ -substituted  $\alpha$ -methyl- $\alpha$ -phenethyl radical, is 2 to 3 times as reactive towards peroxy radicals as is styrene (22).

The methylnaphthalenes were slowest to oxidize of the hydrocarbons studied; after the standard 6 hours only a few per cent had been converted to the products shown:

Product	Intensity <sup>a</sup>	
	1-Methylnaphthalene	2-Methylnaphthalene
Aldehyde	4	2
Carbinol	5	2
Carbinyl acetate	13	6
Dinaphthylethane	4	3

<sup>a</sup> Relative to methylnaphthalene = 100.

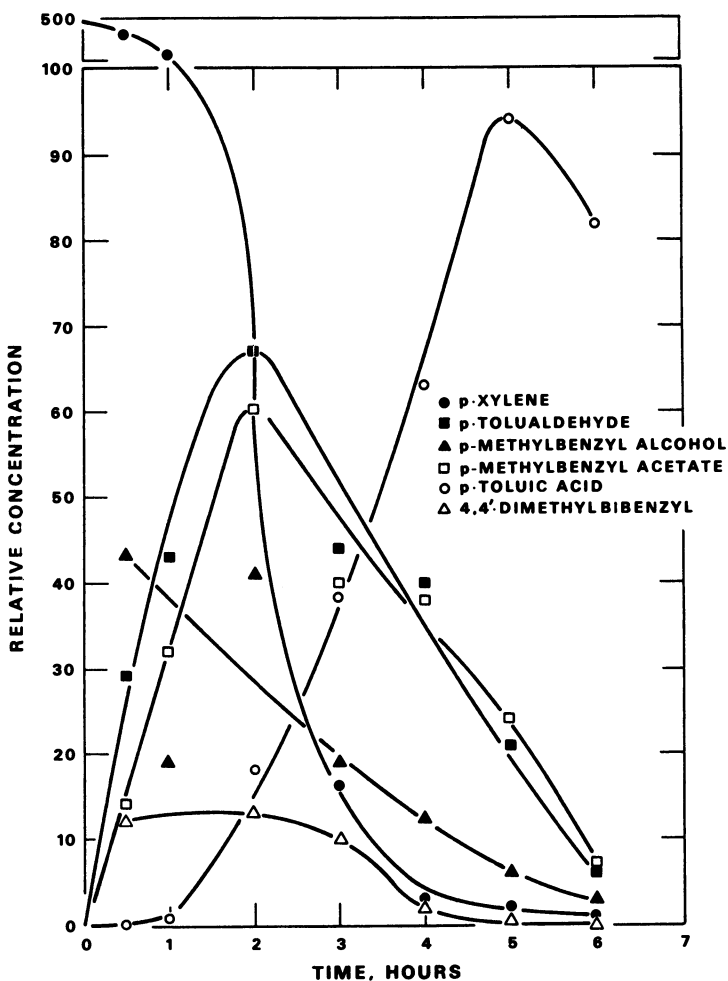


Figure 6. Oxidation of p-xylene

Neither the relative number of benzylic hydrogens nor the base strength accounts for the slow oxidation rate of the methylnaphthalenes. Formation of radicals in the presence of aromatic hydrocarbons can lead to radical attack on the aromatic ring. Addition of phenyl or methyl radical to the ring gives a cyclohexadienyl radical that may disproportionate or dimerize, or undergo hydrogen abstraction by another radical (3, 9, 13).

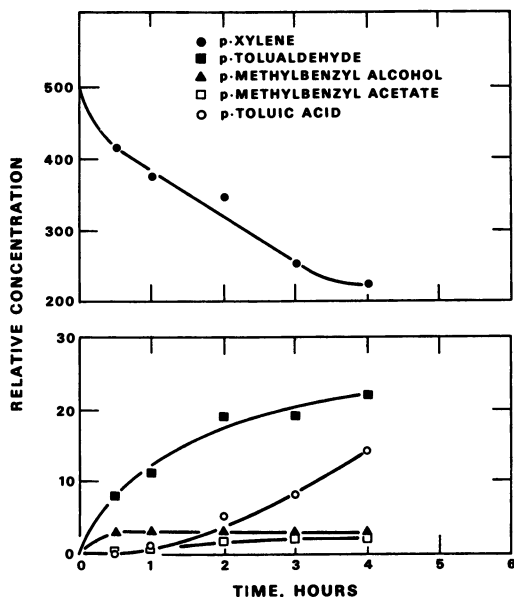
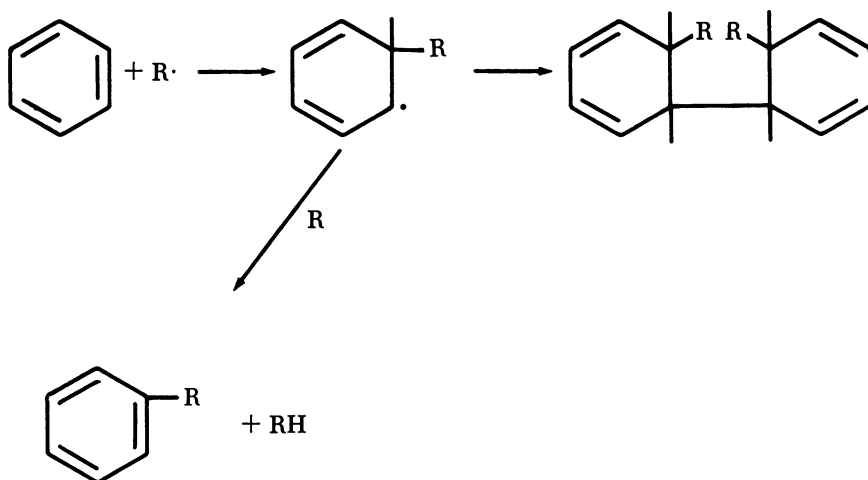
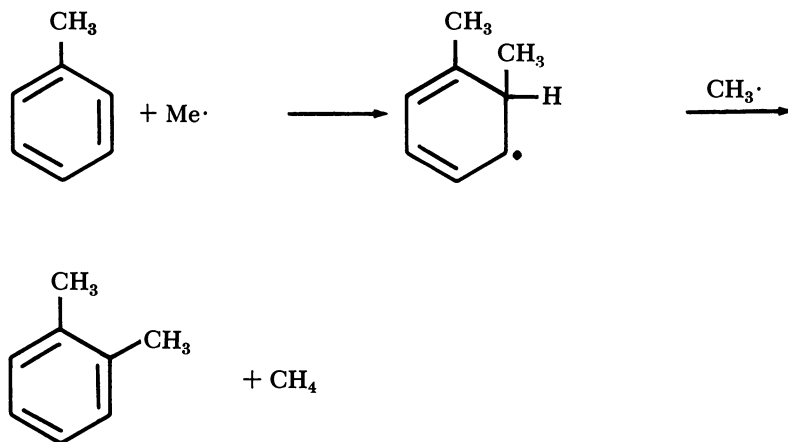
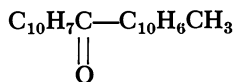


Figure 7. Oxidation of p-xylene (no  $\text{CoBr}_2$ )

Abstraction of ring hydrogen may compete with that of benzylic hydrogen. The decomposition of acetyl peroxide in ring-deuterated toluene, ethylbenzene, and cumene gives rise to methane-*d* (31). Apparent abstraction of ring hydrogen in competition with benzylic hydrogen probably occurs by addition of methyl radical to the benzene ring, followed by abstraction of the cyclohexadienyl hydrogen by another methyl radical.



This process competes favorably with benzylic hydrogen abstraction in toluene, less in ethylbenzene, and least in cumene (31). Such reactions do not seem significant in the oxidation of benzene derivatives. However, naphthalene reacts about 20 times as rapidly with phenyl radical as does benzene (16), and radical addition to the naphthalene nucleus may at least partly account for the slow oxidation rate in the methylnaphthalenes. Among the minor products from both methylnaphthalene oxidations were compounds of molecular weight 296:



probably derived by oxidation of a methyl dinaphthylmethane, which in turn contributes to the intensity at mass 282, along with dinaphthylethane and perhaps dimethyldinaphthyls.

Further evidence of nuclear attack was furnished by the oxidation of toluene-*α-d*<sub>3</sub> under conditions identical to those in Table IV. After 90 minutes the product contained an estimated 6% benzaldehyde-*d*<sub>1</sub> and 11% benzyl alcohol-*d*<sub>2</sub> plus benzyl acetate-*d*<sub>2</sub>. In addition, samples taken at three intervals gave these isotopic analyses for the recovered toluene:

Time, Minutes	0	20	60	90
No. of Deuterium Atoms	Toluene Isotopic Composition			
$d_0$	0	0.1	0.1	0.4
$d_1$	0.2	0.7	1.2	0.8
$d_2$	4.7	6.1	6.6	12.1
$d_3$	91.1	89.1	88.0	82.6
$d_4$	3.1	3.1	3.1	3.3
$d_5$	0.6	0.7	0.7	0.7
$d_6$	0.3	0.2	0.2	0.1

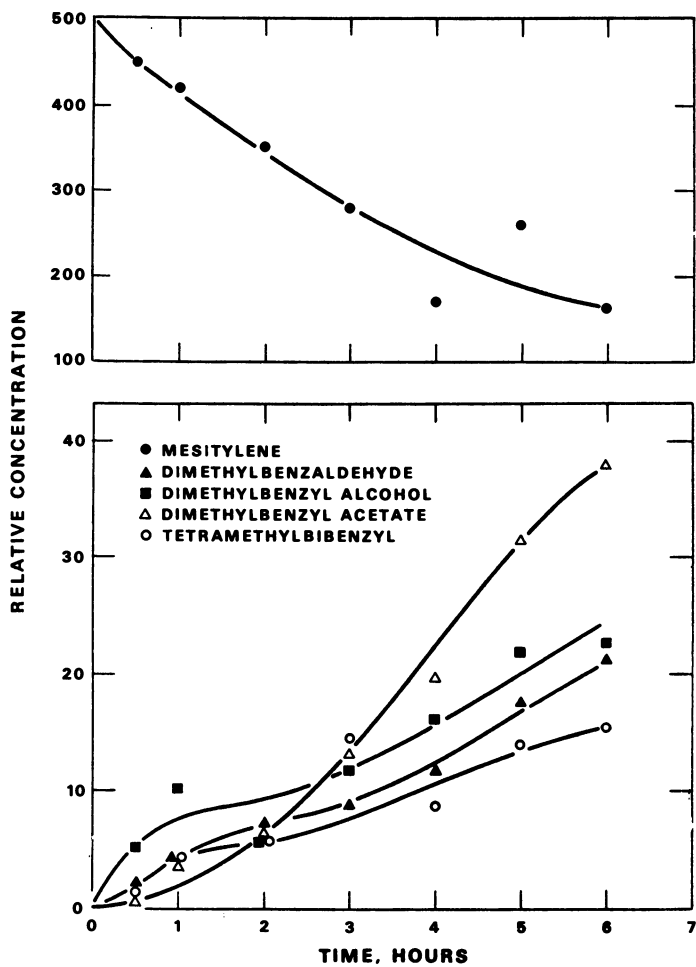


Figure 8. Oxidation of mesitylene

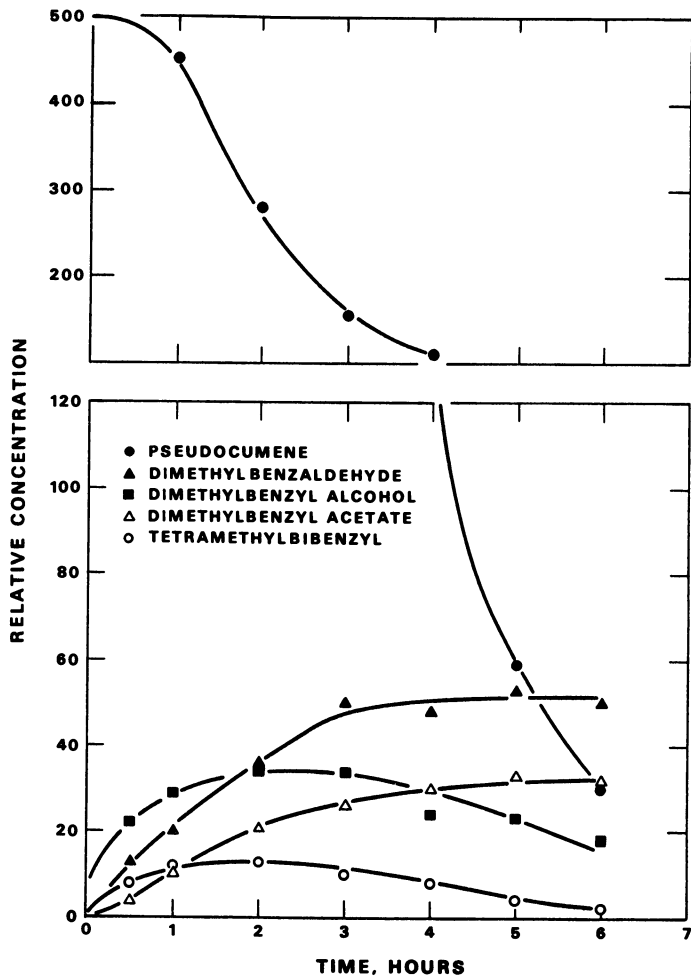


Figure 9. Oxidation of pseudocumene

Toluene- $d_4$ ,  $-d_5$ , and  $-d_6$  remained constant:  $-d_3$  decreased, and  $-d_2$  increased. This indicates some exchange, probably by way of a benzyl radical that abstracts protium in place of the original deuterium. Toluene- $\alpha$ - $d_3$ , refluxed for 2 hours in acetic acid with the same concentration of cobalt acetate and cobalt bromide, was recovered unchanged. Hydrogen, of course, could be furnished by the acetic acid; however, in the  $C_{14}$  hydrocarbons, the product of molecular weight 187 amounted to about 15% of that of 186. Presumably these are chiefly methylphenylmethane and bibenzyl, respectively.

[Relative parent-peak sensitivities of the available  $C_{14}H_{14}$  isomers, measured at the low-voltage conditions used in this study, are bibenzyl, 0.565, and 2-methyldiphenylmethane, 0.825. True concentrations of the  $C_{14}$  and presumably the  $C_{21}$  compounds are therefore somewhat different than estimates derived directly from isotopic distributions of the parent ions.]

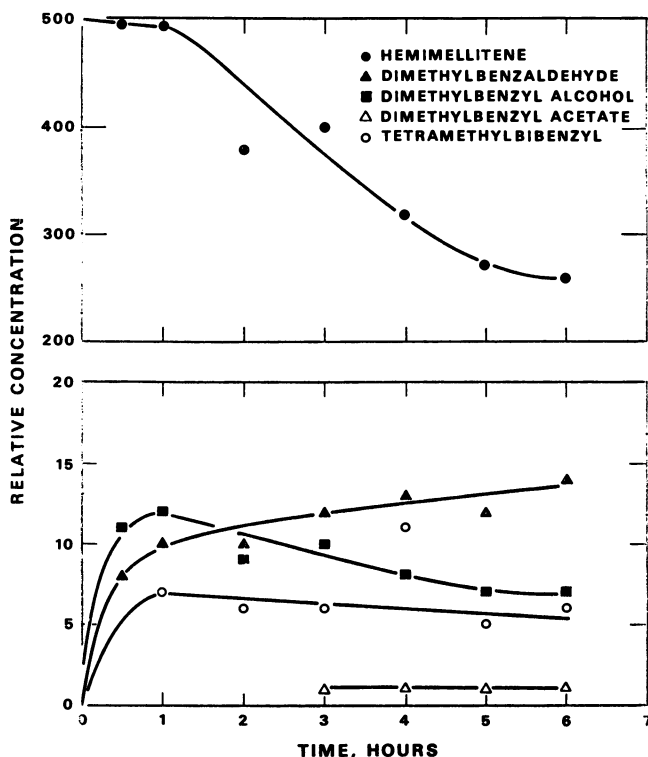


Figure 10. Oxidation of hemimellitene

Also, the peak for a benzyl trimer- $d_8$  was almost as intense as that for bibenzyl- $d_4$ ; the - $d_8$  trimer must have the structure



These products, containing aromatic rings linked directly or through a methylene bridge, give evidence that hydrogen abstraction from the aromatic ring takes place, even though it is a minor reaction.

**Table III. Maximum Conversion of Hydrocarbons to Aldehydes, Alcohols, and Dimers**

<i>Hydrocarbon</i>	% of Original Hydrocarbon		
	<i>Aldehyde (Hr.)</i>	<i>Alcohol + Acetate (Hr.)</i>	<i>Dimer (Hr.)</i>
Toluene	16.9 (2)	12.2 (2)	2.3 (1)
Ethylbenzene	75 <sup>a, b</sup> (6)	39.5 (2)	—
Cumene	20 <sup>c</sup> (2)	15.2 <sup>d</sup> (6)	0.7 (6)
<i>o</i> -Xylene	11.3 (1)	26 (1)	15.3 (1)
<i>m</i> -Xylene	25.7 (5)	21.1 (5)	4.6 (1)
<i>p</i> -Xylene	25.9 (2)	39 (2)	7.5 (1)
Hemimellitene	5.4 (6)	3 (1)	2.8 (4)
Pseudocumene	28.1 (6)	27.8 (3)	2.2 (2)
Mesitylene	6 (6)	16.6 (6)	4 (6)
Durene	5.2 (6)	5.4 (6)	3.5 (6)

<sup>a</sup> Acetophenone.

<sup>b</sup> 11% styrene (1 hr.) formed in addition.

<sup>c</sup>  $\alpha$ -Methylstyrene.

<sup>d</sup> 1-Methyl-1-phenylethylene oxide.

**Table IV. Oxidation of Toluene and *p*-Xylene**

	Yield, Mole %	
	<i>Analysis by Gas Chromatography</i>	<i>Estimate from Low-voltage Mass Spectrum</i>
Toluene		
Benzaldehyde	18.5	16.9
Benzyl alcohol + benzyl acetate	10.8	12.2
<i>p</i> -Xylene		
<p><i>p</i>-Tolualdehyde</p>	26.2	25.9
<p><i>p</i>-Methylbenzyl alcohol + <i>p</i>-methylbenzyl acetate</p>	13.7	23.1

### Conclusions

By adjusting catalyst concentration from the higher value of Hay and Blanchard to that used in this study, we can direct the oxidation of aromatic hydrocarbons to increase the yields of alcohols and aldehydes. The oxidation period for optimum conversion can readily be determined by low voltage mass spectrometry.

**Table V. Maximum Concentrations of the Minor Oxidation Products from Aromatic Hydrocarbons<sup>a</sup>**

Hydrocarbon Oxidized	Product		
	Bibenzyl or Methylated Bibenzyl	Stilbene or Methylated Stilbene	Other
Toluene	13	2	—
Ethylbenzene	6.2	22	$\alpha$ -Hydroxyacetophenone, 47; C <sub>16</sub> H <sub>11</sub> OBr, 33
Cumene	5		2-Phenylacrolein, 25; $\alpha$ -bromo-methylstyrene, 10; 2-phenylallyl acetate, 5
<i>o</i> -Xylene	102	12.4	<i>o</i> -Methylbenzyl acetate, 4; phthalide, 15; C <sub>24</sub> H <sub>24</sub> , 17; C <sub>24</sub> H <sub>26</sub> , 5.1
<i>m</i> -Xylene	29.2	7.9	3-Methyl-3'-formylstilbene, 1.1; 3-methyl-3'-formylbibenzyl, 4.4; C <sub>24</sub> H <sub>24</sub> , 1; C <sub>24</sub> H <sub>26</sub> , 1.4
<i>p</i> -Xylene	46	7.3	4-Methyl-4'-formylstilbene, 2.8; 4-methyl-4'-formylbibenzyl, 2.8; C <sub>24</sub> H <sub>24</sub> , 0.4; C <sub>24</sub> H <sub>26</sub> , 0.4
Mesitylene	15.4	3.5	Formyltrimethylstilbene, 0.1; formyltrimethylbibenzyl, 1.6; C <sub>27</sub> H <sub>32</sub> , 0.7
Hemimellitene	12	2	Formyltrimethylstilbene, 0.1; formyltrimethylbibenzyl, 0.3
Pseudocumene	12.6	4.2	Formylmethylbenzyl alcohol, 34.1; formyltrimethylstilbene, 1.5; formyltrimethylbibenzyl, 2.0
Durene	7.6	1.3	Formylpentamethylbibenzyl, 0.5

<sup>a</sup> Numbers are maximum intensities in low-voltage (7.5 volts, uncorrected) mass spectra, scaled to original intensity of hydrocarbon = 500.

In many studies precise quantitative data are not needed to clarify the chemistry under study. Especially in a series of related samples, low voltage mass spectrometry can quickly and easily furnish data that parallel changes in concentration and are entirely adequate for the purpose of the study. This analytical tool has enabled us to follow readily the formation and disappearance of products, instead of being limited to observing the rate of oxygen absorption; we expect it to be at least equally useful in determining rates and analyzing products of co-oxidations now under way.

**Table VI. Relative Rates of Oxidation of Aromatic Hydrocarbons<sup>b</sup>**

<i>Hydrocarbon</i>	$k \times 10^4 \text{ Sec.}^{-1} \text{ }^a$
<i>p</i> -Xylene	4.49
Ethylbenzene	2.92
<i>o</i> -Xylene	2.84
Toluene	2.4
<i>m</i> -Xylene	1.98
Pseudocumene	1.65
<i>p</i> -Xylene (no CoBr <sub>2</sub> )	0.74
Durene	0.58
Mesitylene	0.5
Hemimellitene	0.4
Cumene	0.34
1-Methylnaphthalene	0.17
2-Methylnaphthalene	0.11

<sup>a</sup> Based on rate of hydrocarbon consumption, measured by intensities in low-voltage (7.5 volts, uncorrected) mass spectra.

<sup>b</sup> Conditions: 5 moles of acetic acid, 0.5 mole of hydrocarbon, 0.01 mole of CoBr<sub>2</sub>·6H<sub>2</sub>O, 0.03 mole of CoAc<sub>2</sub>·4H<sub>2</sub>O; 113°C.; O<sub>2</sub> 0.6 cu. ft./hr. at 1-atm. pressure, over a 6-hour period.

Labeled compounds should prove valuable in studying liquid-phase oxidations, as they have in vapor-phase research, especially at low conversions where scrambling of protium and deuterium is avoided or held to a minimum.

### Literature Cited

- (1) Aczel, T., Lumpkin, H. E., *Anal. Chem.* **32**, 1819 (1960).
- (2) Anderson, H. R., Scheraga, H. A., Van Artsdalen, E. R., *J. Chem. Phys.* **21**, 1258 (1952).
- (3) Augood, D. R., Williams, G. H., *Chem. Rev.* **57**, 123 (1957).
- (4) Bateman, L., *Quart. Rev. (London)* **8**, 147 (1954).
- (5) Bawn, C. E. H., *Discussions Faraday Soc.* **14**, 181 (1953).
- (6) Bawn, C. E. H., Pennington, A. A., Tipper, C. F. H., *Ibid.*, **10**, 282 (1951).
- (7) Blanchard, H. S., *J. Am. Chem. Soc.* **77**, 4035 (1955).
- (8) Bolland, J. L., *Quart. Rev. (London)* **3**, 1 (1949).
- (9) Cadogan, J. T., Hey, D. H., Williams, G. H., *J. Chem. Soc.* **1954**, 794.
- (10) Crable, G. F., Kearns, G. L., Norris, M. S., *Anal. Chem.* **32**, 13 (1960).
- (11) Fields, E. K., Meyerson, S., *J. Org. Chem.* **31**, 3307 (1966).
- (12) Hay, A. S., Blanchard, H. S., *Can. J. Chem.* **43**, 1306 (1965).
- (13) Heilman, W. J., Rembaum, A., Szwarc, M., *J. Chem. Soc.* **1957**, 1127.
- (14) Huisgen, R., Sorge, G., *Ann.* **566**, 162 (1950).
- (15) Kharasch, M. S., Engelmann, W., Mayo, F. R., *J. Org. Chem.* **2**, 288 (1937).
- (16) Kharasch, M. S., Fono, A., Nudenberg, W., Bischof, B., *Ibid.* **17**, 1207 (1952).
- (17) Koltzoff, I. M., Willman, A., *J. Am. Chem. Soc.* **56**, 1007 (1934).
- (18) Landau, R., Brown, D., Russell, J. L., Kollar, J., Preprints, *7th World Petroleum Congress*, Mexico City, May 1967, p. 141 (P.D. 18).

- (19) McCaulay, D. A., private communication.
- (20) McCaulay, D. A., Lien, A. P., *J. Am. Chem. Soc.* **73**, 2013 (1951).
- (21) Mayo, F. R., private communication.
- (22) Mayo, F. R., Miller, A. A., Russell, G. A., *J. Am. Chem. Soc.* **80**, 2500 (1958).
- (23) Meyerson, S., Fields, E. K., *Chem. Commun.* **1966**, 275.
- (24) Meyerson, S., Grubb, H. M., Vander Haar, R. W., *J. Chem. Phys.* **39**, 1445 (1963).
- (25) Ravens, D. A. S., *Trans. Faraday Soc.* **55**, 1768 (1959).
- (26) Robertson, A., Waters, W. A., *Ibid.* **42**, 201 (1946).
- (27) Russell, G. A., *J. Am. Chem. Soc.* **79**, 3781 (1957).
- (28) *Ibid.* **80**, 4987 (1958).
- (29) Rust, F. F., Vaughan, W. E., *Ind. Eng. Chem.* **41**, 2595 (1949).
- (30) Van Helden, R., Bickel, A. F., Kooyman, E. C., *Rec. Trav. Chim.* **80**, 1257 (1961).
- (31) Wilen, S. H., Eliel, E. L., *J. Am. Chem. Soc.* **80**, 3309 (1958).

RECEIVED September 29, 1967.

## Discussion

**Allan S. Hay:** During the autoxidation of *p*-xylene catalyzed by cobalt acetate bromide, a potentiometric titration for bromide ion of an aliquot of the reaction mixture at 0°C. shows that only a fraction of the bromide is present in ionic form. If the titration is performed at room temperature, there is a gradual drift of the end point until it finally corresponds to the calculated total amount of bromide. The implication thus is that benzylic bromides are present during the reaction, and at room temperature during the titration they are slowly solvolyzed.

Is it possible that the unexpectedly slow oxidations of molecules such as mesitylene, durene, and the methylnaphthalenes which the author has described are caused by the depletion of the bromide portion of the catalyst? In these cases, bromination of the activated nuclei could occur and the bromide would be lost permanently.

**Ellis K. Fields:** We have found *o*-methylbenzyl bromide among the oxidation products of *o*-xylene. Even though this bromide persists during the oxidation period and appears to solvolyze somewhat more slowly than other benzyl bromides, it releases its bromine eventually to initiate and propagate free radical chains.

In a forthcoming paper we discuss the formation of arenes containing nuclear bromine in our oxidation system; however, this involves a transition metal catalyst other than cobalt. The latter apparently results in little or no nuclear substitution by bromine.

# Hydroperoxide Oxidations Catalyzed by Metals

## I. The Epoxidation of Olefins

M. N. SHENG and J. G. ZAJACEK

Research and Development Department, ARCO Chemical Co., A Division of Atlantic Richfield Co., Glenolden, Pa.

*The reaction of olefins with organic hydroperoxides in the presence of vanadium, molybdenum, and tungsten catalysts gives excellent yields of epoxides. Propylene, cis- and trans-2-butene, 2-methyl-2-pentene, cyclohexene, 1-octene, and 2-octene were studied using hydroperoxides of aromatic and aliphatic hydrocarbons. Molybdenum compounds are the most active catalysts. The reaction rate is faster at higher temperatures, high catalyst concentration, and with a greater number of substitution of electron-donating groups around the double bond. The conversion and epoxide yield are higher, in general, as the polarity of the solvent decreases. Kinetic data were obtained for the system tert-butyl hydroperoxide, molybdenum hexacarbonyl, and both 1-octene and 2-octene. These data suggest that the reaction is first order in peroxide, in olefin, and in molybdenum hexacarbonyl.*

The epoxidation of olefins using organic hydroperoxides has been studied in detail in this laboratory for a number of years. This general reaction has also recently been reported by other workers (6, 7). We now report on the effects of five reaction variables and propose a mechanism for this reaction. The variables are catalyst, solvent, temperature, olefin structure, and hydroperoxide structure. Besides these variables, the effect of oxygen and carbon monoxide, the stereochemistry, and the kinetics were studied. This work allows us to postulate a possible mechanism for the reaction.



### Experimental

**General Procedure.** Infrared spectra data were obtained with a Perkin-Elmer Infracord. Gas-liquid partition chromatography was conducted using either an Aerograph model A-90-P or a Perkin Elmer/Model 226. Columns used in the Aerograph were 10 ft.  $\times$  1/4 inch packed with 20% Carbowax 20M on 30-60 mesh acid washed Firebrick, or 15% SE 30 silicone rubber gum on 60-80 mesh Gaspac F, and a 12 ft.  $\times$  1/4 inch column packed with 5% SE-200 silicone oil on Haloport F. The stainless steel capillary column used in the Perkin-Elmer chromatograph was 100 ft.  $\times$  0.02 inch coated with Carbowax 15-40 M. Hydroperoxide and epoxide concentrations were analyzed by standard titration procedures (4, 11). Reagent grade chemical were used when available without further purification. Commercially available cumene hydroperoxide was purified according to Davies (3), *p*-Nitrocumene hydroperoxide was prepared by a literature procedure (2). *tert*-Butyl hydroperoxide (94% purity) was obtained from the Lucidol Division, Wallace and Tiernan, Inc. and purified to 97% by drying over anhydrous magnesium sulfate. Olefins were purified by distillation. Molybdenum hexacarbonyl was purified by sublimation.

**1,2-Epoxypropane.** A solution of 100 ml. of liquified propylene, 25 grams of *tert*-butyl hydroperoxide (94% purity), 125 grams of benzene, and 0.05 grams of molybdenum hexacarbonyl was charged into a 500-ml. Magne-drive autoclave and heated to 105°C. for 1 hr. The reactor was cooled to room temperature. Gaseous products were collected in a dry ice-acetone trap. Liquids were collected in an ice-water cooled trap. The products were analyzed for hydroperoxide by standard iodometric titration and epoxide by gas-liquid chromatography (GLC). There was a 92% conversion of the hydroperoxide and an 86% yield of the epoxide based on the conversion of hydroperoxide. GLC analysis showed no acetone or propionaldehyde.

**1,2-Epoxyoctane.** A solution of 1 gram of *tert*-butyl hydroperoxide (97% purity), 3 ml. of octene-1, 3 ml. of benzene, and 0.005 gram of molybdenum hexacarbonyl was sealed in a pressure tube and allowed to react for 1 hr. in a constant temperature bath at 90°C. The tube was removed and cooled in ice water. Hydroperoxide and epoxide were analyzed by iodometric titration and GLC. There was a 75% conversion of the hydroperoxide and a 92% yield of the epoxide based on the hydroperoxide conversion.

**Kinetic Method.** 1-Octene (73.6 grams), 0.01 gram of  $\text{Mo}(\text{CO})_6$ , and 200 ml. of benzene were placed in a 500-ml. three-necked flask equipped with a septum, thermometer, condenser, magnetic stirrer, and addition funnel wrapped with a heating tape. The solution was brought

to reflux. A solution of 6 grams of *tert*-BuOOH and 28.1 grams of 1-octene was placed in the addition funnel and heated to the reflux temperature, then added into a flask. The mole ratio of 1-octene to *tert*-BuOOH was 13.6 to 1. Samples were withdrawn periodically through the septum into a hypodermic syringe and cooled. Each sample was analyzed for unreacted hydroperoxide by iodometric titration. First order plots of  $\log c$  vs. time were made. The same type of experiments were carried out to determine the order in olefin concentration and catalyst concentration.

### Results

**Catalyst Effect.** The effectiveness of various transition metal compounds as catalysts for the epoxidation reaction was studied (Tables I and II). A mixture of catalyst, cumene hydroperoxide, and 2-methyl-2-pentene in methanol reacted at 110°C. in a series of sealed tubes. In the

Table I. Catalytic Activity of Various Compounds

Catalyst	Amount, gram	Time, hr.	Epoxide Yield, % <sup>a</sup>
None	—	15½	29
Sodium molybdate	0.02	15½	70
Sodium tungstate	0.02	15½	35
Sodium vanadate	0.02	15½	52
Molybdenum sulfide	0.01	2½	68
Molybdenum dioxide	0.01	1½	88
Molybdenum trioxide	0.02	2½	81
Silicomolybdic acid	0.005	¾	53
Phosphomolybdic acid	0.005	¾	59
Phosphomolybdic acid	0.005	¾	86
Sodium molybdate	0.02		
Sodium silico-12-molybdate	0.01	¾	85
Sodium molybdate	0.02		
Sodium phospho-12-molybdate	0.01	¾	62
Sodium phospho-12-molybdate	0.01	¾	73
Sodium molybdate	0.02		
Sodium phospho-18-molybdate	0.01	1	84
Sodium phospho-18-molybdate	0.01	1½	84
Sodium molybdate	0.02		
Ethylphosphomolybdate	0.005	¾	81
Sodium molybdate	0.02		
Monoethyldihydrophosphomolybdate	0.005	¾	83
Sodium molybdate	0.02		
Molybdenum oxyacetylacetonate	0.005	¾	86
Molybdenum hexacarbonyl	0.005	¾	81
Molybdenum hexacarbonyl	0.005	¾	86
Sodium molybdate	0.02		
Molybdenum pentachloride	0.002	¾	87
Vanadium oxyacetylacetonate	0.01	1	75

<sup>a</sup> Based on hydroperoxide conversion.

reactions in Table I the activity of various catalysts is compared at 90 mole % conversion of the hydroperoxide. The reaction time required for this conversion of hydroperoxide, the catalyst concentration, and the percent of the epoxide are shown. In Table II, compounds of other transition metals that were tested as possible catalysts for this reaction are listed. They showed essentially no catalytic activity, the yields being below 5%.

**Table II. Transition Elements Tested as Catalysts**

Manganous acetylacetonate  
Manganic acetylacetonate  
Ferrous acetylacetonate  
Ferric acetylacetonate  
Cobaltic acetylacetonate  
Rhodium chloride  
Nickel acetylacetonate  
Potassium platinous chloride  
Tetrammine copper(II) sulfate  
Potassium gold cyanide

The experimental data indicate that molybdenum compounds, including oxides, sulfides, halides, acids, salts, heteropolymolybdc acids, salts of heteropolymolybdc acids, esters of heteropolymolybdc acids, and molybdenum coordination compounds are catalysts for the epoxidation reaction. However, certain compounds such as sodium silicomolybdate, esters of heteropolymolybdc acids, and the coordination compounds (molybdenum hexacarbonyl and molybdenum oxyacetylacetonate) were more effective catalysts.

In all cases molybdenum compounds were the superior catalysts. Coordination compounds of these catalysts are more effective than the simple salts of the acids.

**Temperature Effect.** The rate of hydroperoxide conversion depends on the reaction temperature. It is slow at temperatures below 90°C. but increases rapidly with increasing temperature. However, the epoxide yield at constant hydroperoxide conversion tends to decrease at temperatures greater than optimum (Table III).

**Solvent Effect.** The effect of solvent when using an organic soluble molybdenum catalyst is shown in Table IV. Nonpolar solvents such as benzene and methylcyclohexane give higher conversions and yields than polar solvents such as ethyl alcohol and *tert*-butyl alcohol. Acetone is an especially poor solvent. The low conversion is caused by competition between the solvent and hydroperoxide for molybdenum catalyst. The poor yield of epoxide is primarily caused by hydroperoxide decomposition

—because no by-products derived from a solvent—hydroperoxide reaction are observed.

**Table III. Temperature Effect on Hydroperoxide Conversion and Epoxide Yield**

Sample, <sup>a</sup> ml.	Sodium Molybdate gram	Sodium Silico- molybdate gram	Temp., °C.	Time, hr.	Conver- sion, <sup>b</sup> %	Epoxide Yield, <sup>c</sup> %
5	0.5	—	100	30	89	80
5	0.1	—	100	30	92	92
5	0.1	—	130	8	100	74
5	0.02	—	130	8	100	80
3	0.01	0.04	100	2	96	98
3	0.01	0.04	110	¾	94	98
3	0.01	0.04	118	½	93	96
3	0.01	0.04	128	¼	95	75

<sup>a</sup> Sample was 2 ml. (0.011 mole) cumene hydroperoxide, 2 ml. (0.0163 mole) 2-methyl-2-pentene, and 1 ml. methanol.

<sup>b</sup> % hydroperoxide converted.

<sup>c</sup> Based on hydroperoxide conversion.

**Table IV. Effect of Solvent on the Epoxidation Reaction**

Solvent <sup>a</sup>	Conversion, %	Epoxide Yield, %
Benzene	75	92
Methylcyclohexane	72	84
Ethyl alcohol	40	37
<i>tert</i> -Butyl alcohol	16	58
Acetone	39	5

<sup>a</sup> Experiments were run in sealed tubes at 90°C. for 1 hour. Reagents were 1 gram *tert*-butyl hydroperoxide (97% purity), 3 ml. 1-octene, 3 ml. solvent, and 0.005 gram molybdenum hexacarbonyl.

The solvent effect was also shown in the reaction of propylene, *tert*-butyl hydroperoxide, and molybdenum hexacarbonyl in a mixed solvent of benzene and *tert*-butyl alcohol (Figure 1). The epoxide yield increases rapidly as the benzene-to-*tert*-butyl alcohol ratio increases up to 1:4, thereafter the hydroperoxide conversion increases more rapidly with an increase in this ratio.

**Effect of Olefin Structure.** The reaction rate of the epoxidation depends on olefin structure. In general, the more alkyl substituents bonded to the carbon atoms of the double bond, the faster the reaction rate. This was shown by a reaction of 2-methyl-2-pentene, cyclohexene, and 2-octene with cumene hydroperoxide under the same conditions (Table V). The yield of epoxide was quantitative. The results indicate that 2-methyl-2-pentene reacts faster than cyclohexene and 2-octene.

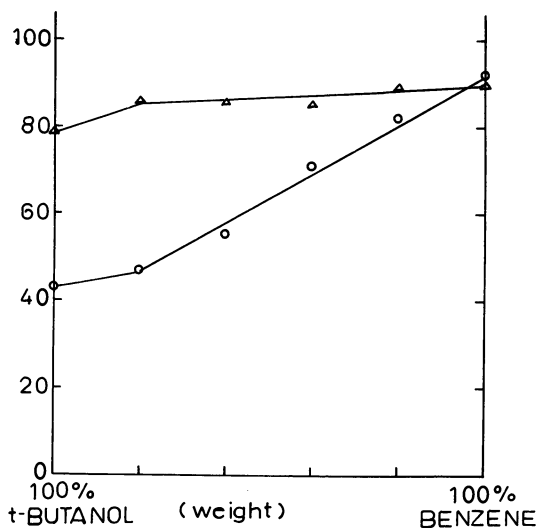


Figure 1. Epoxidation of propylene in *tert*-butyl alcohol and benzene at 110°C.

○: % conversion  
 △: % epoxide yield

Table V. Effect of Substituents on Olefin Reactivity

Olefin <sup>a</sup>	Hydroperoxide Conversion, %
2-Methyl-2-pentene	52
Cyclohexene	30
2-Octene	23

<sup>a</sup> Reagents and conditions were 2 ml. cumene hydroperoxide (82% purity), 2 ml. olefin, 1 ml. methanol, and 0.05 gram sodium molybdate in a sealed tube for 5 hr. at 101°C.

In another series of experiments, 1-octene, 2-octene, and cyclohexene reacted with *tert*-butyl hydroperoxide under identical conditions (Table VI). The yield of epoxide was quantitative.

Table VI. Effect of Substituents on Olefin Reactivity

Olefin <sup>a</sup>	Hydroperoxide Conversion, %
1-Octene	36
2-Octene	76
Cyclohexene	77

<sup>a</sup> Reagents and conditions were 5 ml. solution prepared from 17 ml. *tert*-butyl hydroperoxide (97% purity), 100 ml. olefin, and 0.02 gram molybdenum hexacarbonyl in a sealed tube for 30 minutes.

**Effect of Hydroperoxide Structure.** The reactivity of various hydroperoxides was studied with 2-octene and 2-methyl-1-pentene (Table VII). The yield of epoxide was quantitative. The data show that the substitution of the electron-withdrawing nitro groups in the para-position of cumene hydroperoxide markedly increases the reaction rate. The order of reactivity is *p*-nitrocumene > cumene > *tert*-butyl hydroperoxide.

**Table VII. Effect of the Hydroperoxide Structure on the Rate of Reaction**

Olefin	Hydroperoxide <sup>a</sup>	Time, min.	Hydroperoxide Conversion, %
2-Octene	<i>p</i> -Nitrocumene	15	83
	Cumene	15	60
	<i>tert</i> -Butyl	15	54
	<i>p</i> -Nitrocumene	30	92
	Cumene	30	84
	<i>tert</i> -Butyl	30	78
2-Methyl-1-pentene	Cumene	15	48
	<i>tert</i> -Butyl	15	39
	Cumene	30	68
	<i>tert</i> -Butyl	30	63

<sup>a</sup> Reagents were a 5-ml. solution prepared from 0.011 mole hydroperoxide (99% purity), 0.033 mole olefin, 0.008 gram molybdenum hexacarbonyl diluted to 12 ml. with benzene. The conditions were a sealed tube at 80.5°C.

**Effect of Oxygen.** The reaction of 1-octene with *tert*-butyl hydroperoxide and molybdenum hexacarbonyl catalyst was chosen as the model system to study the effect of oxygen. Oxygen can affect the epoxidation reaction in at least two ways. It could retard the rate if the reaction mechanism involves free radicals, or it could react with the catalyst and convert it to an inactive form. The first set of experiments was done under a nitrogen atmosphere which was the standard. After the first reaction was completed, the organic material was stripped off under high vacuum to leave only the catalyst and any residue. Fresh solution was added, and the reaction was run again. Three more cycles were carried out. The data (Table VIII) show that there is a gradual loss of catalytic activity but no abrupt change. The second set of experiments was run in air. In the fourth run of this set air was bubbled through the solution during the reaction. The third set of experiments was carried out by bubbling oxygen through the solution during the runs. The first run in each set gave 90% conversion of the hydroperoxide. The epoxide yield is quantitative, based on the hydroperoxide converted. Thus, oxygen does not lower the reaction rate, but it does reduce the life of the catalyst.

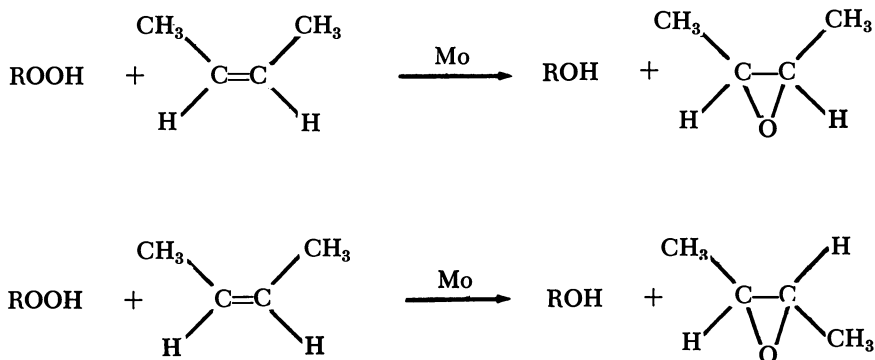
Table VIII. Effect of Oxygen on the Epoxidation Reaction

Run No. <sup>a</sup>	Epoxide Yield, %		
	Set I, Nitrogen	Set II, Air	Set III, Oxygen
1	87	85	83
2	85	85	74
3	86	70	50
4	75	70	

<sup>a</sup> Reagents were 21 grams *tert*-butyl hydroperoxide (95% purity), 62 grams 1-octene, and 0.01 gram molybdenum hexacarbonyl; the conditions were 1 hr. at 105-110°C.

**Effect of Carbon Monoxide.** According to our proposed mechanism (*see discussion*), the hydroperoxide coordinates with molybdenum first and then epoxidizes the olefin; accordingly for molybdenum hexacarbonyl catalyst at least one or two carbon monoxide ligands must be replaced by hydroperoxide. Therefore, the reaction rate should be slower under a carbon monoxide atmosphere than under a nitrogen atmosphere. To test this, two identical experiments with 1-octene, *tert*-butyl hydroperoxide, and molybdenum hexacarbonyl were run in an autoclave under 200 p.s.i.g. of nitrogen and carbon monoxide at 90°C. for 1 hour. The reaction under nitrogen gave a 54% conversion of hydroperoxide. The reaction under carbon monoxide gave a 31% conversion. Thus, the reaction rate appears to be retarded in the carbon monoxide atmosphere.

**Stereospecific Epoxidation of 2-Butene.** The hydroperoxide epoxidation reaction is stereospecific. Pure *cis*- and *trans*-2-butene were epoxidized separately by cumene hydroperoxide. The *cis* olefin gave exclusively *cis* epoxide, and the *trans* olefin gave exclusively *trans* epoxide. In both cases, the epoxide was the sole product formed from the olefin. They can be distinguished easily by their different retention times on a gas chromatography column of 20% diisodecyl phthalate on Chromosorb W(60-80 mesh). They were also identified by comparing their infrared spectra with authentic samples.



**Kinetics.** The kinetics of the epoxidation of olefins with *tert*-butyl hydroperoxide in the presence of molybdenum hexacarbonyl have been studied. The reaction rate is first order in *tert*-butyl hydroperoxide, in olefin, and in molybdenum hexacarbonyl. Olefins substituted near the double bond by electron-releasing alkyl groups react more rapidly than the corresponding unsubstituted olefins. The kinetic data indicate that the epoxidation reaction proceeds according to the rate law,

$$\text{Rate} = k[\textit{tert}\text{-BuOOH}][\text{Olefin}][\text{Mo}(\text{Co})_6]$$

The decomposition rate of *tert*-butyl hydroperoxide is much slower than the epoxidation rate. When *tert*-butyl hydroperoxide and molybdenum hexacarbonyl are refluxed in a mixture of toluene and benzene at 87°C. for 1 hr., only 6.2% of the hydroperoxide decomposes. Under the same conditions with 2-octene present in large excess, 80% of the hydroperoxide is converted, and a quantitative yield of the epoxide results. Thus, the decomposition of *tert*-butyl hydroperoxide is insignificant when the olefin is present.

When the epoxidation reaction was run in a large excess of the olefin, a first-order plot of  $\log C_{\textit{tert}\text{-BuOOH}}$  vs. time gave a straight line (Figure 2), but the second-order plot of  $1/c$  vs. time was a curve during the entire reaction. At 85.5°C., the rate constants are  $0.78 \times 10^{-4} \text{ sec.}^{-1}$  for 1-octene and  $2.0 \times 10^{-4} \text{ sec.}^{-1}$  for 2-octene.

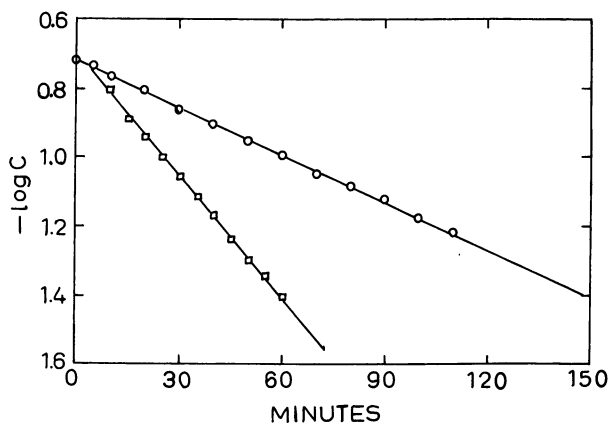


Figure 2. First-order plot for the epoxidation of 1-octene (O) and 2-octene (□) at 85.5°C.

The order with respect to olefin was determined by experiments with 2-octene and *tert*-butyl hydroperoxide in benzene. The mole ratio of reactants was 1.5 to 1 and 2 to 1. The first-order plot of  $\log C_{\textit{tert}\text{-BuOOH}}$

vs. time was a curve; the second-order plot of  $1/a - b \ln b(a-x)/a(b-x)$  vs. time gave a straight line (Figure 3).

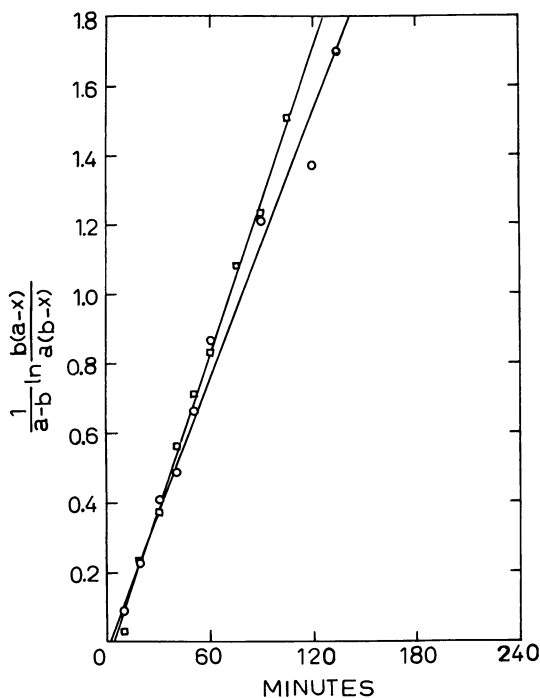


Figure 3. Second-order plot for the epoxidation of 2-octene at 79°C. Mole ratio of tert-butyl hydroperoxide:2-octene = 1:2 ( $\square$ ) and 1:1.5 ( $\circ$ )

Parallel experiments with the same initial concentration of hydroperoxide but different molybdenum hexacarbonyl concentrations indicated a first-order dependence on molybdenum concentration (Table IX). The order was determined by relating the change in slope of the first-order hydroperoxide time plots to the variation in catalyst concentration.

Table IX. First-Order Dependence of Catalyst Concentration

	<i>Experimental Rate Constant<sup>a</sup></i>
Mo(CO) <sub>6</sub> , mole	$k \times 10^4, \text{sec.}^{-1}$
$\frac{7.577 \times 10^{-5}}{3.789 \times 10^{-5}} = 2.00$	$\frac{1.6}{0.78} = 2.04$
Apparent order in Mo(CO) <sub>6</sub>	1.0

<sup>a</sup> At 85.5°C., with large excess of 1-octene.

### Discussion

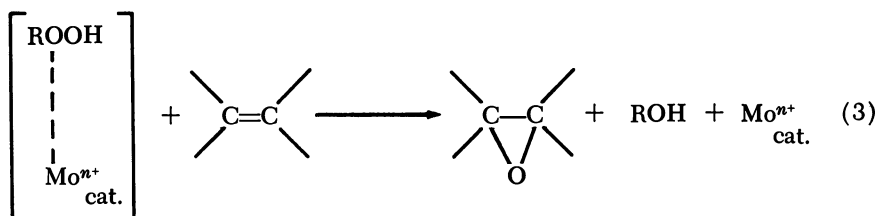
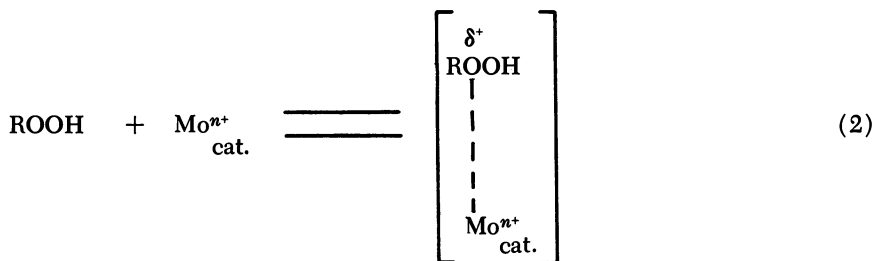
In view of the data, this novel reaction is unlikely to proceed by any mechanism known for other epoxidation reactions. There are several facts that argue strongly against a free radical mechanism. Our data show that the reaction is not affected by the presence of oxygen in contrast to the work of Indictor and Brill (6). Complexes of cobalt, manganese, and iron, which are most effective in converting peroxides to radicals (5, 8), are not catalysts for this reaction. This reaction is stereospecific, and therefore must proceed by an ionic mechanism.

Two ionic mechanisms are known for epoxidation reactions: nucleophilic and electrophilic reactions. Examples of the nucleophilic reactions are the base-catalyzed reactions of hydrogen peroxide or organic hydroperoxides with olefins (1, 12). Examples of the electrophilic reactions are epoxidations of olefins with organic and inorganic peroxyacids (9, 10). A nucleophilic reaction mechanism is very unlikely. Our reaction is accelerated by substituting the olefin with electron-donating groups, whereas nucleophilic additions are accelerated by the presence of electron-withdrawing groups. Thus, the reactive intermediate formed in our system has electrophilic character and outwardly resembles the organic and inorganic peroxyacid reactions. However, it is different from the organic peracid epoxidations which are carried out at low temperatures and in the absence of metal catalysts. Our system is also different from that encountered in the aqueous hydrogen peroxide epoxidations catalyzed by oxides of vanadium, molybdenum, and tungsten. In these systems, tungsten is a much better catalyst than molybdenum or vanadium. Furthermore, water and alcohols are the best solvents. In contrast to this, molybdenum is the best catalyst in our reaction, and water and alcohols retard the reaction.

To generalize a mechanism based on a specific system can be dangerous since other mechanisms may be applicable in the broad framework. Among these one could visualize the formation of a  $\pi$ -complex between the metal and the olefin which is then oxidized by the hydroperoxide.

However, our kinetic data with molybdenum hexacarbonyl and other observations appear more consistent with a mechanism which proceeds through a polarized hydroperoxide complex. Reaction 2 appears to be faster than Reaction 3.

$\text{Mo}^{m+}$  and  $\text{Mo}^{n+}$  are written to indicate forms of molybdenum present during the reaction without specifying an exact oxidation level of structure. The number of molybdenum compounds of various valences (Table I) which catalyze this reaction suggest that the initial molybdenum compound may be converted to the same active forms (Step 1). These active forms then complex with the hydroperoxide rapidly (Step 2).



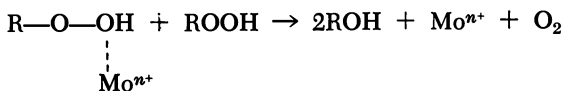
The molybdenum–hydroperoxide complex (Step 3) reacts with the olefin in the rate-determining step to give the epoxide, alcohol, and molybdenum catalyst. This mechanism explains the first-order kinetic dependence on olefin, hydroperoxide, and catalyst, the enhanced reaction rate with increasing substitution of electron-donating groups around the double bond, and the stereochemistry of the reaction.

The two possible transition states for this mechanism are shown below.

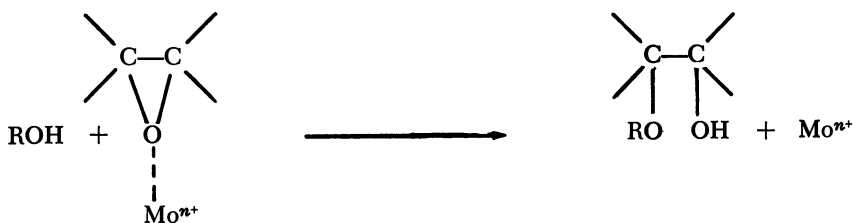


This mechanism also explains why alcohols and carbon monoxide, which would compete with hydroperoxide for the catalyst, retard the reaction rate.

The fact that the epoxide yield decreases at higher temperatures, longer reaction time, higher catalyst concentration, and lower olefin concentration may be caused by two possible side reactions—decomposition of the hydroperoxide and addition of the alcohol to the epoxide. Initial kinetic studies of the decomposition of *tert*-butyl hydroperoxide in the presence of molybdenum hexacarbonyl showed second-order dependence on hydroperoxide and first-order dependence on catalyst concentration. These results indicate that the decomposition of hydroperoxide is caused by the reaction between the hydroperoxide-metal complex and another molecule of hydroperoxide. With higher temperature, higher



catalyst concentration, and lower olefin concentration this decomposition becomes more important. The addition of alcohol to the epoxide also becomes more important at higher temperature, higher catalyst concentration, and longer reaction time. The metal complex can be visualized as a catalyst for the addition of alcohol or the hydroperoxide to the epoxide.



The postulated hydroperoxide-molybdenum complex indicates that there should be a steric and an electronic effect by the alkyl and aryl groups of the hydroperoxide. The steric effect is important in the transition state. The electronic effect will influence the rate of complex formation and the epoxidation reaction. Some data (Table VII) were obtained for these effects, but a clear distinction or evaluation of their role cannot be made at this time.

### Acknowledgments

The authors are grateful to G. A. Bonetti and J. E. Connor for helpful discussions and encouragement and to J. I. Stroud and F. J. Hilbert for their experimental work.

**Literature Cited**

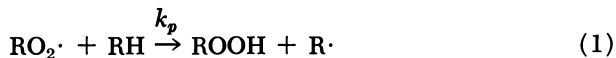
- (1) Bunton, C. A., Minkoff, G. J., *J. Chem. Soc.* **1949**, 665.
- (2) Conner, J. C., Jr., U. S. Patent **2,718,530** (1955).
- (3) Davies, A. G., "Organic Peroxides," p. 114, Butterworth & Co., London, 1961.
- (4) Durbetaki, A. J., *Anal. Chem.* **28**, 2000 (1956).
- (5) Hawkins, E. G. E., "Organic Peroxides," p. 17, D. Van Nostrand, New York, 1961.
- (6) Indictor, N., Brill, W. F., *J. Org. Chem.* **30**, 2074 (1965).
- (7) Kollar, J., Belgian Patent **657838** (1964).
- (8) Richardson, W. H., *J. Am. Chem. Soc.* **87**, 1096 (1965).
- (9) Smith, C. W., Payne, G. B., U. S. Patent **2,786,854** (March 26, 1957).
- (10) Swern, D., "Organic Reactions," Vol. 7, p. 378, Wiley, New York, 1953.
- (11) Weeler, D. H., *Oil Soap* **9**, 89 (1932).
- (12) Yang, N. C., Finnegan, R. A., *J. Am. Chem. Soc.* **80**, 5845 (1958).

RECEIVED September 29, 1967.

**Discussion**

**C. Walling:** The following is a general comment concerning technical autoxidations run in the liquid phase at moderate temperature, which have often been interpreted in terms of hydroperoxide chains.

We now have accurate values for the ratio  $k_p^2/2k_t$  for a number of hydrocarbons, which fixes a maximum possible chain length (defined as the relative rates of Reactions 1 and 2)



for the simple hydroperoxide chain process.

$$\nu = (k_p^2/2k_t) [\text{RH}]^2 / (-d[\text{RH}]/dt) \quad (3)$$

Thus, for toluene at 30°C.  $k_p^2/2k_t = 2 \times 10^{-10}$ , and if we assume, rather generously,  $E_t = 4$  kcal.,  $E_p = 12$  kcal., the value at 120°C. becomes approximately  $5 \times 10^{-7}$ . This predicts a maximum kinetic chain length of unity in 1M toluene being oxidized at 0.18% per hour. (If toluene is also consumed in the initiation step, the rate could be at most doubled.) Technical autoxidations—e.g., in the presence of metal catalysts, run far

faster than this, and one is forced to the conclusion that the classical hydrogen abstraction step (Reaction 1) makes a negligible contribution to the over-all process! In short, these reactions must require attack on hydrocarbon by quite different reagents—alkoxy radicals, metal ions, halogen atoms, etc.—and must be thought of in these terms (as has been pointed out in connection with bromide ion-catalyzed processes.)

On the one hand, this complicates the problem of understanding such fast oxidations, but on the other, it points up the possibility of a much wider range of control and selectivity than would be possible if only a single chain-carrying species were involved. It may well be that the autoxidations of cumene and acetaldehyde are the only technical processes in operation to which the classical hydroperoxide (or peracid) long-chain mechanisms truly apply.

**F. R. Mayo:** I endorse Dr. Walling's ideas that chain lengths in technical oxidations are short and that many reactions are important besides the conventional propagation and termination steps of alkylperoxy radicals. However, I think that he has overstated his case enough that it may be misleading. First, we should distinguish between the early and late stages of a technical autoxidation. At the start, we are dealing with (say) nearly pure toluene, air, and added catalysts. I suspect that this reaction has an initial slow stage, where the conventional propagation and termination reactions are important. However, after a few percent of the toluene has oxidized, we are dealing with a co-oxidation of toluene with benzyl hydroperoxide, benzyl alcohol, benzaldehyde, perbenzoic acid, benzoic acid, and perhaps other compounds. At a near steady state, the intermediate compounds together are responsible for most of the oxygen absorption; three of them alone have so much more favorable ratios of  $k_p/(2k_t)^{1/2}$  that this ratio for pure toluene is a poor guide to kinetic chain lengths. Further, as the oxidation accelerates, depletion of the oxygen supply introduces more complications.

The implications of Dr. Walling's conclusion that the reaction of peroxy radicals with substrate "makes a negligible contribution to the over-all process" suggest that his conclusion must be an exaggeration. Although attack of toluene and of all its intermediates presumably yields free radicals which react with oxygen, he states that reactions of these with toluene, the predominant organic species is "negligible." He also implies that the hydroperoxides which might result are not needed and not used in initiating the many and short chains which we agree are involved.

# INDEX

<b>A</b>	
Absorption spectra .....	169
Acetaldehyde .....	363, 369
Acetone .....	42, 98, 122
Activation energies .....	48, 80
for C and O .....	149
Active sites .....	309
Air oxidation of alcohols to esters ..	389
Aldehyde formation in oxidation ..	146
Alkane oxidation, mechanism of ..	70
<b>Alkanes</b>	
gas-phase oxidation of .....	1
O-heterocycles from the gaseous	
oxidation of .....	86
on hydrogen-oxygen reaction,	
effect of added .....	11
large .....	77
mercury-photosensitized	
oxidation of .....	3
small .....	79
Alkenes .....	71, 95
addition of peroxy radicals to ..	74
Alkoxy radicals, gas-phase	
reactions of .....	23
Alkylaromatic hydrocarbon,	
autoxidation of .....	382
Alkylated aromatic hydrocarbons..	395
Alkyl free radicals .....	58
Alkyl hydroperoxides,	
degenerate branching by ....	105
Alkylperoxy radicals .....	72, 86, 96
gas-phase reactions of .....	23
isomerization of .....	72, 76, 104
<b>Alkyl radicals</b>	
chain propagation in the	
oxidation of .....	69
gas-phase oxidation of .....	1
large .....	79
plus oxygen .....	131, 138
regeneration of .....	72
small .....	80
Allylic intermediate .....	249
Alumina catalysts, chromia- .....	256
Anthracene oxidation .....	387
Antimony-vanadium catalysts .....	288
Antioxidant concentration, critical .	176
Antioxidants .....	168
<b>Aromatic hydrocarbons</b>	
to alcohols and aldehydes .....	395
minor oxidation products from .	414
nitric acid catalysis in the	
oxidation of .....	382
oxidation rates of .....	415
Aromatic ring, radical attack on ..	408
Aromatic side chains, free-radical	
bromination of .....	399
Aromatics .....	261
Arrhenius parameters .....	33, 105
Atmospheric pollutants .....	58
Autocatalysis in gas-phase	
oxidation .....	3
<b>Autoxidation</b>	
of alkylaromatic hydrocarbon ..	382
of hydrocarbons .....	193
initiation of .....	161
of olefins .....	352
scheme .....	398
Azoalkanes, photo-oxidation of ...	3
1,1-Azoisobutane,	
photo-oxidation of .....	58
Azo-2-methylpropane,	
photo-oxidation of .....	4
<b>B</b>	
Benzene .....	226
Benzoyl peroxide .....	211
Benzyl acetate- <i>d</i> <sub>2</sub> .....	409
Benzyl alcohol .....	400
Benzyl alcohol- <i>d</i> <sub>2</sub> .....	409
Benzylic bromides, reaction of	
indium and .....	397
Benzyl trimer- <i>d</i> <sub>8</sub> .....	412
Bibenzyl- <i>d</i> <sub>4</sub> .....	412
Bis(1-methyl-2-	
acetoxypropyl)selenide .....	347
Bismuth molybdate catalyst .....	252
1,2-Bis(salicylidene amino)ethane	
iron(III) chloride .....	209
Bond strength .....	81
Bromide catalysts .....	193
Bromination of aromatic side	
chains, free-radical .....	399
Bromine oxidation of alcohols ....	389
Bromoform .....	226
$\alpha$ -Bromo- <i>o</i> -xylene .....	397
Butadiene .....	264
Butane .....	87, 95, 111
1-Butanol .....	392
1-Butene .....	262
2-Butene .....	346
stereospecific epoxidation of ..	425
<i>N</i> -Butylacetamide .....	165
<i>tert</i> -Butyl alcohol .....	42
<i>tert</i> -Butyl hydroperoxide .....	42
2- <i>n</i> -Butyloxiran .....	87

C	
Calorimetry .....	304
Carbon dioxide, chemisorption of ..	297
Carbon monoxide	
chemisorption of .....	296
vs. epoxidation .....	425
on nickel oxide, mechanisms of	
oxidation of .....	292
Carbon tetrachloride .....	226
Carbonyl compounds .....	78
Catalysis	
bromine-nitric acid .....	389
electron theory of .....	281
metal salt .....	193
in the oxidation of aromatic	
hydrocarbons, nitric acid ..	382
platinum .....	248, 258, 313
silver .....	244, 258
Catalyst	
activity, influence of environ-	
mental factors on .....	156
inhibitor conversion .....	163
in autoxidation reactions ..	160
metal chelate .....	163
Catalysts	
antimony-vanadium .....	288
bromide .....	193
chromia-alumina .....	256
chromium-vanadium .....	288
cobalt .....	193
copper oxide .....	276
metal .....	258
metal complex oxidation .....	182
molybdenum .....	421
organoselenides as .....	345
surface of solid oxidation .....	254
Catalytic oxidation	
effect of oxygen concentration on	317
heterogeneous .....	242
of hydrocarbons .....	313
ionization from .....	313
Chain	
branching by formaldehyde .	101, 108
carriers, interconversion of .....	72
length in oxidation .....	5, 431
mechanism, hydroperoxide .....	69
oxidation, low temperature .....	144
oxidation, multistep .....	207
propagation, general scheme for	75
propagation in the oxidation of	
alkyl radicals .....	69, 79
termination by mutual reaction of	
peroxy radicals .....	13
Chelate catalyst, metal .....	163
Chelates	
cobalt and copper .....	166
metal salicylaldimine .....	164
zinc .....	165
Chemi-ionization .....	314
Chemisorption	
of carbon dioxide .....	297
of carbon monoxide .....	296
of oxygen .....	294
Chloroform .....	226
CH <sub>3</sub> O with radicals, reactions of ..	37
CH <sub>3</sub> O <sub>2</sub> with radicals, reactions of .	28
C <sub>2</sub> H <sub>5</sub> O with molecules,	
reactions of .....	36
Cobalt(II) acetate in	
acetaldehyde oxidation .....	366
Cobalt	
catalysts .....	193
catalyzed oxidation of <i>p</i> -xylene	
to terephthalic acid .....	383
complexes .....	166, 188
CO on catalysts, heats of	
adsorption of .....	297
CO <sub>2</sub> on catalysts, heats of	
adsorption of .....	297
Combustion	
mechanism of action of halogen	
compounds on .....	236
processes vs. halogen compounds	226
pyrolysis of radicals in .....	10, 14
Cool-flame combustion .....	87
Cool flame limits .....	99
Cool flames .....	20, 71, 108
Co-oxidation, iron-catalyzed .....	221
Copper(II) acetate in acetaldehyde	
oxidation .....	366
Copper	
chelates .....	166
oxide catalysts .....	252, 276
selenite .....	276
Coupled oxidation .....	247
Cumene .....	195
Cyclic transition state .....	81
Cyclization .....	82
Cyclohexane .....	352
Cyclohexene .....	353
Cyclohexenyl radicals .....	359
Cyclohexyl radicals .....	359
<i>p</i> -Cymene oxidation .....	387
D	
Decompositions of RO,	
unimolecular .....	28
Degenerate branching intermediates	105
Di- <i>tert</i> -butyl peroxide .....	42
<i>N,N'</i> -Di- <i>sec</i> -butyl- <i>p</i> -	
phenylenediamine .....	208
2,3-Diethyloxiran .....	87
Dihydroperoxide .....	75
Diisobutylene .....	226
Diisopropyl salicylates .....	166
Dimethylaniline .....	211
Dimethylbibenzyl .....	400
2,2-Dimethylbutane .....	226, 316
Dimethyldinaphthyls .....	409
2,6-Dimethylnaphthalene oxidation	387
2,4-Dimethyloxetan .....	87
2,3-Dimethyloxiran .....	95
4,4-Dimethyl-2-pentene .....	316
2,2-Dimethylpropane .....	315
Dimethyltetrahydrofurans .....	78
Dinaphthylethane .....	409
Dinaphthylmethane .....	409

- Diolefins ..... 242  
 Disproportionation ..... 37, 151  
*n*-Dodecane ..... 195  
 Dodecanol ..... 392  
 Dual effect of halogen compounds 156
- E**
- Electron theory of catalysis ..... 281  
 Energy chains ..... 247  
 Entropy of activation ..... 81  
 Epoxidation  
   carbon monoxide *vs.* ..... 425  
   hydroperoxide structure *vs.* .... 424  
   of olefins ..... 418  
     kinetics of ..... 426  
   olefin structure *vs.* ..... 422  
   oxygen *vs.* ..... 424  
   solvent effect on ..... 422  
 Epoxide formation ..... 149  
 Epoxides ..... 95  
   from ketone slow combustion .. 104  
 Ethane ..... 111  
   high temperature combustion of .. 11  
   oxidation ..... 127, 130, 132  
 Ethanethiol oxidation ..... 182  
 Ethanol ..... 392  
 Ethylbenzene ..... 195, 226  
 Ethyl bromide ..... 226  
 Ethylene ..... 101  
   dibromide, dichloride ..... 226  
   oxidation ..... 135  
   over silver ..... 245  
 2-Ethylhexanol ..... 392  
 Ethyl iodide ..... 226  
 2-Ethyl-4-methyloxetan ..... 87  
 3-Ethylloxiran, 2-methyl- ..... 87  
 Evans-Polanyi relation for  
   peroxy radicals ..... 15
- F**
- Falling cloud reactor ..... 87  
 Fatty acid ..... 193  
 Fermi level ..... 284, 293  
 Ferric acetylacetonate ..... 209  
 Ferric chloride ..... 217  
 Five-membered rings, RO<sub>2</sub>'  
   isomerization *via* ..... 148  
 Flame speeds, halogen compounds  
   *vs.* ..... 235  
 Formaldehyde, chain branching  
   by ..... 101, 108  
 Four-step chain ..... 217  
 Free-radical bromination of  
   aromatic side chains ..... 399  
 Free radical oxidations,  
   mechanism of ..... 143
- H**
- H-abstraction by peroxy radicals,  
   rate constants for ..... 14  
 Halogenated hydrocarbons ..... 317  
 Halogen compounds ..... 227  
   on combustion, action of ..... 236  
   *vs.* combustion processes ..... 226  
   dual effect of ..... 156  
   *vs.* flame speeds ..... 235  
   *vs.* ignition ..... 233  
 H atoms, reactions of ..... 131  
 Heats of adsorption of O<sub>2</sub>, CO, and  
   CO<sub>2</sub> on catalysts ..... 297  
 Heneicosanol ..... 392  
 Heptane ..... 226  
   1-Heptane, formation of hydro-  
     peroxides in oxidation of .... 20  
 Heterocycles in gas-phase oxidation,  
   formation of ..... 10, 20  
 Heterogeneous catalytic oxidation . 242  
   of hydrocarbons ..... 313  
 Hexadec-1-ene ..... 160  
*n*-Hexane ..... 87, 226  
 Hex-1-ene ..... 226  
 H<sub>2</sub>O<sub>2</sub> decomposition ..... 145  
 Homogeneous catalysis ..... 207  
   in gas-phase oxidation ..... 156  
   of liquid-phase oxidation ..... 157  
 H-transfer ..... 78  
 Hydrocarbon oxidation, radical re-  
   actions in gas-phase ..... 111  
 Hydrocarbon reactions in H-O  
   mixtures ..... 124  
 Hydrocarbons  
   to alcohols and aldehydes,  
     oxidation of aromatic ..... 395  
   to aldehydes, alcohols, and  
     dimers, conversion of ..... 413  
   autoxidation of ..... 193  
   catalytic oxidation of ..... 313  
   combustion of ..... 226  
   heterogeneous catalytic  
     oxidation of ..... 313  
   minor oxidation products from  
     aromatic ..... 414  
   nitric acid catalysis in the  
     oxidation of aromatic ..... 382  
   noncatalytic oxidative  
     dehydrogenation of ..... 326  
   oxidation rates of aromatic .... 415  
   slow oxidation of ..... 23  
   vapor-phase oxidation of ..... 313  
 Hydrogen abstraction by methyl  
   peroxy radical ..... 107  
 Hydrogen peroxide from propane . 326  
 Hydrogen-oxygen reaction .... 124, 126  
   effect of added alkanes on .... 11  
 Hydrogen shift ..... 79  
 Hydrogen transfer in silent  
   discharge ..... 352  
 Hydroperoxide  
   in gas-phase oxidation ..... 17  
   in oxidation of 1-heptane ..... 20  
 Hydroperoxyalkylperoxy radicals .. 75  
 Hydroperoxyalkyl radicals ..... 72, 96  
 Hydroperoxy radicals, rate constants  
   for reactions of ..... 13, 16  
 Hydroxyl radical ..... 75

<b>I</b>		<b>Mechanism</b>	
Ignition, halogen compounds vs. . .	233	of alkane oxidation . . . . .	70
Ignition, oxidation leading to . . .	226	of free radical oxidations . . . . .	143
Indene and thiophenol, co-oxidation of . . . . .	207	of methane plus oxygen reaction of oxidation of carbon monoxide on nickel oxide . . . . .	147 292
Indium and benzylic bromides, reaction of . . . . .	397	of oxidation, high temperature . .	145
Inhibition by metal complexes . . .	179	Mercury-photosensitized oxidation of alkanes . . . . .	3
Inhibition of oxidation . . . . .	226	Metal catalysts . . . . .	163, 182, 258
Inhibitor conversion in autoxidation reactions, catalyst . . . . .	160	Metal complexes, inhibition by . . .	179
Inhibitor sweetening . . . . .	214	Metal oxide surfaces, oxidation of . .	261
Initiated oxidation of 2-methylpropane . . . . .	5	Metal salicylaldehyde chelates . . . .	164
Initiation of autoxidation . . . . .	161	Metal salt catalysis . . . . .	193
Initiation, termolecular . . . . .	161	Metals with a filled <i>d</i> -shell, oxides of . . . . .	261
Inorganic oxides . . . . .	261	Metals, hydroperoxide oxidations catalyzed by . . . . .	418
Intermediary complex . . . . .	181	Metal-thiol complexes . . . . .	185
Ionization . . . . .	313	Methacrolein . . . . .	276
from catalytic oxidation . . . . .	313	Methane . . . . .	111
effect of oxygen concentration on . .	317	oxidation . . . . .	127, 130
Iron-catalyzed co-oxidation . . . . .	221	plus oxygen reaction . . . . .	147
Isobutane low temperature oxidations of . .	40	Methyl ethyl ketone . . . . .	99
rate constants in oxidation of . . .	48	iodide . . . . .	226
Isobutene . . . . .	276	linoleate . . . . .	160
Isobutyl free radical . . . . .	58	peroxy radical, hydrogen abstraction by . . . . .	107
with oxygen, rate constants for the primary reactions of the . . . . .	61	vinyl ketone . . . . .	104
Isobutyl peroxy radical, reactions of . .	66	<i>p</i> -Methylbenzyl alcohol . . . . .	400
Isomerization . . . . .	271	<i>o</i> -Methylbenzyl radical . . . . .	402
alkylperoxy radical . . . . .	72, 76	2-Methyl-2-butene . . . . .	347
radical . . . . .	86	Methylcyclohexane . . . . .	226
Isooctane . . . . .	220	Methylene dichloride . . . . .	226
<b>K</b>		2-Methyl-3-ethyloxiran . . . . .	87
3-Keto-2-butylperoxy radical . . . . .	103	Methyl hydroperoxide . . . . .	105
3-Keto-2-butyl radicals . . . . .	101	Methylnaphthalenes . . . . .	407
Ketones, slow combustion of . . . . .	98	2-Methyloxetan . . . . .	87
Kinetic parameters . . . . .	80	2-Methylpentane . . . . .	19, 96, 226
Kinetics of ammoxidation of xylenes over vanadium catalysts . . . . .	288	gas-phase oxidation of . . . . .	20
of epoxidation of olefins . . . . .	426	3-Methylpentane, products from . .	19
of peracetic acid decomposition . . . .	368	2-Methylpropane . . . . .	40
of propane oxidation . . . . .	113, 337	initiated oxidation of . . . . .	5
<b>L</b>		2-Methylpropene . . . . .	5, 276
Lachrymator . . . . .	397	2-Methyl-3- <i>n</i> -propyloxiran . . . . .	87
Lattice oxygen . . . . .	269	$\alpha$ -Methylstyrene . . . . .	404
Lauryl aldehyde . . . . .	390	Molecular structure on platinum- catalyzed oxidation, effect of . .	314
Light emission . . . . .	111	Molecules reactions of C <sub>2</sub> H <sub>5</sub> O with . . . . .	36
Linear energy transfer . . . . .	359	reactions of RO with . . . . .	31
Liquid-phase oxidation, homogene- ous catalysis of . . . . .	157	reactions of RO <sub>2</sub> with . . . . .	26
Low temperature chain oxidation . . . .	144	Molybdenum catalysts . . . . .	421
Low temperature oxidations of isobutane . . . . .	40	Multistep chain oxidation . . . . .	207
<b>M</b>		Mutual reactions of ROO . . . . .	13
Manganese(II) acetate in acetaldehyde oxidation . . . . .	366	<b>N</b>	
		Negative temperature coefficient . . .	11
		in oxidation . . . . .	144
		in slow combustion . . . . .	105
		Neopentane, gas-phase oxidation of . . . . .	7, 20, 136

Neopentyl glycol . . . . . 390, 392  
 Nickel chelates . . . . . 167  
 Nickel oxide, mechanisms of oxidation of carbon monoxide on . . 292  
 Nitric acid catalysis, bromine- . . . . 389  
 Nitric acid catalysis in the oxidation of aromatic hydrocarbons . . . . 382  
 Nitrosyl radical . . . . . 217  
 Noncatalytic oxidative dehydrogenation of hydrocarbons . . . . 326  
 Non-stationary state . . . . . 212

## O

OH radicals, reactions of . . . . . 131, 136  
 Olefin formation from  $RO_2^{\cdot}$   
 isomerization . . . . . 148  
 Olefins . . . . . 242, 261  
 autoxidation of . . . . . 352  
 catalyzed by selenium, oxidation of . . . . . 345  
 epoxidation of . . . . . 418  
 in gas-phase oxidation . . . . . 7, 16, 20, 426  
 Olefin structure vs. epoxidation . . . . 422  
 Organoselenides as catalysts . . . . 345  
 Oxidation  
 of aromatic hydrocarbons to alcohols and aldehydes . . . . 395  
 of metal oxide surfaces . . . . . 261  
 of neopentane in the gas-phase . . . . 7  
 of olefins catalyzed by selenium . . . . 345  
 of polymers . . . . . 200  
 products from aromatic hydrocarbons, minor . . . . 414  
 Oxides, transition metal . . . . . 255, 261  
 Oxygenated products . . . . . 71  
 Oxygen  
 bonding on silver . . . . . 244  
 chemisorption of . . . . . 294  
 concentration on catalytic oxidation and ionization, effect of . . . . . 317  
 vs. epoxidation . . . . . 424  
 heterocycles . . . . . 19, 79, 96  
 from the gaseous oxidation of *n*-alkanes . . . . . 86  
 in gas-phase oxidation, formation of . . . . . 10, 20  
 lattice . . . . . 269  
 reaction, effect of added alkanes on hydrogen . . . . . 11  
 singlet . . . . . 60

## P

*n*-Pentane . . . . . 87, 96, 111  
 1-Pentane, gas-phase oxidation of . . . . 20  
 1-Pentane, products from . . . . . 19  
 Pentavalent carbon . . . . . 149  
 Peracetic acid . . . . . 347  
 with acetaldehyde, reaction of . . . . 369  
 decomposition, kinetics of . . . . . 368  
 degenerate branching by . . . . . 105  
 Peroxide radical ions . . . . . 272

Peroxy radicals  
 to alkenes, addition of . . . . . 74  
 chain termination by mutual reaction of . . . . . 13  
 Evans-Polanyi relation for . . . . . 15  
 rate constants for  
 H-abstraction by . . . . . 14  
 rate constants for reactions of . . . . 12, 17  
 rearrangements of . . . . . 19  
 Phase change in oxidation of isobutane . . . . . 40  
 Photo-oxidation  
 of azoalkanes . . . . . 3  
 of 1,1-azoisobutane . . . . . 58  
 of azo-2-methylpropane . . . . . 4  
 Photolytic oxidation, wall after-effects in . . . . . 151  
 Phthalocyanines . . . . . 189  
*Pic d'arrêt* . . . . . 111  
 Platinum catalysis . . . . . 248, 258  
 Platinum-catalyzed oxidation, effect of molecular structure on . . . . 314  
 Platinum as oxidation catalyst . . . . 313  
 Polyamides . . . . . 160  
 Polyethylene . . . . . 160  
 Polyhydroperoxides . . . . . 20  
 Polymers, oxidation of . . . . . 200  
 Polyolefins . . . . . 160  
 Polypropylene . . . . . 160  
 Porphyrin ligands . . . . . 184  
 Pre-exponential factor . . . . . 81  
 Preflame oxidation . . . . . 236  
 Preflame studies . . . . . 227  
 Primary  $RO_2^{\cdot}$ , disproportionation of . . . . 151  
 Propane . . . . . 111  
 hydrogen peroxide from . . . . . 326  
 oxidation, kinetics of . . . . . 337  
 Propylene . . . . . 353  
 oxidation . . . . . 249  
 1,2-Propylene oxide . . . . . 104  
 2-*n*-Propyloxiran . . . . . 87  
 3-*n*-Propyloxiran, 2-methyl- . . . . . 87  
 Pseudocumene oxidation . . . . . 387  
 Pseudo-steady state . . . . . 220  
 Pyrolysis of radicals in  
 combustion . . . . . 10, 14  
 in gas-phase oxidation . . . . . 18  
 Pyrophosphates . . . . . 189

## R

Radical  
 attack on the aromatic ring . . . . . 408  
 isomerization . . . . . 86  
 reactions in gas-phase hydrocarbon oxidation . . . . . 111  
 Radicals  
 alkylperoxy . . . . . 86, 96  
 in combustion, pyrolysis of . . . . . 10, 14, 18  
 hydroperoxylalkyl . . . . . 96  
 reactions of  $CH_3O^{\cdot}$  with . . . . . 37  
 reactions of  $CH_3O_2^{\cdot}$  with . . . . . 28  
 reactions of  $RO^{\cdot}$  with . . . . . 35  
 reactions of  $RO_2^{\cdot}$  with . . . . . 27

